LEABHARLANN CHOLÁISTE NA TRÍONÓIDE, BAILE ÁTHA CLIATH | TRINITY COLLEGE LIBRARY DUBLIN
Ollscoil Átha Cliath | The University of Dublin

Terms and Conditions of Use of Digitised Theses from Trinity College Library Dublin

Copyright statement

All material supplied by Trinity College Library is protected by copyright (under the Copyright and Related Rights Act, 2000 as amended) and other relevant Intellectual Property Rights. By accessing and using a Digitised Thesis from Trinity College Library you acknowledge that all Intellectual Property Rights in any Works supplied are the sole and exclusive property of the copyright and/or other IPR holder. Specific copyright holders may not be explicitly identified. Use of materials from other sources within a thesis should not be construed as a claim over them.

A non-exclusive, non-transferable licence is hereby granted to those using or reproducing, in whole or in part, the material for valid purposes, providing the copyright owners are acknowledged using the normal conventions. Where specific permission to use material is required, this is identified and such permission must be sought from the copyright holder or agency cited.

Liability statement

By using a Digitised Thesis, I accept that Trinity College Dublin bears no legal responsibility for the accuracy, legality or comprehensiveness of materials contained within the thesis, and that Trinity College Dublin accepts no liability for indirect, consequential, or incidental, damages or losses arising from use of the thesis for whatever reason. Information located in a thesis may be subject to specific use constraints, details of which may not be explicitly described. It is the responsibility of potential and actual users to be aware of such constraints and to abide by them. By making use of material from a digitised thesis, you accept these copyright and disclaimer provisions. Where it is brought to the attention of Trinity College Library that there may be a breach of copyright or other restraint, it is the policy to withdraw or take down access to a thesis while the issue is being resolved.

Access Agreement

By using a Digitised Thesis from Trinity College Library you are bound by the following Terms & Conditions. Please read them carefully.

I have read and I understand the following statement: All material supplied via a Digitised Thesis from Trinity College Library is protected by copyright and other intellectual property rights, and duplication or sale of all or part of any of a thesis is not permitted, except that material may be duplicated by you for your research use or for educational purposes in electronic or print form providing the copyright owners are acknowledged using the normal conventions. You must obtain permission for any other use. Electronic or print copies may not be offered, whether for sale or otherwise to anyone. This copy has been supplied on the understanding that it is copyright material and that no quotation from the thesis may be published without proper acknowledgement.

Investigation into the mechanism by which a novel series of pyrrolo-1,5-benzoxazepine compounds induce apoptosis in chronic myelogenous leukaemia cells

Thesis submitted to the
University of Dublin
for the Degree of
Doctor of Philosophy

by

Margaret Mc Gee
Department of Biochemistry
Trinity College
Dublin

August 2001

TRINITY COLLEGE
0 4 DEC 2001
LIBRARY DUBLIN
Thesis
6433

Declaration

I certify that the work herein is entirely my own and has not been submitted for a degree at this, or any other, University. The library at Trinity College Dublin has my full permission to lend or copy this thesis upon request.

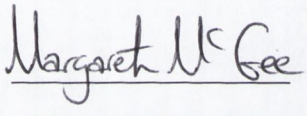

Margaret Mc Gee

Acknowledgements

Firstly, a heartfelt thanks to Dr. Daniela Zisterer and Professor D. Clive Williams for their invaluable advice and encouragement throughout the entire project. Your friendship and knowledge was a tremendous support.

What fun would work have been without lab members past and present? Thanks to Marina, Severene, Stephen, Patrick, Monica, Siobhan, Jude, Anna, Jana, Anne-Marie, Francesca, Gordon, Elena and Grace. Thanks also to other members of the department for their help and friendship especially Roisin and Bernie.

Thanks to Professor Luke O'Neill and members of his research group, especially Kate, Ashley, Andrew, Eva, and Caroline, for much help and for borrowing an unending list of items.

I would also like to mention Professor Giuseppe Campiani for synthesising the compounds used in this study, Dr. Mark Lawler for advice and the use of facilities in his laboratory, and BioResearch Ireland for financial support.

A big thanks to my friends Fiona, Sheila and Sinead for their support and encouragement and for our many nights out on the town!

Thanks to all my family for being so supportive throughout and finally, a special thanks to Don, who at this stage could almost master a Western blot himself – thanks for always being there.

Table of Contents

Table of contents *i*

List of illustrations *ix*

List of tables *x*

Abbreviations *xi*

Abstract *xiv*

Chapter 1 General Introduction

1.1 Chronic myelogenous leukaemia **1**

1.2 Regulation of hematopoiesis **3**

1.3 The *abl* gene **4**

1.4 The *bcr* gene **5**

1.5 Bcr-Abl genes and proteins **6**

1.6 Mechanisms of Bcr-Abl-mediated transformation **7**

1.7 Bcr-Abl activated signalling pathways **9**

1.7.1 Bcr-Abl and mitogen-activated protein (MAP) kinase pathways 9

1.7.2 Bcr-Abl and STAT signalling 9

1.7.3 Bcr-Abl and phosphoinositide 3-kinase (PI-3 kinase) signalling 10

1.7.4 Bcr-Abl and interaction with SHIP proteins 11

1.7.5 Bcr-Abl and *c-myc* signalling 11

1.8 Diagnosis of CML **11**

1.9 Conventional chemotherapy in the treatment of CML **12**

1.10 Bone marrow transplantation as a therapy for CML **13**

1.11 Molecular targets for CML therapy **14**

1.12 Experimental models of CML **17**

1.13 Cell death: characteristics of apoptosis and necrosis **18**

1.14 *Caenorhabditis elegans* and apoptosis **19**

1.15 Caspases: apoptotic proteases **20**

1.16 Mitochondria and apoptosis **24**

1.17 Bcl-2 proteins and the regulation of apoptosis 26
1.18 Oxidative stress and apoptosis 28
1.19 Tyrosine phosphorylation and apoptosis 29
1.20 Mitogen-activated protein (MAP) kinase signalling 30
1.21 GTP binding proteins 33
1.22 Farnesyl transferase inhibitors and prevention of Ras transformation 36
1.23 Induction of apoptosis by DNA damaging drugs 39
1.24 Peripheral-type benzodiazepine receptor 41
1.25 Aims of this study 44

Chapter 2 Materials and Methods

2.1 Materials 46
2.2 Cell Culture 52
2.2.1 Growth and maintenance of the Human Leukaemic HL60 cell line, Jurkat T cells and the Chronic Myeloid Leukaemia cell lines K562, KYO.1 and LAMA 84 52
2.2.2 Cryo-preservation of cells 52
2.3 Determination of protein concentration 53
2.3.1 Bradford protein assay 53
2.3.2 Markwell protein assay 53
2.4 Cytospin preparation and RapiDiff staining of cells 54
2.5 Detection of DNA Fragmentation by agarose gel electrophoresis 54
2.6 Measurement of levels of Bcr-Abl expression by Western blotting 55
2.6.1 Preparation of cell extracts for measurement of Bcr-Abl expression 55
2.6.2 Sodium dodecyl sulphate-polyacrylamide gel electrophoresis (SDS-PAGE) 55
2.6.3 Western blotting 56
2.6.4 Stripping and re-probing of blots 57
2.7 Measurement of protein tyrosine phosphorylation by Western blot 57
2.8 Western blot to measure cytochrome c release 58

2.9 Measurement of caspase-3 activity **59**
2.9.1 Fluorogenic assay to measure caspase-3-like protease activity 59
2.9.2 Preparation of AMC standard curve 59
2.10 Fluorogenic assay to measure caspase-6-like protease activity **60**
2.11 Determination of caspase-7-like protease activity using Western blotting **60**
2.12 Western blot analysis of poly (ADP-ribose) polymerase (Parp) cleavage **61**
2.13 Western blot to detect activation of mitogen-activated protein (MAP) kinases and their substrates **62**
2.14 Detection of Bcl-2 family members by Western blotting **63**
2.14.1 Subcellular fractionation of K562 cells to yield cytosolic and mitochondrial fractions 63
2.14.2 Western blot to detect Bcl-2, Bcl-$_{XL}$ and Bax 64
2.15 Radioligand binding assay **64**
2.15.1 Measurement of [^{3}H] PK11195 binding to CML cell homogenates 64
2.15.2 Liquid scintillation counting 65
2.15.3 Analysis of binding data 65
2.16 Measurement of DNA strand breaks **67**
2.16.1 Alkaline elution assay to measure DNA strand breaks 67
2.17 Determination of farnesyl protein transferase activity **68**
2.17.1 Partial purification of farnesyl protein transferase from cells 68
2.17.2 Assay for farnesyl protein transferase activity 68
2.18 Statistical analysis of data **69**
2.19 Electrophoretic mobility shift assay (EMSA) **69**
2.19.1 Preparation of nuclear extracts for the detection of nuclear factor kappa B (NFκB) activation 69
2.19.2 Labelling of oligonucleotides for EMSA assay 70
2.19.3 EMSA assay 70
2.20 Lactate Dehydrogenase (LDH) assay **71**
2.21 Preparation of LB medium **72**
2.22 Preparation of competent *E.coli* **72**

2.23 Preparation of antibiotic stock solutions 73
2.24 Transformation of competent *E.coli* 73
2.25 Extraction and ethanol precipitation of plasmid DNA from *E.coli* (Mini-prep) 73
2.26 Quantification and analysis of DNA by agarose electrophoresis 74
2.27 Spectrometric quantification of DNA 74
2.28 Preparation of Maxiprep plasmid DNA 74
2.29 Transient transfection of K562 cells 75
2.30 Determination of luciferase reporter gene activity 75
2.31 Determination of β-galactosidase activity 76
2.32 Plasmid constructs 76

Chapter 3 Investigation into the apoptotic effects of a novel series of pyrrolo-1,5-benzoxazepine compounds in chronic myelogenous leukaemia cells

3.1 Introduction 77
3.2 Results 84
3.2.1 Pyrrolo-1,5-benzoxazepines induce apoptosis in K562 cells 84
3.2.2 K562 cells are resistant to the induction of apoptosis by many commonly used chemotherapeutic drugs 84
3.2.3 PBOX-6 induces apoptosis in K562, LAMA 84 and KYO.1 cells in a dose- and time-dependent manner 85
3.2.4 PBOX-6 induces DNA fragmentation in K562, LAMA 84 and KYO.1 cells 85
3.2.5 PBOX-6-induced apoptosis is not preceded by a down-regulation in Bcr-Abl expression 85
3.2.6 Investigation into the tyrosine phosphorylation status of the Abl tyrosine kinase and other proteins during PBOX-6-induced apoptosis in CML cells 86

3.2.6.1 PBOX-6-induced apoptosis is not mediated by a decrease in protein tyrosine phosphorylation 86
3.2.6.2 PBOX-6 increases the tyrosine phosphorylation of two proteins in K562 cells 87
3.2.6.3 Genistein prevents tyrosine phosphorylation and the induction of apoptosis by PBOX-6 87
3.2.6.4 Investigation into the identity of two tyrosine phosphorylated proteins (63 kDa and 71 kDa) using specific tyrosine kinase inhibitors 88
3.2.7 PBOX-6-induced apoptosis does not result in an increase in cytoplasmic cytochrome c levels in CML cells 88
3.2.8 Antioxidants do not protect against PBOX-6-induced apoptosis in K562 cells 89
3.2.9 Investigation into the role of cysteine proteases during PBOX-6-induced apoptosis in CML cells 90
3.2.9.1 Caspase-3-like proteases become activated to a small extent in K562 and LAMA 84 cells, but not in KYO.1 cells, in response to PBOX-6 90
3.2.9.2 Activation of caspase-3-like proteases is not essential in PBOX-6-mediated apoptosis in CML cells 91
3.2.9.3 Caspase-6-like proteases are not activated during PBOX-6-induced apoptosis in CML cells 92
3.2.9.4 Lack of involvement of caspase-7 during PBOX-6-induced apoptosis in CML cells 93
3.2.9.5 The general caspase inhibitor, z-VAD-fmk, does not protect against PBOX-6-induced apoptosis in CML cells 93
3.2.10 Caspase-3 is not necessarily required for poly (ADP-ribose) polymerase (Parp) cleavage in CML cells 94
3.3 Discussion 95

Chapter 4 Investigation into the events that trigger the apoptotic cascade induced by PBOX-6 in K562 cells

4.1 Introduction **106**

4.2 Results **112**

4.2.1 Saturable binding of [^{3}H] PK11195 to K562, KYO.1 and LAMA 84 cell homogenates 112

4.2.2 Displacement of [^{3}H] PK11195 by PBOX-6 from K562, KYO.1 and LAMA 84 cell homogenates 112

4.2.3 Displacement of [^{3}H] PK11195 from K562 cell homogenates by the non-apoptotic pyrrolo-1,5-benzoxazepines, PBOX-1 and -2, and the apoptotic pyrrolo-1,5-benzoxazepines, PBOX-4, -5 and –7 113

4.2.4 Peripheral-type receptor ligands, Ro5-4864 and PK11195, have no effect on PBOX-6-induced apoptosis in K562 cells 113

4.2.5 Investigation into the effect of PBOX-6 on farnesyl protein transferase activity by measuring H-Ras farnesylation 114

4.2.5.1 Optimisation of experimental conditions to measure farnesyl protein transferase activity in K562 cells 114

4.2.5.2 Inhibition of farnesyl protein transferase activity from K562 cell extracts using manumycin A, FTI (II) and FTI-276 115

4.2.5.3 Lack of effect of PBOX-6 on K562 farnesyl protein transferase activity from K562 cell extracts 116

4.2.6 Determination of the apoptotic activity of farnesyl protein transferase inhibitors, manumycin A, FTI (II) and FTI-276 on K562 cells 116

4.2.7 Pretreatment of K562 cells with various topoisomerase II inhibitors prevents PBOX-6-induced apoptosis 117

4.2.8 Alkaline elution assays to determine whether PBOX-6 acts as a topoisomerase II poison by inducing DNA strand breaks 118

4.2.9 Alkaline elution assays to determine whether PBOX-6 acts as a catalytic inhibitor of topoisomerase II 119

4.3 **Discussion** **121**

Chapter 5 Characterisation of the biochemical signalling pathway initiated during PBOX-6-induced apoptosis in K562 cells

5.1 Introduction **131**

5.2 Results **140**

5.2.1 PBOX-6 induces transient activation of c-Jun N-terminal kinase (JNK) in K562 cells, but has no effect on extracellular signal-regulated kinase (ERK) or p38 140

5.2.2 The JNK signalling inhibitor, CEP-1347, inhibits JNK activation and blocks apoptosis induced by PBOX-6 in K562 cells 140

5.2.3 PBOX-6 induces phosphorylation of the c-Jun transcription factor in a dose-and time-dependent manner in K562 cells 141

5.2.4 PBOX-6 induces phosphorylation of activating transcription factor 2 (ATF-2) in K562 cells in a dose- and time-dependent manner 141

5.2.5 The JNK signalling inhibitor, CEP-1347, inhibits activation of c-Jun and ATF-2 in K562 cells following treatment with PBOX-6 142

5.2.6 The JNK signalling inhibitor, dicumarol, prevents phosphorylation of c-Jun and ATF-2, and apoptosis induced by PBOX-6 in K562 cells 142

5.2.7 Manumycin A induces activation of the JNK MAP kinase in K562 cells, which is not essential for the induction of apoptosis 143

5.2.8 The topoisomerase II inhibitors, etoposide and ICRF-187, do not inhibit PBOX-6-induced JNK activation in K562 cells 144

5.2.9 Phosphorylation of the anti-apoptotic proteins, Bcl-2 and Bcl-$_{XL}$, in K562 cells in response to PBOX-6 treatment 144

5.2.10 Inhibition of PBOX-6-induced phosphorylation of Bcl-2 and Bcl-$_{XL}$ in K562 cells using the JNK inhibitors CEP-1347 and dicumarol 145

5.2.11 PBOX-6 has no effect on expression levels and on subcellular localisation of Bax in K562 cells 146

5.2.12 Activation of c-Jun- and ATF-2-dependent reporter genes following stimulation of K562 cells with PBOX-6 147

5.2.13 Expression of the JNK signalling inhibitor, JIP-1, prevents activation

of the ATF-2-dependent reporter gene and apoptosis induced by PBOX-6 148
5.2.14 PBOX-6 activates the NFκB-dependent reporter gene in K562 cells 149
5.2.15 PBOX-6 induces a time-dependent increase in NFκB activation in K562 cells 149
5.2.16 Effect of RasV12 and RasN17 on PBOX-6-induced activation of the ATF-2-dependent reporter gene 150
5.2.17 Effect of RacV12 and RacN17 on PBOX-6-induced activation of the ATF-2-dependent reporter gene 150
5.2.18 Effect of wild type Cdc42 and Cdc42N17 on PBOX-6-induced activation of the ATF-2-dependent reporter gene 151
5.2.19 Lethal toxin, which inhibits the activity of Ras and Rac, does not prevent PBOX-6-induced JNK activation in K562 cells 152
5.3 Discussion 154

Chapter 6 Concluding Remarks 165

References 172

Publications 206

List of illustrations

Chapter 1

1.1	Schematic representation of the p145 c-Abl protein	4
1.2	Schematic representation of the p160 Bcr protein	6
1.3	Schematic representation of the p210 Bcr-Abl fusion protein	6
1.4	Signalling pathways with mitogenic potential in Bcr-Abl transformed cells	9
1.5	Schematic representation of pathways describing the caspase cascades that result in apoptosis	22
1.6	GTP-binding proteins and their regulation of MAP kinase signalling cascades	30
1.7	Regulation of GTP-binding proteins	34
1.8	The catalytic cycle of topoisomerase II	39
1.9	General formula of pyrrolo-1,5-benzoxazepine compounds	43

Chapter 2

2.1	AMC standard curve	60
2.2	Plasmid structure for *Trans*-Reporting system	76
2.3	Schematic map of expression vectors for RacV12 and RacN17	76
2.4	Schematic diagram of expression vectors for wild type Cdc42 and N17Cdc42	76
2.5	Schematic diagram of the point mutations in RasV12 and RasN17	76
2.6	Schematic illustration of JIP-1 and its interaction with components of the JNK MAP kinase pathway	76
2.7	Graphical representation of the β-Galactosidase vector	76
2.8	Graphical representation of pGL3Luc vector used to construct the NFκB-luciferase reporter plasmid	76

Chapter 3

3.1	Structure of pyrrolo-1,5-benzoxazepines	84
3.2	Morphological features of K562 cells undergoing apoptosis following treatment with PBOX-6	84
3.2	Primary myeloid cells derived from normal bone marrow do not undergo apoptosis following treatment with PBOX-6	84

Chapter 5

5.26	Schematic representation of the proposed pathway of PPOX-6-induced apoptosis in K562 cells	164

List of Tables

4.1	Summary of the displacement of [^{3}H] PK11195 binding to the PBR by a range of PBOX compounds	113

Abbreviations

Abl	Abelson
AIF	Apoptosis-inducing factor
AMC	Amino methyl coumarin
ANT	Adenine nucleotide translocator
AP-1	Activator protein-1
Apaf-1	Protease activating factor-1
APS	Ammonium persulphate
ATF-2	Activating transcription factor 2
ATP	Adenosine triphosphate
Bcr	Breakpoint cluster region
B_{max}	Maximal binding capacity
BSA	Bovine serum albumin
CAD	Caspase-activated DNase
CAM	Cell adhesion molecule
CARD	Caspase recruitment domain
CFU	Colony forming unit
CML	Chronic myelogenous leukaemia
Cpm	Counts per minute
CRIB	Cdc42/Rac interactive binding
CSF	Colony stimulating factor
DBI	Diazepam binding inhibitor
DED	Death effector domain
DFF	DNA fragmentation factor
DMSO	Dimethyl sulphoxide
DTT	Dithiothreitol
EDTA	Ethylenediaminetetraacetic acid
EMSA	Electrophoretic mobility shift assay
EndoG	Endonuclease G
ERK 1/ 2	Extracellular signal-regulated kinase 1/ 2

FAD	Flavin adenine dinucleotide
FADD	Fas associated protein with death domain
FCS	Foetal calf serum
FISH	Fluorescence in situ hybridisation
Fmk	Fluoromethyl ketone
FPP	Farnesyl pyrophosphate
FPTase	Farnesyl protein transferase
GAP	GTPase activating protein
GCK	Germinal centre kinase
GDI	Guanine nucleotide dissociation inhibitor
GDP	Guanine diphosphate
GEF	Guanine nucleotide exchange factor
GGPTase	Geranyl geranyl protein transferase
GTP	Guanine triphosphate
HEPES	N-[2-Hydroxyethyl]piperazine-N'-[2-ethanesulphonic acid]
ICAD	Inhibitor of caspase-activated DNase
ICE	Interleukin-1β-converting enzyme
IGF	Insulin-like growth factor
IκB	Inhibitory κB
IL	interleukin
JIP	JNK-interacting protein
JNK	c-Jun N-terminal kinase
K_D	Equilibrium dissociation constant
KDa	Kilodalton
K_i	Inhibition constant
LB	Lauria-Bertani
LDH	Lactate dehydrogenase
MAPK	Mitogen-activated protein kinase
MAPK K	Mitogen-activated protein kinase kinase
MAPKKK	Mitogen-activated protein kinase kinase kinase
MLK	Mixed-lineage kinase

Mr	Relative molecular mass
NAC	*N*-acetylcystine
NFκB	Nuclear factor kappa B
ODN	Oligodeoxynucleotide
PAGE	Polyacrylamide gel electrophoresis
PAK	p21-activated kinase
Parp	Poly (ADP-Ribose) polymerase
PBOX	Pyrrolobenzoxazepine
PBR	Peripheral-type benzodiazepine receptor
PBS	Phosphate buffered saline
PGDF	Platelet derived growth factor
Ph	Philadelphia
PI3-K	Phosphatidylinositol 3-kinase
PKC	Protein kinase C
PMSF	Phenylmethylsulphonyl fluoride
PT	Permeability transition
PTK	Protein tyrosine kinase
PVDF	Polyvinylidene difluoride
Rb	Retinoblastoma protein
ROI	Reactive oxygen intermediate
ROS	Reactive oxygen species
SCID	Severe combined immunodeficiency
SDS	Sodium dodecyl sulphate
S.E.M	Standard error of mean
TCA	Trichloroacetic acid
TEMED	*N, N, N', N'*,-Tetramethylethylenediamine
TNF	Tumour necrosis factor
Topo II	Topoisomerase II
TRAF	TNF-receptor associated factor
VDAC	Voltage-dependent anion channel
UV	Ultra-violet

Abstract

Some members of a novel series of pyrrolo-1,5-benzoxazepine compounds induce apoptosis in human chronic myeloid leukaemia (CML) cells. A representative compound, PBOX-6, induces apoptosis in a dose- and time-dependent manner, in three CML cell lines; K562, KYO.1 and LAMA 84. The morphological criteria associated with apoptosis including cell shrinkage, chromatin condensation and DNA fragmentation was observed in these cells in response to PBOX-6. In this study, the mechanism by which PBOX-6 induces apoptosis in CML cells was investigated.

The anti-apoptotic property of CML cells has been attributed to the expression of a Bcr-Abl fusion protein. PBOX-6-induced apoptosis in CML cells does not result in a down-regulation of Bcr-Abl or its tyrosine kinase activity, suggesting that PBOX-6 bypasses the apoptotic suppressor, Bcr-Abl, in the mechanism in which it induces apoptosis.

Apoptosis induced by PBOX-6 in CML cells does not result in the alteration of mitochondrial events such as cytochrome c release or the generation of reactive oxygen intermediates. However, the induction of apoptosis in K562 cells is accompanied by an increase in the tyrosine phosphorylation status of two, as yet unidentified proteins, of approximately 63 kDa and 71 kDa.

PBOX-6 induces a small amount of caspase-3-like protease activity in K562 and LAMA 84, but not in KYO.1 cells. Inhibition of caspase-3-like protease activity failed to protect against PBOX-6-induced apoptosis, suggesting that activation of caspase-3-like proteases is not an essential part of the apoptotic pathway induced by PBOX-6 in CML cells. Alternative executioner caspases, such as caspase-6 and caspase-7, are not activated in response to PBOX-6, suggesting that caspases are dispensable for apoptosis induced by PBOX-6 in CML cells. Induction of apoptosis by PBOX-6 results in a small degree of Parp cleavage. Detection of Parp cleavage in the KYO.1 cells, in which caspase-3-like protease activity was not detected, suggests that caspase-3 is not required for Parp cleavage, and that alternative caspases or proteases may be responsible for Parp cleavage in these cells.

The mechanism in which PBOX compounds induce apoptosis does not involve their specific interaction with the PBR, which they bind to with high affinity. In addition, the

inability of PBOX-6 to inhibit farnesylation of H-Ras suggests that PBOX-6 does not function as a farnesyl protein transferase inhibitor.

The DNA binding protein, Topo II, is the target for many anti-cancer drugs. Some compounds act as Topo II poisons and induce DNA strand breaks. PBOX-6 does not induce DNA strand breaks in K562 cells, suggesting that it does not act as a Topo II poison. Catalytic inhibitors of Topo II attenuate strand breaks induced by Topo II poisons. PBOX-6 does not attenuate DNA strand breaks induced by Topo II poisons, suggesting that it does not operate in a manner similar to these compounds. However, the ability of a number of Topo II inhibitors to prevent PBOX-6-induced apoptosis suggests that Topo II is involved in the apoptotic pathway induced by PBOX-6.

MAP kinases play a critical role in the regulation of apoptosis. In this study, PBOX-6 induces the rapid and transient activation of two JNK isoforms in K562 cells. Activation of p38 and ERK was not detected in K562 cells following PBOX-6 treatment. The JNK inhibitors, CEP-1347 and dicumarol, prevent PBOX-6-induced JNK activation and apoptosis, suggesting that activation of JNK is an essential component of the apoptotic pathway. PBOX-6 phosphorylates and activates the JNK substrates c-Jun, ATF-2 and NFκB in K562 cells. In addition, JNK phosphorylates and inactivates the anti-apoptotic Bcl-2 family members, Bcl-2 and Bcl-$_{XL}$.

GTP-binding proteins play a regulatory role in MAP kinase signalling cascades. Expression of dominant negative mutants of Ras, Rac and Cdc42 in K562 cells does not prevent PBOX-6-induced activation of an ATF-2-dependent reporter gene, suggesting that PBOX-6-induced activation of JNK occurs independent of GTPase activity.

Overexpression of the scaffold protein, JIP-1, which selectively scaffolds the MLK-MKK7-JNK pathway, has been previously shown to inhibit the JNK signalling pathway. In the present study, expression of JIP-1 in K562 cells inhibits phosphorylation of ATF-2 and apoptosis induced by PBOX-6, confirming the importance of JNK in the apoptotic pathway. These results also support a role for the MLK family of MAPKKKs and the MAPKK MKK7, in the regulation of JNK activity in K562 cells. Furthermore, an alternative JNK inhibitor, CEP-1347, has recently been found to selectively target members of the MLK and germinal centre kinase (GCK) families. Together these reports strongly support a role for these kinases in the upstream signalling pathway leading to JNK activation and apoptosis in K562 cells in response to PBOX-6 treatment.

Chapter 1

General Introduction

1.1 Chronic myelogenous leukaemia

Chronic myelogenous leukaemia (CML) is probably the most extensively studied human malignancy. It is a member of a group of diseases classed as myeloproliferative disorders, which account for 20% of all leukaemias. CML has an incidence of 1 to 2 cases per 100,000 of the population, and has a male-to-female ratio of 1.3-1. Incidence increases with age, the median age at presentation is 45-55 years (Faderl *et al.*, 1999).

CML is a myeloproliferative disorder with clonal expansion of transformed primitive hematopoietic progenitor cells. The disorder is easily recognised because the leukaemia cells of more than 95% of patients have a distinctive cytogenetic abnormality known as the Philadelphia (Ph) chromosome. This discovery by Baikie *et al.* (1960), which was the first consistent chromosomal abnormality associated with a specific type of leukaemia, was a breakthrough in cancer biology. The Philadelphia chromosome results from a reciprocal translocation between the long arms of chromosomes 9 and 22. This translocation results in the transfer of the abelson (*abl*) oncogene on chromosome 9 to an area of chromosome 22 termed the breakpoint cluster region (*bcr*) [t (9; 22) (q34; q11)]. This in turn results in the fused *bcr-abl* gene and in the production of an abnormal tyrosine kinase protein that may be related to the disordered myelopoiesis found in CML (Clarkson *et al.*, 1997; Cortez *et al.*, 1997). This fusion converts c-Abl tyrosine kinase from a tightly regulated, predominantly nuclear, protein into a constitutively active, abnormally regulated, cytoplasmic tyrosine kinase. Because of its increased activity and new location in the cell, Bcr-Abl gains access to a wide range of cytoplasmic substrates, which may function in mediating its anti-apoptotic effect (Evans *et al.*, 1993; Mc Gahon *et al.*, 1994a).

The Bcr-Abl gene transcribes a novel 8.5 kb mRNA, which in turn encodes a p210 kDa protein that is present in most CML patients. It is now well established that the breakpoint within Bcr can be variable. Three major forms of Bcr-Abl fusion proteins are now recognised, and it appears that the inclusion or exclusion of Bcr exons is largely responsible for determining the disease phenotype caused by these proteins. In most patients with CML and in approximately one-third of patients with Ph-positive acute lymphoblastic leukaemia (ALL), the break occurs within a 5.8 kb area spanning Bcr exons 12-16, and is defined as the major breakpoint cluster region (M-*bcr*). A 210 kDa chimeric protein (p210 Bcr-Abl) is derived from this mRNA. In the remaining patients with ALL, and rarely associated with

CML or acute myelocytic leukaemia (AML), the breakpoints occur further upstream in the 54.4 kb region, which is termed the minor breakpoint cluster region (m-*bcr*). This mRNA produces the smallest fusion protein, p190 Bcr-Abl. Recently, a third breakpoint cluster region (μ-*bcr*) has been identified, which gives rise to a 230 kDa Bcr-Abl fusion protein that has been observed in cells from patients with Chronic Neutrophilic Leukaemia (CNL) (Cortez *et al.*, 1997; Deininger *et al.*, 2000).

Clinically, CML follows a triphasic course. In the initial chronic phase there is an elevated white cell count, the blood film shows an increase in morphologically normal myeloid cells at all stages of differentiation but with greatest numbers of myelocytes and neutrophils. During this stage of the disease, therapeutic intervention is usually reasonably successful. However, after an unpredicted period, which can be weeks, months, or even years, the disease progresses to a more aggressive phase of accelerated growth. The accelerated phase is characterised by an increase in the number of immature cells in the peripheral blood that have lost their capacity for terminal differentiation. The accelerated phase is followed after 3 to 18 months by a blastic phase, where the bone marrow consists of myeloid and lymphoid cells, which fail to mature fully, and these eventually spill over into the blood. The latter resembles acute leukaemia and causes death within 3 to 6 months (Faderl *et al.*, 1999). The immature blast cells in the bloodstream invade other organs and tissues and disrupt their normal function. From a clinical viewpoint, blast crisis is particularly resistant to therapeutic intervention and is almost invariably fatal. CML myeloid precursors display normal mitotic indices, normal responses to colony-stimulating factors and do not proliferate faster than their normal counterparts. Taken together, these observations suggest that the myeloid expansion in CML may occur via prolongation of cell survival rather than excessive proliferation (Mc Gahon *et al.*, 1994a).

It is thought that 50-80% of patients acquire additional genetic alterations and chromosomal abnormalities that precede the progression of CML from the chronic phase of the disease to induce the phenotype of blast crisis (Deininger *et al.*, 2000). Genes known to be altered in the progression of CML include p53, retinoblastoma protein (Rb), c-myc and Ras. Loss of function of p53 has been associated with suppression of apoptosis and progression into blast crisis (Faderl *et al.*, 1999). One recent article has reported a down-regulation of the major mammalian DNA repair protein, DNA-dependent protein kinase

(DNA-PK) by Bcr-Abl (Deutsch *et al.*, 2001). Although little is known about the possible implication of Bcr-Abl in the DNA repair processes, the fact that CML cells are both deficient in DNA repair and refractory to apoptosis may explain how genetic abnormalities can accumulate in leukaemic cells and why this myeloproliferative disorder constantly progresses to a blast crisis. While the underlying genetic abnormality in CML is now quite well defined, the critical biochemical aberrations caused by p210 Bcr-Abl that can result in the expansion of the myeloid compartment are still largely unknown (Clarkson *et al.*, 1997).

1.2 Regulation of hematopoiesis

Hematopoiesis means the formation of blood. All cells recognisable in blood are ultimately derived from pluripotential stem cells. Stem cells are not detectable by microscopic techniques, but their existence can be inferred from culturing them. Cultures of these early cells on agar generate groups of more mature, and thus recognizable, progenitor cells known as colony forming units (CFUs) (Clarkson *et al.*, 1997). For myeloid development, the earliest detectable precursor cell creates granulocytes, erythrocytes, monocytes and megakaryocytes and is thus called CFU-GEMM. Pluripotential cells have the capacity for self-renewal as well as differentiation and the system allows enormous amplification. A lifetime of human hematopoiesis with the generation of incalculable numbers of mature cells may rely on only a few thousand stem cells present at birth. Once committed to differentiate, all hematopoietic cells have finite life spans and normally undergo programmed cell death at prescribed times depending on the lineage and environmental factors (Clarkson *et al.*, 1997). The localisation of hematopoiesis to the bone marrow involves developmentally regulated adhesive interactions between primitive hematopoietic cells and the stromal-cell-mediated hematopoietic microenvironment. Primitive hematopoietic progenitor cells exhibit a wide range of cell adhesion molecules (CAMs) and ligands for many of these CAMs are expressed by bone marrow stromal cells (To *et al.*, 1997). The regulation of hematopoiesis is influenced by a number of growth factors, including stem cell factor, erythropoietin, colony stimulating factors, and thrombopoietin. In addition to stimulating the proliferation of hematopoietic progenitors, hematopoietic growth factors are required to support the survival of their target cells. For example, granulocyte-macrophage colony stimulating factor (GM-CSF), macrophage CSF,

and granulocyte CSF have all been used to promote the recovery of granulocyte and macrophages after systemic chemotherapy for cancer (Steller, 1995). Bcr-Abl expression alters the normal developmental controls in leukaemic-progenitor cells by suppressing apoptosis, effectively increasing the pool of cells susceptible to other mutagenic events, which ultimately lead to progression to blast crisis (Fardel *et al.*, 1999; Laurent *et al.*, 2001).

1.3 The *abl* gene

The *c-abl* non-receptor tyrosine kinase was identified as the cellular homologue of the *v-abl* oncogene from the Abelson murine leukaemia virus (A-MuLV). The A-MuLV was generated from the recombination between M-MuLV and a processed form of the *c-abl* protooncogene (Samali *et al.,* 1997). Mammalian *c-abl* is a member of a family of cellular genes that exhibit structural conservation in the sea urchin (*e-abl*), fruit fly (*d-abl*) and nematode (*n-abl*) (Kharbanda *et al.*, 1997). The *c-abl* gene is ubiquitously expressed and encodes two 145 kDa isoforms (1a and 1b) as a result of alternative splicing of the first two exons (1a and 1b). The c-Abl protein contains at least four functional domains: the N-terminal variable domain encoded by the two alternative first exons, a kinase regulatory domain which includes two regions of homology to the *src* tyrosine kinase (*src* homology regions 3 and 2, or SH3 and SH2), the tyrosine kinase domain, and a large C-terminal segment that is unique to the Abl subfamily of tyrosine kinases (Fig. 1.1). The nuclear localisation of the c-Abl protein is determined primarily by the C-terminal segment, which contains a nuclear translocation signal and a DNA binding domain, which is necessary for association with chromatin (McWhirter and Wang, 1993). The presence of an F-actin binding domain at the C-terminus as well as a DNA binding domain implies that the protein has both a cytoplasmic and a nuclear function. In fact, c-Abl is found in both of these subcellular locations, although it is mainly found in the nucleus (Samali *et al.*, 1997).

Many oncogenic kinases contain an N-terminal sequence that can be modified by the addition of the fatty acid myristate. These *N*-myristoylation signals are believed to target the kinases to cellular membranes, and in some cases, to specific membrane receptors (Resh, 1990). The *v-abl* gene product from the Abelson murine leukaemia virus is known as the Gag-v-Abl protein. Its Abl tyrosine kinase is deregulated by deletion of the variable and SH3 domains, and an *N*-myristoylation signal is provided by the retroviral Gag sequence (Samali

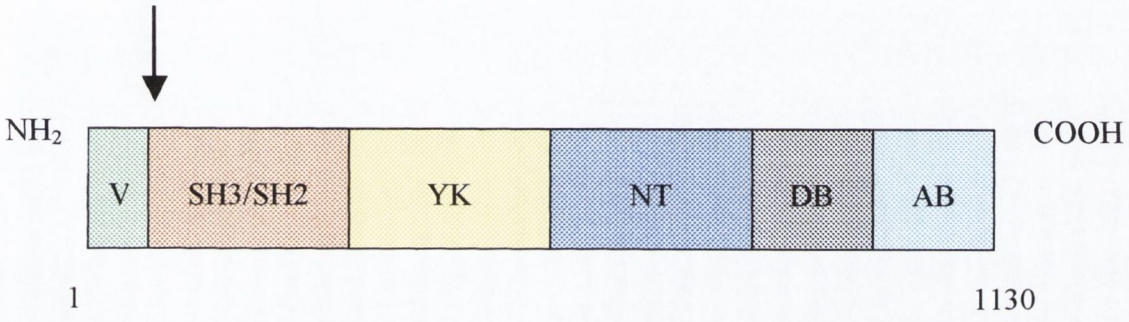

Fig 1.1 Schematic representation of the p145 c-Abl protein

The c-Abl protein is composed of an N-terminal variable domain (V), a kinase regulatory domain, which includes two regions of homology to the src tyrosine kinase (SH3 and SH2), the tyrosine kinase domain (YK), nuclear translocation signal (NT), DNA-binding domain (DB) and an actin-binding domain (AB). The arrowhead indicates the position of the breakpoint in the Bcr-Abl fusion protein.

et al., 1997). The mouse c-Abl protein already contains an *N*-myristoylation signal and it can be converted to an oncogene simply by mutating the SH3 domain. Therefore, the SH3 domain is a negative regulator of the Abl tyrosine kinase. In CML the *c-abl* gene is activated by an entirely different mechanism. It involves a chromosome translocation, which causes the *c-abl* gene on chromosome 9 to become fused to the *bcr* gene on chromosome 22, resulting in the expression of a unique fusion protein called Bcr-Abl, in which the variable domain of c-Abl is replaced by N-terminal Bcr sequences. The Bcr-Abl proteins differ from the Gag-v-Abl protein, in two ways; their SH3 domains remain intact, and they are not *N*-myristoylated. Therefore, it appears that Bcr sequences must override the negative regulatory activity of the SH3 domain (Fernandes *et al.*, 1996). It is thought that Bcr sequences interact with the SH2 domain of Abl and this somewhat blocks the negative regulation by the SH3 domain, perhaps by preventing binding of an inhibitory molecule (Samali *et al.*, 1997).

Several fairly diverse functions have been attributed to Abl. The normal Abl protein is involved in the regulation of the cell cycle (Cortez *et al.*, 1997) and in cellular response to genotoxic stress (Kharbanda *et al.*, 1997). Overall, it appears that the Abl protein serves a complex role as signal integrator, from various extracellular and intracellular sources, involved in the cell cycle and apoptosis.

1.4 The *bcr* gene

The *bcr* gene spans 130 kb and contains 23 exons. Two transcripts, 4.5 kb and 7.0 kb long, have been found. While a number of Bcr-related pseudogenes (*bcr2, bcr3* and *bcr4*) have been described (Croce *et al.*, 1987), the normal *bcr* gene is known to encode two major proteins, 160 kDa and 130 kDa, which are possibly derived from the 7.0 kb and 4.5 kb transcripts, respectively (Laurent *et al.*, 2001). The Bcr proteins, like Abl, are ubiquitously expressed. The *bcr* gene is known to be a complex molecule with many different functional domains. Within the first N-terminal exon resides a structurally novel serine-threonine kinase domain. Also present within the first exon are several SH2-binding domains. SH2 domains are highly conserved, non-catalytic regions of approximately 100 amino acids that bind SH2-binding sites consisting of three to five amino acids including a phosphotyrosine. A coiled domain at the N-terminus of Bcr allows dimer formation *in vivo* and is thought to be partially responsible for the cytoplasmic localisation of Bcr-Abl, by enhancing F-actin binding. The

centre of the molecule contains a region that stimulates the exchange of guanidine triphosphate (GTP) for guanidine diphosphate (GDP) on Rho guanidine exchange factors, which may in turn activate transcription factors. This is known as the GEF binding domain. The C-terminus has GTPase activity for Rac, a small GTP binding protein of the Ras superfamily that regulates actin polymerisation (Fig. 1.2). In addition, Bcr can be phosphorylated on several tyrosine residues, especially tyrosine 177 within the first exon. There are 11 tyrosines in total within the Bcr first exon. This data implicates the participation of Bcr in two major intracellular signalling mechanisms in eukaryotic cells, phosphorylation and GTP-binding (reviewed by Laurent *et al.,* 2001). The first exon of the *bcr* gene is of critical significance because it is the one exon of *bcr* included in all known Bcr-Abl fusion proteins. The first two domains of the Bcr sequence appear to be necessary for the transforming ability of Bcr-Abl and will be discussed in the next section.

1.5 Bcr-Abl genes and proteins

The hallmark of CML is the Ph chromosome, which is a shortened chromosome 22 resulting from the translocation, t (9; 22)(q34; q11), between chromosomes 9 and 22. The breakpoints within the a*bl* gene at 9q34 can occur anywhere over a large area, greater than 300 kb, at its 5' end. The breakpoints are either upstream of the first alternative exon 1b, downstream of the second alternative exon 1a, or, more frequently, between the two (Deininger *et al.*, 2000). Regardless of the exact location of the breakpoint, splicing of the primary hybrid transcripts yields a mRNA molecule in which *bcr* sequences are fused to *abl* (Fig. 1.3). In contrast to *abl*, breakpoints within *bcr* localise to one of three so-called breakpoint cluster regions. In CML the break on chromosome 22 is restricted in most patients to an area of 5.8 kb termed M-bcr. M-bcr consists of five exons located within the central region of the *bcr* gene, equivalent to exons 11-15. Most breaks occur downstream of exon 2 or 3 of the M-bcr region. Breakpoints occurring outside the M-bcr region, which produce alternative fusion proteins, 160 kDa and 230 kDa in size, are responsible for acute lymphoblastic leukaemia (ALL) and chronic neutrophilic leukaemia (CNL), respectively (Cortex *et al.,* 1997).

The fusion of *bcr* and *abl* on the Ph chromosome occurs in a head-to-tail manner, with the 3' end of *bcr* joined to the 5' end of *abl*. This configuration places the fusion gene

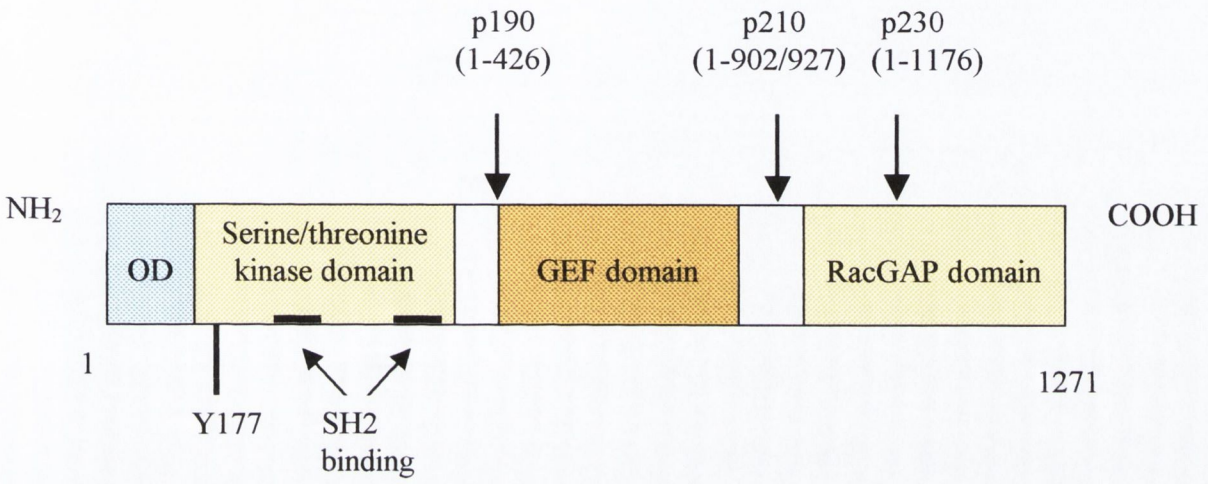

Fig. 1.2 Schematic representation of the p160 Bcr protein

The Bcr protein is composed of an oligomerisation domain (OD), a serine/threonine kinase domain, two serine-rich boxes containing SH2-binding domains and a tyrosine phosphorylation site (Y177). The central part contains a GEF binding domain, whereas the C-terminus contains GTPase activity. Arrowheads indicate the position of the breakpoints in the Bcr-Abl fusion proteins.

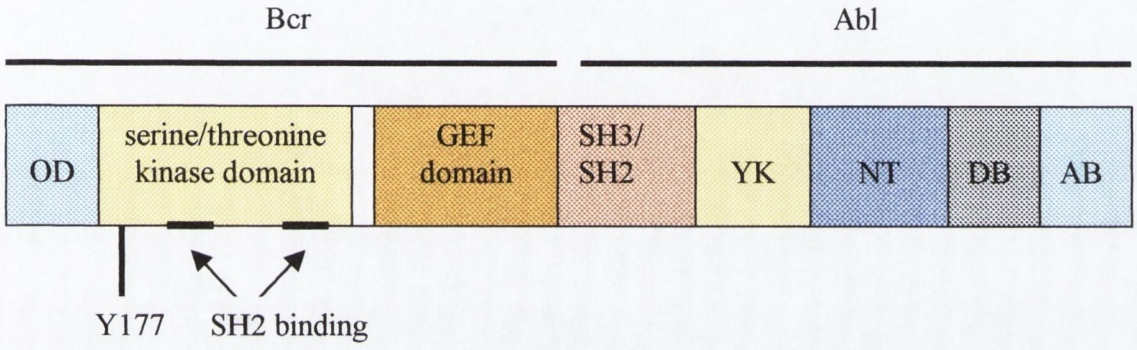

Fig. 1.3 Schematic representation of the p210 Bcr-Abl fusion protein

The fusion of *bcr* and *abl* on the Ph chromosome occurs in a head-to-tail manner, with the 3' end of *bcr* joined to the 5' end of *abl*. This configuration places the fusion gene under the control of the BCR promoter, which produces an 8.5 kb mRNA transcript that encodes a protein, M_r 210,000, designated p210 Bcr-Abl.

under the control of the BCR promoter, which produces an 8.5 kb mRNA transcript that encodes a protein (M_r 210,000) designated p210 Bcr-Abl (Laurent *et al.*, 2001). Based on the observation that the *abl* part in the chimeric protein is almost invariably constant while the *bcr* portion varies greatly, it has been suggested that *abl* is likely to carry the transforming principle whereas the different sizes of the *bcr* sequence may dictate different disease phenotypes.

The Abl protein is a non-receptor tyrosine kinase that is localised primarily to the nucleus and normally has very little constitutive kinase activity. The p210 Bcr-Abl fusion protein has constitutively activated tyrosine kinase activity and is normally found in the cytoplasm. This tyrosine kinase activity is attributable to the kinase domain found within the Abl segment of the fusion protein. However, Bcr-Abl fusion transcripts are detectable in low frequency in the blood of many healthy individuals. It has been suggested that the translocation occurs in cells committed to terminal differentiation that are thus eliminated by an immune response (Deininger *et al.*, 2000).

1.6 Mechanisms of Bcr-Abl-mediated transformation

Mutational analysis identified several features in the chimeric protein that are essential for cellular transformation. In Abl, they include the SH1, SH2 and actin-binding domains and, in Bcr, they include a coiled-coil motif contained in amino acids 1-63, the tyrosine at position 177, and the phosphoserine-threonine-rich sequences between amino acids 192-242 and 298-413, all of which lie within the first exon of *bcr* (Deininger *et al.*, 2000). The degree of transforming activity of Bcr-Abl correlates with the degree of tyrosine kinase activity (Evans *et al.*, 1993). Furthermore, Bcr-Abl induces the tyrosine phosphorylation of many cellular proteins, including Crk1, Shc, Syp, Fes, Vav and paxillin (Laurent *et al.*, 2001).

The serine-threonine rich region of Bcr binds to the SH2 domain of Abl in a high-affinity, phosphotyrosine-independent manner and contributes to deregulation of the tyrosine kinase. Deletion of Bcr sequences essential for Abl SH2-binding renders Bcr-Abl non-transforming (Pendergast *et al.*, 1991). An F-actin binding domain is found at the C-terminus of the Abl protein. The affinity for F-actin is increased by the addition of Bcr sequences that are required for transformation by Bcr-Abl. The mechanism by which Bcr enhances F-actin

binding involves the oligomerisation domain located in the first 63 amino acids of Bcr to a consensus sequence found on Abl (McWhirter and Wang, 1993). Although normal Abl protein can be found in the nucleus and the cytoplasm, the enhanced F-actin binding by Bcr sequences is partly responsible for the cytoplasmic localisation of the Bcr-Abl fusion protein. This is consistent with the fact that the DNA binding function of Abl is not required for transformation and the role of actin-association by Bcr-Abl may be analogous to that of *N*-myristoylation in transformation by the v-Abl oncoproteins (McWhirter and Wang, 1993).

Ras activation has been shown to be necessary for transformation by both p210 Bcr-Abl and p190 Bcr-Abl. The mechanisms by which Bcr-Abl interacts with the Ras pathway are complex. Ras activity is regulated by the opposing actions of GTPase-activating proteins (GAPs), which exchange GTP for GDP and are negative regulators, and guanine nucleotide exchange factors (GEFs), which exchange GDP for GTP. Bcr-Abl exists in a complex with the adaptor protein Grb-2 *in vivo*. Binding of Grb-2 to Bcr-Abl is mediated by the direct interaction of the Grb-2 SH2 domain with a phosphorylated tyrosine, Y177, within the Bcr first exon. Grb-2 functions as a molecular link between oncogenic tyrosine kinases and the Ras activator SOS-1, through its SH3 domain. SOS-1 stimulates conversion of inactive GDP-bound Ras to the active GTP-bound state. A substitution of phenylalanine for tyrosine 177 in Bcr-Abl abolished Grb-2 binding and abrogated Bcr-Abl induced Ras activation, suggesting that up-regulation of the Ras signalling pathway may be a key component for Bcr-Abl-mediated transformation of hematopoietic cells (Million and Van Etten, 2000; Pendergast *et al.,* 1993; Puil *et al.,* 1994). It has been reported that dominant negative H-Ras induces apoptosis in K562 CML cells, suggesting that activation of Ras by Bcr-Abl may be responsible for the anti-apoptotic properties of these cells (Sakai *et al.*, 1994).

While the importance of the Ras pathway in Bcr-Abl transformation is well understood, alternative signals from Bcr-Abl to Ras activation have been suggested. Bcr-Abl tyrosine kinases can also phosphorylate Shc adaptor proteins on tyrosine, inducing the formation of an Shc-Grb2 complex that also has potential to stimulate Ras. The adaptor molecule Crk1 is a likely candidate since it has been implicated in connecting Bcr-Abl with downstream effectors such as Ras (Goga *et al.*, 1995; Puil *et al.*, 1994).

1.7 Bcr-Abl activated signalling pathways

Expression of Bcr-Abl in growth factor-dependent cell lines prevents apoptosis after growth factor withdrawal, an effect that is dependent on tyrosine kinase activity and correlates with the activation of Ras. However, the underlying biological mechanisms are still not well understood. Numerous substrates of the Bcr-Abl kinase have been identified in various cell lines. The majority of proteins phosphorylated by Bcr-Abl are components of pathways activated in normal cells by normal growth factor signalling, or involved in cell adhesion. It is not clear which of these intracellular pathways are responsible for the anti-apoptotic effects of Bcr-Abl. Fig. 1.4 summarises the potential signalling pathways involved in Bcr-Abl transformation.

1.7.1 Bcr-Abl and mitogen-activated protein (MAP) kinase pathways

Deregulated Ras signalling is associated with a wide variety of human leukaemias and as discussed earlier, activation of the Ras pathway by Bcr-Abl is an important event in its transforming ability. Ras activation leads to signal transduction through downstream mitogen-activated protein (MAP) kinase pathways. There is still dispute as to which MAP kinase pathway lies downstream of Ras in Ph-positive cells, and it seems that activation of individual paths depend on the cell type (Deininger *et al.*, 2000). The best-defined Ras-mediated signalling pathway activates Raf-1 and the extracellular signal-regulated kinase (ERK) group of MAP kinases and usually affects the expression of genes that control cell proliferation. It has been suggested that the activated ERK pathway stimulated by Bcr-Abl could be responsible for the resistance to apoptosis in CML cells (Kang *et al.*, 2000). In contrast, activation of the Jun N-terminal kinase (JNK) substrate c-Jun by Bcr-Abl has been demonstrated and is required for malignant transformation (Raitano *et al.*, 1995).

1.7.2 Bcr-Abl and STAT signalling

The growth of normal hematopoietic cells is controlled by the action of cytokines, which activate intracellular signal transduction pathways. For example, in myeloid cells, growth factors and cytokines such as interleukin 3 (IL-3) and granulocyte/macrophage-colony stimulating factor (GM-CSF) regulate growth by binding to their respective receptors. A cardinal feature of Bcr-Abl positive cells is growth factor independence. One mechanism

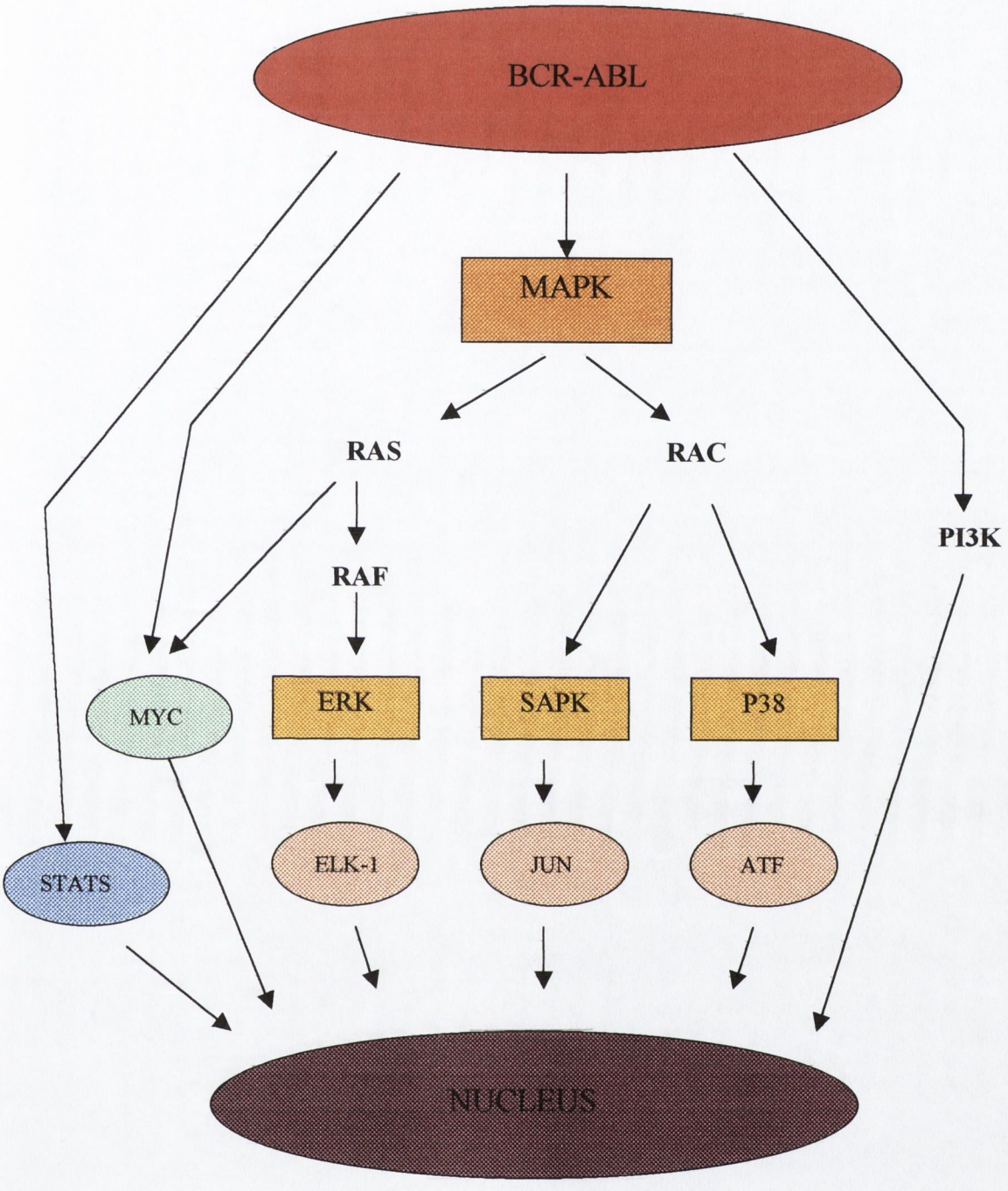

Fig. 1.4 Signalling pathways with mitogenic potential in Bcr-Abl transformed cells

The activation of individual pathways depends on the cell type, but the MAP kinase system appears to play a central role. Activation of p38 has been demonstrated in v-abl transformed cells but not for Bcr-Abl expressing cells.

for this phenomenon might be the constitutive activation of cytokine signal transduction pathways. Cytokines such as GM-CSF signal through the Janus (JAK) family of cytoplasmic tyrosine kinases, which in turn phosphorylates STAT proteins, a family of transcription factors (Shuai *et al.*, 1996). Tyrosine phosphorylated STAT proteins translocate to the nucleus and stimulate transcription of target genes. It has indeed been found that STAT5 is constitutively activated in CML cells, through JAK kinase, and activation of STAT5 correlates directly with the ability of Bcr-Abl to confer cytokine independent growth (Shuai *et al.*, 1996; Sillaber *et al.*, 2000). Only a small number of STAT5 regulated genes are known, incuding β-casein, CIS-1 and the Bcl-2 anti-apoptotic family member, Bcl-$_{XL}$. It has been shown that Bcr-Abl induced STAT5 activity contributes to an increased expression of Bcl-$_{XL}$, which may be responsible for the enhanced viability of these cells (Gesbert and Griffin, 2000). Inhibition of Bcr-Abl kinase activity by the novel compound, STI571, has recently been shown to result in a decrease of Bcl-$_{XL}$, which preceded apoptotic cell death, further supporting the role of Bcl-$_{XL}$ as a target for the transforming function of Bcr-Abl (Oetzel *et al.*, 2000).

1.7.3 Bcr-Abl and phosphoinositide 3-kinase (PI-3 kinase) signalling

PI-3 kinases are a family of lipid kinases defined by their ability to phosphorylate the 3'-OH group of the inositol ring in inositol phopholipids (Blume-Jensen and Hunter, 2001). PI-3 kinase activity is required for the proliferation of Bcr-Abl-positive cells. Bcr-Abl forms multimeric complexes with PI-3 kinase, Cbl, and the adapter molecules crk and Crkl, in which PI-3 kinase is activated (Deininger *et al.*, 2000). The serine threonine kinase, Akt, is activated downstream of PI-3 kinase and has been previously implicated in anti-apoptotic signalling pathways. Akt, in turn, has been reported to phosphorylate and inactivate the pro-apoptotic Bcl-2 family member, Bad, at serine 136, causing its binding to 14-3-3 family proteins and thus preventing it from binding to anti-apoptotic proteins such as Bcl-$_{XL}$ (Cross *et al.*, 2000). Bad has been shown to be constitutively active in Bcr-Abl expressing cells, and Bcr-Abl mutants that fail to phosphorylate Bad are also unable to protect transfected cells from apoptosis. Akt also promotes cell survival in hematopoietic cells by neutralising the pro-apoptotic activity of Bad, through an increase in expression levels of Bcl-2 and Bcl-$_{XL}$ (Salomoni *et al.*, 2000). Raf-1, which is immediately downstream of Ras, also

phosphorylates Bad and it has been reported that the survival signal provided by Bcr-Abl requires targeting of Raf-1 to the mitochondria (Salomoni *et al.*, 1998). Furthermore, Akt phosphorylates and activates IKK-α, the kinase that regulates IκB and leads to activation of nuclear factor kappa B (NFκB), which in turn regulates the transcription of a variety of survival factors (Cross *et al.*, 2000).

1.7.4 Bcr-Abl and interaction with SHIP proteins

The phosphatidylinositol polyphosphate 5-phosphatase SHIP proteins, SHIP 1 and SHIP 2, are downstream targets of Bcr-Abl and are thought to play a negative regulatory role in signalling by downregulating the action of PI-3 kinase. Bcr-Abl negatively regulates the activity of SHIP 1 by reducing its half-life (Laurent *et al.,* 2001). A major phosphoprotein found in hematopoietic cells is a 62 kDa RasGAP-associated protein, Dok 1. Phosphorylation of Dok proteins induces association with RasGAP, implying that Dok proteins might play a role in the regulation of Ras signalling. SHIP 1 has been found to interact with the Dok1 phosphoprotein in Bcr-Abl transformed cells suggesting that this complex formation may be involved in mediating the effects of Bcr-Abl activity (Dunant *et al.*, 2000).

1.7.5 Bcr-Abl and *c-myc* signalling

The *c-myc* oncogene has been shown to co-operate in Bcr-Abl and v-Abl transformation. For example, colony formation of fibroblasts expressing Bcr-Abl is increased if c-myc proteins are overexpressed (Lugo and Witte, 1989). The oncogene is believed to function downstream of the Bcr-Abl signal, because dominant negative forms of myc block Bcr-Abl-mediated transformation and it has been suggested that Bcr-Abl activates at least two independent pathways for transformation (Afar *et al.*, 1994).

1.8 Diagnosis of CML

CML is usually diagnosed in the chronic phase. Typical symptoms include fatigue, abdominal fullness, weight loss, anorexia, bleeding and sweats. Splenomegaly is the most common physical finding, often causing pain and bloating. Leukocytosis, anaemia and thrombocytosis are typical laboratory features at presentation. Diagnostic testing for CML consists of a complete blood count, including a differential and platelet count. A bone

marrow aspiration is taken, which involves removing a sample of cells or tissue from the bone marrow, for microscopic examination. Histopathologic examination of the bone marrow aspirate demonstrates a shift in the myeloid series to immature forms that increase in number as the patient progresses towards the blast crisis phase of the disease. The diagnosis is usually confirmed by the presence of the Philadelphia chromosome in the cells. Cytogenetic analysis is the gold standard diagnostic test in CML. Genomic PCR and Southern blot assay can determine the exact breakpoints of the fusion genes, whereas RT-PCR and Northern blot analysis detect Bcr-Abl transcripts at the RNA level. RT-PCR and fluorescence in situ hybridization (FISH) are used to detect the Ph chromosome during diagnosis and in monitoring the disease course following treatment (Faderl *et al.,* 1999).

1.9 Conventional chemotherapy in the treatment of CML

Although CML is not currently curable with conventional chemotherapy, the natural history of the disease has changed significantly over the years. In the past, the average survival period was 3 years and less than 20% of patients would live 5 years after diagnosis. Survival duration has since doubled to 5 to 7 years, with 50-60% of patients alive 5 years after diagnosis and more than 30% alive after 10 years. Several reasons account for this change, including earlier diagnosis, more effective therapies such as allogenic bone marrow transplantation, and better supportive care (Faderl *et al.*, 1999).

Total body or splenic radiation therapy was the main therapy for CML until the 1950's. However, it did not effect overall survival and is rarely used today, if at all. Busulfan, which was introduced in the 1950s, controls hematologic variability. It is administered orally at 0.1 mg/kg until the leukocyte count decreases by 50%, at which point the dose of busulfan is reduced. Side effects include severe, prolonged myelosuppression, marrow fibrosis and endocardial fibrosis (Faderl *et al.*, 1999).

In 1972, hydroxyurea, a cell cycle-specific inhibitor of DNA synthesis, became available for the treatment of CML. Administered orally at 40mg/kg per day, hydroxyurea allows rapid but transient hematologic control, is well tolerated and has few side effects (nausea, vomiting, diarrhoea, mucosal ulcers and skin manifestations). Hydroxyurea and busulfan produce complete hematologic remission in 50-80% of patients. Although hydroxyurea therapy is superior to busulfan therapy, cytogenetic remissions are rare, neither

drug affects progression of the disease and patients will inevitably experience transformation to blast crisis (Faderl *et al.,* 1999).

Interferon-α is a type I interferon produced mainly by leukocytes. These bind to cell surface receptors and act through intracellular signalling pathways to modulate the expression of genes involved in cell proliferation. Interferon-α therapy in CML has consistently produced high rates of complete hematologic (46-80% of patients) and cytogenetic responses (complete remission in 13-32% of patients and partial response in 15%). A number of trials, which compared cytogenetic responses in patients receiving different treatments, reported a better response with interferon-α than with hydroxyurea or busulfan. However, therapy with interferon-α does not appear to be curative, and side effects, which include influenza-like symptons, nausea, anorexia and weight loss, can result in discontinuation of therapy in many cases (Bhatia *et al.,* 1997; Faderl *et al.,* 1999).

Many of the drugs used in conventional chemotherapy are only effective in delaying clonal expansion during chronic phase CML and cannot modify the natural disease course, which ultimately results in blast crisis. The side effects that accompany many treatments for CML also highlight the need for the development of new therapeutic drugs, which target the cancerous cells whilst having a minimal effect on normal progenitor cells in the hematopoietic system. New targets for therapy are being identified through better definitions of molecular events involved in the initiation and progression of chronic myelogenous leukaemia. These novel therapies and concepts will be discussed later.

1.10 Bone marrow transplantation as a therapy for CML

An alternative therapy for the treatment of CML is bone marrow transplantation. A number of different transplantations may be performed which include, allogenic, syngeneic and autologous. The most successful and commonly practiced transplantation is allogenic, in which bone marrow from a donor is transplanted into a patient. In syngeneic bone marrow transplantation, the bone marrow donor is the patient's identical twin. Finally, patients who undergo autologous bone marrow transplantation use their own bone marrow for the transplant, which is usually removed during the chronic phase and undergoes several *ex vivo,* purging strategies to reduce Ph-positive cells. Autologous 'peripheral blood stem cell transplantation' is also an option. In this procedure, stem cells, which repopulate the bone

marrow and bloodstream, are collected from peripheral blood. Regardless of the type of transplantation, the procedure is essentially the same. Bone marrow is extracted or harvested from the rear hip of the donor (or the patient in autologous bone marrow transplant). If the patient is undergoing peripheral blood stem cell transplantation, cells are collected by extracting blood from the patient's arm, filtering it to remove the stem cells and returning the remaining blood components to the patient through a needle in the other arm. Prior to transplantation, the patient undergoes a preparative regimen to destroy leukaemia cells in the bone marrow and organs. The preparative regimen for CML patients typically consists of high dose chemotherapy followed by total body irradiation. The bone marrow or peripheral blood stem cells are then re-infused or transplanted into the patient in a manner similar to that used for a blood transfusion (Bhatia *et al.*, 1997).

Allogenic bone marrow transplantation in the chronic phase represents the only known curative therapy for CML. It produces disease-free survival in 30-70% of patients. However, the option of allogenic bone marrow transplantation is not available to the majority of patients, primarily because of the lack of a suitable donor and because of age restrictions. Several factors influence the outcome of stem cell transplantations. For instance, younger patients benefit more due to an increase in treatment-related mortality with increased age. In addition, results are more favourable if patients undergo transplantation during chronic phase instead of during transformation. For example, between 10-20% of patients transplanted during the chronic phase of CML relapse following transplantation, whereas up to 80% of patients transplanted during blast crisis suffer relapse. Chemotherapy before transplantation has been shown to affect disease-free survival, where survival rates after transplantation vary significantly with the different chemotherapeutic agents administered (Faderl *et al.*, 1999).

1.11 Molecular targets for CML therapy

Deregulated cell proliferation together with suppressed apoptosis, constitutes a common platform upon which all neoplastic evolution occurs. The critical issue is to identify how tumour cells differ from normal cells and how those differences can be exploited therapeutically (Evan and Vousden, 2001). The Philadelphia (Ph) chromosome provided the first example of a consistent chromosomal abnormality associated with a specific type of

leukaemia. The requirement for Bcr-Abl kinase activity in transformation made this oncoprotein an ideal candidate for therapeutic targeting. Synthetic compounds were developed through a rational design of chemical structures capable of competing with the ATP or substrate binding sites of the kinase. One such molecule that has aroused interest is the recently developed Bcr-Abl-specific kinase inhibitor, STI571. A 2-phenylaminopyrimidine derivative, STI571 functions as an ATP-competitive inhibitor of the Abl tyrosine kinase and induces apoptosis in CML cells (Gambacorti-Passerini *et al.,* 1997; Oetzel *et al.*, 2000). Investigations have demonstrated Bcr-Abl-specific inhibition of cellular proliferation and tumour formation by both primary CML cells and Bcr-Abl-expressing cell lines (Drucker *et al.*, 1996). STI571 has also been found to inhibit the kinase activity of platelet derived growth factor (PDGF) receptor (Buchdunger *et al.,* 2000), and c-Kit, the receptor for stem cell factor, a cytokine involved in hematopoiesis (Heinrich *et al.*, 2000), suggesting that in addition to CML, STI571 may have clinical potential in the treatment of diseases that involve abnormal activation of c-Kit or PDGF receptor tyrosine kinases. However, recent data have indicated that patients in the blast crisis stage of CML are beginning to acquire increased resistance to STI571, a characteristic that is common with conventional anti-cancer drug treatments. Evaluation of patients who relapsed while being treated with STI571 showed that, in some cases, relapse was due to *bcr-abl* gene amplification, whereas in other cases, acquired resistance was due to a point mutation that changed a single amino acid in the enzymes active site that hinders STI571 binding to Bcr-Abl (Gorre *et al.,* 2001).

Suppression of Bcr-Abl by interference with downstream pathways critical to transformation merits exploration. Upregulation of the Ras signalling pathway is reportedly a key component for Bcr-Abl-mediated transformation of hematopoietic cells (Pendergast *et al.,* 1993). Activation of Ras depends on the addition of a farnesyl group, which allows it to attach to the cell membrane. The enzyme that catalyses this reaction, farnesyl protein transferase (FPTase) has been the focus for the development of inhibitors as potential anticancer drugs, and molecules that inhibit enzyme activity are now entering clinical trials in CML (Oliff, 1999; Prendergast *et al.*, 2000).

Altering the expression of key molecular components of the cell death machinery is an attractive strategy. Antisense therapy is one approach for altering gene expression.

Antisense oligodeoxynucleotides (ODNs) are pieces of nucleic acid, usually 15-20 bases long, with a sequence complementary to part of the mRNA of a target nucleotide sequence. Thus, antisense ODNs are capable of hybridising specifically to the target sequence, forming an mRNA-DNA duplex, which prevents translation of the targeted message into protein. ODNs directed against the Bcr-Abl junction were first reported in 1991 as being inhibitory to the growth of CML cell lines (Szczylik *et al.*, 1991). Several groups have subsequently reported that treatment of CML cell lines with ODN targeting Bcr-Abl restores the sensitivity of CML cell lines to apoptosis-inducing chemotherapeutic agents (McGahon *et al.*, 1994b).

Allogenic stem-cell transplant and, more recently, STI571 are considered to be front line in the treatment of CML (Bhatia *et al.*, 1997; Mauro and Drucker, 2001). Antisense ODNs have also been studied as agents for *ex vivo* purging of hematopoietic cell harvests, aimed at reducing the number of cancerous cells in bone marrow or blood, prior to autologous transplantation. Although few clinical reports are currently available, a karyotypic response was observed in some patients (Clark, 2000). However, antisense therapeutics has not been without its problems. Phosphodiester linked ODN are easily degraded by nucleases and degradation products may themselves be non-specifically toxic or growth inhibitory to a variety of hematological cells. Degradation products of Bcr-Abl ODNs have been implicated as being responsible for non-specific antiproliferative effects in CML (Vaerman *et al.*, 1995). Phosphorothioate ODNs may have reduced penetration into the cell unless targeted using vehicles such as liposomes. The targeted sequence may be rendered inaccessible by steric configurations (Bhatia *et al.*, 1997; Clark, 2000). However, the observations that patients with CML may derive some clinical benefit, and the greater specificity of antisense oligodeoxynucleotides compared to many of the chemotherapeutic agents used at present, will most certainly maintain continued research into the field. At present, further clinical studies appear justified to improve our knowledge of how antisense ODNs work *in vivo*.

Specific RNA sequences, termed ribozymes, have the ability to cleave other RNA molecules in a catalytic manner and have been adapted to create antisense molecules that specifically bind and cleave RNA molecules. Such ribozymes have been shown to inhibit Bcr-Abl gene expression under various culture conditions (Bhatia *et al.*, 1997).

Further *ex vivo* manipulation of bone marrow or peripheral blood stem cells is based on physical separation of normal cells from Philadelphia (Ph) positive cells. This approach

takes advantage of differences in expression of certain cell surface proteins between Ph-positive and Ph-negative cells to physically isolate a population of Ph-negative stem cells that might be used in autologous bone marrow transplantations (Senechal and Sawyers, 1996).

Another potentially unique direction, which uses Bcr fragments as a therapy, is based on the observation that first exon Bcr sequences, when phosphorylated on serine residues, attenuate the kinase activity of Bcr-Abl. In contrast, tyrosine- phosphorylated Bcr lacks this inhibitory effect (Liu *et al.*, 1996; Wu *et al.*, 1999). These findings raise the possibility that Bcr fragments could form the basis of a therapeutic agent for the treatment of CML.

New molecular based medicines founded on the genetic understanding of cancer are promising. Some of the most exciting results are obtained with agents directed against tyrosine kinases. However, some of the complications inherited with these new strategies and the problem of tumour instability that might lead to resistance are important issues to be considered (Mauro and Drucker, 2001). This highlights the need to develop new chemotherapeutic agents, with improved and durable anti-tumour activity, reduced toxicity and prevention of drug resistance (Gibbs, 2000).

1.12 Experimental models of CML

Over the years, the study of Ph positive cell lines has significantly increased our understanding of CML. The number of Bcr-Abl positive cell lines available has grown considerably and they include cell lines with myeloid differentiation, such as the well known K562 cell line, and with lymphoid phenotype, such as BV173. These cell lines have been isolated from patients suffering from CML and represent the different phases in the progression of the disease. K562 and KYO.1 cells were derived from the blastic phase of CML, whereas LAMA 84 cells were derived from the accelerated phase. K562 cells were isolated in 1970 from the pleural effusion of a 53-year-old female with CML in terminal blast crisis (Lozzio and Lozzio, 1975; 1979). KYO.1 cells were also derived from the peripheral blood of a 22-year-old male with CML in blast crisis (Ohkbuo *et al.,* 1985). These cell lines contain genetic alterations in addition to Bcr-Abl, and consequently reflect blast crisis better than chronic phase CML. So far, no cell line from chronic phase CML has been established, just as no cell line could be derived from normal human bone marrow. The use of these cell

lines have, without doubt, proven invaluable as model systems for studying Bcr-Abl transformation and the resulting biochemical abnormalities. In particular, many of the proteins that interact with Bcr-Abl were identified in Ph- positive cell lines, where they are more abundantly expressed than in primary cells (Deininger *et al.*, 2000).

The study of material from patients and its comparison with normal hematopoietic progenitor cells is certainly the gold standard of CML research, particularly in the chronic phase of the disease. However, studying primary cells does have its problems. These cells do not survive in culture for long, therefore, the window of time for *ex vivo* studies is narrow. Furthermore, there is considerable variation between patients and it is difficult to distinguish between normal and CML cells. Nonetheless, it is important to confirm results obtained from cell lines in these primary cells (Deininger *et al.*, 2000).

The main aims of using animal models to study CML are to establish a disease phenotype that resembles chronic phase CML and to test the efficacy of new drugs *in vivo*. A number of approaches have been taken, which include the engraftment of immunodeficient mice, such as SCID (severe combined immunodeficiency) mice, with human Bcr-Abl positive cells. It was shown that SCID mice can be engrafted with chronic phase CML cells if the inoculum is large enough, which will be useful for studying the response to novel forms of treatment. Another approach involves the engraftment of Bcr-Abl transformed cell lines in syngeneic mice. Transgenic mouse models, which use Bcr-Abl constructs to induce leukaemia, and the transduction of murine bone marrow cells with Bcr-Abl retroviruses, have also proved useful in studying the effect of novel drugs on CML (Deininger *et al.*, 2000).

1.13 Cell death: characteristics of apoptosis and necrosis

The term apoptosis first appeared in the biomedical literature in 1972, to delineate a structurally distinctive mode of cell death responsible for cell loss within living tissues (Kerr *et al.*, 1972). Although most of the observable events that define apoptosis were well documented as early as the 1950s, and its role in embryonic development was understood, the importance of apoptosis to the daily maintenance of the fully formed organism would not gain recognition for another 20 years. Apoptosis, or programmed cell death, is an evolutionarily conserved and genetically regulated biological process that plays an important role in the development and homeostasis of multicellular organisms. (Duke *et al.*, 1996).

Apoptosis, from the direct translation of the Greek, means "dropping off", as in the dropping off of flower petals or falling leaves. The cardinal morphological features of apoptosis are cell shrinkage, accompanied by transient bubbling and blebbing from the surface, which culminates in separation of the cell into a cluster of membrane-bound bodies, known as apoptotic bodies. Organellar structure is usually preserved intact, but the nucleus undergoes a characteristic condensation of chromatin initiated at sublamellar foci and often extending to generate cap-like, densely heterochromatic, regions. Endonucleolytic cleavage of genomic DNA into nucleosomal-size fragments, approximately 180 bases long, yields a DNA laddering pattern, the hallmark of apoptosis. The barrier function of the plasma membrane is maintained throughout, avoiding pathogenic spillover of the cell's soluble components into the tissue. Nevertheless, subtle changes in the membrane cause neighbouring scavenger cells to engulf and phagocytose the dying cells, without inciting an inflammatory response. To facilitate such engulfment, apoptotic cells reduce their volume by pumping out ions (mainly K^+) and contract their reorganized cytoskeleton (Zamzami and Kroemer, 1999; Singh, 2000). Apoptosis, an ATP-dependent active process, is easily morphologically distinguished from necrosis.

Necrotic cell death occurs as a result of injury, such as a physical insult or by oxygen deprivation. Morphological features of necrosis include loss of cellular ion homeostasis. Increased intracellular calcium concentrations result in activation of calcium-dependent DNAses, phospholipases and proteases. Swelling of internal organelles, most obviously the mitochondria, leads to swelling of the entire cell, which will lyse, emptying its cytoplasmic and nuclear content into the intercellular space, sparking an inflammatory response. Circulating macrophages and other white blood cells of the immune system converge on the necrotic cell and ingest it. The activities and secretions of the white cells can in turn damage normal cells in the vicinity (Duke *et al.*, 1996; Balla *et al.*, 2001).

1.14 *Caenorhabditis elegans* and apoptosis

Apoptotic cell death machinery is conserved throughout evolution and invertebrate model systems have been invaluable in identifying and characterising the genes that control apoptosis. The nematode worm *Caenorhabditis elegans*, whose invariant, lineage-restricted development makes this organism particularly advantageous for the study of the

developmental process, has served as a model system for defining core components of the apoptotic death process (Pan *et al.*, 1998).

During development of the adult hermaphrodite worm, 131 of the 1,090 somatic cells die by apoptosis, leaving an adult comprising 959 cells (Meier *et al.*, 2000). Investigations of programmed cell death in *C. elegans* identified a gene, *ced-3* (*ced* for cell death abnormal) that is essential for apoptosis (Ellis and Horvitz, 1986). The protein encoded by the *ced-3* gene was found to be very similar to a human protein called interleukin-1-converting enzyme (ICE), a mammalian cysteine protease also known as caspase-1. The similarity between the ced-3 and ICE proteins was the first indication that the cell death programme depends on protein cleavage. In *C. elegans*, ced-3 becomes activated through a physical interaction between pro-ced-3 and another protein known as ced-4, a homologue of the human Apaf-1 protein. If either gene is inactivated by mutation in *C. elegans*, the 131 cell deaths that normally happen during the development of the worm fail to occur (Raff, 1998). A third gene, *ced-9*, was found to be important in the regulation of nematode cell death. By contrast, *ced-9* encodes a negative regulator that functions to suppress inappropriate cellular suicide, and was found to be similar to the human Bcl-2 gene. Remarkably, the human Bcl-2 gene is so similar to ced-9 that it can suppress apoptosis in *C. elegans* when artificially introduced into the worm (Vaux *et al.*, 1992). Ced-9 acts as an apoptosis suppressor in worms in two ways: it binds directly to the ced-3 protease, blocking its activity, and it binds to ced-4, blocking its ability to activate the ced-3 pro-caspase (Raff, 1998). A fourth gene, *egl-1*, was found to inhibit anti-apoptotic ced-9 protein and is a homologue of the mammalian BH3 domain pro-apoptotic Bcl-2 family members. Regulation seems elegantly simple in *C. elegans*, where apoptosis requires only *egl-1*, *ced-3*, *ced-4* and *ced-9*, whereas an increased complexity is apparent in mammals, which possess multiple caspases and Bcl-2 homologues (Cory and Adams, 1998; Meier *et al.*, 2000).

1.15 Caspases: apoptotic proteases

Apoptotic death requires special machinery, which is always in place and only requires a trigger to activate it. The central component of this machinery is a proteolytic system involving a family of proteases called caspases (cysteine-dependent aspartate-directed proteases). Caspases were implicated in apoptosis with the discovery that ced-3, found in *C.*

elegans, is related to the mammalian interleukin-1β-converting enzyme (ICE or caspase-1). Although caspase-1 has no obvious role in cell death, it is the first identified member of a large family of proteases whose members have distinct roles in inflammation and apoptosis (Thornberry and Lazebnik, 1998). This family of proteases, which contains at least 12 human members, shares a common structure (Wolf and Green, 1999) and each cysteine protease shares specificity for aspartate in the P1 position of substrates (Talanian *et al.*, 1997). Recognition of at least four amino acids, NH_2-terminal to the cleavage site, is a necessary requirement for efficient catalysis. The preferred tetrapeptide recognition motif differs significantly among caspases and explains the diversity of their biological function (Thornberry and Lazebnik, 1998). To date, the 12 distinct human caspases identified can be grouped into 3 subfamilies based on their substrate specificity. Group 1 caspases prefer bulky hydrophobic residues in the P4 position. Group 2 caspases require an aspartate at P4, while those in group 3 favor a branched chain aliphatic residue (Cory and Adams, 1998). Group 1 caspases (caspases-1, -4 and -5) are thought to play a role in inflammation, whereas group 2 (caspases-2, -3 and -7) and group 3 (caspases -6, -8, -9 and -10) are mainly involved in apoptosis (Janicke *et al.*, 1998).

Caspases are synthesised as inactive precursors (zymogens), 30-50 kDa in size, each containing a short or a long N-terminal prodomain, a large subunit (20 kDa) containing the active site cysteine within the conserved QACXG motif, and a C-terminal small subunit (10 kDa). The aspartate cleavage site separates the prodomain from the large subunit, and an interdomain linker containing one or two aspartate cleavage sites separates the large and small subunits. Sequential cleavage of the pro-enzyme at specific Asp residues releases the small and large subunits that associate to form a heterodimer. Two such heterodimers associate to form a tetramer, primarily via interactions of the small subunits, to produce the active form of the enzyme (Cory and Adams, 1998; Wolf and Green, 1999).

Caspase prodomains vary in length and sequence. Long prodomain caspases function as signal integrators for apoptotic signals, are known as "initiator" caspases and include caspases -2, -8, -9 and -10. The long prodomain allows them to interact with specific adaptor molecules. Such interactions bring initiator caspases in close proximity and allow autoactivation to occur. Active "initiator" caspases are responsible for directly or indirectly

activating various downstream "effector" caspases (caspases -3, -6 and -7), which contain short prodomains (Bratton *et al.,* 2000).

Current understanding suggests that the protein-protein interactions leading to activation of caspase-8 and caspase-9 are the end result of two very distinct signalling processes. Different initiator caspases mediate distinct sets of signals: caspase-8 has been suggested to be associated with "death receptor" induced apoptosis, such as that induced by CD95 (Fas/Apo-1) (Juo *et al.,* 1998). On the other hand, caspase-9 has been reported to be involved with cell death induced by cytotoxic agents (Sun *et al.,* 1999). Both pathways are demonstrated in Fig. 1.5. Activation of initiator caspase, pro-caspase-8, requires association with its cofactor FADD (Fas associated protein with death domain) through the DED (death effector domain). Because FADD is a multimeric protein, it can act as a molecular scaffold that juxtaposes multiple pro-caspase-8 molecules. Caspase-8 then becomes activated by self-catalysis and, in turn, cleaves pro-caspase-3 and -7, thus activating them; and active caspase-3 cleaves pro-caspase-6. Although the ligands and adaptor molecules are different for other death receptors, such as that of the TNF receptor, similar pathways appear to ultimately be activated (Kaufmann and Earnshaw, 2000; Sun *et al.,* 1999). Alternatively, active caspase-8 can cleave the pro-apoptotic Bcl-2 family member, Bid, resulting in its translocation to the mitochondria where it promotes cytochrome c release. The release of cytochrome c into the cytosol results in activation of caspase-9 and subsequent activation of effector caspases-3, -7 and -6 (Hengartner, 2000).

Less is known about non-receptor signal transduction pathways that operate within the cytoplasm to activate caspases. At least one apoptotic pathway operates through the mitochondria and causes the release of cytochrome c into the cytosol, where it binds to the scaffold protein, Apaf 1 (protease activating factor 1), which is homologous to the *ced-4* gene found in *C. elegans* (Li *et al.,* 1997). The NH_2 region of Apaf-1 shares sequence similarity with the pro-domain of ced-3 and other caspases with long prodomains. This domain serves as a caspase recruitment domain (CARD) by binding to caspases that have similar CARDs at their NH_2 termini. The binding of cytochrome c to Apaf-1 induces a conformational change in the Apaf 1/cytochrome c complex, thus exposing the CARD of Apaf 1, and allowing pro-caspase-9 to bind in the presence of ATP to form the "apoptosome" complex. Subsequent oligomerisation of pro-caspase-9 facilitates caspase autoactivation, and active caspase-9 in

Fig. 1.5 Schematic representation of pathways describing the caspase cascades that result in apoptosis

Apoptosis involving death receptors such as TNF or Fas involves association with the co-factor, FADD, which juxtaposes multiple pro-caspase-8 molecules, which become activated by self-catalysis. Active caspase-8 in turn can directly cleave pro-caspase-3 and -7, thus activating them, or can act indirectly by cleaving cytosolic Bid, which translocates to the mitochondria and promotes cytochrome c release followed by activation of caspase-9 and subsequent activation of effector caspases-3, -6 and -7. Non-receptor signal transduction pathways, which are triggered in response to stress, such as that caused by cytotoxic agents and DNA damaging agents, operate via undefined signals through the mitochondria causing the release of cytochrome c into the cytosol. Cytochrome c binds Apaf-1 causing a conformational change in the cytochrome c-Apaf-1 complex, thus allowing pro-caspase-9 to bind in the presence of ATP. Oligomerization of pro-caspase-9 facilitates auto-activation, and active caspase-9 in turn cleaves and activates pro-caspases-3 and -7. Active caspase-3 will subsequently cleave and activate pro-caspase-6.

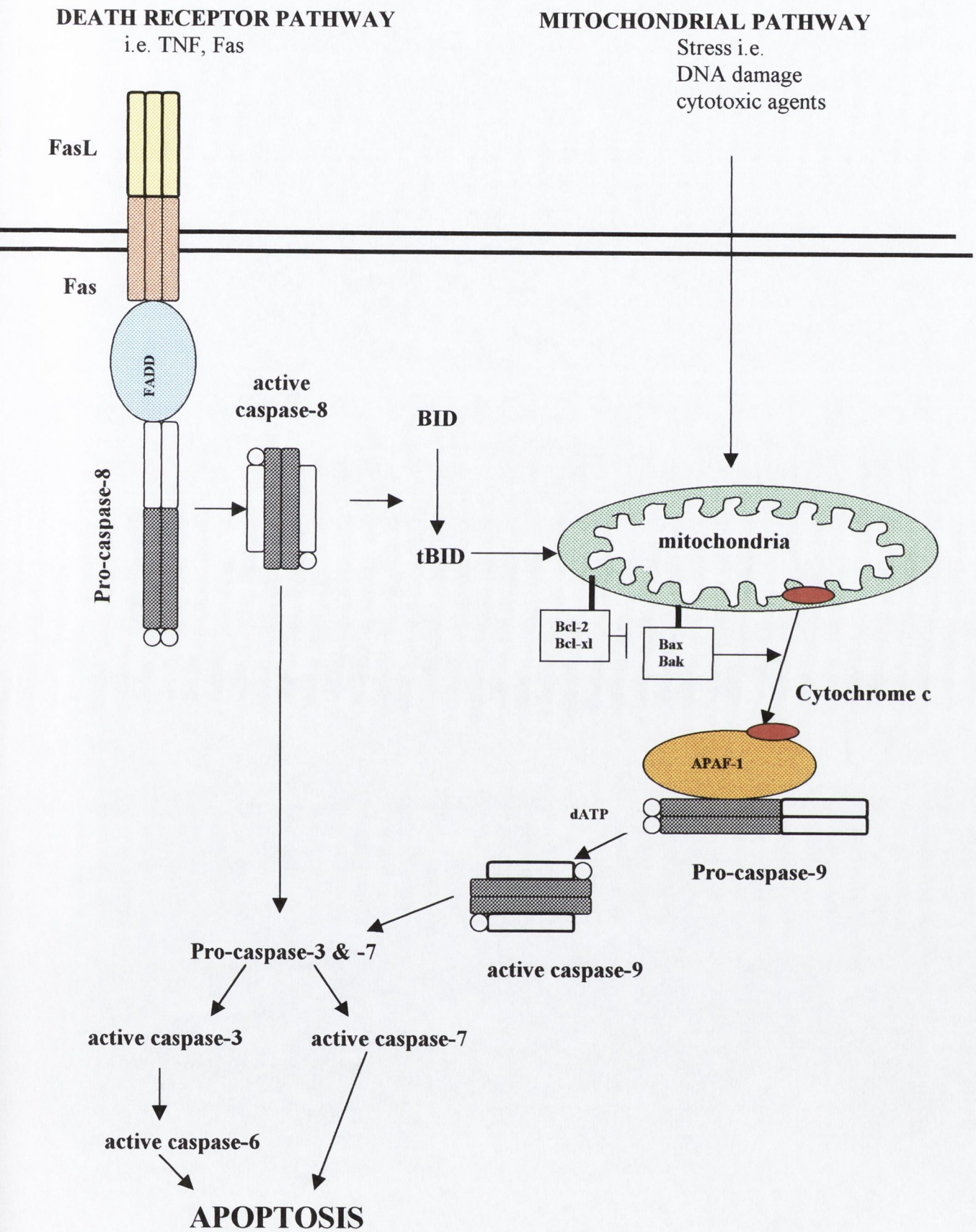
DEATH RECEPTOR PATHWAY
i.e. TNF, Fas
MITOCHONDRIAL PATHWAY
Stress i.e.
DNA damage
cytotoxic agents
FasL
Fas
FADD
Pro-caspase-8
active
caspase-8
BID
tBID
mitochondria
Bcl-2
Bcl-xl
Bax
Bak
Cytochrome c
APAF-1
dATP
Pro-caspase-9
active caspase-9
Pro-caspase-3 & -7
active caspase-3
active caspase-7
active caspase-6
APOPTOSIS

turn cleaves and activates pro-caspases-3 and -7, and active caspase-3 will subsequently cleave and activate pro-caspase-6 (Li *et al.,* 1997; Wolf and Green, 1999).

Caspase-mediated cleavage of specific substrates explains several characteristic features of apoptosis. For example, cleavage of nuclear lamins is required for nuclear shrinking (Orth *et al.,* 1996). Loss of overall cell shape and membrane blebbing is caused by cleavage of cytoskeletal proteins such as fodrin (Martin *et al.,* 1995). Caspase-3 cleaves death substrates, including proteins involved in regulation of the cell cycle such as retinoblastoma protein (pRb) and protein kinase c (PKC) (Nicholson and Thornberry, 1997). Poly (ADP-ribose) polymerase or Parp cleavage has been linked to endonuclease activation, with Parp demonstrated to negatively regulate endonuclease activity. On cleavage of Parp, this block is removed and the endonuclease is re-activated (McGowan *et al.*, 1996, Nicholson *et al.,* 1995). A caspase substrate discovered in recent years has led to the elucidation of the mechanism of activation of the nuclease responsible for producing the DNA laddering pattern. DNA fragmentation is believed to result from protease-mediated cleavage of a nuclease inhibitor called ICAD (inhibitor of caspase-activated DNAse), which releases a unique endonuclease called CAD (caspase-activated DNAse) from its inactive complex with ICAD, leaving it free to act as a nuclease (Enari *et al.,* 1998; Kaufmann and Earnshaw, 2000; Wolf *et al.,* 1999). Close to 100 additional caspase substrates have been reported and, although some of the key apoptotic events are still poorly understood, it is possible that many of the described caspase substrates are "innocent bystanders" in the process (Hengartner, 2000).

Although caspases have been shown to play a central role in cell death pathways in a wide variety of systems, caspase-independent mechanisms for commitment to cell death have also been reported. For example, over-expression of a pro-apoptotic protein, Bax, in mammalian cells, can induce DNA condensation and membrane alterations leading to apoptosis, without any caspase activation (Xiang *et al.,* 1996). More recently, a caspase-independent commitment to cell death has been described by Kroemer and co-workers, which involves the activation of a novel apoptosis inducing factor (AIF) (Dumont *et al.,* 2000; Loeffler and Kroemer, 2000; Susin *et al.*, 1999b).

1.16 Mitochondria and apoptosis

It is widely reported that mitochondria play a critical role in many forms of apoptosis. One of the mechanisms that demonstrate mitochondrial involvement has been the release of apoptogenic factors, such as cytochrome c and apoptosis-inducing factor (AIF), from the intermembrane space into the cytosol, activating the downstream executioner phase of apoptosis (Tsujimoto and Shimizu, 2000).

Cytochrome c, the first apoptogenic intermembrane protein to be identified, is a soluble protein located in the mitochondrial intermembrane space. In response to various apoptotic stimuli, cytochrome c is released from the mitochondria. Cytosolic cytochrome c forms an essential part of the vertebrate "apoptosome", which is composed of cytochrome c, Apaf 1 and pro-caspase-9. The result is activation of caspase-9, which will subsequently process and activate downstream caspases to orchestrate the biochemical execution of cells (Green and Reed, 1998). The mechanism of cytochrome c release and its regulation remains unclear (Scarlett and Murphy, 1997), but Bcl-2 family members are thought to play an intimate role in this process and their involvement will be discussed later.

Whether the release of cytochrome c from the mitochondria reflects rupture of the outer membrane or formation of specific channels remains controversial (Martinou, 1999; Shimizu *et al.*, 1999). In many apoptotic pathways, it has been suggested that the mitochondrial inner transmembrane potential ($\Delta\psi_m$) collapses as a result of opening of the large conductance channel known as the mitochondrial permeability transition (PT) pore (Scarlett and Murphy, 1997). The structure and composition of the PT pore remains only partially defined, but it is thought to consist of inner and outer membrane proteins, which operate together and create a channel through which molecules less than 1.5 kDa pass. These proteins include VDAC (voltage-dependent anion channel), ANT (adenine nucleotide translocator), cyclophilin D and the peripheral-type benzodiazepine receptor (PBR) (Bono *et al.*, 1999; Green and Reed, 1998). It has been suggested that opening of this non-selective channel in the inner membrane results in a volume dysregulation of mitochondria due to the hyperosmolarity of the matrix, causing it to expand. The inner membrane consists of folded cristae and therefore possesses a larger surface area than the outer membrane. This volume expansion can eventually cause rupture of the outer membrane, releasing apoptogenic proteins (Green and Reed, 1998). Interaction of a Bcl-2 family member, Bax, with ANT is

reported to result in cytochrome c release, presumably by inducing mitochondrial-swelling leading to outer membrane rupture (Marzo *et al.,* 1998). In contrast, Shimizu *et al.* (1999) demonstrated that the Bcl-2 family members, Bax and Bak, target VDAC directly, inducing a conformational change in VDAC so that cytochrome c can pass through the channel. Inhibitors of PT pore-opening, such as bongkrekic acid, appear to block apoptosis in some systems, thus providing support for the idea that the PT is central to some apoptotic processes (Tafani *et al.*, 2001).

However, it has also been proposed that alternative permeabilisation mechanisms must exist. According to Eskes *et al.* (1998), the mitochondrial effects of Bax, which releases cytochrome c into the cytosol, are not inhibited by the PT pore inhibitors, cyclosporin A or bongkrekic acid. Some studies have reported cytochrome c release from mitochondria of apoptotic cells without any apparent changes in mitochondrial potential, which normally accompanies PT pore opening (Gross *et al.,* 1998). In addition, no evidence for mitochondrial membrane permeabilisation has been reported in *C. elegans*. Moreover, the *C. elegans* apoptosome does not require cytochrome c, further evidence to suggest that mitochondria may not always be involved in cell death (Loeffler and Kroemer, 2000).

Recent findings have uncovered that cytochrome c is not the only pro-apoptotic protein released by mitochondria. It has been shown that, upon induction of apoptosis, mitochrondria also release pro-caspase-2, -3 and -9. These pro-caspases redistribute from the mitochondria to the cytosol and are processed to generate enzymatically active caspases (Mancini *et al.,* 1998; Susin *et al.*, 1999a).

Recently another apoptogenic protein, known as apoptosis-inducing factor (AIF), was found to be released from the mitochondria in response to apoptotic stimuli (Susin *et al.,* 1999b). AIF is a flavoprotein with a significant homology to bacterial oxidoreductases. It is located in the mitochondrial intermembrane space and is released into the cytosol and translocates to the nucleus in response to death stimuli. Release of AIF is dependent upon the occurrence of membrane permeability transition characterized by loss in membrane potential ($\Delta\psi_m$). When added to purified nuclei, AIF induces partial chromatin condensation and large scale (50 kbp) DNA fragmentation, but not oligonucleosomal DNA fragmentation. DNA fragmentation is not inhibited by the caspase-inhibitor, z-VAD-fmk, and translocation of AIF to the nucleus, which appears to occur before cytochrome c release, is ATP-

independent (Daugas *et al.*, 2000; Loeffler and Kroemer, 2000). Bcl-2 inhibits the mitochondrial release of AIF but has no cytoprotective effect once AIF is present in the cytosol. Thus, it is likely that AIF acts beyond or independently of the Bcl-2 and caspase checkpoints in the cell death process (Susin *et al.*, 1999b). How AIF mediates its apoptogenic function remains entirely elusive. AIF interacting proteins in the cytosol and the nuclear AIF target(s) have not yet been identified. AIF, which lacks flavin adenine dinucleotide (FAD) and therefore has no NADH oxidase activity, exhibits a similar apoptosis-inducing potential when microinjected into the cytoplasm of intact cells. This indicates that the oxidoreductase activity of AIF can be dissociated from its apoptosis-inducing function (Miramar *et al.*, 2001). However, deletion mutants affecting parts of the oxidoreductase domain abolished the apoptogenic potential of AIF, indicating that at least some of the structural features of the oxidoreductase domain are important for the apoptogenic effect of AIF (for review, Daugas *et al.*, 2000).

1.17 Bcl-2 proteins and the regulation of apoptosis

In recent years, it has been well established that Bcl-2 prevents most forms of cell death and some forms of necrotic cell death. A large number of Bcl-2-related proteins have been isolated and divided into three categories (Tsujimoto and Shimizu, 2000).

1. Anti-apoptotic members such as Bcl-2, Bcl-$_{XL}$, Bcl-$_{w}$ and Mcl-1. These members exert their anti-apoptotic activity and share sequence homology, particularly within 4 regions, Bcl-2 homology (BH) 1 through to BH4.
2. Pro-apoptotic members such as Bax, Bak, Bad, Bok, which primarily share homology in BH1, BH2 and BH3 although some homology in BH4 has been noticed.
3. 'BH3-only proteins', the pro-apoptotic proteins that include Bik, Bid and Bim, and these share sequence homology only in BH3 domains.

Apoptotic mitochondrial changes, including the release of cytochrome c and AIF, are central to signal transduction. Bcl-2 family members regulate apoptogenic mitochondrial changes independently or by interacting with each other. One of the striking features of Bcl-2 family proteins is their ability to form homodimers and heterodimers (Oltvai *et al.*, 1993). Heterodimerisation between opposing family members is thought to inhibit the biological

activity of their partners. This is mediated by the insertion of the BH3 domain of a pro-apoptotic protein into a hydrophobic pocket composed of BH1, BH2 and BH3 from an anti-apoptotic protein (Sattler *et al.,* 1997). In addition, BH1, BH2, BH3 and BH4 are required for anti-apoptotic activity, while BH3 is essential for pro-apoptotic activity (Tsujimoto, 1998).

In addition to the regulation of apoptosis by heterodimerisation of anti-apoptotic and pro-apoptotic members, alternative independent mechanisms also exist. A variety of apoptotic stimuli activate a number of caspases, leading to apoptosis. Bcl-2 prevents cell death by blocking a step that leads to activation of caspases (Chinnaiyan *et al.*, 1996). Two independent mechanisms in which Bcl-2 prevents caspase activation have been considered. These include the prevention of release of mitochondrial apoptogenic factors, such as cytochrome c, and the sequestration of pro-caspases.

Mechanisms that regulate mitochondrial cytochrome c release remain controversial and a number of theories are discussed. Based on the structural similarity of Bcl-$_{XL}$ to the pore forming subunit of diphtheria toxin (Muchmore *et al.*, 1996), it has been suggested that Bcl-2 proteins might act by inserting, following a conformational change, into the outer mitochondrial membrane where they could form channels. Bcl-2 family members, including Bcl-$_{XL}$, Bax and Bcl-2, have been shown to insert into synthetic lipid bilayers and form channels (Nouraini *et al.*, 2000; Schendel *et al.,* 1997). However, it remains to be determined if Bcl-2 family proteins actually form ion channels *in vivo* and if these proteins regulate apoptosis via the creation of ion channels.

Bcl-2 family members interact with many proteins and it has been proposed that regulation of apoptosis may occur by controlling the opening of the permeability transition pore. Bax and Bak have been shown to interact directly with VDAC and induce mitochondrial cytochrome c release (Shimizu *et al.*, 1999). It is thought that Bax/Bak induces a conformational change in VDAC so that cytochrome c can pass through the channel, or that these three proteins interact to form a larger channel. Inhibition of PT by Bcl-2 or Bcl-$_{XL}$ has been shown to prevent apoptosis by as yet unidentified methods (Fulda *et al.*, 1998).

In addition, it has been suggested that Bcl-2 and Bcl-$_{XL}$ can bind indirectly to and therefore sequester cytosolic caspases, via Apaf-1, thereby preventing their activation (Pan *et al.*, 1998, Hengartner, 2000). It is thought that BH3 proteins operate as death ligands and their targets are classified as death receptors. Death receptors might be members of the Bax

subfamily or totally unrelated proteins with a BH3-binding structure similar to that of Bcl-2. The activity of some Bcl-2 family members appears to be regulated by phosphorylation. For instance, the activity of Bad and its binding to Bcl-$_{XL}$ seems to be regulated by phosphorylation and dephosphorylation (Tsujimoto, 1998). In addition, a number of workers have reported the inactivation of Bcl-2 by phosphorylation, which occurs within an unstructured loop and involves several sites, the principal ones being serine 70, serine 87 and threonine 69 (Haldar *et al.,* 1995; Yamamoto *et al.*, 1999). It has been shown that deletion of the loop region of Bcl-2 completely blocks phosphorylation (Srivastava *et al.,* 1999). A mechanism of activation of pro-apoptotic members of the Bcl-2 family involves proteolytic cleavage by caspases. A BH3 protein, Bid, has been shown to be cleaved by caspase-8 to become active in inducing mitochondrial cytochrome c release (Li *et al.,* 1998).

It appears that the regulation of the activities of Bcl-2 family members is modulated by heterodimerisation with other family members, post-translational modifications, such as phosphorylation, and proteolytic cleavage. The life-death signals transmitted to the Bcl-2 family proteins eventually converge on the mitochondria to determine whether the release of apoptogenic factors to the cytosol is induced or prevented (Tsujimoto and Shimizu, 2000).

1.18 Oxidative stress and apoptosis

Cellular energy metabolism is based on the production of ATP through the electron transport reaction during oxidative phosphorylation and this process is usually extraordinarily efficient. However, 1-2% of electrons are leaked to generate $O_2^{\cdot}$. These molecules are readily converted into the hydroxyl radical, $OH^{\cdot}$, which is highly reactive and induces serious oxidative damage. Thus, mitochondria are believed to be the primary site of reactive oxygen species (ROS) production within the cell (Kamata and Hirata, 1999). Under normal conditions, aerobic cells are endowed with an extensive biochemical defense mechanism to counteract the damaging effect of ROS. This is composed of glutathione peroxidase, glutathione reductase, superoxide dismutase, NADP dehydrogenase (NADPH), Vitamins E and C. For example, superoxide radicals are scavenged by superoxide dismutase, leading to the production of hydrogen peroxide, which again is detoxified by glutathione peroxidase or catalase. When pro-oxidants overwhelm antioxidant defense mechanisms, oxidative stress occurs (Kannan and Jain, 2000). Experimental evidence suggests an increase in the

production of ROS such as peroxides and superoxides during apoptosis and pretreatment with a number of antioxidants, such as *N*-acetylcysteine, and the free-radical scavenger Tempo, prevent apoptosis mediated through ROS (Mc Gowan *et al.*, 1996). It has also been reported that moderate oxidative radical stress induces apoptosis through alteration of cellular signalling, whereas necrosis occurs when the cells are exposed to a higher dose of ROS (Kamata and Hirata, 1999; Lennon *et al.,* 1991). Indeed Ras is suspected to activate a cascade of kinases via ROS production (Kannan and Jain, 2000). An increase in cytosolic Ca^{2+} by oxidants may lead to apoptosis due to stimulation of intracellular proteases, nucleases and other enzyme activities. Current chemotherapeutic drugs, such as the anthracycline-derivative, adriamycin, are known to chelate iron and generate ROS that results in apoptosis of cancer cells (Kannan and Jain, 2000).

1.19 Tyrosine phosphorylation and apoptosis

Intracellular signal transduction involving protein tyrosine kinase cascades is a fundamental cellular mechanism regulating cell survival, growth, differentiation and migration. Deregulated cell growth is the defining feature of all neoplasms and some classes of signalling proteins and pathways are targeted more frequently by oncogenic mutations than others. For example, receptor protein tyrosine kinases (RPTKs), a subclass of transmembrane-spanning receptors, can become potent oncoproteins when mutated. In addition, of the 32 known cytoplasmic, non-receptor, protein tyrosine kinases, almost half have been implicated in human cancer (Blume-Jensen and Hunter, 2001). Signalling by RPTKs requires ligand-induced receptor oligomerisation, which results in tyrosine autophosphorylation of the receptor subunits. This both activates catalytic activity and generates phosphorylated tyrosine residues that mediate the specific binding of cytoplasmic signalling proteins containing protein tyrosine binding domains. As a result of the increased or constitutive activity of these normally, tightly regulated proteins, in many types of cancer, protein tyrosine kinases have become important targets for drug development efforts (Bergamaschi *et al.,* 1993). The recent development of a series of relatively specific PTK inhibitors, and their ability to inhibit the proliferation of tumour cells expressing the target PTK is often enough to slow down progression of cancer. For example, the synthetic compound STI571, a 2-phenylaminopyrimidine derivative, is an ATP-competitive inhibitor

of the Abl tyrosine kinase that has been shown to inhibit the kinase activity of Abl both *in vivo* and *in vitro* and to inhibit the growth of v-Abl and Bcr-Abl transformed cells (Buchdunger *et al.*, 1996; Gambacorti-Passerini *et al.*, 1997). These results suggest that compounds that exploit the distinctive inactivation mechanisms of individual protein kinases can achieve both high affinity and high specificity.

1.20 Mitogen-activated protein (MAP) kinase signalling

The mitogen-activated protein (MAP) kinases are a group of protein serine/threonine kinases that are activated in response to a variety of extracellular stimuli and mediate signal transduction from the cell surface to the nucleus. These signalling cascades have important roles in the regulation of cell growth, differentiation, cell survival, apoptosis, stress and inflammatory responses (Chan-Hui and Weaver, 1998). In mammalian systems, the biochemical properties of three MAP kinases have been characterised in detail, the extracellular signal-regulated kinases (ERKs; also known as p42-44 MAP kinases), the c-Jun N-terminal kinases (JNKs; also referred to as stress-activated protein kinases, or SAPKs) and the p38 MAP kinases (Ichijo, 1999). Components and activators of the three MAP kinase cascades are summarised in Fig. 1.6.

All MAP kinases are serine/threonine kinases that are activated in response to their phosphorylation on invariant threonine and tyrosine, within a TXY motif, by dual specificity MAP kinase kinases (MAPKKs). The MAPKKs also form a highly conserved group that are activated through phosphorylation of conserved serine and threonine residues by a somewhat more diverse group of MAP kinase kinase kinases (MAPKKKs). The latter group receive signals from cell surface receptors through a variety of intermediates, including other protein kinases such as PAKs (p21-activated kinases), scaffold proteins such as JNK interacting protein-1 (JIP-1) that increase the local concentration of cascade components, adaptor proteins such as TRAFs (TNF receptor-associated factors) that form oligomers and interact with receptors, and small GTP binding proteins including Rac and Cdc42 (Ichijo, 1999). In the different MAP kinase pathways, the MAPK, MAPKK and the MAPKKK are usually highly conserved in their catalytic domains, but can differ considerably in their regulatory domains and their substrate specificities. Specific MAPKKs will recognise specific sequences at sites of regulatory phosphorylation on the MAPK, for example, amino acids

Fig 1.6 GTP-binding proteins and their regulation of MAP kinase signalling cascades

Three MAP kinase cascades have been characterised in mammalian cells. Activation of the signalling cascade involves dual phosphorylation and activation of MAPKKKs, which in turn will dually phosphorylate MAPKKs, which phosphorylate and activate either the ERK, JNK or p38 MAP kinases on specific tyrosine and threonine residues. These MAP kinases activate transcription factors and increase their transcriptional activity. While MAPKKs are specific for their substrates, a large extent of crosstalk takes place at the MAPKKK level. MAP kinase signalling cascades are regulated by upstream GTP-binding proteins from the Ras (primarily regulates the ERK pathway) and Rho (Cdc42 and Rac, which primarily regulate the JNK and p38 pathways) subfamilies.

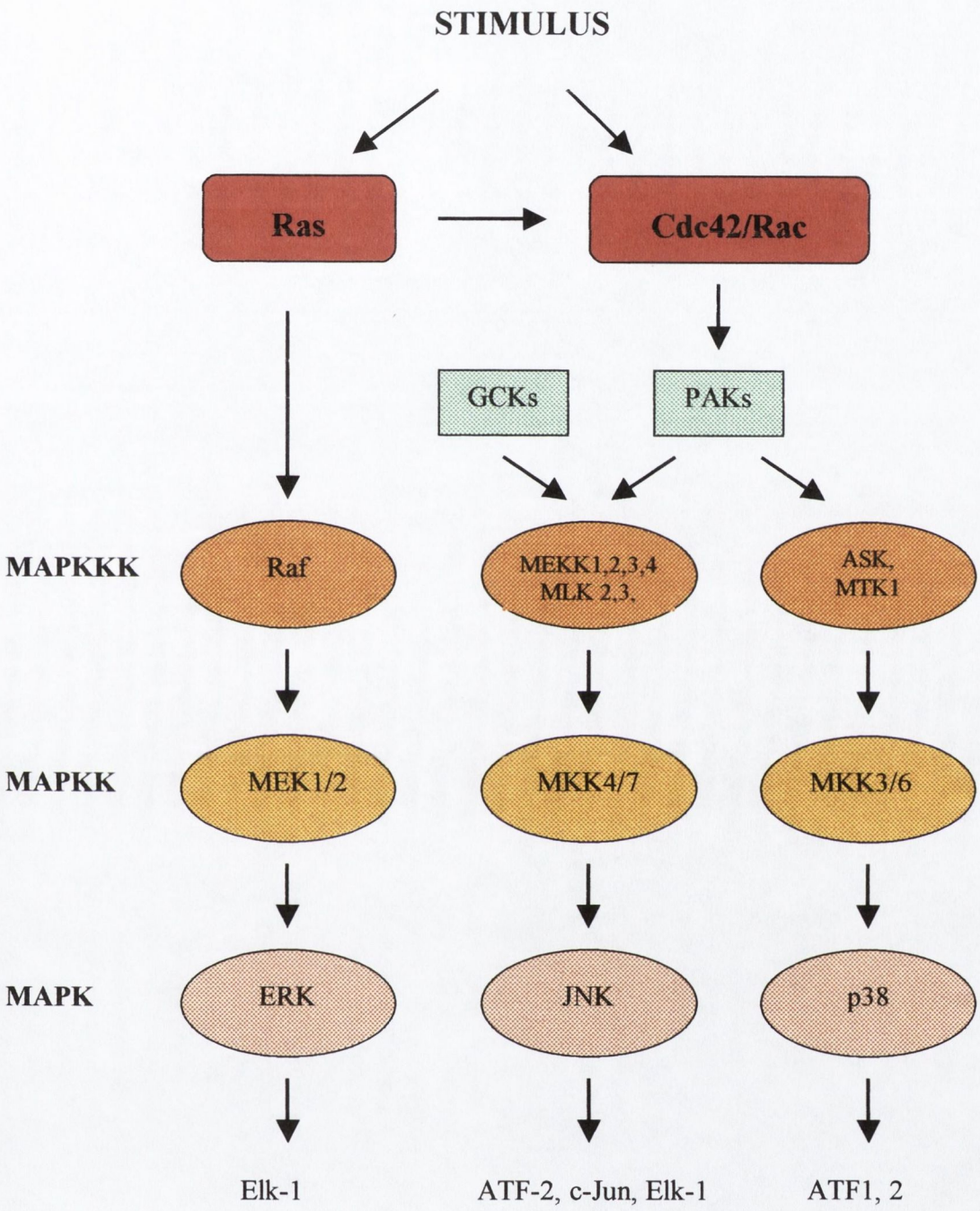
STIMULUS
Ras
Cdc42/Rac
GCKs
PAKs
MAPKKK
Raf
MEKK1,2,3,4
MLK 2,3,
ASK,
MTK1
MAPKK
MEK1/2
MKK4/7
MKK3/6
MAPK
ERK
JNK
p38
Elk-1
ATF-2, c-Jun, Elk-1
ATF1, 2

TEY on ERK1/2, amino acids TPY on the JNK subgroup and amino acids TGY on p38 MAPKs (Kyriakis and Avruch, 1996; Minden and Karin, 1997). MAP kinases phosphorylate proteins located at the plasma membrane, cytoplasm and nucleus. In unstimulated cells, MAPKs are largely cytoplasmic. Upon activation, a portion of the MAP kinase translocates to the nucleus. The duration of MAP kinase activation influences the extent of their nuclear translocation and thus their access to transcription factors. Activated MAP kinases regulate the activities of transcription factors or kinases further downstream by phosphorylation, and thereby control gene expression and cellular function (Buschmann *et al.*, 2000; Ichijo, 1999).

The first mammalian MAP kinase cascade to be characterised in detail was the pathway leading to activation of the extracellular signal-regulated kinase (ERK) subgroup of MAP kinases (Payne *et al.*, 1991). The ERK subgroup of MAP kinases is activated most potently by mitogenic stimuli such as growth factors, which bind to cell surface receptors. Ligand-induced receptor-clustering results in autophosphorylation of the receptor cytoplasmic domain on tyrosine residues. The recruitment of additional proteins results in a complex formation. Recruitment of the exchange factor, SOS, results in activation of H-Ras by catalysing GDP:GTP exchange. Once activated, Ras binds and recruits the serine/threonine kinase Raf-1 to the membrane. Raf-1 functions as the MAPKKK in the ERK cascade. Once Raf-1 is activated, it phosphorylates and activates the MAPKKs, MEK1 and MEK2. Once activated, either MEK1 or MEK2 can directly activate the ERKs, which comprise ERK1 and ERK2, by phosphorylating their conserved threonine and tyrosine activation sites. Once the ERKs are activated, a fraction of the enzyme translocates to the nucleus where it phosphorylates and thereby regulates transcription factors that mediate changes in gene expression (Minden and Karin, 1997).

Unlike the ERK signalling pathway, the JNK and p38 pathways are preferentially activated by inflammatory cytokines such as TNFα and IL-1β, and a diverse array of cellular stresses, including UV irradiation, heat, osmotic shock and growth factor withdrawal. In the JNK subgroup, three genes (*jnk1, jnk2* and *jnk3*) have been described. JNK1 and JNK2 protein kinases are expressed ubiquitously, while JNK3 is expressed primarily in the brain (Yasuda *et al.*, 1999). The family comprises at least 8 isoforms derived by differential splicing from three or more genes, to generate proteins of 54 kDa and 46 kDa (Zanke *et al.*, 1996). JNKs are activated by phosphorylation on threonine 183 and tyrosine 185 residues by

two distinct MAPKKs, MKK4/SEK1 and MKK7 (Sanchez *et al.*, 1994). These MAPKKs are activated in turn by phosphorylation by a wide number of MAPKKKs including ASK1, TPL2, TAK1, members of the MEKK (MEKK-1, -2, -3, -4), and mixed-lineage protein kinase (MLK-2, -3) groups of MAPKKKs (Ichijo, 1999; Yasuda *et al.*, 1999). While MAPKKs are specific for their respective downstream targets, a certain amount of crosstalk occurs between the MAPKKKs (Ichijo, 1999). Unlike the ERKs, JNK is activated upstream by two H-Ras related GTP-binding proteins of the Rho family, namely Rac and Cdc42 (Bagrodia *et al.*, 1995; Coso *et al.*, 1995; Teramoto *et al.*, 1996). However it is unclear how these GTP-binding proteins can activate the JNK pathway. It is thought that p21-activated kinases (PAKs) act as mediators between the GTP-binding proteins and JNK (Knaus and Bokoch, 1998). Another kinase, germinal centre kinase (GCK) has been shown to activate JNK, however, unlike PAK, it does not appear to be activated by Rac and Cdc42, suggesting that G-protein independent activation of JNK may occur (Pombo *et al.*, 1995). Other stimuli reported to activate JNK include heterotrimeric G-proteins, UV and ionizing radiation and DNA damaging agents (Minden and Karin, 1997).

Activated JNK phosphorylates transcription factors such as activating transcription factor-2 (ATF-2) (Gupta *et al.*, 1995), c-Jun and Elk1 (Minden and Karin, 1997) and strongly augments their transcriptional activity. c-Jun, encoded by *c-jun* proto-oncogene, is a sequence specific transcription factor whose function has been implicated in various cellular events ranging from cell proliferation and differentiation to neoplastic transformation. c-Jun, together with ATF-2 and Fos, is a component of the activator protein-1 (AP1) transcription factor, which is composed of a collection of dimers of DNA-binding proteins. The exact function and target gene of AP-1 is determined by their composition (Minden and Karin, 1997; Leppa and Bohmann, 1999). JNK phosphorylates serine 63 and 73 on the c-Jun activation domain. Mammalian Jun proteins include c-Jun, JunB and JunD, but only c-Jun is an efficient JNK substrate (Leppa and Bohmann, 1999; Minden and Karin, 1997). Phosphorylation of Elk1 at specific sites in its transactivation domain by JNK stimulates its ability to activate transcription of genes such as *c-fos* (Minden and Karin, 1997). Phosphorylation of ATF-2 at residues threonine 69 and 71 is mediated by JNK (Gupta *et al.*, 1995) and although the physiological role of ATF-2 remains largely uncharacterised, in addition to c-Jun, it is thought to interact with the tumour suppressor gene product,

retinoblastoma protein (Rb) and the transcription factor nuclear factor-κB (NFκB) (Du *et al.*, 1993). JNK has also been shown to phosphorylate and inactivate the anti-apoptotic Bcl-2 protein (Yamamoto *et al.*, 1999) and the pro-apoptotic p53 protein (Milne *et al.*, 1995). While activation of JNK serves as a major pro-apoptotic switch in many cellular instances (Minden and Karin, 1997), JNK activation leading to suppression of apoptosis has also been reported (Krause *et al.*, 2001).

A third mammalian MAP kinase pathway leads to p38 activation and is thought to play an important role in inflammation and apoptosis. The p38 group of MAP kinases, which consists of 4 isoforms, was originally identified as a kinase that is activated by lipopolysaccharide (LPS). The p38 MAP kinase is phosphorylated and activated by the MAPKKs, MKK3 and MKK6, which are in turn phosphorylated by a number of MAPKKKs such as MTK-1 and MLK-2 and -3, ASK1, DLK and TAK1. Overexpression of a number of these MAPKKKs also leads to JNK activation, which may be a reason why p38 and JNK are often co-activated (Ono and Han, 2000; Minden and Karin, 1997). Downstream substrates of p38 include the MAP kinase interaction protein kinase (MNK1), the p38 regulated/activated kinase (PRAK), mitogen and stress-activated kinase (MSK) and the transcription factors ATF1, ATF-2, AP-1 and CHOP (Ono and Han, 2000).

1.21 GTP binding proteins

Small GTP-binding proteins are monomeric G-proteins with molecular masses of 20-30 kDa. More than 100 small G-proteins have been identified in eukaryotes from yeast to human and they comprise a superfamily. Members of the superfamily are structurally classified into at least five subfamilies: the Ras, Rho, Rab, Sar1/Arf, and Ran families. Members of the Ras subfamily (H-Ras, K-Ras, Rap1A, Rap1B, Rap2A, Rap2B and Ral) mainly regulate gene expression, members of the Rho subfamily, including Rho, Rac, Cdc42, regulate both cytoskeletal reorganisation and gene expression, the Rab, Sar1/Arf family members regulate intracellular vesicle trafficking and the Ran family members regulate nucleocytoplasmic transport and microtubule organisation during the cell cycle (Matozaki *et al.*, 2000).

Small G-proteins act as molecular switches that cycle between two interconvertible forms: GDP-bound inactive and GTP-bound active forms. Upstream events lead to the

exchange of GDP for GTP, leading to the conformational change of the downstream effector-binding region allowing it to interact with downstream effectors (Kjoller and Hall, 1999). At least three classes of molecules are capable of interacting with GTPases and regulating their activation state. Guanine nucleotide exchange factors (GEFs) catalyse the exchange of GDP for GTP resulting in activation, GTPase activating proteins (GAPs) stimulate the intrinsic GTPase activity, thus GTP hydrolysis, and guanine nucleotide dissociation inhibitors (GDIs) inhibit the exchange of GDP for GTP. The cycling and regulation of GTP-binding proteins are summarised in Fig 1.7. Activation of GTPases requires interaction with molecules and it is presumed that such interactions take place at the plasma membrane. GTPases are capable of interacting with membranes through a lipid residue attached to the C-terminus (Denhardt, 1996).

Activation of Ras induces proliferation in many cell types and, in its mutant oncogenic form, Ras transforms many cell lines, conferring on them a malignant phenotype (Denhardt, 1996). The 21 kDa Ras protein also plays an integral role in signal transduction pathways, connecting events at many cell surface receptors to intracellular processes. The principle role of Ras in cell signalling is as a regulator of the ERK MAP kinase pathway, with Ras lying upstream of the MAPKKK Raf. Activation of Raf by Ras involves relocation to the cell membrane where it undergoes further conformational changes and phosphorylation by protein kinase C (PKC) and a protein tyrosine kinase, which enhances its ability to phosphorylate MAPKKs (Denhardt, 1996). Ras has also been reported to play a role in PI3-K activation (Heimbrook and Oliff, 1998).

The Rho subfamily of G-proteins consists of seven distinct proteins: Rho (A, B and C isoforms), Rac (1 and 2 isoforms), Cdc42 (Cdc42Hs and G25K isoforms), RhoD, RhoG, RhoE and TC10 (Mackey and Hall, 1998). The Rho subfamily was initially described for their ability to control the actin cytoskeletal compartment in all eukaryotic cells. Activation of Rho in fibroblasts causes bundling of actin filaments into stress fibres and the clustering of integrins into focal adhesion complexes. Activation of Rac promotes actin polymerisation to form lamellipodial extensions and membrane ruffles, and activation of Cdc42 triggers actin polymerisation to form filopodia or microspikes (Mackay and Hall, 1998; Matozaki *et al.*, 2000).

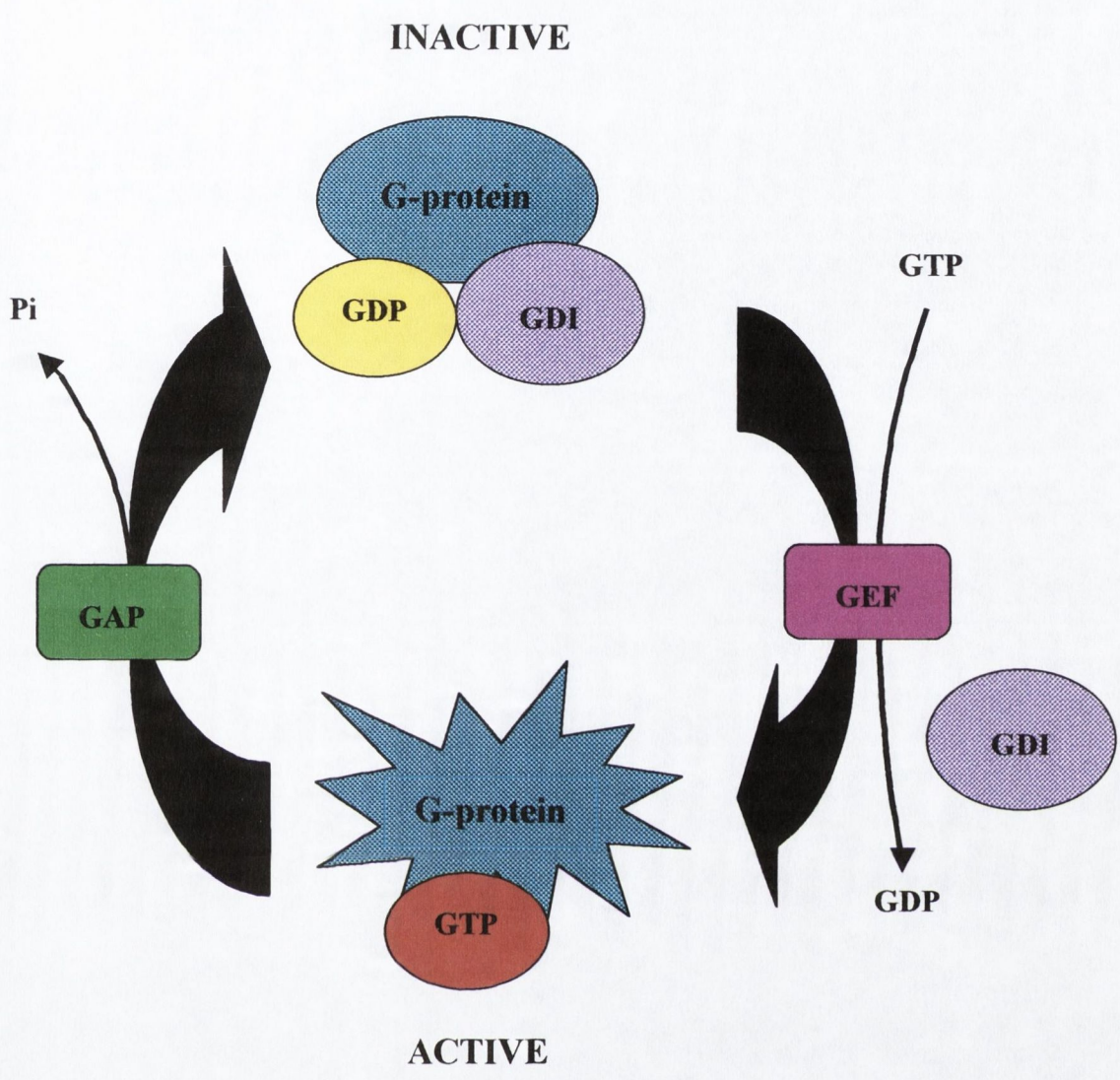

Fig. 1.7 Regulation of GTP-binding proteins

Schematic representation of the regulation of GTP-binding proteins by (1) guanine nucleotide exchange factors (GEFs) that catalyse the exchange of GDP for GTP resulting in activation of G-proteins, (2) inactivating GTPase activating proteins (GAPs) that catalyse the hydrolysis of GTP to GDP, and (3) guanine nucleotide dissociation inhibitors (GDIs), that inhibit the exchange of GDP for GTP. In its active GTP-bound form, the G-proteins can interact with downstream effectors and initiate signalling cascades.

Rho family proteins such as Rac and Cdc42 have also been implicated in the regulation of JNK and p38 MAP kinase cascades, suggesting an analogous role to that played by Ras in the ERK MAP kinase cascade (Bagrodia *et al.,* 1995; Coso *et al.*, 1995; Teramoto *et al.*, 1996; Zhang *et al.*, 1995). The identity of molecules communicating Rac and Cdc42 to JNK and p38 activation is poorly understood. However, a group of 65-68 kDa serine/threonine protein kinases, termed PAKs (p21-activated kinases), were found to bind Rac and Cdc42 in mammalian cells (Knaus and Bokoch, 1998) and couple to JNK and p38 MAP kinase signalling pathways. These kinases contain a conserved binding motif called a CRIB (Cdc42/Rac interactive binding) domain (Bagrodia *et al.*, 1995; Zhang *et al.*, 1995). Mixed-lineage kinases (MLKs), also known as src homology 3 domain (SH3)-containing proline-rich protein kinase (SPRK), also contain a CRIB domain. Overexpression of MLK3 in mammalian cells activates the JNK MAP kinase-signalling pathway through phosphorylation and activation of MKK4 or MKK7 (Bock *et al.*, 2000). Interestingly, activation of JNK by TNFα and IL-1 appears to be Cdc42/Rac-dependent in some cases (Bagrodia *et al.*, 1995; Coso *et al.*, 1995) but not in others (Davis *et al.*, 1999; Puls *et al.*, 1999), which suggest the possibility that alternative mechanisms may exist which relay signals from the cell surface to nuclear events. The MAP kinase pathways and their regulation by G-proteins from the Ras and Rho subfamilies are summarised in Fig 1.6.

Rac and Cdc42 are reported to interact with PI3-K signalling, and PI3-K is thought to act upstream of Rac in some cases (Missy *et al.*, 1998; Tolias *et al.*, 1995). Rho family GTP-binding proteins are also involved in the Ras protein-induced transformation (Qiu *et al.*, 1997). In addition to receptors that recognise soluble ligands, adhesion receptors, in particular integrins, are able to activate Rho GTPases although the mechanism remains unclear (Kjoller and Hall, 1999).

In the last few years, considerable progress has been made towards understanding the signalling networks and downstream pathways of small G-proteins. However, it remains largely unknown at the molecular level how extracellular signals activate these small G-proteins and how crosstalk and signalling cascades are regulated. It is clear however that we are still some way off a biochemical description of the pathways linking Rac and Cdc42 to p38 and JNK activation and further work is required to uncover further participants in this pathway (Mackay and Hall, 1998; Matozaki *et al.,* 2000).

1.22 Farnesyl transferase inhibitors and prevention of Ras transformation

Mutated *ras* genes exist in 20-30% of all human cancers and the highest incidence of *ras* mutations are found in adenocarcinoma of the pancreas (90%), colon (50%), and lung (30%) (Shao *et al.*, 2000). Three *ras* genes are transcribed in human cells, these being Harvey, Kirsten and N-*ras*. Although all three types of mutated *ras* gene are capable of transforming mammalian cells in culture, the Kirsten-*ras* gene is by far the most commonly mutated form of *ras* found in human cancers. Mutations arising in oncogenes generally result in 'gain of function' changes for their encoded proteins. Oncogenes harbouring 'gain of function' mutations are more attractive targets for pharmaceutical intervention than 'loss of function' changes that occur in cancer-causing mutations of tumour suppressor genes and DNA repair enzymes (Oliff, 1999).

Ras proteins cycle between GDP- and GTP-bound forms. When *ras* becomes mutated, it loses its GTPase activity and remains trapped in the GTP-bound form. The pathophysiological consequence of these mutations is that the Ras-driven cell proliferation signal is constitutively active and inappropriately stimulates continuous cell proliferation. For example, activation of Ras function is an important component of Bcr-Abl-mediated transformation of hematopoietic cells (Pendegast *et al.*, 1993).

Ras proteins are synthesised in the cytoplasm as biologically inactive precursor molecules. These precursors undergo a complex series of post-translational modifications to become mature Ras proteins capable of mediating intracellular signal transduction and stimulating cell proliferation (Oliff, 1999). The initial post-translational event is the transfer of a 15-carbon isoprene farnesyl from farnesyl pyrophosphate to a cysteine residue (Cys^{186} in H-Ras) in the conserved carboxyl-terminal "CAAX" motif (where A is an aliphatic residue) (Bishop *et al.*, 1995). This reaction is followed by proteolytic cleavage of three carboxy-terminal AAX residues and carboxymethylation of the now carboxy-terminal prenylated cysteine residue (Oliff, 1999). Of these three reactions, isoprenylation is required for Ras proteins to become membrane-associated and to induce cellular transformation. The proteolytic and carboxymethylation reactions are not required for Ras-induced transformation. These observations immediately suggest that interference with the prenylation of Ras proteins might be an effective means of inhibiting Ras-driven transformation. This may be performed by blocking the synthesis of the farnesyl

pyrophosphate with an inhibitor of 3-hydroxy-3-methylglutaryl coenzyme A reductase using compounds such as lovastatin, or alternatively, by inhibiting the enzyme that catalyses the farnesylation reaction, farnesyl protein transferase (FPTase). FPTase has been purified and has been the focus for the development of inhibitors as potential anticancer drugs (Gibbs *et al.*, 1994).

Three enzymes have been described that catalyse prenylation reactions: farnesyl protein transferase (FPTase), geranylgeranyl protein transferase I (GGPTase I), and geranylgeranyl protein transferase II (GGPTase II). Each is a heterodimeric protein composed of common α-subunits and divergent, albeit homologous, β-subunits. FPTase catalyses the transfer of a 15-carbon isoprenyl group derived from farnesyl pyrophosphate (FPP) to the appropriate substrate via the formation of a covalent thio-ether bond. GGPTase catalyses the transfer of a 20-carbon isoprenyl group to its target protein. A preference for farnesylation over geranylgeranylation is dictated by the sequence of its CAAX box. FPTases prefer substrates with serine, methionine or glutamine in the X position, whereas GGPTase I prefer substrates with leucine in the X position and GGPTase II modifies proteins terminating in XXCC and XCXC. However, while all three species of Ras are preferentially farnesylated, both K- and N-Ras can also serve as substrates for geranylgeranylation (Gibbs *et al.*, 1994; Oliff, 1999).

Since farnesylation of Ras is the preferred prenylation modification, over the past number of years, a series of small molecule inhibitors of FPTase have been developed. Two moieties that are recognised by the enzyme and that are used as models for drug design are the CAAX carboxy terminus of Ras and the other substrate of FPTase, farnesyl pyrophosphate (FPP) (Qian *et al.*, 1994). Some of these have been discovered by the screening of natural products, for example, the antibiotic manumycin A, which is a structural homologue of FPP (Hara *et al.*, 1993). Manumycin A has been shown to inhibit Ras farnesylation and phosphorylation of the downstream MAP kinase pathway, thus inhibiting proliferation of rat vascular smooth muscle cells (Kouchi *et al.*, 1999). An alternative strategy has focused on molecules that resemble the structure of the CAAX tetrapeptide found at the carboxy-terminus of the Ras protein. These act as alternative substrates *in vitro*, thereby competitively inhibiting Ras farnesylation. With structural and conformational characteristics being of high importance, a number of inhibitors have been synthesised (Qian

et al., 1994). However, due to the presence of amide bonds and other peptide features, these compounds are vulnerable to proteolytic degradation and have shown slow cellular uptake, which has limited their use. As a result, a number of non-peptide analogues were synthesised, for example, a group of compounds known as benzodiazepine peptidomimetics, which are non-peptide scaffolds that replace all or part of the tetrapeptide. These were designed with the initial hypothesis that the tetrapeptide substrate binds to the FPTase in a turn conformation, which would place the N-terminal cysteine and the C-terminal methionine in close approximation where they can interact with a Zn^{2+} atom that is known to be essential for peptide binding (James *et al.*, 1993). Over the years, a wide range of non-peptide mimetic inhibitors of Ras have been synthesised (Bishop *et al.*, 1995; Nigam *et al.*, 1993; Vogt *et al.*, 1994).

Although these compounds have shown considerable promise as anti-cancer agents based on their ability to inhibit transformation induced by oncogenic Ras proteins, a number of issues need to be addressed, including the ability of FPTase inhibitors to block the farnesylation of several proteins in addition to Ras, such as the lamins (James *et al.*, 1993). Thus, FPTases are not Ras-specific. There are at least 18 mammalian proteins known to undergo farnesylation during their post-translational maturation, with some of these proteins known to participate in the regulation of cell growth (H-, K- and N-Ras, RhoB, lamins A and B) (Oliff, 1999). In the presence of FPTase inhibitors, some protein substrates become alternatively prenylated by geranylgeranyl protein transferases, and it has been suggested that an alternatively prenylated form of RhoB exerts anti-proliferative effects on transformed cells (Prendergast, 2000). Some FPTase inhibitors reveal remarkable biological selectivity in that geranylgeranylation of cellular proteins was not inhibited by the inhibitor BZA-5B at concentrations that were fully inhibitory of farnesylation (James *et al.*, 1994). Thus, FPTase inhibitors appear to have multiple potential targets of action besides Ras to account for anti-proliferative activity in transformed cells. Although the mechanism of action of FPTase inhibitors is complicated, they have shown potent inhibitory effects on FPTase activity in cell-based assay and are useful tools in understanding Ras signal transduction pathways, and some of these compounds have entered clinical trials on patients with solid tumours (Adjei *et al.*, 2000).

1.23 Induction of apoptosis by DNA damaging drugs

Antitumour drugs from many chemical classes that are routinely used in the treatment of various cancers have been shown to function by inducing DNA damage, which accumulates and ultimately results in the induction of apoptosis. Many of these clinically effective antineoplastic agents, such as etoposide, the anthracyclines mitoxanthrone and daunorubicin, merbarone, m-AMSA and many others have been found to target the mammalian DNA topoisomerase II enzyme while carrying out their function (Khelifa and Beck, 1999; Rowe *et al.*, 1986).

Topoisomerases are nuclear enzymes that function in a variety of cellular processes requiring DNA separation and play important roles in regulating DNA topology (Azumu *et al.,* 1995). Topoisomerases are divided into two classes in mammalian cells i.e., types I and II. Topo I is involved in the relaxation of DNA, and in the knotting and unknotting of single stranded circular DNA. The enzyme introduces a transient single-strand break through which another DNA strand can pass. Type I topoisomerases change the linking number of covalently closed circular DNA (Liu and Miller, 1981). Mammalian cells express two topoisomerase II genes, α and β. Topoisomerase II catalyses the relaxation of supercoiled DNA and separate intertwined DNA duplexes (decatenation), such as those formed during DNA replication. Topo II binds its double stranded DNA substrate, and relaxation and separation is achieved by the formation of two protein-linked breaks in the DNA where the 5' phosphoryl group on deoxyribose is covalently joined to a tyrosine residue in the topoisomerase. Topo II acts as a homo-dimer with each subunit joining to one of the DNA strands (Kaufmann, 1998). This Topo II-DNA complex is called the cleavable complex. ATP binding induces a conformational change in the enzyme, which converts Topo II into a "protein clamp" on the DNA. One double stranded DNA segment is transported through the broken DNA strand and the enzyme then re-ligates the break in the cleaved helix. Upon ATP hydrolysis, the protein clamp opens, releasing the DNA, and the enzyme is recycled (Fortune and Osheroff, 1998). The catalytic cycling of topoisomerase II is summarised in Fig 1.8. Topo II is phosphorylated almost exclusively on serine residues *in vivo* (Ritke *et al.,* 1994a) and binding to DNA is sequence specific (Kaufmann, 1998).

Topoisomerase II (*Mr* 170,000 isoform) is a target for several clinically effective anticancer drugs (Ritke *et al.,* 1995). Among the Topo-II-targeted agents currently in clinical

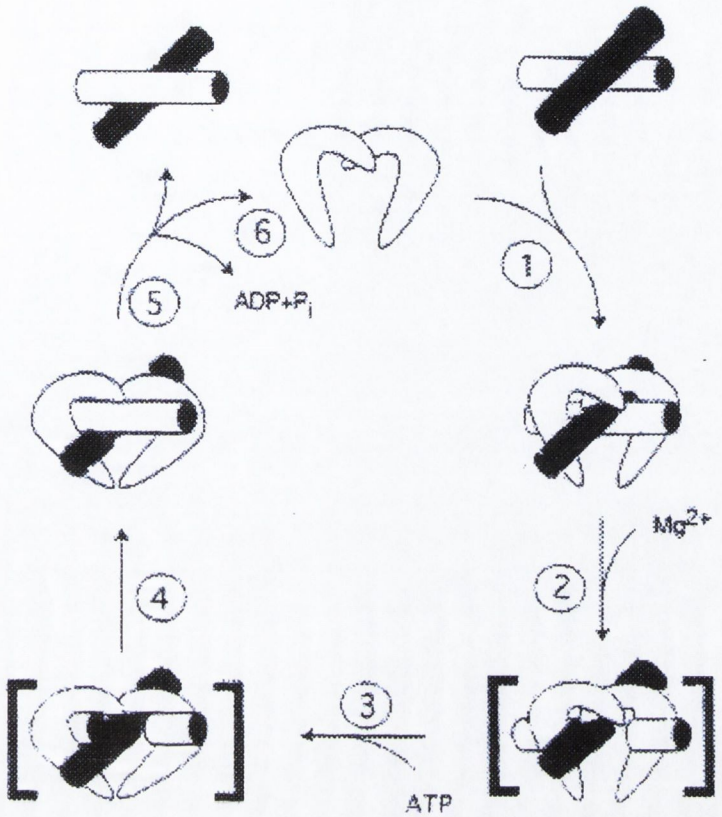

Fig. 1.8 The catalytic cycle of topoisomerase II

The individual steps of the catalytic cycle of topoisomerase II are shown. These are (1) DNA binding; (2) pre-strand passage cleavage/religation; (3) DNA strand passage; (4) post-strand passage cleavage/religation; (5) ATP hydrolysis; and (6) enzyme recycling. Brackets are used to indicate that the cleavage complex is a short-lived intermediate. Diagram taken from Burden and Osheroff, 1998.

use are the non-DNA intercalators etoposide and teniposide, and the DNA intercalators, doxorubicin, mitoxanthrone and amsacrine. These drugs kill cells in an unusual way. They prevent the release of covalently bound topoisomerase, which results in stabilisation of the cleaved complex. This in turn prevents re-ligation of DNA and results in the accumulation of DNA strand breaks, which, in turn, leads to apoptosis. Thus, by increasing levels of Topo-II-mediated DNA cleavage, this essential enzyme is converted into a potent cellular toxin. These compounds are referred to as topoisomerase poisons (Fortune and Osheroff, 1998; Kaufmann, 1998).

A second class of compounds affect the activity of Topo II, but not Topo I, and are called catalytic inhibitors. In contrast to poisons, these agents act by inhibiting the catalytic activity of the enzyme. They do not intercalate into the DNA or stabilise the Topo II-DNA covalent complexes (Fattman *et al.*, 1996; Tanabe *et al.*, 1991). These include drugs such as merbarone, the bis-2,6-dioxopiperazine derivatives ICRF-193, ICRF-154, ICRF-159, aclarubicin, fostriecin, staurosporine and mitindomide, which reflect a variety of inhibitory mechanisms. Merbarone acts by blocking the DNA cleavage reaction of Topo II (Fortune and Osheroff, 1998). Aclarubicin is thought to block binding of the enzyme to its DNA substrate, the initial step of the Topo II catalytic cycle (Fortune and Osheroff, 1998). As described earlier, binding of ATP to Topo II closes the two jaws of the clamp, and hydrolysis of the bound ATP precedes the re-opening of the clamp (Roca *et al.,* 1994). The bis-2,6-dioxopiperazine derivative, ICRF-193, blocks the catalytic activity of the enzyme by inducing a conformational change in Topo II and trapping it in the inactive, closed-clamp form, thus preventing it from re-opening, by blocking ATP hydrolysis and ultimately re-cycling of the enzyme (Roca *et al.,* 1994). These compounds presumably kill cells by preventing separation of intertwined daughter duplexes (Kaufmann, 1998). Bisdioxopiperazine derivatives such as ICRF-193 and ICRF-187 have also been shown to inhibit strand breakage induced by other cleavable complex forming agents such as etoposide and amsacrine (Fattman *et al.*, 1996; Tanabe *et al.,* 1991) by reducing the amount of available target for poisons such as etoposide.

Although this nuclear enzyme is the target of several clinically effective anti-cancer drugs, exposure of cells to Topo II-inhibitory drugs ultimately results in acquired resistance. Multiple targets for mutations may be present in cells exposed to these agents and of most

interest have been the nucleotide binding domains and the active site tyrosine (Ritke *et al.*, 1994a)

1.24 Peripheral-type benzodiazepine receptor

Benzodiazepines are amongst the most highly prescribed drugs due to their sedative, anxiolytic and relaxant effects. These drugs are known to exert their pharmacological effects through binding to the benzodiazepine receptor that is associated with the neuronal GABA-gated chloride channel (see Zisterer and Williams, 1997). This is known as the central-type benzodiazepine receptor and is present exclusively in the central nervous system. This GABA/benzodiazepine receptor complex is a hetero-oligomer composed of five subunits, α-, β-, γ- , δ- and ρ-polypeptides. Benzodiazepines bind to the α-subunit and facilitate the inhibitory effect obtained by GABA.

A second distinct class of receptor through which benzodiazepines bind is the peripheral-type benzodiazepine receptor (PBR), so called because it was initially discovered in peripheral tissue (Braestrup and Squires, 1977), but was later found to be present in the CNS. PBRs are composed of at least three subunits: the binding sites for isoquinolines, with a molecular mass of 18 kDa; the voltage-dependent anion channel (VDAC) with a molecular mass of 32 kDa; and the adenine nucleotide carrier, with a molecular mass of 30 kDa. This complex is located on the outer and inner mitochondrial membrane contact sites (Gavish *et al.*, 1999). In studies on the PBR using MA-10 Leydig cells' mitochondrial membrane, Papadopoulous *et al.* (1994, 1997) showed that the 18 kDa protein is organised in clusters of four to six molecules associated with one VDAC molecule in such a way as to favour the formation of what they called "single pores".

A number of compounds have been developed for studying the PBR, and PK11195, an isoquinoline carboxamide compound, which has great selectivity for the PBR in all species, is the most widely used ligand. Although the 18 kDa protein responsible for the drug-binding activity has been identified and cloned, little is known about the exact molecular structure and the true physiological role of the receptor. The fact that benzodiazepine receptors are so well conserved throughout evolution may imply that the functions of this gene must be fundamental to the cell (Gavish *et al.*, 1999). However, a quest for an endogenous ligand for this receptor is still underway. One of the best candidates is a

peptide known as diazepam binding inhibitor (DBI), which competes for [^{3}H] diazepam binding and is located close to the PBR at the outer mitochondrial membrane. Porphyrins, which also interact with the PBR, are selectively associated with the inner mitochondrial membrane and are involved in steroidogenesis, which is one of the suggested functions of the PBR.

A wide variety of physiological functions have been attributed to the PBR over the years. These include effects on cell growth and differentiation, effects on mitochondrial respiration, steroidogenesis (Zisterer and Williams, 1997) and, more recently, an involvement in apoptosis (Hirsch *et al.*, 1998).

Many reports suggest that PBR ligands affect cell growth and differentiation in a number of cell systems. However, it has been argued that these anti-proliferative effects are unrelated to a specific interaction of these drugs with the PBR, because these ligands exhibit nanomolar affinities for PBRs whereas micromolar concentrations are required to elicit the anti-proliferative properties (Zisterer and Williams, 1997).

The biosynthesis of steroids in all steroidogenic tissues begins with the enzymatic conversion of the precursor cholesterol to form pregnenolone. The rate-limiting step in this process is the transport of cholesterol from cellular stores across the aqueous intermembrane space of the mitochondria to the inner mitochondrial membrane. It has been suggested that PBRs play a major role in this mitochondrial cholesterol transport and the presence of a cholesterol recognition/interaction amino acid consensus sequence (CRAC) at the C-terminus of PBR has been proposed (Li and Papadopoulous, 1998; Li *et al.*, 2001a). Two more important observations suggest that PBRs may be involved in steroidogenesis. First, PBRs are found primarily on the outer mitochondrial membrane, and secondly, PBRs are extremely abundant in the steroidogenic endocrine tissue (Gavish *et al.*, 1999). However, considering the ubiquitous expression of the PBR, it has also been suggested that the PBR plays a more general role in intracellular cholesterol transport and compartmentalisation (Li and Papadopoulous, 1998).

The PBR has also been reported to be involved in immune response, behavioural conditions, cellular respiration and calcium channels (Gavish *et al.*, 1999). However, there appears to be much ambiguity about these proposed roles of the PBR. Much still remains to be learned about the structure of the PBR as well as its cellular location, regulation of gene

expression and interaction between PBR subunits. Recently a series of novel compounds were synthesised as high affinity PBR ligands based on the pyrrolobenzoxazepine skeleton (Campiani *et al.,* 1996). These compounds, which are known as pyrrolobenzoxazepine (PBOX) compounds, are selective for the PBR and do not interact with the central-type benzodiazepine receptor (CBR) (Campiani *et al.*, 1996). In addition, these novel ligands have been shown to bind to the PBR in steroidogenic tissue with nanomolar affinities (Campiani *et al.*, 1996), and have been shown to elicit similar biological effects, such as regulation of steroidogenesis, to the classically used PBR ligands, PK11195 and Ro5-4864 (Zisterer *et al.*, 1998). It was thought that these PBOX compounds would prove useful as probes for determining the structure and function of the PBR. The general structure of pyrrolo-1,5-benzoxazepines is outlined in Fig. 1.9.

Three compounds from this series, PBOX-1, PBOX-2 and PBOX-21, exhibited anti-proliferative effects in rat C6 glioma and human 1321N1 astrocytoma cells, at micromolar concentrations. These compounds were found to induce a specific accumulation of C6 glioma and 1321N1 cells in the G1 phase of the cell cycle. In both cell types, there was a significant decrease in the proportion of cells in the S and G2 + M phases of the cell cycle, with a concomitant increase in cells in the G0-G1 phase. These compounds were not cytotoxic to the cells, and the anti-proliferative effects did not appear to be mediated through binding to the PBR, as 1000-fold higher concentrations of the drugs were required to produce the anti-proliferative effects than were required to saturate the PBR (Zisterer *et al.,* 1998).

It has recently been found that some, but not all, of these PBOX compounds induce apoptosis in a number of cancerous cells such as the human promyelocytic leukaemia HL-60 cell line, the human lymphoma Hut-78 cell line, and the human lympoblast Jurkat cell line (Zisterer *et al.,* 2000). Although the mechanism in which these compounds induce apoptosis in these cancerous cells remains unclear, it was reported that apoptosis induced in HL-60 cells was accompanied by the release of mitochondrial cytochrome c and activation of caspase-3-like proteases (Zisterer *et al.*, 2000). In recent years, other workers have also reported the possible role of PBR ligands as apoptotic inducers. For example, it has been shown that PK11195, while having no cytotoxic effect itself, enhances apoptosis induced by the chemotherapeutic agents etoposide and doxorubicin. This synergism between PK11195 and several pro-apoptotic agents extended to all hallmarks of apoptosis, including loss of

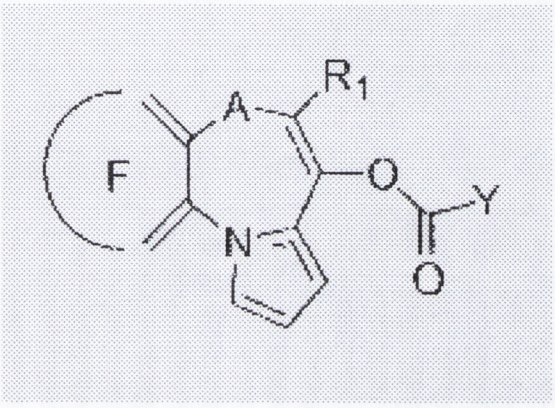

Fig 1.9 General formula of pyrrolo-1,5-benzoxazepine compounds

A schematic representation of the general structure of pyrrolo-1,5-benzoxazepines wherein R_1 represents an unsubstituted C6 or C10 aryl group; or a C6 aryl group substituted with Me or OMe. A represents O, S or S partially oxidized to sulfoxide. The cyclic group labelled F represents an unsubstituted C6 or C10 aryl-fused group or a C5 heteroaryl-fused group (nitrogen as heteroatom) or a benzo-fused system substituted with ethoxycarbonyl function. R_2 and R_3 are independently hydrogen or methyl.

mitochondrial transmembrane potential ($\Delta\psi_m$), an increase in the generation of ROIs, exposure of phosphatidylserine on plasma membrane surface and nuclear DNA fragmentation (Hirsch *et al.*, 1998). More recently, work by Chelli *et al.* (2001) supports this role for PBR ligands as apoptotic inducers. They have shown that exposure of rat mitochondria to various PBR ligands, including PK11195, produces a dose-dependent and cyclosporin-A-sensitive permeability transition, and supernatants from these mitochondria induced apoptotic changes in isolated cardiac nuclei.

It is evident that apoptosis-inducing drugs have diverse chemical structures and different mechanism of action, such as the topoisomerase II inhibitor, etoposide, and the DNA intercalator, daunorubicin. All these drugs have been shown to induce apoptosis in cancerous cells derived from the hematopoietic system, such as HL-60 cells. Due to their potent apoptotic effect on numerous cancerous cell lines, it has been proposed that these PBOX compounds, which are ligands to the peripheral type receptor, may be potential novel anti-cancer drugs.

1.25 Aims of this study

Conventional therapies for the treatment of CML are often non-specific with severe side effects, whereas novel therapies focus on targeting components of the molecular pathway that are critical for transformation. While some of these novel approaches, such as inhibition of the Abl tyrosine kinase and antisense treatment to down-regulate Bcr-Abl, have shown promising results, acquired resistance and non-specific toxic side effects have been reported (Gorre *et al.*, 2001). This highlights the need for the development of new therapies for the treatment of CML and related diseases.

Recently, a novel series of pyrrolo-1,5-benzoxazepine (PBOX) compounds were synthesised and it was found that some of these compounds induce apoptosis in cells derived from the hematopoietic system. In this study, the potential of these novel compounds as anti-cancer agents in the treatment of CML is investigated. Thus, the aims of the project are as follows;

(1) To investigate the apoptotic effects of this series of pyrrolo-1,5-benzoxazepine compounds in three CML cell lines, K562, KYO.1 and LAMA 84, which represent different stages in the progression of CML.

(2) To investigate the involvement of the PBR, to which PBOX compounds bind with high affinity, in the mechanism by which these compounds induce apoptosis in CML cells.

(3) To determine the effect of a representative compound, PBOX-6, on the expression and activity of Bcr-Abl in CML cells, as Bcr-Abl is thought to mediate the anti-apoptotic properties of these cells.

(4) To dissect the biochemical components of the apoptotic cascade initiated by PBOX-6 in K562 cells. This involves assessing the involvement of mitochondrial events, caspases and signal transduction cascades during PBOX-6-induced apoptosis.

Chapter 2

Materials and Methods

2.1 Materials

The full names and addresses of the sources listed below are given at the end of the list.

Ac-DEVD-AMC	Alexis
Ac-VEID-AMC	Alexis
5'-AGT TGA GGG GAC TTT CCC AGG C-3' consensus sequence for NFκB (underlined)	Promega
Agarose	Promega
AMC	Sigma
Anisomycin	Sigma
Anti-ATF-2 phospho antibody	New England Biolabs
Anti-Bax antibody	Pharmingen
Anti-Bcl-2 antibody	Santa Cruz
Anti-Bcl_{xl} antibody	Pharmingen
Anti-c-abl antibody	Calbiochem
Anti-c-jun antibody	New England Biolabs
Anti-cytochrome c antibody	Pharmingen
Anti-JNK antibody	New England Biolabs
Anti-JNK phospho antibody	New England Biolabs
Anti-p38 phospho antibody	New England Biolabs
Anti-p42-44 phospho antibody	New England Biolabs
Anti-phosphotyrosine antibody	Calbiochem
Aprotinin	Sigma
Ammonium persulphate	Sigma
Ara-C	Sigma
β-Actin	Sigma
BSA	Sigma
Centricon concentrators	Amicon
CHAPS	Sigma
Cryotubes	Biosciences
Cytocentrifuge filters	Shandon

Cytochrome c	Sigma
Damnacanthal	Calbiochem-Novabiochem
DMSO	Sigma
DTT	Sigma
ECL detection system	Amersham International
Ecoscint	National Diagnostics
EDTA	Sigma
Ethidium bromide tablets	Sigma
Etoposide	Sigma
FCS	Greiner
[^{3}H] Farnesyl pyrophosphate	Sigma
Filter paper	Whatman
Folin's reagent	Sigma
FTI (II)	Calbiochem
FTI-276	Calbiochem
FuGENE 6	Roche
Geldanamycin	Calbiochem-Novabiochem
Genistein	Sigma
Gentamicin	Sigma
Glass fibre filters (GF/B)	Whatman
Glutamine	Gibco
Glycerol	Sigma
Glycine	Merck
D-Glucose	Sigma
Goat anti-mouse IgG peroxidase conjugate	Sigma
Goat anti-rabbit IgG peroxidase conjugate	Sigma
Herbimycin A	Sigma
HEPES	Sigma
HL-60 cells	E.C.A.C.C.
[^{3}H] Thymidine	Sigma
Jurkat T cells	E.C.A.C.C.
Kodak X-Omat™ LS film	Sigma

Leupeptin	Sigma
Manumycin A	Sigma
β-Mercaptoethanol	Sigma
Mitoxanthrone	Sigma
Nitrocellulose	Sigma
Pepstatin A	Sigma
Piceatannol	Calbiochem
Pipettes, sterile	Sterilin
[^{3}H] PK11195	New England Nuclear
PMSF	Sigma
[γ-^{32}P]ATP	Promega
Poly-L-Lysine coated slides	Sigma
Protein molecular weight standards	New England Biolabs
Proteinase K	Sigma
Protogel™	National Diagnostics
PVDF	Sigma
RapiDiff Kit	Diagnostic Developments
Ras, human recombinant	Calbiochem
RNAase A	Sigma
RPMI medium	Sigma
SDS	BDH
Sodium lauryl sarcosinate	NBS Biologicals
Sodium orthovanadate	Sigma
Staurosporine	Sigma
Sucrose	Sucrose
TEMED	Sigma
Tetrapropylammonium hydroxide	Sigma
Thymidine	Sigma
Tissue culture flasks and plates	Griener
Tris	Sigma
Triton X-100	Sigma

Trypsin	Sigma
Tween 20	Sigma
Tyrphostin	Calbiochem
z-DEVD-fmk	Calbiochem
z-VAD-fmk	Calbiochem

CML cells, K562, KYO.1 and LAMA 84 were kindly supplied by Dr. Mark Lawler, Central Pathology Lab, St. James's Hospital and Trinity College, Dublin 2. Anti-Parp antibody was a gift from Mark Dempsey, Pharmacology Dept., University College Dublin. Anti-caspase-3 antibody, ICRF 187 and CEP1347 were gifts from Professor Luke O'Neill, Biochemistry Dept., Trinity College Dublin. Anti-caspase-7 antibody was a gift from Professor Seamus Martin, Dept. of Genetics, Trinity College Dublin. Pyrrolo-1,5-benzoxazepine compounds were gifts from Professor Giuseppe Campiani, Department of Pharmaceutical Chemistry, University of Siena, Italy. All other reagents were of analytical grade, where possible, and were obtained from BDH and Sigma.

Addresses of Suppliers:

Alexis Corporation, (U.K.) Ltd, 3, Moorbridge Court, Moorbridge Road East, Bingham, Nottingham NG138QG, U.K.

Amersham International Plc., Amersham Place, Little Chalfont, Buckinghamshire, HP7 9NA, U.K.

Amicon Ltd., Upper Mill, Stonehouse, Gloucestershire GL10 2BJ, England, U.K.

Biosciences, 3 Charlemont Tce., Crofton Road, Dun Laoghaire, Co. Dublin, Ireland.

Boehringer Mannheim, Bell Lane, Lewes, East Sussex, BN7 1LG, U.K.

British Drugs House (BDH), Chemicals Ltd., c/o Lennox Chemicals, J.F. Kennedy Drive, Dublin 12, Ireland.

Calbiochem-Novabiochem, Boulevard Industrial Est., Padge Road, Beeston, Nottingham NG9 2JR, U.K.

Diagnostic Developments, Burscough, Lancashire, L408JY, U.K.

European Collection of Animal Cell Cultures (E.C.A.C.C.), PHLS Centre for Applied Microbiology and Research, Porton Down, Salisbury SP4 0JG, U.K.

Greiner, GmbH, Maybachstrasse 2, P.O.Box 1162, D-7443 Frickenhausen, Germany.

Merck, Merck KgaA, 64271 Darmstradt, Germany.

National Diagnostics, 305 Patton Drive, Atlanta, Georgia 30336, U.S.A.

New England Biolabs, (UK) Ltd, Knowl Piece, Wilburg Way, Hitchin, Herts SG40TY, U.K.

New England Nuclear, c/o Med Labs, Stillorgan Industrial Estate, Co. Dublin, Ireland.

NBS Biologicals, 14 Tower Square, Huntingdon, Cambs PE18 7DT, U.K.

Pharmacia Biosystems Ltd, Pharmacia LKB Biotechnology AB, Davy Avenue, Knowhill, Milton Keynes MK5 8PH, U.K.

Pharmingen, 10975, Torreyana Road, San Diego, CA 92121 U.S.A.

Promega Corporation, 2800 Woods Hollow Road, Madison, WI 53711-5399, U.S.A.

Roche Diagnostics GmbH, Roche Molecular Biochemicals, Mannheim, Germany.

Sigma Chemical Co. Ltd., Fancy Road, Poole, Dorset, U.K.

Sterilin, Bibby Sterilin Ltd., Stone, Staffs., U.K.

Whatman Ltd., Maidstone, Kent, U.K.

2.2 Cell Culture

2.2.1 Growth and maintenance of the Human Leukaemic HL60 cell line, Jurkat T cells and the Chronic Myeloid Leukaemia cell lines K562, KYO.1 and LAMA 84

Cells were grown in suspension at 37°C under a humidified atmosphere of 95% O_2, 5% CO_2, in 75 cm^2 flasks containing RPMI 1640 medium supplemented with 20% (v/v) foetal calf serum (FCS) for the HL60 cells and 10% (v/v) foetal calf serum (FCS) for the Jurkat and CML cells, 2mM L-glutamine and 100µg/ml gentamicin (complete medium).

Cells were passaged twice weekly. The cells were centrifuged at 500xg for 5 min, the medium was removed and the pellet was resuspended in 1ml of complete medium. Cell numbers were counted using a haemocytometer. An aliquot of cells (1 x 10^6 cells) was seeded in 75 cm^2 flasks in 20ml of complete medium. After approximately 50 passages, cells were discarded and a new batch grown from liquid nitrogen stocks.

2.2.2 Cryo-preservation of cells

HL60, Jurkat and CML cells, grown to a state of subconfluency were harvested and counted as previously described (Section 2.2.1). The cells were centrifuged and the pellet was resuspended in 5ml of complete medium plus 10% (v/v) dimethylsulphoxide (DMSO) and 25% (v/v) FCS for Jurkat and CML cells, and in 5 ml of complete medium plus 10% (v/v) glycerol for HL60 cells. An aliquot (1ml) was transferred into 1.5ml cryotubes and placed at -20°C for 1h. The cryotubes were then transferred to -70°C for 1h, before storing them in a liquid nitrogen vessel.

When required, an aliquot of cells was removed from the liquid nitrogen vessel, rapidly thawed and resuspended in 10ml of complete medium. This cell suspension was centrifuged at 500xg for 5 min, the medium containing DMSO or glycerol was discarded and the pellet was resuspended in complete medium. Cells were then seeded in tissue culture flasks as previously described (Section 2.2.1).

2.3 Determination of protein concentration

2.3.1 Bradford protein assay

Protein concentration of cell lysates was determined using a modification of the method of Bradford (1976).

Reagent A (200µl) (0.01% (w/v) Coomassie Brilliant Blue G-250, 4.7% (v/v) ethanol and 8.5% (w/v) orthophosphoric acid) was added to 18µl of H_2O and 2µl of the protein sample in a 96-well microtitre plate and left at room temperature for 5 min. The absorbance at a wavelength of 595 nm was measured using a Dynatech MR5000 plate reader and the results were compared to the standard curve prepared using known concentrations of bovine serum albumin (BSA). All protein determinations were performed in triplicate.

2.3.2 Markwell protein assay

Protein concentration of cell lysates was determined using the method described by Markwell *et al.*, (1978).

Stock solution A (2% (w/v) sodium carbonate; 0.4% (w/v) sodium hydroxide; 0.16% (w/v) potassium sodium tartrate and 1% (w/v) sodium dodecyl sulphate (SDS) and stock solution B (4% copper sulphate) were mixed (100:1 (v/v)) prior to use, to obtain solution C. Solution C (1.5ml) was added to each of the protein samples and samples were incubated at room temperature for 15 min. An aliquot (0.15ml) of Folin-Ciocalteau's reagent, diluted 1:1 (v/v) with distilled water, was added to each sample, mixed and incubated at room temperature for 1h.

The absorbance at a wavelength of 650 nm was measured using a Dynatech MR5000 plate reader. Results were compared to the standard curve prepared using known concentrations of BSA. All protein determinations were performed in triplicate from samples that were diluted 1:100 with distilled water.

2.4 Cytospin preparation and RapiDiff staining of cells

Cells, grown as described in Section 2.2.1, were seeded at a density of $3x10^5$ cells/ml, treated with the indicated compounds, and incubated at 37°C, 95% O_2 and 5% CO_2 for the outlined time. Following incubation with the various compounds, an aliquot of cells (150µl), was cytocentrifuged onto poly-L-lysine coated slides at 500xg for 2 min using a Cytospin 3 (Shandon). The slides were removed and left to air-dry at room temperature for approximately 2 min. Staining was carried out using the RapiDiff kit, containing solution A, 100% methanol, solution B, eosin-Y and solution C, methylene blue. The cells were fixed by dipping them 10 times in solution A. The nucleus of the cells was stained pink by dipping the slide 10 times in solution B and the cytoplasm was stained blue by dipping the slide 8 times in solution C. Excess dye was washed off with H_2O. After allowing the slides to air dry, the percentage of apoptosis and necrosis was determined by counting approximately 300 cells under a light microscope (Nikon) using 40x magnification. At least three fields of view per slide, with an average of approximately 100 cells per field, were counted. Apoptotic cells were shrunken with an intact outer membrane, condensed or fragmented chromatin and often contained membrane blebs and/or the presence of apoptotic bodies. Necrotic cells were swollen and often the outer membrane had ruptured resulting in the release of cellular contents. Normal healthy cells had an even intact outer membrane with a large regular shaped nucleus.

The percentage apoptosis/necrosis was determined as follows:

% apoptosis = (no. of apoptotic cells/total no. of cells) x 100;

% necrosis = (no. of necrotic cells/total no. of cells) x 100.

2.5 Detection of DNA Fragmentation by agarose gel electrophoresis

Cells were grown as described in Section 2.2.1 and seeded at a density of $1x10^7$ cells in 20ml of growth medium. Cells were treated with the indicated compound and incubated at 37°C in 95% O_2, 5% CO_2 for 48h. Following incubation, cells were centrifuged at 500xg for 5 min and the supernatant removed. The pellet was resuspended in lysis buffer (1ml) (20mM EDTA, 100mM Tris pH 8.0, 0.8% (w/v) sodium lauryl sarcosinate) and incubated at 37°C for 1h. RNAse A (0.5mg/ml) was added to each tube and left at 37°C for a further 2h. Proteinase K (6mg/ml) was then added to each sample and tubes were incubated overnight at 37°C. An aliquot of each sample (45µl) was mixed with loading dye (5µl) (0.25% Bromophenol blue,

30% glycerol in Tris borate EDTA (TBE) and samples were resolved on a 1.5% agarose gel in TBE, prestained with ethidium bromide (10µl of a 10mg/ml stock into 100ml of agarose). DNA was electrophoresed at a constant voltage of 55V for 4h and a DNA laddering pattern was visible under UV light using a UVP gel documentation system.

2.6 Measurement of levels of Bcr-Abl expression by Western blotting

2.6.1 Preparation of cell extracts for measurement of Bcr-Abl expression

Cells were grown as described in Section 2.2.1 and seeded at $7x10^6$ cells/flask. Following treatment with either vehicle or the indicated drug for the outlined time, cells were harvested by centrifugation at 500xg for 5 min followed by washing in ice-cold phosphate buffered saline (PBS). Pellets were resuspended in Harvesting Buffer (200µl) (20mM Hepes pH 7.5, 10% (w/v) sucrose, 0.1% (w/v) CHAPS, 2mM dithiotreitol, 0.1% (v/v) Nonidet NP40, 1mM sodium EDTA and 1mM phenylmethylsulfonyl fluoride) supplemented with protease inhibitors (1µg/ml pepstatin A and 1µg/ml leupeptin). Samples were incubated on ice for 10 min followed by passage 12 times through a 21gauge needle. Following a further 10 min incubation on ice, the homogenates were centrifuged at 20,000xg for 20 min at 4°C, and the supernatants were removed. A Bradford assay was performed to determine protein concentration of the resulting supernatants (Section 2.3.1).

2.6.2 Sodium dodecyl sulphate-polyacrylamide gel electrophoresis (SDS-PAGE)

Levels of Bcr-Abl expression were determined by SDS-PAGE followed by Western blotting.

Sodium dodecyl sulphate-polyacrylamide gel electrophoresis (SDS-PAGE) was carried out as described by Laemmli (1970), using an ATTO electrophoresis unit (model AE 6450) with 8% resolving and 5% stacking gels. The 8% resolving gel consisted of: H_20 (6.9ml), Protogel™, (Ultra-pure 30% (w/v) acrylamide and 0.8% (w/v) bisacrylamide) (4.0ml), 1.5 M Tris-HCl pH 8.8 (3.8ml), 10% (w/v) SDS (150µl), 10% (w/v) ammonium persulphate (APS) (150µl) and *N,N,N',N'*-tetramethylethylenediamine (TEMED) (9µl). The 5% stacking gel consisted of: H_2O (3.4ml), Protogel™ (830µl), 1 M Tris-HCl pH 6.8 (630µl), 10% SDS (w/v) (50µl), 10% (w/v) APS (50µl) and TEMED (6µl).

Equal amounts of protein (40μg), prepared as described in Section 2.6.1, were electrophoresed at 80V until the tracker dye reached the resolving gel. The voltage was then increased to 100V for 150-180 min, until the tracker dye reached the bottom of the resolving gel. Proteins were then transferred onto polyvinylidene difluoride (PVDF) membrane as described in Section 2.6.3.

2.6.3 Western blotting

Proteins resolved by SDS-PAGE were transferred onto 0.2μm PVDF membrane using a wet transfer apparatus (BioRad mini trans blot), at 30V, 90mA overnight at 4°C. Prior to transfer, the PVDF membrane, cut to size, was soaked for 15 sec in 100% methanol, followed by 2 min wash in distilled water and allowed to equilibrate in transfer buffer (25mM Tris-HCl, 192mM glycine and 10% (v/v) methanol) for 10-15 min. The gel, also equilibrated for 10-15 min, was placed on a layer of filter paper and sponge and overlaid with PVDF. A second piece of filter paper was placed on top followed by the second sponge. The entire assembly was placed in a cassette and the electric current applied.

Following the transfer of proteins, the PVDF membrane was blocked by incubation with gentle agitation in blocking buffer containing 5% (w/v) dry milk in TBST (0.1% (v/v) Tween 20 in Tris buffered saline (TBS)) for 2h at room temperature. The membrane was washed briefly in TBST (2 x 2 min), followed by incubation in anti-c-abl primary antibody (1:1000 dilution in TBST containing 1% dry milk) for 1h at room temperature. The membrane was washed again in TBST (2 x 5min, 1 x 10 min) followed by incubation in secondary antibody, goat anti-mouse horseradish peroxidase (HRP)-conjugated (1:1000 in TBST containing 1% dry milk) for 1h at room temperature. The blot was then washed in TBST (2 x 5 min, 1 x 10 min, 2 x 5 min) before a final 5 min wash in TBS.

Membranes were developed using electrochemiluminescence (ECL) detection system, which detected the secondary antibody by means of a HRP-catalysed oxidation of luminol under alkaline conditions. Results were recorded on Kodak X-Omat LS film and developed using an X-ray processor (Fuji).

2.6.4 Stripping and re-probing of blots

Membranes were incubated with stripping buffer (62.5 mM Tris-HCl, pH 7.8, 100mM β-Mercaptoethanol, 2% (w/v) SDS) for 30 min at 50°C followed by several washes in TBS at room temperature. The membrane was blocked by incubation with gentle agitation in blocking buffer (5% dry milk in TBST (0.1% (v/v) Tween 20 in TBS) for 2h at room temperature or overnight at 4°C. The blot was washed briefly (2 x 2 min), followed by incubation in anti-β-actin antibody diluted 1:5000 in TBST containing 1% (w/v) dry milk. Following washing for 20 min in PBST, the membrane was incubated with goat anti-mouse horseradish peroxidase (HRP)-conjugated secondary antibody (1:1000 in TBST containing 1% (w/v) dry milk) for 1h at room temperature. The blot was then washed in TBST (2 x 5 min, 1 x 10 min, 2 x 5 min) before a final 5 min wash in TBS. Membranes were developed using ECL detection as described in Section 2.6.3.

2.7 Measurement of protein tyrosine phosphorylation by Western blot

Cells were seeded at a density of $5x10^6$ cells/flask and treated with either vehicle or the indicated drug for the required time at 37°C in 95% O_2 and 5% CO_2. Following a treatment period, cells were harvested by centrifugation at 500xg for 5 min and pellets were washed with ice-cold phosphate buffered saline containing sodium orthovanadate (Na_3VO_4) (1mM). The pellets were resuspended in ice-cold lysis buffer (150mM NaCl, 50mM Tris/Cl pH 8.0, 0.1% (w/v) SDS, 1% (w/v) Triton X-100, 1mM sodium orthovanadate, 1μg/ml leupeptin, 1mM phenylmethylsulfonyl fluoride and 10μg/ml aprotinin). Samples were incubated on ice for 20 min followed by centrifugation at 20,000xg for 10 min at 4°C. The resultant supernatants were removed and used to measure tyrosine phosphorylation status. Protein concentration was determined using a Bradford assay, as described in Section 2.3.1. Equal amounts of protein was resolved by SDS-PAGE and transferred onto PVDF membrane as described in Section 2.6.2 and 2.6.3, with a few modifications. The 10% resolving gel consisted of: H_20 (5.9ml), Protogel™, (Ultra-pure 30% (w/v) acrylamide and 0.8% (w/v) bisacrylamide) (5ml), 1.5M Tris-HCl pH 8.8 (3.8ml), 10% (w/v) SDS (150μl), 10% (w/v) APS (150μl) and TEMED (8μl). The 5% stacking gel consisted of: H_2O (3.4ml), Protogel™ (830μl), 1M Tris-HCl pH 6.8 (630μl), 10% SDS (w/v) (50μl), 10% (w/v) APS (50μl) and TEMED (6μl). Proteins were transferred onto PVDF membrane using a wet transfer

apparatus (BioRad mini trans blot), at 60V, 160 mA for 90 min at room temperature. Following transfer, membranes were blocked overnight with Tris buffered saline (TBS) containing 5% (w/v) fatty acid free BSA. Membranes were washed briefly in TBS containing 0.1% v/v Tween 20 (TBST) and probed for 1h at room temp with anti-phosphotyrosine primary antibody diluted 1:100 in TBST containing 1% (w/v) BSA. Membranes were washed in TBST for 20 min (2 x 5 min, 1 x 10 min) and incubated for 1h with goat anti-mouse horseradish peroxidase coupled secondary antibody, diluted 1:1000 in TBST containing 1% (w/v) BSA. Membranes were washed for 30 min in TBST (2 x 5 min, 1 x 10 min, 2 x 5 min) followed by ECL development as described in Section 2.6.3.

2.8 Western blot to measure cytochrome c release

Cells were grown as described in Section 2.2.1 and seeded in 75 cm^2 flasks at a density of 20 x 10^6 cells/flask. Flasks were treated with the indicated compound and incubated at 37°C in 95% O_2, 5% CO_2 for 16h. Following the treatment period, cells were harvested by centrifugation at 500xg for 5 min, pellets were washed in PBS and resuspended in 100µl Buffer A (20mM Hepes pH 7.5, 10mM KCl, 1.5mM $MgCl_2$, 1mM EDTA, 1mM EGTA, 1mM dithiotrietol, and 0.1mM PMSF) supplemented with protease inhibitors inhibitors (5µg/ml pepstatin A, 2µg/ml leupeptin, 2µg/ml aprotinin). Cells were incubated on ice for 15 min followed by centrifugation at 20,000xg for 20 min at 4°C. The resultant supernatant was stored at -70°C until use. Protein concentration was determined using the Bradford assay as described in Section 2.3.1.

Equal amounts of protein (30µg) were resolved on a 15% SDS-polyacrylamide gel. The 15% resolving gel consisted of: H_20 (3.4ml), Protogel™, (Ultra-pure 30% (w/v) acrylamide and 0.8% (w/v) bisacrylamide) (7.5ml), 1.5M Tris-HCl pH 8.8 (3.8ml), 10% (w/v) SDS (150µl), 10% (w/v) APS (150µl) and TEMED (8µl). The 5% stacking gel consisted of: H_2O (3.4ml), Protogel™ (830µl), 1M Tris-HCl, pH 6.8 (630µl), 10% SDS (w/v) (50µl), 10% (w/v) APS (50µl) and TEMED (6µl).

Protein was electrophoresed at 80V until the tracker dye reached the bottom of the stacking gel and was then increased to 110V for 120-150 min, until the tracker dye reached the bottom of the resolving gel. Proteins were then transferred onto nitrocellulose using a semi-dry transfer apparatus (Hoefer Semi-Phor TE-70 apparatus) at 5V, 110mA for 2h.

Membranes were blocked overnight at 4°C with PBS containing 5% (w/v) dry milk and probed for 1h with anti-cytochrome c monoclonal antibody diluted 1:150 in PBS containing 0.05% (v/v) Tween 20 (PBST) and 1% (w/v) dry milk. Following washing for 20 min (2 x 5 min, 1 x 10 min) in PBST, membranes were incubated with goat-anti mouse IgG HRP conjugate diluted 1:1000 in PBST containing 1% (w/v) dry milk. Membranes were washed in PBST (2 x 5 min, 1 x 10 min, 2 x 5 min) followed by ECL development as described in Section 2.6.3.

2.9 Measurement of caspase-3 activity

2.9.1 Fluorogenic assay to measure caspase-3-like protease activity

Cells were grown as described in Section 2.2.1 and seeded at $5x10^6$ cells/flask. Following treatment with either vehicle or the indicated drug for the outlined time, cells were harvested as described in Section 2.6.1. A Bradford assay was performed on resulting supernatants as outlined in Section 2.3.1.

Enzyme activity was determined by a fluorometric assay using the substrate Ac-Asp-Glu-Val-Asp (DEVD)-AMC. The substrate is specifically cleaved by caspase 3-like proteases resulting in release of the fluorescent leaving group, amino-4-methyl coumarin (AMC). Cell extracts (100μg) were incubated with 100mM HEPES, pH 7.5, containing 10% (w/v) sucrose, 0.1% (w/v) CHAPS, 10mM dithiotreitol and 20μM substrate in a total reaction volume of 3ml. Following incubation for 60 min at 25°C, fluoresence was monitored continuously using a spectrofluorimeter (Perkin Elmer, Luminescence Spectrometer, LS50B) at an excitation wavelength of 380 nm and an emission wavelength of 460 nm. The amount of AMC released was determined by comparison with a standard curve generated with known amounts of AMC (see Section 2.9.2), and fluorescence units were converted to nmol AMC released per min per mg of protein.

2.9.2 Preparation of AMC standard curve

A stock of AMC (10mM) was prepared and dissolved in 2N HCl. From this stock the following 100x standards were prepared; 50μm, 35μM, 25μM, 10μM. These standards were diluted 1:100 with incubation buffer (100mM Hepes, pH 7.5, containing 10% (w/v) sucrose,

0.1% (w/v) CHAPS, 10mM dithiotreitol) in a final volume of 3ml and the fluoresence was measured using a spectrofluorimeter (see Fig. 2.1)

2.10 Fluorogenic assay to measure caspase-6-like protease activity

Cells were grown as described in Section 2.2.1 and seeded at $5x10^6$ cells/flask. Following treatment with vehicle or drug for 16h cell extracts were prepared as described in Section 2.6.1. Enzyme activity was measured using a fluorometric assay as described in Section 2.9.1, and the substrate Ac-Val-Glu-LIE-Asp (VEID)-AMC. Caspase-6-like proteases specifically cleave the Ac-VEID-AMC and release the fluorescent leaving group, AMC. Cell lysates (100μg) were incubated for 60 min at 25°C, with 100mM Hepes, pH 7.5, containing 10% (w/v) sucrose, 0.1% (w/v) CHAPS, 10mM dithiotreitol and 20μM substrate in a total reaction volume of 3ml. Following incubation fluoresence was monitored continuously using a spectrofluorimeter (Perkin Elmer, Luminescence Spectrometer, LS50B) at an excitation wavelength of 380 nm and an emission wavelength of 460 nm. The amount of AMC released was determined by comparison with an AMC standard curve as described in Section 2.9.2 and fluorescence units were converted to nmol AMC released per min per mg of protein.

2.11 Determination of caspase -7-like protease activity using Western blotting

Cells were grown as described in Section 2.2.1 and seeded at $1x10^6$ cells/ml in a 6 well plate in a total volume of 2ml. Cells were treated with either vehicle or the indicated drug and incubated at 37°C in 95% O_2 and 5% CO_2 for 16h. Following the incubation period, cells were harvested by centrifugation at 500xg for 5 min and the pellet was resuspended in SDS lysis buffer (200μl) (62.5 mM Tris-HCl, pH 6.8, 2% w/v SDS, 10% (w/v) glycerol, 50mM DTT, 0.1% (w/v) bromophenol blue). Extracts were transferred to a minifuge tube and sonicated for 15 sec to shear DNA and reduce sample viscosity. Samples were then heated to 95°C for 5-7 min and placed directly on ice for 5 min. An aliquot of protein (30μl) was resolved by SDS-PAGE, on 12% resolving and 5% stacking gels followed by Western blot analysis. The 12% resolving gel consisted of: H_20 (4.9ml), Protogel™, (Ultra-pure 30% (w/v) acrylamide and 0.8% (w/v) bisacrylamide) (6.0ml), 1.5M Tris-HCl, pH 8.8 (3.8ml), 10% (w/v) SDS (150μl), 10% (w/v) APS (150μl) and TEMED (6μl). The 5% stacking gel

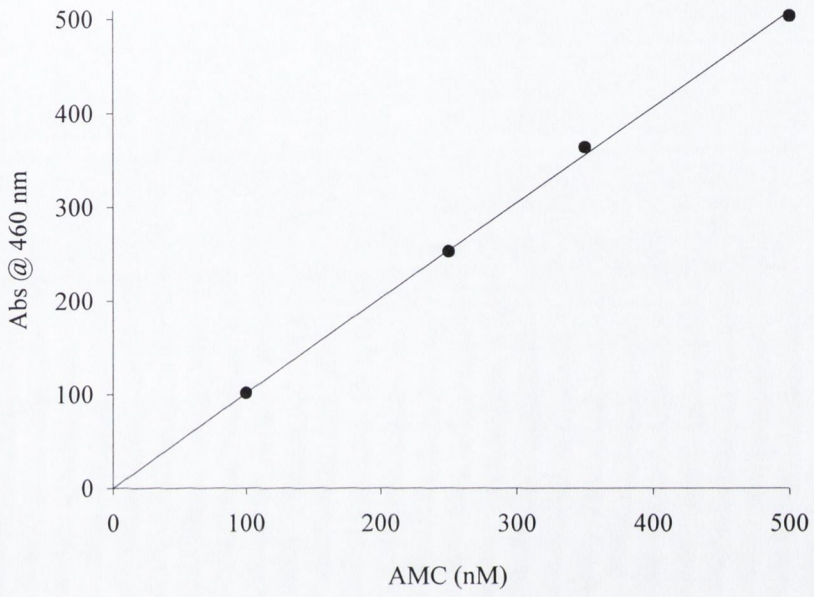

Fig. 2.1 AMC standard curve

A stock solution of AMC (10mM) was used to prepare a concentration range (100-500nM) of AMC in final volume of 3 ml, and the absorbance @ 460 nm was read using a spectrofluorimeter.

consisted of: H_2O (3.4ml), Protogel™ (830µl), 1M Tris-HCl, pH 6.8 (630µl), 10% SDS (w/v) (50µl), 10% (w/v) APS (50µl) and TEMED (6µl). Proteins were electrophoresed at 80V until the tracker dye reached the resolving gel and was then increased to 110V for 120-150 min, until the tracker dye reached the bottom of the resolving gel. Proteins were then transferred onto PVDF membrane overnight at 4°C using the wet transfer apparatus as described in Section 2.6.3. The membrane was blocked for 1h at room temperature, by incubation with gentle agitation in blocking buffer containing 5% (w/v) dry milk in TBST (0.1% (v/v) Tween 20 in TBS). The membrane was washed briefly in TBST (2 x 2 min), followed by incubation in primary anti-caspase-7 antibody (1:1000 dilution in blocking buffer) for 1h at room temperature. The membrane was washed again in TBST (2 x 5 min, 1 x 10 min) followed by incubation in secondary antibody, goat anti-mouse HRP-conjugated (1:1000 dilution in blocking buffer) for 1h at room temperature. The blot was then washed in TBST (2 x 5 min, 1 x 10 min, 2 x 5 min) before a final 5 min wash in TBS.

Membranes were developed using electrochemiluminescence (ECL) detection system as described in Section 2.6.3.

2.12 Western blot analysis of poly (ADP-ribose) polymerase (Parp) cleavage

Cells, grown as described in Section 2.2.1, were seeded at a density of $2x10^6$ cells/flask and treated with either vehicle or the outlined drug for 16h at 37°C. Following treatment, cells were harvested by centrifugation at 500xg for 5 min, the supernatant was removed and the pellets resuspended in Parp sample buffer (200µl) (62.5mM Tris/HCl pH 6.8, 6M urea, 10% (w/v) glycerol, 2% (w/v) SDS, 0.00125% bromophenol blue and 5% (v/v) β-mercaptoethanol added immediately before use). Samples were sonicated for 15 sec and heated at 65° for 15 min before aliquoting into 15µl volumes. Samples were stored at –20°C until use. Thawed samples (15µl) were resolved directly by SDS-PAGE. The 10% resolving gel consisted of: H_20 (5.9ml), Protogel™, (Ultra-pure 30% (w/v) acrylamide and 0.8% (w/v) bisacrylamide) (5ml), 1.5M Tris-HCl, pH 8.8 (3.8ml), 10% (w/v) SDS (150µl), 10% (w/v) APS (150µl) and TEMED (8µl). The 5% stacking gel consisted of: H_2O (3.4ml), Protogel™ (830µl), 1M Tris-HCl, pH 6.8 (630µl), 10% SDS (w/v) (50µl), 10% (w/v) APS (50µl) and TEMED (6µl). Samples were then electrophoresed, transferred onto PVDF and blocked by gentle agitation in PBST containing 5% (w/v) dry milk, overnight at 4°C. Membranes were

then washed briefly in PBST (2 x 2 min) before incubating with anti-Parp antibody (2μg/ml in PBST containing 1% dry milk) for 1h at room temperature. Following incubation the membrane was washed for 20 min in PBST and incubated for 1h with goat anti-mouse HRP-conjugated secondary antibody (1:1000 dilution in PBST containing 1% (w/v) dry milk). After washing in PBST for 30 min, ECL was used to visualise the proteins. The antibody recognises the full enzyme, which is represented by a 116kDa band, and the 87 kDa cleavage product.

2.13 Western blot to detect activation of mitogen-activated protein (MAP) kinases and their substrates

Cells were grown as described in Section 2.2.1 and seeded at a density of $5x10^6$cells/flask. Cells were treated with either vehicle or PBOX-6 and incubated at 37°C in 95% O_2 and 5% CO_2 for the required time. Following treatment, cells were harvested by centrifugation at 500xg for 5 min. For determination of MAPK activation, pellets were washed with ice-cold PBS and resuspended in ice-cold lysis buffer (100μl) (150mM NaCl, 50mM Tris/Cl pH 8.0, 0.1% (w/v) SDS, 1% (w/v) Triton X-100, 1mM sodium orthovanadate, 1μg/ml leupeptin, 1mM PMSF and 10μg/ml aprotinin). Samples were incubated on ice for 20 min followed by centrifugation at 20,000xg for 10 min at 4°C. The resultant supernatants were removed and used to measure the phosphorylated form of ERK, p38 and JNK MAP kinases. A Bradford assay was used to determine protein concentration as described in Section 2.3.1. To determine the activation of the Jun N-terminal kinase (JNK) substrates, c-Jun and ATF-2, the pellets were resuspended in SDS sample buffer and sonicated as described in Section 2.11.

Equal amounts of protein were resolved on a 10% SDS-polyacrylamide gel. The 10% resolving gel consisted of: H_20 (5.9ml), Protogel™, (Ultra-pure 30% (w/v) acrylamide and 0.8% (w/v) bisacrylamide) (5ml), 1.5M Tris-HCl, pH 8.8 (3.8ml), 10% (w/v) SDS (150μl), 10% (w/v) APS (150μl) and TEMED (8μl). The 5% stacking gel consisted of: H_2O (3.4ml), Protogel™ (830μl), 1M Tris-HCl, pH 6.8 (630μl), 10% SDS (w/v) (50μl), 10% (w/v) APS (50μl) and TEMED (6μl). Proteins were electrophoresed at 80V until the tracker dye reached the resolving gel and was then increased to 110V for 120-150 min, until the tracker dye reached the bottom of the resolving gel. Proteins were then transferred onto PVDF

membrane as described in Section 2.6.3 except that the transfer was carried out at 60V, 160mA for 90 min at room temperature. Western blotting was carried out as described in Section 2.6.3. Anti-ERK-phospho, anti-JNK phospho, anti-p38 phospho and anti-c-Jun antibodies were diluted 1:000 in TBST containing 5% (w/v) BSA whereas the anti-ATF-2 antibody was diluted 1:500.

2.14 Detection of Bcl-2 family members by Western blotting

2.14.1 Subcellular fractionation of K562 cells to yield cytosolic and mitochondrial fractions

K562 cells were grown as described in Section 2.2.1 and seeded at a density of $2x10^6$ cells/flask and treated with either vehicle (1% (v/v) ethanol) or PBOX-6 for 16h at 37°C. Following treatment the cells were collected by centrifugation at 500xg for 5 min and resuspended in isotonic lysis buffer (100µl) (200mM mannitol, 70mM sucrose, 1mM EGTA and 10mM Hepes, pH6.9). Cells were incubated on ice for 5-10 min and repeatedly drawn through a 21-gauge syringe for 2-3 min to rupture the cells. Following a further incubation on ice for 10 min, unbroken cells, nuclei and heavy membranes were separated by centrifugation at 1000xg for 5 min, and the resulting pellet was discarded. The supernatant was centrifuged 12,000xg for 20 min at 4°C to produce mitochondrial enriched and cytosolic fractions. The supernatant was removed and represents the cytosolic fractions. The remaining pellet, which represents the mitochondrial enriched fraction, was washed one time in isotonic buffer (200µl) followed by centrifugation at 12,000xg for 5 min followed by a final resuspension in hypotonic lysis buffer (20µl) 10mM Tris-Cl, pH7.5, 5mM $MgCl_2$, 1mM EGTA and 1mM dithiotrietol) supplemented with the protease inhibitors (5µg/ml pepstatin A, 2µg/ml leupeptin, 2µg/ml aprotinin). A Bradford assay was performed on all fractions to determine the protein concentration, as outlined in Section 2.3.1 and levels of expression of the various Bcl-2 family members was performed by Western blot analysis as described in Section 2.14.2.

2.14.2 Western blot to detect Bcl-2, Bcl-$_{XL}$ and Bax

Cells were grown as described in Section 2.2.1 and seeded at a density of $2x10^6$ cells/flask and treated with either vehicle or the outlined drug at 37°C. Following treatment for the indicated time, whole cell lysates were prepared using an SDS sample buffer as described in Section 2.11. Proteins were resolved on a 12% SDS-PAGE gel in a manner similar to that described in Section 2.11. Proteins were then transferred onto PVDF membrane using the wet transfer apparatus at 60V, 160 mA for 75 min at room temperature. Membranes were blocked by gentle agitation in TBST containing 5% (w/v) dry milk for 2h at room temperature. Membranes were then washed briefly in PBST (2 x 2 min) before incubating overnight with primary antibody at 4°C. Anti-Bcl-2 antibody was diluted 1:100, anti-Bcl-$_{xl}$ antibody was diluted 1:250 and anti-Bax antibody was diluted 1:200 in TBST containing 5% (w/v) dry milk. Following incubation the membrane was washed for 20 min in TBST and incubated with goat anti-mouse HRP-conjugated secondary antibody (1:1000 dilution in TBST containing 5% (w/v) dry milk). After washing in TBST for 30 min, ECL was used to visualise the proteins.

2.15 Radioligand binding assay

2.15.1 Measurement of [^{3}H] PK11195 binding to CML cell homogenates

CML cells were grown as described in Section 2.2.1 and harvested by centrifugation at 500xg for 5 min. Following a wash in PBS, the cell pellet was homogenised in 50mM Tris-HCl, pH 7.4 (Incubation Buffer) (2ml), using an Ultraturrax homogeniser (10 sec) and then passed 5 times through a 21 gauge needle. Cell homogenates were incubated on ice with 0.5-50nM [^{3}H] PK11195 (86.5 Ci/mmol) in incubation buffer, in a total volume of 0.5ml. Total and non-specific/non-saturable binding in each case was determined in the absence and presence of 10μM unlabelled PK11195 respectively. All samples were incubated in triplicate for 60 min on ice. The incubation mixtures were then rapidly diluted with ice-cold incubation buffer (1.5ml) and immediately filtered through Whatman glass fibre filters (2.5cm diameter) pre-soaked in 0.15 (v/v) polyethyleneimine, followed by rapid rinsing of the test tubes with 1.5ml of ice-cold incubation buffer. The filters were rapidly washed twice with ice-cold incubation buffer (5ml). When dry, the filters were transferred to plastic vials and

scintillation fluid (10ml) was added and the radioactivity remaining on the filters was determined by liquid scintillation counting as described in Section 2.13.2

When testing the potency of a compound to inhibit [^{3}H] PK11195 binding, samples were incubated with a 4nM [^{3}H] PK11195 and varying concentrations (0.1nM-1μM) of compound, and samples were subsequently treated as above.

2.15.2 Liquid scintillation counting

The [^{3}H] radioactivity was measured using either a Packard Tricarb 300 or a Packard 1500 scintillation counter. The scintillant cocktail used was the commercial scintillant Ecoscint. The average counting efficiency for [^{3}H] counting in the Packard Tricarb 300 was calculated to be 45%, based on a quench-correction curve relating counting efficiency to channels ratio. The same counting efficiency was achieved in the 1500 model scintillation counter and this was calculated from a quench curve relating counting efficiency to the spectral index of the external standard.

2.15.3 Analysis of binding data

Binding values were obtained as counts per min (cpm) and were converted to pmol of bound radioligand using counting efficiency and specific radioactivity values. The mean values and the standard error values (S.E.M.) were calculated for total and non-specific values of pmol bound ligand and the following formula was employed to obtain standard errors for specific values:

$$S.E.M. = ((E_1)^2 + (E_2)^2)$$

E_1 = S.E.M. for total binding

E_2 = S.E.M. for non-specific binding

Specific binding was calculated from the difference between total and non-specific binding. The equilibrium dissociation constant (K_D) and the maximal binding capacity (B_{max}), describing the saturable binding of [^{3}H] PK11195 to a single class of binding sites, were obtained by fitting the mean values for specific binding and free ligand concentration using the method of Wilkinson (1961), and the computer program Sigma plot. This program

first plots binding data as the double reciprocal form to obtain initial estimates for K_D and B_{max} for a single site-binding curve. The data are then fitted directly as [bound ligand] versus [free ligand] to the equation describing rectangular hyperbola

$[Bound] = B_{max}.[Free]/([Free]+K_D)$

by non weighted non-linear least squares regression.

Single site displacement curves describing the competition of [^{3}H] PK11195 binding by tested compounds were generated by use of the computer program Graph Pad. Graph Pad uses a sigmoidal curve-fitting programme to fit the displacement curve. Logit-log transformation of the data is performed (i.e linear regression of log [% bound/100-%bound]) against log [concentration of displacer] to obtain initial estimates of certain parameters including IC_{50} (concentration of displacer inhibiting 50% of specific binding). These are then fed to the iterative portion of the program to obtain final estimates of the parameters. The equation used to fit the competitive displacement curve is

$$\text{Bound (dpm)} = \frac{(Bmax-BG)}{(1 + [\text{Displacer concentration} / IC_{50}]^P)} + BG$$

where:

B_{max}: the total amount of radioligand bound (dpm) in the absence of any displacer

BG: the estimate of non-specific binding (dpm)

P: the slope factor (Hill coefficient)

The calculated IC_{50} value is then used to determine K_i (inhibition constant describing potency of inhibition) by applying the equation

$$IC_{50} = K_i (1 + [L]/K_D)$$

Where [L] is the concentration of [^{3}H] ligand and the K_D is its dissociation constant for the binding site.

2.16 Measurement of DNA strand breaks

2.16.1 Alkaline elution assay to measure DNA strand breaks

The alkaline elution assay for measurement of DNA strand breaks was set up as described by Kohn *et al.* (1976) with some modifications.

Cells, grown as described in Section 2.2.1, were seeded at a density of $0.4x10^6$ cells/ml and were in the logarithmic phase of growth. The doubling time was approximately 20h. Cells harvested for the alkaline elution experiments were at a density of $2x10^6$ cells/ml.

Cells ($1x10^6$) were labelled with [^{3}H] thymidine (sp. act. 2Ci/mmol) (0.2μCi/ml) and 1μM unlabelled thymidine, and incubated for 20h at 37°C in 95% O_2 and 5% CO_2. Cells were harvested by centrifugation at 500xg for 5 min followed by two washes in PBS and the pellet was resuspended in 3ml of PBS. Cells were aliquoted into 1ml amounts in a 24-well plate and allowed to recover for 1h at 37°C in 95% O_2 and 5% CO_2 before treating with the indicated compound. Following this treatment period, cells were washed once in PBS, centrifuged at 500xg for 5 min and the resulting pellet was resuspended in 250μl of PBS. An aliquot of cells (200μl) was loaded directly onto a 25 mm diameter glass fibre filter, pore size of 0.2μm. The cells were lysed on the filter by the addition of lysis buffer (5ml) (2% (w/v) SDS, 10mM disodium EDTA, pH 10.0) supplemented with 0.5mg/ml proteinase K. The lysis buffer was allowed to flow slowly through the filter without suction. Filters were washed using wash solution (3ml) (0.02M Na_3EDTA, pH 10.0) allowing it to flow through without suction. DNA was eluted in the dark with an alkaline solution (0.04M EDTA plus tetrapropylammonium hydroxide (10% (v/v) in H_20) added in the amount required to give pH 12.1). The elution apparatus consisted of a filter funnel with output tubing passing through a peristaltic pump to a collector. Elution took place overnight at a flow rate of 0.05 ml/min. Following elution, filters were removed from the elution apparatus and placed in plastic scintillation vials and treated with 0.4ml HCl (1N) for 1h at 70°C to depurinate the DNA. This was followed by the addition of 2.5ml NaOH (0.4N) for 30 min at room temperature, to release the DNA from the filters into solution and allow maximum counting efficiency. Aqueous-based scintillation fluid (Ecoscint) (10ml) was added, the contents were mixed by rigorous vortexing and radioactivity remaining on the filters was determined by liquid scintillation counting as described in Section 2.15.2.

2.17 Determination of farnesyl protein transferase activity

2.17.1 Partial purification of farnesyl protein transferase from cells

A large culture (250ml) of cells grown to confluency at 37°C in 95% O_2 and 5% CO_2 in complete medium were collected by centrifugation at 500xg for 5 min. The pellet was washed in PBS (50ml) and lysed in lysis buffer (10mM HEPES, pH 7.4, 1mM $MgCl_2$, 1mM EDTA, 0.1mM DTT, 0.1mM PMSF) (1ml) on ice for 5 min. The cells were drawn through a 21gauge needle 25-30 times to aid in rupture of the cell wall, followed by incubation on ice for a further 20 min. The cell extract was centrifuged at 60,000xg for 1h at 4°C and the recovered supernatant was further concentrated by ultrafiltration using a Centricon 30 concentrator (Amicon). The supernatant was added to the centricon reservoir and centrifuged at 5000xg for 1h at 4°C. Solvents and low molecular weight solutes in the filtrate were discarded and the concentrate, which contained the farnesyl transferase protein was eluted by centrifugation at 1000xg for 2 min. Protein determination was performed using a Bradford assay as described in Section 2.3.1 and the partially purified farnesyl transferase was aliquoted and stored at -70°C until required.

2.17.2 Assay for farnesyl protein transferase activity

Farnesyl protein transferase activity was determined using the method described by Reiss *et al.* (1990), which measures the amount of [^{3}H] farnesyl transferred from [^{3}H] farnesyl pyrophosphate (FPP) to human recombinant Ras.

The standard reaction mixture contained the following concentrations of components in a final volume of 25µl: 50mM Tris-HCl, pH 7.5, 50µM $ZnCl_2$, 20mM KCl, 3mM $MgCl_2$ and 1mM DTT containing 1µM recombinant wild type H-Ras (Calbiochem), 10 pmols of [^{3}H] FPP (Sigma) and 5µg partially purified farnesyl transferase (see Section 2.17.1). Various different compounds were incubated with the reaction mixture at the concentration outlined in the figure legends. All components were mixed well and incubated in a 37°C waterbath for 1h. The reaction was stopped by the addition of 4% (w/v) SDS (0.5ml). Protein was precipitated with 30% (w/v) trichloroacetic acid (TCA) (0.5ml), tubes were vortexed to mix and incubated on ice for 1h. Solution A (6% (w/v) TCA, 2% (w/v) SDS) (2ml) was added to each tube and the contents were mixed. The cocktail was then filtered directly onto

glass fibre filters (2.4 cm diameter) and tubes were rinsed twice with Solution A (2ml). Each filter was washed 5 times with 6% (w/v) TCA (5 x 2ml), removed from the filter unit and dried at 37°C for 30 min. Filters were placed in a plastic vial and scintillation fluid (10ml) added, and each vial was vortexed vigorously and allowed to stand at room temperature for 1h. Radioactivity remaining on the filters was determined by liquid scintillation counting as outlined in Section 2.15.2. One unit of activity is defined as the amount of enzyme that transfers 1 pmol of [^{3}H] farnesyl from [^{3}H] FPP into acid precipitable H-Ras per hour under standard conditions. Results were expressed as % farnesyl transferase activity over control samples in which drug was not added.

2.18 Statistical analysis of data

A Student's t-test was carried out using the Macintosh Instat program. A p value of < 0.05 was considered significant.

2.19 Electrophoretic mobility shift assay (EMSA)

2.19.1 Preparation of nuclear extracts for the detection of nuclear factor kappa B (NFκB) activation

Nuclear extracts for the determination of NFκB activation were prepared by a modification of the method described by Osborn *et al.* (1989).

Cells, grown as described in Section 2.2.1, were seeded in 6-well plates at a density of $3x10^6$ cells in 5ml of complete growth medium and treated with the indicated compound at 37°C in 95% O_2 and 5% CO_2 for the relevant time. Following treatment, cells were harvested by centrifugation at 500xg for 5 min. The pellets were resuspended in 5ml of ice-cold PBS and re-centrifuged to obtain a pellet. All subsequent steps were performed on ice. The pellet was resuspended in 0.8ml hypotonic buffer (10mM HEPES-NaOH, 1.5mM $MgCl_2$, 10mM KCl, 0.5 mM DTT, 0.5 mM PMSF, pH 7.9) and centrifuged at 13,000xg for 10 min at 4°C. The supernatants were discarded and the cells were lysed for 10 min on ice in 20µl of hypotonic buffer containing 0.1% (v/v) Nonidet P-40. The lysates were centrifuged for a further 10 min at 4°C, the pelleted nuclei were resuspended in 15µl of nuclear extract buffer (20mM HEPES-NaOH, 420 mM NaCl, 1.5mM $MgCl_2$, 0.2 mM EDTA, 25% (v/v) glycerol,

0.5mM PMSF, pH 7.9) and incubated on ice for 15 min. Lysed nuclei were centrifuged at 4°C for 10 min and supernatants (nuclear extracts) were removed to clean minifuge tubes.

Protein determinations were carried out using the Bradford assay, as described in Section 2.3.1. Extracts were stored at -70°C and activation of nuclear NFκB was assessed by the electrophoretic mobility shift assay as described in Section 2.19.3.

2.19.2 Labelling of oligonucleotides for EMSA assay

5' end-labelling of the 22 base pair oligonucleotides containing the NFκB consensus sequence was based on the method of Sambrook *et al.* (1989).

The reaction mixture containing 10pmol of the DNA probe, 50pmol (150μCi) [γ-^{32}P]ATP, 20U T4 polynucleotide kinase and 5μl of 10x kinase buffer (100mM $MgCl_2$, 50mM DTT, 1mM spermidine, 500mM Tris-Cl, pH 7.5) was made up to 50μl with H_2O and incubated at 37°C for 10 min. The reaction was terminated with 2μl of 0.5M EDTA. Phenol:chloroform solution (50μl; 1:1 Tris-EDTA (TE)-saturated phenol:chloroform-isoamyl alcohol (24:1)) was added to extract the DNA. After vortex-mixing for 1 min, the solution was centrifuged at 13,000xg for 2 min. The resulting top aqueous layer was transferred to a fresh tube, 2μl of 5M NaCl added, the tube vortexed and 100μl of ethanol added. This was incubated at -70°C for 30 min to effect ethanol precipitation of the DNA. After centrifugation at 13,000xg for 5 min, the supernatant was carefully removed and discarded. The pellet was dried in an oven at 30°C for 45 min, and then resuspended in 50μl TE buffer (10mM Tris-HCl, pH 8.0, 1mM EDTA). This solution (1μl) was counted in 5ml scintillation fluid, and the stock solution subsequently diluted to 10,000 cpm/μl immediately before use in the EMSA assay, as described in Section 2.19.3.

2.19.3 EMSA assay

Nuclear extracts were analysed for NFκB by electrophoresis, as described by Sen and Baltimore (1986). The principle of this assay is that NFκB, present in nuclear extracts, will bind to a labelled probe containing the NFκB binding motif, thus retarding the electrophoretic mobility of this DNA in a polyacrylamide gel.

Nuclear extracts (2-4 μg protein), prepared as described in Section 2.19.1, were incubated with 10,000 cpm of the labelled 22 base pair oligonucleotide containing the NFκB

consensus sequence, 5'-AGT TGA GGG GAC TTT CCC AGG C-3' (underlined) (for labelling of the probe see Section 2.19.2). Incubations were performed for 30 min at room temperature, in the presence of 2μg poly (dI-dC) as a non-specific competitor, and 10mM Tris-HCl, pH 7.5, containing 100mM NaCl, 1mM EDTA, 5mM DTT, 4% (v/v) glycerol and 100μg/ml nuclease-free bovine serum albumin (binding buffer). Poly (dI-dC) and binding buffer were always added before the radiolabelled probe.

The binding reaction was terminated by addition of one tenth of a volume of loading buffer (final concentration 0.025% (w/v) bromophenol blue, 0.025% (w/v) xylene cyanole FF, 33% (v/v) glycerol in TBE). Samples were then loaded onto a 5% native polyacrylamide gel. The gel was prepared using 2.5ml of 10x TBE (0.89M Tris-HCl, pH 7.5, 0.89M Boric acid, 0.02M EDTA), 3.125ml of 40% acrylamide:bisacrylamide mix (29:1) ratio), 5μl of 1M DTT, 15μl TEMED and 0.05g APS, made up to 25ml with H_2O. Gels were run for 120-160 min at 120-180 V with 0.5x TBE as running buffer.

The gels were dried and autoradiographed using Kodak diagnostic film (X-Omat LS) in autoradiography cassettes with intensifying screens for 16-48h at -70°C. The films were developed using an X-ray processor (Fuji).

2.20 Lactate Dehydrogenase (LDH) assay

Whole cell extracts were prepared as described in Section 2.17 and protein determination was performed using a Bradford assay as described in Section 2.3.1.

An aliquot of protein (1μg diluted in complete growth medium) from each subcellular fraction was placed in a 96-well microtitre plate in a final volume of 100μl. NADH solution containing the catalyst (100μl of a 1mg/ml stock) was added to each of the wells and the plate was covered and incubated at room temperature for 20 min. All enzyme assays were performed in triplicate and the absorbance was read at a wavelength of 340 nm using a Dynatech MR5000 plate reader.

Lactate dehydrogenase activity reduces NAD^+ to NADH + H^+ by oxidation of lactate to pyruvate. In a second enzymatic step, the catalyst converts the yellow tetrazolium salt INT to a formazan salt. The presence of lactate dehydrogenase in the subcellular fraction directly correlates to the amount of formazan formed.

% LDH activity is calculated by

$$\frac{\text{Experimental value} - \text{low control}}{\text{High control} - \text{low control}} \times 100$$

2.21 Preparation of LB medium

LB (Lauria-Bertani) medium

1% (w/v) bacto-tryptone

0.5% (w/v) bacto-yeast extract

1% (w/v) NaCl

Autoclaved for 20 min at 20 lb/sq.in.

LB agar plates: LB medium containing 1.5% (w/v) bacto-agar

2.22 Preparation of competent *E.coli*

A single colony of *E.coli* SCS-1 was inoculated into LB medium (5ml) and grown overnight at 37°C, at 250 rpm in an orbital shaker.

A portion of this overnight culture (1ml) was inoculated into LB medium (50ml) in a 100ml flask and incubated at 37°C, 250 rpm in the orbital shaker. Growth was monitored by measuring the absorbance at a wavelength of 600 nm at regular intervals. When an absorbance of OD_{600} reached 0.3-0.5, the flask was removed from the incubator and 2 x 20ml cultures were collected and centrifuged at 3000xg for 5 min in a Sorvall RC 5B centrifuge using the SS34 rotor. Following centrifugation, cells were placed on ice, supernatant was discarded and each pellet was resuspended in ice-cold 100mM $MgCl_2$ (5ml). Samples were centrifuged again at 3000xg for 5 min at 4°C and the supernatant discarded. Pellets were resuspended in ice-cold 100mM $CaCl_2$ (5ml) and incubated on ice for 20-60 min followed by centrifugation at 3000xg for 5 min at 4°C. The final pellet was resuspended in ice-cold 100mM $CaCl_2$ (1ml) and cells were transformed immediately.

2.23 Preparation of antibiotic stock solutions

Antibiotics were prepared as a stock solution, filter-sterilised, covered and stored at 4°C.

Antibiotic	Stock solution in H_2O	Working concentration (μg/ml)
Ampicillin	100mg/ml	100
Kanamycin	50mg/ml	30

2.24 Transformation of competent *E.coli*

Competent *E.coli* SCS-1 (200μl), prepared as described in Section 2.22, were incubated with plasmid DNA (0.5μg) in a minifuge tube and placed on ice for 1-2h. Following incubation, each tube was heat shocked by placing it in a water bath at 37°C, for 2 min and immediately followed by incubation on ice. LB medium (0.8ml) was added and tubes were incubated at 37°C for 60-90 min, to allow cells to recover and express antibiotic resistant genes. An aliquot of cells (100μl), from various dilutions, was then spread onto LB agar plates containing the appropriate antibiotic and incubated overnight at 37°C.

2.25 Extraction and ethanol precipitation of plasmid DNA from *E.coli* (Mini-prep)

LB medium (3ml) containing the appropriate antibiotic was inoculated with a single colony from the transformation plate (see Section 2.24), and incubated overnight at 37°C, 250rpm. Overnight culture (1.5ml) was placed in a minifuge tube and centrifuged at 12,000xg for 2 min and the supernatant was discarded. Each pellet was resuspended in freshly prepared Solution C (0.5ml) which consisted of a 1:1 mix of Solution A (50mM Tris-HCl, pH 8.0, 20% w/v sucrose) and Solution B (10% w/v Triton X-100, 50mM EDTA). Tubes were gently vortexed to release the pellet. Lysozyme (50mg/ml stock in 20mM NaOAc, pH 4.6/50% (v/v) Isopropanol) (10μl) was added, tubes were mixed gently, and heated to 100°C for 90 sec, followed by centrifugation at 12,000xg for 15 min. The supernatant was collected and transferred to a clean tube. Ice-cold isopropanol (0.7ml) was added and incubated for at least 1h at -20°C. Samples were centrifuged at 12,000xg for 30 min and the supernatant was gently removed using a pipette. The resulting pellets were

washed with ice-cold 70% ethanol (100µl), followed by 100% ethanol (100µl) with a 3 min centrifugation at 12,000xg between each wash and the supernatant was removed taking care not to disturb the pellet. The DNA pellet was allowed to air dry at room temperature for 15-30 min, and resuspended in TE buffer (10mM Tris-HCl, pH 8.0 containing 1mM EDTA) (20µl). An aliquot of the DNA sample was quantified by agarose gel analysis.

2.26 Quantification and analysis of DNA by agarose electrophoresis

Agarose electrophoresis was carried out using an ATTO electrophoresis apparatus (model AE-6100). Agarose gels (1% w/v) were prepared in, and run with, TBE buffer (0.9 M Tris-HCl, pH 8.2, 0.9 M Boric acid and 25 mM EDTA). DNA samples were mixed with loading buffer (0.25% bromophenol blue, 30% w/v glycerol) (5µl) loaded on the gel and electrophoresed at 60V until the samples entered the gel matrix and voltage was increased to 120 V for 1.5-2h.

2.27 Spectrometric quantification of DNA

An aliquot of DNA was diluted in H_2O in a final volume of 1ml and placed in a quartz cuvette. Absorbance was measured at a wavelength of 260 nm using a Unicam UV-Visible spectrometer (UVG 053713) and the following calculation was used to quantify the DNA: 1 OD = 50µg DNA/ volume DNA added per cuvette.

2.28 Preparation of Maxiprep plasmid DNA

LB medium (100ml), containing the appropriate antibiotic, was inoculated with a single colony from a transformation plate (see Section 2.24) and incubated overnight at 37°C, 250rpm in the oribital shaker.

The GenElute™ Plasmid Maxiprep Kit from Sigma (PLX-10) was used to isolate plasmid DNA. Overnight recombinant *E.coli* cultures (100ml) were pelleted by centrifugation at 5,000xg for 10 min and the supernatant was discarded. The bacterial pellet was resuspended with resuspension solution (6ml) and lysed by adding lysis solution (6ml). The tube was inverted 8-10 times until the mixture became clear and viscous. Cell debris was precipitated by adding neutralisation buffer (8ml), tubes were inverted 4-6 times and centrifuged at 12,000xg for 10 min. The resulting cleared lysate was transferred onto a

binding column and centrifuged at 5,000xg for 2 min and the flow through liquid was discarded. Wash solution (15ml) was added to the column, which was centrifuged at 5,000xg for a further 5 min, DNA was eluted with elution solution (1-5ml depending on concentration required) and stored at -20°C. DNA concentration was estimated using agarose electrophoresis as described in Section 2.26 and/or spectometrically as described in Section 2.27.

2.29 Transient transfection of K562 cells

FuGENE 6 transfection reagent was used to transfect K562 cells. Cells were grown as described in Section 2.2.1 and plated one day before the transfection experiment at a density that allowed them to reach subconfluency after overnight incubation.

FuGENE 6 reagent was diluted by pipetting directly into serum-free medium. For each well of a 24 well plate, 1.5µl of FuGENE was added dropwise into 20µl serum-free medium, mixed gently and incubated at room temperature for 5 min. The diluted FuGENE was then added dropwise to DNA (0.4µg in 100µl serum-free medium), the tube was gently tapped to mix contents and incubated at room temperature for 15 min. The FuGENE:DNA complex was added to K562 cells ($4x10^5$ cells/400µl complete medium) and cells were allowed to recover overnight at 37°C in 95% O_2 and 5% CO_2. Following overnight incubation, cells were stimulated with the relevant compound for the required time. To prepare transfection complexes for many parallel experiments, the quantity of all components was increased proportionally.

2.30 Determination of luciferase reporter gene activity

Cells transfected with a luciferase reporter gene were collected by centrifugation at 500xg for 5 min, the supernatant was discarded and cells were washed once in PBS at room temperature. The cell pellets were lysed using passive lysis buffer from Promega (diluted 1:5 with sterile H_2O) (50µl) and incubated at room temperature with gentle agitation for 15 min. A portion of the lysed sample (20µl) was transferred to a 96-well luminometer plate to determine luciferase activity and the remainder was retained to determine β-galactosidase activity. Luciferase activity was assayed by the addition of 40µl of luciferase assay mix (20mM tricine, 1.07mM $(MgCO_3)_4Mg(OH)_2.5H_2O$, 2.67mM $MgSO_4$, 0.1mM EDTA,

33.3mM DTT, 270mM coenzyme A, 470mM luciferin, 530mM ATP) to each sample and luminescence was read using Mediators PHL luminometer. Luminescence readings were corrected for β-galactosidase activity and expressed as fold increase over control values.

2.31 Determination of β-galactosidase activity

β-galactosidase (β-gal) activity was assayed by the addition of O-nitrophenylgalactosidase (4mg/ml stock) (40μl) to an aliquot (20μl) of cell lysate prepared as described in Section 2.30, followed by the addition of 140μl of β-gal buffer (23mM NaH_2PO_4, 77mM Na_2HPO_4, 0.1mM $MnCl_2$, 2mM $MgSO_4$, 40mM β-mercaptoethanol, pH 7.3) in a 96-well microtitre plate. The plate was covered and incubated at 37°C until a yellow colour appeared (2-12h), and absorbance was read at a wavelength of 405nm using a Dynatech MR5000 plate reader.

2.32 Plasmid constructs

The *Trans* activator plasmid consists of the activation domain sequence of the c-jun or AFT-2 transcription activator, which is fused to the DNA binding domain of the yeast GAL4 and is driven by the human cytomegalovirus (CMV) (Fig. 2.2A). This is inserted into the multiple cloning site of the mammalian expression vector, pFA-CMV plasmid (Fig 2.2C). The Luciferase reporter plasmid consists of a luciferase reporter gene fused to five tandem repeats of the yeast GAL4 binding sites that control expression of photinus pyrolis (American fruitfly) (Fig. 2.2B). These plasmids constitute the *Trans* reporting system and were a gift from Professor Luke O'Neill, Biochemistry Dept., Trinity College Dublin. The ATF2 trans activator plasmid was purchased from Strategene.

The pEF expression vector encoding N terminal myc-tagged constitutively active RacV12 and dominant negative RacN17 (Fig. 2.3) were also generous gifts from Professor Luke O'Neill. The pRK5 expression vector encoding N terminal myc-tagged wild type Cdc42 and dominant negative Cdc42 N17 (Fig. 2.4) were a kind gift from Professor Alan Hall, MRC laboratory for molecular cell biology, University College London. The expression vectors encoding RasV12 and Ras N17 (Fig 2.5), the JNK inhibitor, JIP1 (Fig. 2.6), the β-Galactosidase vector (Fig. 2.7) and the κB-luciferase reporter gene (pGL3-5xκB-luc) (Fig. 2.8) were all gratefully received from Professor Luke O'Neill.

Fig. 2.2 Plasmid structure for *Trans*-Reporting system

Diagrams represent (A) fusion trans activator plasmids, pFA-cJun and pFA-ATF2 which were inserted into the multiple cloning site (mcs) of the CMV expression vector (C), and (B) is the luciferase reporter plasmid which contains a synthetic promoter with five tandem repeats of the yeast GAL4 binding sites that control expression of the *Photinus pyralis* (American firefly) luciferase gene.

(A) Fusion *trans*-activator plasmid

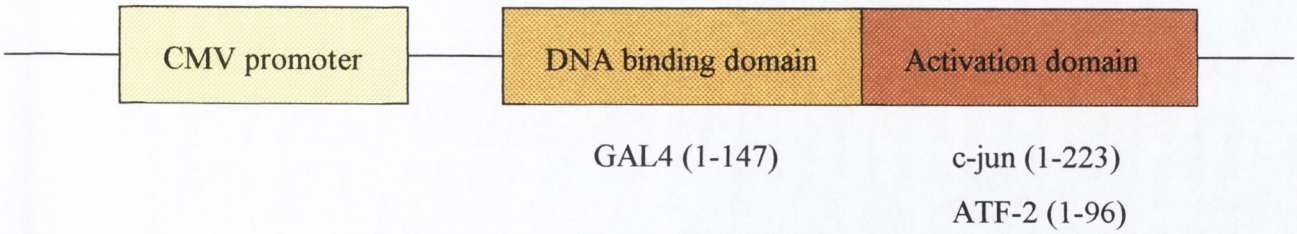

(B) pFR-Luc plasmid

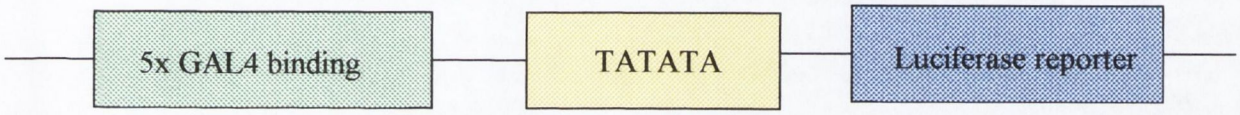

(C) pFA-CMV expression vector

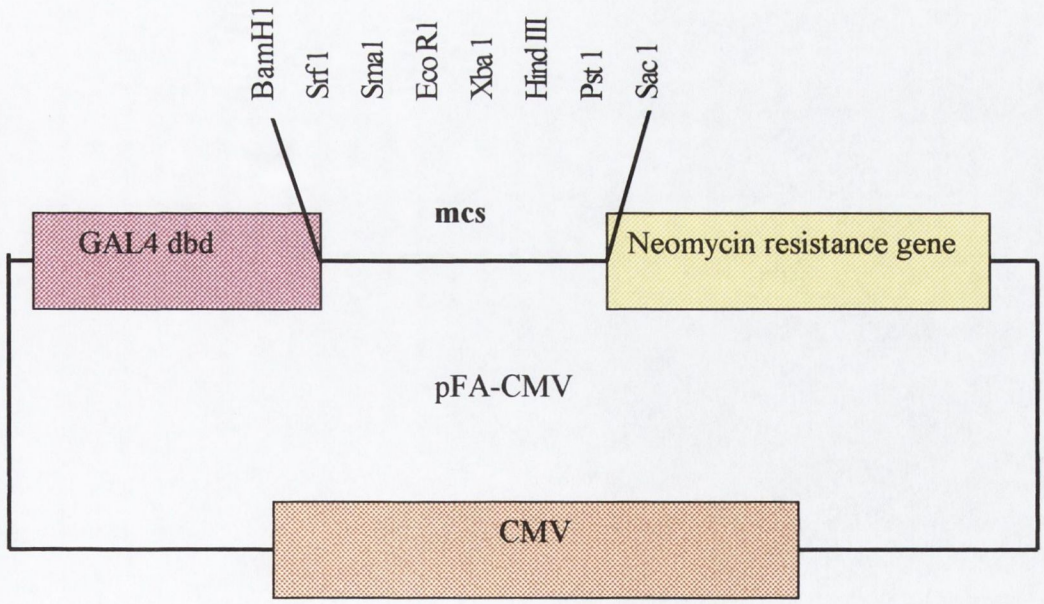

Fig. 2.3 Schematic map of expression vectors for RacV12 and RacN17

Diagrams represent (A) RacV12 and (B) RacN17, indicating N terminal Myc tag, GTP-binding domain and site of point mutation. RacV12 and RacN17 were cloned into the insert region of the mammalian expression vector pEF-BOS (C), which is shown here with elongation factor promoter region, restriction sites and insert region outlined.

(A) Constitutively active Rac V12

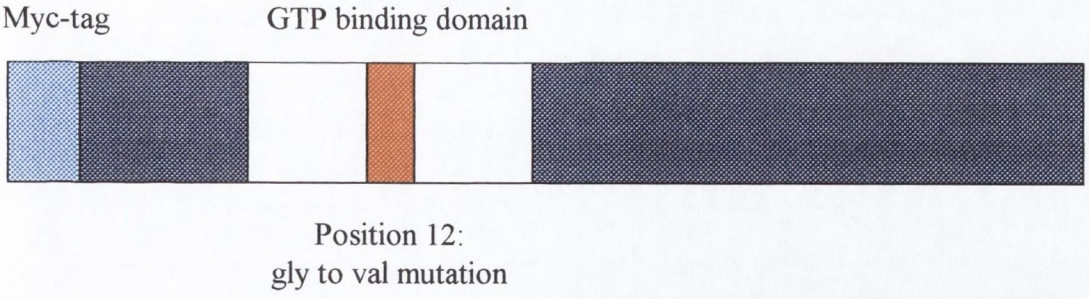

(B) Dominant negative Rac N17

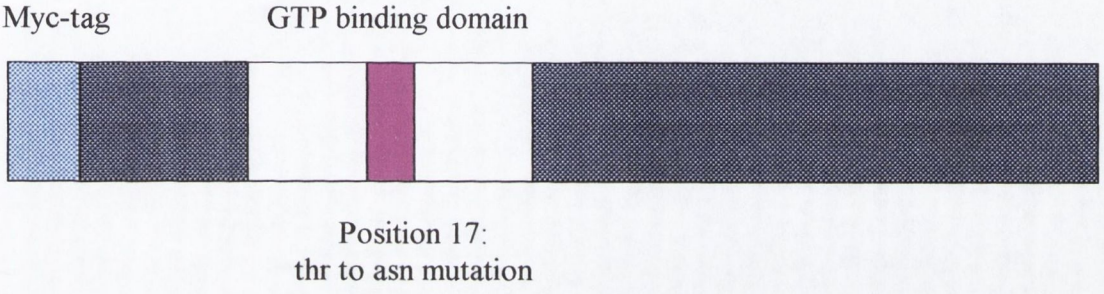

(C) pEF BOS expression vector

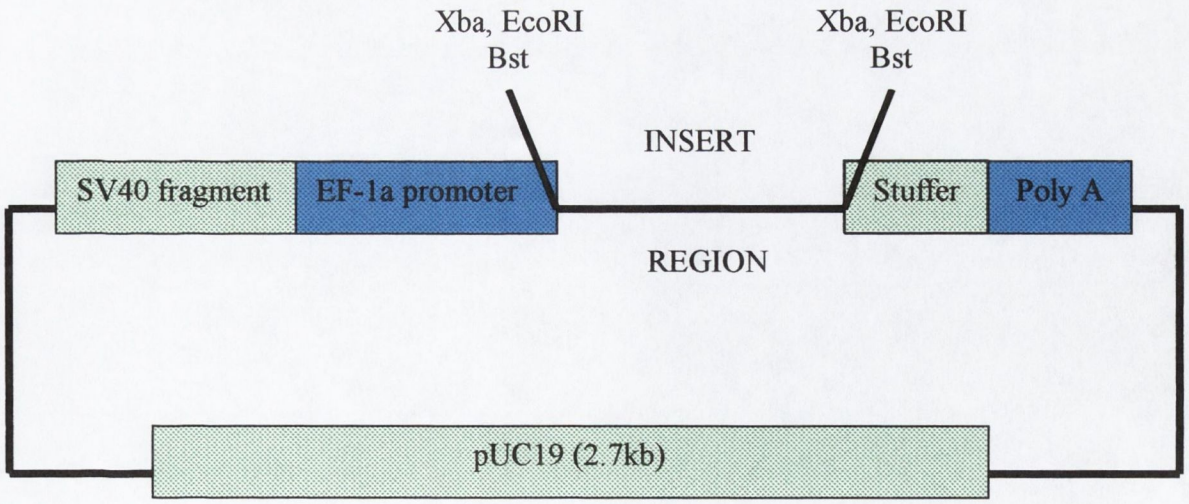

Fig. 2.4 Schematic diagram of expression vectors for wild type Cdc42 and N17Cdc42

Diagram represents (A) wild type Cdc42 and (B) dominant negative N17Cdc42, indicating N terminal myc tag, GTP binding domain and site of point mutation. Wild type and N17Cdc42 were cloned into the multiple cloning site (mcs) of the mammalian expression vector pRK5 (C), which is shown with CMV promoter, insert region and restriction sites.

(A) wild type Cdc42

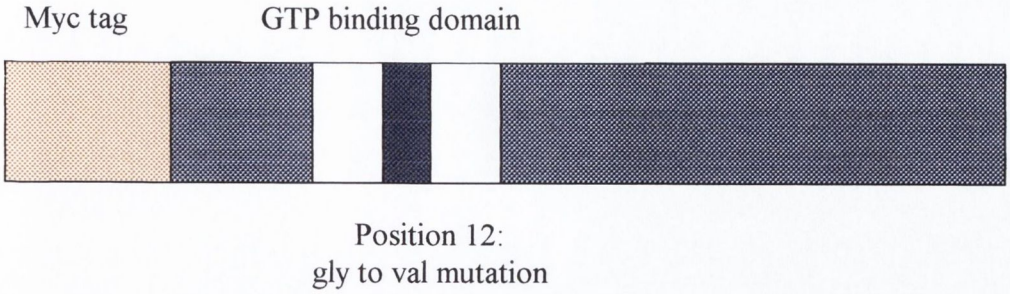

(B) dominant negative N17Cdc42

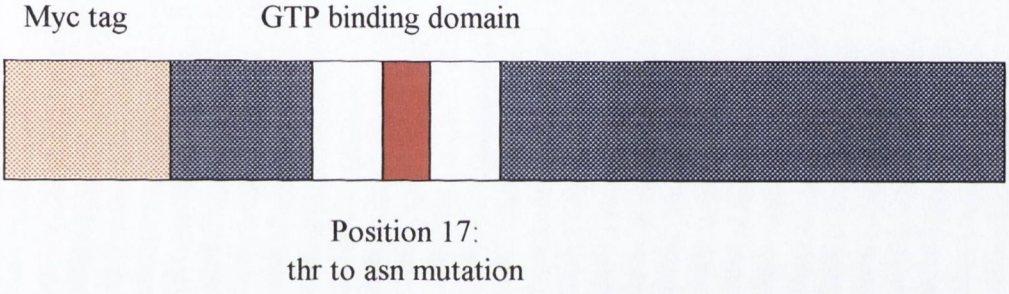

(C) pRK5 expression vector

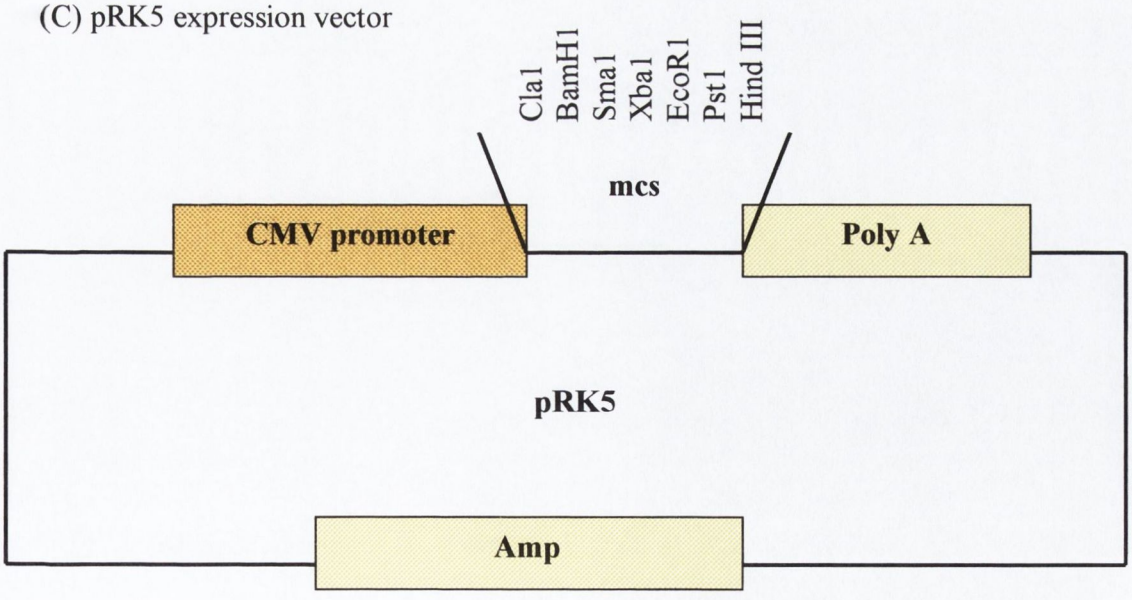

(A) Constitutively active RasV12

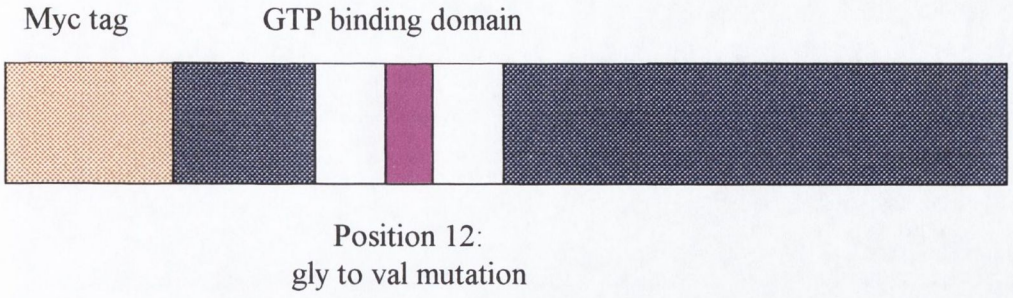

(B) Dominant negative RasN17

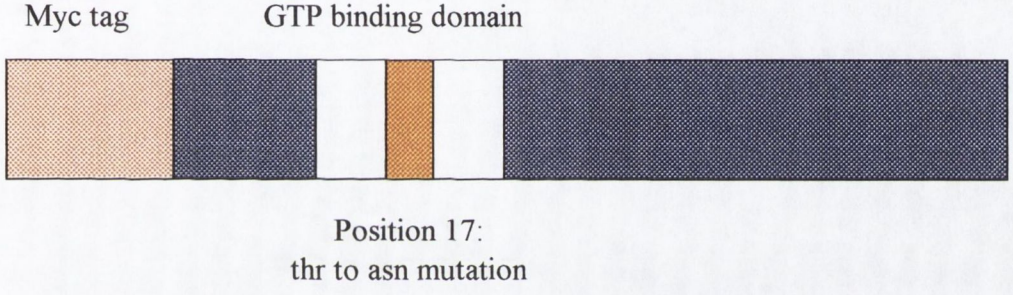

Fig. 2.5 Schematic diagram of the point mutations in RasV12 and RasN17

The diagram represents site of point mutation in the GTP binding domain, which produces (A) constitutively active RasV12 and (B) dominant negative RasN17. These sequences were cloned into the multiple cloning site of the RSV mammalian expression vector.

(A) Structure of JIP-1

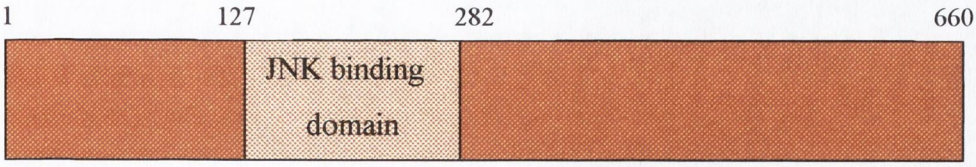

(B) Interaction of JIP-1 with components of the JNK MAP kinase module

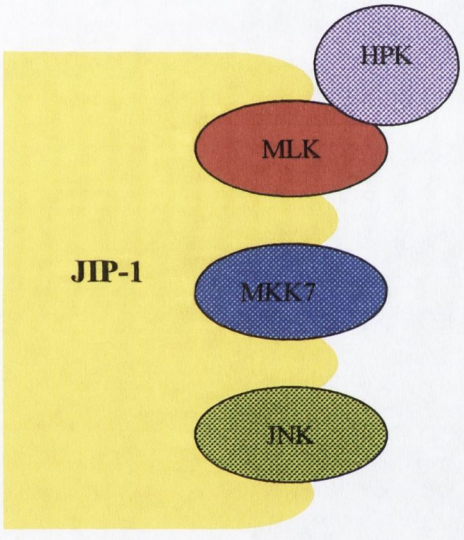

Fig. 2.6 Schematic illustration of JIP-1 and its interaction with components of the JNK MAP kinase pathway

Diagrams represent (A) JIP-1, indicating the JNK binding domain, and (B) JIP-1 scaffold complex which includes the Ste20p-like protein kinase HPK, the MLK group of MAP-kinase-kinase kinases (MKKK), the MAP-kinase kinase (MKK) isoform MKK7, and the MAP-kinase JNK.

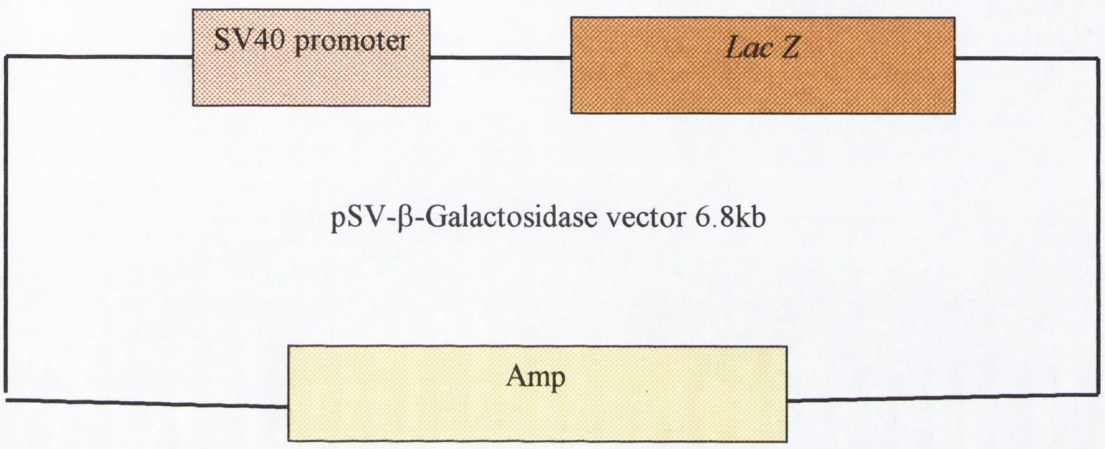

Fig 2.7 Graphical representation of the β-Galactosidase vector

The β-Galactosidase vector consists of a SV40 early promoter and enhancer to drive transcription of the bacterial *lacZ* gene, which encodes β-galactosidase and is used as a reporter enzyme to normalise transfection efficiency.

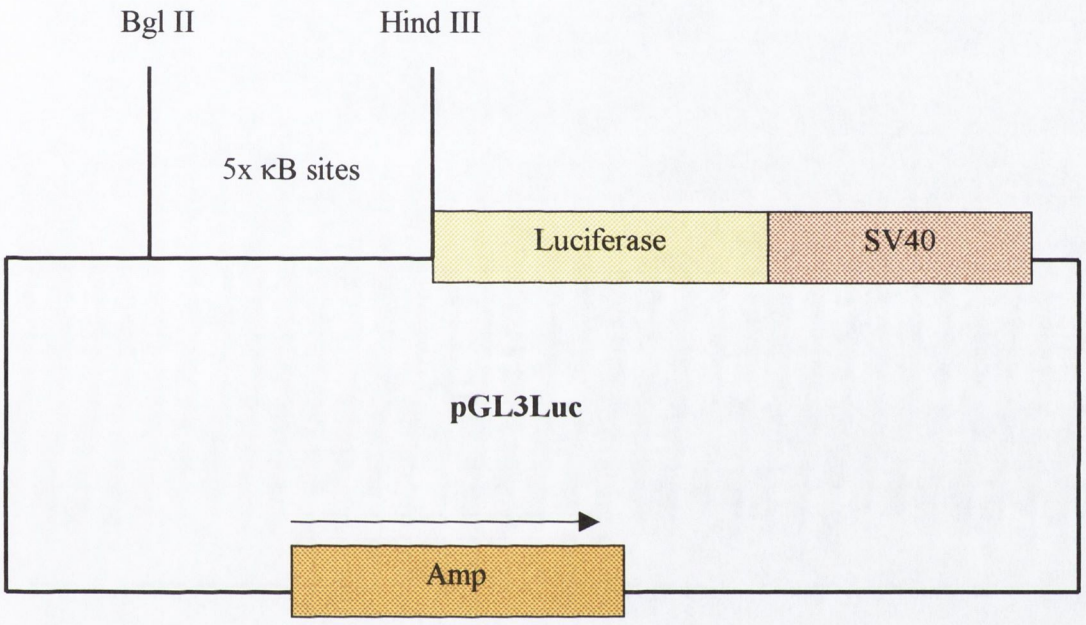

Figure 2.8 Graphical representation of pGL3Luc vector used to construct the NFκB-luciferase reporter plasmid

Five copies of the canonical consensus site for the transcription factor NFκB were cloned into the insert region of the reporter vector, pGL3-Luc. The restriction sites used to insert the sequence are as shown.

Chapter 3

Investigation into the apoptotic effects of a novel series of pyrrolo-1,5-benzoxazepine compounds in chronic myelogenous leukaemia cells

3.1 Introduction

Programmed cell death, or apoptosis, can be induced by a variety of drugs with diverse chemical structure and with different mechanisms of action. Among the list of apoptotic stimuli are a wide range of anti-cancer drugs such as daunorubicin and doxorubicin. Although the mechanism of anti-tumour action of these chemotherapeutic drugs has not been fully elucidated they have been shown to induce apoptosis in cancerous cells derived from the hematopoietic system, such as HL-60 cells. Recently a series of novel compounds, known as PBOX compounds have been synthesised as high affinity ligands to the peripheral-type benzodiazepine receptor (PBR) (Campiani *et al.*, 1996). Although a wide variety of functions have been attributed to the PBR over the years, including inhibition of cell proliferation, effects on mitochondrial respiration and on steroidogenesis, the true physiological role of the receptor remains to be discovered (Gavish *et al.*, 1999). It was thought that this group of novel PBOX compounds would help in probing the true physiological function of the receptor. These compounds have been shown to elicit similar biological effects to the classically used PBR ligands, PK11195 and Ro5-4864, such as anti-proliferative effects on cell growth and effects on steroidogenesis (Zisterer *et al.*, 1998).

In recent years it has been suggested that the PBR may play a role in mitochondrial events associated with the induction of apoptosis. It has been shown that PK11195 facilitates the induction of mitochondrial permeability transition and subsequent apoptosis induced by a number of chemotherapeutic agents such as etoposide and doxorubicin, and it partially reverses Bcl-2 mediated inhibition of apoptosis (Hirsch *et al.*, 1998). More recently, Chelli *et al.* (2001) has shown that PK11195 induces mitochondrial permeability transition in isolated cardiac mitochondria, as demonstrated by a decrease in absorbance associated with mitochondrial swelling. Using a cell free system, supernatants from swollen mitochondria caused apoptotic changes in cardiac nuclei. These reports strongly support the potential of PBR ligands as inducers of apoptosis. Zisterer *et al.* (2000), have shown that some members from this series of novel PBOX compounds induce apoptosis in a number of cancerous cell lines, such as the human promyelocytic leukaemia HL-60 cell line, the human lymphoma Hut-78 cell line and the human lympoblast Jurkat cell line at concentrations 10-fold lower than that used with PK11195. It has thus been proposed that these novel PBOX compounds

may be potential anti-cancer drugs and further study is warranted into their mechanism of action.

Chronic myelogenous leukaemia (CML) has been reported to be resistant to the induction of apoptosis by many chemotherapeutic agents such as etoposide and mitoxanthrone. The myeloid expansion characteristic of chronic phase CML results from the ability of these cells to suppress apoptosis (Kabarowski *et al.*, 1994; Rowley *et al.*, 1996). The Philadelphia chromosome is the cytogenetic hallmark of CML and produces a chimeric protein, p210 Bcr-Abl. This event is generally accepted to be the primary initiating event in the genesis of CML. Overexpression of Bcr-Abl in the K562 CML cell line and in leukaemia cells from patients with CML may in part account for the resistance of these cells to induction of apoptosis, leading to the accumulation of leukaemic blasts in patients with chronic myeloid leukaemia (Urbano *et al.*, 1998).

Over the years, a number of cell lines have been isolated from patients suffering from CML, which represent the different phases in the progression of the disease. K562 and KYO.1 cells are derived from the blastic phase of CML, whereas LAMA 84 cells are derived from the accelerated phase. K562 cells were isolated in 1970, from the pleural effusion of a 53-year-old female with CML in terminal blast crisis (Lozzio and Lozzio, 1975, 1979). KYO.1 cells were also derived from the peripheral blood of a patient with CML in blast crisis (Ohkubo *et al.,* 1985). These cell lines reflect blast crisis very well, but because they contain genetic lesions in addition to Bcr-Abl, they do not reflect chronic phase CML quite so well. Until now, no cell line from chronic phase CML has been established, just as no cell line could be derived from normal human bone marrow (Deininger *et al.*, 2000). However, the use of these cell lines has proved invaluable as a model system for improving our understanding of CML and in the ongoing search for novel drugs for the treatment of CML.

In the present chapter, the ability of PBOX compounds to induce apoptosis in CML cells was investigated. It was determined as to whether the induction of apoptosis by PBOX-6 results in down-regulation of Bcr-Abl expression in CML cells. In addition, the components of the apoptotic pathway by which a representative apoptotic member of these compounds, namely PBOX-6, induces apoptosis were dissected.

Programmed cell death, or apoptosis, occurs in cells in response to a wide variety of stimuli including chemotherapeutic drugs, UV irradiation and death receptors such as Fas

ligand and TNF. The morphological changes which accompany apoptosis, such as cell shrinkage, chromatin condensation, DNA fragmentation and membrane blebbing make it quite distinct from necrotic cell death, in which the cell ruptures releasing its contents (Steller, 1995). Many apoptotic pathways are also accompanied by the activation of caspases. Caspases are cysteine proteases, which cleave proteins after certain aspartate residues. These enzymes participate in a cascade that is triggered in response to pro-apoptotic signals and culminates in the cleavage of a set of proteins, resulting in the disassembly of the cell. Caspases are synthesised as inactive precursors having either a long or short prodomain, and two mature subunits. Cleavage of the inactive enzyme at specific aspartate residues generates a large and a small subunit (20 kDa and 10 kDa), which associate to form a heterodimer. Two such heterodimers associate to form a tetramer, to produce the active form of the enzyme (Adams and Cory, 1998). To date, at least 12 distinct human caspases have been identified that are grouped into three subfamilies based on their substrate specificities. Recognition of at least four amino acids NH_2-terminal to the cleavage site is a necessary requirement for the efficient catalysis. The preferred tetrapeptide recognition motif differs significantly among caspases and explains the diversity of their biological function (Thornberry and Lazebnik, 1998). Group 1 caspases (caspases-1, -4 and -5) play a role in inflammation, whereas group 2 (caspases-2, -3 and -7) and group 3 (caspases-6, -8, -9 and -10) have a role to play in apoptosis (Janicke *et al.*, 1998).

Since all caspases are cleaved at specific aspartic acid residues, it raises the possibility that some caspases sequentially activate others thereby establishing a hierarchy of caspases. Thus, caspases that are involved in upstream regulatory events are known as 'initiator caspases'. These initiator caspases (caspases-2, -8, -9 and -10) cleave and activate downstream 'effector' caspases such as caspases -3, -6 and -7. Effector caspases, are capable of cleaving a number of structural and regulatory proteins such as ICAD (inhibitor of caspase-activated DNAse), Parp (poly ADP-Ribose polymerase), lamins and fodrin, and are directly responsible for many of the morphological features of apoptosis (Bratton *et al.*, 2000). For example, DNA fragmentation results from cleavage of a nuclease inhibitor, ICAD, which forms a complex with and inhibits the endonuclease CAD. Cleavage results in the release of CAD allowing it to act as a nuclease (Enari *et al.*, 1998). Parp has also been

demonstrated to negatively regulate endonuclease activity. On cleavage of Parp, this block is removed and the endonuclease is re-activated (Mc Gowan *et al.*, 1996).

At least two major mechanisms exist whereby initiator caspases are activated, one involves activation of caspase-8 and the other involves activation of caspase-9. Apoptosis induced by death receptors such as Fas (CD95/Apo-1) or TNF involves activation of caspase-8, whereas cell death induced by cytotoxic agents involves caspase-9. These two pathways ultimately result in activation of effector caspases, which in turn cleave death substrates producing the morphological features of apoptosis (Kauffman and Earnshaw, 2000).

The evidence for a central role of caspases in apoptosis and inflammation was obtained using potent peptide-based inhibitors. Design of caspase inhibitors was based on the specific tetrapeptide recognition sequence and cleavage after aspartate groups. Caspase inhibitors act by binding to the active site of caspases and form either a reversible or an irreversible linkage. Caspase inhibitor design includes a peptide recognition sequence attached to a functional group such as an aldehyde (CHO), chloromethylketone (CMK), fluoromethylketone (FMK) or fluoroacyloxymethylketone (FOAM). Inhibitors with a CHO group are reversible whereas those with a CMK, FMK or FOAM group are irreversible. The peptide recognition sequence corresponding to that found in endogenous substrates determines the specificity of a particular caspase. The use of these specific inhibitors has helped in investigating apoptotic signalling cascades involving caspases and to predict the biological role of these enzymes in whole cells and *in vivo*. For example, Ac-YVAD-CHO is a potent inhibitor of caspase-1, Ac-DEVD-CHO inhibits caspase-3 and caspase-7, whereas Ac-VAD-FMK is a competitive and irreversible inhibitor of all caspases (Garcia-Calvo *et al.*, 1998; Talanian *et al.*, 1997). The use of these specific caspase inhibitors has also led to the discovery of caspase-independent pathways. For example, Susin *et al.* (1999b) described the induction of apoptosis by microinjection of a novel apoptogenic protein, apoptosis-inducing factor (AIF), into Rat-1 cells. The general caspase inhibitor, z-VAD-fmk, did not inhibit the hallmarks of apoptosis, including chromatin condensation, DNA loss, and dissipation of the transmembrane potential ($\Delta\psi_m$) and exposure of phosphatidylserine on the outer leaflet of the plasma membrane. In the present study, the involvement of caspases in the mechanism of PBOX-6 induced apoptosis in CML cells was determined.

It is widely reported that mitochondria play a critical role in apoptosis. In response to a variety of apoptosis-inducing agents, cytochrome c is released into the cytosol (Scarlett and Murphy, 1997). Cytosolic cytochrome c forms an essential part of the vertebrate "apoptosome", which is composed of cytochrome c, Apaf 1 and pro-caspase 9. Creation of the apoptosome complex ultimately results in activation of caspase-9 which then processes and activates effector caspases, to orchestrate the biochemical execution of cells (Green and Reed, 1998; Li *et al.,* 1997). The mechanism of cytochrome c release from the mitochondria remains unclear. Many apoptotic pathways result in loss of mitochondrial transmembrane potential ($\Delta\psi_m$) as a result of opening of the permeability transition pore through which cytochrome c is released (Scarlett and Murphy, 1997) whereas others failed to observe changes in mitochondrial potential suggesting an alternative method of cytochrome c release exists (Gross *et al.*, 1999). In contrast, Chauhan *et al.* (1997) reported the induction of apoptosis in multiple myeloma cells using dexamethasone, and anti-Fas mAb, which occurred independent of the accumulation of cytosolic cytochrome c (Chauhan *et al.*, 1997). This evidence, and the lack of involvement of cytochrome c during cell death in *C. elegans* suggest the existence of cytochrome c independent pathways (Loeffler and Kroemer, 2000). In the current study the possible release of mitochondrial cytochrome c into the cytosol during PBOX-6-induced apoptosis was investigated.

Mitochondria are the primary site of reactive oxygen species (ROS) production within the cell. Under normal conditions, mitochondria possess an efficient biochemical defense mechanism to neutralise the effects mediated by reactive oxygen intermediates (ROI), such as production of the antioxidants superoxide dimutase, vitamin E and C, which can scavenge superoxide radicals. When produced in low concentrations, ROI can act as a second messenger in signal transduction pathways. However, when produced in excess, ROI can react with biological macromolecules such as lipids, proteins, nucleic acids and carbohydrates leading to the production of radicals. These hydroxy radicals cause oxidative damage to the cell, which may result in mitochondrial permeability transition and ultimately apoptosis (Kannan and Jain, 2000). Many reports suggest an increase in the production of ROI such as peroxides and superoxides during apoptosis. For example, Mc Gowan *et al.* (1996), reported the production of ROI during UV and drug-induced apoptosis in HL-60 and U937 cells. Apoptosis was accompanied by Parp cleavage and DNA fragmentation.

Pretreatment with antioxidants such as PDTC and the free radical scavenger Tempo, prevented Parp cleavage, DNA fragmentation and apoptosis in these cells. These workers concluded that production of ROI might act as common mediators for Parp cleavage, DNA fragmentation and apoptosis. In the present study we used a number of antioxidants to determine whether PBOX-6 induced apoptosis in CML cells was accompanied by an increase in ROS production.

The development of many types of cancer results from genetic alterations which lead to inhibition of apoptosis and the production of tumour cells. The products of several proto-oncogenes are tyrosine kinases, with kinase activities either increased or constitutively activated in the corresponding oncogene. For example, the Bcr-Abl fusion protein found in CML, which has increased tyrosine kinase activity, confers on hematopoietic cells the ability to survive treatments such as growth factor deprivation and cytotoxic drugs (Dubrez *et al.,* 1998). Tyrosine phosphorylation cascades play a fundamental part in the regulation of cell survival, growth and differentiation. Two antagonistic families of enzymes regulate the tyrosine kinase activity of proteins: tyrosine kinases, which add phosphate, and tyrosine phosphatases, which remove phosphate. A decrease in tyrosine phosphorylation during induction of apoptosis has been reported. For example, inhibitors of tyrosine phosphorylation, including genistein and tyrophostin, induce apoptosis in HL-60 and M07e human leukaemia cell lines (Yousefi *et al.,* 1994). However, the increased tyrosine phosphorylation of various proteins during apoptosis has also been described. Uckun *et al.* (1992) reported that ionising radiation induces enhanced tyrosine phosphorylation of multiple substrates in human-B-lymphocyte precursors, triggering apoptosis. An increase in tyrosine phosphorylation may become apparent within seconds to minutes after initiating the apoptotic cascade (Eischen *et al.,* 1994). This enhanced tyrosine phosphorylation, observed as part of a signal cascade may be due to protein tyrosine kinase activation, phosphatase inactivation, or a combination of these two mechanisms. In the current study the role played by tyrosine kinases in the apoptotic process was investigated with the use of a number of specific inhibitors including herbimycin A, tryphostin and genistein and, in particular, the tyrosine kinase activity of p210 Bcr-Abl was evaluated following treatment with PBOX-6.

Aims of this chapter

The present study indicates that some members of a novel series of pyrrolo-1,5-benzoxazepine compounds, induce apoptosis in three CML cell lines. Whether the apoptosis induced by a representative compound, PBOX-6, causes down-regulation of Bcr-Abl or its tyrosine kinase activity is investigated. Events associated with apoptosis such as DNA fragmentation, cytochrome c release, caspase activation, Parp cleavage and the generation of reactive oxygen intermediates are investigated in CML cells in response to PBOX-6 treatment.

3.2 Results

3.2.1 Pyrrolo-1,5-benzoxazepines induce apoptosis in K562 cells

The CML cell line, K562, was treated with some members of a series of pyrrolo-1,5-benzoxazepines (Fig. 3.1) and the extent of apoptosis was determined by centrifuging the cells onto a slide and staining with the RapiDiff kit. The characteristic morphological features of apoptosis such as cell shrinkage, chromatin condensation, nuclear fragmentation and membrane blebbing were visible in these cells. Fig 3.2 A and B are representative of K562 cells treated with either vehicle or PBOX-6 for 16h respectively. Vehicle treated cells have a large nucleus, whereas in PBOX-6 treated cells the nuclear DNA has become condensed and fragmented. In contrast, primary myeloid cells derived from normal bone marrow do not undergo apoptosis following treatment with PBOX-6 for 72h. Fig 3.2 C and D are representative of primary myeloid cells treated with either vehicle or PBOX-6 (10μM) for 72h respectively. To make a direct comparison of apoptotic potencies in K562 cells, these PBOX compounds were tested at the same time point (16h) and at the same concentration (10μM). Of the PBOX compounds tested, PBOX-3, -4, -5, -6 and -7 were found to induce apoptosis, exhibiting between 40-50% cell death, whereas other members of the PBOX series, PBOX-1 and -2, have no effect on cell viability (Fig. 3.3), suggesting a structure-activity relationship. Subsequent experiments were performed using PBOX-6 as the representative pro-apoptotic pyrrolo-1,5-benzoxazepine.

3.2.2 K562 cells are resistant to the induction of apoptosis by many commonly used chemotherapeutic drugs

It has previously been reported that K562 cells are highly resistant to many chemotherapeutic drugs (Martins *et al.,* 1997, Amarante-Mendes *et al.,* 1998b). To confirm this, K562 cells were treated with PBOX-6 (10μM), or various concentrations of the following commonly used chemotherapeutic agents: etoposide (50, 100 or 150μM), mitoxanthrone (0.5, 1.5 or 5μM) or ara-C (1, 3 or 10 μM), for 16h and the extent of apoptosis was determined by centrifuging an aliquot of cells onto a slide followed by RapiDiff staining and morphological examination. Treatment of K562 cells with PBOX-6 has been shown to

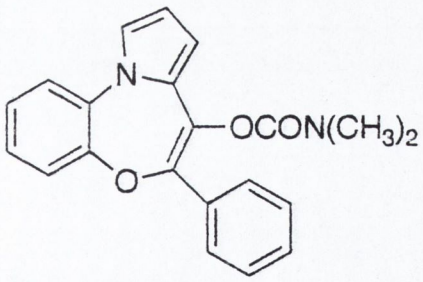

PBOX-1

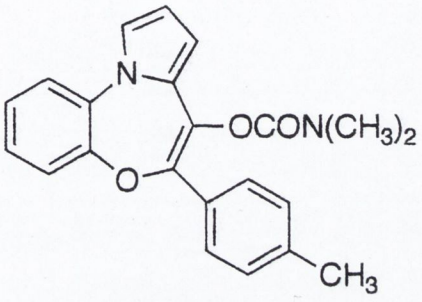

PBOX-2

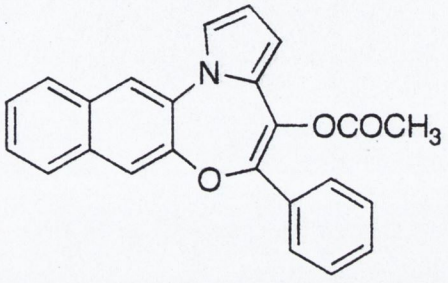

PBOX-3

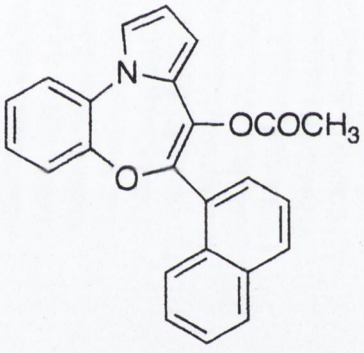

PBOX-4

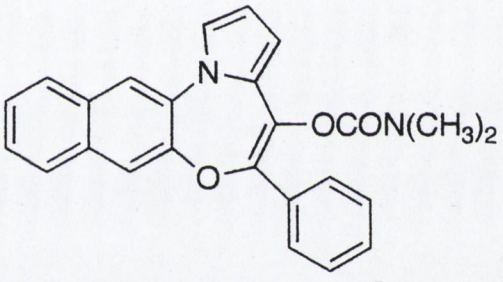

PBOX-5

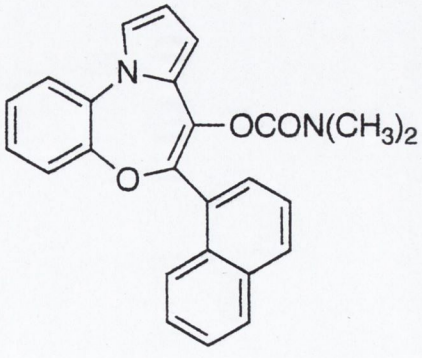

PBOX-6

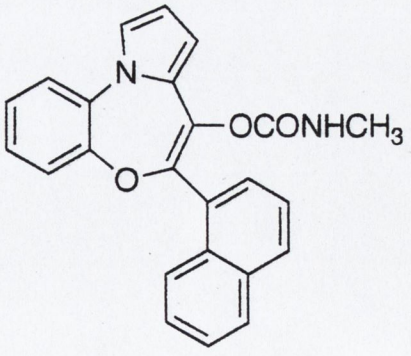

PBOX-7

Fig. 3.1 Structure of pyrrolo-1,5-benzoxazepines

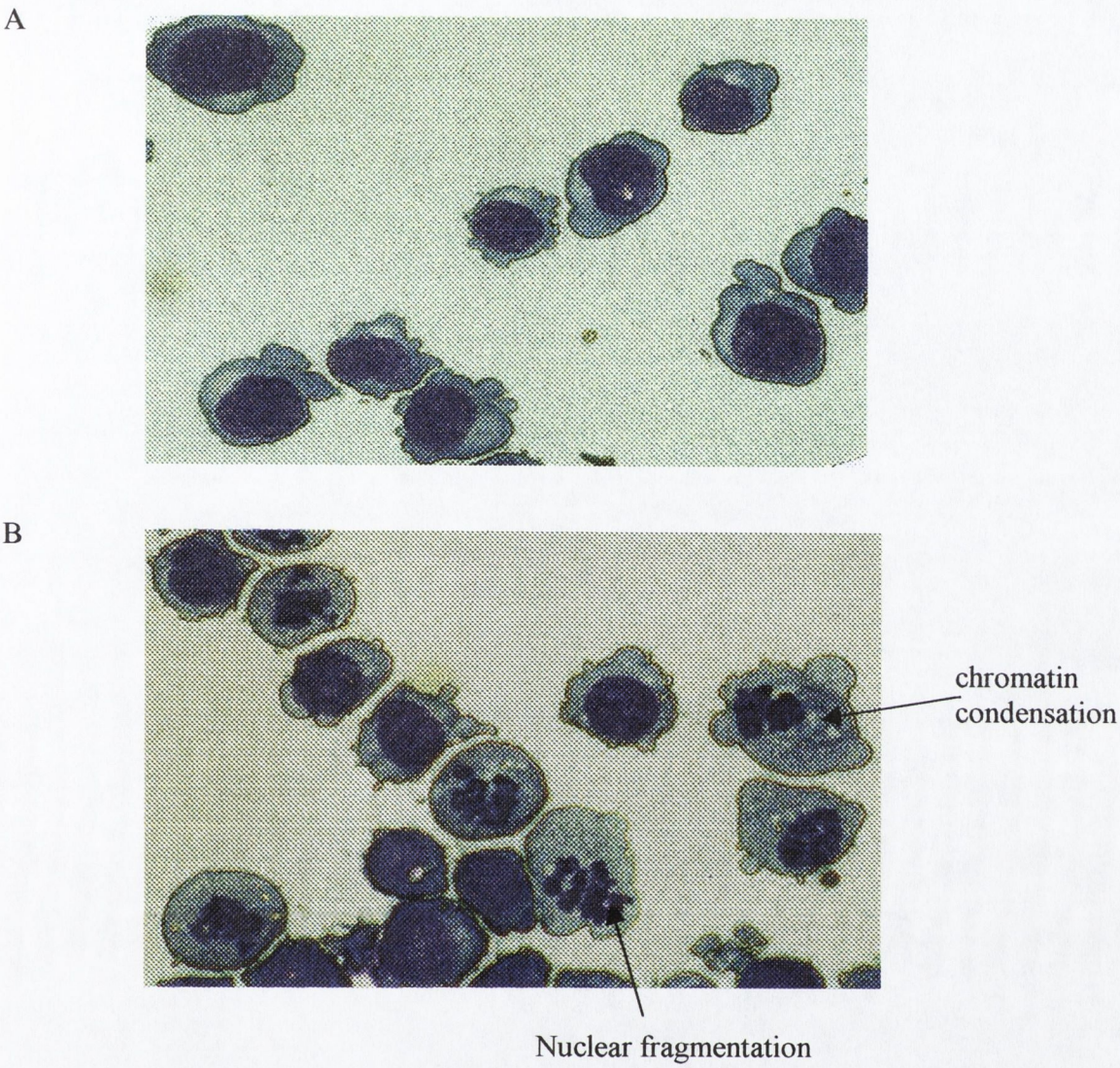

Fig. 3.2 Morphological features of K562 cells undergoing apoptosis following treatment with PBOX-6

Microscopic analysis of K562 cells was performed following treatment with either vehicle (1% (v/v) ethanol) or PBOX-6 (10μM) for 16h. Following treatment, cells were centrifuged onto a glass slide and stained using the RapiDiff kit. The nucleus of the cells was stained pink by dipping the slide 10 times in eosin Y and the cytoplasm was stained blue by dipping the slide 8 times in methylene blue. Vehicle treated cells (A) are characterised by a continuous plasma membrane and an intact nucleus. PBOX-6 treated cells (B) display the morphological features of apoptosis, which includes chromatin condensation and nuclear fragmentation.

C

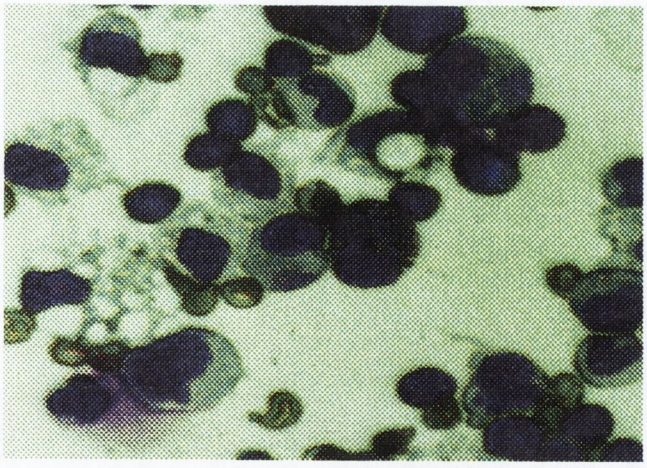

D

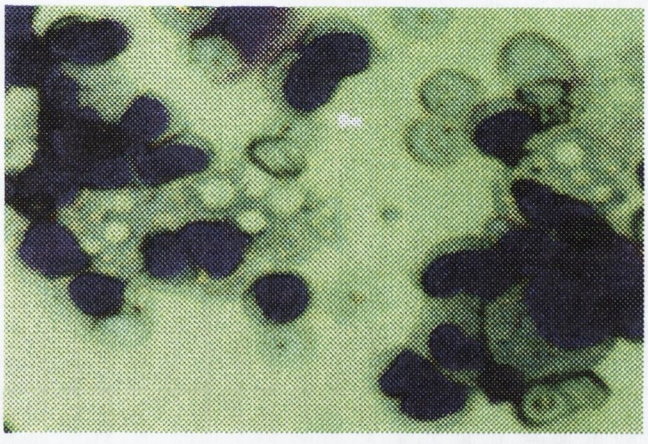

Fig. 3.2 Primary myeloid cells derived from normal bone marrow do not undergo apoptosis following treatment with PBOX-6

Microscopic analysis of primary bone marrow cells of the myeloid lineage, consisting of granulocyte, macrophage, monocyte and megakarayocytes, was performed following treatment with either (C) vehicle (1% (v/v) ethanol) or (D) PBOX-6 (10μM) for 72h. Cells were centrifuged onto a glass slide and stained using the RapiDiff kit as described in Section 2.4.

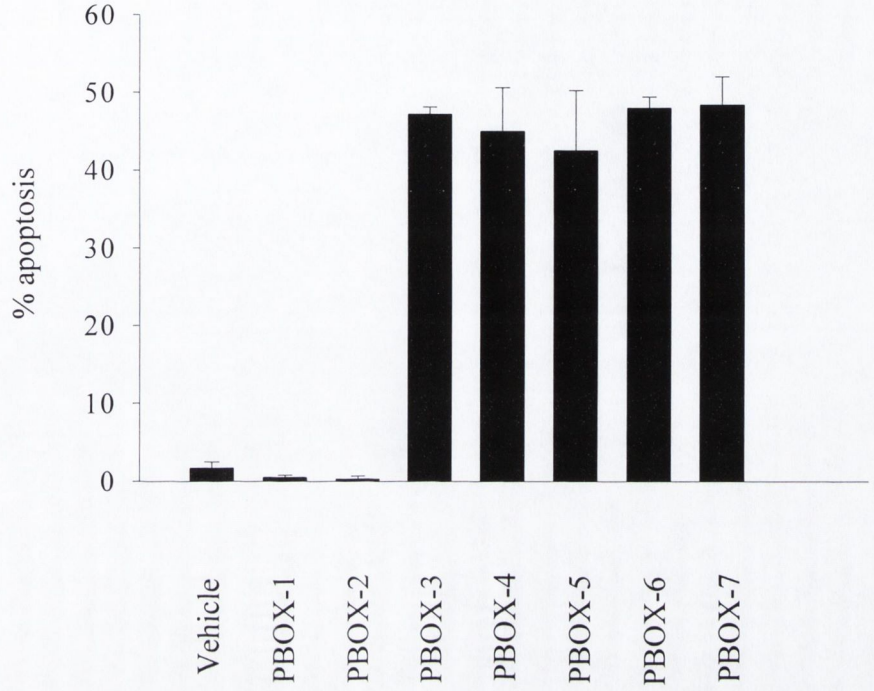

Fig. 3.3 Some pyrrolo-1, 5-benzoxazepines induce apoptosis in K562 cells

K562 cells were seeded at $3x10^5$ cells per ml and treated with the indicated PBOX compound (10μM) for 16h. Vehicle represents cells that were treated with ethanol (1% v/v). An aliquot of cells (150μl) was centrifuged onto a glass slide and stained using the RapiDiff kit. The extent of apoptosis was determined by microscopic examination of the morphological features as described in Section 2.4. Values represent the mean +/- the range of two separate experiments.

induce approximately 45% apoptosis, whereas treatment with etoposide, mitoxanthrone or ara-C does not induce apoptosis (Fig. 3.4).

3.2.3 PBOX-6 induces apoptosis in K562, LAMA 84 and KYO.1 cells in a dose- and time-dependent manner

In the three CML cell lines examined, K562, LAMA 84 and KYO.1, induction of apoptosis by PBOX-6 occurs in a dose- and time-dependent manner (Fig. 3.5A and B). The morphological features of apoptosis, which include cell shrinkage, chromatin condensation, DNA fragmentation and the production of apoptotic bodies, become apparent following a 4h treatment with PBOX-6 (10μM) and levels rise linearly until 16h, where approximately 40-50% of cells display apoptotic features. When CML cells were treated with a concentration range of PBOX-6 for 16h, apoptotic features were not visible with concentrations of 1μM or less.

3.2.4 PBOX-6 induces DNA fragmentation in K562, LAMA 84 and KYO.1 cells

DNA fragmentation is considered to be the hallmark of apoptosis, and produces 180-200 bp internucleosomal DNA fragments, which are visible as 'DNA ladders' on an agarose gel. DNA, extracted from all three CML cells following treatment with vehicle (1% (v/v) ethanol) or PBOX-6 (10μM) for 48h, was electrophoresed as described in Section 2.5 and a DNA laddering pattern was clearly visible in all three cell lines (Fig. 3.6).

3.2.5 PBOX-6-induced apoptosis is not preceded by a down-regulation in Bcr-Abl expression

Expression of the Bcr-Abl fusion protein in CML cells has been suggested to be responsible for the resistance of CML cells to many apoptotic agents (Martins *et al.*, 1997). It is widely agreed that the mechanism by which Bcr-Abl may cause the accumulation of leukaemic blasts is by inhibition of apoptosis, rather than by increasing the rate of cell division (Kabarowski *et al.*, 1994; Rowley *et al.*, 1996).

To investigate the effect of PBOX-6 on Bcr-Abl expression, levels of p210 were determined by Western blot analysis of protein extracts isolated from control and PBOX-6 treated CML cells. In the three CML cell lines, any down-regulation of Bcr-Abl is not be

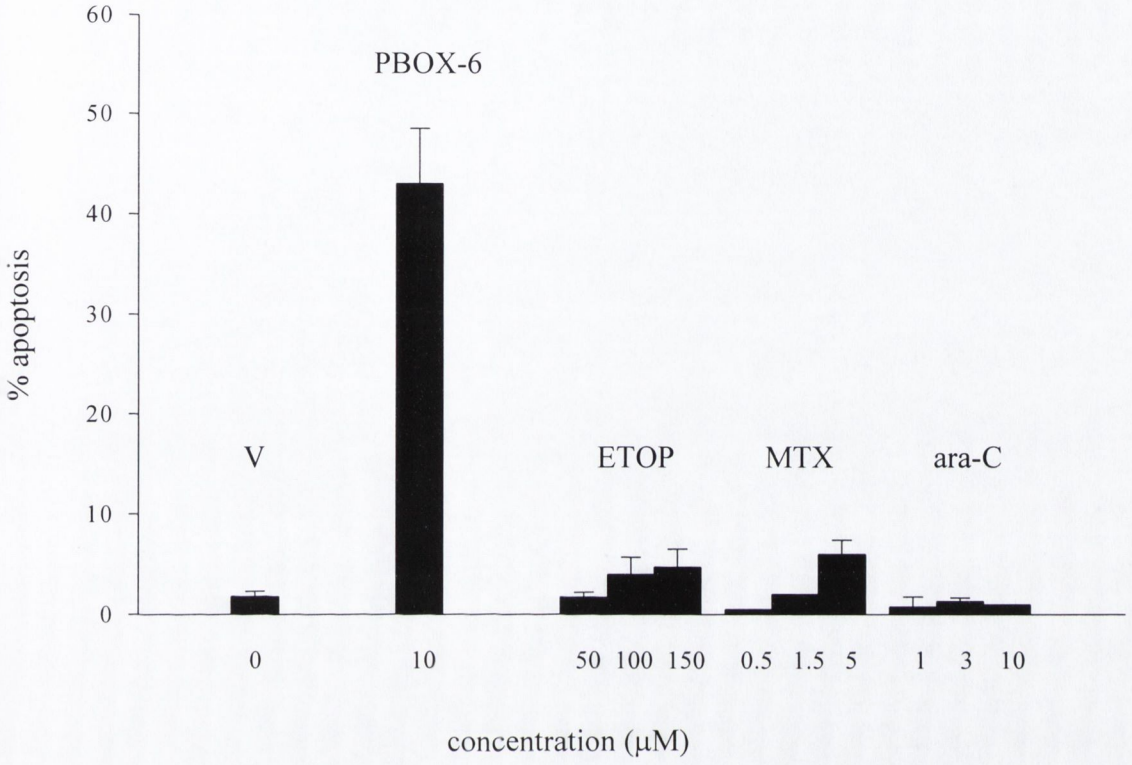

Fig. 3.4 K562 cells are resistant to apoptosis induced by etoposide, mitoxanthrone and ara-C

K562 cells were seeded at a density of $3x10^5$ cells per ml and treated for 16h with vehicle (1% (v/v) ethanol) (V), PBOX-6 (10μM), etoposide (ETOP) (50, 100 or 150μM), mitoxanthrone (MTX) (0.5, 1.5 or 5μM) or ara-C (1, 3 or 10μM). The extent of apoptosis was determined by centrifuging an aliquot of cells (150μl) onto a glass slide and staining the cells using the RapiDiff kit as described in Section 2.4. Results represent the mean +/- S.E.M. of three separate experiments.

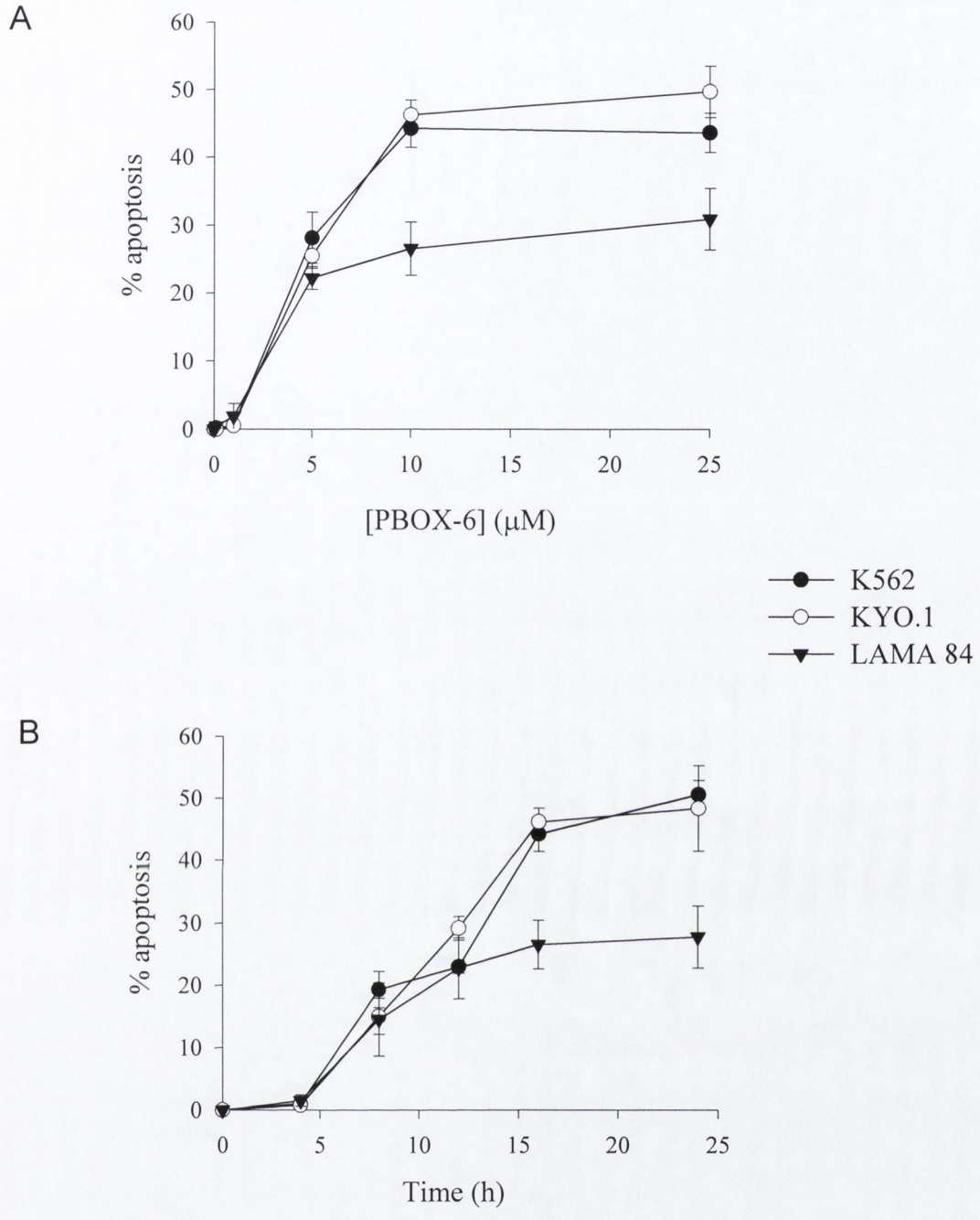

Fig. 3.5 PBOX-6-induced apoptosis in CML cells is dose- and time-dependent

Cells were seeded at $3x10^5$ cells per ml and were treated with (A) a range (0-25μM) of concentrations of PBOX-6 for 16h, or (B) PBOX-6 (10μM) for a period of 4, 8, 12, 16 and 24h. The percent apoptosis was determined by centrifugation onto glass slides followed by staining with the RapiDiff kit as described in Materials and Methods. Values represent the mean +/- S.E.M of three separate experiments.

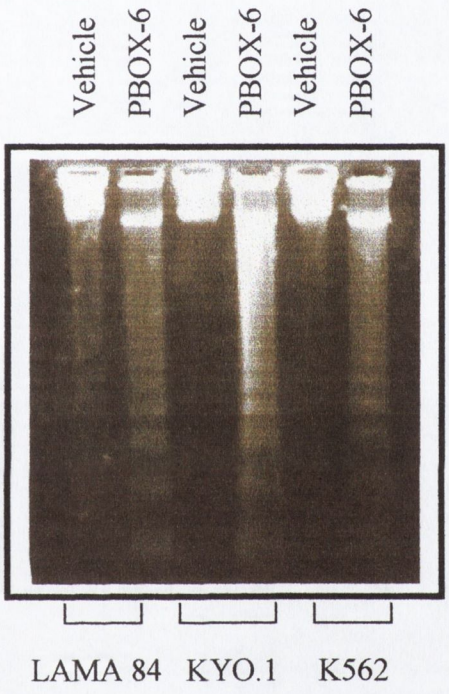

Fig. 3.6 PBOX-6 induces internucleosomal DNA fragmentation in CML cells

Cells ($1x10^7$/flask) were treated with either vehicle (1% (v/v) ethanol) or PBOX-6 (10μM) for 48h. Cells were lysed and the DNA was extracted as described in Section 2.5. An aliquot of DNA (45μl) was mixed with loading dye (5μl) and resolved on an agarose gel (1.5%) for 4h at a constant voltage of 55V. DNA ladders were visible under UV light using a UVP gel documentation system. Results are representative of at least three separate experiments.

detected up to 24h following treatment with PBOX-6 (Fig.3.7A, 3.8A and 3.9A), where approximately 50% of cells have undergone apoptosis. A decrease in Bcr-Abl expression is detected in K562 and LAMA 84 cells, but only after a 24h treatment. To ensure that an equal amount of protein was loaded, blots were stripped and re-probed with an antibody against β-actin as a loading control (Fig. 3.7B, 3.8B and 3.9B). These results suggest that down-regulation of Bcr-Abl is not involved in the induction of apoptosis by PBOX-6.

3.2.6 Investigation into the tyrosine phosphorylation status of the Abl tyrosine kinase and other proteins during PBOX-6 induced apoptosis in CML cells

3.2.6.1 PBOX-6-induced apoptosis is not mediated by a decrease in protein tyrosine phosphorylation

Tyrosine phosphorylation is involved in the regulation of many apoptotic pathways. Protein tyrosine kinases and phosphatases jointly maintain the tyrosine phosphorylation status of cellular proteins (Yousefi *et al.,* 1994). Transformation by the *bcr-abl* oncogene is absolutely dependent on its tyrosine kinase activity, and the recently discovered Abl tyrosine kinase inhibitor, STI571, has been shown to induce apoptosis in Bcr-Abl positive cell lines (Weisberg and Griffin, 2000).

To determine the effect of PBOX-6 on the tyrosine phosphorylation status of proteins in CML cells, and whether it causes inhibition of the Abl tyrosine kinase, a Western blot assay was set up using an antibody directed against the phosphorylated form of tyrosine residues. In the three CML cells examined, the tyrosine phosphorylation status of proteins remain unchanged up to 24h following treatment with PBOX-6 (Fig. 3.10). A decrease in tyrosine phosphorylation is not visible in K562 and KYO.1 cells even up to 48h following treatment with PBOX-6. In LAMA 84 cells, a decrease in the tyrosine phosphorylation status of some proteins is visible after a 24h treatment with PBOX-6, at which point approximately 50% of the cells have undergone apoptosis.

Having already established that down-regulation of Bcr-Abl expression is not involved in the induction of apoptosis by PBOX-6, these results further suggest that inhibition of the Abl tyrosine kinase activity is not part of the upstream events associated with PBOX-6-induced apoptosis.

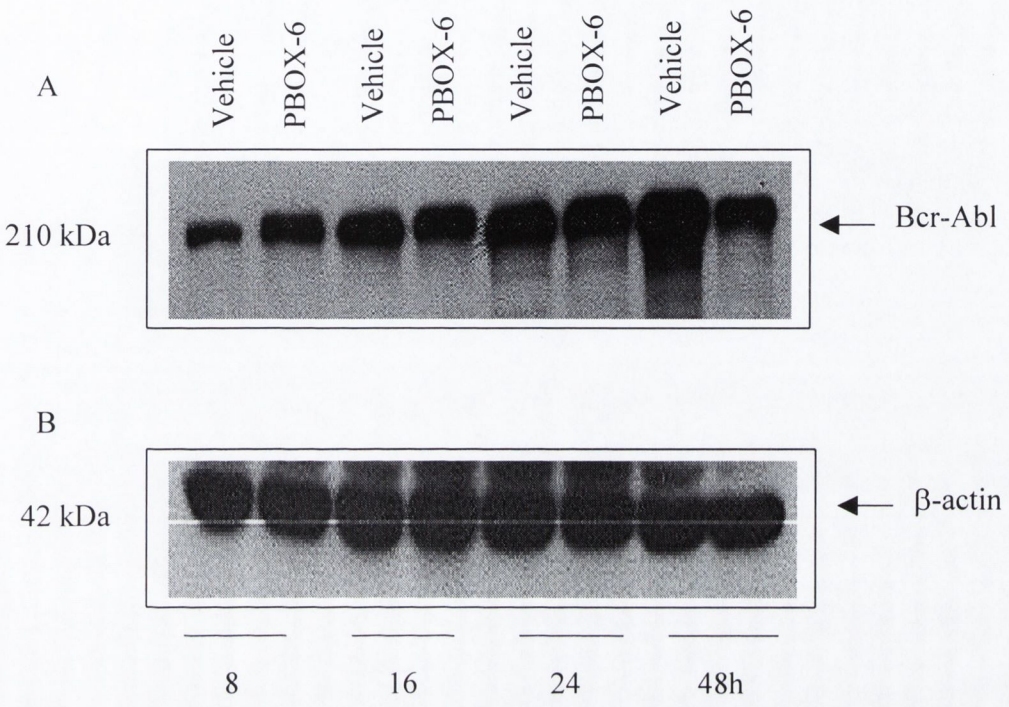

Fig. 3.7 PBOX-6-induced apoptosis in K562 cells is not preceded by the down-regulation of Bcr-Abl

Cytosolic extracts were prepared from K562 cells following treatment with either vehicle (1% (v/v) ethanol) or PBOX-6 (10μM) for 8, 16, 24 and 48h. Protein (40μg) was resolved by SDS-PAGE, transferred onto PVDF membrane overnight and probed with anti-c-abl antibody (A). Blots were stripped and re-probed with an antibody against β-actin as a loading control as described in Section 2.6.4 (B). Results are representative of at least two separate experiments.

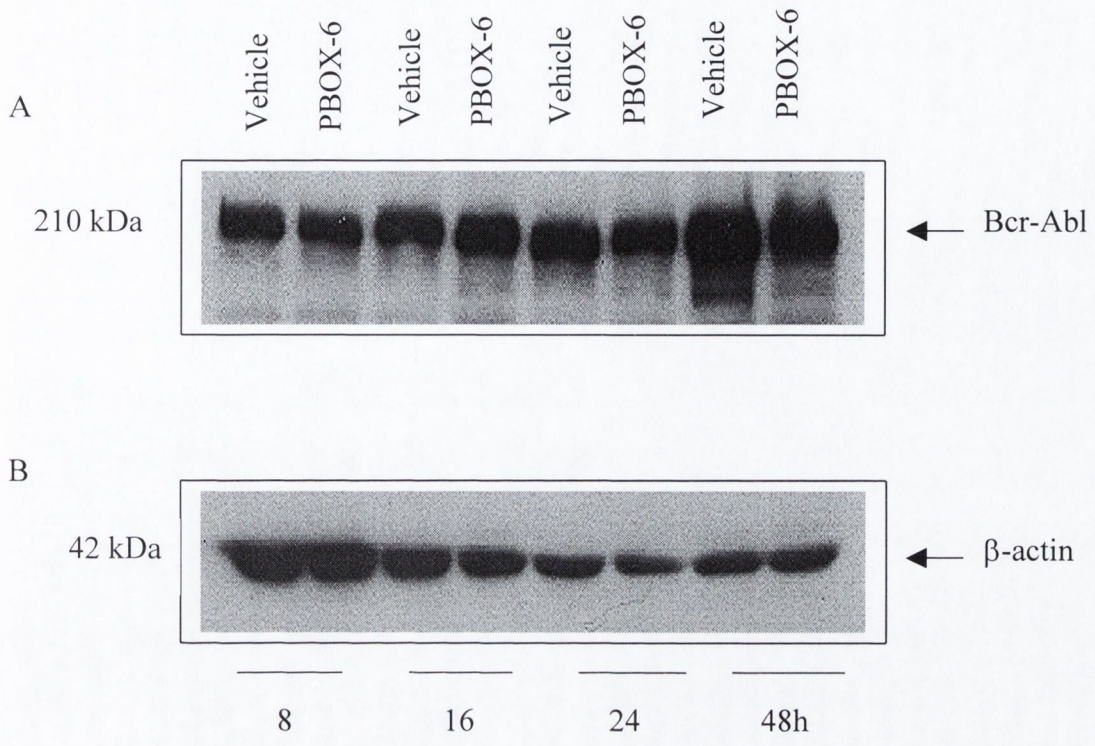

Fig. 3.8 PBOX-6-induced apoptosis in KYO.1 cells is not preceded by the down-regulation of Bcr-Abl

Cytosolic extracts were prepared from KYO.1 cells following treatment with either vehicle (1% (v/v) ethanol) or PBOX-6 (10μM) for 8, 16, 24 and 48h. Cytosolic extracts were prepared and protein (40μg) was resolved by SDS-PAGE, transferred onto PVDF membrane overnight and probed with anti-c-abl antibody (A). Blots were stripped and re-probed with an antibody against β-actin as a loading control as described in Section 2.6.4 (B). Results are representative of at least two separate experiments.

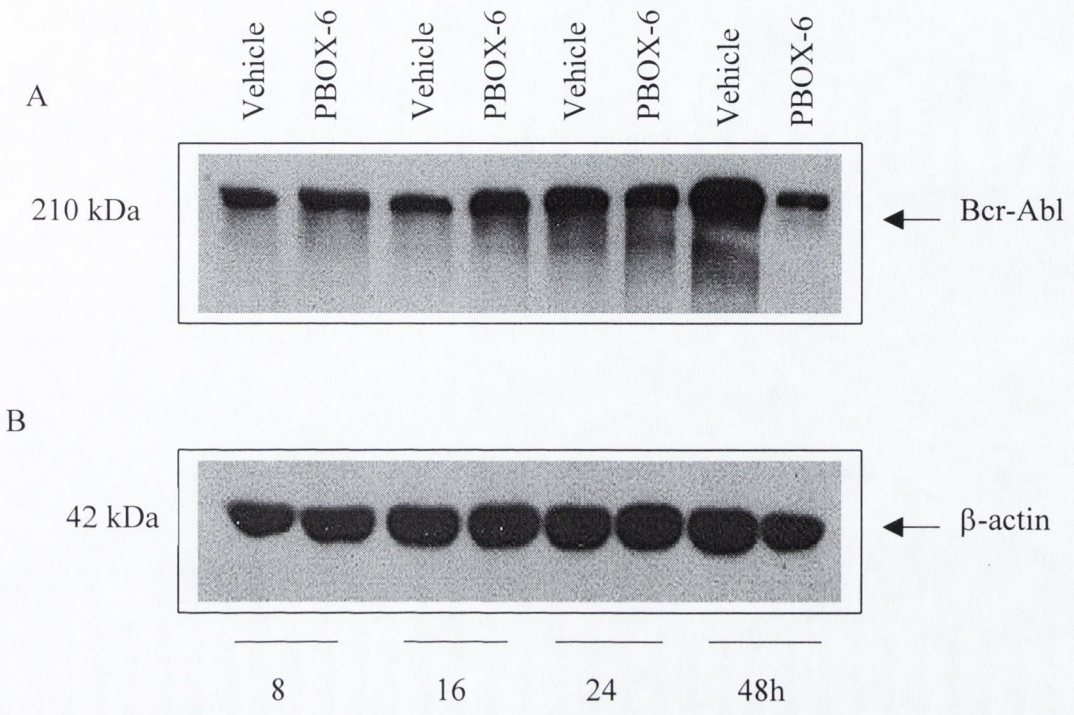

Fig. 3.9 PBOX-6-induced apoptosis in LAMA 84 cells is not preceded by the down-regulation of Bcr-Abl

Cytosolic extracts were prepared from LAMA 84 cells following treatment with either vehicle (1% (v/v) ethanol) or PBOX-6 (10μM) for 8, 16, 24 and 48h. Protein (40μg) was resolved by SDS-PAGE, transferred onto PVDF overnight and probed with anti-c-abl antibody (A). Blots were stripped and re-probed with an antibody against β-actin as a loading control as described in Section 2.6.4 (B). Results are representative of at least two separate experiments.

Fig. 3.10 PBOX-6-induced apoptosis in CML cells is not mediated by a change in the tyrosine phosphorylation status of proteins

Whole cell extracts were prepared from (A) K562, (B) KYO.1 and (C) LAMA 84 cells following treatment with either vehicle (1% (v/v) ethanol) or PBOX-6 (10μM) for 8, 16, 24 and 48h. Protein (40μg) was resolved by SDS-PAGE, transferred onto PVDF membrane and probed with anti-phosphotyrosine antibody. Results are representative of at least two separate experiments

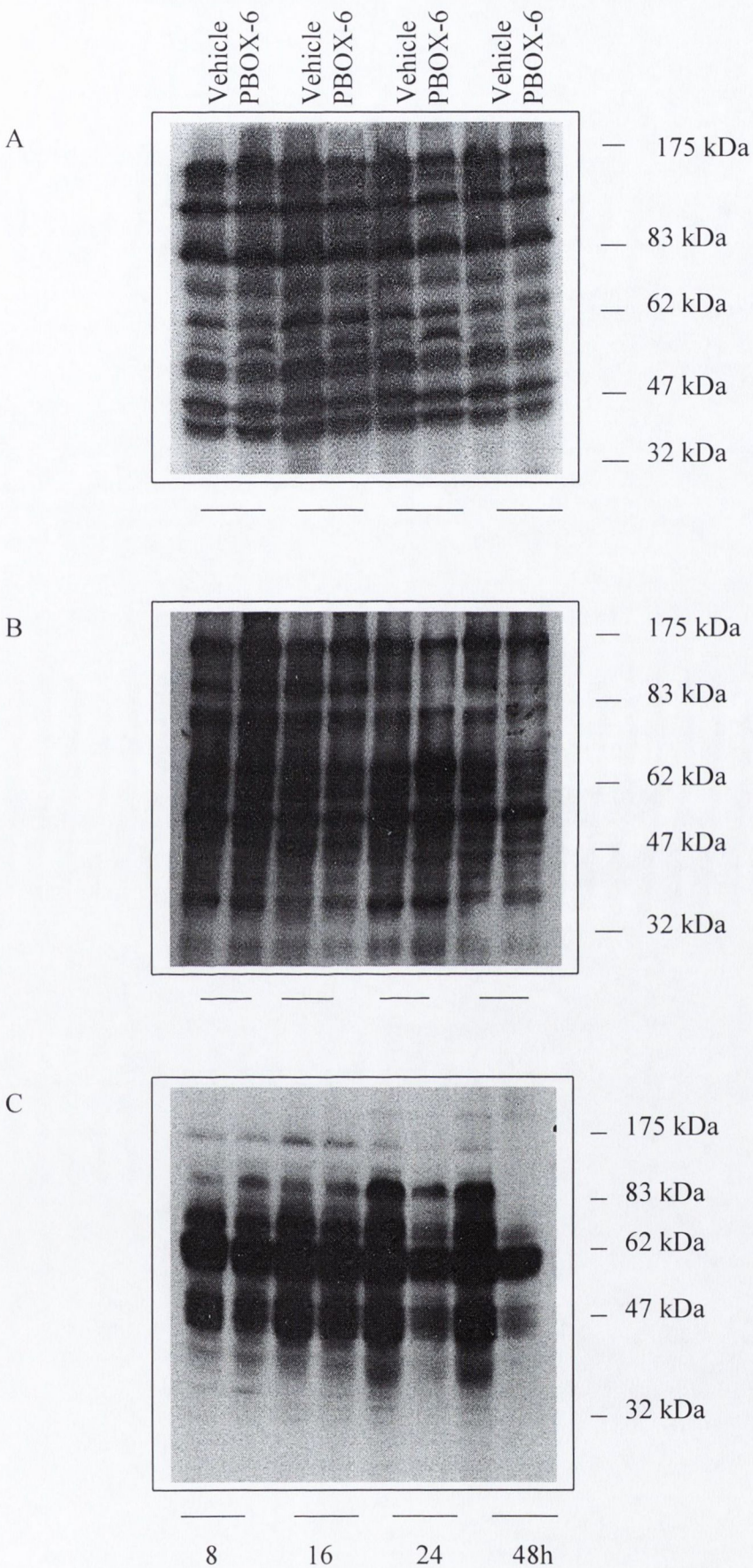
Vehicle
PBOX-6
Vehicle
PBOX-6
Vehicle
PBOX-6
Vehicle
PBOX-6
A
175 kDa
83 kDa
62 kDa
47 kDa
32 kDa
B
175 kDa
83 kDa
62 kDa
47 kDa
32 kDa
C
175 kDa
83 kDa
62 kDa
47 kDa
32 kDa
8
16
24
48h

3.2.6.2 PBOX-6 increases the tyrosine phosphorylation of two proteins in K562 cells

Close examination of tyrosine phosphorylation blots from K562 cells treated with PBOX-6 showed an increase in the phosphorylation status of proteins, approximately 60-70 kDa, following treatment with PBOX-6 for 8h and 16h. In order to investigate this further, shorter time courses were performed. A time course ranging from 5 min up to 16h was thus carried out. Treatment of K562 cells with PBOX-6 (10μM) for 5, 15 or 30 min, does not have any effect on the tyrosine phosphorylation status of proteins (Fig. 3.11A). However, an increase in the tyrosine phosphorylation status of two proteins has been detected in K562 cells following treatment with PBOX-6 for 16h (Fig. 3.11B). These two proteins, as yet unidentified, are approximately 63 kDa and 71kDa in size.

In order to ensure that proteins observed are indeed phosphorylated specifically on tyrosine residues, a control experiment was performed in which the membrane was incubated with a solution containing anti-phosphotyrosine antibody and an excess of phosphotyrosine (1mM). The excess phosphotyrosine in solution will bind to the anti-phosphotyrosine antibody, thus preventing it from binding to tyrosine-phosphorylated proteins on the membrane. Results show the disappearance of all tyrosine-phosphorylated bands following the addition of excess phosphotyrosine (Fig. 3.12), indicating the specificity of the antibody for tyrosine-phosphorylated residues.

3.2.6.3 Genistein prevents tyrosine phosphorylation and the induction of apoptosis by PBOX-6

Pretreatment of K562 cells with the broad range phosphotyrosine kinase inhibitor, genistein (100μM in DMSO) for 1h prior to treatment with PBOX-6 (10μM) for a further 16h prevents the phosphorylation of these two proteins (Fig. 3.13A) as shown by Western blot analysis. An aliquot of cells (150μl) was centrifuged onto a glass slide, stained using the RapiDiff kit and the extent of apoptosis was determined by morphological examination. Results demonstrate that pretreatment of K562 with genistein prior to treatment with PBOX-6 completely inhibits the induction of apoptosis (Fig. 3.13B). Pretreatment of K562 cells with herbimycin A (5μM in DMSO) and tyrophostin (200μM in DMSO), also commonly used tyrosine kinase inhibitors, reduces the extent of apoptosis induced by PBOX-6 (Fig. 3.14), as shown by the centrifugation of cells and RapiDiff staining, although they are themselves

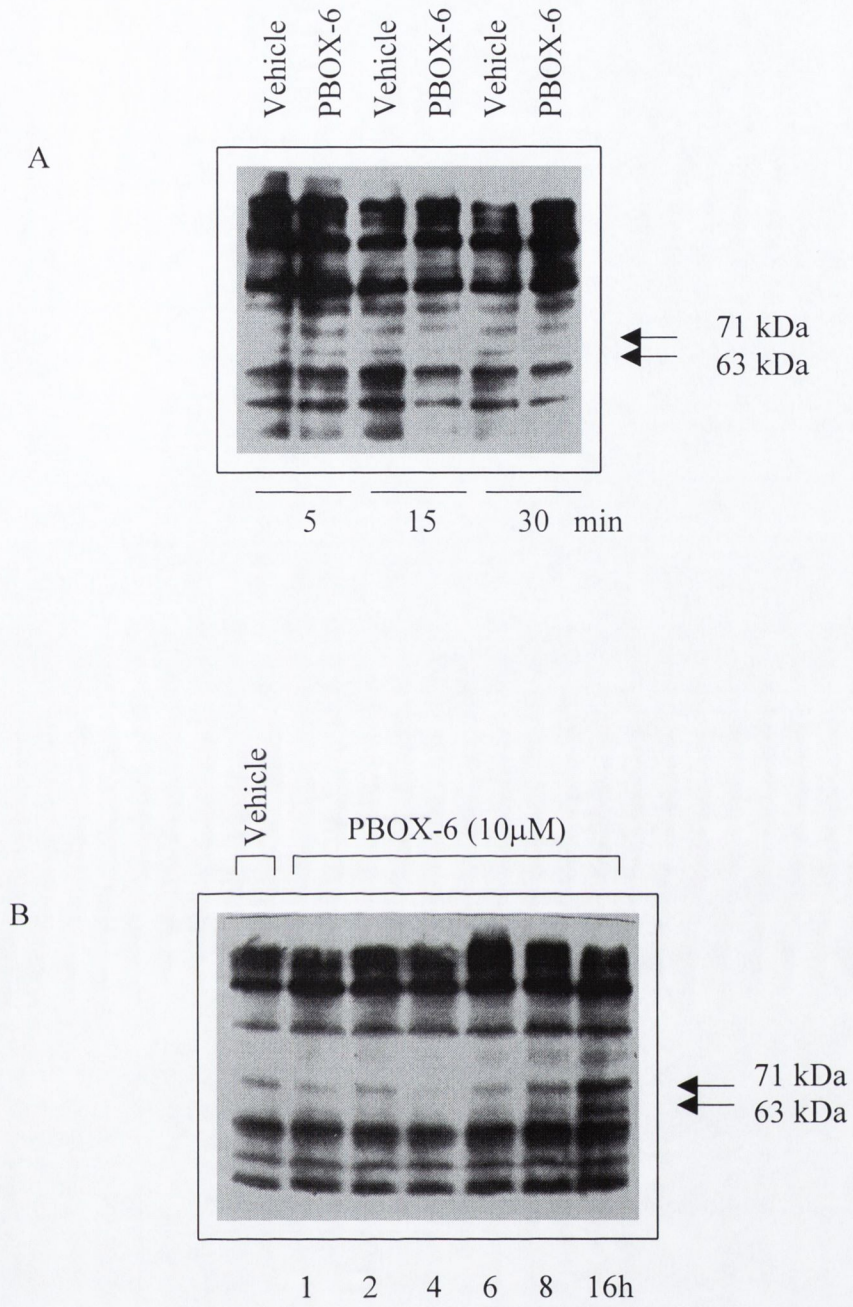

Fig. 3.11 PBOX-6 alters the tyrosine phosphorylation status of proteins in K562 cells

K562 cells ($5x10^6$/flask) were treated with vehicle (1% (v/v) ethanol) or PBOX-6 (10μM) for either (A) 5, 15 and 30 min or (B) 1, 2, 4, 6, 8, and 16h. Cytosolic extracts were prepared as described in Section 2.10. Protein (40μg) was resolved by SDS-PAGE, transferred onto PVDF membrane and probed with anti-phosphotyrosine antibody. Results are representative of at least two separate experiments.

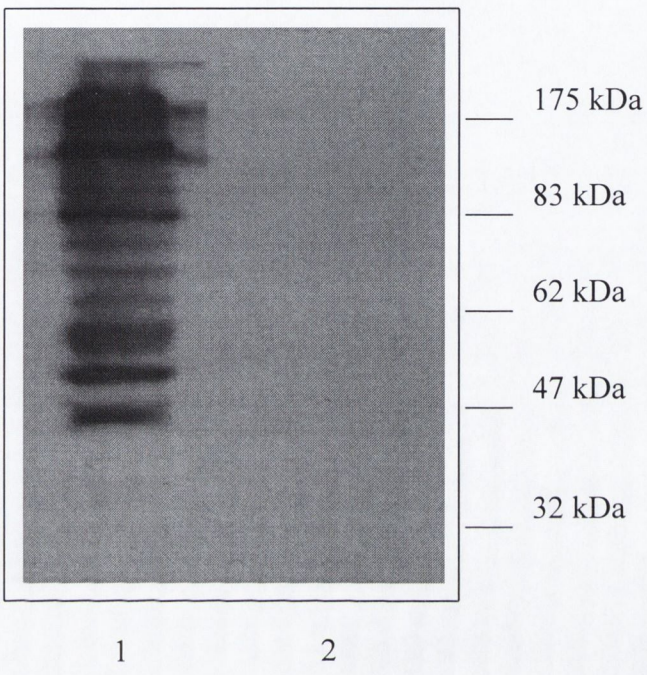

Fig. 3.12 Anti-phosphotyrosine antibody binds specifically to tyrosine phosphorylated residues

Whole cell extracts from untreated K562 cells were prepared as described in Section 2.7. Protein (40μg) was resolved by SDS-PAGE, transferred onto PVDF membrane and probed for 1h with either anti-phosphotyrosine antibody (lane 1) or anti-phosphotyrosine antibody plus an excess phosphotyrosine (1mM) (lane 2). Both membranes were washed and probed with goat anti-mouse-HRP-conjugated secondary antibody. Results are representative of at least two separate experiments.

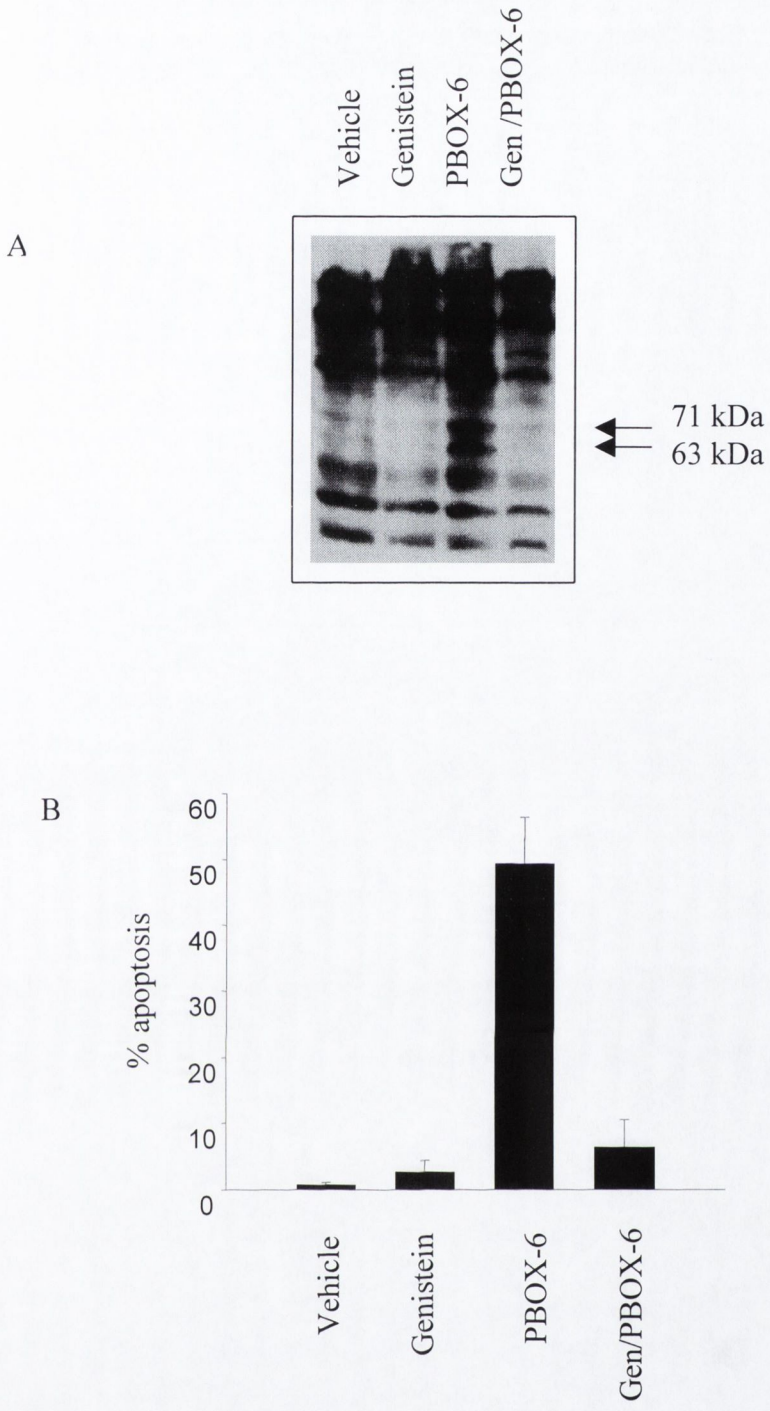

Fig. 3.13 Pretreatment of K562 cells with the tyrosine kinase inhibitor, genistein, prevents protein tyrosine phosphorylation and inhibits apoptosis induced by PBOX-6

K562 cells were seeded at (A) $5x10^6$ cells per sample or (B) $3x10^5$ cells per ml and pretreated with genistein (100μM) for 1h prior to treatment with PBOX-6 (10μM) for a further 16h. Vehicle treatment represents cells treated with ethanol (1% v/v), DMSO (0.5% v/v) for 17h. In (A) cytosolic extracts were prepared and protein (40μg) was resolved by SDS-PAGE and probed with anti-phosphotyrosine antibody as described in Section 2.7. Results are representative of at least 3 separate experiments. In (B) the extent of apoptosis was determined by staining the cells using the RapiDiff kit, followed by morphological examination as described in Section 2.4. Results represent the mean +/- S.E.M of three separate experiments.

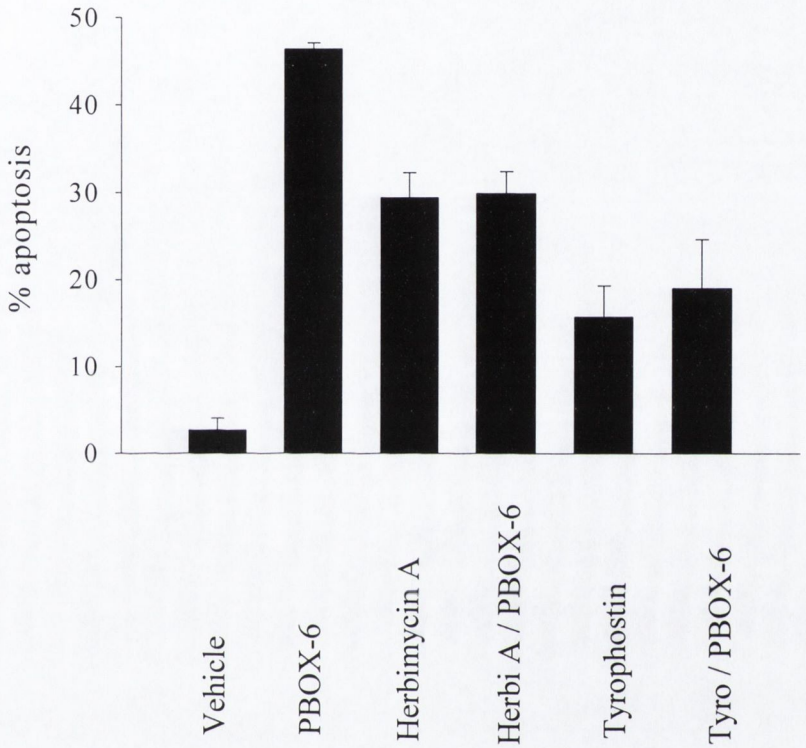

Fig. 3.14 Herbimycin A and tyrophostin reduce but do not completely inhibit PBOX-6 induced apoptosis in K562 cells

Cells were seeded at $3x10^5$ cells per ml and were pretreated with either herbimycin A (5μM) or tyrophostin (200μM) for 1h prior to treatment with PBOX-6 (10μM) for a further 16h. Vehicle represents cells treated with ethanol (1% v/v) and DMSO (0.5% v/v) for 17h. The extent of apoptosis was determined by centrifuging the cells onto a slide and staining with the RapiDiff kit, followed by morphological examination as described in Section 2.4. Results represent the mean +/- S.E.M of three separate experiments.

somewhat cytotoxic to the cells. Herbimycin A and tyrophostin alone induce approximately 30% and 15% apoptosis respectively. Therefore, it was decided that Western blot analysis of K562 cells treated with these two compounds would be unsuitable. However, these results suggest that an increase in the tyrosine phosphorylation status of the two proteins, or other proteins inhibited by genistein, may be involved in the pathway in which PBOX-6 induces apoptosis in K562 cells.

3.2.6.4 Investigation into the identity of two tyrosine phosphorylated proteins (63 kDa and 71 kDa) using specific tyrosine kinase inhibitors

In an attempt to identify the proteins phosphorylated by PBOX-6, which may include tyrosine kinases which are themselves phosphorylated on tyrosine residues, K562 cells were pretreated for 1h with a series of specific tyrosine kinase inhibitors, prior to treatment with PBOX-6 (10μM) for a further 16h. Morphological examination of the cells was carried out and the extent of apoptosis was determined. Three tyrosine kinase inhibitors were used which inhibit the tyrosine kinase activity of proteins close to the approximate size of the proteins phosphorylated by PBOX-6. These inhibitors included damnacanthal (p56 LCK inhibitor), geldanamycin (p60 SRC inhibitor) and piceatannol (p72 SYK inhibitor). Results reveal that pretreatment of K562 cells with these inhibitors failed to protect against PBOX-6 induced apoptosis (Fig. 3.15) suggesting that the tyrosine kinases inhibited by these compounds are not involved in the pathway in which PBOX-6 induces apoptosis. However, it was found that geldanamycin and piceatannol themselves induce a small extent of apoptosis in these cells.

3.2.7 PBOX-6-induced apoptosis does not result in an increase in cytoplasmic cytochrome c levels in CML cells

Release of cytochrome c from mitochondria has been shown to be an important event in triggering apoptosis in many cell systems (Scarlett and Murphy, 1997). However, in recent years other workers have shown that the release of cytochrome c is not necessarily an obligatory event in the apoptotic process (Chauchan *et al.*, 1997).

It has previously been shown that staurosporine treatment of HL-60 cells causes the release of cytochrome c into the cytosol (Yang *et al.*, 1997). Therefore, treatment of HL-60 cells with staurosporine (1μM) for 6h was used as a positive control in setting up the assay

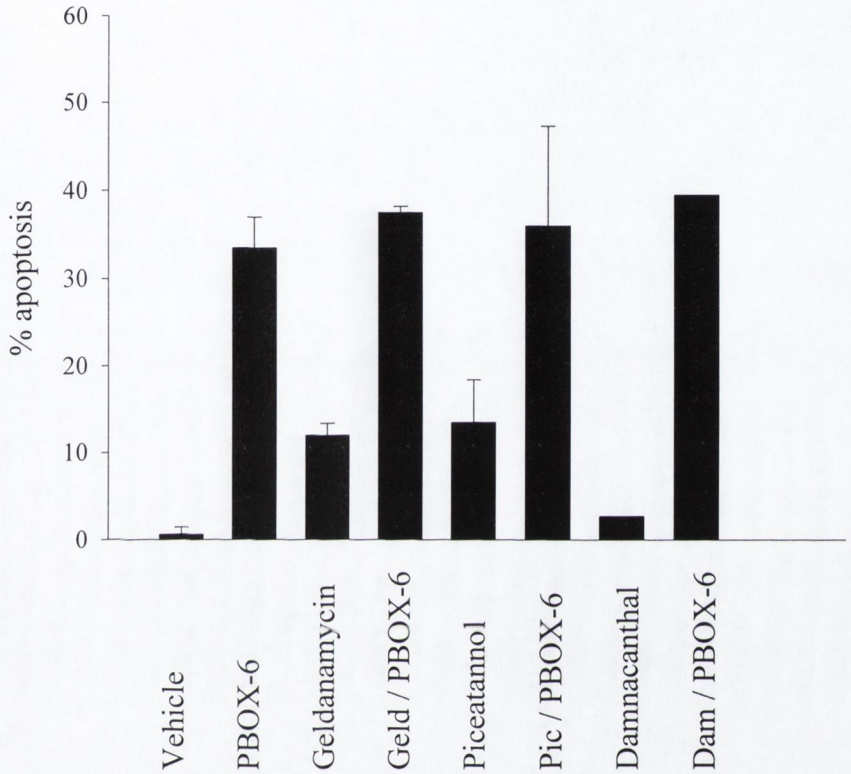

Fig. 3.15 Three tyrosine kinase inhibitors fail to prevent PBOX-6 induced apoptosis in K562 cells

K562 cells were seeded at $3x10^5$ cells per ml and pretreated with geldanamycin (2μM), piceatannol (20μM) or damnacanthal (1μM) for 1h prior to treatment with PBOX-6 (10μM) for a further 16h. Vehicle represents cells treated with ethanol (1% v/v), DMSO (0.5% v/v) for 17h. The extent of apoptosis was determined by centrifuging an aliquot of cells (150μl) onto a slide and staining with the RapiDiff kit as described in Section 2.4. Results represent the mean +/- the range of two separate experiments.

(Fig. 3.16). To determine whether cytochrome c release is involved in PBOX-6-mediated apoptosis in CML cells, K562, KYO.1 and LAMA 84 cells were exposed to the compound for 16h, and its effect on the accumulation of cytochrome c in the cytosol was determined. Cytosolic fractions were isolated and analysed for levels of cytochrome c by Western blotting. Results demonstrate that levels of cytochrome c in the cytosol remain unchanged in CML cells following a 16h treatment with PBOX-6 (Fig. 3.17 A, B, C).

Cytochrome c is evident in the cytosol of untreated and vehicle treated CML cells. In order to ensure that cytochrome c is not all non-specifically released during preparation of the cytosolic fractions, the remaining pellet was solubilised. Western blot analysis shows that the majority of cytochrome c remains in the pellet (Fig. 3.18). This suggests that the cytochrome c present in the cytosolic fractions of untreated and vehicle treated cells is only a small fraction of the unreleased protein present in the mitochondria. The cytochrome c detected in the cytosol of untreated and treated samples is probably due to some non-specific leakage of the protein from the mitochondria during sample preparation.

3.2.8 Antioxidants do not protect against PBOX-6-induced apoptosis in K562 cells

Several observations suggest an involvement of reactive oxygen intermediates (ROI) in the signal transduction pathway leading to apoptosis and antioxidants such as *N*-acetylcysteine (NAC) have been shown to block apoptosis in a variety of cell systems (Jacobson, 1996).

To determine whether the induction of apoptosis in K562 cells by PBOX-6 involves the production of ROIs, cells were pretreated with Vitamin E or *N*-acetylcysteine for 24h or 1h respectively, prior to treatment with PBOX-6 for a further 16h. The extent of apoptosis was determined by centrifuging the cells onto slides and staining with the RapiDiff kit as described in Section 2.4. Results show that pretreatment of cells with these antioxidants, does not protect against PBOX-6-induced apoptosis (Fig. 3.19 A and B) suggesting that the production of ROI is not involved in the mechanism by which PBOX-6 induces apoptosis in K562 cells. As a positive control, HL-60 cells were pretreated with the antioxidants Vitamin E or *N*-acetylcysteine prior to treatment with the apoptosis inducing agents, UV irradiation or H_2O_2 respectively. Results show that pretreatment of HL-60 cells with these antioxidants

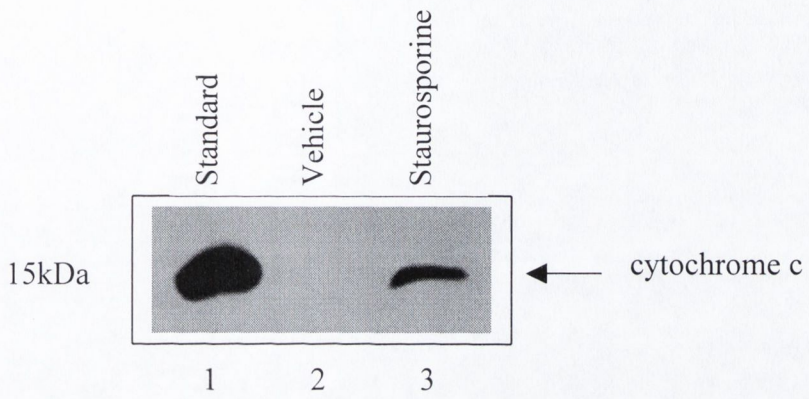

Fig. 3.16 Mitochondrial cytochrome c is released into the cytosol during staurosporine induced apoptosis in HL-60 cells

HL-60 cells were treated with either (lane 2-3), vehicle (0.1% (v/v) DMSO) or staurosporine (1μM) for 6h and cytosolic extracts were prepared as described in Section 2.8. Protein (30μg) was resolved by SDS-PAGE, transferred onto PVDF membrane and probed with anti-cytochrome c antibody. Horse cytochrome c (10μg/ml) was used as a standard (lane 1). Results are representative of at least two separate experiments.

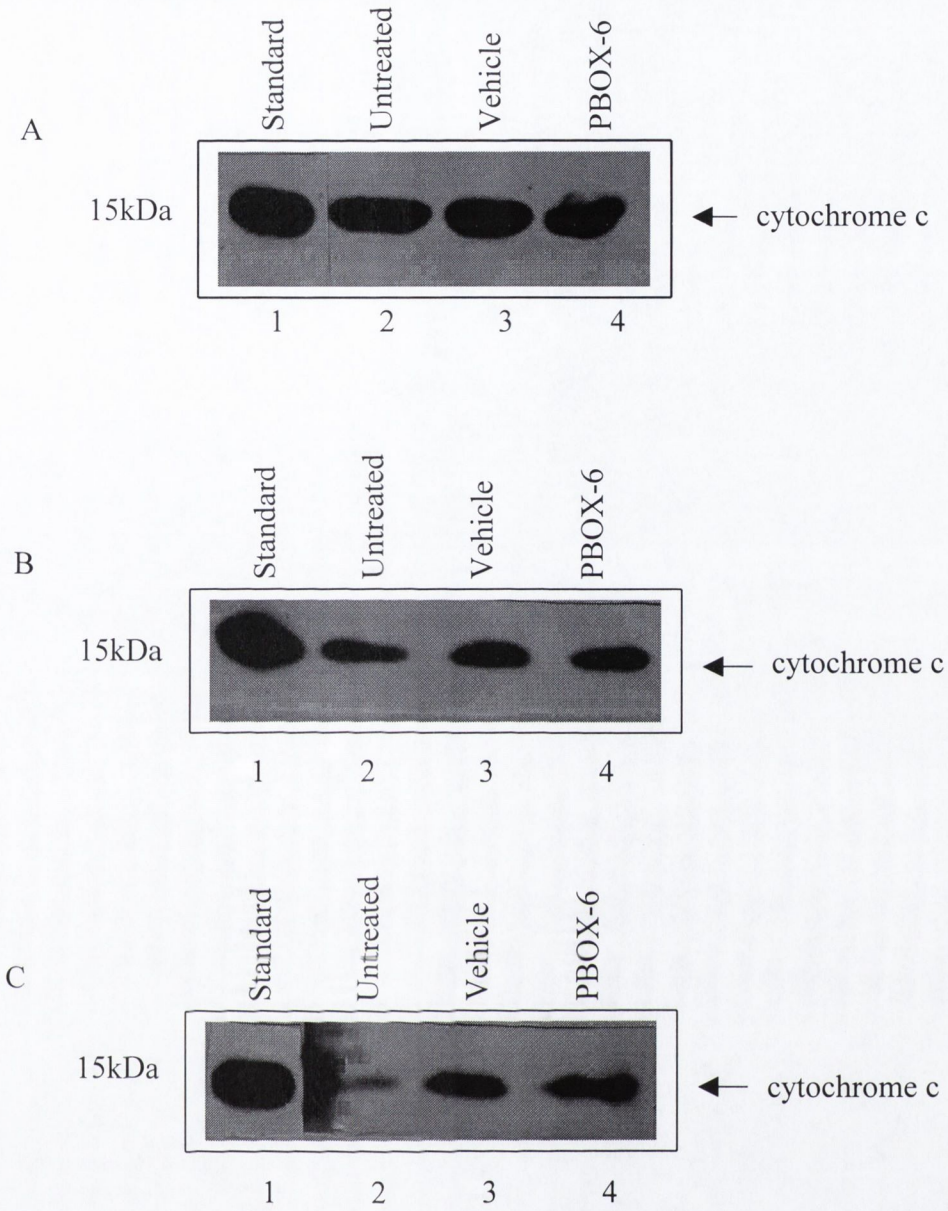

Fig. 3.17 Mitochondrial cytochrome c is not released into the cytoplasm during PBOX-6 induced apoptosis in CML cells

Cytosolic extracts were prepared from K562 cells (A), KYO.1 (B) and LAMA 84 cells (C) following treatment with either (lanes 2-4) control (untreated), vehicle (1% (v/v) ethanol) or PBOX-6 (10μM) for 16h. Protein (30μg) was resolved by SDS-PAGE, transferred onto PVDF membrane and probed with anti-cytochrome c antibody. Horse cytochrome c (10μg/ml) was used as a standard in each case (lane 1). Results are representative of at least two separate experiments.

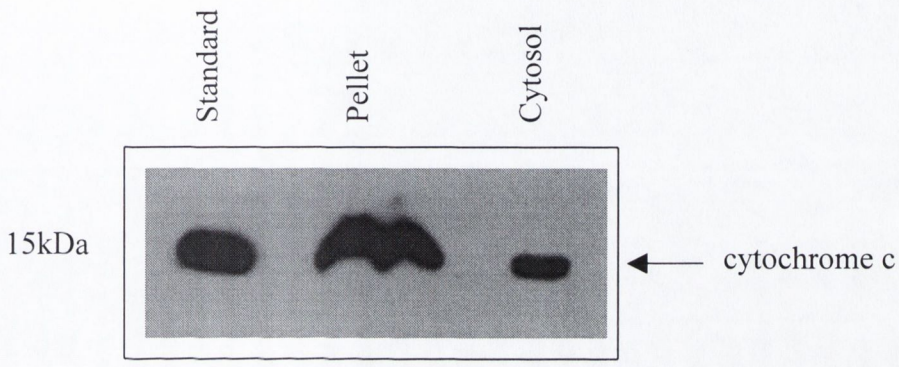

Fig. 3.18 Cytochrome c is not all non-specifically released from mitochondria during sample preparation

Cytosolic extracts from untreated K562 cells were prepared as described in Section 2.8. The remaining pellet was solubilised in 100µl of lysis buffer and incubated on ice for 30 min. Samples were centrifuged and the resulting supernatant was removed. Protein (30µg) from the solubilised pellet (lane 2) and from the cytosol (lane 3) were resolved by SDS-PAGE, transferred onto PVDF membrane and probed with anti-cytochrome c antibody. Horse cytochrome c (10µg/ml) was used as a standard (lane 1). Results are representative of at least two separate experiments.

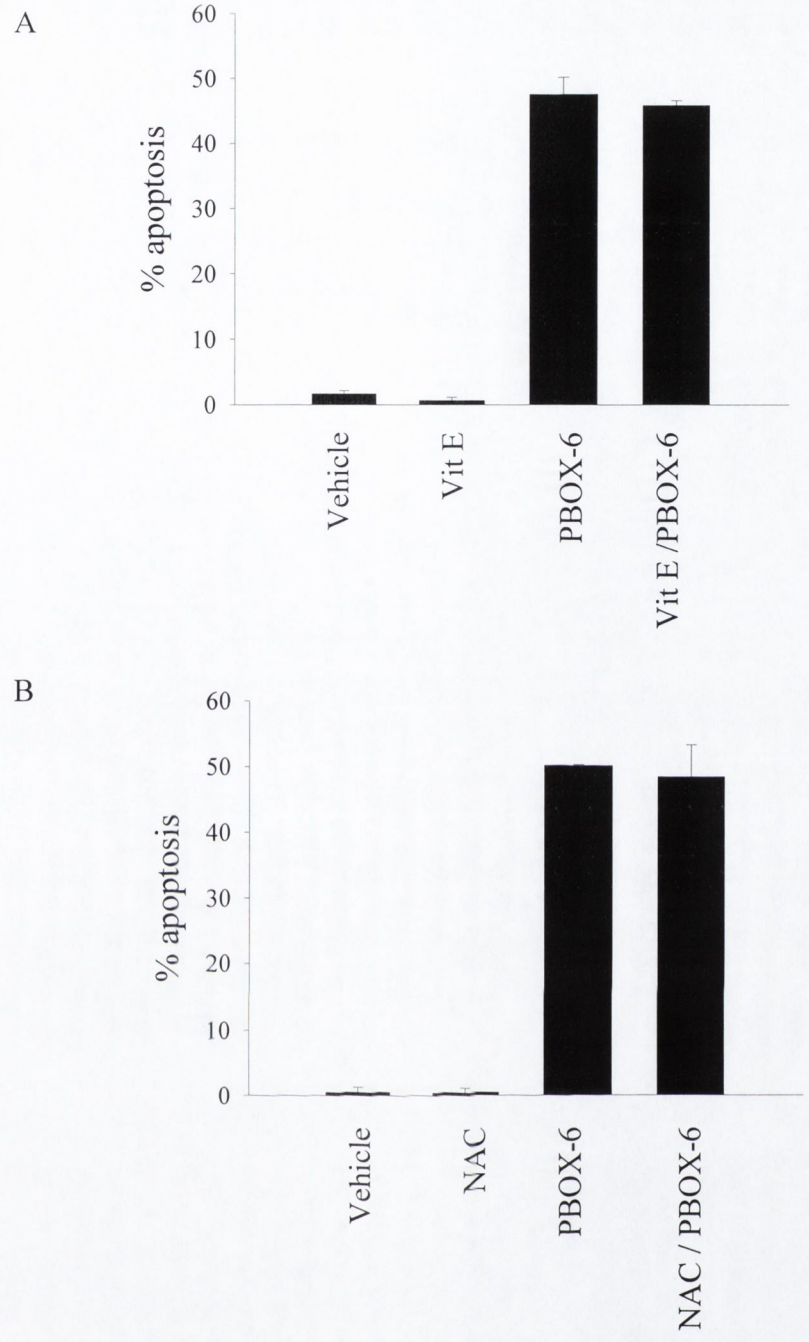

Fig. 3.19 The antioxidants, Vitamin E and *N*-acetylcysteine, fail to protect against PBOX-6 induced apoptosis in K562 cells

K562 cells were seeded at $3x10^5$ cells per ml and treated with (A) either vehicle (1% (v/v) PBS, 0.1% (v/v) ethanol), Vitamin E (100μM) for 40h, PBOX-6 (10μM) for 16h or a pretreatment of Vitamin E for 24h followed by PBOX-6 for a further 16h. In (B) cells were treated with either vehicle (1% (v/v) 25mM Tris, 0.1% (v/v) ethanol), *N*-acetylcysteine (NAC) (5mM) for 17h, or a pretreatment of NAC for 1h followed by PBOX-6 for a further 16h. The extent of apoptosis was determined by RapiDiff staining followed by microscopic examination as described in Section 2.4. Results represent the mean +/- S.E.M of three separate experiments.

prior to either UV irradiation or H_2O_2 treatment, reduces the level of apoptosis induced in these cells (Fig. 3.20A and B).

3.2.9 Investigation into the role of cysteine proteases during PBOX-6 induced apoptosis in CML cells

3.2.9.1 Caspase-3-like proteases become activated to a small extent in K562 and LAMA 84 cells, but not in KYO.1 cells, in response to PBOX-6

Caspase-3 is a member of the caspase family of cysteine proteases. These enzymes are synthesised as zymogens and are capable of being processed to form active heterodimeric enzymes in response to apoptotic stimuli (Duan *et al.*, 1996). This family, which consists of at least 12 human members, possesses very unusual substrate specificity in that they cleave substrates following an aspartate residue (Orth *et al.*, 1996). Caspases can be grouped into three subfamilies based on their substrate specificities. Caspase-3, along with caspases-2 and -7, are members of Group 2 caspases, which require an aspartate at P4. Caspase-3 is one of the most intensely studied and is believed to play a role of downstream executioner in many apoptotic pathways.

Cytosolic extracts were isolated from CML cells as described in Section 2.9 following treatment with either vehicle or PBOX-6 (10μM) for 16h. Caspase-3-like protease activity was examined using a fluorogenic assay in which active caspase-3-like proteases will cleave a substrate, the fluorescent peptide Ac-Asp-Glu-Val-Asp- (7-amino-4-methylcoumarin) (DEVD-AMC), and release the fluorogenic group (AMC), which can subsequently be measured using a spectrofluorimeter. This tetrapeptide (DEVD) mimics the target sequence cleaved by caspase-3-like proteases. The amount of AMC released is calculated from a standard curve of AMC, prepared using known concentrations of AMC as described in Section 2.9.2. Cytosolic extracts (100μg) were incubated with substrate (20μM) for 1h and protease activity was measured. A small increase in fluorescence, indicative of a low level of caspase-3-like protease activity, was detected in K562 and LAMA 84 cells following treatment with PBOX-6 for 16h. Caspase-3-like protease activity was not detected in KYO.1 cells following treatment with PBOX-6 for 16h (Fig. 3.21), although apoptosis was induced by PBOX-6 to the same extent in this cell line.

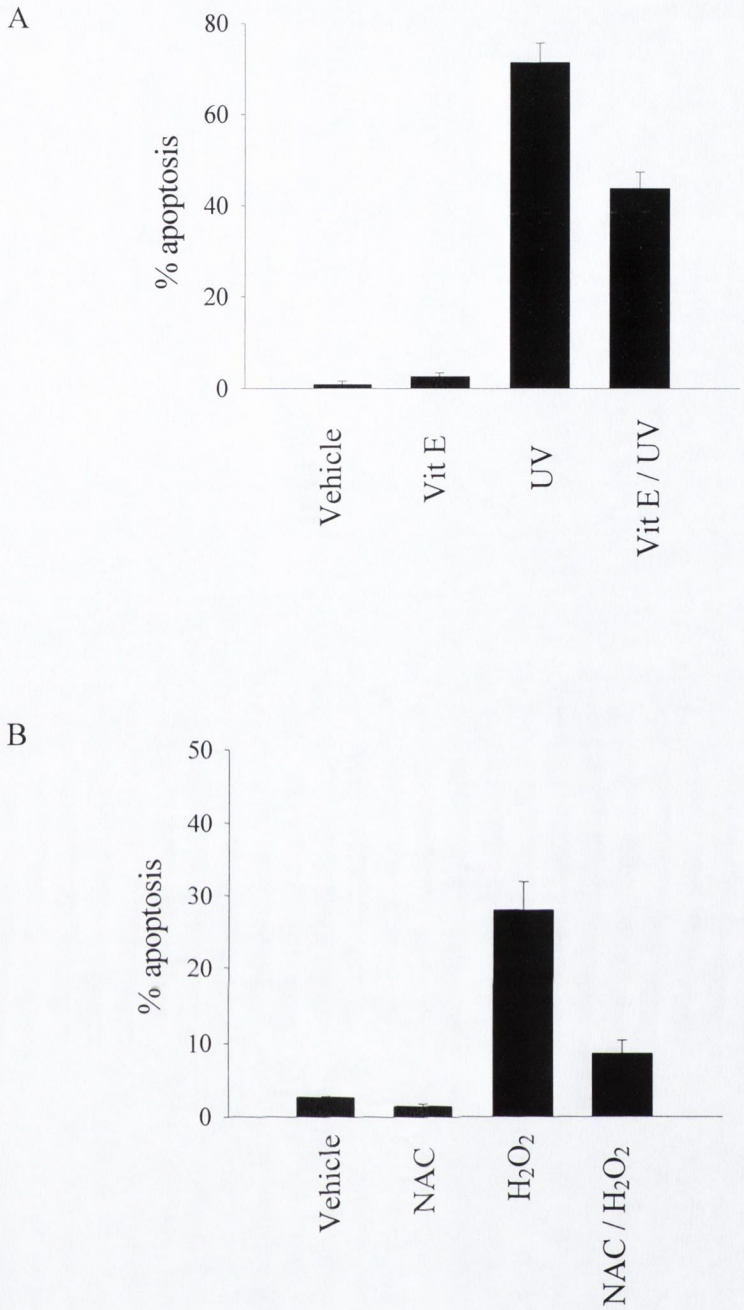

Fig. 3.20 The antioxidants, Vitamin E and *N*-acetylcysteine, reduce the level of apoptosis induced in HL-60 cells by UV irradiation and H_20_2 treatment respectively

HL-60 cells were seeded at $3x10^5$ cells per ml and treated with (A) either vehicle (1% (v/v) PBS), Vitamin E (100μM) for 24h, UV irradiation for 90 sec or a pretreatment with Vitamin E for 24h followed by UV irradiation for 90 sec. Cells were then incubated at 37°C for a further 2h. In (B) cells were treated with either vehicle (1% (v/v) 25mM Tris), *N*-acetylcysteine (NAC) (5mM) for 5h, H_2O_2 (0.01μM) for 4h or a pretreatment of NAC for 1h followed by H_2O_2 for a further 4h. The extent of apoptosis was determined by RapiDiff staining followed by microscopic examination as described in Section 2.4. Results represent the mean +/- S.E.M of three separate experiments.

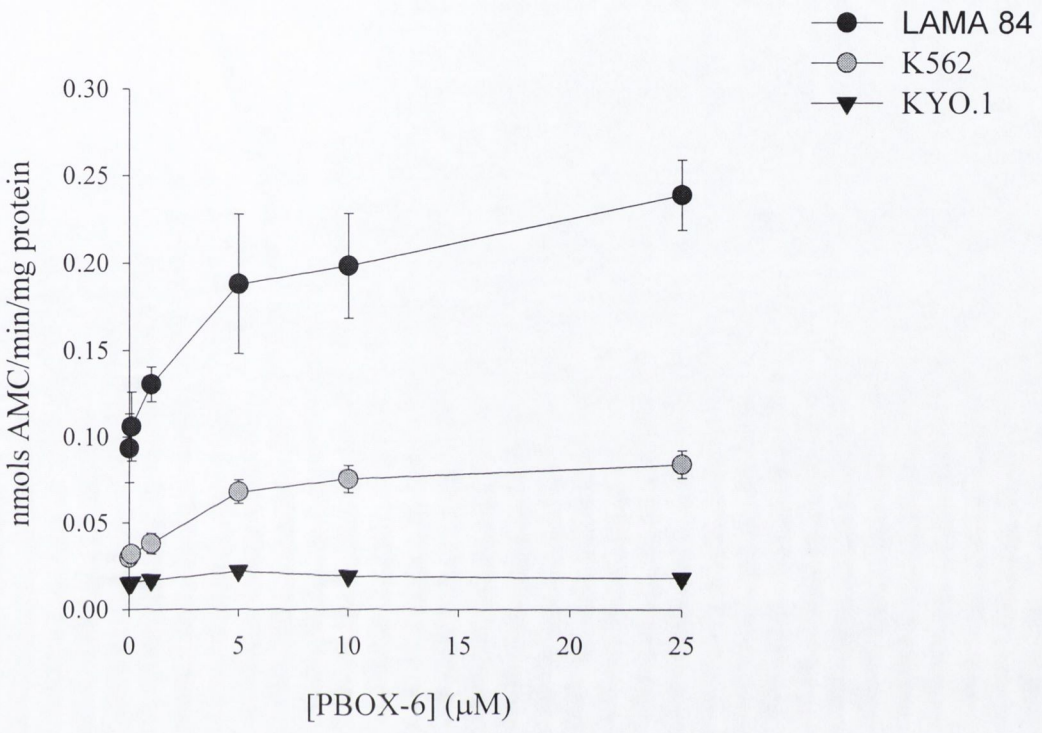

Fig. 3.21 Caspase-3-like proteases become activated to a small extent in K562 and LAMA 84 cells, but not in KYO.1 cells, in response to PBOX-6

CML cells were seeded at $5x10^6$/flask and treated with a range (0-25μM) of PBOX-6 concentrations for 16h. Cytosolic extracts were prepared as described in Section 2.9. Extracts (100μg) were incubated with substrate (20μM) for 60 min at 25°C in a total volume of 3 ml and fluorescence was monitored continuously using a spectrofluorimeter. All values represent the mean +/- S.E.M of three separate experiments.

The human breast carcinoma cell line (MCF-7), has previously been shown be deficient in the caspase-3 pro-enzyme, and thus during apoptosis caspase-3 cannot become activated (Janicke *et al.,* 1998). To ensure that KYO.1 cells contain pro-caspase-3, a Western blot using an antibody directed against this pro-enzyme was set up. Results demonstrate the presence of this pro-enzyme in all three CML cell lines (Fig. 3.22).

3.2.9.2 Activation of caspase-3-like proteases is not essential in PBOX-6-mediated apoptosis in CML cells

Although this unique family of cysteine proteases reportedly play a critical role in initiating and sustaining the biochemical events that occur during some apoptotic processes, other workers have shown that activation of caspase-3-like proteases are not essential for tumor necrosis factor-, staurosporine-, or Fas-induced apoptosis (Janicke *et al.,* 1998). In fact, in recent years a caspase-independent commitment to cell death has been described by Kroemer and co-workers, which involves the activation of a novel apoptosis inducing factor (AIF) (Loeffler and Kroemer, 2000).

In order to determine if caspase-3-like protease activity is an essential step in the apoptotic pathway in which it was detected following PBOX-6 treatment, a caspase-3-like protease inhibitor, z-DEVD-fluoromethylketone (fmk) was utilised. This irreversible inhibitor is of the general structure peptide-CO-CH_2-X, where X is a halide ion. It contains a peptide-recognition element corresponding to that found in endogenous substrates. CML cells were pretreated with the caspase-3-like protease inhibitor, z-DEVD-fmk (200μM), for 1h prior to treatment with PBOX-6 (10μM) for a further 8h. Caspase-3-like protease activity was measured using the fluorogenic substrate, Ac-DEVD-AMC, and results reveal that pretreatment of K562 and LAMA 84 cells with the inhibitor, z-DEVD-fmk, inhibited the activity of caspase-3-like proteases (Fig. 3.23A). To determine the effect of the caspase-3-like protease inhibitor on the extent of apoptosis induced by PBOX-6, cells were seeded at 3 x 10^5 cells/ml and treated in a similar manner to that described above. Following treatment, an aliquot of cells was removed, centrifuged onto a glass slide and stained using the RapiDiff kit as described in Section 2.4. The extent of apoptosis was determined by analysis of the morphological features of apoptosis. Results demonstrate that pretreatment of cells with the caspase-3-like protease inhibitor fails to prevent the induction of apoptosis by PBOX-6 (Fig.

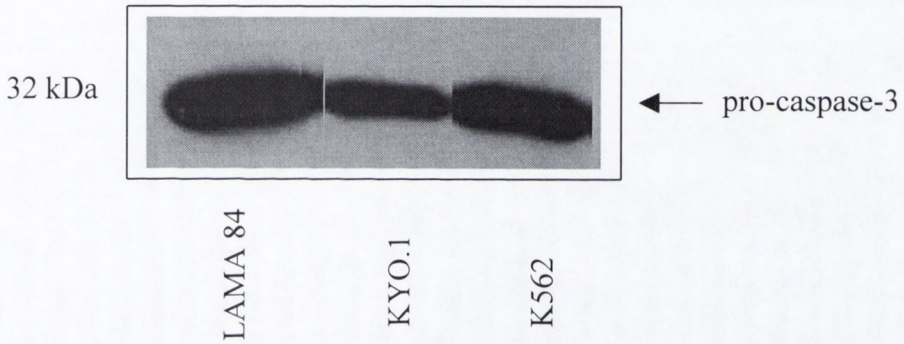

Fig. 3.22 Procaspase-3 is present in LAMA 84, KYO.1 and K562 cells

Cytosolic extracts from untreated CML cells ($5x10^6$) were prepared as described in Section 2.9. Protein (45μg) was resolved by SDS-PAGE, transferred onto PVDF membrane and probed with anti-pro-caspase-3 antibody. Results are representative of two separate experiments.

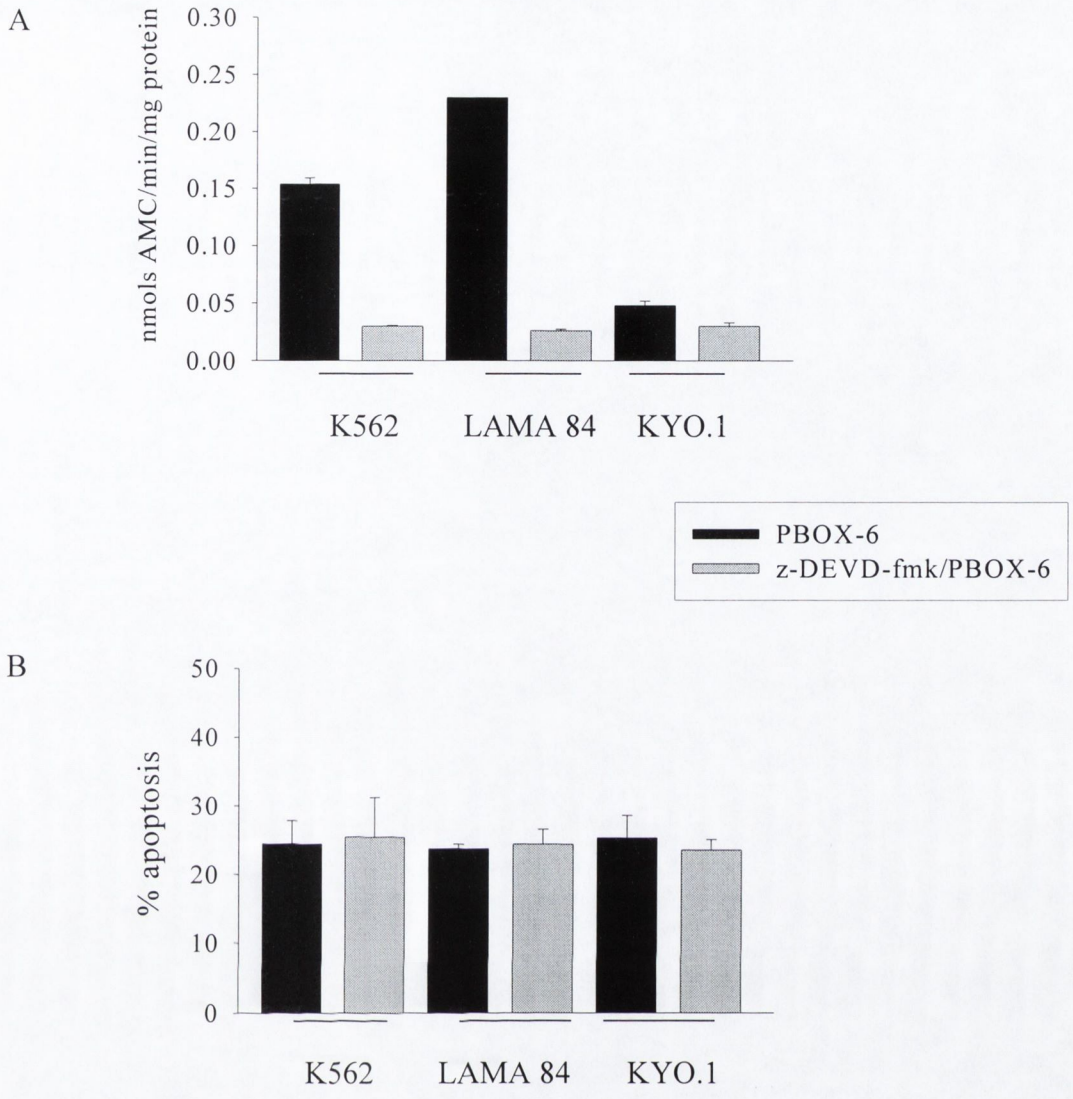

Fig. 3.23 The caspase-3-like protease inhibitor, z-DEVD-fmk, inhibits caspase-3-like protease activity but fails to protect against PBOX-6 induced apoptosis in CML cells

CML cells were seeded at (A) $5x10^6$ cells per ml and pretreated with or without z-DEVD-fmk (200μM) for 1h prior to treatment with PBOX-6 (10μM) for 8h. Cytosolic extracts were prepared and protein (100μg) was incubated with the caspase-3 substrate; Ac-DEVD-AMC (20μM) for 60 min at 25°C in a total volume of 3ml. Caspase-3-like protease activity was determined as described in Section 2.9. CML cells were seeded at (B) $3x10^5$ cells per ml and pretreated with z-DEVD-fmk (200μM) for 1h prior to treatment with PBOX-6 (10μM) for a further 8h. The extent of apoptosis was determined by RapiDiff staining followed by morphological examination as described in Section 2.4. Values represent the mean +/- S.E.M of three separate experiments.

3.23B). These results suggest that although during apoptosis caspase-3-like protease activity is detected in two of the CML cell lines, this activity is not an essential step in the pathway under which PBOX-6 induces apoptosis in these cells.

It has previously been reported that caspase-3-like protease activity is essential for etoposide-induced apoptosis in HL-60 cells. A control was set up where HL-60 cells were pretreated with the inhibitor, z-DEVD-fmk (200μM), prior to treatment with etoposide (50μM) for 8h. Cells were stained using the RapiDiff kit and results demonstrate that inhibition of caspase-3-like protease activity using the inhibitor z-DEVD-fmk, prevents the induction of apoptosis (Fig. 3.24).

3.2.9.3 Caspase-6-like proteases are not activated during PBOX-6-induced apoptosis in CML cells

Caspases can be divided into subfamilies based on a number of different criteria. For example, caspases can be subdivided into three groups according to substrate specificity (Janicke *et al.,* 1998). Alternatively, caspases can be subdivided into two different groups, the initiator caspases (caspases-2, -8, -9 and -10) which are found upstream in apoptotic pathways, and whose main function is to activate effector caspases (such as caspases-3, -6 and -7). These effector caspases are found further downstream in apoptotic pathways and are responsible for dismantling cellular proteins resulting in apoptosis (Mehmet, 2000).

In order to determine whether the effector protease, caspase-6, is involved in the mechanism in which PBOX-6 induces apoptosis in CML cells, a fluorogenic assay was set up using the substrate Ac-Val-Glu-Ile-Asp-7-amino-4-methylcoumarin (Ac-VEID-AMC), which is recognised by caspase-6 (Talanian *et al.,* 1997). As a positive control HL-60 cells were treated with etoposide (68μM) for 6h and cytosolic extracts were prepared as described in Section 2.10. Cytosolic extract (100μg) was incubated with substrate (20μM) for 1h and fluorescence was monitored using a spectrofluorimeter. An increase in fluorescence, indicative of protease activity, was detected in HL-60 cells following etoposide treatment (Fig. 3.25). Cytosolic extracts were prepared from CML cells following treatment with either vehicle (1% (v/v) ethanol) or PBOX-6 (10μM) for 16h. Protein (100μg) was incubated with substrate (20μM) and the fluorogenic assay was performed. Some non-specific, background fluorescence was detected in vehicle treated cells, which may be due to breakdown of the

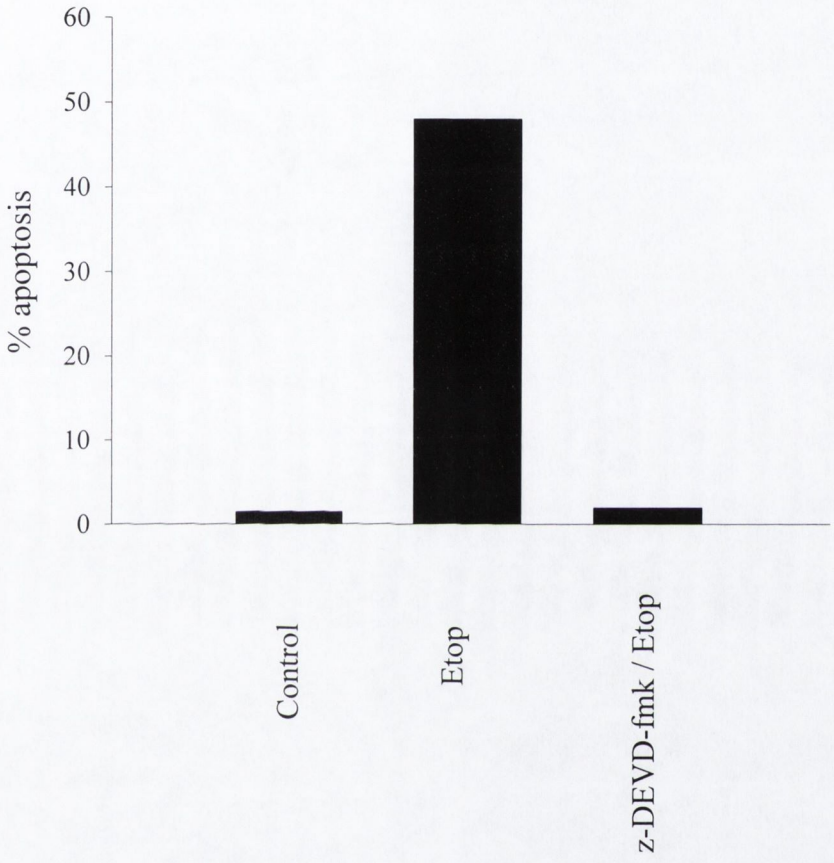

Fig. 3.24 The caspase-3-like protease inhibitor, z-DEVD-fmk, protects against etoposide-induced apoptosis in HL-60 cells

HL-60 cells were seeded at $3x10^5$ cells per ml and pretreated with z-DEVD-fmk (200μM) for 1h prior to treatment with etoposide (Etop) (50μM) for a further 8h. The extent of apoptosis was determined by centrifuging an aliquot of cells (150μl) onto a glass slide followed by RapiDiff staining and morphological examination as described in Section 2.4. Results are representative of an experiment performed twice.

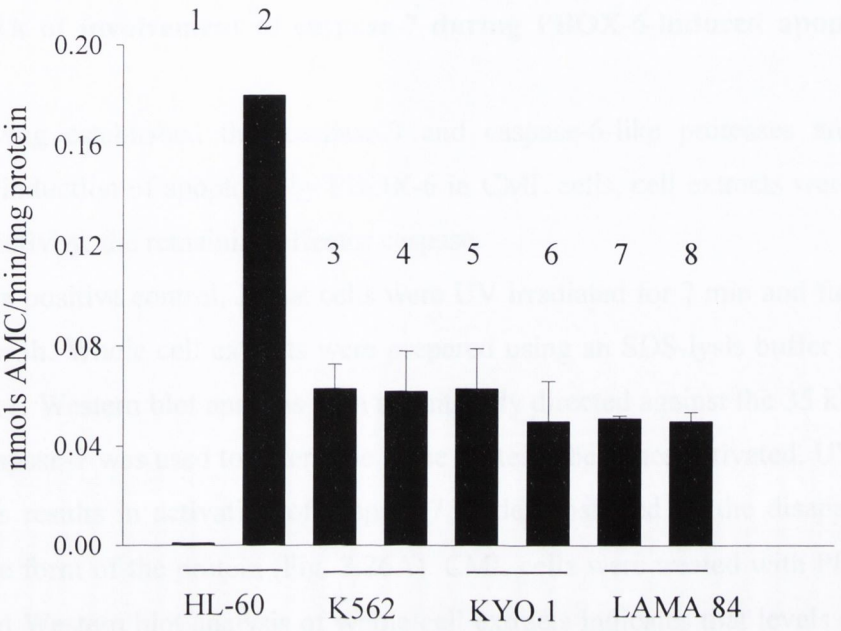

Fig. 3.25 Caspase-6-like proteases are not activated during PBOX-6 induced apoptosis in CML cells

Caspase-6-like protease activity was measured in cell extracts (100μg) isolated from either HL-60 cells following treatment with either vehicle (1% (v/v) DMSO) (lane1) or etoposide (68μM) (lane 2) for 6h, or from CML cells; K562 (lanes 3 and 4), KYO.1 (lanes 5 and 6) and LAMA 84 (lanes 7 and 8), following treatment with either vehicle (1% (v/v) ethanol) or PBOX-6 (10μM) respectively, for 16h. Cell extracts were incubated at 25°C for 60 min with the caspase-6 fluorogenic substrate, Ac-VEID-AMC (20μM), in a total volume of 3ml and fluorescence was monitored using a spectroflourimeter. Results represent the mean +/- S.E.M of three separate experiments.

substrate as a result of freeze-thawing. However, an increase in fluorescence was not observed for the three CML cells following treatment with PBOX-6 (Fig. 3.25), suggesting that caspase-6-like proteases are not involved in the apoptotic pathway leading to apoptosis.

3.2.9.4 Lack of involvement of caspase-7 during PBOX-6-induced apoptosis in CML cells

Having established that caspase-3 and caspase-6-like proteases are not required during the induction of apoptosis by PBOX-6 in CML cells, cell extracts were examined for caspase-7 activity, the remaining effector caspase.

As a positive control, Jurkat cells were UV irradiated for 2 min and further incubated at 37°C for 3h. Whole cell extracts were prepared using an SDS-lysis buffer as described in Section 2.11. Western blot analysis with an antibody directed against the 35 kDa pro-enzyme form of caspase-7 was used to determine if the protease becomes activated. UV irradiation of Jurkat cells results in activation of caspase-7 as demonstrated by the disappearance of the pro-enyzme form of the protein (Fig. 3.26A). CML cells were treated with PBOX-6 (10μM) for 16h and Western blot analysis of whole cell extracts indicates that levels of pro-caspase-7, from vehicle and drug treated samples, remains unchanged suggesting that caspase-7 does not become activated in response to PBOX-6 (3.26B).

3.2.9.5 The general caspase inhibitor, z-VAD-fmk does not protect against PBOX-6-induced apoptosis in CML cells

So far, it has been shown that the three downstream effector caspases (caspases-3, -6 and -7) are not required for PBOX-6-induced apoptosis in CML cells. The possibility that apoptosis occurs via a caspase-independent pathway was addressed using a general caspase inhibitor, z-VAD-fmk.

CML cells were pretreated with z-VAD-fmk (200μM), for 1h prior to treatment with PBOX-6 (10μM) for a further 8h. The extent of apoptosis was determined by centrifuging an aliquot of cells onto a slide and stained using the RapiDiff kit. Pretreatment of CML cells with the general caspase inhibitor does not prevent against PBOX-6 induced apoptosis (Fig. 3.27A), suggesting that the cysteine proteases inhibited by z-VAD-fmk are not required for PBOX-6-induced apoptosis. Since z-VAD-fmk inhibits the activity of all known cysteine

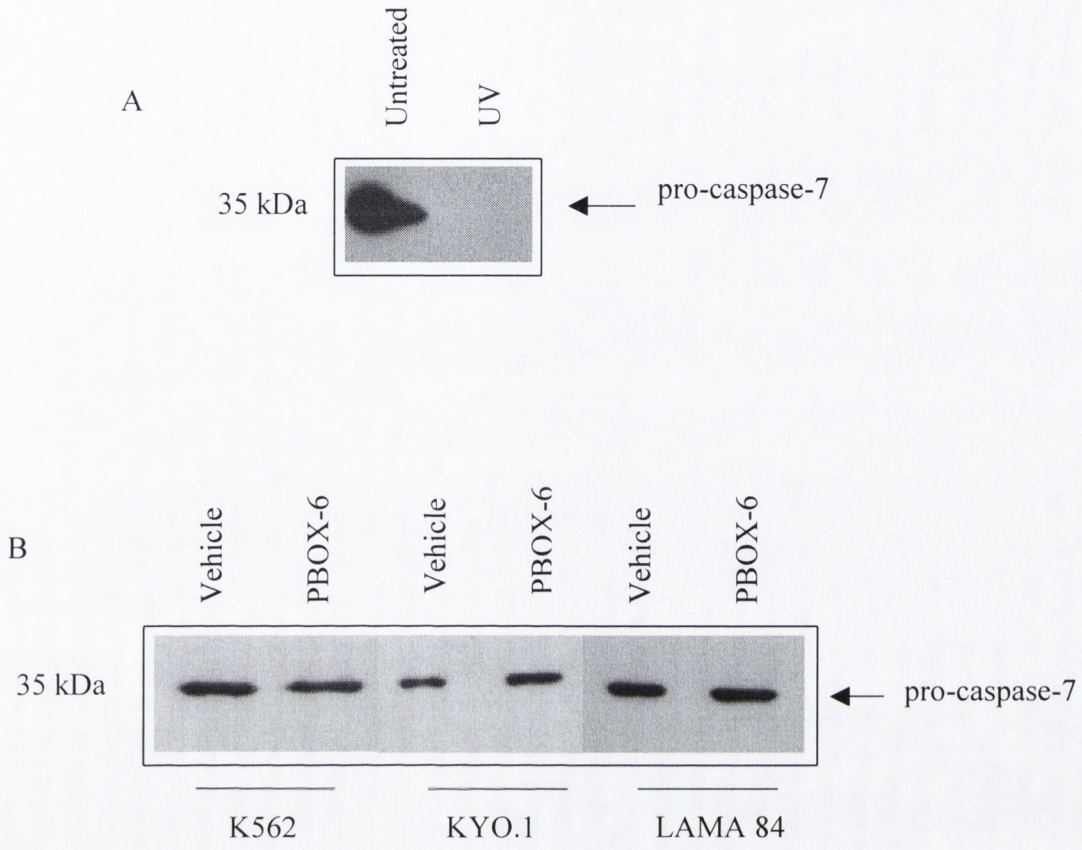

Fig. 3.26 Lack of involvement of caspase-7 during PBOX-6 induced apoptosis in CML cells

Whole cell extracts were prepared from (A) Jurkat cells, which were untreated or UV irradiated for 2 min and incubated at 37°C for a further 3h, or (B) CML cells; K562 (lanes 1 and 2), KYO.1 (lanes 3 and 4) and LAMA 84 (lanes 5 and 6) which were treated with either vehicle (1% (v/v) ethanol) or PBOX-6 (10μM) respectively, for 16h. Equal amounts of protein were resolved by SDS-PAGE, transferred onto PVDF membrane and probed with anti-pro-caspase-7 antibody as described in Section 2.11. A disappearance of the 35 kDa pro-caspase form of the enzyme is indicative of caspase-7 activation. Results are representative of at least three separate experiments.

Fig. 3.27 The general caspase inhibitor, z-VAD-fmk, does not protect against PBOX-6 induced apoptosis in CML cells

Cells were seeded at $3x10^5$ cells per ml and (A) CML cells; K562, KYO.1 and LAMA 84 with pretreated with or without the caspase inhibitor, z-VAD-fmk (200μM), for 1h prior to treating with PBOX-6 (10μM) for a further 8h. HL-60 cells (B) were pretreated with or without the caspase inhibitor, z-VAD-fmk (200μM), for 1h prior to treatment with etoposide (50μM) for 4h. An aliquot of cells (150μl) was centrifuged onto a slide and the extent of apoptosis was determined by counting apoptotic cells following RapiDiff staining, as described in Section 2.4. Results represent the mean +/- S.E.M of three separate experiments.

A

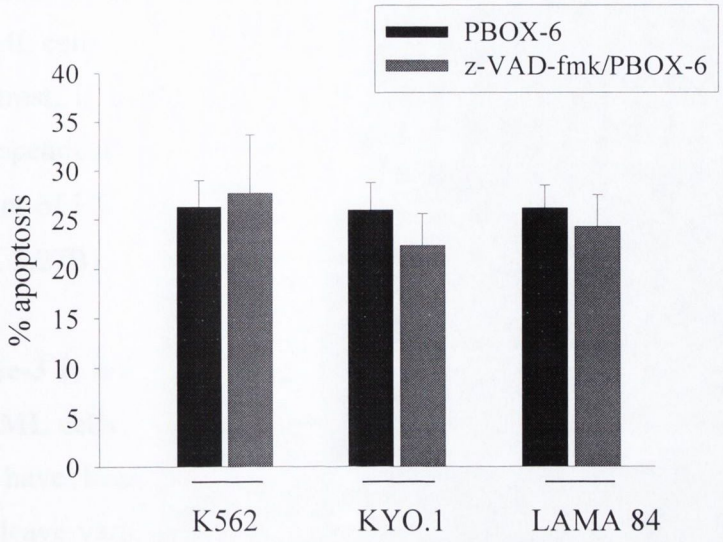
PBOX-6
z-VAD-fmk/PBOX-6
% apoptosis
40
35
30
25
20
15
10
5
0
K562
KYO.1
LAMA 84

B

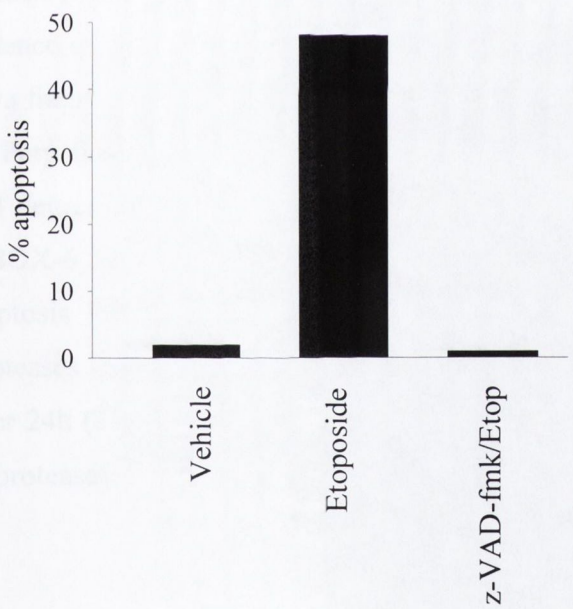
% apoptosis
50
40
30
20
10
0
Vehicle
Etoposide
z-VAD-fmk/Etop

proteases (Garcia-Calvo *et al.,* 1998), these results suggest that the induction of apoptosis by PBOX-6 in CML cells is not dependent on the activation of caspases.

In contrast, it has been reported that induction of apoptosis in HL-60 cells using etoposide is dependent on caspase activity. Therefore, as a control, it has been shown that the pretreatment of HL-60 cells with z-VAD-fmk (200μM) for 1h blocks etoposide-induced apoptosis (Fig. 3.27B).

3.2.10 Caspase-3 is not necessarily required for poly (ADP-ribose) polymerase (Parp) cleavage in CML cells

There have been conflicting reports regarding the requirement of caspase-3-like proteases to cleave various death substrates (Martins *et al.*, 1997; Mc Gowan *et al.*, 1996; Janicke *et al.*, 1998). However Cullivier *et al.,* (1998) reported that Parp can be cleaved by a number of caspases, and of these caspase-3 is thought to be the most efficient. Having established that activation of caspase-3-like proteases is not necessarily a requirement for the induction of apoptosis in CML cells, control and apoptotic cell lysates from CML cells were examined for evidence of Parp cleavage. Parp (116 kDa) is cleaved during apoptosis into its 87 kDa and 29 kDa fragments. The Parp antibody specifically recognises the intact protein as well as the large Parp fragment (87 kDa) by Western blot analysis of cell lysates. Results show that a small degree of Parp cleavage occurs in K562 and LAMA 84 cells following treatment with PBOX-6 for 24 and 16h respectively (Fig. 3.28A and 3.28B). However, the induction of apoptosis by PBOX-6 in KYO.1 cells, which does not involve activation caspase-3-like proteases (see Fig. 3.19), has also been shown to result in a small degree of Parp cleavage after 24h (Fig. 3.28C), suggesting Parp cleavage may occur without activation of caspase-3-like proteases.

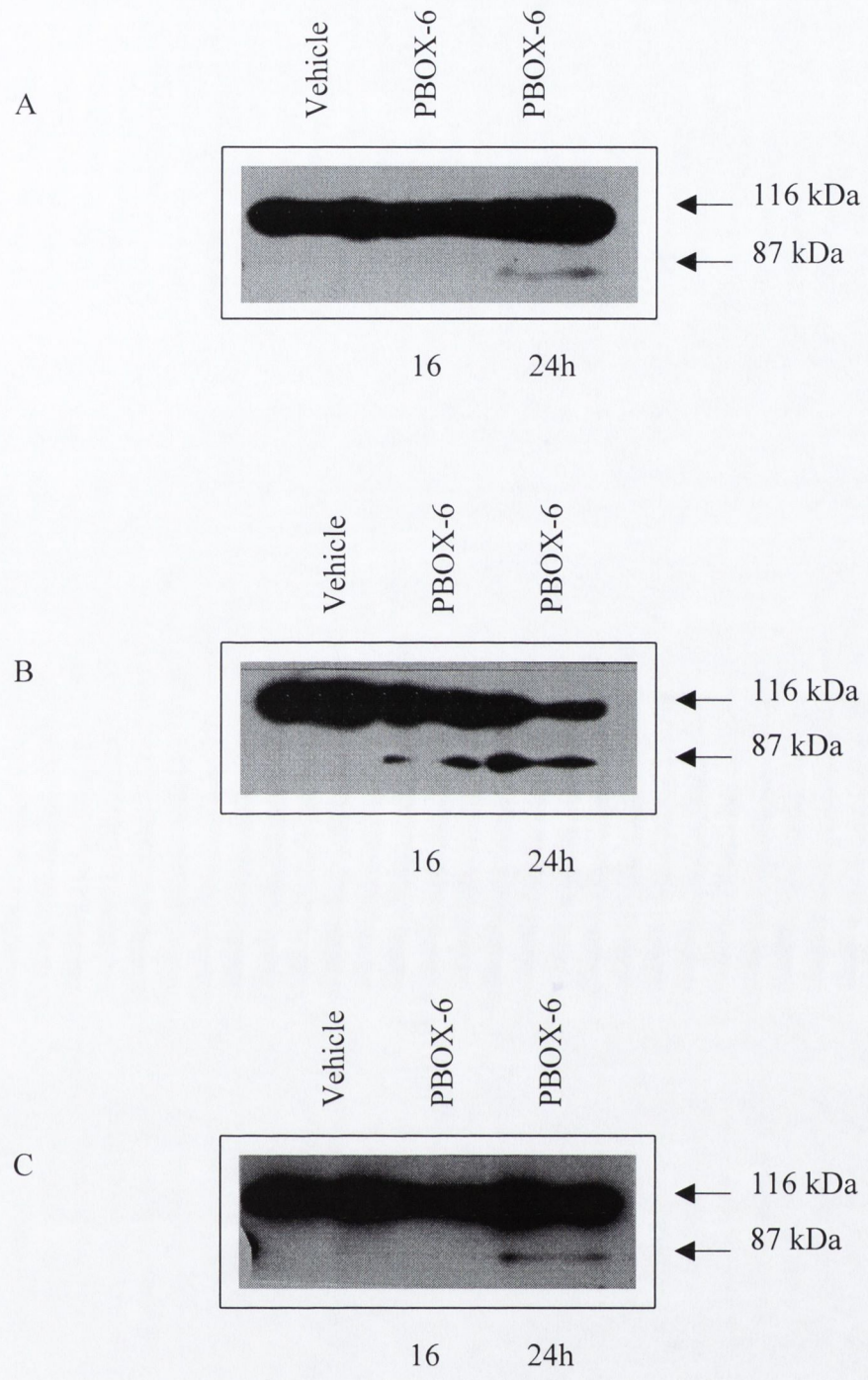

Fig. 3.28 PBOX-6 induces Parp cleavage in CML cells

Whole cell extracts from K562 (A), LAMA 84 (B), and KYO.1 (C) cells were prepared as described in Section 2.12 following treatment with either vehicle (1% (v/v) ethanol) for 24h or PBOX-6 (10μM) for 16 and 24h. Samples were resolved by SDS-PAGE, transferred onto PVDF membrane and probed with anti-Parp antibody. Results are representative of at least two separate experiments.

3.3 Discussion

Recently a novel series of pyrrolo-1,5-benzoxazepines were synthesised (Campiani *et al.,* 1996), and some of these have been shown to induce apoptotic cell death in a variety of human cell lines derived from the hematopoietic system such as the human promyelocytic leukaemia HL-60 cells, Jurkat T lymphoma and subcutaneous Hut-78 lymphoma cells (Zisterer *et al.,* 2000). This may suggest the potential of these compounds as novel anti-cancer drugs.

Leukaemia and lymphoma are diseases of the hematopoietic system, which are characterised in many cases by acquired genetic changes including expression of anti-apoptotic genes. Although a variety of chemotherapeutic agents have been used in the treatment of these diseases, many forms such as chronic myeloid leukaemia are resistant to chemotherapy-induced cell death (Martins *et al.,* 1997). Previous reports have shown that expression of the transforming oncogene, *bcr-abl*, in CML cells confers resistance against apoptosis. The mechanism or the step at which this anti-apoptotic effect is exerted has not been clearly defined but it is thought that Bcr-Abl exerts its effects upstream of events that result in cytochrome c release and caspase activation (Amarante-Mendes *et al.,* 1998b; Dubrez *et al.,* 1998). The search for novel compounds that induce apoptosis in CML cells and that may be used in the treatment of CML patients is of importance.

In the present study it has been shown that some members from this novel series of PBOX compounds induce apoptosis in CML cells, including the extremely resistant K562 cell line. Not all members from this series induced apoptosis in these cells suggesting a structure-activity relationship. From the seven pyrrolo-1,5-benzoxazepine compounds tested, the pro-apoptotic members (PBOX-3, -4, -5, -6 and -7) were all found to contain a naphthyl side-chain, suggesting the possible importance of this side-chain in the induction of apoptosis. A representative pro-apoptotic pyrrolo-1,5-benzoxazepine, PBOX-6, has been shown to induce apoptosis in a dose- and time-dependent manner in 3 CML cell lines, K562, KYO.1 and LAMA 84. The morphological criteria used to identify apoptotic cells included cell shrinkage, chromatin condensation, DNA fragmentation and membrane blebbing. These findings are similar to those reported by Zisterer *et al.* (2000), where it was discovered that a number of these pyrrolo-1,5-benzoxazepine compounds induce apoptosis in HL-60 cells, and of these PBOX-6 was one of the most potent, inducing approximately 40% apoptosis

following treatment with the compound at a similar concentration of 10μM for 16h. Apoptosis induced in CML cells reaches a maximum level of approximately 50% following a 16h treatment with PBOX-6. A possible explanation for this may be the metabolism of the drug, or the possible existence of a subclone of cells that have increased resistance to PBOX-6.

In the present study it was confirmed that K562 cells are resistant to the induction of apoptosis by many chemotherapeutic agents such as etoposide, mitoxanthrone and ara-C. The resistance of the K562 cell line to apoptosis has been reported to be reversed by down-regulation of Bcr-Abl using synthetic oligomers targeted against the tumour specific gene, known as antisense oligodeoxynucleotides (ODNs) (Martins *et al.*, 1997). Colony formation was suppressed in leukaemia blast cells from CML patients exposed to Bcr-Abl antisense oligonucleotides, whereas normal marrow progenitors were unaffected (Szczylik *et al.,* 1991) providing evidence that leukaemia growth can be selectively inhibited by synthetic oligomers targeted against the tumour specific gene. Antisense treatment is thought to induce apoptosis in K562 cells or render the cells more susceptible to apoptosis induced by other chemotherapeutic agents. Mc Gahon *et al.* (1994b) demonstrated that susceptibility of K562 cells to apoptosis induced by serum deprivation or chemotherapeutic agents is restored in the presence of antisense oligonucleotides which down-regulate Bcr-Abl protein expression. However, Bcr-Abl antisense treatment of CML cells has had different results in the hands of different investigators. Some of these differences may be explained by the use of different types of CML cells, different types of oligonucleotides or the choice of the target sequence within the Bcr-Abl mRNA sequence, but other differences remain unexplained (Rowley *et al.*, 1996). K562 cells are derived from a patient in the blastic phase of the disease and contain mutations in addition to the Bcr-Abl translocation. Findings from antisense treatment of K562 cells may not apply to cells in the chronic phase of the disease or to primary cells derived from patients at different stages of CML. In addition, an oligonucleotide may have effects due to binding, not to its complementary sequence, but to a protein such as a tyrosine kinase (Bergan *et al.*, 1995). Different types of oligonucleotide can also be used which may explain some inconsistencies between workers. These include oligonucleotides with phosphodiester, phosphoorothioate, or methylphosphonate backbones. The length of the oligomers is also of concern with shorter oligomers possibly binding to unintended targets. It

has in fact been reported that down-regulation is not caused by an antisense mechanism, and it was found that some antisense ODNs and several control ODNs inhibit the proliferation of leukaemic cells lines. This non-specific effect is thought to be caused by a 3' terminal TAT sequence and is an example of phosphodiester sequence-specific toxicity (Vaerman *et al.*, 1995).

The 26S proteasome is a large multicatalytic protease that regulates several cell cycle and apoptosis regulatory proteins. A recent report suggests that inhibition of the proteasome activity, using selective inhibitors, causes the induction of apoptosis in K562 cells. Proteasome inhibition resulted in a reduction of Bcr-Abl protein expression, which occurred several hours before the onset of apoptosis. Furthermore, reduced Bcr-Abl expression resulted in significant attenuation of Bcr-Abl-mediated protein tyrosine phosphorylation. These workers concluded that proteasome inhibitors that lead to a reduction in levels of the Bcr-Abl oncoprotein might have potential as chemotherapeutic agents for treating CML and related diseases (Dou *et al.*, 1999).

STI571, previously known as CGP57148B, a 2-phenylaminopyrimidine derivative, is a selective ATP inhibitor of the Abl protein kinase (Schindler *et al.*, 2000). STI571 has been shown to inhibit the tyrosine phosphorylation of Bcr-Abl within minutes, in K562 and LAMA 84 cells, resulting in apoptosis (Gambacorti-Passerini *et al.*, 1997). It has also been reported that Bcr-Abl-mediated resistance to apoptosis is in part attributable to an up-regulation of the anti-apoptotic Bcl-2 family member, Bcl-$_{XL}$ (Amarante-Mendes *et al.*, 1998a). The pro-apoptotic effect of STI571 is accompanied by down-regulation of Bcl-$_{XL}$ (Oetzel *et al.*, 2000), further supporting the role of Bcl-$_{XL}$ as a target for the transforming function of Bcr-Abl. A few CML cell lines and primary progenitors from peripheral blood or bone marrow are, however, resistant to this compound (Deininger *et al.*, 1997), which is an important issue as the compound enters clinical trials. It was recently found that Bcr-Abl positive cell lines that evade the inhibitory effect of STI571 do so by different mechanisms, which include overexpression of Bcr-Abl or reduced uptake due to P-glycoprotein overexpression (Mahon *et al.*, 2000). Although preliminary results from STI571 treatments have resulted in complete remission in a large proportion of patients, a recent article reports that patients in the blast crisis stage of CML are gaining increased resistance to STI571

(Gorre *et al.*, 2001). This highlights the need for a continual search for new drugs, with minimal side effects, for use in the treatment of CML and related illnesses.

In contrast to results found with STI571 and with proteasome inhibition, in the current study, it has been found that the representative pyrrolo-1,5-benzoxazepine, PBOX-6, can by-pass Bcr-Abl-mediated resistance to apoptosis in the three CML cell lines examined. This is the first report of a compound that can potently induce apoptosis in CML cells by by-passing the apoptotic suppressor, Bcr-Abl. Any down-regulation of Bcr-Abl that was observed does not accompany, but rather follows apoptosis in these cells. Down-regulation was not detected until after a 24-hour treatment with PBOX-6 when approximately 50% of cells displayed the morphological features of apoptosis. This down-regulation is probably due to the large extent of apoptosis present at this time. The tyrosine phosphorylation status of the Abl tyrosine kinase remained unchanged up to 24 hours following treatment with PBOX-6, suggesting that inhibition of Bcr-Abl tyrosine kinase activity is not responsible for execution of the apoptotic cascade following PBOX-6 treatment. Results from this study suggest that a reduction in Bcr-Abl expression, or inhibition of its tyrosine kinase activity, is not the only mechanism by which cells can escape the anti-apoptotic effect of the *bcr-abl* gene. Moreover, this may suggest that *bcr-abl* itself might not be solely responsible for the anti-apoptotic properties of these cells.

Phosphorylation and dephosphorylation of cellular proteins is implicated in many biologically important processes such as cell growth and differentiation (Weng *et al.*, 1998). Protein tyrosine kinases (PTKs) and phosphatases (PTPases) jointly maintain the tyrosine phosphorylation status of cellular proteins in homeostasis (Yousefi *et al.*, 1994). Alteration in the tyrosine phosphorylation status of proteins has previously been implicated in apoptotic cell death. For example, ionising radiation induces enhanced tyrosine phosphorylation of multiple substrates in human-B-lympocyte precursors, triggering apoptosis (Uckun *et al.*, 1992). There also appears to be conflicting reports as to whether an increase or decrease in the tyrosine phosphorylation status of proteins results in apoptosis. For example, on the one hand, inhibitors of tyrosine phosphorylation, genistein and tyrophostin, have been shown to induce apoptosis in HL-60 and MO7e human leukaemia cell lines (Bergamaschi *et al.*, 1993), while on the other hand they have been shown to prevent didemnin B-induced apoptosis in HL-60 cells (Johnson *et al.*, 1996).

In the present study it has been shown that treatment of K562 cells with PBOX-6 induced an increase in the tyrosine phosphorylation status of two, as yet unidentified proteins, approximately 63 kDa and 71 kDa in size. The increased phosphorylation of these proteins did not become apparent until 16 hours following treatment with PBOX-6 when approximately 50% of cells had undergone apoptosis, suggesting that increased phosphorylation of these two proteins does not trigger the induction of apoptosis but rather accompanies apoptosis induced in K562 cells. Pretreatment of K562 cells with the broad range tyrosine kinase inhibitor, genistein, prevented the phosphorylation of these two proteins and inhibited the induction of apoptosis, suggesting that phosphorylation of these proteins may be important in the pathway in which PBOX-6 induces apoptosis. Pretreatment of cells with alternative tyrosine kinase inhibitors, herbimycin A and tyrophostin, also reduced the extent of apoptosis induced by PBOX-6, although they were themselves somewhat cytotoxic to the cells. Although these molecules are usually considered specific inhibitors of tyrosine kinases, they may also have other, as yet unidentified effects. For example, genistein is also known as an inhibitor of topoisomerase I and II. In addition, it has been reported by Riordan *et al.* (1998), that herbimycin A irreversibly inhibits tyrosine kinases, including those encoded by Bcr-Abl, whereas genistein does not preferentially inhibit the Bcr-Abl tyrosine kinase. These workers have shown that pretreatment of K562 cells with herbimycin A enhanced apoptosis following treatment with the DNA damaging agent, etoposide, whereas pretreatment with genistein failed to enhance the activity of etoposide. In contrast, the current study has revealed that pretreatment of K562 cells with genistein, prior to treatment with PBOX-6, results in complete protection from apoptosis, whereas pretreatment with herbimycin A results in a protection of approximately 10%. These results, which correlate with results reported earlier from Western blot assays, suggest that PBOX-6 induces apoptosis in K562 cells by bypassing the apoptotic suppressor, Bcr-Abl. If it was the case that PBOX-6 required inhibition of Bcr-Abl in order to induce apoptosis in these cells, it would be expected that pretreatment with herbimycin A would enhance the extent of apoptosis induced by PBOX-6, rather than reducing the extent of apoptosis, as observed.

An attempt to identify the two proteins phosphorylated by PBOX-6 involved the use of specific tyrosine kinase inhibitors, which inhibit the phosphorylation of proteins close to

the approximate size of the two unidentified proteins. These included damnacanthal (p56 LCK inhibitor), geldanamycin (p60 SRC inhibitor) and piceatannol (p72 SYK inhibitor). P60 SRC and p56 LCK are members of the SRC family of tyrosine kinases and have been reported to be involved in the activation of the Ras signalling pathway, which is also thought to play a role in Bcr-Abl transformation. P56 LCK and p72 SYK have been implicated in T cell activation and selective inhibitors of these may have efficacy in the treatment of T cell leukaemias and lymphomas (Faltynek *et al.,* 1995). However, these inhibitors failed to protect against PBOX-6 induced apoptosis in K562 cells suggesting that the proteins inhibited by these compounds are not phosphorylated by PBOX-6. Further work is required to elucidate the identity of these proteins.

A number of studies report as critical the release of cytochrome c from the mitochondrial intermembrane space into the cytosol, where it activates cysteine proteases, leading to cell death in receptor and chemical induced apoptosis (Scarlett and Murphy, 1997). However, it has also been reported that cytochrome c release is not necessarily a requirement for all cells undergoing apoptosis. For example, it has been shown that induction of apoptosis in Multiple Myeloma cells using three distinct stress inducers, infa-red radiation (IR), dexamethasone (Dex), and anti-Fas mAb, resulted in the accumulation of cytosolic cytochrome c in IR, but not in Dex and anti-Fas mAb induced apoptosis (Chauhan *et al.*, 1997). It was also shown that caspase-3 was cleaved and activated not only in IR-mediated apoptosis, but also in Dex and anti-Fas mAb mediated apoptosis. These results suggest that in Multiple Myeloma cells, there are at least two different pathways that lead to apoptosis, one correlated and the other not correlated with the release of cytochrome c from mitochondria. Hishita *et al.* (2001) reported that caspase-3 activation in P39 cells following etoposide treatment was not accompanied by mitochondrial dysfunction or subsequent cytochrome c release. They suggested that cytochrome c independent activation of caspase-3 may be due to leakage of lysosomal cysteine proteases into the cytosolic compartment and the lysosomal enzyme, cathepsin L, may be involved in the activation of caspase-3. A recent article by Finkel, (2001) reviewed the current situation with regard to the central player in programmed cell death. Reports are split into two competing camps, one that argues a central role for mitochondria, which release apoptogenic proteins including cytochrome c, AIF and three caspases, triggering the apoptotic cascade with some reports suggesting that caspases are

dispensable for apoptosis. The other camp reports that the mitochondria are secondary agents of the cell's demise, and that primary apoptotic signals route directly to the caspases without first involving the mitochondria. Many questions remain unanswered and given the complexity of apoptosis, which can be triggered by many different stimuli, it may turn out that cells can employ different mechanisms in different circumstances.

The results presented in this study show that the induction of apoptosis in CML cells by PBOX-6 is independent of the accumulation of cytochrome c in the cytosol. These results confirm the existence of apoptotic pathways that lead to the execution of apoptosis in which the release of mitochondrial cytochrome c is not an obligatory event. The results presented here are in direct contrast to that reported by Zisterer *et al.* (2000) where PBOX-6-induced apoptosis in HL-60 cells was accompanied by the accumulation of cytochrome c in the cytoplasm, suggesting that the mechanism in which PBOX-6 induces cell death differs in HL-60 and CML cells.

Several studies have demonstrated that the production of ROI and the resulting oxidative stress play a pivotal role in apoptosis. The addition of various exogenous antioxidants, such as *N*-acetylcysteine (NAC) and the free radical scavenger, Tempo, can block or delay apoptosis (Chen *et al.*, 1998; McGowan *et al.*, 1996). In the present work it has been shown that PBOX-6-induced apoptosis in K562 cells is unaffected by the presence of NAC or Vitamin E. This would suggest that PBOX-6-induced apoptosis is not mediated by ROI. Similar findings were reported by Zisterer *et al.* (2000) following treatment of HL-60 cells with PBOX-6. This is in agreement with reports, which indicate that ROI are not necessarily a requirement for apoptosis. For example, Fas ligand- or staurosporine-induced apoptosis do not appear to require the generation of ROI and are not inhibited by the use of antioxidants (Jacobson and Raff, 1995).

A unique family of cysteine proteases called caspases appears to play a critical role in initiating and sustaining the biochemical events that occur in apoptotic cell death. This family of proteases, which contain at least 12 human members, cleave polypeptides on the carboxyl side of aspartate residues (Martins *et al.*, 1997). These caspases are grouped into 3 subfamilies based on their substrate specificities. Group I (caspases-1, -4 and -5) caspases are believed to play a role in inflammation whereas group II (caspases-2, -3, and -7) and group III (caspases -6, -8, -9, and -10) are mainly involved in apoptosis (Garcia-Calvo *et al.*, 1998).

Janicke *et al.* (1998) has shown that caspase-3 is required for apoptosis induced by cytochrome c, but is not essential for TNF-, staurosporine-, or Fas-induced apoptosis. Although the cellular mechanisms that account for caspase-independent apoptosis are still elusive, evidence from an increasing number of experimental systems support the existence of caspase-independent pathways (Dumont *et al.,* 2000). TRAIL induced JNK activation in HeLa cells can occur via a caspase-dependent or caspase-independent pathway (Muhlenbeck *et al.,* 1998). It has also been shown that over-expression of the pro-apoptotic protein Bax in mammalian cells induces DNA condensation and membrane alterations leading to cell death, without any caspase activation (Xiang *et al.*, 1996). In recent years one of the proteins thought to be responsible for caspase-independent apoptotic pathways has been identified. This protein, know as apoptosis-inducing factor (AIF), is a flavoprotein, which is released from the mitochondrial intermembrane space and translocates to the nucleus where it causes partial chromatin condensation (Zamzami and Kroemer, 1999). In an attempt to define the ordering of caspase-dependent and caspase-independent apoptogenic events in T lymphocytes, Dumont *et al.* (2000) reported a caspase-independent 'commitment phase' which is characterised by the selective release of AIF from the mitochondria and translocation to the cytosol and the nucleus, cell shrinkage and partial chromatin condensation. This was followed by a caspase dependent 'execution phase', which is characterised by release of cytochrome c, DNA fragmentation and Parp cleavage. In these studies, caspase-dependent and independent cell death was distinguished by the use of the general caspase inhibitor z-VAD-fmk.

It is well known that most caspase substrates are not exclusively cleaved by a specific caspase but only preferentially, while other members of the caspase family act on these substrates to a lower extent. For example, caspases-3 and -7 display similar specificities for the fluorogenic peptide Ac-DEVD-AMC, and the peptide inhibitor, Ac-DEVD-CHO, potently inhibits both enzymes, whereas the primary specificity of caspase-6 is the tetrapeptide, VEID, and this is only poorly cleaved by other caspases (Talanian *et al.*, 1997). Although the use of these substrates and inhibitors has lead to a generalisation that, for example, DEVD-based reagents are 'caspase-3-specific' this is an oversimplification and therefore, throughout the current study these reagents have been referred to as 'caspase-3-like-protease' substrates or inhibitors. Western blotting is not suitable for the quantitative

measurement of caspase activity, therefore, these tetrapeptide fluorogenic substrates, which are more sensitive, are widely used.

In this study it has been shown that activation of caspase-3-like proteases are not required for the induction of apoptosis by PBOX-6 in CML cells. Although activation of caspase-3-like proteases was detected to a small extent in K562 and LAMA 84, inhibition of this caspase-3-like activity using the inhibitor z-DEVD-fmk, did not inhibit the induction of apoptosis, suggesting that caspases are dispensable for PBOX-6-induced cell death in these cells. In addition, caspase-3-like protease activity was not detected in KYO.1 cells undergoing apoptosis, further evidence to suggest that apoptosis can occur independent of caspase-3-like protease activation. These results are in contrast to that reported by Zisterer *et al.* (2000), where PBOX-6 was found to induce a large extent of caspase-3-like protease activity in HL-60 cells, which was shown to be an essential step in the apoptotic pathway. The possibility that other downstream 'executioner' caspases may be activated in response to PBOX-6 treatment was investigated. Activation of caspase-6 or -7-like proteases was not detected, suggesting that alternative, as yet unknown, effector caspases may be involved in the induction of apoptosis or a caspase-independent mechanism for commitment to cell death may exist. The latter possibility was further corroborated when the competitive and irreversible broad-spectrum caspase inhibitor, z-VAD-fmk (Garcia-Calvo *et al.*, 1998), failed to protect against PBOX-6-induced apoptosis. Therefore, it seems likely that PBOX-6-induced apoptosis in CML cells occurs via a cytochrome c-independent mechanism, and that caspase activation is dispensable. These results suggest that induction of apoptosis could possibly involve the release of AIF from the mitochondrial intermembrane space.

Caspases have been known to cleave a variety of death substrates. An early biochemical event that accompanies apoptosis in many cell types is the proteolytic cleavage of the DNA repair enzyme, Parp, from a 116 kDa polypeptide to an approximately 29 kDa fragment containing the N-terminal DNA binding domain and an approximately 87 kDa polypeptide containing the automodification domain and the NAD-binding domain (Kaufmann *et al.*, 1993). Parp cleavage has been linked to endonuclease activation, with Parp demonstrated to act as a negative regulator. On cleavage of Parp, this block is removed and the endonuclease is re-activated. Cleavage of Parp results in decreased enzyme activity, which precludes binding of the enzyme to the damaged site and thus compromises the

response to DNA damage (Mc Gowan *et al.,* 1996). It has indeed been reported that Parp cleavage can be catalysed by several caspases, including caspases-1, -2, -3, -4, -6, -7 (Gu *et al.*, 1995; Orth *et al.*, 1996) and of these caspase-3 is thought to be the most efficient Parp protease, followed by caspase-7 (Cuvillier *et al.,* 1998). However, the MCF-7 human breast carcinoma cell line lacks caspase-3 owing to the functional deletion of the Casp-3 gene (Janicke *et al.*, 1998). It has been shown that TNF- or staurosporine-induced apoptosis of caspase-3-deficient MCF-7 cells resulted in the cleavage of the death substrates Parp, Rb (retinoblastoma protein), PAK 2 (p21-activated kinase 2 binding protein), DNA-PK (DNA-dependent protein kinase catalytic subunit), DFF-45 (DNA fragmentation factor), but not fodrin. Introduction of the Casp-3 gene into MCF-7 cells resulted in the cleavage of fodrin into its 120 kDa fragment. These results show that caspase-3 is not required for the cleavage of Parp, Rb, PAK2, DNA-PK and DFF-45. In the present study, Western blot analysis has shown Parp cleavage in all three cell lines, but only to a small degree. This low level of Parp cleavage is consistent with low or no caspase-3-like protease activation and no caspase-6 or -7 activity. The lack of activation of caspase-3 in KYO.1 cells is not due to the absence of the pro-enzyme form of caspase-3, as demonstrated by Western blotting. The results presented herein suggest that caspase-3-like protease activity is not necessarily required for the Parp cleavage observed in CML cells. It has been shown that caspase-6 or caspase-7-like proteases are not activated during PBOX-6-induced apoptosis. Therefore, alternative caspases or proteases may be responsible for Parp cleavage in these cells. As mentioned earlier, caspase-independent apoptosis can occur, which would in turn suggest that Parp cleavage is not essential for apoptosis in these cases. Therefore, it seems that extensive Parp cleavage or Parp cleavage per se is not essential for commitment to apoptosis in CML cells. It has been reported that Parp cleavage and endonuclease activity resulting in DNA fragmentation appear as closely associated events (Mc Gowan *et al.,* 1996). The occurrence of Parp cleavage at a later stage during PBOX-6-induced apoptosis may be responsible for some of the characteristic morphological features, such as oligonucleosomal DNA fragmentation, or another protein may be responsible for the DNA fragmentation in these cells. A recent article reported the activation of endonuclease G (endoG) in response to apoptotic stimuli. EndoG, a mitochondrion-specific nuclease, translocates to the nucleus during apoptosis causing DNA fragmentation, which is not blocked by the broad-spectrum caspase inhibitor z-

VAD-fmk, thus representing a caspase-independent pathway leading to DNA fragmentation (Li *et al.*, 2001b).

In summary it has been shown that some members of a novel series of pyrrolo-1,5-benzoxazepines potently induce apoptosis in chemotherapy resistant CML cells. The potent apoptotic activity of these novel compounds suggests their potential use in the treatment of CML and related diseases. Cell death induced by a representative pyrrolo-1,5-benzoxazepine, PBOX-6, in three CML cell lines, K562, KYO.1 and LAMA 84, was accompanied by the morphological features of apoptosis including DNA fragmentation, the biochemical hallmark of apoptosis. Induction of apoptosis by PBOX-6 was not accompanied by either the down-regulation of Bcr-Abl or attenuation of its tyrosine kinase activity. This demonstrates that PBOX-6 can by-pass Bcr-Abl-mediated suppression of apoptosis, suggesting an important potential use of these compounds in the treatment of CML. Part of the mechanism by which this novel compound executes the apoptotic cascade has been characterised and it has been shown that apoptosis is independent of events that lead to the release of mitochondrial cytochrome c and caspases are dispensable for apoptosis induced by PBOX-6 in CML cells.

The results presented in the current study suggest the potential of PBOX-6 as a chemotherapeutic agent for the treatment of CML. A number of currently used chemotherapeutic agents, such as etoposide, ara-C and doxorubicin, induce apoptosis in hematopoietic cells with distinct mechanisms of action. The mechanism of action of PBOX-6 is investigated in the next two Chapters.

Chapter 4

Investigation into the events that trigger the apoptotic cascade induced by PBOX-6 in K562 cells

4.1 Introduction

In the previous chapter, it has been shown that some members of a novel series of pyrrolo-1,5-benzoxazepine compounds potently induce apoptosis in CML cells. Pyrrolo-1,5-benzoxazepines are high affinity ligands for the peripheral-type benzodiazepine receptor (PBR) (Campiani *et al.*, 1996). In recent years a number of reports suggest a role for the PBR in the induction of apoptosis (Bono *et al.*, 1999; Chelli *et al.*, 2001; Hirsch *et al.*, 1998). The PBR is conserved throughout evolution suggesting that the functions of this gene must be fundamental to the cell (Gavish *et al.,* 1999). Although a number of functions besides apoptosis have been attributed to the PBR over the years including roles in steroidogenesis and cell proliferation, the true physiological role of the receptor remains unclear (Gavish *et al.*, 1999).

Evidence supporting a role of the PBR in the induction of apoptosis includes the protein complex in which it exists and its cellular location. The PBR appears to be a heteromeric complex of at least three different subunits, including the 18 kDa isoquinoline binding subunit, the 32 kDa voltage dependent anion channel (VDAC) and the 30 kDa adenine nucleotide carrier (ANT) (Gavish *et al.*, 1999). Along with cyclophilin D, these components are thought to form part of the permeability transition (PT) pore, which is believed to play a critical role in a number of apoptotic pathways (Finkel, 2001; Tafani *et al.,* 2001). Although molecular components of the PT pore have not been definitively established, it appears to consist of a multiprotein complex formed at the contact sites between the mitochondrial inner and outer membranes forming a large conductance channel. It is believed that during apoptosis the PT pore opens allowing water and solutes to enter. The mitochondria swells and its outer membrane ruptures allowing apoptogenic factors such as cytochrome c and apoptosis-inducing factor to escape (Martinou, 1999). Members of the Bcl-2 protein family regulate opening of the PT pore, although the mechanism in which they do so remains controversial. Some reports suggest that Bcl-2 family members target VDAC and cause PT opening (Shimizu *et al.,* 1999), whereas others suggest they form ion channels allowing the release of apoptogenic agents (Marzo *et al.*, 1998). The peripheral-type benzodiazepine receptor is found primarily on the outer mitochondrial membrane (Gavish *et al.*, 1999) and its close association with the PT pore has lead a number of groups to investigate its possible involvement in PT pore opening and the induction of apoptosis. For example, it has been reported that the isoquinoline carboxamide, PK11195, a prototypic

ligand of the 18 kDa PBR subunit, facilitates the induction of apoptosis by a number of different stimuli including agonists of the glucocorticoid receptor, the chemotherapeutic agents etoposide and doxorubicin, gamma irradiation and the second messenger ceramide. It was found that PK11195, which itself is not toxic, can reverse Bcl-2 mediated inhibition of apoptosis. The synergism between PK11195 and these pro-apoptotic agents extended to all hallmarks of apoptosis, namely loss of mitochondrial transmembrane potential, generation of reactive oxygen intermediates, exposure of phosphatidylserine on the plasma membrane and DNA fragmentation (Hirsch *et al.*, 1998). Chelli *et al.* (2001) reported that PBR ligands including PK11195, Ro5-4864 and diazepam induce PT pore opening in a cell-free system using heart mitochondria. It has also been reported that PK11195 significantly enhanced the pro-apoptotic effect of TNFα in U937 cells (Bono *et al.*, 1999) and TNFα-induced necrotic cell death in fibroblast cells (Pastorino *et al.*, 1996). However, in contrast, it has been suggested that the PBR may function in protecting against TNFα induced cell death as the resistance of Leydig cells to TNFα correlates with up-regulation of PBR expression (Rey *et al.*, 2000). In the present study, the possibility that the pro-apoptotic effect of pyrrolo-1,5-benzoxazepine compounds in CML cells is mediated through their interaction with the PBR was investigated.

It is widely agreed that Bcr-Abl oncoproteins bind directly to activators of the Ras signalling pathway, and activation of Ras function is an important component in Bcr-Abl-mediated transformation (Goga *et al.*, 1995; Million and Van Etten, 2000; Pendergast *et al.*, 1993; Puil *et al.*, 1994). Ras is a small GTP-binding protein that acts as a molecular switch cycling between active GTP-bound and inactive GDP-bound forms. Three different interacting molecules regulate G-protein activation. Guanine nucleotide exchange factors (GEFs) catalyse the exchange of GDP for GTP resulting in activation. GTPase activating proteins (GAPs) stimulate the intrinsic GTPase activity, thus inactivation, and guanine nucleotide dissociation inhibitors (GDIs), inhibit the exchange of GDP for GTP (Denhardt, 1996). Bcr-Abl binds to the adaptor protein Grb2 through its SH2 domain and this binding requires phosphorylation of tyrosine 177 (Million and Van Etten, 2000; Pendergast *et al.*, 1993). Grb-2 binding to Bcr-Abl potentiates oncogenic transformation through direct stimulation of Ras via Sos-1, a guanine nucleotide exchange factor, which activates Ras (Pendergast *et al.*, 1993; Puil *et al.*, 1994). The pathophysiological consequence of Ras up-

regulation is constitutive signalling thereby stimulating cell proliferation and inhibiting apoptosis (Adjei *et al.*, 2000).

Several small G-proteins involved in cell signalling, including Ras and Rho, as well as several polypeptides of diverse functions such as lamins A and B and rhodopsin kinase, are synthesised as cytoplasmic precursors that require posttranslational modification for conversion to mature membrane bound forms (Adjei *et al.*, 2000). The first step in this process is the transfer of a 15-carbon isoprene unit, farnesyl, from the substrate farnesyl pyrophosphate (FPP) onto the cysteine residue located in the CAAX tetrapeptide at the C-terminus of these proteins, where C is cysteine, A is an aliphatic residue and X is methionine or serine. An enzyme known as farnesyl protein transferase (FPTase) catalyses this process. Farnesylation is required for Ras proteins to become membrane-associated and induce cellular transformation (Oliff, 1999) and inhibition of farnesyl protein transferase was envisioned as a strategy for interfering with Ras-dependent transformation. In recent years a series of small molecular inhibitors of FPTase have been developed. Some FPTases have been discovered by the screening of natural products, for example, the antibiotic manumycin A is a structural homologue to the substrate FPP. Manumycin A has been shown to inhibit Ras farnesylation and phosphorylation of the downstream MAP kinase pathway, thus inhibiting proliferation of rat vascular smooth muscle cells (Kouchi *et al.*, 1999). A second strategy involved the development of peptides that mimic the CAAX tetrapeptide found at the C-terminus of Ras, known as peptidomimetics. A number of these compounds have been shown to be effective in inhibiting the farnesylation of Ras (Bishop *et al.*, 1995; Emanuel *et al.*, 2000; James *et al.*, 1993; Lerner *et al.*, 1995; Peters *et al.*, 2001). For example, the FPTase inhibitor SCH66336 has recently been shown to inhibit colony formation in soft agar and proliferation of Bcr-Abl transformed BaF3 cells in a dose-dependent manner. The compound sensitised cells to apoptotic stimuli such as serum withdrawal and irradiation, and also abrogated Bcr-Abl induced leukaemia *in vivo* (Peters *et al.*, 2001). Results from phase 1 clinical trials of SCH66336 in twenty patients with solid tumours revealed that the compound is well tolerated with reversible and manageable toxicity, and provided the first evidence of clinical activity of this class of agent in humans *in vivo* (Adjei *et al.*, 2000). In addition, the FPTase inhibitors L-739, 749 and L-744, 832 have been shown to inhibit CFU-GM colony growth using primary cells from patients with confirmed juvenile myelomonocytic leukaemia (JMML). As in the case of CML, the pathogenesis of JMML has been linked to deregulated

signal transduction through the Ras signalling pathway (Emanuel *et al.*, 2000). A variety of FPTase inhibitors have also been shown to induce mitochondrial cytochrome c release, caspase-3 activation, chromatin condensation and DNA fragmentation, under conditions of reduced serum and with specificity for transformed cell (Suzuki *et al.*, 1998). Based on the novel mechanism of action, FPTase inhibitors present a promising class of anti-cancer agents. Anti-tumour efficacy in a large number of animal studies has been demonstrated and at least six FPTase inhibitors are currently in phase I trials (Crul *et al.*, 2001). Pyrrolo-1,5-benzoxazepines share structural similarities with a series of compounds known as benzodiazepines, which also bind to the PBR (Braestrup and Squires, 1977). A novel series of benzodiazepine-based peptidomimetics have been synthesised and some members including BZA-5B, act as potent farnesyl transferase inhibitors (James *et al.*, 1994). In the current study, the pyrrolo-1,5-benzoxazepine, PBOX-6, has been shown to induce apoptosis in CML cells by bypassing the apoptotic suppressor, Bcr-Abl. In an attempt to investigate whether PBOX-6 targets molecular components involved in Bcr-Abl-mediated transformation, the ability of the compound to act as a molecular inhibitor of Ras farnesylation was determined.

A wide variety of chemotherapeutic agents are currently used in the treatment of diseases of the hematopoietic system. These include the DNA intercalators amsacrine, mitoxanthrone and doxorubicin, and the non-DNA intercalators, etoposide and teniposide. Although these chemotherapeutic agents function through diverse mechanisms, they have all been shown to inhibit the mammalian topoisomerase II enzyme, ultimately inducing DNA strand breaks and apoptosis (Kaufmann, 1998). Topoisomerases are nuclear enzymes that play a role in the regulation of DNA topology and are required for replication and transcription (Azumu *et al.*, 1995; Mo and Beck, 1999). Two classes are found in mammalian cells, type I and type II. Type I topoisomerase is involved in relaxation of DNA and the unknotting of single stranded circular DNA (Liu and Miller, 1981). Type II topoisomerase (Topo II) catalyses the relaxation of supercoiled DNA and separates intertwined DNA duplexes. This is accomplished by the formation of two protein-linked breaks in the DNA where the 5' phosphoryl group on deoxyribose is covalently attached to a tyrosine residue in the topoisomerase. Topo II acts as a homodimer, with each subunit joining to one of the DNA strands. This Topo II-DNA complex is known as the cleavable complex. ATP binding induces a conformational change in the enzyme, which converts Topo II into a clamp on the

DNA. The DNA strands are passed between the two subunits, thus strand passage will relieve supercoiling tension. The break in the cleaved helix is re-ligated and upon ATP hydrolysis, the clamp is removed releasing the DNA and the enzyme is re-cycled (Fortune and Osheroff, 1998; Kaufmann, 1998).

Topoisomerase II is the target of several clinically effective anti-cancer agents, which are divided into two classes depending on the mechanism in which they inhibit the activity of Topo II. These are known as either Topo II poisons or catalytic inhibitors of the enzyme. Topo II poisons kill cells by stabilising the Topo II-DNA cleavable complex and increasing the amount of Topo II-mediated DNA cleavage, thus converting this essential enzyme into a potent cellular toxin (Fortune and Osheroff, 1998). Among the Topo II poisons currently is use are mitoxanthrone, doxorubicin and amsacrine (Perez *et al.*, 1997), which intercalate into the DNA and prevent the release of covalently bound topoisomerase (Kaufmann, 1998; Lown *et al.,* 1985), and the non-DNA intercalators such as the epipodophyllotoxins etoposide and teniposide which interfere with the release reaction by binding to the enzyme directly (Kaufmann, 1998). Etoposide has been shown to induce DNA strand breaks and internucleosomal DNA damage resulting in apoptosis in HL-60 cells. Interestingly, etoposide was also found to induce DNA strand breaks in K562 cells, however, these cells were resistant to the induction of apoptosis (Ritke *et al.*, 1994b).

In contrast to Topo II poisons, catalytic inhibitors of Topo II inhibit the catalytic activity of the enzyme without stabilising the Topo II-DNA complex or intercalating into the DNA (Fatmann *et al.,* 1996). These include compounds such as merbarone, aclarubicin, staurosporine and the bis-2,6-dioxopiperazine derivatives ICRF-187, ICRF-193 and ICRF-154. It is believed that these inhibitors exert their effects through diverse mechanisms. The bisdioxopiperazine derivatives appear to induce a conformational change in Topo II that results in the enzyme being trapped in an inactive closed protein clamp form. The inhibition of the closed clamp structure inhibits the intrinsic ATPase activity of topoisomerase II and prevents recycling of the enzyme (Fatmann *et al.*, 1996). These agents presumably kill cells by preventing separation of intertwined daughter duplexes (Kaufmann, 1998). Aclarubicin blocks binding of Topo II to its DNA substrate, the initial step in the catalytic cycle, while merbarone and staurosporine are thought to operate by blocking cleavage of its DNA substrate, thus disrupting chromosome separation during mitosis (Fortune and Osheroff, 1998). In addition to their differential cellular effects, drugs that act at or before the DNA

cleavage step in the catalytic cycle are likely to attenuate the actions of topoisomerase poisons. This is indeed the case with merbarone, which diminishes DNA cleavage stimulated by etoposide (Fortune and Osheroff, 1998). Similar results were found with the bisdioxopiperazine derivative ICRF-193 (Tanabe *et al.*, 1991) and aclarubicin (Jensen *et al.*, 1990), which have been shown to block etoposide-induced DNA cleavage suggesting that these compounds interfere with some earlier step before the formation of the cleavable complex in the catalytic cycle (Tanabe *et al.*, 1991). In the current study, it was determined whether PBOX-6-induced apoptosis is mediated by inhibition of topoisomerase II activity, by inducing DNA strand breaks in a manner similar to the Topo II poisons, or at an earlier stage in the catalytic cycle similar to the catalytic inhibitors.

Aims of this chapter

CML cells, in particular the K562 cell line, are refractory to apoptosis induced by most chemotherapeutic agents and expression of the transforming oncogene, *bcr-abl*, is believed to confer resistance on these cells. In the present study, it has been shown that a series of novel pyrrolo-1,5-benzoxazepine compounds potently induce apoptosis in three CML cell lines by by-passing this apoptotic suppressor. The aim of the current chapter is to further elucidate the molecular mechanism in which these compounds induce apoptosis in CML cells. Investigations were initially carried out to determine whether interaction of these pyrrolo-1,5-benzoxazepine compounds with the peripheral-type benzodiazepine receptor is responsible for the pro-apoptotic effects. Then, in an attempt to further dissect the pathway in which these compounds function, their effect on Ras farnesylation was determined. Finally, investigative work was carried out to determine whether these compounds function in a manner similar to many conventional chemotherapeutic agents, which inhibit Topo II activity and induce DNA damage with subsequent apoptosis.

4.2 Results

4.2.1 Saturable binding of [^{3}H] PK11195 to K562, KYO.1 and LAMA 84 cell homogenates

A number of ligands have been used for studying the peripheral-type benzodiazepine receptor (PBR) and the high affinity carboxamide isoquinoline, PK11195, is one of the most widely used. Preliminary experiments were carried out to characterise the binding of PK11195 to the receptor in CML cells.

Cell homogenates were prepared as described in Section 2.15.1 and the protein concentration was determined using a Markwell assay as outlined in Section 2.3.2. Cell homogenates were incubated with [^{3}H] PK11195 (0.5-50nM) and binding was allowed to take place. Total and non-specific binding in each case was determined by the absence and presence of 10μM unlabelled PK11195, respectively. Results show saturable binding of [^{3}H] PK11195 to a single class of binding site in K562, KYO.1 and LAMA 84 cell homogenates (Fig. 4.1, 4.2 and 4.3, respectively). K562 cells displayed K_D and B_{max} values of 16 +/- 7.3 nM and 2.3 +/- 0.14 pmols/mg protein, respectively (Fig. 4.1A). Minimum variation was observed between experiments as indicated on Fig. 4.1B where K562 cells displayed a K_D and B_{max} values of 12.0 +/- 2.0 nM and 1.04 +/- 0.06 pmols/mg protein, respectively. Similarly, KYO.1 cells displayed K_D and B_{max} values of 17.1 +/- 5.1 nM and 3.8 +/- 0.5 pmols/mg protein, and LAMA 84 cells displayed K_D and B_{max} values of 9.4 +/- 3.4nM and 5.2 +/-0.5 pmols/mg protein, respectively.

4.2.2 Displacement of [^{3}H] PK11195 by PBOX-6 from K562, KYO.1 and LAMA 84 cell homogenates

In order to determine the affinity of PBOX-6 for binding to the PBR, cell homogenates were incubated with a constant amount of [^{3}H] PK11195 (4nM) and a range of PBOX-6 concentrations (0.1-100nM). Results show that PBOX-6 causes a dose-dependent displacement of [^{3}H] PK11195 from K562, KYO.1 and LAMA 84 cell homogenates (Fig. 4.4, 4.5 and 4.6 respectively) with K_i values of 0.7 nM, 0.7 nM and 1.0 nM, respectively. Displacement curves, describing the competition of [^{3}H] PK11195 binding to the PBR by PBOX-6 were generated with the use of the computer program Graph Pad, which uses a sigmoidal curve-fitting programme.

A

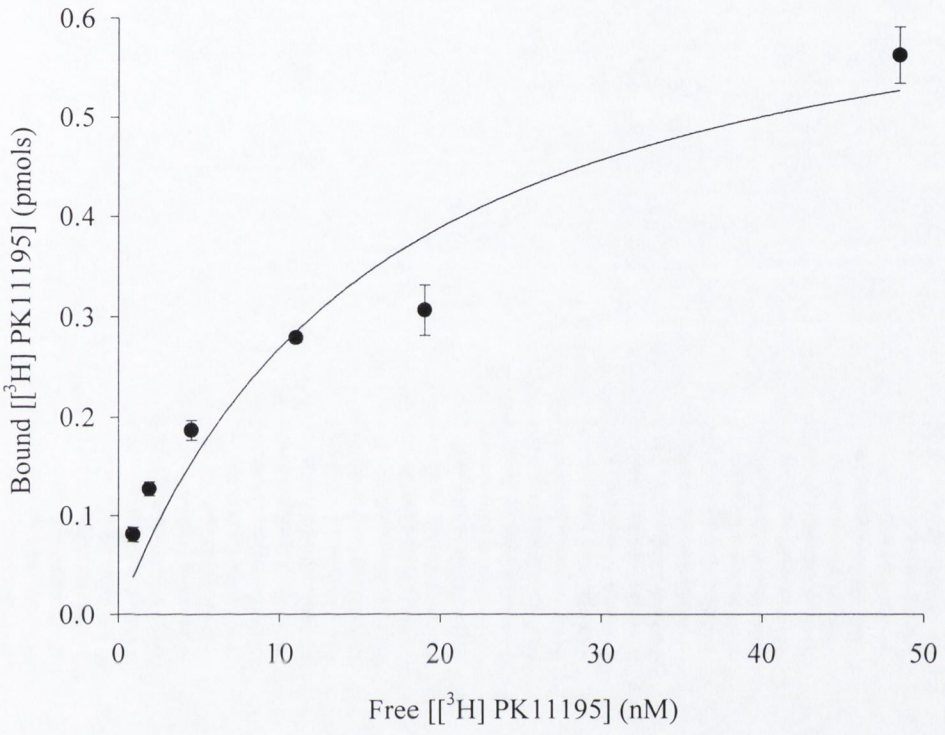

Fig. 4.1 Saturable [^{3}H] PK11195 binding to homogenates of K562 cells

(A) Cell homogenate (300μg) was incubated with [^{3}H] PK11195 (0.5-50nM, 86.5 Ci/mmol) for 60 min at 4°C. Total and non-specific binding in each case was determined by the absence and presence of 10μM unlabelled PK11195, respectively, as described in Section 2.15.1. Specific binding was measured by subtracting non-specific binding from total binding values. Specific [^{3}H] PK11195 binding data was fitted using the Sigma plot computer program, to the equation describing a rectangular hyperbola, yielding K_D and B_{max} values of 16 +/- 7.3 nM and 2.3 +/- 0.14 pmols/mg protein respectively. Each point is the mean +/- S.E.M of triplicate determinations. The absence of error bars indicates that the error was smaller than the size of the symbol. Results are representative of an experiment performed three times.

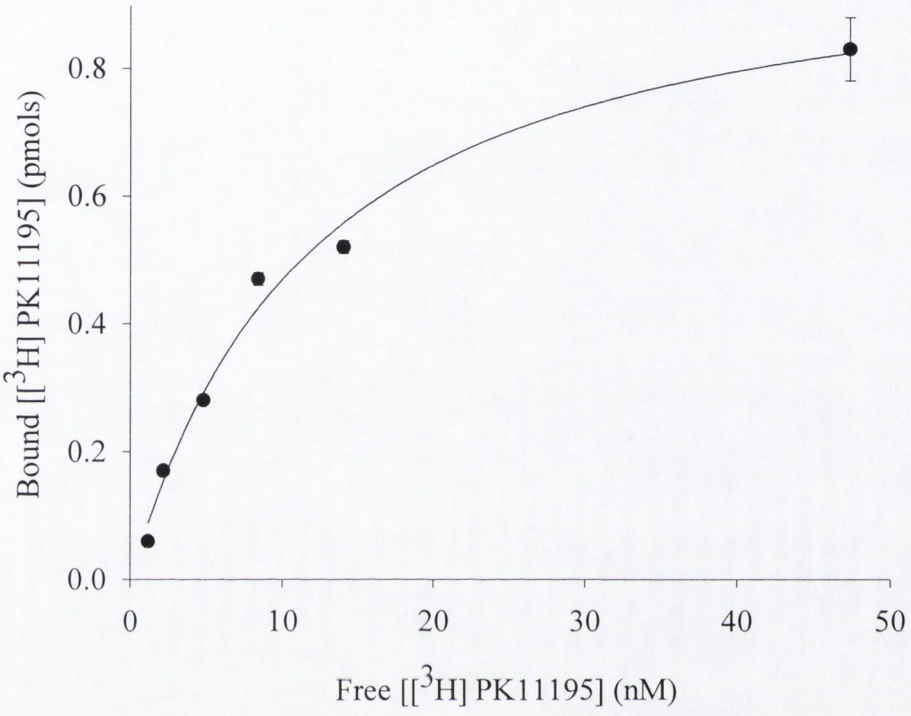

Fig. 4.1 Saturable [^{3}H] PK11195 binding to homogenates of K562 cells

(B) Cell homogenate (330μg) was incubated with [^{3}H] PK11195 (0.5-50nM, 86.5 Ci/mmol) for 60 min at 4°C. Total and non-specific binding in each case was determined by the absence and presence of 10μM unlabelled PK11195, respectively, as described in Section 2.15.1. Specific binding was measured by subtracting non-specific binding from total binding values. Specific [^{3}H] PK11195 binding data was fitted using the Sigma plot computer program, to the equation describing a rectangular hyperbola, yielding K_D and B_{max} values of 12 +/- 2.0 nM and 1.04 +/- 0.06 pmols/mg protein respectively. Each point is the mean +/- S.E.M of triplicate determinations. The absence of error bars indicates that the error was smaller than the size of the symbol. Results are representative of an experiment performed three times.

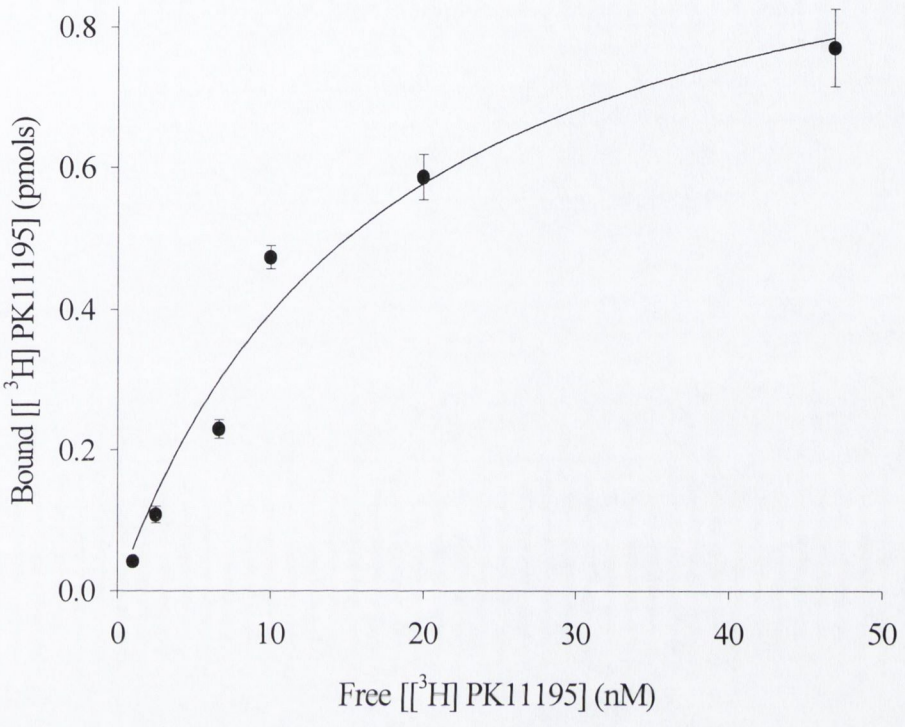

Fig. 4.2 Saturable [^{3}H] PK11195 binding to homogenates of KYO.1 cells

Cell homogenate (280μg) was incubated with [^{3}H] PK11195 (0.5-50nM, 86.5 Ci/mmol) for 60 min at 4°C. Total and non-specific binding in each case was determined by the absence and presence of 10μM unlabelled PK11195, respectively, as described in Section 2.15.1. Specific binding was measured by subtracting non-specific binding from total binding values. Specific [^{3}H] PK11195 binding data was fitted using the Sigma plot computer program, to the equation describing a rectangular hyperbola, yielding K_D and B_{max} values of 17.1 +/- 5.1 nM and 3.8 +/- 0.5 pmols/mg protein respectively. Each point is the mean +/- S.E.M of triplicate determinations. The absence of error bars indicates that the error was smaller than the size of the symbol. Results are representative of an experiment performed three times.

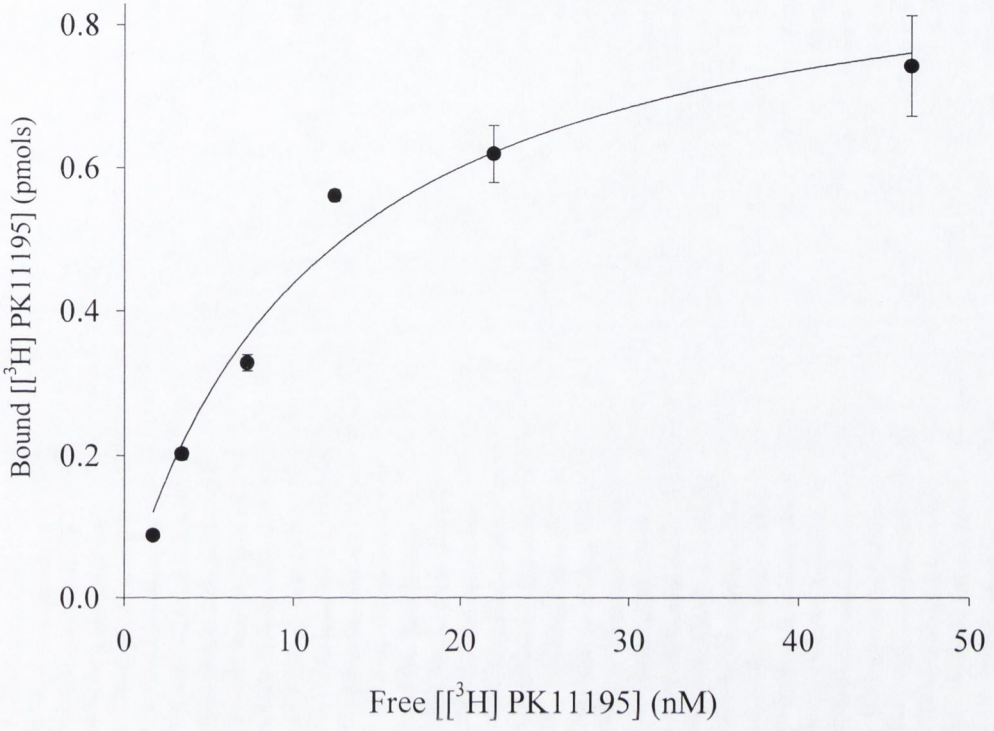

Fig. 4.3 Saturable [^{3}H] PK11195 binding to homogenates of LAMA 84 cells

Cell homogenate (172μg) was incubated with [^{3}H] PK11195 (0.5-50nM, 86.5 Ci/mmol) for 60 min at 4°C. Total and non-specific binding in each case was determined by the absence and presence of 10μM unlabelled PK11195, respectively, as described in Section 2.15.1. Specific binding was measured by subtracting non-specific binding from total binding values. Specific [^{3}H] PK11195 binding data was fitted using the Sigma plot computer program, to the equation describing a rectangular hyperbola, yielding K_D and B_{max} values of 9.4 +/-3.4 nM and 5.2 +/- 0.5 pmols/mg protein respectively. Each point is the mean +/- S.E.M of triplicate determinations. The absence of error bars indicates that the error was smaller than the size of the symbol. Results are representative of an experiment performed three times.

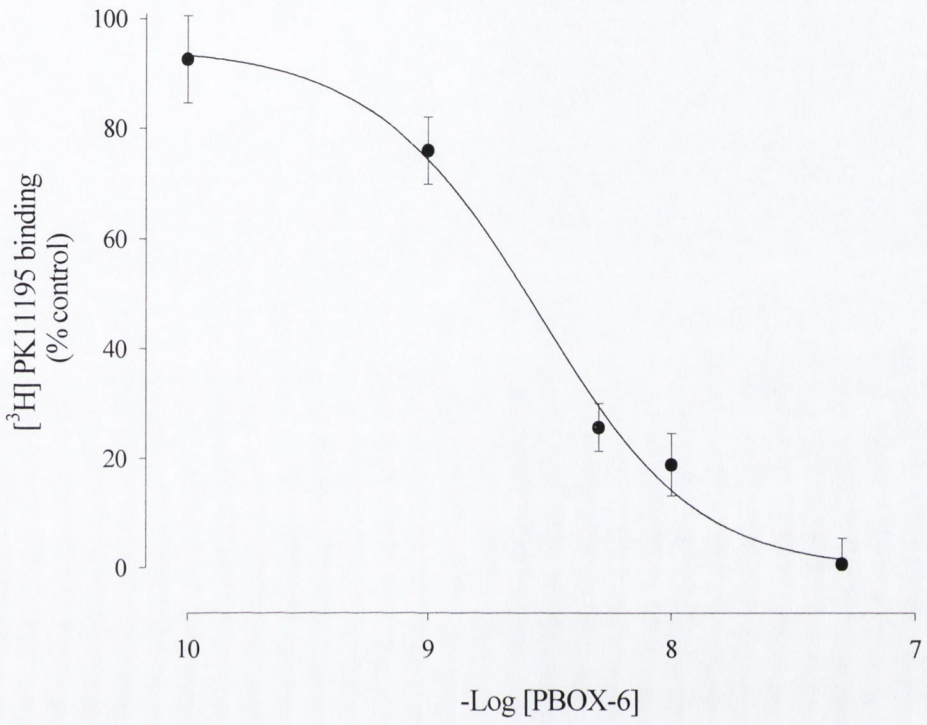

Fig. 4.4 Displacement of [^{3}H] PK11195 specific binding to K562 cell homogenates by PBOX-6

K562 cell homogenates (200μg) were assayed for specific binding of [^{3}H] PK11195 (4nM; 86.5 Ci/mmol) in the absence and presence of a range of concentrations of PBOX-6 (0.1-100nM), as described in Section 2.15.1. Control binding was defined as specific binding in the absence of PBOX-6. Non-specific binding was measured in the presence of 10μM unlabelled PK11195. The displacement curve was generated assuming a mutually exclusive binding site and the best fit was obtained using the computer program Graph Pad, yielding a K_i value of 0.7 nM. Each point represents the mean +/- S.E.M of incubations performed in triplicate. Results are representative of an experiment performed three times.

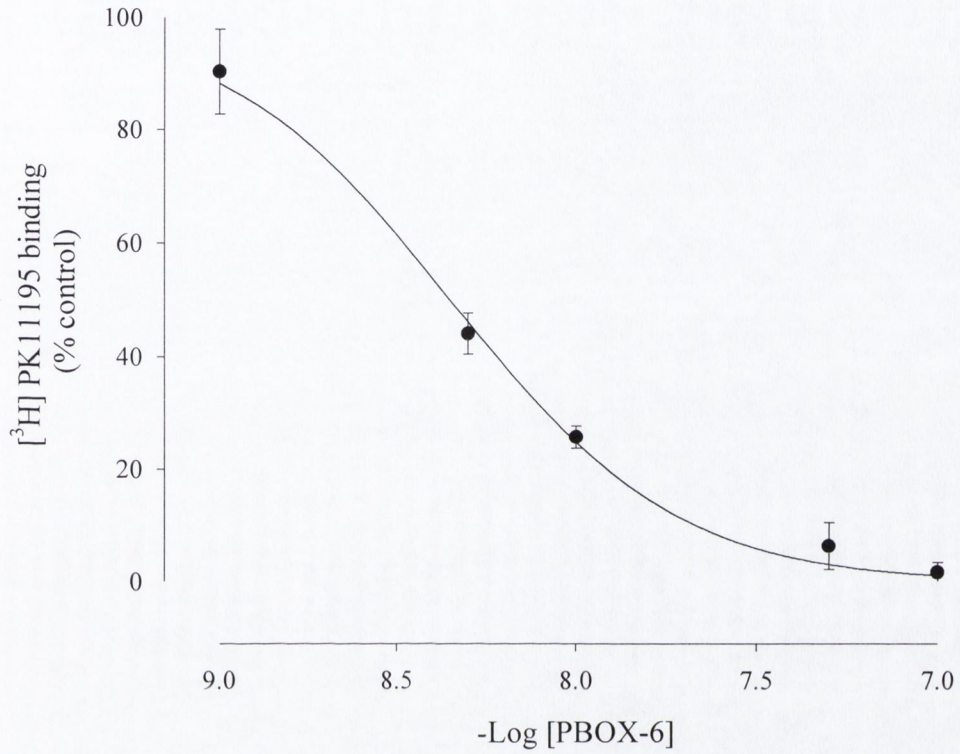

Fig. 4.5 Displacement of [^{3}H] PK11195 specific binding to KYO.1 cell homogenates by PBOX-6

Cell homogenates (160μg), prepared from KYO.1 cells were assayed for specific binding of [^{3}H] PK11195 (4nM; 86.5 Ci/mmol) in the absence and presence of a range of concentrations of PBOX-6 (0.1-100nM), as described in Section 2.15.1. Non-specific binding was measured in the presence of 10μM unlabelled PK11195. Control binding was defined as specific binding in the absence of PBOX-6. The displacement curve was generated assuming a mutually exclusive binding site and the best fit was obtained using the computer program Graph Pad, yielding a K_i value of 0.7 nM. Each point represents the mean +/- S.E.M of incubations performed in triplicate. Results are representative of an experiment performed three times.

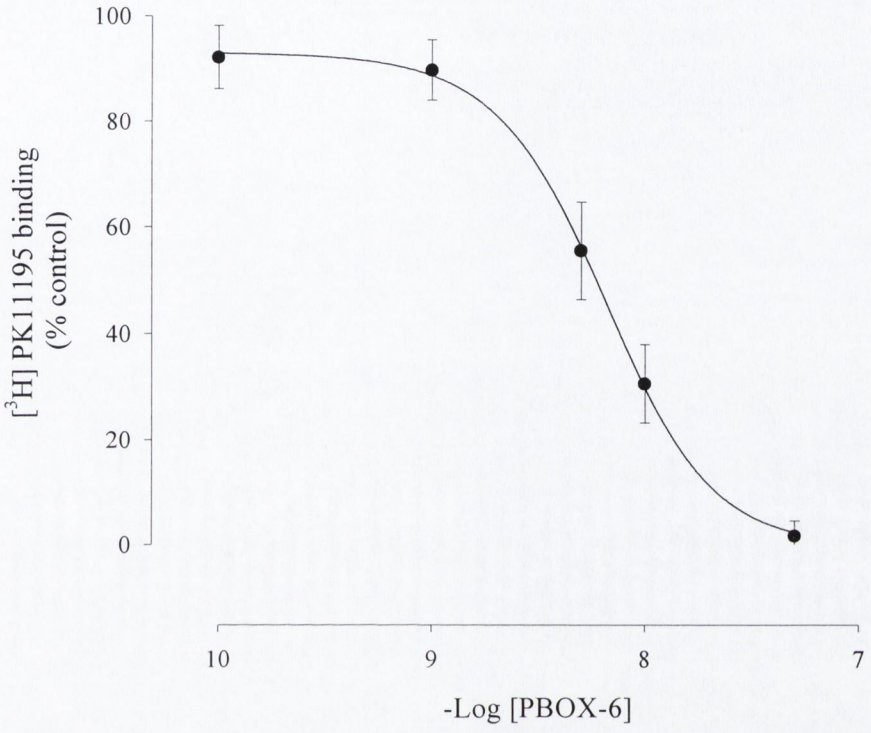

Fig. 4.6 Displacement of [^{3}H] PK11195 specific binding to LAMA 84 cell homogenates by PBOX-6

Cell homogenates (160μg) were prepared from LAMA 84 cells and assayed for specific binding of [^{3}H] PK11195 (4nM; 86.5 Ci/mmol) in the absence and presence of a range of concentrations of PBOX-6 (0.1-100nM), as described in Section 2.15.1. Control binding was defined as specific binding in the absence of PBOX-6. Non-specific binding was measured in the presence of 10μM unlabelled PK11195. The displacement curve was generated assuming a mutually exclusive binding site and the best fit was obtained using the computer program Graph Pad, yielding a K_i value of 1.0 nM. Each point represents the mean +/- S.E.M of incubations performed in triplicate. Results are representative of an experiment performed three times.

4.2.3 Displacement of [^{3}H] PK11195 from K562 cell homogenates by the non-apoptotic pyrrolo-1,5-benzoxazepines, PBOX-1 and -2, and the apoptotic pyrrolo-1,5-benzoxazepines, PBOX-4, -5 and -7

In order to determine whether the pro-apoptotic effect observed with some members of this pyrrolo-1,5-benzoxazepine series was mediated through binding to the PBR, a comparison was made of the binding affinities of a number of apoptotic and non-apoptotic compounds. It has already been shown in Chapter 3 that PBOX-4, -5, -6 and -7 potently induce apoptosis in K562 cells, whereas PBOX-1 and -2 do not induce apoptosis at a similar concentration. Cell homogenates were incubated with a constant amount of [^{3}H] PK11195 (4nM) and a range of concentrations (0.1-100nM) of either PBOX-1, -2, -4, -5 and -7. Results show that PBOX-1, -2, -4, -5 and -7 induces a dose-dependent displacement of [^{3}H] PK11195 from K562 cell homogenates (Fig. 4.7, 4.8, 4.9, 4.10 and 4.11 respectively) yielding K_i values of 0.7 nM, 0.7 nM 0.8 nM, 0.4 nM and 0.9nM respectively. This data, which is summarised in Table 4.1, indicates that all the PBOX compounds tested bind to the PBR with similar affinities. Thus there is no correlation between affinity for the PBR and ability to induce apoptosis. This would suggest that the pro-apoptotic effect observed with some PBOX compounds is not mediated through binding to the PBR.

4.2.4 Peripheral type receptor ligands, Ro5-4864 and PK11195, have no effect on PBOX-6-induced apoptosis in K562 cells

A number of recent reports suggest that the PBR ligand PK11195 enhances the pro-apoptotic effect of a number of chemotherapeutic agents including etoposide and doxorubicin (Hirsch *et al.*, 1998). Furthermore, an alternative PBR ligand, Ro5-4864, has also been reported to induce apoptosis in some systems (Chelli *et al.*, 2001), while having anti-apoptotic effects in other systems (Bono *et al.*, 1999).

The effect of the PBR ligands on PBOX-6-induced apoptosis was examined by the pretreatment of K562 cells with Ro5-4864 and PK11195 at concentrations much greater than necessary to saturate the receptor, and greater than concentrations used by Bono *et al.*, (1999), in which an anti-apoptotic effect was observed. Cells were pretreated with the PBR ligands for 1h prior to treatment with PBOX-6 for a further 16h and the extent of apoptosis was determined. Results, presented in Fig. 4.12, show that treatment of K562 cells with either Ro5-4864 or PK11195 for 17h does not induce apoptosis itself, whereas similar

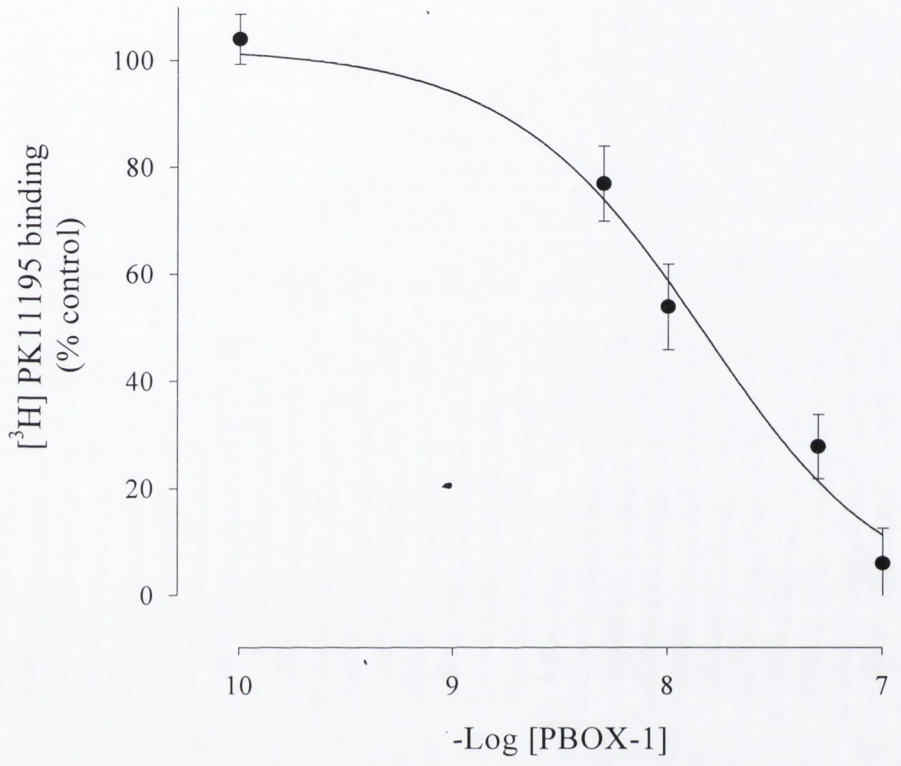

Fig. 4.7 Displacement of [^{3}H] PK11195 specific binding to K562 cell homogenates by PBOX-1

K562 cell homogenates (200μg) were assayed for specific binding of [^{3}H] PK11195 (4nM; 86.5 Ci/mmol) in the absence and presence of a range of concentrations of PBOX-6 (0.1-100nM), as described in Section 2.15.1. Control binding was defined as specific binding in the absence of PBOX-1. Non-specific binding was measured in the presence of 10μM unlabelled PK11195. The displacement curve was generated assuming a mutually exclusive binding site and the best fit was obtained using the computer program Graph Pad, yielding a K_i value of 0.7 nM. Each point represents the mean +/- S.E.M of incubations performed in triplicate. Results are representative of an experiment performed three times.

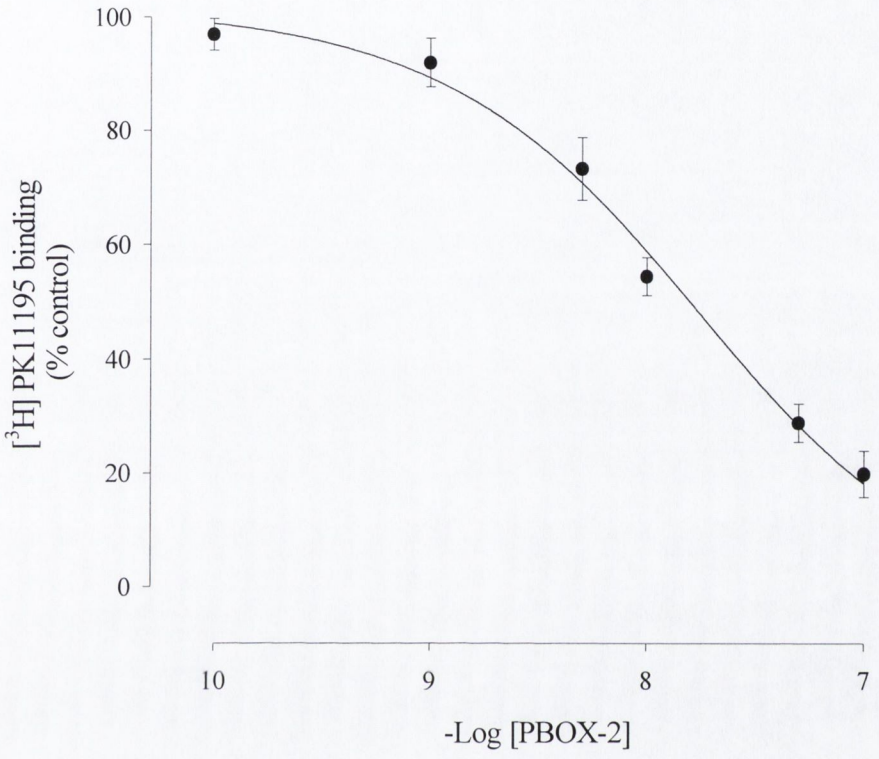

Fig. 4.8 Displacement of [^{3}H] PK11195 specific binding to K562 cell homogenates by PBOX-2

K562 cell homogenates (170μg) were assayed for specific binding of [^{3}H] PK11195 (4nM; 86.5 Ci/mmol) in the absence and presence of a range of concentrations of PBOX-2 (0.1-100nM), as described in Section 2.15.1. Control binding was defined as specific binding in the absence of PBOX-6. Non-specific binding was measured in the presence of 10μM unlabelled PK11195. The displacement curve was generated assuming a mutually exclusive binding site and the best fit was obtained using the computer program Graph Pad, yielding a K_i value of 0.7 nM. Each point represents the mean value +/- S.E.M of incubations performed in triplicate. Results are representative of an experiment performed three times.

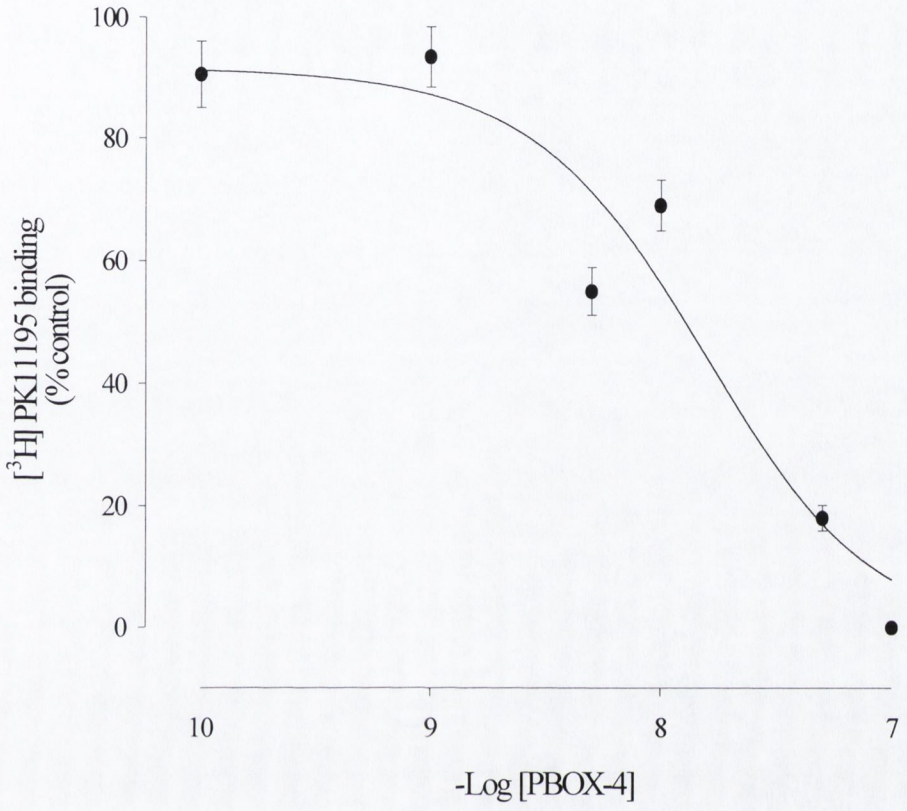

Fig 4.9 Displacement of [^{3}H] PK11195 specific binding to K562 cell homogenates by PBOX-4

K562 cell homogenates (132μg) were assayed for specific binding of [^{3}H] PK11195 (4nM; 86.5 Ci/mmol) in the absence and presence of a range of concentrations of PBOX-4 (0.1-100nM), as described in Section 2.15.1. Control binding was defined as specific binding in the absence of PBOX-4. Non-specific binding was measured in the presence of 10μM unlabelled PK11195. The displacement curve was generated assuming a mutually exclusive binding site and the best fit was obtained using the computer program Graph Pad, yielding a K_i value of 0.8 nM. Each point represents the mean +/- S.E.M of incubations performed in triplicate. Results are representative of an experiment performed three times.

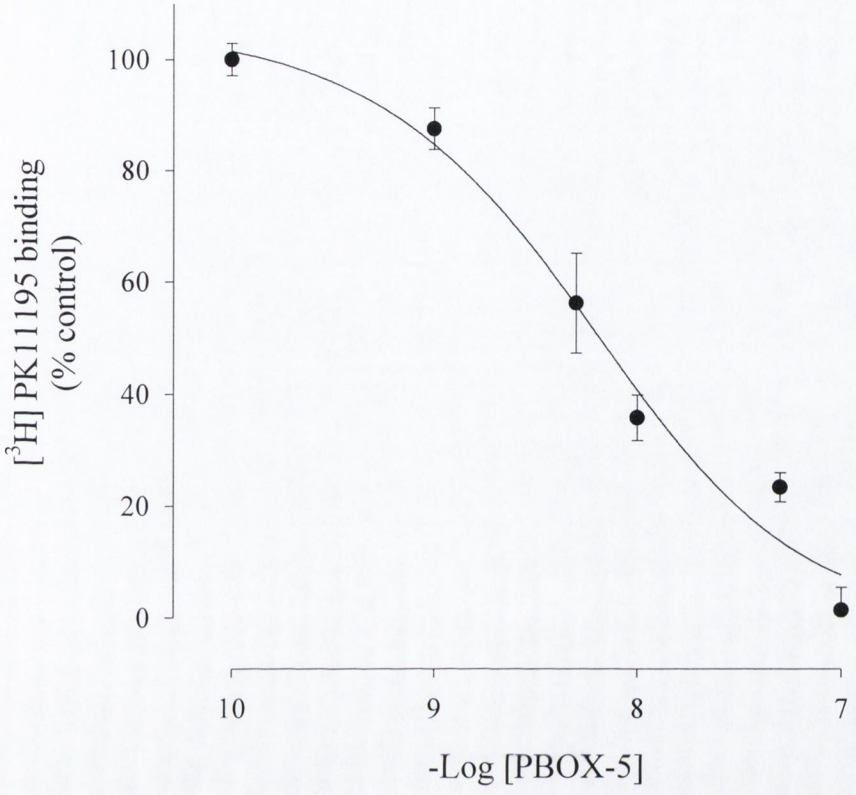

Fig. 4.10 Displacement of [^{3}H] PK11195 specific binding to K562 cell homogenates by PBOX-5

Cell homogenates (132μg) were prepared from K562 cells and assayed for specific binding of [^{3}H] PK11195 (4nM; 86.5 Ci/mmol) in the absence and presence of a range of concentrations of PBOX-5 (0.1-100nM), as described in Section 2.15.1. Control binding was defined as specific binding in the absence of PBOX-6. Non-specific binding was measured in the presence of 10μM unlabelled PK11195. The displacement curve was generated assuming a mutually exclusive binding site and the best fit was obtained using the computer program Graph Pad, yielding a K_i value of 0.4 nM. Each point represents the mean +/- S.E.M of incubations performed in triplicate. Results are representative of an experiment performed three times.

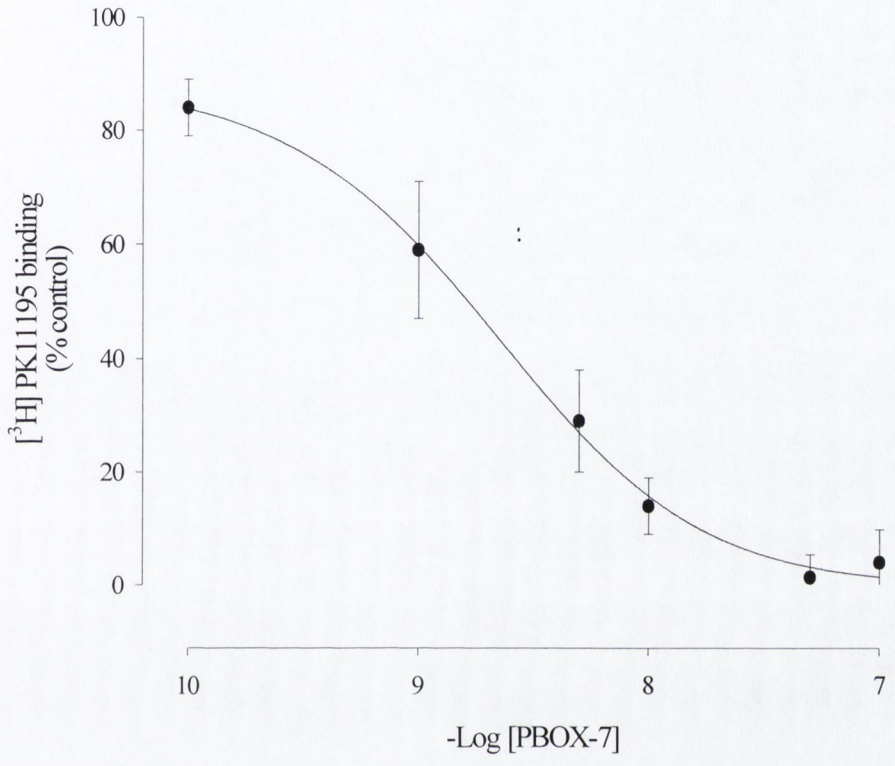

Fig. 4.11 Displacement of [^{3}H] PK11195 specific binding to K562 cell homogenates by PBOX-7

K562 cell homogenates (160μg) were assayed for specific binding of [^{3}H] PK11195 (4nM; 86.5 Ci/mmol) in the absence and presence of a range of concentrations of PBOX-7 (0.1-100nM), as described in Section 2.15.1. Control binding was defined as specific binding in the absence of PBOX-6. Non-specific binding was measured in the presence of 10μM unlabelled PK11195. The displacement curve was generated assuming a mutually exclusive binding site and the best fit was obtained using the computer program Graph Pad, yielding a K_i value of 0.9 nM. Each point represents the mean value +/- S.E.M of incubations performed in triplicate. Results are representative of an experiment performed three times.

PBOX compound	Inhibition of [^{3}H] PK11195 binding to the PBR K_i values (nM)
PBOX-1	0.7
PBOX-2	0.7
PBOX-4	0.8
PBOX-5	0.4
PBOX-6	0.7
PBOX-7	0.9

Table 4.1 Summary of the displacement of [^{3}H] PK11195 binding to the PBR by a range of PBOX compounds

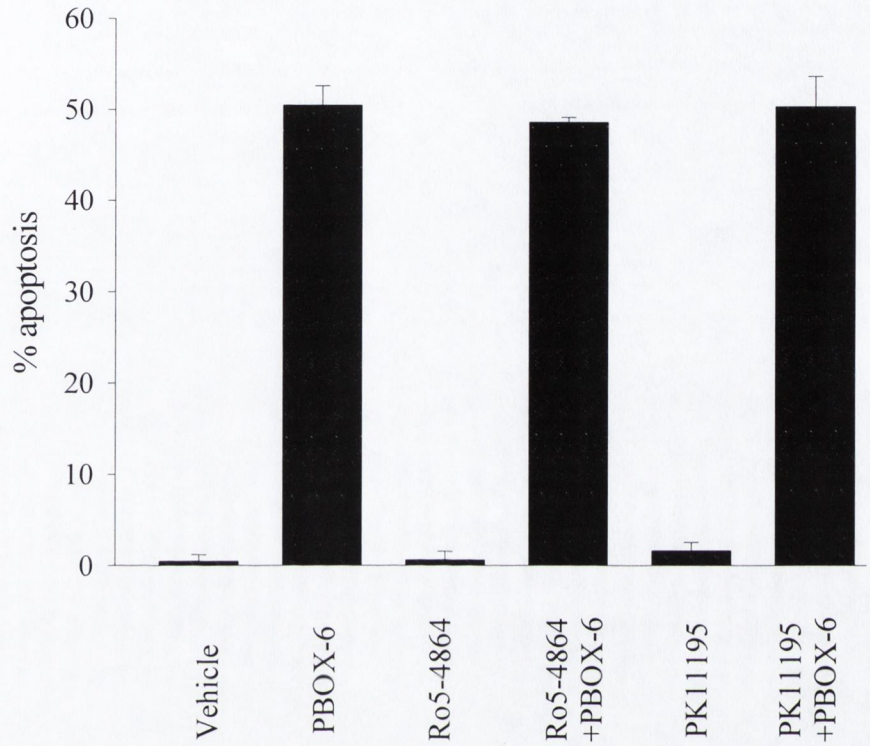

Fig. 4.12 The PBR ligands, Ro5-4864 and PK11195, have no effect on PBOX-6 induced apoptosis in K562 cells

K562 cells were seeded at 3 x 10^5 cells per ml and were either treated with vehicle (1% (v/v) ethanol), PBOX-6 (10μM), the PBR ligands Ro5-4864 (10μM) and PK11195 (10μM) or were pretreated with Ro5-4864 (10μM) or PK11195 (10μM) for 1h prior to treatment with PBOX-6 (10μM) for a further 16h. An aliquot of cell suspension (150μl) was centrifuged onto a slide and stained using the RapiDiff kit as described in Section 2.4. The extent of apoptosis was determined by morphological examination of cells. Results represent the mean +/- S.E.M of three separate experiments.

concentrations of PBOX-6 induces approximately 50% apoptosis. In addition, pretreatment of K562 cells with the PBR ligands did not enhance or inhibit PBOX-6-induced apoptosis in K562 cells and provide further evidence of a lack of involvement of the PBR in PBOX-6-induced apoptosis.

4.2.5 Investigation into the effect of PBOX-6 on farnesyl protein transferase activity by measuring H-Ras farnesylation

The post-translational modification of Ras, which is required for cellular transformation, involves the transfer of a 15-carbon isoprene farnesyl from farnesyl pyrophosphate to a cysteine residue in the conserved C-terminal "CAAX" motif (Oliff, 1999). A number of compounds have been developed that inhibit farnesylation of Ras and other intracellular polypeptides. In principle, any of these could serve as an indicator of farnesyl transferase inhibition (Adjei *et al.,* 2000). In order to determine whether PBOX-6 acts as a farnesyl transferase inhibitor, H-Ras was chosen as the substrate to measure enzyme activity.

4.2.5.1 Optimisation of experimental conditions to measure farnesyl protein transferase activity in K562 cells

Farnesyl protein transferase activity was determined by measuring the amount of farnesyl transferred from [^{3}H] farnesyl pyrophosphate (FPP) onto human recombinant H-Ras. In order to optimise experimental conditions, an assay was set up as described in Section 2.17.2 in which the reaction mix contained fixed concentrations of [^{3}H] FPP (10 pmols, 16 Ci/mmol) and H-Ras (1μM) and varying amounts of farnesyl protein transferase (Fig. 4.13A). Farnesyl transferase was partially purified from K562 cells as outlined in Section 1.17.1 and the protein concentration was determined using the Bradford assay. K562 lysate containing 6μg/μl of partially purified farnesyl transferase protein was isolated. Using lysis buffer, various working stock solutions were prepared, to yield final concentrations of 0, 1.5μg, 3μg, 6μg, 9μg and 12μg of FPTase in the complete reaction mix. Mean cpm values obtained from duplicate samples were plotted against FPTase concentration (Fig. 4.13A) and 5μg of partially purified FPTase was chosen as optimal and used in all future experiments. A similar assay was set up in which the reaction mix contained [^{3}H] FPP (10 pmols, 16 Ci/mmol), FPTase (5μg) and a range of H-Ras concentrations (0-15μM). The reaction was

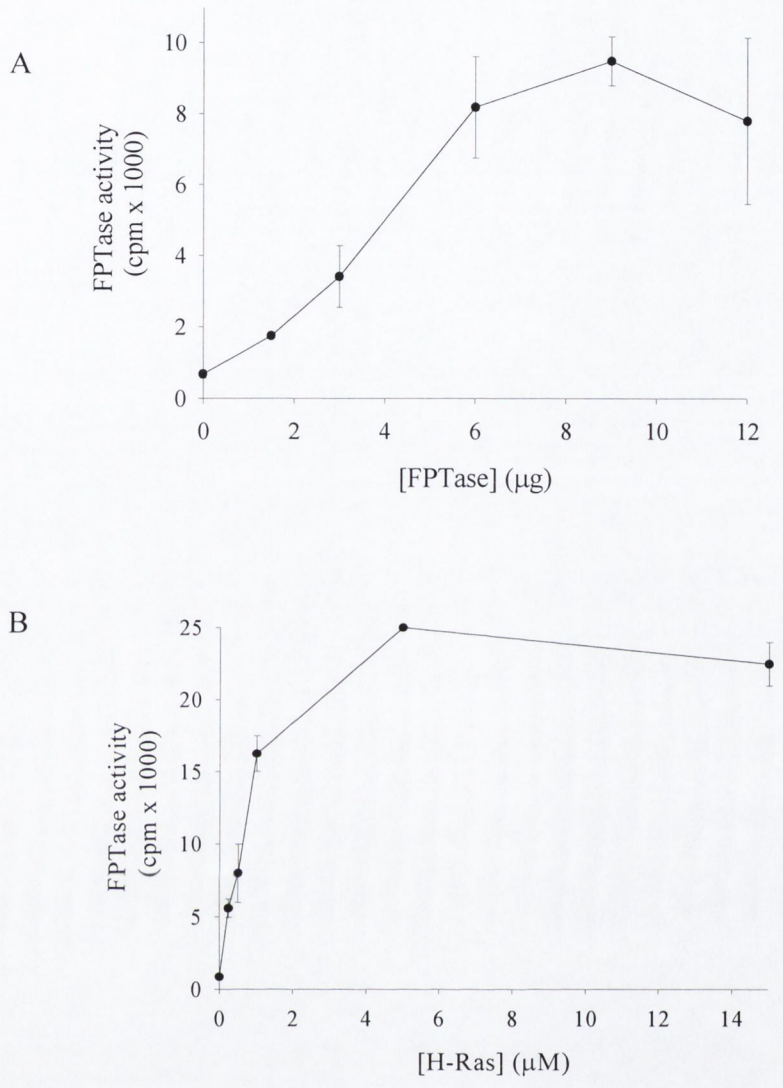

Fig. 4.13 Optimisation of assay conditions for measurement of farnesyl protein transferase activity

A reaction mix was set up as outlined in Section 2.17 containing either (A) [^{3}H] FPP (10 pmols; 16 Ci/mmol), H-Ras (1μM) and a range of concentrations (0-12μg) of FPTase, partially purified from K562 cells, or (B) [^{3}H] FPP (10 pmols), FPTase (5μg) and a range of concentration (0-15μM) of H-Ras. The reaction was allowed to take place for 1h at 37°C and proteins were precipitated by trichloroacetic acid (TCA) and filtered onto glass fibre filters. The filters were washed thoroughly and the radioactivity remaining was determined by scintillation counting. [^{3}H] FPP bound to H-Ras was retained on the filter and is a measure of FPTase activity. Each point represents the mean +/- the range of incubations performed in duplicate. Results are representative of an experiment performed at least twice.

allowed to take place for 1hr, followed by TCA precipitation and scintillation counting. Mean cpm values were plotted against increasing Ras concentrations (Fig. 4.13B) and 1μM of H-Ras was chosen as optimal and used to measure activity of FPTase.

The concentration of FPP in the reaction mix was maintained at its K_m value (0.5μM) and therefore, 10 pmols FPP was added into 25μl reaction mix.

4.2.5.2 Inhibition of farnesyl protein transferase activity from K562 cell extracts using manumycin A, FTI (II) and FTI-276

Molecular inhibitors of farnesylation inhibit one of two moieties recognised by farnesyl protein transferase, the C-terminal CAAX motif on Ras, or the substrate farnesyl pyrophosphate (FPP). The antibiotic manumycin A is a structural homologue of FPP and has been shown to inhibit farnesylation of Ras (Kouchi *et al.*, 1999). On the other hand, peptidomimetics such as FTI (II) and FTI-276 are non-peptide analogues of the Ras CAAX tetrapeptide, which also inhibit Ras farnesylation (Lerner *et al.*, 1995).

In the current study, the three FPTase inhibitors were used as positive controls to show inhibition of human recombinant H-Ras farnesylation. The reaction mix containing H-Ras (1μM), [^{3}H] FPP (10 pmols) and FPTase (5μg) was set up as described in Section 2.17.2 in the presence or absence of a range of concentrations of either manumycin A (0-100μM), FTI (II) (0-1μM) or FTI-276 (0-10nM). In the case of manumycin A, DTT was omitted from the reaction mix as it reportedly affects the activity of manumycin A (personal communication). Mean cpm values were obtained from duplicate samples and farnesyl transferase activity was expressed as a percentage of vehicle treated (0.1% (v/v) DMSO) cells. Results indicate that the addition of increasing concentrations of the manumycin A caused a dose-dependent inhibition of FPTase activity resulting in almost complete inhibition of H-Ras farnesylation (Fig. 4.14). Similarly, the addition of increasing concentrations of the peptidomimetics FTI (II) and FTI-276 caused a dose-dependent inhibition of FPTase activity in K562 (Fig. 4.15A and B respectively). These results indicate that compounds that are homologous to the substrate, FPP, such as manumycin A and molecules that resemble the Ras C-terminal CAAX tetrapeptide, such as FTI (II) and FTI-276, can potently inhibit FPTase activity, and subsequently blocks Ras farnesylation.

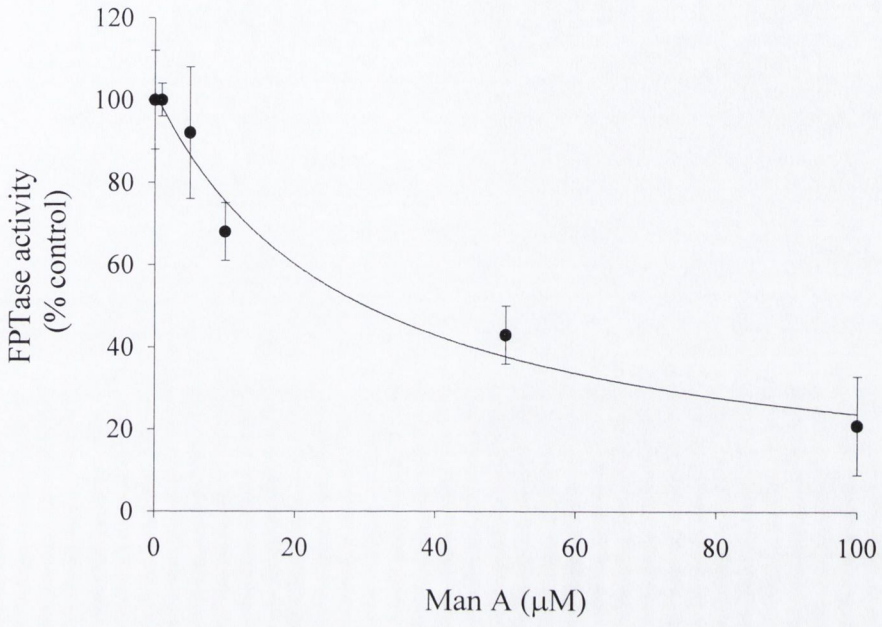

Fig. 4.14 Manumycin A inhibits the activity of farnesyl protein transferase (FPTase) from K562 cell lysates in a dose-dependent manner

FPTase (5μg), which was partially purified from K562 cell lysates, was incubated in the standard reaction mix with DTT omitted, along with human recombinant H-Ras (1μM) and [^{3}H] FPP (10 pmols; 16 Ci/mmol) as described in Section 2.17.2 in the presence and absence of a range of concentrations of manumycin A (0-100μM). The reaction was allowed to take place at 37°C for 1h and proteins were precipitated by trichloroacetic acid and deposited onto glass fibre filters. Filters were thoroughly washed and the radioactivity remaining was determined by scintillation counting. FPTase activity was expressed as a percentage of vehicle treated (0.1% (v/v) DMSO) cells, which were taken as 100%, and values represent the mean +/- the range of duplicate samples. Results are representative of an experiment performed at least twice.

Fig. 4.15 The peptidomimetic inhibitors, FTI (II) and FTI-276, inhibit the activity of farnesyl protein transferase (FPTase) from K562 cell lysates in a dose-dependent manner

FPTase (5μg), which was partially purified from K562 cell lysates as described in Section 2.17.1 was incubated in the standard reaction mix containing H-Ras (1μM) and [^{3}H] FPP (10 pmols; 16 Ci/mmol) as outlined in Section 2.17.2, in the absence and presence of a concentration range of FTI (II) (0-1μM) or FTI-276 (0-10nM). The reaction was allowed to take place at 37°C for 1h and proteins were precipitated by trichloroacetic acid and deposited onto glass fibre filters. Filters were thoroughly washed and the radioactivity remaining was determined by scintillation counting. FPTase activity was expressed as a percentage of vehicle treated cells, which was 0.1% (v/v) sterile distilled water in the case of FTI (II) and 0.1% (v/v) DMSO in the case of FTI-276. Cpm values represent the mean +/- the range of duplicate samples. Results are representative of an experiment performed at least twice.

A

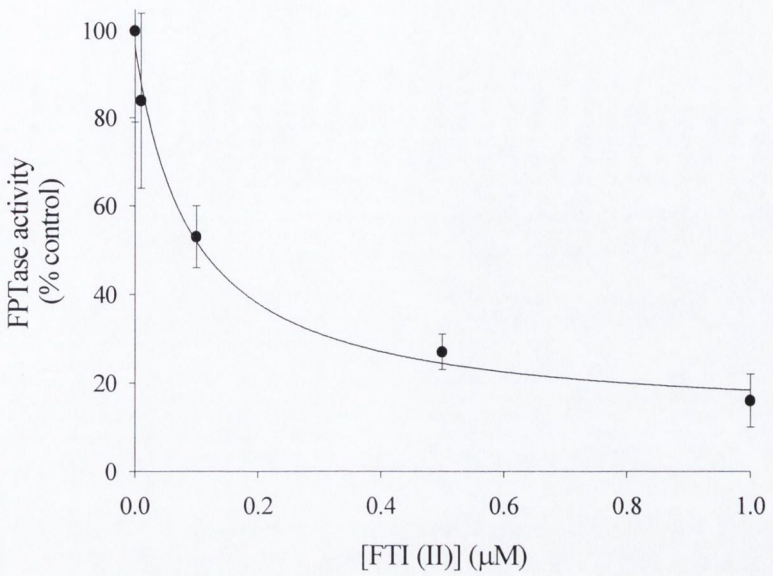
100
80
60
40
20
0
FPTase activity
(% control)
0.0
0.2
0.4
0.6
0.8
1.0
[FTI (II)] (μM)

B

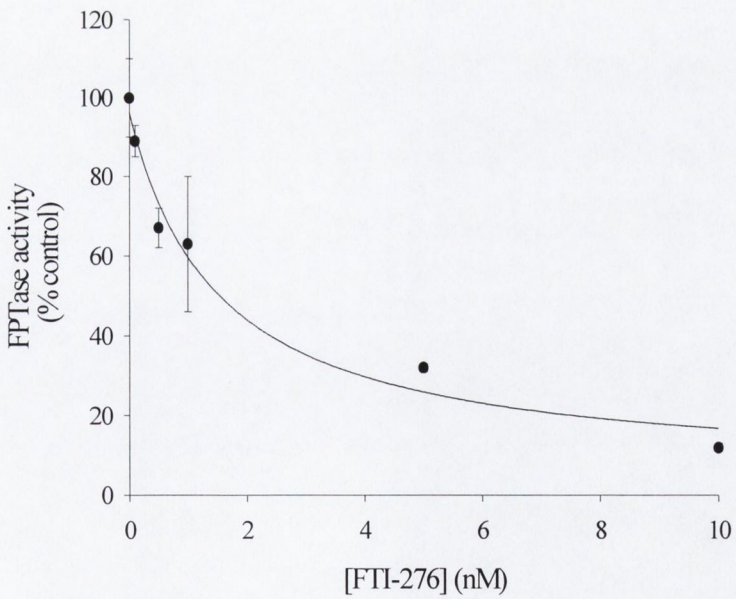
120
100
80
60
40
20
0
FPTase activity
(% control)
0
2
4
6
8
10
[FTI-276] (nM)

4.2.5.3 Lack of effect of PBOX-6 on K562 farnesyl protein transferase activity from K562 cell extracts

To determine whether PBOX-6 acts in a manner similar to the natural inhibitor manumycin A or the peptidomimetics FTI (II) or FTI-276, and inhibits Ras farnesylation, the reaction mix was incubated with either vehicle (1% (v/v) ethanol) or a range of PBOX-6 concentrations (0-20μM) and the assay was performed as described in Section 2.17.2. Results obtained from scintillation counting did not show a significant decrease in cpm values when compared with vehicle treated control samples (Fig. 4.16). An assay was also carried out using PBOX-6 in which DTT was omitted, however, the outcome remained unchanged. Clearly, PBOX-6 fails to inhibit H-Ras farnesylation, indicating that it does not behave as a farnesyl protein transferase inhibitor similar to that observed with the three control compounds, manumycin A, FTI (II) and FTI-276, which show almost complete inhibition of farnesyl transferase activity. These results suggest that direct inhibition of farnesyl protein transferase activity is not the mechanism by which this compound induces apoptosis in K562 cells.

4.2.6 Determination of the apoptotic activity of farnesyl protein transferase inhibitors manumycin A, FTI (II) and FTI-276 on K562 cells

K562 cells ($3x10^5$ cells per ml) were treated with PBOX-6 (10μM), manumycin A (10μM), FTI (II) (200μM) or FTI-276 (20μM) for 16h. An aliquot of cells (150μl) was centrifuged onto a slide and stained with the RapiDiff Kit as described in Section 2.4. The extent of apoptosis was determined by morphological examination of cells. Results indicate that treatment of K562 cells with FTI (II) and FTI-276 failed to induce apoptosis at concentrations above that used to show almost complete inhibition of farnesyl transferase activity (Fig. 4.17). The lack of apoptotic effect of the peptidomimetic inhibitors indicates that inhibition of Ras farnesylation by competitive inhibition of the CAAX motif does not induce apoptosis in these cells. Pretreatment of K562 cells with FTI (II) or FTI-276 for 1h prior to treatment with PBOX-6 (10μM) for a further 16h failed to prevent PBOX-6 induced apoptosis (Fig. 4.17). This suggests that PBOX-6 induces apoptosis via a pathway independent of Ras farnesylation. These results are consistent with the results in Fig. 4.16, which suggests that PBOX-6 does not act as a farnesyl transferase inhibitor. Manumycin A, on the other hand, inhibits farnesyl protein transferase activity by competitively inhibiting

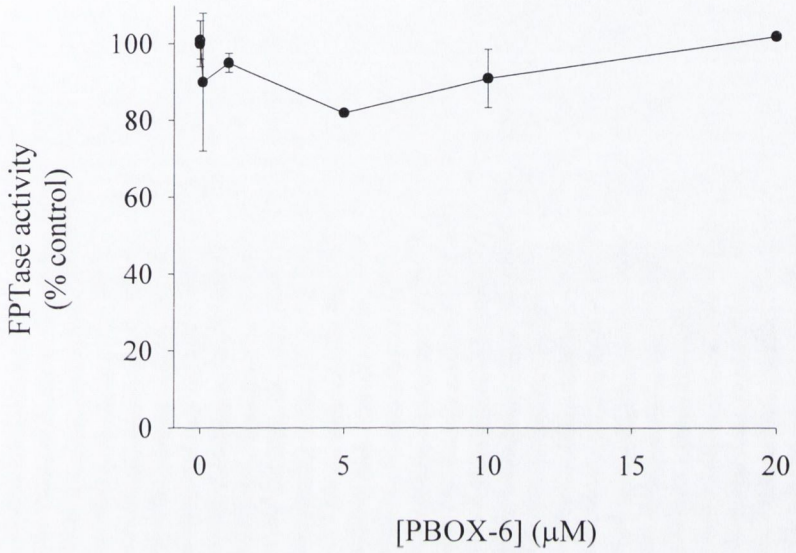

Fig. 4.16 PBOX-6 does not inhibit the activity of farnesyl protein transferase (FPTase) in K562 cell lysates

FPTase (5μg), partially purified from K562 cell lysates, was incubated in the standard reaction mix that included H-Ras (1μM) and [^{3}H] FPP (10 pmols; 16 Ci/mmol) as described in Section 2.17.2, in the absence or presence of a concentration range of PBOX-6 (0-20μM). The reaction was allowed to take place at 37°C for 1h and proteins were precipitated by trichloroacetic acid and deposited onto glass fibre filters. Filters were thoroughly washed and the radioactivity remaining was determined by scintillation counting. Cpm values represent the mean +/- the range of duplicate samples. FPTase activity was expressed as a percentage of vehicle (1% (v/v) ethanol) treated cells. Results are representative of an experiment performed at least four times.

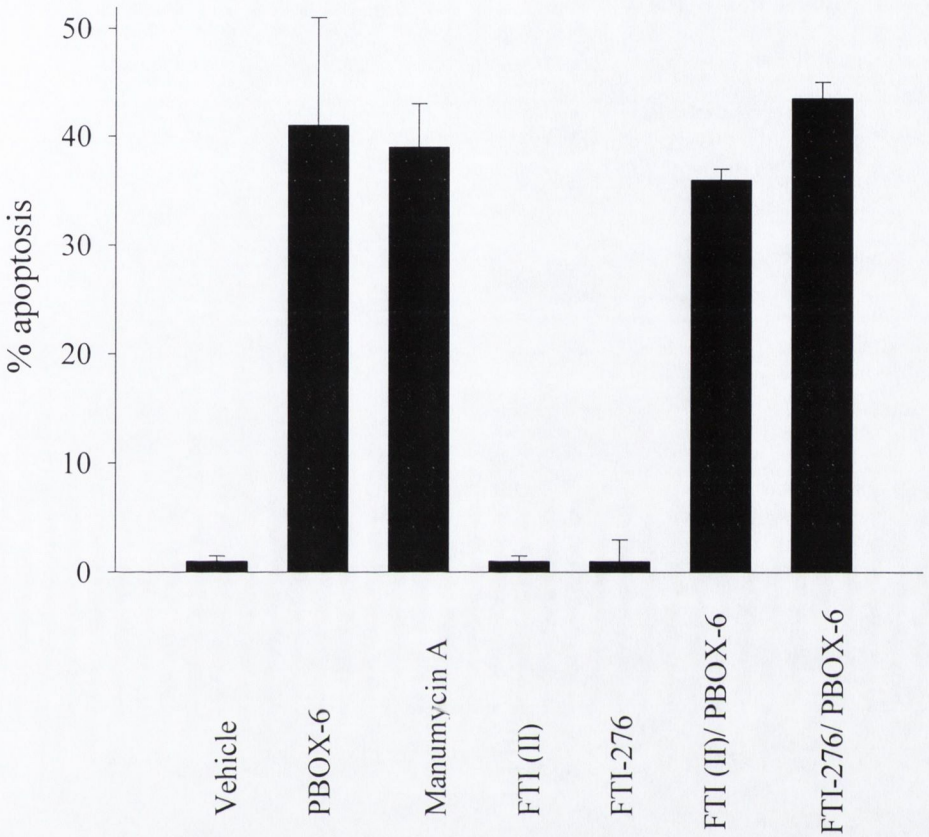

Fig. 4.17 Apoptotic activity of the farnesyl transferase inhibitors, manumycin A, FTI (II) and FTI-276 in K562 cells

K562 cells were seeded at $3x10^5$ cells per ml and treated either with vehicle (1% (v/v) ethanol and 0.1% (v/v) DMSO), PBOX-6 (10μM), manumycin A (10μM), FTI (II) (200μM) or FTI-276 (20μM) for 16h, or a combination of FTI (II) (200μM) or FTI-276 (20μM) for 1h followed by PBOX-6 (10μM) for a further 16h. An aliquot of cells (150μl) was centrifuged onto a glass slide and stained using the RapiDiff kit as described in Section 2.4. The extent of apoptosis was determined by morphological examination of cells. Results represent the mean +/- the range of two separate experiments.

enzyme binding to the FPP substrate. Treatment of K562 cells with manumycin A was found to induce approximately 40% apoptosis, an extent similar to that induced by PBOX-6 (Fig. 4.17). It should be noted that at this concentration, manumycin A also induced approximately 20% necrosis. These results are in contrast to that obtained with FTI (II) and FTI-276. In principle, inhibition of Ras by whatever method should yield similar results and this was found by inhibition of FPTase activity using the three different FPTase inhibitors. It is thus likely that the induction of apoptosis in K562 cells is due to a non-specific effect of this compound and is not due to inhibition of farnesyl transferase activity.

4.2.7 Pretreatment of K562 cells with various topoisomerase II inhibitors prevents PBOX-6-induced apoptosis

Etoposide and mitoxanthrone are commonly used chemotherapeutic agents. These compounds induce apoptosis by inhibiting the mammalian topoisomerase II enzyme and are known as Topo II poisons. They stabilise the Topo II-DNA complex causing the accumulation of DNA strand breaks, which ultimately results in cell death (Ritke *et al.*, 1995). In the present study, K562 cells were pretreated with etoposide (50μM) or mitoxanthrone (500nM) for 1h prior to treatment with PBOX-6 for a further 16h. An aliquot of cells (150μl) was centrifuged onto a glass slide and stained using the RapiDiff kit as described in Section 2.4. Morphological examination of K562 cells indicated that treatment with etoposide and mitoxanthrone alone does not induce apoptosis (Fig. 4.18), which is in agreement with previous reports (Martins *et al.*, 1997). However, it was found that the pretreatment of K562 with these Topo II poisons protects against PBOX-6 induced apoptosis (Fig. 4.18). Therefore, it is feasible to hypothesise that PBOX-6 may induce apoptosis by acting as a Topo II inhibitor, and pretreatment with alternative Topo II inhibitors such as etoposide and mitoxanthrone reduces the amount of target available for PBOX-6, thus preventing apoptosis.

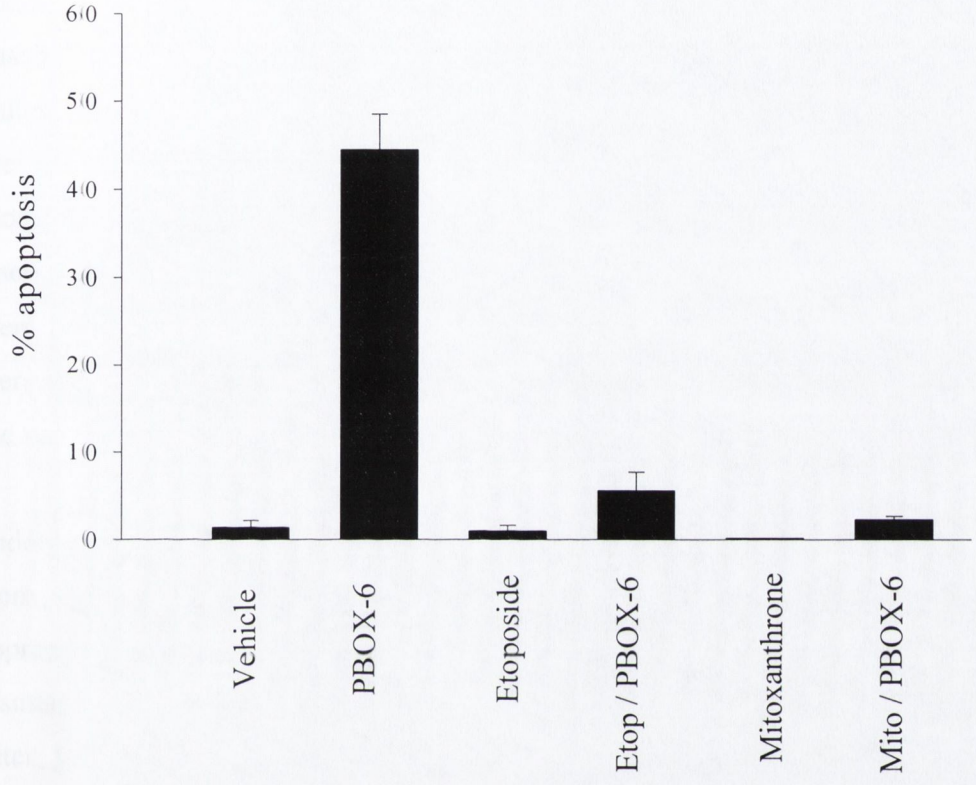

Fig. 4.18 Topoisomerase II poisons, etoposide and mitoxanthrone, protect against PBOX-6 induced apoptosis in K562 cells

K562 cells were seeded at a density of $3x10^5$ cells per ml and treated with vehicle (1% (v/v) ethanol and 0.1% (v/v) DMSO: ethanol (1:1)), PBOX-6 (10μM) for 16h, etoposide (50μM) or mitoxanthrone (500nM) for 17h, or a pretreatment of etoposide (50μM) or mitoxanthrone (500nM) for 1h prior to treatment with PBOX-6 (10μM) for a further 16h. The extent of apoptosis was determined by centrifuging the cells onto a slide and staining with the RapiDiff kit followed by morphological examination as described in Section 2.4.Values represent the mean +/- S.E.M of three separate experiments.

4.2.8 Alkaline elution assays to determine whether PBOX-6 acts as a topoisomerase II poison by inducing DNA strand breaks

Topo II poisons induce apoptosis by causing DNA strand breaks (Ritke *et al.*, 1995). In order to determine whether PBOX-6 functions as a Topo II poison in these cells, an alkaline elution assay was developed which measures DNA strand breaks. The procedure is based on a previously reported finding that DNA from mammalian cells, lysed on filters, is eluted only very slowly by alkaline solutions, and that substantial increases in elution rates are produced by a relatively small extent of DNA strand breaks. This assay was a modification of that described by Kohn *et al.* (1976) and is outlined in detail in Section 2.16. Each assay consisted of the following samples set up in parallel; vehicle treated cells which were lysed on the filter but had not undergone alkaline elution, vehicle treated cells which were lysed on the filter and had undergone alkaline elution, and cells which were treated with the various compounds and had undergone the alkaline elution procedure.

As a control in setting up this assay, human Jurkat T lymphoblast cells, which readily undergo apoptosis upon treatment with etoposide, were examined. It was found that DNA from vehicle treated Jurkat cells was sensitive to the process of alkaline elution, where approximately 25% +/- 5% of the DNA from control cells was eluted when compared to results obtained with the control sample in which vehicle treated cells were lysed on the filter, but did not undergo the alkaline elution procedure. K562 cells were also found to be sensitive to the alkaline elution process, although not to the same extent as Jurkat cells, where approximately 10% of the DNA from control cells was eluted when compared to values obtained with control cells, which did not undergo alkaline elution. This observation was not due to the vehicle treatment (0.1% (v/v) ethanol: DMSO (1:1) in Jurkat cells and 1% (v/v) ethanol in K562 cells) as a similar effect was observed with untreated cells. Therefore, values obtained from vehicle treated cells, which had undergone alkaline elution were taken as 100% and values obtained from the treatment of cells with either PBOX-6 or various Topo II inhibitors were compared directly to this.

As a positive control for the development of the assay to measure DNA strand breaks, Jurkat cells were labeled with [^{3}H] thymidine followed by treatment with either vehicle (0.1% (v/v) ethanol: DMSO (1:1)) or etoposide (2.5μM) for 1h as described in Section 2.16. Cell extracts were prepared and DNA was lysed onto filters followed by an overnight elution with an alkaline solution. Following elution, filters were removed and following treatment

with various solutions to depurinate and release DNA, the radioactivity remaining on the filters was determined by scintillation counting as described in Section 2.15. Results showed a large decrease in the amount of radioactivity remaining on filters following etoposide treatment, when compared to vehicle-treated cells (Fig. 4.19) indicating that etoposide induces a significant amount of DNA strand breaks in Jurkat cells. In contrast, K562 cells treated with PBOX-6 (10μM) for 3h, did not show any significant induction of DNA strand breaks (Fig. 4.20). These results suggest that PBOX-6 does not induce DNA strand breaks and therefore does not function in a manner similar to Topo II poisons.

4.2.9 Alkaline elution assays to determine whether PBOX-6 acts as a catalytic inhibitor of topoisomerase II

A series of compounds that are members of the bisdioxopiperazine family of anti-cancer drugs, including ICRF-154 and its derivative ICRF-193, have been shown to inhibit calf thymus DNA topoisomerase II activity, but without intercalation into the DNA or stabilisation of the Topo II-DNA complex. These are known as catalytic inhibitors of Topo II as opposed to Topo II poisons, which were described earlier (Ishida *et al.*, 1991). It has been reported that these ICRF compounds and the catalytic inhibitors merbarone and aclarubicin, inhibit Topo II mediated DNA breaks induced by etoposide (Fattman *et al.*, 1996; Fortune and Osheroff, 1998; Jensen *et al.*, 1990; Tanabe *et al.*, 1991) by reducing the amount of available target for etoposide, suggesting that they inhibit the catalytic cycle at some step before the formation of the intermediate cleavable complex.

In the present study, Jurkat cells, which were labelled with [^{3}H] thymidine as before, were pretreated with ICRF-187 (200μM) for 1h prior to treatment with etoposide (2.5μM) for a further 1h. Cell extracts were prepared, deposited onto filters and the DNA was lysed and eluted overnight with an alkaline solution as described in Section 2.16. The radioactivity remaining on the filters was calculated and results revealed that pretreatment of Jurkat cells with ICRF-187 prevented etoposide-induced DNA strand cleavage (Fig.4. 21A). Jurkat cells, treated in a similar manner, were centrifuged onto slides and stained using the RapiDiff kit as described in Section 2.4. Microscopic examination of the morphological features revealed that ICRF-187 pretreatment also inhibited apoptosis induced by etoposide (Fig. 4.21B). These results are in agreement with others, which report that the bisdioxopiperazine compounds, merbarone and aclarubicin, inhibit DNA strand breaks and apoptosis induced by

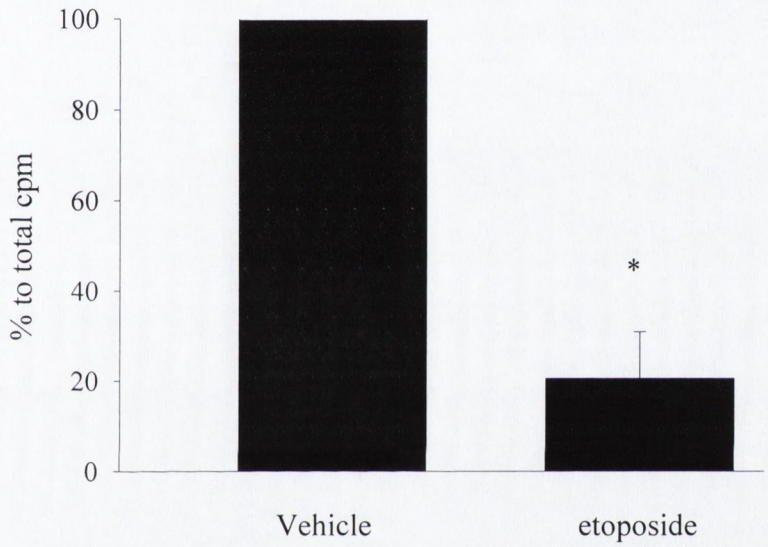

Fig. 4.19 Etoposide induces DNA strand breaks in Jurkat cells

Jurkat cells were labelled with [^{3}H] thymidine as outlined in Section 2.16 and treated with either vehicle (0.1% (v/v) ethanol: DMSO (1:1)) or etoposide (2.5μM) for 1h. Cells were lysed onto filters and DNA was eluted overnight at 0.05ml/min using an alkaline solution. The amount of DNA remaining on the filters was determined by scintillation counting. The extent of DNA stand breaks induced by etoposide was estimated by a comparison of the amount of DNA remaining on the filters of treated an untreated cells. Results represent the mean +/- S.E.M of three separate experiments. Statistics were carried out using the computer program Instat.

* $p < 0.001$ with respect to vehicle treatment; Students t-test.

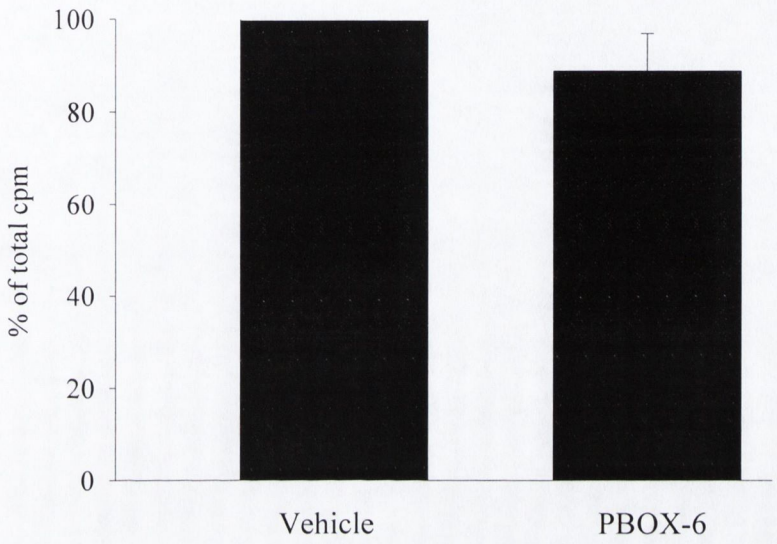

Fig. 4.20 PBOX-6 does not induce DNA strand breaks in K562 cells

K562 cells were labelled with [^{3}H] thymidine as described in Section 2.16 and treated either with vehicle (1% (v/v) ethanol) or PBOX-6 (10μM) for 3h. Cells were lysed onto filters and the DNA was eluted in the dark overnight at a rate of 0.05ml/min with an alkaline solution. Following DNA elution the amount of DNA retained on the filters was determined by scintillation counting. The extent of strand breaks induced was estimated by comparison of the amount of DNA retained on filters from treated and untreated cels. Results represent the mean +/- S.E.M of three separate experiments.

Fig. 4.21 The topoisomerase II catalytic inhibitor, ICRF-187, inhibits etoposide-induced DNA strand breaks and protects against apoptosis in Jurkat cells

(A) Jurkat cells were labelled with [^{3}H] thymidine as described in Section 2.16 and treated with vehicle (0.1% (v/v) ethanol: DMSO (1:1)), ICRF-187 (200μM) or etoposide (2.5μM) for 1h, or cells were pretreated with ICRF-187 for 1h prior to treatment with etoposide for a further 1h. Cells were lysed onto filters and DNA was eluted overnight with an alkaline solution. The DNA remaining on filters was estimated by scintillation counting and the extent of DNA damage was determined by comparison of filters from cells untreated and those treated with the various compounds. (B) Jurkat cells ($3x10^5$cells/ml) were treated with either vehicle (0.1% (v/v) ethanol: DMSO (1:1)), ICRF-187 (200μM) for 17h or etoposide (2.5μM) for 16h, or cells were pretreated with ICRF-187 for 1h followed by etoposide for a further 16h. The extent of apoptosis was determined by staining cells using the RapiDiff kit as outlined in Section 2.4. Values represent the mean +/- range of two separate experiments.

A

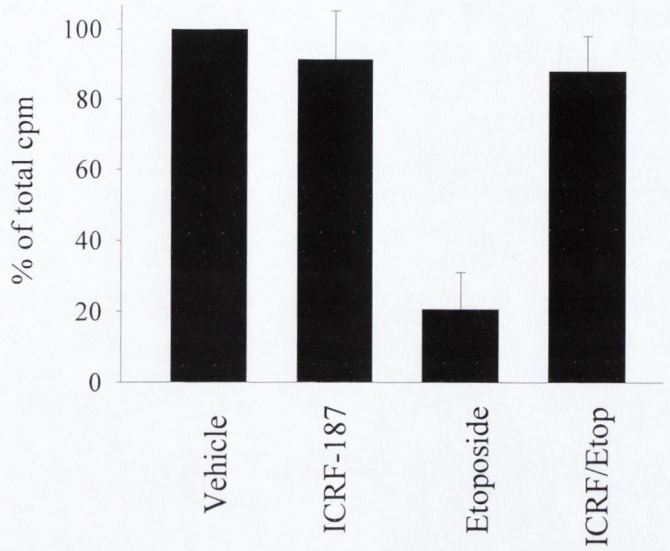
% of total cpm
100
80
60
40
20
0
Vehicle
ICRF-187
Etoposide
ICRF/Etop

B

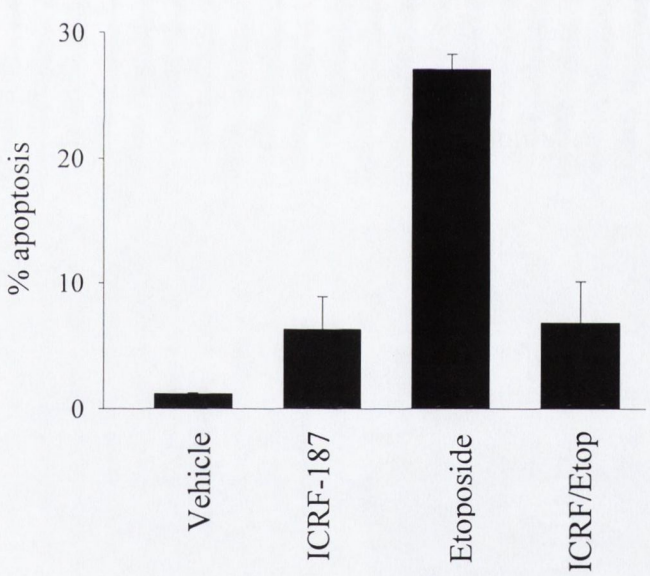
% apoptosis
30
20
10
0
Vehicle
ICRF-187
Etoposide
ICRF/Etop

etoposide (Fattman *et al.*, 1996; Fortune and Osheroff, 1998; Jensen *et al.*, 1990; Tanabe *et al.*, 1991). Pretreatment of K562 cells with ICRF-187 (200μM) for 1h prior to treatment with PBOX-6 (10μM) for a further 16h reduced but did not completely inhibit PBOX-6 induced apoptosis, as determined by RapiDiff staining (Fig. 4.22). In order to determine whether PBOX-6 operates in a manner similar to the ICRF compounds, Jurkat cells were pretreated with a sub-cytotoxic concentration of PBOX-6 (0.5μM) for 1h prior to treatment with etoposide (2.5μM) for a further 1h and the alkaline elution procedure was performed. Results showed that pretreatment with PBOX-6 did not prevent the induction of DNA strand breaks by etoposide (Fig. 4.23A). In order to determine whether PBOX-6 inhibits etoposide-induced apoptosis, Jurkat cells were pretreated with a sub-cytotoxic concentration of PBOX-6 (0.5μM) for 1h prior to treatment with etoposide (2.5μM) for a further 16h. The extent of apoptosis was determined by RapiDiff staining as described in Section 2.4. Results showed that pretreatment with PBOX-6 does not protect against etoposide-induced apoptosis in Jurkat cells (Fig. 4.23B). These results are in direct contrast to those reported with ICRF compounds merbarone and aclarubicin, suggesting that PBOX-6 does not function in a manner similar to these catalytic inhibitors of topoisomerase II.

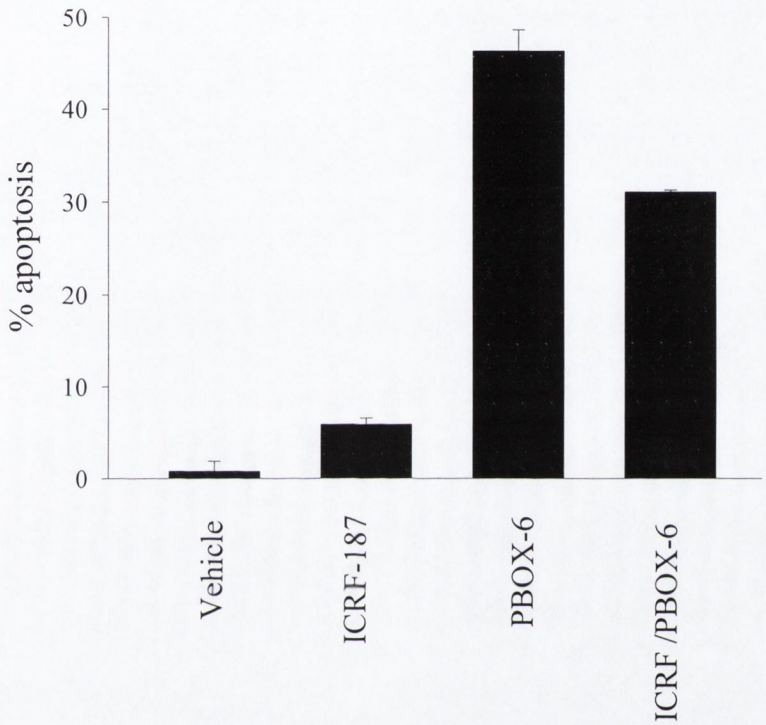

Fig. 4.22 The bisdioxopiperazine derivative, ICRF 187, reduces the level of apoptosis induced by PBOX-6 in K562 cells

K562 cells were seeded at $3x10^5$ cells per ml and treated with either vehicle (1% (v/v) ethanol), ICRF-187 (200μM) for 17h, PBOX-6 (10μM) for 16h or a pretreatment of ICRF-187 for 1h prior to treatment with PBOX-6 for a further 16h. An aliquot of cells (150μl) was centrifuged onto slides followed by staining with the RapiDiff kit as described in Section 2.4. The extent of apoptosis was determined by morphological examination of cells. Results represent the mean +/- the range of at least two separate experiments.

Fig. 4.23 PBOX-6 failed to protect against etoposide-induced DNA strand breaks and apoptosis in Jurkat cells

(A) Jurkat cells were labelled with [^{3}H] thymidine and treated with either vehicle (1% (v/v) ethanol and 0.1% (v/v) DMSO: ethanol (1:1)), PBOX-6 (10μM) for 3h or etoposide (2.5μM) for 1h, or cells were pretreated with PBOX-6 (0.5μM) for 1h followed by etoposide for a further 1h. Cells were lysed onto filters and DNA was eluted overnight in the dark with an alkaline solution. The DNA remaining on the filters was estimated by scintillation counting and the extent of DNA strand breaks induced was determined by a comparison of DNA retained on the filters from untreated cells and cells treated with the various compounds. (B) Jurkat cells ($3x10^5$ cells/ml) were treated with vehicle (1% (v/v) ethanol and 0.1% (v/v) DMSO: ethanol (1:1)), PBOX-6 (0.5μM) for 17h or etoposide (2.5μM) for 16h or a pretreatment of PBOX-6 for 1h followed by etoposide for a further 16h. An aliquot of cells (150μl) was centrifuged onto glass slides and stained using the RapiDiff kit as outlined in Section 2.4. The extent of apoptosis was determined by morphological examination of cells. Values represent the mean +/- S.E.M of three separate experiments.

B
% apoptosis
0
10
20
30
Vehicle
PBOX-6
Etoposide
PBOX-6/Etop
A
% of total cpm
0
20
40
60
80
100
Vehicle
PBOX-6
Etoposide
PBOX-6/Etop

4.3 Discussion

Chemotherapeutic agents used in the treatment of neoplastic diseases elicit their anti-tumour effect through a variety of mechanisms and the development of novel agents that will demonstrate greater efficacy and lower toxicity than currently available cytotoxic drugs is ongoing. Without a doubt, our increasing knowledge of the biological complexities of cancer and the molecular genetic defects underlying tumourigenesis has provided new opportunities for anti-cancer drug discovery and development (Gibbs, 2000). This includes the development of compounds that inhibit the activity of oncogenic proteins involved in transformation such as Ras (Crul *et al.,* 2001) and compounds that induce DNA damaging effects such as those that target the mammalian topoisomerase enzyme (Kaufmann, 1998).

A series of novel compounds, known as pyrrolo-1,5-benzoxazepines, have been synthesised and some members have been previously shown to induce apoptosis in a variety of cancerous cells such as the HL-60, Jurkat and Hut 78 cell lines (Zisterer *et al.,* 2000). In the present study, it has been shown that some members of this novel pyrrolo-1,5-benzoxazepine series potently induce apoptosis in CML cells, although the mechanism in which they do so has not been fully elucidated. Pyrrolo-1,5-benzoxazepines are high affinity ligands to the PBR receptor, whose physiological function remains unclear (Campiani *et al.*, 1996; Gavish *et al.*, 1999). In recent years it has been suggested that the PBR may be involved in the induction of apoptosis. For example, it has been shown that the PBR ligand, PK11195, while having no cytotoxic effect itself, enhances apoptosis induced by the chemotherapeutic agents etoposide and doxorubicin (Hirsch *et al.*, 1998) and by TNFα (Bono *et al.*, 1999). The mitochondrial location of the PBR and its interaction with VDAC (Gavish *et al.,* 1999), a component of the permeability transition (PT) pore, supports a role for the PBR in the induction of apoptosis (Finkel, 2001; Tafani *et al.,* 2001). It has been previously shown that pyrrolo-1,5-benzoxazepines elicit similar effects to the classical PBR ligands, PK11195 and Ro5-4864 (Zisterer *et al.*, 1998). It was reported that three members from the pyrrolo-1,5-benzoxazepine series, PBOX-1, -2 and -21, elicit anti-proliferative effects similar to that observed with PK11195 and Ro5-4864 in rat C6 Glioma and human 132IN1 astrocytoma cells. However, due to a lack of correlation observed between anti-proliferative effects and affinity of these ligands for the receptor, these workers concluded that the anti-proliferative effects observed were independent of PBR binding. In the present study, the involvement of the PBR in mediating the apoptotic effect observed with a number

of PBOX compounds in CML cells was determined. The three CML cell lines, K562, KYO.1 and LAMA 84, all contain the peripheral-type benzodiazepine receptor as shown by the high affinity, saturable binding of [^{3}H] PK11195. It has been shown that the three CML cell lines contain similar levels of receptor density, with B_{max} values of 2-5 pmol/mg protein, which is similar to levels found in other cells such as C6 glioma and 1321N1 cells (Zisterer *et al.*, 1998). Results yielding K_D values in the range of 9.4-17 nM were obtained, which is similar to dissociation constants for PK11195 binding to the PBR in other tissues and cells (Zisterer *et al.*, 1998).

The PBR binding affinity of a range of PBOX compounds, including both apoptotic and non-apoptotic members, was tested and a comparison of the affinity of ligands for the PBR and their apoptotic activity was made, to help determine the involvement of the receptor in this process. It was found that all pyrrolo-1,5-benzoxazepine compounds tested bind to the receptor with similar affinity, yielding K_i values in the range of 0.4-1.0 nM. Of these PBOX-4, -5, -6 and -7 were found to induce apoptosis in K562 cells whereas PBOX-1 and -2 did not show any apoptotic activity. Thus there is no correlation between the affinity of pyrrolo-1,5-benzoxazepines for the receptor and their ability to induce apoptosis. These results suggest that the apoptotic activity of pyrrolo-1,5-benzoxazepine compounds is not mediated by a specific interaction of these ligands with the PBR. Furthermore, these compounds were shown to induce apoptosis at micromolar concentrations in the three CML cell lines whereas nanamolar concentrations are required to saturate the receptor. This discrepancy of approximately 1000-fold in the concentration of drug necessary to produce the apoptotic effects and saturate the receptor argues against these effects being mediated through binding to the PBR and are in agreement with the conclusions made by Zisterer *et al.* (1998). In addition, Zisterer *et al.*, (2000), reported a similar discrepancy between concentrations of pyrrolo-1,5-benzoxazepines required to induce apoptosis and that required to saturate the receptor in HL-60 cells. These workers also described how PBOX-6 potently induced apoptosis in the PBR-deficient Jurkat cell line, whereas a lack of apoptotic induction was observed in PBR-rich rat Leydig cells. These reports further support the suggestion that the mechanism in which pyrrolo-1,5-benzoxazepine compounds induce apoptosis in CML cells does not involve their specific interaction with the PBR.

It has been reported that classical PBR ligands such as PK11195 and Ro5-4864 induce apoptosis in some systems (Chelli *et al.*, 2001; Zisterer *et al.*, 2000) while in other

systems they are appear to be non-toxic themselves but enhance apoptosis induced by other cytotoxic agents, (Hirsh *et al.*, 1998). It has also been reported by Bono *et al.* (1999) that PK11195 enhances TNFα induced apoptosis whereas Ro5-4864 significantly reduced the pro-apoptotic effect of TNFα at concentrations of 100nM. In the present study, it was found that PK11195 and Ro5-4864 did not induce apoptosis in K562 cells following treatment for 17 hours at a concentration of 10μM. Pretreatment of K562 cells with either of the PBR ligands prior to treatment with PBOX-6 did not enhance or inhibit the levels of apoptosis induced, suggesting that the classical PBR ligands do not elicit pro-or anti-apoptotic effects in CML cells. These results would also confirm the suggestion of a lack of involvement of the PBR in PBOX-6-induced apoptosis.

Mutationally activated *ras* genes are the oncogenes most frequently found in human tumours and activated Ras function has been shown to be important in the transforming ability of the *bcr-abl* gene (Pendergast *et al.*, 1993). The post-translational modification of Ras, which is required for transformation, involves the addition of a farnesyl group, a step that is catalysed by farnesyl protein transferase (FPTase) (Oliff, 1999). FPTase inhibitors have been developed, which are a novel class of cancer chemotherapeutic agents in clinical trials, which selectively target the growth and survival of malignant cells (Crul *et al.*, 2001). Natural products such as manumycin A are homologues to the substrate, farnesyl pyrophosphate (FPP) (Kouchi *et al.*, 1999) whereas peptidomimetics were developed that mimic the Ras C-terminal tetrapeptide, CAAX motif, which is the minimal substrate required for interaction with the enzyme (Barrington *et al.*, 1998). However, FPTase inhibitors are not Ras specific, they have also been shown to block farnesylation of nuclear lamin A and B, several retinal proteins, RhoB, the peroxisomal proteins, skeletal muscle phosphorylase kinase and many other uncharacterised polypeptides (Crul *et al.*, 2001). Although FTPase inhibitors inhibit Ras farnesylation, it remains unclear as to whether the anti-proliferative effects of these compounds result exclusively from effects on Ras. Several cell types that lack Ras mutations are sensitive to FPTase inhibitors (Feldkamp *et al.*, 2001). In the presence of inhibitory doses of FPTase inhibitors, some protein substrates can become alternatively prenylated by the geranylgeranyl protein transferase (GGPTase). Of these, RhoB has been identified and FPTase inhibitor treatment elevates the level of geranylgeranylated isoform of RhoB because of its unencumbered action leading to its mislocalisation in cells, and event which is necessary and sufficient to exert anti-proliferative and apoptotic effects on

transformed cells (Liu *et al.*, 2001b; Prendergast, 2000). FPTase inhibitors can also inhibit malignant growth induced by activated K-Ras or N-Ras, even though these proteins are alternatively prenylated by GGPTase in the absence of FPTase activity (Prendergast, 2000). Collectively these findings argue that inhibition of the farnesylation of other proteins might also contribute to the observed anti-tumour properties of FPTase inhibitors.

The involvement of Ras-dependent mechanisms in Bcr-Abl oncogenicity suggested that FPTase inhibitors might be active agents in the treatment of Bcr-Abl-induced leukaemia. Indeed, the FPTase inhibitor SCH66336 has been shown to enhance apoptosis induced by serum withdrawal and irradiation of Bcr-Abl-transformed BaF3 cells *in vitro* and *in vivo* (Peters *et al.*, 2001). These workers have shown that Bcr-Abl activates the Ras/MAP kinase signalling pathway, leading to activation of the transcription factor AP-1 and that SCH66336 treatment inhibits this effect. They also observed that SCH66336 was more effective at inhibiting colony formation in Bcr-Abl-transformed cells than dominant negative Ras despite the inhibition of Raf-1 association and AP1 activity. They concluded that inhibition of other critical farnesylated protein targets by SCH66336 must contribute to the efficacy of this compound against Bcr-Abl transformed cells. Because of the large number of farnesylated mammalian proteins, it was expected that FPTase inhibitors would also elicit serious toxic effects. However, Phase I studies have demonstrated that SCH66336 is well tolerated, with reversible and manageable toxicity (Adjei *et al.*, 2000). SCH66336 selectively inhibits FPTase activity over GGPTase activity. Therefore, geranylgeranylation of other proteins in the presence of FPTase inhibitors may provide an alternative pathway for generating active forms of these proteins to carry out their normal function. It is also possible that survival pathways in normal cells might be less dependent on Ras signalling pathways than those in Ras-transformed cells. Alternative FPTase inhibitors such as L-739,749 and L-744,832, profoundly inhibit cell growth of juvenile myelomonocytic leukaemia (JMML) in which Ras activity is deregulated (Emanuel *et al.,* 2000). Derivatives of the benzodiazepines (BZAs) have also been shown to inhibit FPTase. For example, BZA-5B has been shown to inhibit farnesylation of H-Ras in both transformed and untransformed Rat-1 cells. However, reduction of MAP kinase enzymatic cascades was reduced only in the transformed cells (James *et al.*, 1994). These results were explained by the notion that untransformed cells contain a form of Ras whose farnesylation is not blocked by BZA-5B (James *et al.,* 1995).

However, a disadvantage of the peptidomimetic structure of this compound was found to hinder the development of oral formulations (Crul *et al.*, 2001).

A number of intracellular polypeptides are farnesylated and in principle any one of these could serve as an indicator for FPTase inhibition (Adjei *et al.,* 2000). Under physiological conditions, all three Ras isotypes undergo farnesylation almost exclusively, but when treated with FPTase inhibitors, K-Ras and N-Ras, but not H-Ras can be efficiently geranylgeranylated, providing an alternative pathway for their post translational processing. The alternative prenylation pathway makes these Ras isoforms unsuitable as biochemical markers of FPTase inhibition, whereas H-Ras is not alternatively prenylated and more sensitive to these agents and therefore a more suitable marker of the efficacy of FPTase inhibition (Feldkamp *et al.*, 2001). In the present study the activity of a number of FPTase inhibitors was determined by measuring the inhibition of transfer of farnesyl from [^{3}H] farnesyl pyrophosphate onto human recombinant H-Ras by FPTase partially purified from K562 cell lysates. Previous reports that the natural inhibitor, manumycin A, and the peptidomimetic inhibitor, FTI-276, potently inhibit FPTase activity (Kouchi *et al.,* 1999; Lerner *et al.,* 1995) was confirmed in the present study. In direct contrast to these findings, PBOX-6 failed to significantly inhibit farnesylation of H-Ras, suggesting that this compound does not act as a FPTase inhibitor. Treatment of K562 cells with FTI (II) and FTI-276 at concentrations greater than that used to cause almost complete inhibition of FPTase activity failed to induce apoptosis in these cells, suggesting that disruption of the farnesylation of H-Ras or other polypeptides is not sufficient to induce apoptosis in K562 cells. Furthermore, the extent of apoptosis induced by PBOX-6 in K562 cells remained unchanged following pretreatment with these FPTase inhibitors, indicating that PBOX-6 induces apoptosis via an alternative pathway and that inhibition of the Ras pathway, or that of other farnesylated polypeptides, does not disrupt the pathway that PBOX-6 utilises to induce apoptosis in K562 cells. In contrast, manumycin A, which is a homologue of the FPP substrate and was also shown to inhibit H-Ras farnesylation, was found to induce apoptosis in K562 cells. Manumycin A was also found to induce approximately 20% necrosis in these cells at this concentration. In principle, inhibition of FPTase activity in K562 cells by whatever method should yield a similar result. However, although all three compounds inhibit FPTase activity, manumycin A induced apoptosis whereas FTI (II) and FTI-276 did not. It has been reported that a possible disadvantage of using FPP analogues such as manumycin A to inhibit FPTase

activity is that other cellular enzymes utilising FPP, such as squalene synthetase and farnesyl diphosphate synthetase, may be inhibited aswell, the consequence of which is unclear (Crul *et al.*, 2001). Therefore, non-specific effects due to the inhibition of FPTase activity by competitively inhibiting the substrate FPP may explain the apoptosis induced by manumycin A.

Many conventional chemotherapeutic agents such as etoposide, mitoxanthrone and doxorubicin that are used in the treatment of human malignancies, function by inducing large scale DNA damage, while compounds such as the bisdioxopiperazine derivatives are non-DNA damaging. Although the mechanism of action of these compounds has not been fully elucidated, many have been shown to target the mammalian Topo II enzyme. Topo II catalyses the separation of double stranded DNA by forming a complex with the DNA and causing two protein-linked breaks in the DNA which are religated following the passage of a second double stranded DNA (Kaufmann, 1998) Because of their essential role during DNA replication and cell growth, as well as their high level of expression in proliferating cells, these enzymes are ideal targets for cancer chemotherapy (Mo and Beck, 1999). Topo II inhibitors, which are among the most useful anti-cancer drugs, include Topo II poisons and catalytic inhibitors. Topo II poisons, which stabilise the Topo II-DNA complex, consist of the DNA intercalators, doxorubicin, mitoxanthrone and amsacrine (Lown *et al.*, 1985; Zwelling *et al.*, 1989) and the non-DNA intercalators, etoposide and teniposide (Wang *et al.*, 2001).

Pyrrolo-1,4-benzodiazepines, which share structural similarity with pyrrolo-1,5-benzoxazepines, represent a class of anti-tumour agents that bind to the 2' amino group of guanine within the minor groove of double stranded DNA (Lown and Joshua, 1979). Many anti-tumour agents, including camptothecin and the anthracyclines, bind within the minor groove of DNA, and are potent inhibitors of topoisomerase activity (Capranico and Binaschi, 1998; Pommier *et al.*, 1998).

Previous reports have shown that treatment of HL-60 cells with the Topo II poison etoposide (0-20μM) for 1 hour, caused a significant induction of DNA strand breaks, as shown by alkaline elution and resulted in internucleosomal DNA fragmentation and apoptosis (Ritke *et al.*, 1994b). In the present study it was found that K562 cells are resistant to apoptosis induced by etoposide and mitoxanthrone. However, the pretreatment of cells with these compounds prevented PBOX-6-induced apoptosis. Similarly, in the previous

chapter it was shown that treatment of K562 cells with the tyrosine kinase inhibitor genistein, which also acts as a Topo II inhibitor by binding to the ATP binding site (Bergamaschi *et al.*, 1993), did not induce apoptosis itself, however it blocked PBOX-6-induced apoptosis. The ability of etoposide, mitoxanthrone and genistein to inhibit PBOX-6-induced apoptosis suggested that these Topo II inhibitors might do so by reducing the amount of target available for PBOX-6. This suggested that PBOX-6 itself might act as a Topo II inhibitor. The ability of etoposide to inhibit the activity of Topo II in Jurkat cells was confirmed in the present study using an assay that measured the extent of DNA strand breaks induced by the compound. In contrast, K562 cells which were treated with PBOX-6, failed to induce an increase in DNA strand breaks when compared to vehicle treated cells. These results suggest that PBOX-6 does not induce DNA strand breaks and therefore does not function as a Topo II poison, and this is therefore unlikely to be the mechanism by which this compound induces apoptosis in K562 cells. However, although PBOX-6 does not act as a Topo II poison, a requirement of active Topo II in the apoptotic pathway may explain the ability of Topo II poisons to prevent PBOX-6 induced apoptosis.

In contrast to the Topo II poisons, the catalytic inhibitors of Topo II activity do not intercalate into the DNA or induce DNA strand breaks. These include the bisdioxopiperazine derivatives, which trap the enzyme in a closed clamp form thus preventing it from recycling (Roca *et al.*, 1994) and merbarone, aclarubicin and staurosporine which reflect a variety of inhibitory mechanisms that result in cell death (Fortune and Osheroff, 1998). For example, merbarone-induced apoptosis in CEM cells caused activation of c-Jun N-terminal kinase (JNK), c-Jun gene induction, activation of caspase-3-like proteases and Parp cleavage leading to apoptosis (Khelifa *et al.,* 1999). The bisdioxopiperazine compounds have also been reported to induce apoptosis in CEM cells (Morgan *et al.*, 2000). K562 cells, which are refractory to apoptosis induced by most chemotherapeutic agents, have recently been reported to undergo differentiation and apoptosis following treatment with ICRF-187 (Hasinoff *et al.*, 2001). However, it should be noted that this induction of apoptosis was slow and took place over the course of five days. In the present study, treatment of K562 cells with the bisdioxopiperazine derivative ICRF-187 for 17 hours did not result in the induction of apoptosis. Pretreatment of K562 cells with ICRF-187 prior to treatment with PBOX-6 reduced but did not completely inhibit apoptosis induced by PBOX-6, suggesting that ICRF-187-mediated reduction of available target may be responsible for the observed reduction in

PBOX-6-induced apoptosis and that PBOX-6 may function in a manner similar to these Topo II inhibitors.

It has been reported that catalytic inhibitors of Topo II are likely to attenuate the actions of topoisomerase poisons that induce DNA strand breaks by reducing the amount of available target, suggesting that they inhibit the catalytic cycle at some step before the formation of the intermediate cleavable complex. For example, the bisdioxopiperazine derivative ICRF-193 was shown to inhibit the production of linear DNA following etoposide treatment, indicating that ICRF-193 inhibits DNA strand breaks induced by etoposide (Tanabe *et al.*, 1991). In addition, ICRF-187 and merbarone antagonise etoposide induced Topo II-DNA complex formation in a dose-dependent manner in K562 cells (Fattman *et al.*, 1996; Fortune and Osheroff, 1998). Furthermore, aclarubicin alone had no stimulatory effect on Topo II-mediated DNA cleavage but has been shown to inhibit the increased formation of DNA cleavage induced by the Topo II poisons, etoposide and m-AMSA (Jensen *et al.*, 1990). In the present study, pretreatment of Jurkat cells with ICRF-187 prior to treatment with etoposide has been shown to prevent etoposide-mediated DNA strand cleavage and to completely prevent apoptosis induced by etoposide. These result are consistent with those reported for ICRF-193, ICRF-187, merbarone and aclarubicin. In contrast however, sub-cytotoxic concentrations of PBOX-6 failed to prevent etoposide-induced strand breaks and apoptosis in Jurkat cells. It was not feasible to increase the concentration of PBOX-6 used in the experiment as this compound itself potently induces apoptosis in Jurkat cells (Zisterer *et al.*, 2000). Therefore, the results reported in the current study suggest that PBOX-6 does not operate in a manner similar to the catalytic inhibitors, merbarone, aclarubicin, staurosporine or the bisdioxopiperazine derivatives that inhibit the catalytic cycle at a step before the formation of the intermediate cleavable complex.

Interestingly, an alternative Topo II targeting agent known as fostriecin, which acts as a catalytic inhibitor, has been shown to inhibit growth of K562 cells but does not inhibit etoposide-induced DNA strand cleavage, confirming that mechanistic differences exist between the Topo II catalytic inhibitors. It has been reported that fostriecin exerts its cytotoxic effect primarily by acting as a phosphatase inhibitor (Roberge *et al.*, 1994). Therefore it is possible that PBOX-6 may inhibit the catalytic activity of Topo II by a mechanism distinct from merbarone, aclarubicin, staurosporine or the bisdioxopiperazine derivatives and may inhibit the enzyme activity at some later stage in the catalytic cycle.

Topo II-mediated drug resistance can arise as a result of a many cellular events. These include a decrease in the amount of enzyme, therefore reducing the amount of drug-induced complexes and thus cytotoxicity. Alternatively, the enzyme may be mutated and therefore drug-insensitive. Targets for mutation include the nucleotide binding domain and the active site tyrosine. The role of topoisomerase II phosphorylation in inducing DNA damage remains unclear, however, it seems that phosphorylation of Topo II may affect the sensitivity of cells to Topo II inhibitors (Ritke *et al.*, 1994a, 1995). In addition, overexpression of P-glycoprotein prevents intracellular accumulation of Topo II poisons as well as other cytotoxic drugs (Dubrez *et al.*, 1995). A comparison of etoposide-induced DNA cleavage in HL-60 and K562 cells, reported initial DNA damage and DNA complex formation in both cell lines, however apoptosis was readily apparent only in the HL-60 cells (Ritke *et al.*, 1994b). Similarly, a report outlining the varying sensitivity of five human cell lines to etoposide, reported that three of these cell lines (HL-60, BV173 and U937) were sensitive and two cell lines were resistant (K562 and KCL22), yet DNA strand breaks were induced in all five cell lines (Dubez *et al.*, 1995). These reports of DNA damage that does not translate to *in vitro* cytotoxicity, suggest that other factors subsequent to DNA damage, such as DNA repair and apoptosis function play an important role in determining sensitivity to cytotoxic drugs (Wang *et al.*, 2001). For example, Kamesaki *et al.* (1993) reported that overexpression of the Bcl-2 protein inhibited apoptosis and cytotoxicity in CH31 mouse B-cells with little or no effect on the formation of DNA strand breaks. Thus, Bcr-Abl acts downstream of the drug-target interaction to prevent the coupling of drug-induced DNA damage to apoptosis. This decreased sensitivity to apoptosis induction may explain the inhibitory nature of K562 cells to almost all chemotherapeutic drugs currently in use and contributes to the progression of CML (Dubez *et al.*, 1998). These reports outlining the resistance of K562 cells are consistent with results from the current study, which have shown that these cells are resistant to apoptosis induced by the Topo II poisons etoposide, mitoxanthrone and genistein. The ability of the pyrrolo-1,5-benzoxazepine compound, PBOX-6, to overcome the mechanisms that confer resistance on K562 cells and potently induce apoptosis in these cells suggests the novel potential of this compound in the treatment of CML and related diseases.

In summary, the pyrrolo-1,5-benzoxazepine compound PBOX-6 has been shown to potently induce apoptosis in chemotherapy resistant CML cells. In the present Chapter,

attempts to further elucidate its mechanism of action have revealed that the pro-apoptotic effect of PBOX-6 is not mediated through its binding to the peripheral-type benzodiazepine receptor. Bcr-Abl-mediated resistance of CML cells is thought to involve up-regulation of the Ras pathway. However, it has been shown that PBOX-6-induced apoptosis in CML cells is not mediated through inhibition of Ras function. In addition, it has been found that PBOX-6 seems to require an active form of topoisomerase II in the pathway in which it induces apoptosis, although it does not target this enzyme in a manner similar to many conventional chemotherapeutic agents.

A wide variety of chemotherapeutic agents have been shown to affect the regulation of intracellular signalling pathways. The effect of PBOX-6 on biochemical components of intracellular signal transduction pathways was investigated in the next chapter.

Chapter 5

Characterisation of the biochemical signalling pathway initiated during PBOX-6-induced apoptosis in K562 cells

5.1 Introduction

Deregulated cell growth is the defining feature of all neoplasms, both benign and malignant, and occurs as a result of perturbed signal transduction leading to alteration of signals that modulate cellular behaviour or function (Blume-Jensen and Hunter, 2001). Certain classes of signalling proteins and pathways are targeted more frequently by oncogenic mutations than others and ultimately result in amplified signalling pathways. These include G-proteins such as the Ras superfamily (Crul *et al.*, 2001), protein kinases that normally exert tight control on protein phosphorylation and regulatory proteins such as Bcl-2 family members, (Nicholson, 2000). Targeting different biochemical components of deregulated signal transduction pathways presents promising opportunities for future cancer therapeutics.

Chronic myelogenous leukaemia results from the expression of the Bcr-Abl fusion protein. This fusion converts the Abl tyrosine kinase from a tightly regulated predominantly nuclear tyrosine kinase into an abnormally regulated cytoplasmic protein with increased activity. Because of its new cellular location, the Bcr-Abl tyrosine kinase gains increased access to substrates, which it can phosphorylate unhindered (Deininger *et al.*, 2000). Bcr-Abl oncoproteins bind directly to activators of the Ras signalling pathway, and activation of Ras function is an important component in Bcr-Abl-mediated transformation (Goga *et al.*, 1995; Million and Van Etten, 2000; Pendergast *et al.*, 1993; Puil *et al.*, 1994). Ras activation leads to signal transduction through downstream mitogen-activated protein (MAP) kinase pathways. The downstream signalling from Bcr-Abl responsible for the inherent resistance of CML to cytotoxic therapy remains poorly understood. There is still dispute as to which MAP kinase pathway lies downstream of Ras in Ph-positive cells, and it seems that activation of individual paths depend on the cell type (Deininger *et al.*, 2000).

In mammalian cells, the biochemical properties of three MAP kinases have been characterised in detail, the extracellular signal-regulated kinases (ERKs; also known as p42-44 MAP kinases), the c-Jun N-terminal kinases (JNKs; also referred to as stress-activated protein kinases or SAPKs) and the p38 MAP kinases (Ichijo, 1999). These enzymes are the terminal enzymes in a three-enzyme cascade in which each dually phosphorylates and activates the next in sequence. All MAP kinases are serine/threonine kinases that are activated in response to their phosphorylation on invariant threonine and tyrosine residues, within a TXY motif in the activation loop of the catalytic domain, by dual specificity MAP

kinase kinases (MAPKKs). The MAPKKs are activated through phosphorylation of conserved serine and threonine residues by a somewhat more diverse group of MAP kinase kinase kinases (MAPKKKs). Phosphorylation within the activation loop is sufficient to cause translocation of the MAP kinase to the nucleus in a process involving dimerisation as well as synthesis of labile nuclear retention proteins (Cans *et al.,* 2000).

The ERK subgroup of MAP kinases is activated primarily by mitogenic stimuli such as growth factors. Most commonly, the ERK activated pathway begins with cell surface receptor-mediated activation of Ras. Once activated, Ras binds and recruits the MAPKKK Raf-1 to the membrane (Minden and Karin, 1997). Activated Raf-1 phosphorylates and activates the MAPKKs, MEK1 and MEK2, which directly activate the ERKs, consisting of ERK1 and 2. Once activated, a fraction of ERK translocates to the nucleus where they phosphorylate and thereby regulate transcription factors such as Elk1 (Minden and Karin, 1997; Payne *et al.,* 1991).

In contrast to ERK, the JNK and p38 pathways are activated primarily by cellular inflammatory cytokines such as TNFα and IL-1 and a diverse array of cellular stress including UV irradiation, hydrogen peroxide, DNA damage, heat and osmotic shock (Ichijo, 1999). The p38 MAP kinase is phosphorylated and activated by the MAPKKs, MKK3 and MKK6, which are themselves activated by a diverse range of MAPKKKs including MTK1, MLK2, MLK3, DLK, ASK1 and TAK1. Over-expression of these MAPKKKs leads to activation of both the p38 and JNK pathways, which may explain the regular co-activation of these two pathways (Ono and Han, 2000).

In the JNK subgroup, three genes (*jnk1, jnk2* and *jnk3*) have been described. JNK1 and JNK2 protein kinases are expressed ubiquitously, while JNK3 is expressed primarily in the brain (Yasuda *et al.*, 1999). At least 10 different splice variants have been described that generate proteins of 54kDa and 46kDa (Zanke *et al.,* 1996). JNK is activated by dual phosphorylation by two distinct MAPKKs, MKK4 (Sanchez *et al.*, 1994) or MKK7. A number of MAPKKKs have been identified as upstream activators of the JNK pathway, including MEKK (MEKK-1, -2, -3 and -4 (MTK1)), Tpl-2, and the mixed-lineage protein kinases DLK, LZK, MLK-2 and MLK-3, TAK1, ASK1 and ASK2. Of these, MEKK-1, -2, -3 and Tpl-2 can also activate the ERK pathway, while TAK1, ASK1 and MTK1 have been shown to activate p38 (Ichijo, 1999; Minden and Karin, 1997). Although the three MAP kinase pathways share structural similarity, the outcome of activation is quite different. ERK

activation results in cell division and differentiation whereas growth arrest and cell death is observed following activation of the JNK and p38 pathways (Zanke *et al.*, 1999). In the present study, an involvement of these three parallel MAP kinase pathways in the mechanism by which PBOX-6 induces apoptosis in CML cells was assessed.

The JNK pathway can be activated by a variety of stimuli including growth factors such as angiotensin (Murasawa *et al.*, 2000), cytokines such as TNFα and IL-1 (Bagrodia *et al.*, 1995; Ichijo, 1999) and genotoxic stress such as anti-cancer drugs (Osborne and Chambers; 1996; Seimiya *et al.*, 1997). A number of factors have been implicated in the coupling between activating stimuli and the MAPKKKs. Receptor-mediated signalling by growth factors involves autophosphorylation on tyrosine residues (Minden and Karin, 1997). Alternatively, in the case of cytokines such as TNFα, signalling involves receptor aggregation and recruitment of cytoplasmic signalling proteins such as TNF receptor associated factor 2 (TRAF2). TRAF2 binds directly to the MAPKKK ASK1 and interacts with MEKK1 through germinal centre kinase (GCK) resulting in JNK activation (Ichijo, 1999). Other proteins involved in coupling extracellular signals to MAPKKKs include the small GTP-binding protein Ras (Minden *et al.*, 1994) members from the Rho family of GTPases, Rac and Cdc42 (Murasawa *et al.*, 2000; Puls *et al.*, 1999; Teramoto *et al.*, 1996) and members of the Ste20-related kinase family including the germinal centre kinase (GCK) (Pombo *et al.*, 1995; Yuasa *et al.*, 1998).

The Rho family of GTPases, including Rac and Cdc42, can activate the JNK (Coso *et al.*, 1995; Murasawa *et al.*, 2000; Teramoto *et al.*, 1996) and p38 (Bagrodia *et al.*, 1995; Zhang *et al.*, 1995) MAP kinase pathways, although little is known about how receptors recruit Rac/Cdc42 or stimulate GTP-binding (Kyriakis and Avruch, 1996). Rac and Cdc42 are coupled to the JNK and p38 MAP kinase pathway by serine/threonine protein kinases known as p21-activated kinases (PAKs). PAKs were the first identified mammalian members of a growing class of Ste20-like ser/thr protein kinases. Association between the active GTP form of Rac and Cdc42 and a p21-binding domain of PAK known as Cdc42/Rac interactive binding (CRIB) domain promotes PAK autophosphorylation (Knuas and Bokoch, 1998). Dominant inhibitory mutants of PAK have been shown to inhibit Rac and Cdc42-stimulated activation of p38 in response to IL-1 (Zhang *et al.*, 1995). In addition to PAKs, Rac and Cdc42 interact with the mixed-lineage kinases (MLKs) through a similar CRIB domain. To date, five members of the MLK family have been identified, MLK-1, -2 and -3, DLK and

LZK. With the exception of MLK-1, all family members function as MAPKKKs and predominantly activate the JNK signalling pathway (Leung and Lassam, 2001). Dominant inhibitory mutant forms of MLK3 have been shown to reduce JNK activation by Rac and Cdc42 (Teramoto *et al.*, 1996). However, other members of the MLK family, such as DLK, lack a Rac/Cdc42 binding domain, suggesting that MLKs may mediate JNK activation by Rac- and Cdc42-dependent as well as -independent pathways (Teramoto *et al.*, 1996). Several reports suggest that G-protein independent pathways leading to JNK activation exist (Bird *et al.*, 1994; Coso *et al.*, 1995; Davis *et al.*, 1999; Minden *et al.*, 1994; Puls *et al.*, 1999). One example by Coso *et al.* (1995) demonstrated that dominant negative mutants of Rac and Cdc42 effectively reduced JNK stimulation elicited by both EGF and TNFα but had no effect on JNK activation in response to anisomycin, suggesting that different stimuli activate JNK through distinct pathways.

A second class of mammalian Ste20-related ser/thr kinases has been shown to activate JNK (Pombo *et al.,* 1995). This growing family of Ste20-related kinases include germinal centre kinase (GCK), hematopoietic progenitor kinase-1 (HPK1), HPK/GCK-like kinase (HGK), Nck interacting kinase (NIK), kinase homologous to SPS1/STE20 (KHS), GCK-like kinase (GLK), mammalian Ste20-like kinase-1 and -2 (MST-1 and -2). Germinal centre kinase was the first member shown to activate JNK (Pombo *et al.,* 1995) and subsequently additional members were shown to activate the JNK pathway, however, none of these can activate the ERK or p38 pathways (Yao *et al.*, 1999). These kinases are activated in response to TNFα and UV irradiation, which in part uses the TNF receptor-signalling pathway (Diener *et al.*, 1997; Shi and Kehrl, 1997), and activate JNK through the MKK4 and/or MKK7 pathway (Diener *et al.*, 1997; Yao *et al.*, 1999). Some members have been shown to activate MEKK1 (Diener *et al.*, 1997; Su *et al.*, 1997) or the MLK-3 (Leung and Lassam, 2001) family of MAPKKKs. This second class of Ste20-related kinases do not appear to contain a Cdc42 and Rac binding sites, suggesting that pathways activated by these kinases are independent of Rac and Cdc42 (Pombo *et al.,* 1995). It has been shown that the GCK c-terminal regulatory domain can interact with both the TNF signal transducer, TRAF2 and the MAPKKK, MEKK1, thereby coupling TRAF to the JNK pathway (Yuasa *et al.,* 1998). The regulation of GCK and related kinases remain unclear, but it is suspected to be negatively regulated by an inhibitor that is removed by upstream stimuli (Kyriakis and Avruch, 1996).

Heterotrimeric G proteins mediate a wide range of fundamental cellular events in response to external stimulation of transmembrane spanning receptors, and transduce ligand-mediated signals. Activation of heterotrimeric G-proteins is dependent on GTP binding to their α subunits. Certain stimuli, for example the gonadotrophin-releasing hormone, activate heterotrimeric G protein receptors and ultimately the JNK MAP kinase pathway in a time-, dose- and receptor-dependent manner in primary rat pituitary gonadotrophs (Minden and Karin, 1997; Mulvaney and Roberson, 2000).

The targeting of certain signals to specific MAP kinase modules may be regulated by the presence of scaffold proteins, which facilitate the assembly of regulator-effector complexes by increasing the local concentration of the scaffold components, and by preventing cross-talk with functionally unrelated members of other MAP kinase signalling modules (Whitmarsh *et al.,* 1998). The JIP (JNK-interacting protein) group of scaffold proteins, which consists of JIP-1 and JIP-2 (Yasuda *et al.*, 1999), has been shown to form homo-and hetero-oligomeric complexes with multiple components of the JNK signalling module and facilitates signal transduction mediated by the bound proteins. JIP-1 has been shown to interact with the MAPKK MKK7 but not MKK4, and the MAPKKK from the mixed-lineage kinase family, MLK-2, MLK-3 and DLK, but not the MAPKKK MEKK1 or MEKK4. Signalling molecules that function upstream of MAPKKK, such as the Ste20-related kinase HPK1, were found to bind JIP-1, whereas binding to the PAKs and Rho family proteins Rac and Cdc42 was not detected. Therefore the function of JIP-1 as a scaffold protein is selective for the MLK-MKK7-JNK MAP kinase module (Whitmarsh *et al.*, 1998; Yasuda *et al.*, 1999). Overexpression of the JIP proteins cause cytoplasmic retention of JNK and thereby inhibits gene expression mediated by JNK signalling pathways. Inhibition of JNK signalling may also reflect the sequestration of limiting JNK pathway components into separate complexes by the overexpressed scaffold protein (Dickens *et al.*, 1997; Whitmarsh *et al.*, 1998; Yasuda *et al.*, 1999). Thus, overexpression of the JIP scaffold proteins is a potent and selective inhibitor of the JNK signalling pathway.

A variety of inhibitors specific for the different signalling pathways are available. These include PD98059, a selective and cell-permeable inhibitor of MEK that acts by inhibiting the activation of the ERK MAP-kinase (Kang *et al.*, 2000), and SB203580, a specific enzymatic inhibitor of p38 MAP kinase (Ono and Han, 2000). In addition, CEP-1347, a semi-synthetic derivative of the fermentation product K-252a found in broths of the

Narcodiopsis Bacterium, is a novel inhibitor of the JNK signalling pathway and is believed to target upstream of JNK. It has been shown that CEP-1347-mediated inhibition of motor neuron apoptosis correlated with inhibition of the JNK signalling cascade (Maroney *et al.*, 1998). In addition, it has recently been shown that the coumarin derivative, dicumarol, specifically inhibits activation of the JNK MAP kinase signalling pathways by a variety of stimuli including anisomycin, UV irradiation, ceramide, TNFα (Cross *et al.*, 1999) and the insulin growth factor (IGF) receptor (Krause *et al.*, 2001). NAD(P)H dehydrogenase, also termed quinone reductase, is inhibited by dicumarol. Like other coumarins, dicumarol is used clinically to inhibit coagulation processes dependent on Vitamin K, a biological quinone. It has been suggested that quinone reductases likely provide an intracellular environment permissive to stress signalling rather than themselves being activated during the signalling. Inhibition by dicumarol would interfere with the environment and inhibit the ability of cells to transmit stress signals (Cross *et al.*, 1999).

The identification of receptor-initiated signalling pathways that involve small GTPases, such as Ras and the Rho GTPases Rac and Cdc42, have relied largely on the ability to specifically block individual GTPases and dominant negative versions have been used extensively. These have been designed by analogy with the original dominant negative Ras protein, which involved a serine to asparagine substitution at codon 17, hence RasN17 (Kjoller and Hall, 1999). Dominant negative mutants inhibit the exchange of GDP for GTP by inhibiting the activity of GEFs and hence remain permanently GDP-bound. In contrast, constitutively active versions contain a glycine to valine point mutation at position 12, which prevents hydrolysis of GTP thus rendering the protein permanently active, hence RasV12. These mutants have been extensively used as tools to elucidate the involvement of GTPases in various signalling pathways (Davis *et al.*, 1999).

As an alternative to dominant negative proteins, bacterial toxins that can inactivate GTPases from the Ras and Rho families have been described and provide a useful tool for the investigation of pathways dependent on these signalling molecules. Lethal toxin, originating from *Clostridium sordellii,* has been shown to glycosylate and inactivate Rac, Ras and Rap (Davis *et al.*, 1999). In the present study, many of these molecular tools were used to aid in characterising the upstream signalling cascade initiated by PBOX-6 that ultimately leads to apoptosis in CML cells.

Activation of MAP kinase pathways lead to phosphorylation of a number of targets including several transcription factors involved in cell death, cell growth and differentiation and mediates changes in their gene expression (Minden and Karin, 1997). The AP1 family of transcription factors consists of a collection of dimers of basic region leucine zipper (bZIP) - domain proteins from the Jun, the Fos and the ATF-2 subfamilies (Leppa and Bohmann, 1999). The composition of AP1 subunits, and other transcription factors may determine the effect on activation or repression of the gene (Leppa and Bohmann, 1999) The Jun family comprises c-Jun, JunB and JunD but only c-Jun is efficiently phosphorylated by JNK. Activated JNK translocates to the nucleus and forms a complex with the N-terminal domain of c-Jun and phosphorylates serines 63 and 73 in the c-Jun activation domain, stimulating its transcriptional activity (Minden and Karin, 1997). Many reports have shown that signals that activate the JNK MAP kinase pathway also stimulate c-Jun phosphorylation (Seimiya *et al.*, 1997; Sanchez *et al.*, 1994; Osborn and Chambers; 1996). The JNK MAP kinase has also been shown to phosphorylate ATF-2 (activating transcription factor-2) on amino acids Thr-69 and Thr-71 and phosphorylation of both sites is required for its transcriptional activity (Fuchs *et al.*, 2000; Gupta *et al.*, 1995). Phosphorylation of c-Jun and ATF-2 by JNK occurs while these proteins are bound to the c-Jun promoter in a sequence-specific manner at the cis acting element known as the TRE (TPA response element) and activates transcription leading to *c-jun* induction and thus, AP1 activity (Karin, 1995). ATF-2 also interacts with the transcription factor, nuclear factor kappa B (NFκB) (Du *et al.*, 1993). The most common form of NFκB is a heterodimer composed of p50 and p65 subunits. In resting cells, NFκB is largely cytoplasmic and is sequestered in the cytoplasm by inhibitory proteins known as IκB (inhibitory κB) which mask the NFκB nuclear localisation domain and inhibit DNA binding (Mayo and Baldwin, 2000). In response to a large variety of stimuli, the IκB inhibitor is phosphorylated and degraded, thus allowing nuclear translocation of NKκB where is binds to its consensus sequence upstream of target genes resulting in the transcription of numerous target genes including many pro- and anti-apoptotic genes (Bours *et al.*, 2000). The role of NFκB in apoptosis is controversial, with many reports suggesting an anti-apoptotic role of NFκB in oncogenesis by up-regulating activity of many anti-apoptotic proteins such as the Bcl-2 family members, and members of the IAP family (Mayo and Baldwin, 2000). In contrast, other reports suggest that activation of NFκB is required for, and precedes

apoptosis, induced by etoposide and ara-C in HL-60 cells (Bessho *et al.*, 1994). It seems therefore, that the role of NFκB in apoptosis is determined by the experimental conditions, which include cell type and apoptotic stimulus (Aggarwal, 2000).

In addition to nuclear transcription factors, JNK can phosphorylate non-nuclear substrates such as the Bcl-2 family of regulatory proteins (Fan *et al.*, 2000; Maundrell *et al.*, 1997; Yamamoto *et al.*, 1999). The Bcl-2 family, which plays an important role in the regulation of apoptotic events, possesses both pro- and anti-apoptotic members and the ratio of death agonists to antagonists determines, in part, their response to a death signal. Modifications to Bcl-2 family members include dimerisation, phosphorylation and proteolytic cleavage and often result in subcellular translocation. The ability of Bcl-2 family proteins to form heterodimers with opposing family members is considered to inhibit the biological activity of their partners (Tsujimoto, 1998; Yang *et al.*, 1995). Uncertainty still exists as to whether phosphorylation increases or decreases the anti-apoptotic function of Bcl-2, however, most data support the original hypothesis suggesting that phosphorylation inactivates Bcl-2, thus promoting apoptosis (Fan *et al.*, 2000; Haldar *et al.*, 1996). Phosphorylation of Bcl-2 occurs in an unstructured loop and involves several sites, the principal ones being serine 70, serine 87 and threonine 69 (Yamamoto *et al.*, 1999). Deletion of the loop region has been shown to block apoptosis induced by the microtubule inhibitor, paclitaxel (Srivastava *et al.*, 1999). Furthermore, the ASK1-MKK7-JNK pathway has been shown to be responsible for paclitaxel-induced phosphorylation of Bcl-2 (Yamamoto *et al.*, 1999). Vinblastine, a microtubule inhibitor used in the treatment of many types of cancer, has been shown to phosphorylate Bcl-2 and Bcl-$_{XL}$ in a JNK dependent manner, thus inducing apoptosis in KB-3 human carcinoma cells (Fan *et al.*, 2000). The pro-apoptotic Bcl-2 family member, Bax, in its inactive monomeric form is localised to the cytosol and mitochondria of healthy cells (Gross *et al.*, 1998; Nomura *et al.*, 1999). Following apoptotic stimuli, Bax undergoes a conformational change, which includes its homodimerisation, translocation of cytosolic Bax to the mitochondria and membrane insertion resulting in mitochondrial dysfunction (Goping *et al.*, 1998; Gross *et al.*, 1998; Khaled *et al.*, 1999), a process that can be blocked by the presence of protective levels of Bcl-2. (Gross *et al.*, 1998). Bax forms heterodimers with Bcl-2 and Bcl-$_{XL}$ (Yang *et al.*, 1995), and phosphorylation of Bcl-2 has been shown to result in a reduction of heterodimer complexes with Bax and subsequent apoptosis (Haldar *et al.*, 1996). Furthermore, the pro-apoptotic family member, Bad,

heterodimerises with Bcl-$_{XL}$ in mammalian cells and displaces Bax from Bcl-$_{XL}$ promoting cell death (Yang *et al.*, 1995). Alternatively, it has been suggested that Bcl-2 prevents apoptosis by inhibiting Bax translocation to mitochondria by regulating a cytosolic factor involved in the translocation of Bax (Nomura *et al.*, 1999). In the current study, the effect of PBOX-6 on the phosphorylation status of Bcl-2 family members and on the mitochondrial translocation of Bax was assessed.

Eukaryotic cells respond to extracellular stimuli by recruiting signal transduction pathways, which relay signals to the nucleus and result in changes in gene expression. A number of signalling pathways are probably activated at any given time in a cell in response to extracellular stimulation. Therefore, a combination of signalling pathways probably contributes to any given response. Furthermore, the same signalling pathway can often have different functions depending on the cell context (Minden and Karin, 1997). For example, although JNK activation leading to suppression of apoptosis in FL5.12 lymphocytic cells has been reported (Krause *et al.*, 2001), JNK is primarily activated as a cellular response to a variety of stress stimuli and anti-cancer drugs including etoposide, camptothecin (Seimiya *et al.*, 1997), ara-C (Kuwakado *et al.*, 1995), adriamycin and vinblastine (Osborn and Chambers, 1996), therefore, it is proposed to serve as a major pro-apoptotic switch in many cellular instances (Minden and Karin, 1997).

Aims of this chapter

In the present study, some members of a novel series of pyrrolo-1,5-benzoxazepine compounds have been found to potently induce apoptosis in CML cells. It has been found that PBOX-6 bypasses Bcr-Abl, the apoptotic suppresser associated with CML, and its downstream target Ras, thus representing a novel compound for the treatment of CML. In an attempt to further dissect the biochemical pathways in which PBOX-6 induces apoptosis, the effect of PBOX-6 on a variety of intracellular signal transduction pathways, involving activation of MAP kinase cascades and intracellular G-proteins was examined. The effect of PBOX-6 on the activity of a number of Bcl-2 family members that function in the regulation of apoptosis was also assessed.

5.2 Results

5.2.1 PBOX-6 induces transient activation of c-Jun N-terminal kinase (JNK) in K562 cells, but has no effect on extracellular signal-regulated kinase (ERK) or p38

Mitogen-activated protein (MAP) kinases represent one of the most important signalling cascades in response to extracellular stimuli and it is the dual phosphorylation of MAP kinases by upstream kinases that results in their activation (Chan-Hui and Weaver, 1998). The ability of PBOX-6 to activate intracellular MAP kinase pathways in K562 cells was assessed by Western blot analysis. Cells were treated with vehicle (1% (v/v) ethanol) or PBOX-6 (10μM) for various lengths of time. Whole cell extracts were prepared as outlined in Section 2.13 and proteins were resolved by SDS-PAGE followed by Western blotting. Membranes were probed with phospho-specific antibodies to JNK, ERK and p38. Phospho-JNK antibody detects dual phosphorylated threonine 183 and tyrosine 185 of p46 and p54 JNK isoforms, and does not cross react with non-phosphorylated JNK, ERK or p38. Results clearly indicate that PBOX-6 induces the transient activation of two JNK isoforms, p46 and p54, in K562 cells (Fig. 5.1). JNK activation first becomes visible following a 15 min treatment with PBOX-6, it peaks between 30-45 min and then slowly declines over 8h where it returns close to basal levels. In contrast, although UV irradiation of Jurkat cells for 2 min was shown to activate p38, PBOX-6 (10μM) treatment of K562 cells for up to 8h failed to result in p38 activation (Fig. 5.2). Similarly, PMA (100nM) treatment of K562 cells for 30 min was shown to activate the ERK MAP kinase whereas PBOX-6 (10μM) treatment of cells for up to 8h had no effect (Fig. 5.3). These results suggest that activation of the JNK MAP kinase, and not the p38 or ERK MAP kinase, may be an important intermediate in the pathway in which PBOX-6 induces apoptosis in K562 cells.

5.2.2 The JNK signalling inhibitor, CEP-1347, inhibits JNK activation and blocks apoptosis induced by PBOX-6 in K562 cells

To determine whether the activation of JNK was directly associated with the pro-apoptotic activity of PBOX-6, K562 cells were pretreated with a JNK inhibitor, CEP-1347 (5μM), for 1h prior to treatment with PBOX-6 (10μM) for a further 45 min, and Western blot analysis was performed. With the use of a phospho-specific antibody directed against JNK, results reveal that pretreatment of K562 cells with CEP-1347 prior to treatment with PBOX-6

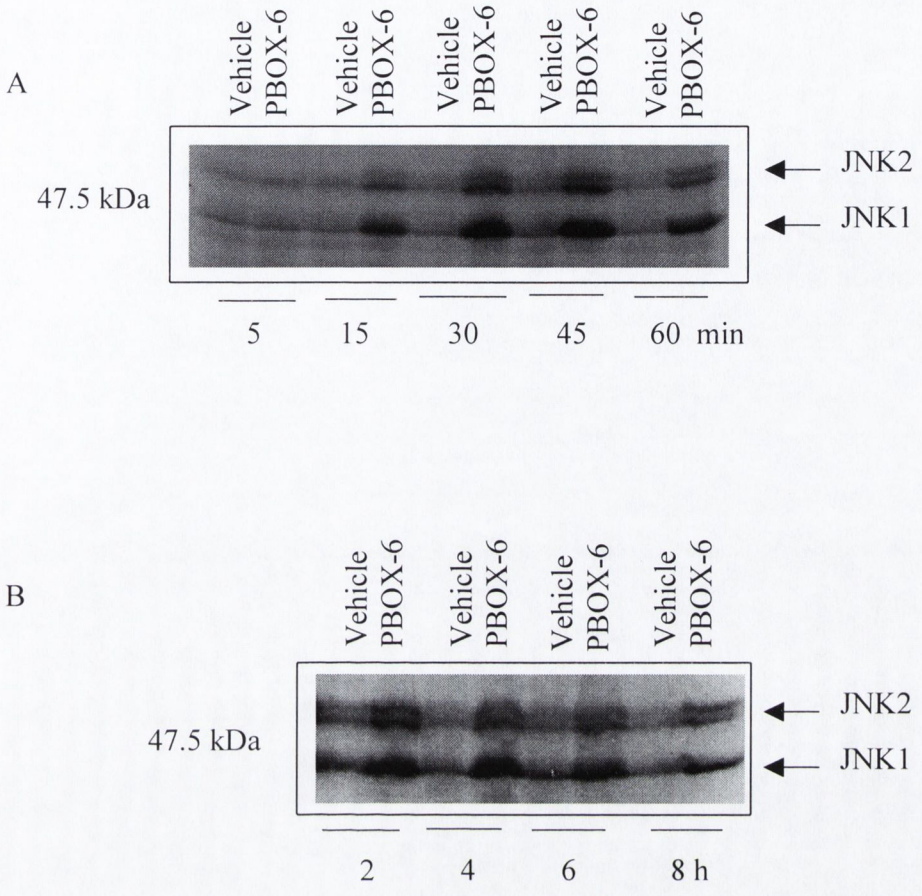

Fig. 5.1 PBOX-6 induces transient activation of two JNK isoforms, p46 and p54, in K562 cells

K562 cells were seeded at $5x10^6$cells/flask and treated with vehicle (1% (v/v) ethanol) or PBOX-6 (10μM) for (A) 5, 15, 30, 45 and 60 min, or (B) 2, 4, 6 and 8h. Whole cell extracts were prepared as described in Section 2.13 and equal amounts of protein (30μg) were resolved by SDS-PAGE and probed with a phospho-specific JNK antibody that recognises only the phosphorylated forms of JNK. Results are representative of two separate experiments.

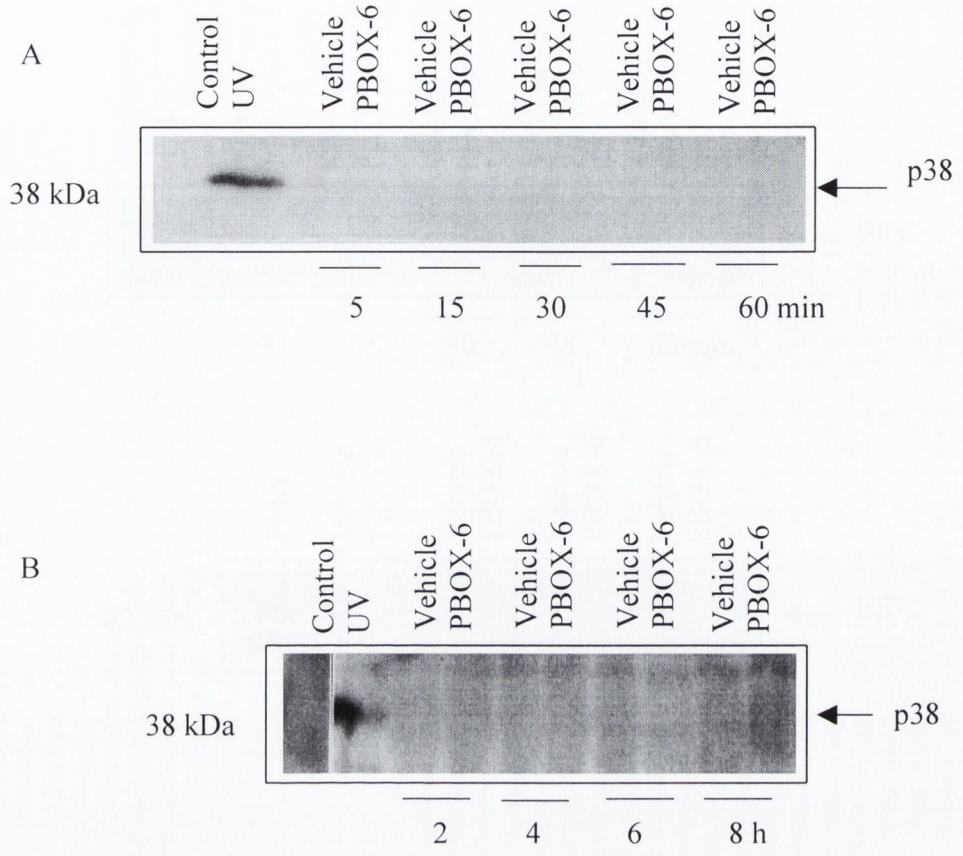

Fig. 5.2 Lack of activation of p38 MAP kinase in K562 cells in response to PBOX-6

Cells were seeded at $5x10^6$cells/flask and Jurkat cells (lanes 1-2) were UV irradiated for 2 min and incubated at 37°C for a further 2h. K562 cells (lanes 3-12) were treated with vehicle (1% (v/v) ethanol) or PBOX-6 (10μM) for either (A) 5, 15, 30, 45 and 60 min or (B) 2, 4, 6 and 8h. Whole cell extracts were prepared as described in Section 2.13 and equal amounts of protein were resolved by SDS-PAGE and probed with a phospho-specific p38 antibody, that cross reacts specifically with the phosphorylated form of p38. Results are representative of two separate experiments. In (B) the samples shown on lanes 1 and 2 were prepared together, however, the sample on lane 1 was resolved on a separate gel.

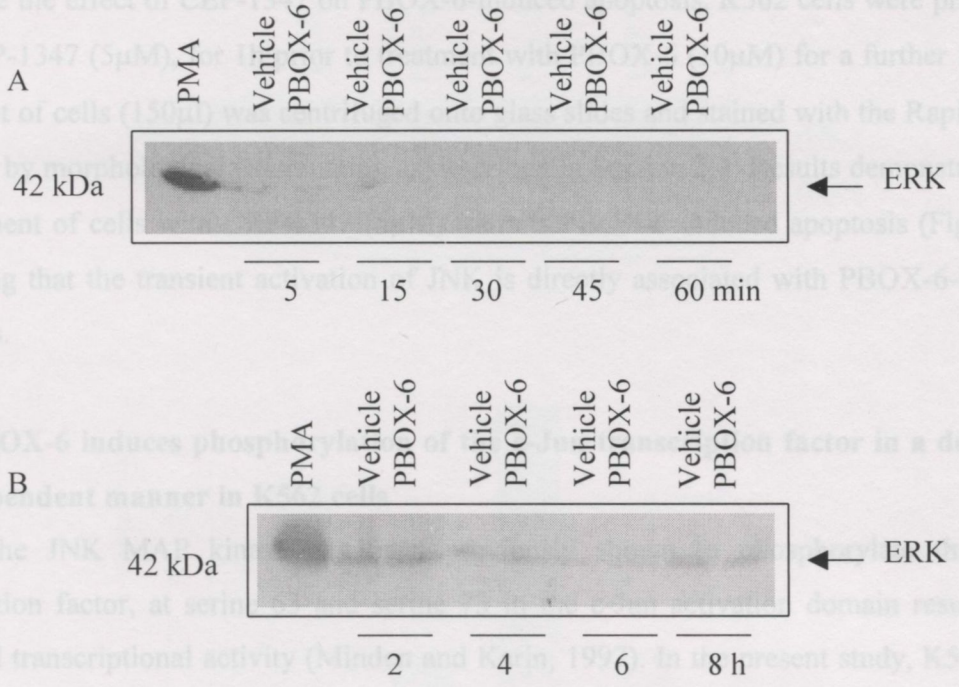

Fig. 5.3 Lack of activation of extracellular-regulated kinase (ERK) kinase in K562 cells in response to PBOX-6

K562 cells were seeded at $5x10^6$cells/flask and treated with PMA (100nM) for 30 min (lane 1) as a positive control or vehicle (1% (v/v) ethanol) or PBOX-6 (10μM) for (A) 5, 15, 30, 45 and 60 min (lanes 2-11) or (B) 2, 4, 6 and 8h (lanes 2-11). Whole cell extracts were prepared as described in Section 2.13 and equal amounts of protein (30μg) were resolved by SDS-PAGE and probed with a phospho-specific ERK antibody that reacts with the phosphorylated form of ERK. Results are representative of two separate experiments.

was sufficient to completely block PBOX-6-induced activation of JNK (Fig. 5.4A). To determine the effect of CEP-1347 on PBOX-6-induced apoptosis, K562 cells were pretreated with CEP-1347 (5μM), for 1h prior to treatment with PBOX-6 (10μM) for a further 16h and an aliquot of cells (150μl) was centrifuged onto glass slides and stained with the RapiDiff kit followed by morphological examination as described in Section 2.4. Results demonstrate that pretreatment of cells with CEP-1347 (5μM) inhibits PBOX-6-induced apoptosis (Fig. 5.4B) suggesting that the transient activation of JNK is directly associated with PBOX-6-induced apoptosis.

5.2.3 PBOX-6 induces phosphorylation of the c-Jun transcription factor in a dose-and time-dependent manner in K562 cells

The JNK MAP kinase has been previously shown to phosphorylate the c-Jun transcription factor, at serine 63 and serine 73 in the c-Jun activation domain resulting in increased transcriptional activity (Minden and Karin, 1997). In the present study, K562 cells were treated with vehicle (1% (v/v) ethanol) or PBOX-6 (10μM) for 1, 4, 8 and 16h, or a range of PBOX-6 concentrations (0.1, 1, 5 and 10μM) for 16h, and whole cell extracts were prepared as described in Section 2.13. Western blot analysis using a phospho-specific antibody that recognises c-Jun only when phosphorylated on serine 73 demonstrates that PBOX-6 induces a dose- and time-dependent phosphorylation of c-Jun in K562 cells (Fig. 5.5A and B respectively). It has been found that c-Jun first becomes activated either following treatment with 1μM PBOX-6 for 16h, or following a 4h treatment with PBOX-6 (10μM) and increases up until 16h. The appearance of c-Jun phosphorylation correlates with the appearance of the morphological signs of apoptosis in these cells.

5.2.4 PBOX-6 induces phosphorylation of activating transcription factor 2 (ATF-2) in K562 cells in a dose- and time-dependent manner

ATF-2, which has been shown to act as a substrate for JNK, is phosphorylated on residues thr-69 and thr-71, which is required for its transcriptional activity (Fuchs *et al.*, 2000; Gupta *et al.*, 1995). To determine whether ATF-2 becomes activated in response to PBOX-6 treatment of K562 cells, whole cell extracts were prepared following treatment with vehicle (1% (v/v) ethanol) or PBOX-6 (10μM) for 1, 4, 8 and 16h, or a range of PBOX

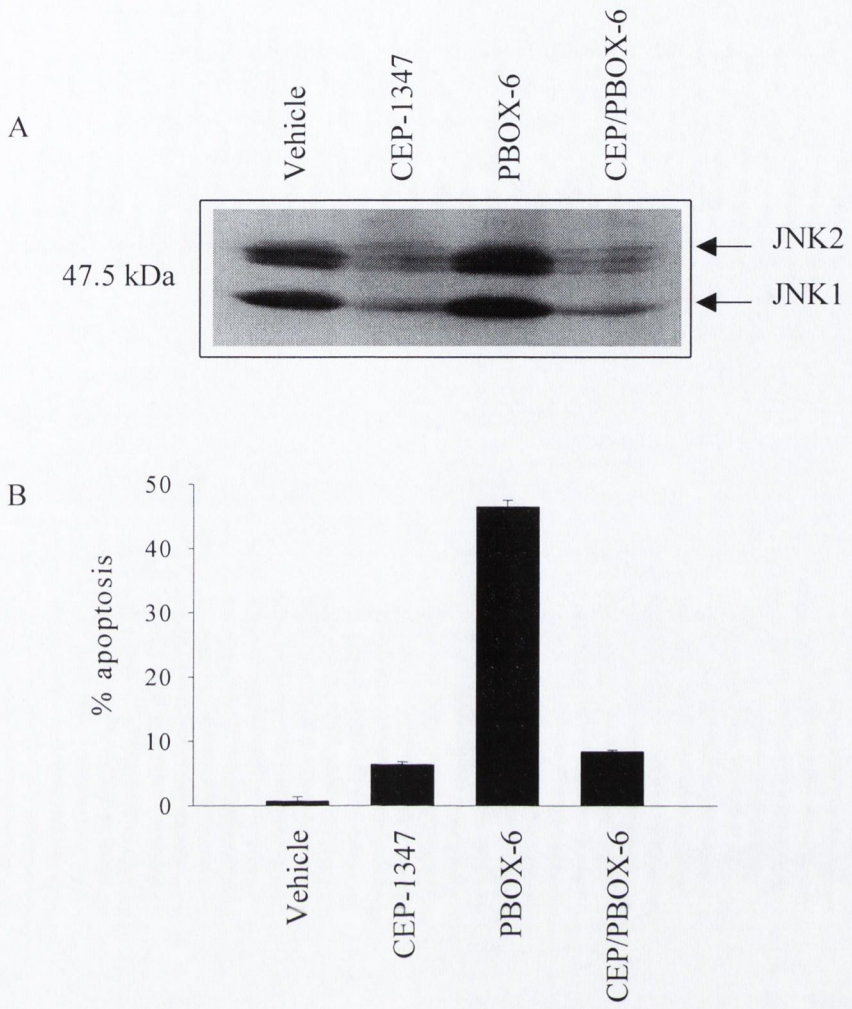

Fig. 5.4 The JNK inhibitor, CEP-1347, inhibits activation of JNK and apoptosis induced by PBOX-6 in K562 cells

(A) K562 cells ($5x10^6$ cells/flask) were treated with vehicle (1% (v/v) ethanol, 0.1% (v/v) DMSO), CEP-1347 (5μM) for 105 min, PBOX-6 (10μM) for 45 min or a pretreatment of CEP-1347 (5μM) for 1h prior to treatment with PBOX-6 (10μM) for a further 45 min. Whole cell extracts were prepared and protein (50μg) was resolved by SDS-PAGE and probed with a phospho-specific JNK antibody. (B) K562 cells (3×10^5 cells/ml) were treated with either vehicle (1% (v/v) ethanol, 0.1% (v/v) DMSO), CEP-1347 (5μM) for 17h, PBOX-6 (10μM) for 16h or a pretreatment of CEP-1347 (5μM) for 1h prior to treatment with PBOX-6 (10μM) for a further 16h. An aliquot of cells (150μl) was centrifuged onto a glass slide and the extent of apoptosis was determined by staining with the RapiDiff kit as described in Section 2.4. Values represent the mean +/- the range of two separate experiments.

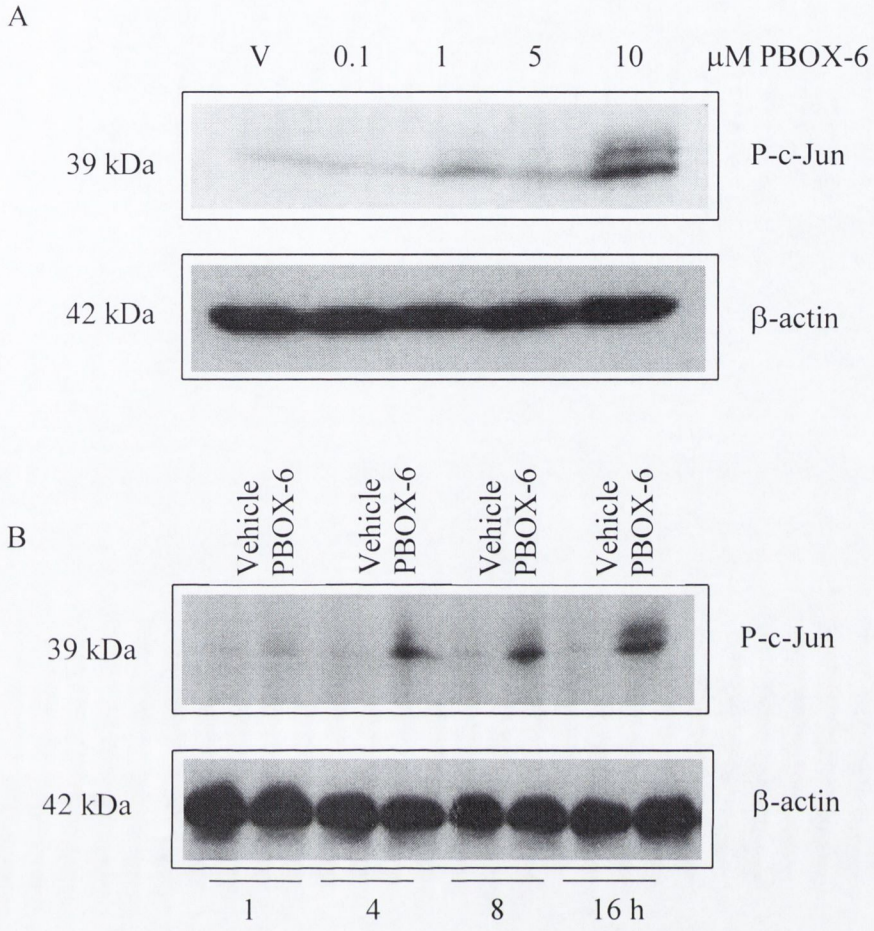

Fig. 5.5 PBOX-6 induces a dose- and time-dependent phosphorylation of c-Jun in K562 cells

K562 cells were seeded at $5x10^6$ cells/flask and treated with either (A) vehicle (1% (v/v) ethanol) or a range (0.1, 1, 5 and 10μM) of PBOX-6 concentrations for 16h or (B) vehicle (1% (v/v) ethanol) or PBOX-6 (10μM) for 1, 4, 8 and 16h. Whole cell extracts were prepared as described in Section 2.13 and protein (30μg) was resolved by SDS-PAGE followed by Western blotting. Membranes were probed with a phospho-specific c-Jun antibody that recognises the phosphorylated form of c-Jun. Blots were stripped and re-probed with an antibody against β-actin as a loading control. Results are representative of at least two separate experiments.

concentrations (0.1, 1, 5 and 10μM) for 16h. Western blot analysis using a phospho-specific antibody that recognises ATF-2 when phosphorylated at thr-69 and thr-71 reveals that PBOX-6 treatment results in a dose- and time-dependent phosphorylation of ATF-2 in K562 cells (Fig. 5.6A and B respectively). Results show that phosphorylation of ATF-2 first becomes apparent either following treatment with 1μM PBOX-6 for 16h or following a 4h treatment with PBOX-6 (10μM) and increases gradually until 16h. This pattern of phosphorylation is similar to that observed with c-Jun, and correlates with the appearance of the morphological signs of apoptosis in K562 cells.

5.2.5 The JNK signalling inhibitor, CEP-1347, inhibits activation of c-Jun and ATF-2 in K562 cells following treatment with PBOX-6

In order to determine whether activation of c-Jun and ATF-2 occurs as a direct consequence of JNK activation in response to PBOX-6 treatment, JNK activity was inhibited in K562 cells and the phosphorylation status of c-Jun and ATF-2 was analysed. K562 cells were pretreated with CEP-1347 (5μM) for 1hr prior to treatment with PBOX-6 (10μM) for a further 16h and whole cell extracts were prepared as described in Section 2.13. Western blot results revealed that CEP-1347 inhibits c-Jun and ATF-2 phosphorylation in response to PBOX-6 treatment (Fig. 5.7A and B respectively). Membranes were stripped and re-probed with an antibody against β-actin as a loading control. These results suggest that the activation of c-Jun and ATF-2 observed following PBOX-6 treatment of K562 cells is a direct consequence of JNK activation.

5.2.6 The JNK signalling inhibitor, dicumarol, prevents phosphorylation of c-Jun and ATF-2, and apoptosis induced by PBOX-6 in K562 cells

An alternative compound known as dicumarol has recently been shown to specifically inhibit activation of the JNK MAP kinase in response to a variety of stress stimuli (Cross *et al.*, 1999; Krause *et al.*, 2001).

In the present study, the activity of dicumarol as a JNK signalling inhibitor in K562 cells was assessed. Cells were pretreated with dicumarol (200μM) for 1h prior to treatment with PBOX-6 (10μM) for a further 16h and whole cell extracts were prepared as described in Section 2.13. Extracts were analysed for c-Jun and ATF-2 activity by Western blotting and results revealed that while dicumarol has no effect on c-Jun and ATF-2 activity, it inhibits c-

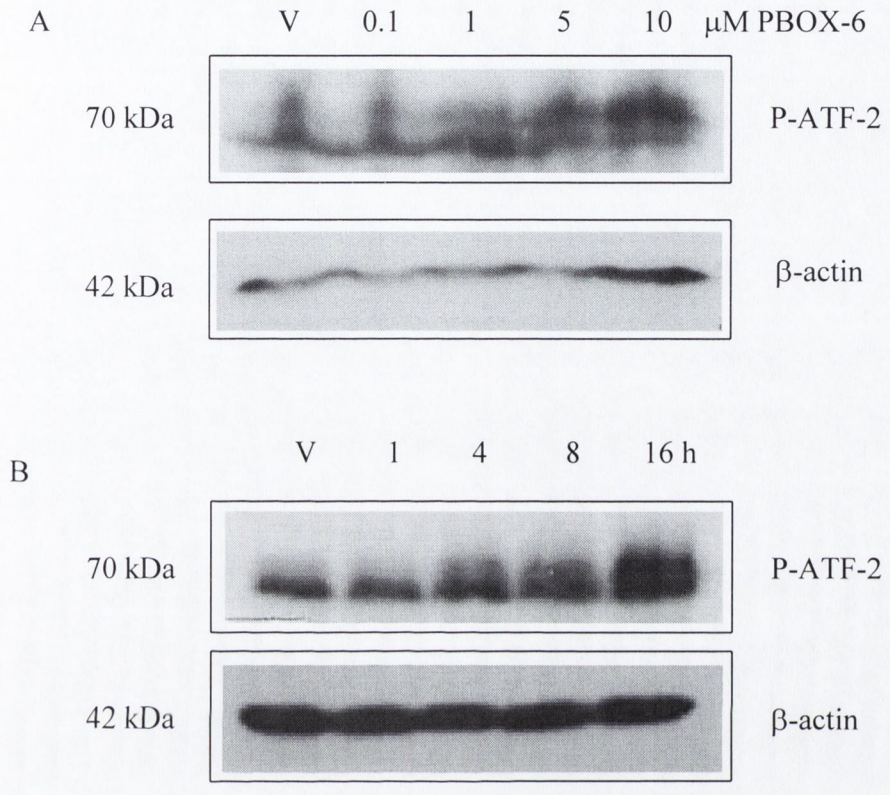

Fig. 5.6 PBOX-6 induces a dose- and time-dependent phosphorylation of ATF-2 in K562 cells

K562 cells were seeded at $5x10^6$ cells/flask and treated with vehicle (1% (v/v) ethanol) or (A) a range (0.1, 1, 5 and 10μM) of PBOX-6 concentrations for 16h or (B) PBOX-6 (10μM) for 1, 4, 8 and 16h. Whole cell extracts were prepared as described in Section 2.13 and protein (30μg) was resolved by SDS-PAGE followed by Western blotting. The membrane was probed with a phospho-specific ATF-2 antibody. Blots were stripped and re-probed with an antibody against β-actin as a loading control. Results are representative of at least two separate experiments.

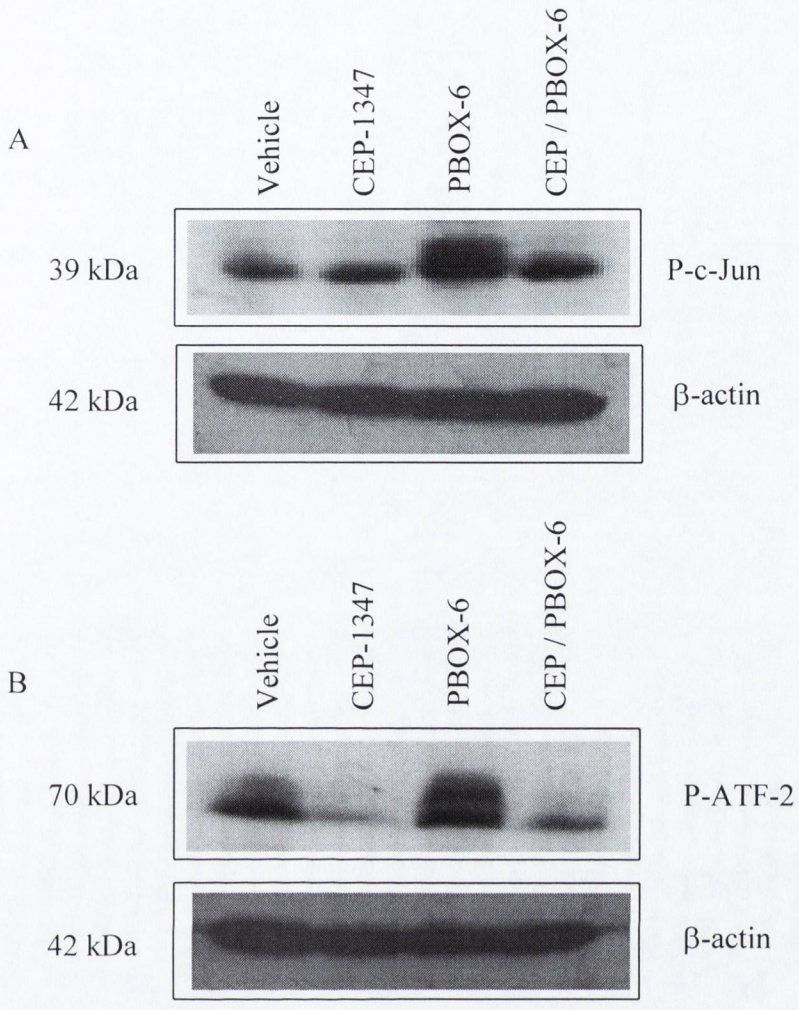

Fig. 5.7 The JNK inhibitor, CEP-1347, prevents PBOX-6-induced phosphorylation of c-Jun and ATF-2 in K562 cells

K562 cells were suspended at $1.5x10^6$ cells in 1ml of growth medium and treated with either vehicle (1% (v/v) ethanol, 0.1% (v/v) DMSO) for 17h, CEP-1347 (5μM) for 17h, PBOX-6 (10μM) for 16h, or a pretreatment of CEP-1347 (5μM) for 1h prior to treatment with PBOX-6 (10μM) for a further 16h. Whole cell extracts were prepared as outlined in Section 2.13 and equal amounts of protein (30μg) were resolved by SDS-PAGE followed by Western blotting. Membranes with probed with (A) phospho-specific c-Jun antibody and (B) phospho-specific ATF-2 antibody. Blots were stripped and re-probed with an antibody against β-actin as a loading control. Results are representative of at least two separate experiments.

Jun and ATF-2 activity in response to PBOX-6 (Fig. 5.8A and B respectively). Membranes were stripped and re-probed with an antibody against β-actin as a loading control. In order to determine the effect of dicumarol on PBOX-6-induced apoptosis, K562 cells were treated with dicumarol (200μM) for 1h prior to treatment with PBOX-6 (10μM) for a further 16h. An aliquot of cells (150μl) was centrifuged onto a glass slide and stained using the RapiDiff kit as described in Section 2.4. The extent of apoptosis was determined by morphological examination of cells. Results illustrate that dicumarol itself does not induce apoptosis in K562 cells, however, pretreatment with dicumarol completely abolishes PBOX-6-induced apoptosis in these cells (Fig. 5.9). These results correlate with those obtained using CEP-1347, which suggest that JNK activation is essential in the pathway in which PBOX-6 induces apoptosis in K562 cells and that activation of the transcription factors, c-Jun and ATF-2, occurs as a direct consequence of JNK activation.

5.2.7 Manumycin A induces activation of the JNK MAP kinase in K562 cells, which is not essential for the induction of apoptosis

In the previous chapter it has been reported that the FPTase inhibitor manumycin A induces apoptosis in K562 cells, although it also induced approximately 20% necrosis. It was thus determined whether the apoptotic effect observed in response to manumycin A treatment resulted in JNK activation in a similar manner to PBOX-6-induced apoptosis. K562 cells were treated with manumycin A (10μM) for various lengths of time (5min-8h). Whole cell extracts were prepared and Western blot analysis revealed that manumycin A induces the transient activation of JNK in K562 cells (Fig. 5.10). Activation of JNK becomes apparent following a 5 min treatment with PBOX-6, and increases gradually until it peaks at 4h and declines slightly at 8h. To ensure equal amounts of protein was resolved, the membrane was stripped and re-probed with an antibody that recognises the total JNK protein. K562 cells were then pretreated with the JNK inhibitor CEP-1347 (5μM) for 1 hr prior to treatment with manumycin A for a further 2h, and whole cell extracts were prepared. Western blot analysis revealed that CEP-1347 completely blocks JNK activation in response to manumycin A treatment (Fig. 5.11A). The membrane was stripped and re-probed with an antibody against JNK as a loading control. The effect of CEP-1347 on the extent of apoptosis induced by manumycin A was examined by staining an aliquot of cells (150μl) with the RapiDiff kit as described in Section 2.4. Percent apoptosis was determined by the morphological

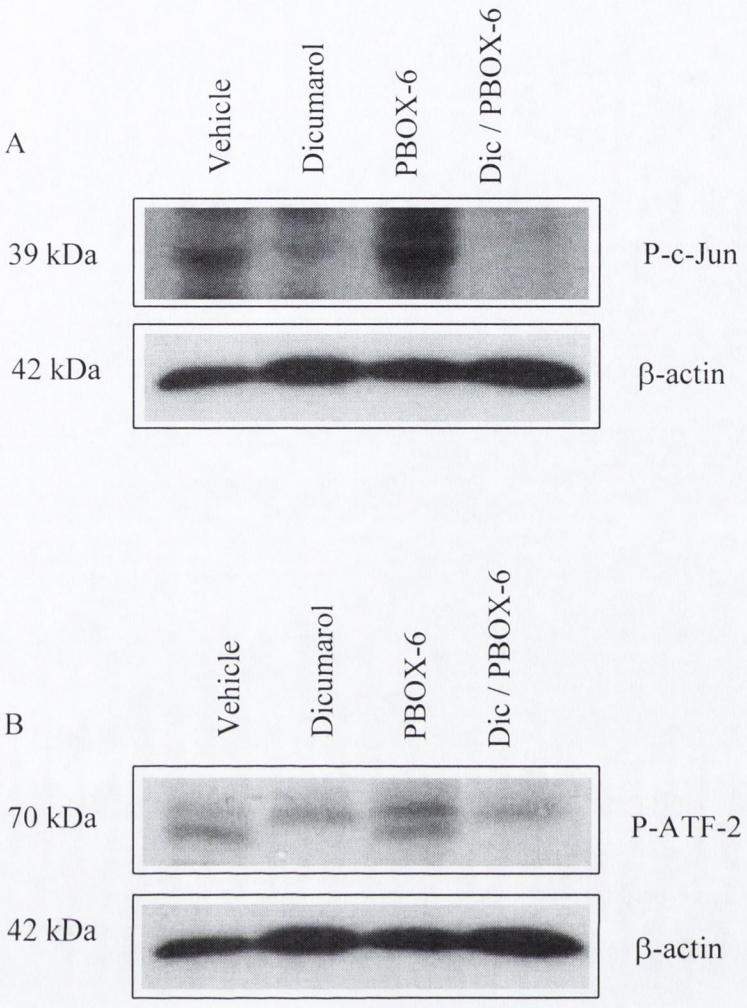

Fig. 5.8 The JNK signalling inhibitor, dicumarol, inhibits PBOX-6-induced phosphorylation of c-Jun and ATF-2 in K562 cells

K562 cells were suspended at $1.5x10^6$ cells in 1ml of growth medium and treated with either vehicle (1% (v/v) ethanol) for 17h, dicumarol (200μM) for 17h, PBOX-6 (10μM) for 16h, or a pretreatment of dicumarol (200μM) for 1h prior to treatment with PBOX-6 (10μM) for a further 16h. Whole cell lysates were prepared as outlined in Section 2.13 and an equal amount of protein (30μg) was resolved by SDS-PAGE followed by Western blotting. Membranes with incubated with (A) phospho-specific c-Jun antibody and (B) phospho-specific ATF-2 antibody. Blots were stripped and re-probed with β-actin as a loading control. Results are representative of at least two separate experiments.

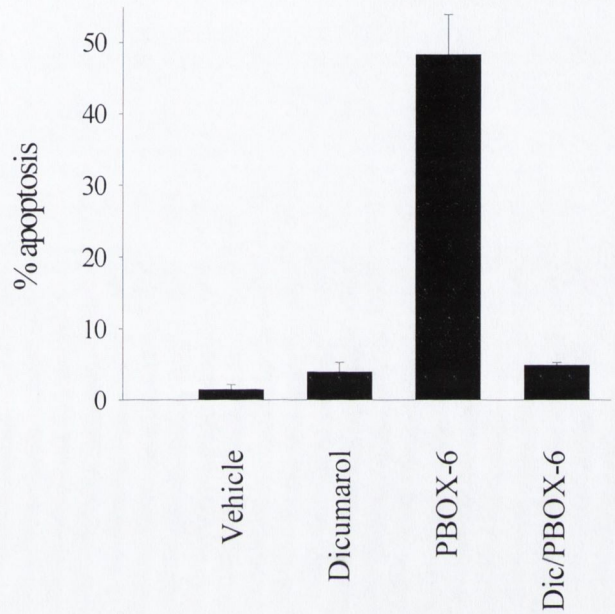

Fig 5.9 The JNK inhibitor, dicumarol, inhibits apoptosis induced by PBOX-6 in K562 cells

K562 cells were seeded at $3x10^5$ cells/ml and treated with vehicle (1% (v/v) ethanol) for 17h, dicumarol (200μM) for 17h, PBOX-6 (10μM) for 16h, or a pretreatment of dicumarol (200μM) for 1h prior to treatment with PBOX-6 (10μM) for a further 16h. The extent of apoptosis was determined by centrifuging an aliquot of cells (150μl) onto a slide and staining with the RapiDiff kit followed by morphological examination as outlined in Section 2.4. Results represent the mean +/- the range of two separate experiments.

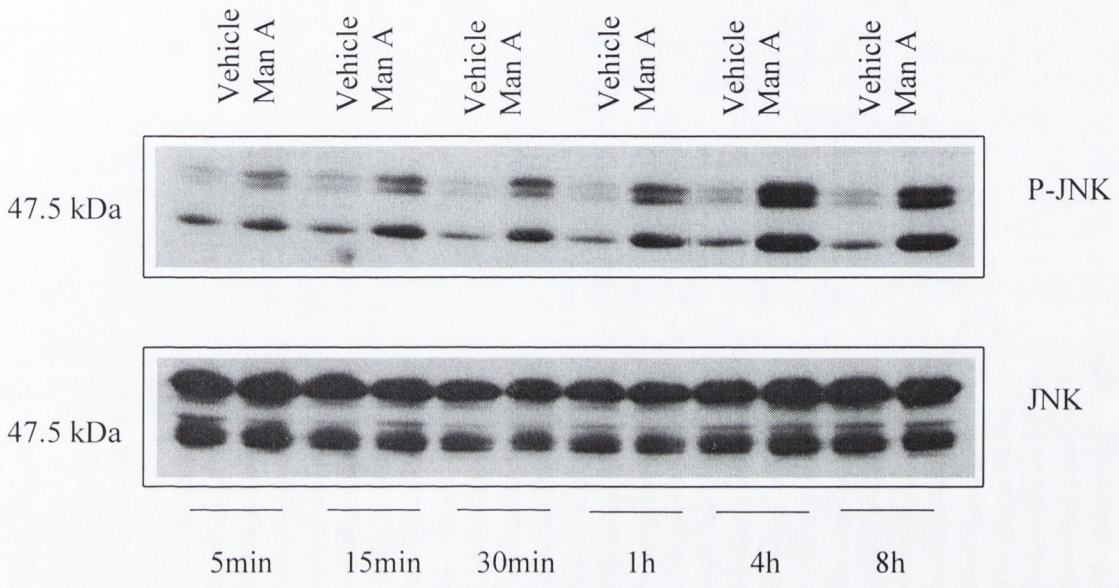

Fig. 5.10 The FPTase inhibitor, manumycin A, induces transient activation of JNK in K562 cells

K562 cells ($1.5x10^6$ cells/ml) were treated with vehicle (0.1% (v/v) DMSO) or manumycin A (Man A) (10μM) for 5 min, 15 min, 30 min, 1h, 4h and 8h. Whole cell extracts were prepared as described in Section 2.13 and an equal amount of protein (30μg) was resolved by SDS-PAGE followed by Western blotting. Membranes were probed with a phospho-specific JNK antibody (P-JNK), which recognises the phosphorylated form of JNK only. As a loading control, blots were stripped and re-probed with anti-JNK antibody, which recognises total JNK. Results are representative of at least two separate experiments.

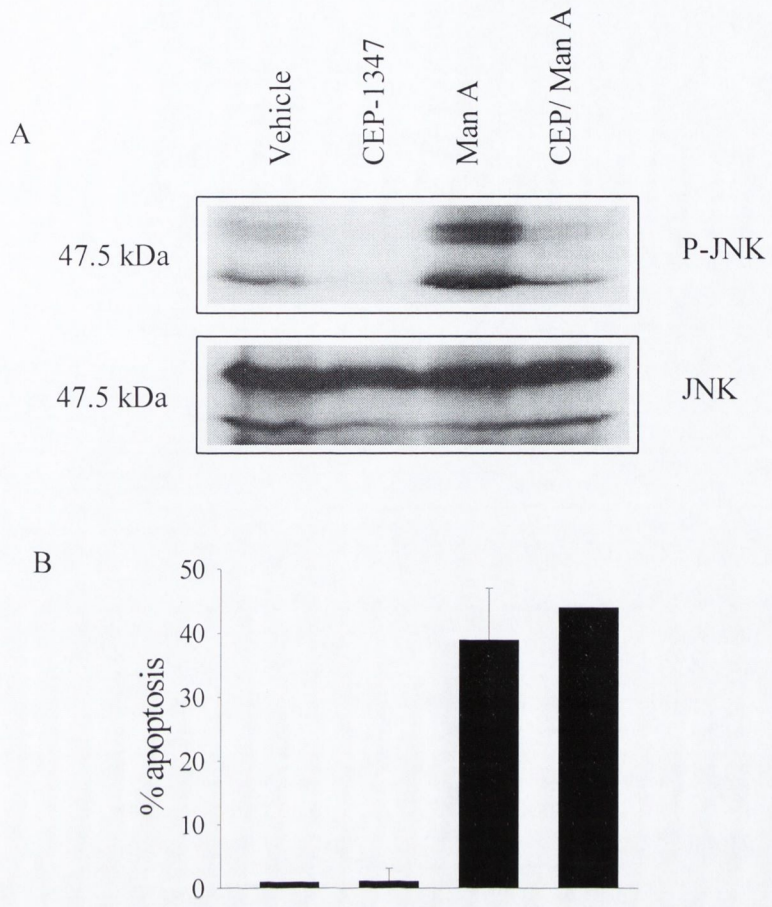

Fig 5.11 The JNK inhibitor, CEP-1347, inhibits JNK activation but not apoptosis induced in K562 cells in response to manumycin A treatment

K562 cells were seeded at either (A) $1.5x10^6$ cells/ml or (B) $3x10^5$ cells/ml and treated with either vehicle (0.2% (v/v) DMSO) for 3h, CEP-1347 (5μM) for 3h, manumycin A (Man A) (10μM) for 2h or a pretreatment of CEP-1347 (5μM) for 1h prior to treatment with manumycin A (10μM) for a further 2h. In (A) whole cell extracts were prepared as described in Section 2.13 and protein (30μg) was resolved by SDS-PAGE, followed by Western blotting. The membrane was incubated with an antibody (P-JNK) that only recognises the phosphorylated form of JNK. As a loading control, membranes were stripped and re-probed with anti-JNK-antibody that recognises unphosphorylated JNK. In (B) an aliquot of cells (150μl) was centrifuged onto a glass slide and the extent of apoptosis was determined by RapiDiff staining followed by morphological examination as described in Section 2.4. Results represent the mean +/- the range of two separate experiments.

examination of cells. Results demonstrated that pretreatment of K562 cells with CEP-1347 fails to protect against manumycin A-induced apoptosis in these cells (Fig. 5.11B). These results demonstrate that JNK activation is not an essential step in the pathway in which manumycin A induces apoptosis in K562 cells. These results, which are in contrast to that found with PBOX-6 treatment of K562 cells, suggest that these two compounds, PBOX-6 and manumycin A, do not induce apoptosis in a similar manner.

5.2.8 The topoisomerase II inhibitors, etoposide and ICRF-187, do not inhibit PBOX-6-induced JNK activation in K562 cells

In the previous chapter it was found that pretreatment of K562 cells with the topoisomerase II inhibitors, etoposide and mitoxanthrone, completely inhibited PBOX-6-induced apoptosis, whereas ICRF-187 reduced apoptosis mediated by PBOX-6 in K562 cells (Fig. 4.18 and Fig. 4.22, respectively). Although it was found that PBOX-6 does not function in a manner similar to either etoposide or ICRF-187, it was concluded that PBOX-6-induced apoptosis seems to require active topoisomerase II. To determine whether a possible PBOX-6-Topo II interaction occurs upstream or downstream of JNK in the apoptotic pathway, K562 cells were pretreated with etoposide (50μM) or ICRF-187 (200μM) for 1h prior to treatment with PBOX-6 (10μM) for a further 45 min, and the effect of JNK activation was analysed by Western blotting. Results show that pretreatment of K562 cells with etoposide does not prevent PBOX-6-induced JNK activation (Fig. 5.12A). Similarly, pretreatment of K562 cells with ICRF-187 does not prevent JNK activation in response to PBOX-6 treatment (Fig. 5.12B). ICRF-187 itself induces activation of JNK, probably as a result of stress inflicted on the cells, however, it does not induce apoptosis in these cells, as outlined in the previous chapter (Fig. 4.22). These results suggest that a possible involvement of Topo II in the apoptotic pathway initiated by PBOX-6 in K562 cells occurs downstream of JNK activation.

5.2.9 Phosphorylation of the anti-apoptotic proteins, Bcl-2 and Bcl-$_{XL}$, in K562 cells in response to PBOX-6 treatment

In addition to nuclear transcription factors, JNK has been shown to phosphorylate non-nuclear substrates such as members of the Bcl-2 protein family, which is believed to result in their inactivation (Fan *et al.*, 2000).

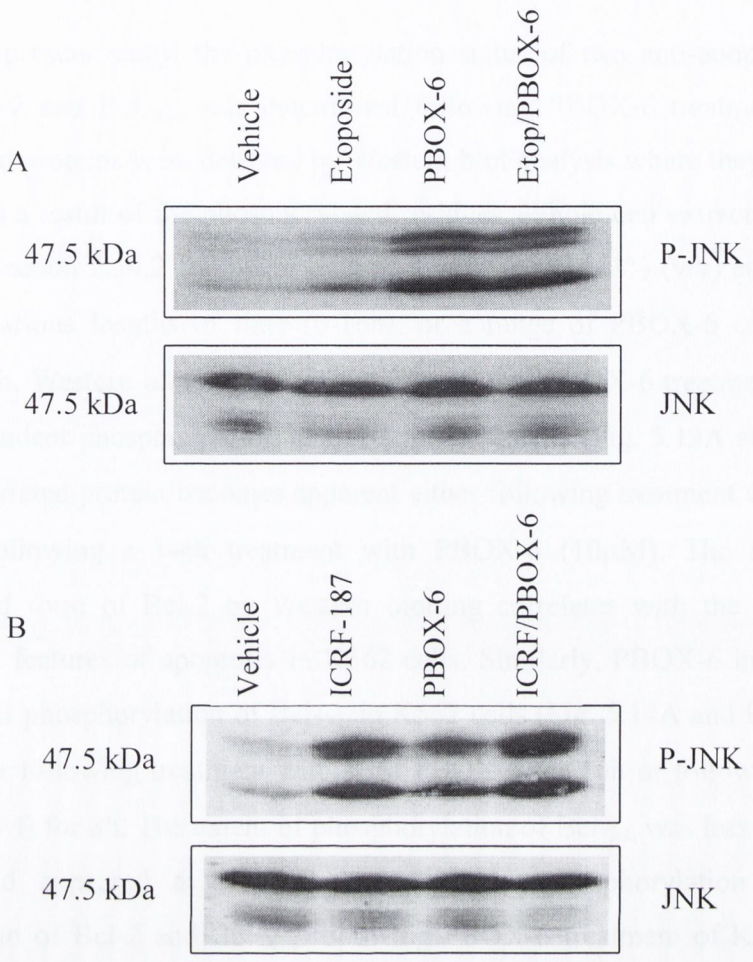

Fig. 5.12 The topoisomerase II inhibitors, etoposide and ICRF-187, do not inhibit PBOX-6-induced activation of JNK in K562 cells

K562 cells were seeded at $5x10^6$ cells/flask and treated with (A) vehicle (1% (v/v) ethanol, 0.1% ethanol: DMSO (1:1)) for 105 min, etoposide (50μM) for 105 min, PBOX-6 (10μM) for 60 min or a pretreatment of etoposide (50μM) for 60 min prior to PBOX-6 (10μM) for a further 45 min, or (B) vehicle (1% (v/v) ethanol) for 105 min, ICRF-187 (200μM) for 105 min, PBOX-6 (10μM) for 60 min or a pretreatment of ICRF-187 (200μM) for 60 min prior to PBOX-6 (10μM) for a further 45 min. Whole cell extracts were prepared as described in Section 2.13 and protein (30μg) was resolved by SDS-PAGE followed by Western blotting. Membranes were incubated with an antibody (P-JNK) that only recognises the phosphorylated form of JNK. As a loading control, membranes were stripped and re-probed with an antibody that recognises total JNK. Results are representative of at least two separate experiments.

In the present study, the phosphorylation status of two anti-apoptotic Bcl-2 family members, Bcl-2 and Bcl-$_{XL}$, was determined following PBOX-6 treatment of K562 cells. Phosphorylated proteins were detected by Western blot analysis where they migrate slower in SDS-PAGE as a result of the phosphorylated residues. Whole cell extracts were prepared as described in Section 2.14.2 following treatment with vehicle (1% (v/v) ethanol) or PBOX-6 (10μM) for various lengths of time (0-16h), or a range of PBOX-6 concentrations (0.1-10μM) for 16h. Western blot analysis demonstrated that PBOX-6 treatment induces a dose- and time-dependent phosphorylation of Bcl-2 in K562 cells (Fig. 5.13A and B respectively). The phosphorylated protein becomes apparent either following treatment with 1μM PBOX-6 for 16h or following a 1-4h treatment with PBOX-6 (10μM). The appearance of the phosphorylated form of Bcl-2 by Western blotting correlates with the appearance of the morphological features of apoptosis in K562 cells. Similarly, PBOX-6 induces a dose- and time-dependent phosphorylation of Bcl-$_{XL}$ in K562 cells (Fig. 5.14A and B), which becomes apparent either following treatment with 5μM PBOX-6 for 16h or following treatment with PBOX-6 (10μM) for 8h. The extent of phosphorylation of Bcl-$_{XL}$ was less than that observed for Bcl-2 and appeared at a later time than the phosphorylation of Bcl-2. The phosphorylation of Bcl-2 and Bcl-$_{XL}$, following PBOX-6 treatment of K562 cells suggests that these anti-apoptotic proteins may be inactivated in response to PBOX-6.

5.2.10 Inhibition of PBOX-6-induced phosphorylation of Bcl-2 and Bcl-$_{XL}$ in K562 cells using the JNK inhibitors CEP-1347 and dicumarol

To determine whether phosphorylation of Bcl-2 and Bcl-$_{XL}$ is an integral part of the apoptotic pathway in which PBOX-6 induces apoptosis, the phosphorylation status of Bcl-2 and Bcl-$_{XL}$ was assessed following inhibition of JNK activity. K562 cells were pretreated with the JNK inhibitors, CEP-1347 (5μM) or dicumarol (200μM) for 1h, prior to treatment with PBOX-6 (10μM) for a further 16h and whole cell extracts were prepared as described in Section 2.14.2. Western blot analysis revealed that treatment of K562 cells with CEP-1347 or dicumarol alone has no effect of Bcl-2 phosphorylation. However, pretreatment with these compounds prior to PBOX-6, inhibits PBOX-6-induced phosphorylation of Bcl-2 (Fig. 5.15A and B respectively). In addition, inhibition of JNK activity in K562 cells using CEP-1347 results in inhibition of Bcl-$_{XL}$ phosphorylation (Fig. 5.16). The inhibition of Bcl-2 and

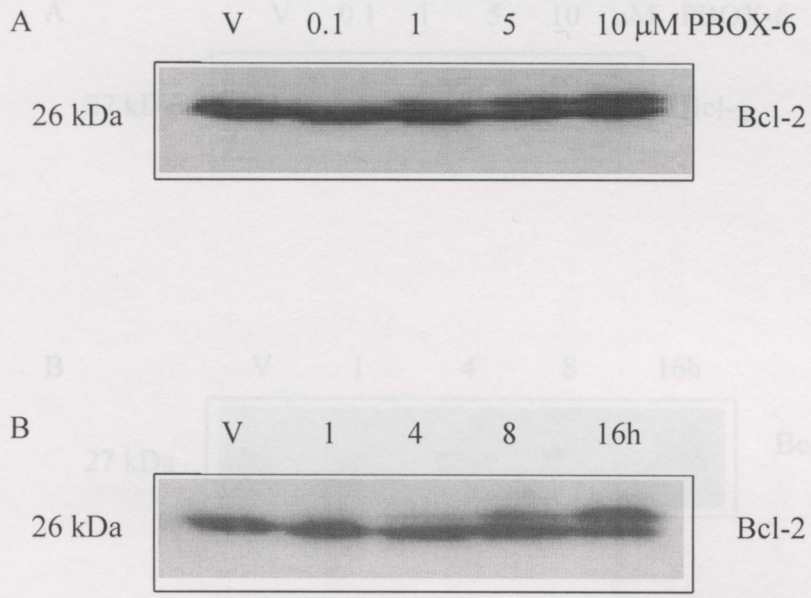

Fig. 5.13 PBOX-6 induces a dose- and time-dependent phosphorylation of Bcl-2 in K562 cells

K562 cells were seeded at $5x10^6$ cells/flask and treated with vehicle (1% (v/v) ethanol) or (A) 0.1, 1, 5 and 10μM PBOX-6 for 16h or (B) PBOX-6 (10μM) for 1, 4, 8 and 16h. Whole cell lysates were prepared as outlined in Section 2.14.2 and equal amounts of protein (30μg) was resolved by SDS-PAGE followed by Western blotting and incubation with anti-Bcl-2 antibody. Results are representative of three separate experiments.

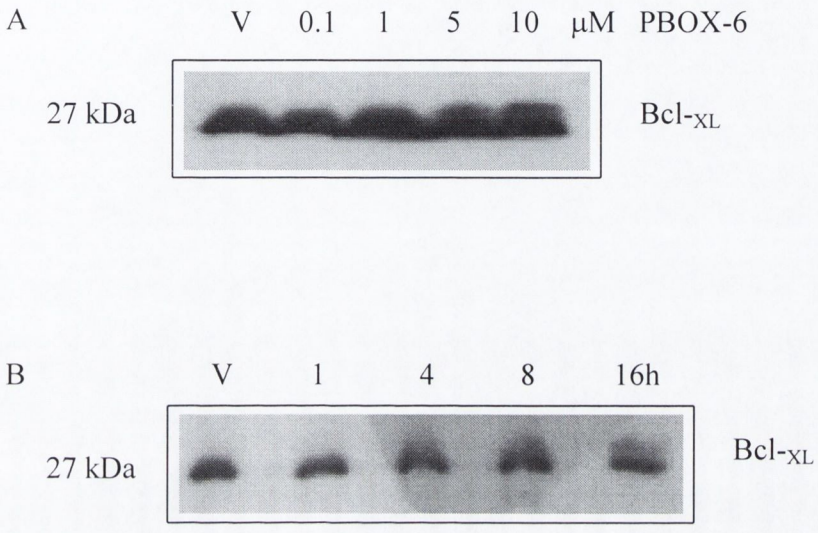

Fig. 5.14 PBOX-6 induces a dose- and time-dependent phosphorylation of Bcl-$_{XL}$ in K562 cells

K562 cells were seeded at $5x10^6$ cells/flask and treated with vehicle (1% (v/v) ethanol) or (A) 0.1, 1, 5 and 10μM PBOX-6 for 16h or (B) PBOX-6 (10μM) for 1, 4, 8 and 16h. Whole cell extracts were prepared as described in Section 2.14.2 and an equal amount of protein (30μg) was resolved by SDS-PAGE followed by Western blotting. Membranes were incubated with anti-Bcl$_{XL}$ antibody. Results are representative of two separate experiments.

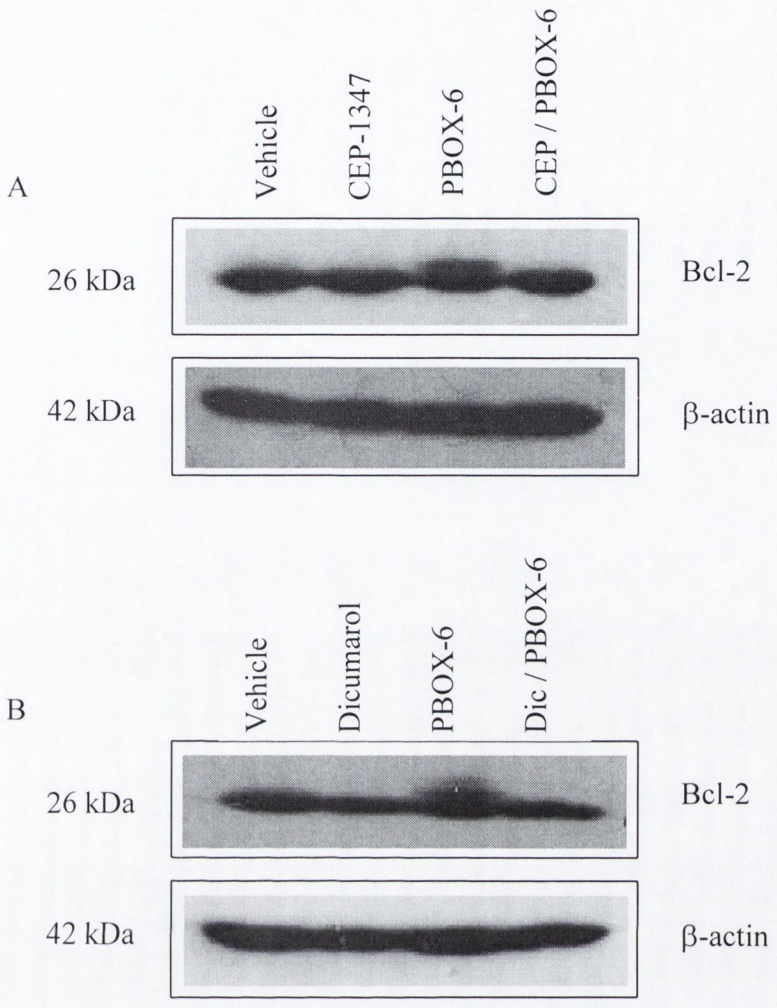

Fig. 5.15 The JNK inhibitors, CEP-1347 and dicumarol, prevent PBOX-6 induced phosphorylation of Bcl-2 in K562 cells

K562 cells ($1.5x10^6$ cells) were treated with (A) vehicle (1% (v/v) ethanol, 0.1% (v/v) DMSO) for 17h, CEP-1347 (5μM) for 17h, PBOX-6 (10μM) for 16h, or a pretreatment of CEP-1347 (5μM) for 1h prior to treatment with PBOX-6 (10μM) for a further 16h, or (B) vehicle (1% (v/v) ethanol) for 17h, dicumarol (200μM) for 17h, PBOX-6 (10μM) for 16h, or a pretreatment of dicumarol (200μM) for 1h prior to treatment with PBOX-6 (10μM) for a further 16h. Whole cell extracts were prepared as outlined in Section 2.14.2 and equal amounts of protein (30μg) were resolved by SDS-PAGE followed by Western blotting. Membranes with probed with anti-Bcl-2 antibody. As a loading control, blots were stripped and re-probed with an antibody against β-actin. Results are representative of at least two separate experiments.

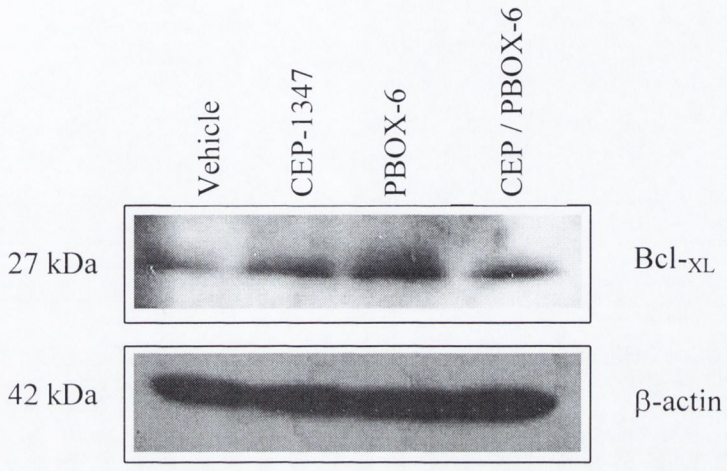

Fig. 5.16 The JNK inhibitor, CEP-1347, prevents PBOX-6 induced phosphorylation of Bcl-$_{XL}$ in K562 cells

K562 cells were suspended at 1.5x10^6 cells in 1ml of growth medium and treated with vehicle (1% (v/v) ethanol, 0.1% (v/v) DMSO) for 17h, CEP-1347 (5μM) for 17h, PBOX-6 (10μM) for 16h, or a pretreatment of CEP-1347 (5μM) for 1h prior to treatment with PBOX-6 (10μM) for a further 16h. Whole cell extracts were prepared as outlined in Section 2.14.2 and equal amounts of protein (30μg) were resolved by SDS-PAGE followed by Western blotting. Membranes with probed with anti-Bcl-$_{XL}$ antibody. As a loading control, blots were stripped and re-probed with an antibody against β-actin. Results are representative of at least two separate experiments

Bcl-$_{XL}$ phosphorylation using compounds that have been previously shown to inhibit JNK activity suggests that phosphorylation of Bcl-2 and Bcl-$_{XL}$ lies downstream of JNK in the apoptotic pathway in which PBOX-6 induces apoptosis in K562 cells.

5.2.11 PBOX-6 has no effect on expression levels and on subcellular localisation of Bax in K562 cells

Bcl-2 family members undergo modification such as dimerisation, phosphorylation and proteolytic cleavage. It has been suggested that Bcl-2 prevents apoptosis by inhibiting the translocation of Bax from the cytosol into the mitochondria where it can carry out its pro-apoptotic function (Nomura *et al.*, 1999). In the present study, the hypothesis that inactivation of Bcl-2 and Bcl-$_{XL}$ by phosphorylation may allow mitochondrial translocation of Bax, which may be responsible for the subsequent apoptosis was investigated.

Levels of Bax expression were monitored in mitochondrial and cytosolic fractions from K562 cells prepared following treatment with PBOX-6. Cells were treated with either vehicle (1% (v/v) ethanol) or PBOX-6 (10μM) for 16h. Two cellular fractions were prepared by centrifugation, a cytosolic fraction, and a mitochondrial-enriched fraction. A Bradford assay was used to determine the protein concentration as described in Section 2.3.1. Equal amounts of protein were resolved by SDS-PAGE and the levels of Bax were determined by Western blot analysis. To determine the purity of the cytosolic and mitochondrial fractions, each fraction was tested for cross-contamination with the other, by measuring the presence or absence of two protein markers. Bcl-2 was chosen as a mitochondrial marker as this is its primary cellular location and it has previously been used as a reliable marker in similar studies (Gross *et al.*, 1998; Khaled *et al.*, 1999). The cytosolic enzyme, lactate dehydrogenase (LDH), was used as a marker of the cytosolic fraction and activity was measured using the LDH assay as described in Section 2.20. Enzyme activity in each fraction was expressed as a percentage of total enzyme activity, measured from whole cell extracts. Results from Western blotting have shown that Bax is present in the cytosolic and mitochondrial fraction of untreated K562 cells. Treatment of cells with PBOX-6 does not alter the distribution of Bax expression in these cells (Fig. 5.17). The membrane was stripped and re-probed with anti-Bcl-2 antibody and results show the presence of Bcl-2 in the whole cell and mitochondrial fraction, whereas it is absent from the cytosolic fraction. These results determine that the cytosolic fraction is not contaminated with components from the

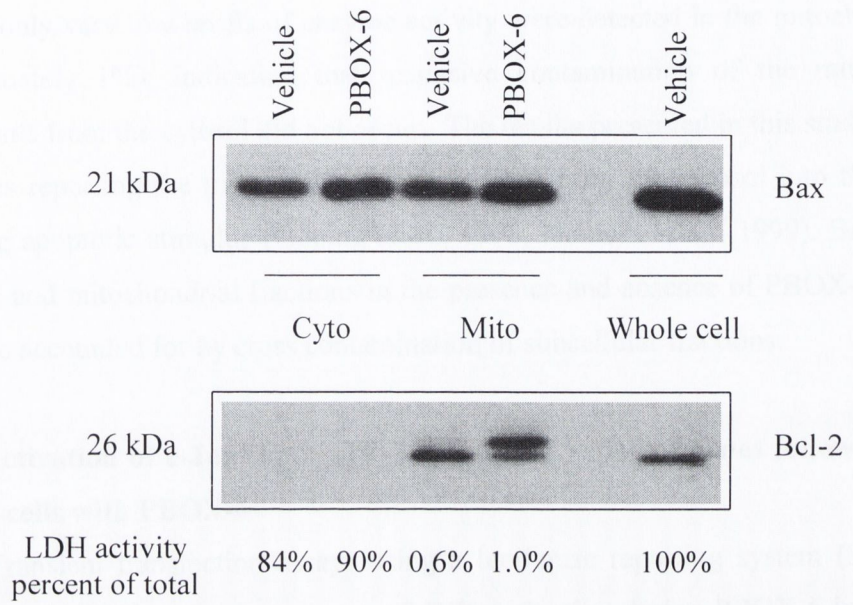

Fig. 5.17 PBOX-6 has no effect on levels of expression of the pro-apoptotic protein, Bax, in K562 cells

K562 cells ($2x10^6$ cells/ml) were treated with either vehicle (1% (v/v) ethanol) or PBOX-6 (10μM) for 16h. Whole cell extracts or subcellular fractions, consisting of cytosolic and mitochondrial-enriched fractions, were prepared as described in Section 2.14.1. Protein concentration was determined using the Bradford technique and an equal amount of protein (30μg) from cytosolic, mitochondrial and whole cell extracts, was resolved by SDS-PAGE followed by Western blotting. Membranes were incubated with anti-Bax antibody and proteins were detected by ECL. Membranes were stripped and re-probed with Bcl-2, which is used as a mitochondrial marker. An LDH assay was performed on an equal amount of protein (1μg) from each subcellular fraction and enzyme activity was expressed as percent of total LDH measured from whole cell extracts. Results are representative of at least three separate experiments.

mitochondrial fraction. In addition, an LDH assay was carried out on equal amounts of protein (1μg) from whole cell extracts and the two subcellular fractions. Results indicate that the majority of LDH activity remained in the cytosolic fraction (approximately 90%), whereas only very low levels of enzyme activity were detected in the mitochondrial fraction (approximately 1%), indicating that extensive contamination of the mitochondria with components from the cytosol did not occur. The results presented in this study are in contrast to articles reporting the translocation of some Bax from the cytosol into the mitochondria following apoptotic stimulus (Goping *et al.*, 1998; Nomura *et al.*, 1999). Bax was found in cytosolic and mitochondrial fractions in the presence and absence of PBOX-6, an effect that cannot be accounted for by cross contamination of subcellular fractions.

5.2.12 Activation of c-Jun- and ATF-2-dependent reporter genes following stimulation of K562 cells with PBOX-6

Transient transfection assays using a luciferase reporting system (Strategene) were carried out to confirm the importance of JNK activation during PBOX-6-induced apoptosis and to investigate events upstream of JNK in the apoptotic signalling pathway.

K562 cells were transiently transfected using the FuGENE6 transfection reagent, a non-liposomal lipid formulation, as described in Section 2.29. All DNA used in the transfection assays was first transformed in *E. coli* SCS-1 cells, grown in culture and purified from *E. coli* cells and the resultant DNA was quantified (Sections 2.21-2.28). K562 cells were transiently transfected with a c-Jun and ATF-2-dependent reporting system. Direct or indirect phosphorylation of the c-Jun or ATF-2 activation domain causes binding of the Gal4 DNA binding domain to the binding sites on the reporter plasmid, thus activating transcription of luciferase. Following transfection of K562 cells ($4x10^5$ cells) in triplicate as described in Section 2.29, and overnight recovery at 37°C, cells were stimulated with vehicle (1% (v/v) ethanol) or PBOX-6 (10μM) for 48h. Cell extracts were prepared and luciferase activity was measured using a luminometer as outlined in Section 2.30. Following each transfection procedure, an aliquot of cell extract was retained for measurement of β-galactosidase activity, which was used to normalise luciferase measurements. ATF-2 activity is determined as a function of luciferase activity and is expressed as fold stimulation over unstimulated cells. Results shown in Fig. 5.18 indicate that vehicle (1% (v/v) ethanol) has no effect on the activation of c-Jun or ATF-2, whereas PBOX-6 stimulates a 3.6-fold increase in

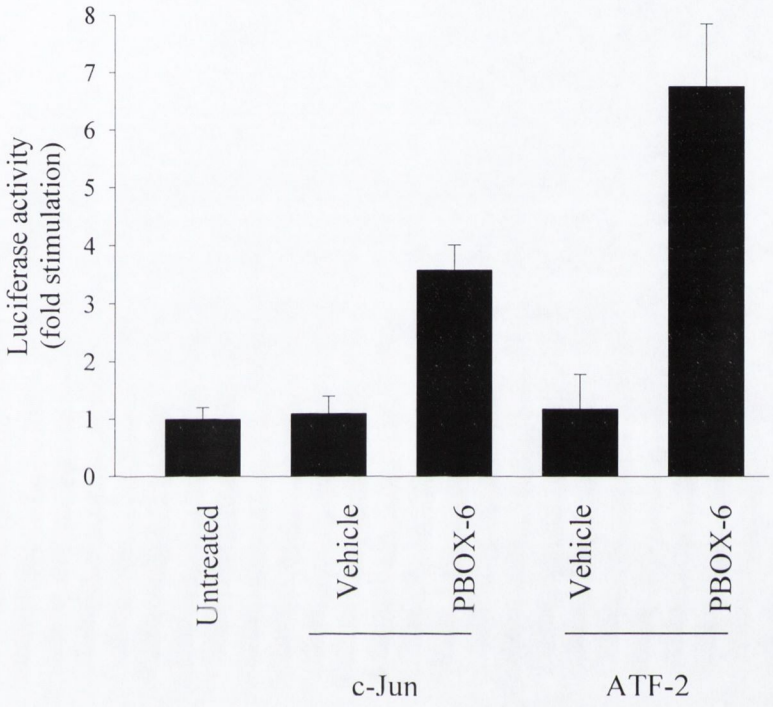

Fig. 5.18 PBOX-6 stimulates activation of c-Jun- and ATF-2-dependent reporter genes in K562 cells

K562 cells ($4x10^5$) were transfected with a luciferase reporting system (400ng) consisting of a plasmid encoding the c-Jun or ATF-2 activation domains (20ng), a luciferase reporter (100ng), β-galactosidase (80ng) and empty vector (200ng). Following overnight recovery at 37°C, cells were treated with vehicle (1% (v/v) ethanol) or PBOX-6 (10μM) for a further 48h. Reporter gene activity was determined as a function of luciferase activity. Results are expressed as fold stimulation over unstimulated cells and represent the mean +/- S.E.M of triplicate determinations performed at least three times.

c-Jun activity and a 6.8-fold increase in ATF-2 activity. These results suggest that PBOX-6 causes phosphorylation of the JNK substrates, c-Jun and ATF-2, and confirms previous results from Western blotting. Since a higher fold increase in ATF-2 activity was detected when compared to c-Jun activity, following PBOX-6 treatment, the ATF-2 reporting system was used in all further studies.

5.2.13 Expression of the JNK signalling inhibitor, JIP-1, prevents activation of the ATF-2-dependent reporter gene and apoptosis induced by PBOX-6

Overexpression of the JNK scaffold protein, JIP-1, acts as a JNK signalling inhibitor due to cytoplasmic retention of JNK and also by the sequestration of limiting JNK pathway components (Dickens *et al.*, 1997; Whitmarsh *et al.*, 1998; Yasuda *et al.*, 1999).

K562 ($4x10^5$) cells were transfected with JIP-1 and the ATF-2 reporting system in a total volume of 400µl as indicated in Section 2.29. Following overnight recovery, cells were stimulated with either vehicle (1% (v/v) ethanol) or PBOX-6 (10µM) for 48h and luciferase activity was determined. Luciferase activity is expressed as fold stimulation over vehicle treated cells and results demonstrate that while PBOX-6 stimulated a 5-fold increase in ATF-2-dependent reporter gene activity, co-transfection of the JIP-1 protein into K562 cells completely inhibits PBOX-6-induced stimulation of the ATF-2 activity (Fig. 5.19A). K562 cells were also transfected with an empty vector ($PCDNA_3$) or JIP-1 in a manner similar to that described above, and treated with either vehicle or PBOX-6 (10µM) for 16h. An aliquot of cells (150µl) was centrifuged onto a glass slide and the extent of apoptosis was determined by staining the cells with the RapiDiff kit followed by morphological examination, as described in Section 2.4. Results show that transfection of JIP-1 into K562 cells significantly reduces the extent of apoptosis induced by PBOX-6 (Fig. 5.19B). Incomplete protection against PBOX-6 induced apoptosis in JIP-1 transfected cells can be explained by incomplete transfection of the total cell population. These results confirm the earlier reports by Yasuda *et al.* (1999) that JIP-1 acts as an inhibitor of the JNK signalling pathway and correlates with results from Western blotting, which illustrate that two different JNK inhibitors block activation of ATF-2 and apoptosis induced by PBOX-6 in K562 cells.

Fig. 5.19 The JNK signalling inhibitor, JIP-1, prevents activation of the ATF-2-dependent reporter gene and apoptosis induced by PBOX-6 in K562 cells

K562 cells ($4x10^5$) were transfected with (A) the ATF-2-luciferase reporting system (400ng) consisting of a plasmid encoding the ATF-2 activation domain (20ng), a luciferase reporter (100ng), β-galactosidase (80ng), in combination with either an empty vector (200ng) (columns 1-3) or a plasmid encoding JIP-1 (200ng) (column 4). Following overnight recovery at 37°C, cells were treated with vehicle (1% (v/v) ethanol) or PBOX-6 (10μM) for a further 48h. ATF-2 activity was determined as a function of luciferase activity. Results are expressed as fold stimulation over unstimulated cells and represent the mean +/- S.E.M of triplicate determinations performed at least three times. In (B) cells were transfected with empty vector (400ng) or a plasmid encoding JIP-1 (200ng) and empty vector (200ng). Following overnight recovery, cells were treated with either vehicle (1% (v/v) ethanol) or PBOX-6 (10μM) for 16h and the extent of apoptosis was determined by RapiDiff staining followed by morphological examination as outlined in Section 2.4. Results represent the mean +/- S.E.M of three separate experiments. Statistical analysis was carried out using the Instat computer program.

* $p<0.001$ with respect to vehicle treatment; Students t-test.

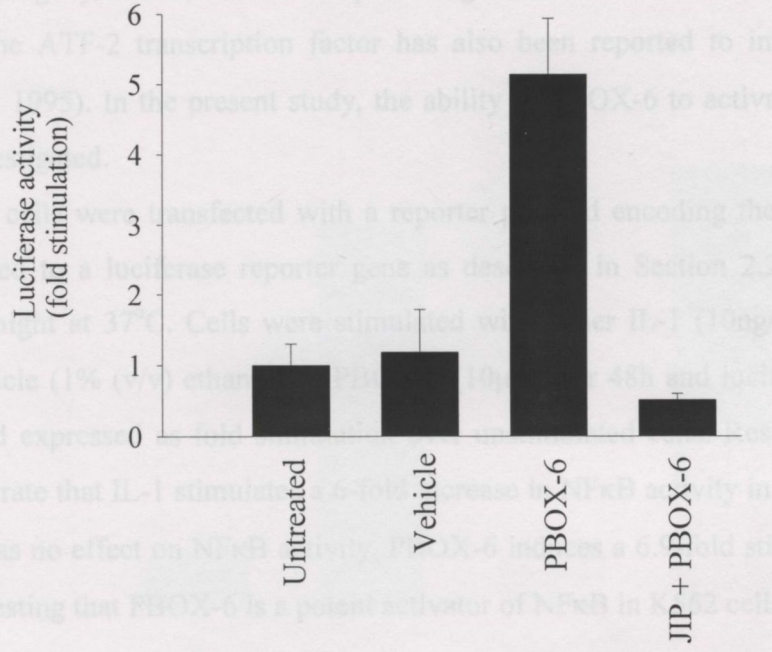
A
Luciferase activity
(fold stimulation)
0
1
2
3
4
5
6
Untreated
Vehicle
PBOX-6
JIP + PBOX-6

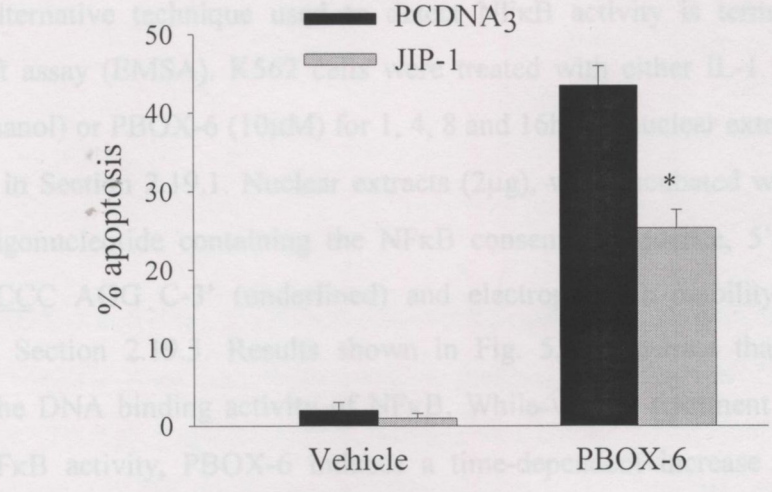
B
PCDNA3
JIP-1
% apoptosis
0
10
20
30
40
50
*
Vehicle
PBOX-6

5.2.14 PBOX-6 activates the NFκB-dependent reporter gene in K562 cells

The NFκB transcription factor is activated in response to a variety of pro-apoptotic stimuli including cytokines, chemotherapeutic agents and oxidative stress (Bours *et al.*, 2000), and the ATF-2 transcription factor has also been reported to interact with NFκB (Gupta *et al.*, 1995). In the present study, the ability of PBOX-6 to activate NFκB in K562 cells was investigated.

K562 cells were transfected with a reporter plasmid encoding the NFκB consensus sequence fused to a luciferase reporter gene as described in Section 2.29 and allowed to recover overnight at 37°C. Cells were stimulated with either IL-1 (10ng/ml) (as a positive control), vehicle (1% (v/v) ethanol) or PBOX-6 (10μM) for 48h and luciferase activity was measured and expressed as fold stimulation over unstimulated cells. Results shown in Fig. 5.20 demonstrate that IL-1 stimulates a 6-fold increase in NFκB activity in K562 cells. While the vehicle has no effect on NFκB activity, PBOX-6 induces a 6.9-fold stimulation of NFκB activity suggesting that PBOX-6 is a potent activator of NFκB in K562 cells.

5.2.15 PBOX-6 induces a time-dependent increase in NFκB activation in K562 cells

An alternative technique used to detect NFκB activity is termed electrophoretic mobility shift assay (EMSA). K562 cells were treated with either IL-1 (10ng/ml), vehicle (1% (v/v) ethanol) or PBOX-6 (10μM) for 1, 4, 8 and 16h and nuclear extracts were prepared as described in Section 2.19.1. Nuclear extracts (2μg), were incubated with the labelled 22 base pair oligonucleotide containing the NFκB consensus sequence, 5'-AGT TGA GGG GAC TTT CCC AGG C-3' (underlined) and electrophoretic mobility was analysed as described in Section 2.19.3. Results shown in Fig. 5.21 illustrate that IL-1 induces an increase in the DNA binding activity of NFκB. While vehicle treatment of cells shows no effect on NFκB activity, PBOX-6 induces a time-dependent increase in activity, which becomes apparent following a 1h treatment with PBOX-6. These results are in agreement with reporter gene experiments that demonstrate NFκB activation in K562 cells in response to PBOX-6.

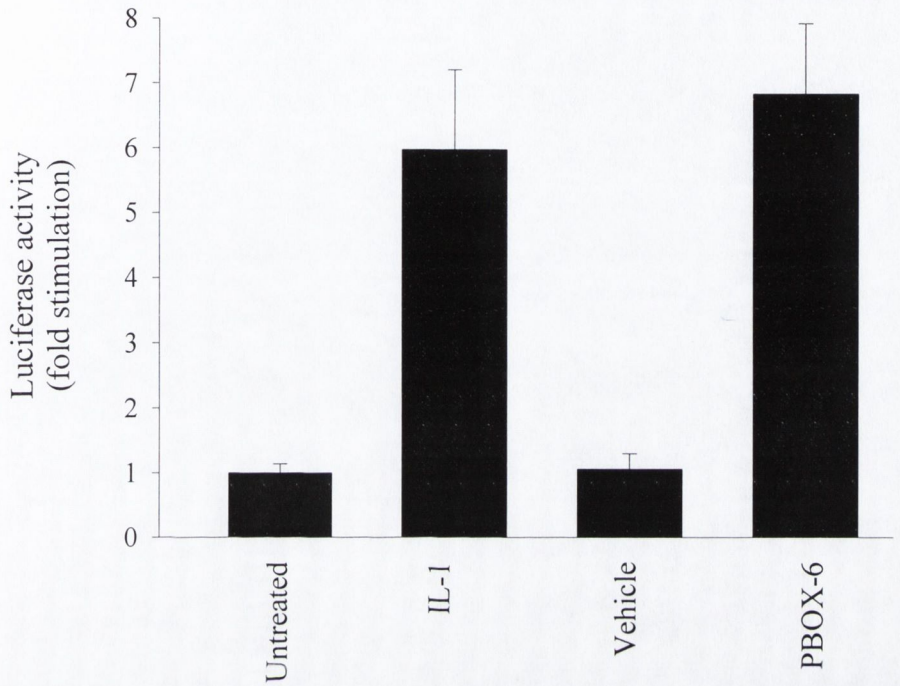

Fig. 5.20 PBOX-6 activates the NFκB-dependent reporter gene in K562 cells

K562 cells ($4x10^5$) were transfected with a plasmid encoding the NFκB-luciferase reporter gene (100ng), β-galactosidase (100ng) and empty vector (200ng). Following overnight recovery at 37°C cells were stimulated with IL-1 (10ng/ml), vehicle (1% (v/v) ethanol) or PBOX-6 (10μM) for 48h. NF-κB activity was determined as a function of luciferase activity, and is expressed as fold stimulation over untreated cells. Results represent the mean +/- S.E.M of triplicate determinations performed at least three times.

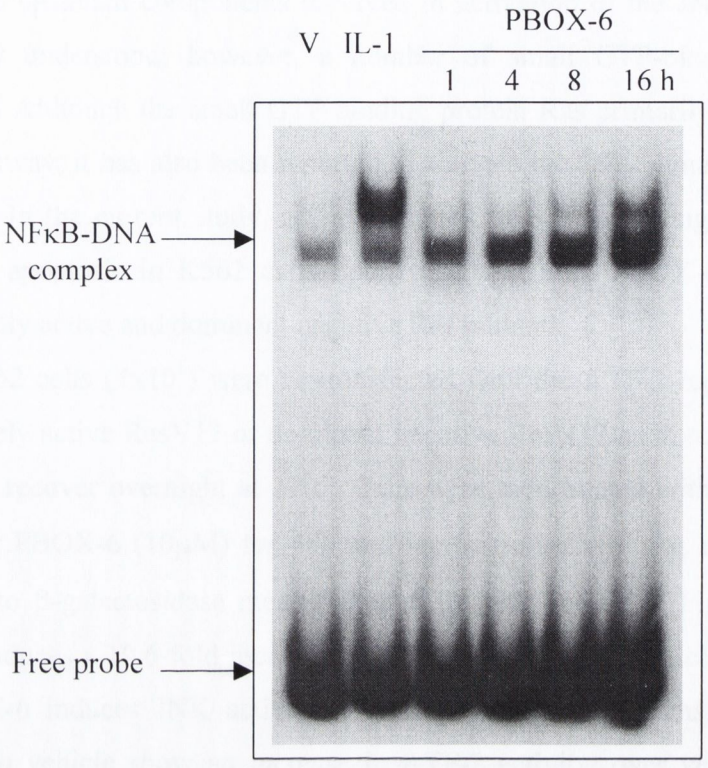

Fig. 5.21 PBOX-6 induces a time-dependent increase in NFκB activation in K562 cells

K562 cells, seeded at a density of $3x10^6$ cells were treated with either vehicle (1% (v/v) ethanol), IL-1 (10ng/ml) or PBOX-6 (10μM) for 1, 4, 8 and 16h and nuclear extracts were prepared as described in Section 2.19.1. Nuclear extracts (2μg), were incubated with the labeled 22 base pair oligonucleotide containing the NFκB consensus sequence, 5'-AGT TGA GGG GAC TTT CCC AGG C-3' (underlined) and the DNA binding activity of NFκB was determined by electrophoretic mobility shift assay as described in Section 2.19.3. Results are representative of two separate experiments.

5.2.16 Effect of RasV12 and RasN17 on PBOX-6-induced activation of the ATF-2-dependent reporter gene

The upstream components involved in activation of the JNK signalling pathway are not clearly understood, however, a number of small GTP-binding proteins have been implicated. Although the small GTP-binding protein Ras primarily activates the ERK MAP kinase pathway, it has also been reported to activate the JNK signalling pathway (Minden *et al.*, 1994). In the current study, an involvement of Ras in the signal transduction pathway leading to apoptosis in K562 cells upon treatment with PBOX-6 was investigated using constitutively active and dominant negative Ras mutants.

K562 cells ($4x10^5$) were co-transfected with the ATF-2 reporting system and either constitutively active RasV12 or dominant negative RasN17 as described in Section 2.29 and allowed to recover overnight at 37°C. Cells were then treated with either vehicle (1% (v/v) ethanol) or PBOX-6 (10μM) for 48h and luciferase activity was measured and normalised according to β-galactosidase measurements. Results, shown in Fig. 5.22, demonstrate that PBOX-6 induces a 10.6-fold increase in ATF-2 activity over vehicle treated cells confirming that PBOX-6 induces JNK activation in K562 cells. Cells transfected with RasV12 and treated with vehicle show an increase in ATF-2 activity, over vehicle treated cells alone, confirming earlier findings that Ras is capable of activating the JNK signalling pathway. Upon treatment of these cells with PBOX-6 an additive increase in ATF-2 activity is observed. On the other hand, cells transfected with dominant negative RasN17, followed by vehicle treatment shows no effect on ATF-2 activation. Treatment of these cells with PBOX-6 still induced a stimulation of ATF-2 activity. The results observed with RasV12 co-transfections indicate that Ras is capable of activating the JNK signalling pathway, whereas the inability of RasN17 to prevent ATF-2 activity induced by PBOX-6 suggests that activation of Ras does not lie upstream of JNK in the signalling pathway in which PBOX-6 induces apoptosis in K562 cells.

5.2.17 Effect of RacV12 and RacN17 on PBOX-6-induced activation of the ATF-2-dependent reporter gene

The small GTP-binding protein, Rac, has been implicated in the signal transduction pathway upstream of JNK in many systems (Murasawa *et al.*, 2000; Teramoto *et al.*, 1996). Constitutively active (RacV12) and dominant negative (RacN17) mutants were used to

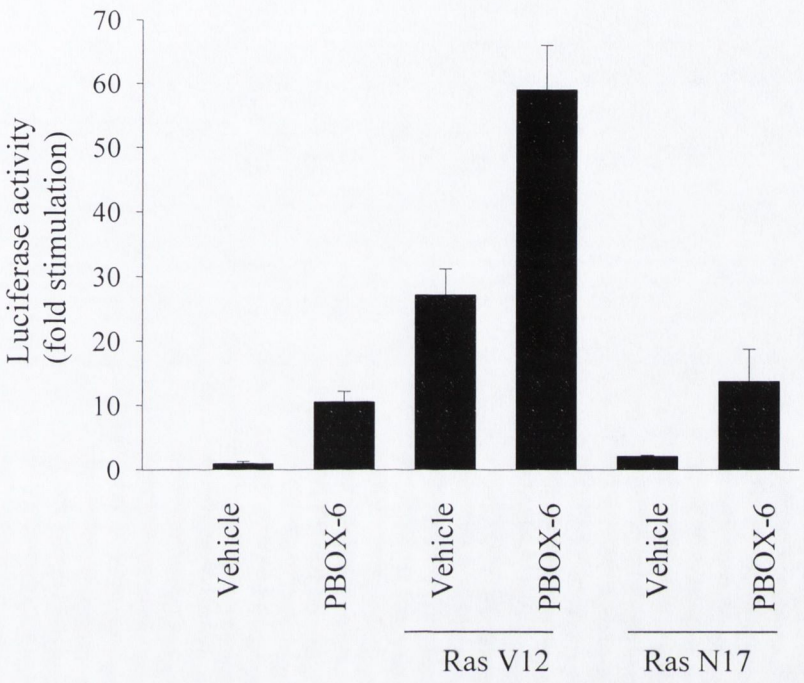

Fig. 5.22 RasN17 does not protect against PBOX-6-induced activation of ATF-2-dependent luciferase reporter gene in K562 cells

K562 cells ($4x10^5$) were co-transfected with the ATF-2-luciferase reporting system (400ng) consisting of a plasmid encoding the ATF-2 activation domain (20ng), a luciferase reporter (100ng), β-galactosidase (80ng), and in some cases, an empty vector (200ng) (column 1-2) or a plasmid encoding RasV12 (200ng) (column 3-4) or RasN17 (200ng) (column 5-6). Following overnight recovery at 37°C, cells were treated with either vehicle (1% (v/v) ethanol) or PBOX-6 (10μM) for a further 48h. ATF-2 activity was determined as a function of luciferase activity. Results are expressed as fold stimulation over vehicle treated cells and represent the mean +/- S.E.M of triplicate determinations performed at least three times.

determine whether Rac is involved in the signal transduction leading to JNK activation during PBOX-6-induced apoptosis.

K562 cells ($4x10^5$) were transfected with the ATF-2 reporting system and either RacV12 or RacN17 as described in Section 2.29. Following overnight recovery at 37°C, cells were then treated with either vehicle (1% (v/v) ethanol) or PBOX-6 (10μM) for 48h and luciferase activity was measured and normalised according to β-galactosidase readings. ATF-2 activity was expressed as fold stimulation over vehicle treated cells. Results shown in Fig. 5.23 demonstrate that PBOX-6 induces a 10.6-fold increase in ATF-2 activity over vehicle treated cells, confirming the activation of JNK by PBOX-6. Transfection of cells with RacV12, which were then treated with vehicle, show an increase in ATF-2 activity over vehicle treated cells alone, confirming earlier findings that Rac is capable of activating the JNK signalling pathway. Upon treatment of these cells with PBOX-6 an additive increase in ATF-2 activity is observed. Transfection of cells with RacN17 followed by treatment with PBOX-6 did not inhibit PBOX-6-induced activation of ATF-2. The ability of RacV12 to activate ATF-2 indicates that it is capable of activating the JNK signalling pathway, whereas the inability of RacN17 to inhibit PBOX-6-induced activation of the ATF-2-dependent reporter gene suggests that activation of Rac does not lie upstream of JNK in the signal transduction pathway in which PBOX-6 induces apoptosis in K562 cells.

5.2.18 Effect of wild type Cdc42 and Cdc42N17 on PBOX-6-induced activation of the ATF-2-dependent reporter gene

In addition to Rac, the small GTP-binding protein, Cdc42 has been implicated upstream of JNK activation in a number of signal transduction pathways (Bagrodia *et al.*, 1995; Teramoto *et al.*, 1996). An involvement of Cdc42 in the signal transduction pathway activated during PBOX-6-induced apoptosis in K562 cells was investigated.

K562 cells ($4x10^5$) were co-transfected with the ATF-2 reporting system and wild type Cdc42 or a dominant negative mutant Cdc42N17 as outlined in Section 2.29. Cells were allowed to recover overnight at 37°C, and treated with vehicle (1% (v/v) ethanol) or PBOX-6 (10μM) for 48h. Cells lysates were prepared for measurement of luciferase activity using a luminometer as outlined in Section 2.30. A portion of lysate was retained and used to measure β-galactosidase activity, which was used to normalise luciferase activity. ATF-2 activity is determined as a function of luciferase activity and expressed as fold stimulation

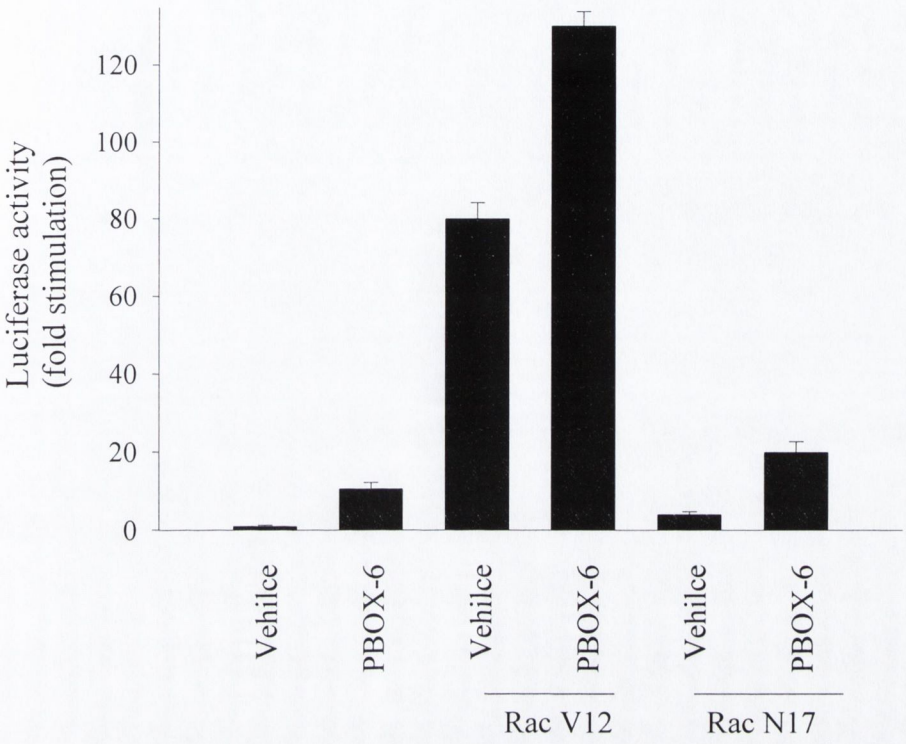

Fig. 5.23 RacN17 does not protect against PBOX-6-induced activation of ATF-2-dependent luciferase reporter gene

K562 cells ($4x10^5$) were co-transfected with the ATF-2-luciferase reporting system (400ng) consisting of a plasmid encoding the ATF-2 activation domain (20ng), a luciferase reporter (100ng), β-galactosidase (80ng), and in some cases, an empty vector (200ng) (column 1-2) or a plasmid encoding RacV12 (200ng) (column 3-4) or RacN17 (200ng) (column 5-6). Following overnight recovery at 37°C, cells were treated with either vehicle (1% (v/v) ethanol) or PBOX-6 (10μM) for a further 48h. ATF-2 activity was determined as a function of luciferase activity. Results are expressed as fold stimulation over vehicle treated cells and represent the mean +/- S.E.M of triplicate determinations performed at least three times.

over vehicle treated cells. Results shown in Fig. 5.24 demonstrate that PBOX-6 stimulates a 6-fold increase in ATF-2 activity when compared to vehicle treated cells. Cells transfected with wild type Cdc42 and treated with vehicle induce an increase in AFT-2 activity over vehicle treated cells alone, demonstrating that Cdc42 is capable of activating the JNK signalling pathway. Upon treatment of these cells with PBOX-6 an additive increase in ATF-2 activity is apparent. On the other hand, cells transfected with dominant negative Cdc42N17 had no effect of ATF-2 activity when treated with vehicle. Treatment of these cells with PBOX-6 still induced a stimulation of ATF-2 activity. Cdc42 is capable of activating the JNK signalling pathway as shown by its ability to increase ATF-2 activity, whereas the inability of Cdc42N17 to protect against ATF-2 activation in response to PBOX-6 suggests that activation of Cdc42 in not involved in the signalling pathway activated by PBOX-6 in K562 cells.

5.2.19 Lethal toxin, which inhibits the activity of Ras and Rac, does not prevent PBOX-6-induced JNK activation in K562 cells

Lethal toxin, which originates from *Clostridium sordellii,* has been shown to glycosylate and inactivate Rac, Ras and Rap (Davis *et al.*, 1999). In the present study, lethal toxin was used to confirm the lack of activation of Rac and Ras in the apoptotic signalling pathway initiated by PBOX-6 in K562 cells.

The phorbol ester, PMA induces activation of the ERK Map kinase pathway via Ras activation, and thus was used as a control to demonstrate the inhibition of Ras activity by lethal toxin. K562 cells were suspended at a density of $1x10^6$ cells in 1ml of growth medium and pretreated with either vehicle (1% (v/v) DMSO) or lethal toxin (500ng/ml) for 3h and then treated with PMA (100nM) for a further 30 min. Similarly, K562 were pretreated with either vehicle (1% (v/v) DMSO) or lethal toxin (500ng/ml) for 3h followed by treatment with PBOX-6 (10μM) for 45 min. Whole cell extracts were prepared as described in Section 2.13 and an equal amount of protein was resolved by SDS-PAGE followed by Western blotting. Levels of ERK activity were measured in PMA treated cells using a phospho-specific ERK antibody (Fig. 5.25A) whereas levels of JNK activity was measured in PBOX-6 treated cells using a phospho-specific JNK antibody (Fig. 5.25B). Results demonstrate that lethal toxin reduces levels of PMA-induced activation of ERK in K562 cells confirming that Ras is involved in activation of ERK MAP kinase pathway. Lethal toxin itself was found to activate

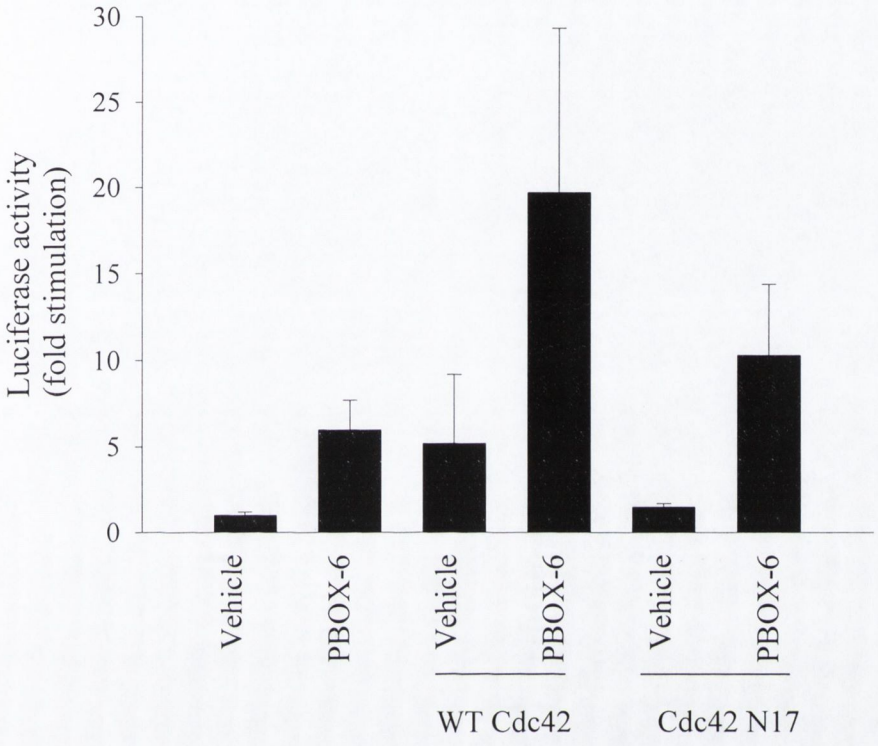

Fig. 5.24 Cdc42N17 does not protect against PBOX-6-induced stimulation of ATF-2-dependent reporter gene activity in K562 cells

K562 cells ($4x10^5$) were co-transfected with the ATF-2-luciferase reporting system (400ng) consisting of a plasmid encoding the ATF-2 activation domain (20ng), a luciferase reporter (100ng), β-galactosidase (80ng), and in some cases, an empty vector (200ng) (column 1-2) or a plasmid encoding wild type (WT) Cdc42 (200ng) (column 3-4) or Cdc42N17 (200ng) (column 5-6). Following overnight recovery at 37°C, cells were treated with either vehicle (1% (v/v) ethanol) or PBOX-6 (10μM) for a further 48h. ATF-2 activity was determined as a function of luciferase activity. Results are expressed as fold stimulation over vehicle treated cells and represent the mean +/- S.E.M of triplicate determinations performed at least three times.

Fig. 5.25 Lethal toxin does not prevent JNK activation or apoptosis induced by PBOX-6 in K562 cells

K562 cells were suspended at a density of $1x10^6$ cells in 1ml of growth medium and treated with (A) vehicle (1% (v/v) PBS, 0.1% DMSO), lethal toxin (LT) (500ng/ml) for 3h, PMA (100nM) for 30 min or pretreated with lethal toxin (500ng/ml) for 3h prior to treatment with PMA for a further 30 min or (B) vehicle (1% (v/v) PBS, 1% (v/v) ethanol), lethal toxin (500ng/ml) for 3h, PBOX-6 (10μM) for 45 min or pretreated with lethal toxin (500ng/ml) for 3h prior to PBOX-6 (10μM) for a further 45 min. Whole cell extracts were prepared as described in Section 2.13 and an equal amount of protein (30μg) was resolved by SDS-PAGE followed by Western blotting. Membranes were incubated with (A) phospho-specific ERK antibody or (B) phospho-specific JNK antibody, which was stripped and re-probed with JNK as a loading control. In (C), K562 cells ($3x10^5$/ml) were treated with vehicle (1% (v/v) ethanol), lethal toxin (500ng/ml) for 1h, PBOX-6 (10μM) for 16h or pretreated with lethal toxin (500ng/ml) for 1h prior to PBOX-6 (10μM) for a further 16h and the extent of apoptosis was determined by RapiDiff staining as described in Section 2.4. Values represent the mean +/- the range of two separate experiments.

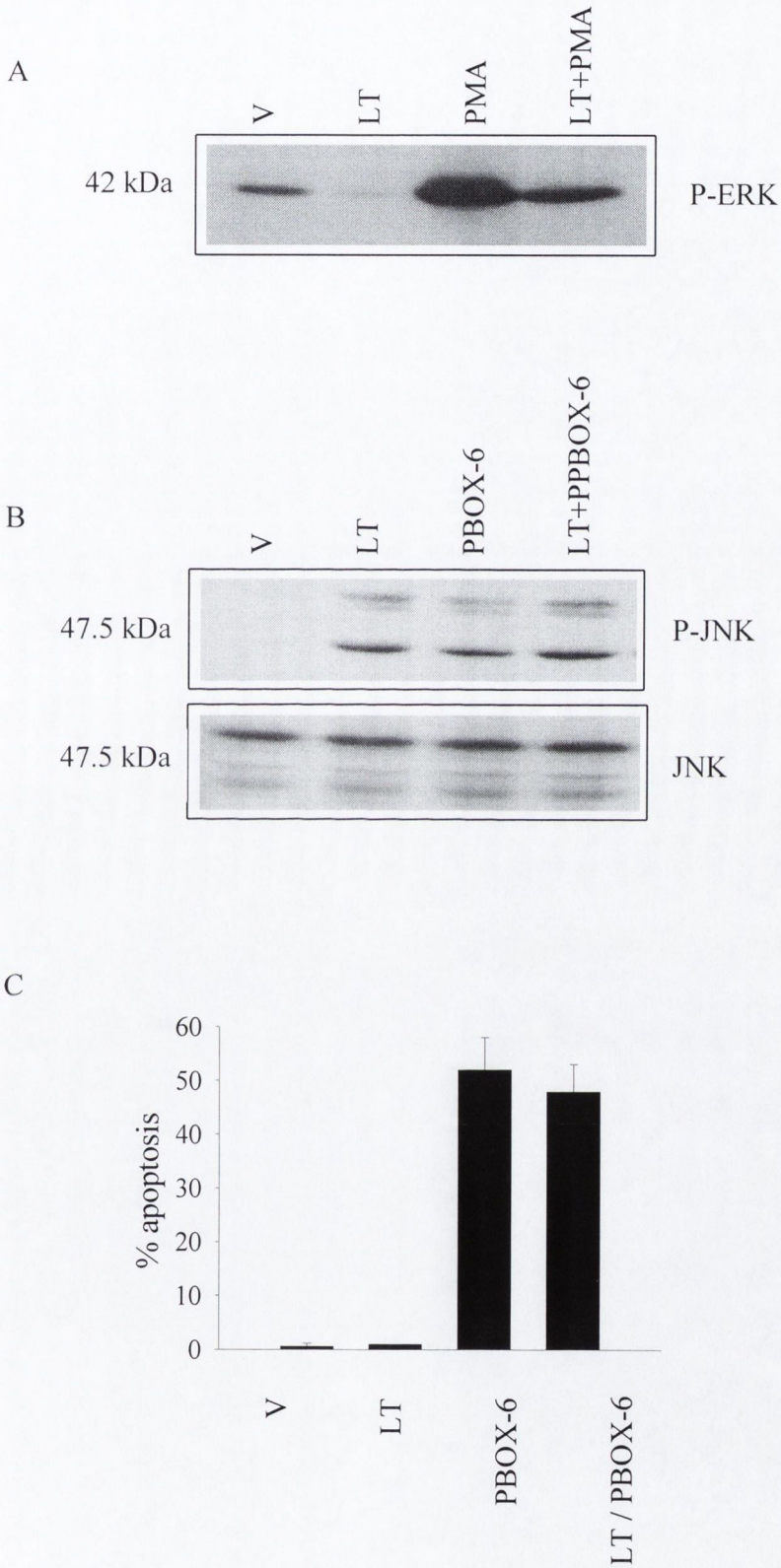
A
V
LT
PMA
LT+PMA
42 kDa
P-ERK
B
V
LT
PBOX-6
LT+PPBOX-6
47.5 kDa
P-JNK
47.5 kDa
JNK
C
% apoptosis
60
50
40
30
20
10
0
V
LT
PBOX-6
LT / PBOX-6

JNK in K562 cells suggesting that at the concentrations used it might induce cellular stress in these cells. However, pretreatment of cells with lethal toxin has no effect on PBOX-6-induced activation of JNK. As a loading control, blots were stripped and re-probed with a JNK antibody, which recognises total JNK. In addition, the effect of lethal toxin on the extent of apoptosis induced by PBOX-6 was examined. Cells were pretreated with either vehicle or lethal toxin (500ng/ml) for 1 hr, following by treatment with PBOX-6 (10μM) for 16h. An aliquot of cells (150μl) was centrifuged onto a glass slide and stained using the RapiDiff kit as described in Section 2.4. The extent of apoptosis was determined by morphological examination of cells. Results shown in Fig. 5.25C demonstrate that lethal toxin itself does not induce apoptosis in these cells and it does not protect against PBOX-6 induced apoptosis. These results correlate with data obtained from using dominant negative mutants and Western blotting, and suggest that Rac and Ras are not involved in the signalling pathway initiated by PBOX-6 in K562 cells.

5.3 Discussion

Three mitogen-activated protein (MAP) kinase cascades constitute one of the major mechanisms of relaying extracellular signals triggered by a variety of stimuli. The ERK MAP kinase pathway is preferentially activated by mitogens whereas the p38 and JNK MAP kinase pathways are primarily activated by cellular stresses and inflammatory cytokines (Kyriakis and Avruch, 1996). These signalling cascades have important roles in the regulation of cell growth, differentiation, cell survival, apoptosis and stress and inflammatory responses (Chan-Hui and Weaver, 1998). Pathologically, failure of an apoptosis programme often leads to an imbalance in cell number and some of these abnormalities may lead to tumourigenesis. Based on this concept, control of apoptosis has emerged as an important strategy for clinical cancer therapy (Seimiya *et al.*, 1997).

Although the three MAP kinase pathways share structural similarity, the outcome of activation is quite different. ERK stimulation by mitogenic and trophic agents results in cell division and differentiation whereas growth arrest and cell death results as an outcome of p38 and JNK activation (Zanke *et al.*, 1996). The function of signal transduction pathways is complicated because a combination of signalling pathways probably contributes to any given response (Minden and Karin, 1997). For example, it has been shown that activation of the JNK and p38 Map kinase pathways and concurrent inhibition of the ERK pathway are critical for nerve growth factor (NGF) withdrawal-induced apoptosis in rat PC12 pheochromocytoma cells (Xia *et al.*, 1995). Furthermore, the same signalling pathway can often have different functions depending on the cell context. However, as JNK is activated by a variety of cellular stresses, it has been proposed to serve as a major apoptosis switch. Activation of the JNK signalling pathway has been shown to result in apoptosis in response to a variety of treatments including *cis*-platinum and heat shock (Zanke *et al.*, 1996), DNA damaging agents such as anisomycin and UV irradiation (Shaulian and Karin, 1999), chemotherapeutic agents such as etoposide and camptothecin (Seimiya *et al.,* 1997), and vinblastine and adriamycin (Osborn and Chambers, 1996). The findings that mechanistically distinct cytotoxic drugs activate the JNK pathway supports the concept that JNK plays an important role in the cell death pathways induced by these agents. In contrast, JNK activation leading to suppression of apoptosis has also been reported. For example, activation of the JNK signalling pathway in FL5.12 lymphocytic cells by insulin-like growth factor (IGF) has been shown to result in suppression of apoptosis (Krause *et al.*, 2001). Furthermore, it has been reported that

inhibition of the ERK MAP kinase pathway, and not the activation of JNK and p38 pathways, is primarily required for herbimycin A-induced apoptosis in K562 cells (Kang *et al.*, 2000).

Production of the Bcr-Abl oncoprotein is the underlying genetic defect found in CML and is responsible for the anti-apoptotic properties of CML cells (Laurent *et al.*, 2001). Bcr-Abl can phosphorylate directly or indirectly a large number of substrates and thereby activate many signal transduction pathways including Ras, ERK, JNK, PI-3 kinase and JAK/STAT pathways (Deininger *et al.*, 2000). These are likely to be important in determining the transformation or the apoptosis-resistant phenotype of CML. However, the precise signalling events that elicit the anti-apoptotic effects of Bcr-Abl remain unclear (Kang *et al.*, 2000). In the present study, a representative pyrrolo-1,5-benzoxazepine compound, PBOX-6, has been found to potently induce apoptosis in the chemotherapy-resistant CML cell line, K562. PBOX-6-induced apoptosis in K562 cells was accompanied by the transient and rapid activation of two JNK isoforms, JNK1 and JNK2. Activation of the ERK and p38 MAP kinase pathways was not detected in response to PBOX-6 treatment. These results correlate with the many reports supporting a role of JNK as the major apoptotic switch in a variety of cells in response to treatment with various cytotoxic agents.

Activated JNK translocates to the nucleus and forms a complex with c-Jun and ATF-2 transcription factors, stimulating their transcriptional activity (Minden and Karin, 1997). In the present study, PBOX-6 treatment of K562 cells was found to result in a dose-and time-dependent phosphorylation of the downstream JNK substrates, c-Jun and ATF-2, which correlates with the appearance of the morphological features of apoptosis in these cells. These results are in agreement with many reports, which have shown that signals leading to activation of the JNK MAP kinase pathway also stimulate c-Jun phosphorylation (Osborn and Chambers; 1996; Sanchez *et al.*, 1994; Seimiya *et al.*, 1997) and ATF-2 phosphorylation (Fuchs *et al.,* 2000; Gupta *et al.*, 1995). For example, treatment of KB-3 cells with adriamycin or vinblastine resulted in JNK activation followed by c-Jun phosphorylation (Osborn and Chambers, 1996).

The importance of JNK in the signalling pathway leading to PBOX-6-induced apoptosis in K562 cells was confirmed using a number of JNK signalling inhibitors. Treatment of cells with CEP-1347, a known inhibitor of JNK (Maroney *et al.,* 1998) was found to prevent activation of JNK and its downstream substrates, c-Jun and ATF-2 and also

to inhibit the induction of apoptosis. In addition, the quinone reductase inhibitor, dicumarol, is an alternative inhibitor of the JNK signalling pathway (Cross *et al.*, 1999; Krause *et al.*, 2001) and has been shown to prevent phosphorylation of c-Jun and ATF-2 and apoptosis induced in response to PBOX-6 treatment of K562 cells. These results suggest that activation of JNK, and not ERK or p38 MAP kinases, is an essential step in the apoptotic pathway leading to apoptosis in K562 cells following treatment with PBOX-6.

In the previous chapter it was found that manumycin A induced apoptosis in K562 cells. In this chapter Western blot analysis revealed that, like PBOX-6, manumycin A induces the transient activation of two JNK isoforms in K562 cells. However, in contrast to results obtained with PBOX-6, pretreatment of K562 cells with CEP-1347 prevented JNK activation but failed to prevent the apoptosis induced by manumycin A, suggesting that although JNK activation was detected in response to manumycin A, it is not an essential step in the pathway in which this compound induces apoptosis in K562 cells. This would suggest that the mechanism by which these two compounds induce apoptosis in K562 cells is not the same. It was also reported in the previous chapter that treatment of K562 cells with the topoisomerase II poisons, etoposide and mitoxanthrone, completely prevented PBOX-6-induced apoptosis, whereas pretreatment with the catalytic inhibitor of topoisomerase II, ICRF-187, reduced the extent of apoptosis induced by PBOX-6. From this work it was concluded that although PBOX-6 does not function in a manner similar to these Topo II inhibitors, it requires active Topo II at some step in the apoptotic pathway. It has been found in the current chapter that activation of the JNK MAP kinase is an essential step in the apoptotic pathway leading to apoptosis in K562 cells following PBOX-6 treatment. In order to determine whether a potential involvement of Topo II during PBOX-6-induced apoptosis occurs upstream or downstream of JNK activation, cells were pretreated with the Topo II inhibitors and the effect on JNK activation was assessed. It was found that pretreatment of K562 cells with etoposide or ICRF-187 did not block PBOX-6-induced phosphorylation of JNK. These results suggest that any involvement of Topo II in the apoptotic pathway induced by PBOX-6 in K562 cells occurs downstream of JNK activation and that inhibition of PBOX-6-induced apoptosis by etoposide and ICRF-187 occurs at a point downstream of JNK activation in the apoptotic pathway.

In addition to phosphorylation and activation of the nuclear transcription factors, c-Jun and ATF-2, the JNK MAP kinase can phosphorylate non-nuclear targets such as

members of the Bcl-2 family. The Bcl-2 family consists of pro-and anti-apoptotic family members, which play an important role in the regulation of apoptosis (Cory and Adams, 1998). Overexpression of Bcl-2 and Bcl-$_{XL}$ is responsible for the anti-apoptotic properties of many cells. The mechanism in which Bcl-2 proteins protect cells from apoptosis remains largely unknown. It has been proposed that Bcl-2 inhibits mitochondrial release of cytochrome c but it has also been suggested that Bcl-2 acts by sequestering and inhibiting caspases via interaction with Apaf-1 (Fadeel *et al.,* 1999). Although the precise signalling events that elicit the anti-apoptotic effects of Bcr-Abl in CML cells remain unclear it seems that activation of individual pathways depends on the cell type (Amarante-Mendes *et al.*, 1998a; Deininger *et al.*, 2000). For example, previous observations have suggested that Bcr-Abl acts through expression of Bcl-2 (Sanchez Garcia and Grutz, 1995). These authors reported that down-regulation of Bcl-2 using antisense oligonucleotides reverted the Bcr-Abl-mediated IL-3 independent phenotype in BaF3 cells. In contrast, it has been found that STAT5 is constitutively activated in CML cells and activation of STAT5 correlates directly with the ability of Bcr-Abl to confer cytokine independent growth (Sillaber *et al.*, 2000; Shuai *et al.*, 1996). The anti-apoptotic Bcl-2 family member Bcl-$_{XL}$ is one of the few known STAT regulated genes. It has been shown that Bcr-Abl-induced STAT5 activity contributes to an increased expression of Bcl-$_{XL}$, which may be responsible for the enhanced viability of these cells (Gesbert and Griffin, 2000). Furthermore, it has recently been reported that the tyrosine kinase inhibitor, STI571, induces apoptosis in Bcr-Abl positive cells by down-regulating expression of Bcl-$_{XL}$ (Oetzel *et al.*, 2000) providing further evidence to support a role of Bcl-$_{XL}$ in the resistant properties of CML cells. These opposing reports outline that in different cell lines it is possible that Bcr-Abl would require the participation of either Bcl-2 or Bcl-$_{XL}$.

Several workers report the phosphorylation and inactivation of Bcl-2 in response to various chemotherapeutic agents, thus promoting apoptosis (Fan *et al.*, 2000; Haldar *et al.,* 1996). It is believed that phosphorylation of Bcl-2 family members results in an inability of the protein to heterodimerise with opposing family members, resulting in inactivation (Tsujimoto, 1998). For instance, Bcl-2 is phosphorylated and inactivated in lymphoid cells in response to the phosphatase inhibitor, okadaic acid, or the chemotherapeutic drug, taxol (Haldar *et al.*, 1995). In addition, Bcl-2 is phosphorylated by the ASK-MKK7-JNK MAP kinase pathway in Jurkat cells following paclitaxel treatment (Yamamoto *et al.*, 1999). This

is in contrast to evidence against a role for JNK in Bcl-2 phosphorylation by transient expression of dominant-negative mutants of ASK1, SEK1 and JNK1, which failed to prevent paclitaxel-induced Bcl-2 phosphorylation (Wang *et al.*, 1999). These results suggest that very specific three-kinase modules may be involved in Bcl-2 phosphorylation and only specific dominant negative combinations are inhibitory. Bcl-2 and Bcl-$_{XL}$ are phosphorylated and inactivated following vinblastine-induced JNK activation in KB-3 cells and antisense oligonucleotides directed against JNK1 and JNK2 significantly inhibited Bcl-2 and Bcl-$_{XL}$ phosphorylation (Fan *et al.*, 2000). In agreement with Fan *et al.* (2000) it has been shown in the present study that Bcl-2 and Bcl-$_{XL}$ are phosphorylated and presumably inactivated in K562 cells during PBOX-6-induced apoptosis. Phosphorylation of Bcl-2 and Bcl-$_{XL}$, which is characterised by the presence of an immunoreactive band of slower mobility, occurred in a time and dose-dependent manner. Phosphorylation of Bcl-2 was more apparent and occurred slightly earlier than the phosphorylation of Bcl-$_{XL}$. Phosphorylation of Bcl-2 and Bcl-$_{XL}$ in K562 cells in response to PBOX-6 was blocked by inhibitors of the JNK signalling pathway, suggesting that phosphorylation occurs as a direct result of JNK activation. These results differ to that reported with STI571-induced apoptosis in Bcr-Abl-positive cells (Oetzel *et al.*, 2000), where down-regulation of Bcl-$_{XL}$ expression was reported rather than phosphorylation of Bcl-$_{XL}$. Both a down-regulation in Bcl-$_{XL}$ expression and phosphorylation of Bcl-$_{XL}$ result in decreased activity of this protein and strongly implicate a role of Bcl-2 family members in the anti-apoptotic properties of Bcr-Abl expressing cells. However, it has also been reported that overexpression of Bcl-$_{XS}$ in K562 cells, which is reportedly antagonistic to the anti-apoptotic effect of Bcl-2 and Bcl-$_{XL}$, only partially reverts the resistance to apoptosis induced by chemotherapeutic drugs, suggesting that other signals probably contribute to the Bcr-Abl-mediated anti-apoptotic phenotype (Ray *et al.*, 1996).

In addition to phosphorylation of Bcl-2 family members, additional modifications include proteolytic cleavage and dimerisation and often result in subcellular translocation. The ability of Bcl-2 family proteins to form heterodimers with opposing family members is considered to inhibit the biological activity of their partners (Tsujimoto, 1998; Yang *et al.*, 1995). For example, Bcl-2 is thought to protect cells from apoptosis by dimerising with Bax. Phosphorylation of Bcl-2 in PC3 prostate cancer cells following treatment with taxol leads to a 50% reduction in Bcl-2/Bax heterodimers, thus driving cells towards apoptosis (Haldar *et al.*, 1996). Enforced dimerisation of Bax is reported to result in translocation from the

cytosol, mitochondrial membrane insertion and homodimerisation resulting in cell death without cytochrome c release, which can be protected by the presence of Bcl-2 but not Bcl-$_{XL}$ (Gross *et al.*, 1998). These workers suggest a model in which cytosolic Bax represents an inactive monomer, perhaps tethered by a chaperone protein. A death stimulus induces a conformational change in Bax releasing it from the cytosolic chaperone and allowing mitochondrial membrane insertion. Furthermore, Nomura *et al.*, (1999) reported similar findings and suggested that Bcl-2 exerts its anti-apoptotic activity by inhibiting the translocation of Bax by modification of the cytoplasmic protein involved in Bax translocation. In the present study, translocation of Bax from the cytosol to the mitochondria was investigated. In agreement with other reports Bax was found to reside in both the cytosolic and mitochondrial fraction of viable cells (Gross *et al.*, 1998). However, levels of Bax in the two subcellular fractions remained unchanged following induction of apoptosis by PBOX-6 treatment. In a manner similar to Fadeel *et al.* (1999) and others, the purity of the various fractions was confirmed by measuring the activity of a cytoplasmic enzyme, lactate dehydrogenase (LDH), as a cytosolic marker. The majority of LDH activity was detected in the cytosolic fraction, whereas very low levels were detected in the mitochondrial fraction. In addition, Western blotting was carried out to determine the levels of cross contamination of cytoplasmic fractions with mitochondrial fragments. Bcl-2 was detected in the mitochondrial fraction in its phosphorylated form following PBOX-6 treatment, which is consistent with earlier results, but was absent from the cytosolic fraction.

The present study therefore demonstrates the phosphorylation of Bcl-2 and Bcl-$_{XL}$ in K562 cells in response to PBOX-6, which occurs downstream of JNK activation in the apoptotic pathway. These results implicate Bcl-2 family members in producing the anti-apoptotic properties of Bcr-Abl positive K562 cells. However, the anti-apoptotic activity of Bcl-2 is not exerted through inhibition of Bax translocation. Although a large number of reports suggest that heterodimerisation of opposing Bcl-2 family members regulates their activity, many additional reports suggest that they are capable of regulating apoptotic function independently of each other (Tsujimoto and Shimizu, 2000).

So far, in the present chapter it has been shown that early activation of the JNK MAP kinase is an essential step in the apoptotic pathway in which PBOX-6 induces cell death in K562 cells. It has also been shown by Western blotting that a number of downstream substrates of JNK are activated in response to PBOX-6 treatment. K562 cells were

transfected with a c-Jun or ATF-2 luciferase reporting system followed by treatment with PBOX-6 and luciferase activity was measured. Results have shown that PBOX-6 induces a 3.6- and 6.8-fold increase in c-Jun and ATF-2 luciferase activity, respectively. These results correlate with that reported earlier using Western blot analysis, which demonstrate activation of the downstream JNK substrates during PBOX-6-induced apoptosis in K562 cells. Although ATF-2 is also known to act as a downstream substrate of p38 (Ono and Han, 2000), in the present study it has been shown that p38 is not activated in K562 cells following PBOX-6 treatment.

ATF-2 has also been reported to interact with NFκB (Du *et al.*, 1993). NFκB is activated in response to several pro-apoptotic stimuli, including cytotoxic drugs, ionising radiation, oxidative stress and TNFα (Bours *et al.*, 2000). In response to these stimuli, NFκB translocates to the nucleus and induces the expression of numerous target genes. However, the role of NFκB in the control of pro- and anti-apoptotic pathways in normal and cancer cells has revealed many contradictory reports, suggesting that NFκB can both induce and protect against cell death (Aggarwal, 2000; Bours *et al.*, 2000). In the present study, K562 cells were transfected with an NFκB-luciferase reporter gene followed by treatment with IL-1 or PBOX-6. It was found that PBOX-6 activated NFκB to the same extent as IL-1. An increase in NFκB DNA binding was visible after a 1-hour treatment with PBOX-6, and this appearance of NFκB activation correlates with the appearance of the morphological features of apoptosis. This is in contrast to reports, which suggest that NFκB activation in response to apoptotic stimuli occurs within minutes and precedes apoptosis (Aggarwal, 2000). The role of NFκB in apoptosis is quite complex and in many instances is determined by the experimental conditions, including cell type and the apoptotic inducer. For instance TNFα induces NFκB activation in most cell types, but not all cell types undergo apoptosis. Thus is seems that NFκB activation alone is not sufficient to induce cell survival or apoptosis (Aggarwal, 2000).

In the present study, the use of several inhibitors of the JNK signalling pathway have demonstrated an essential role for JNK activation in the apoptotic pathway in which PBOX-6 induces apoptosis in K562 cells. In order to confirm these results and to elucidate components of the signalling pathway upstream of JNK, K562 cells were transiently transfected with the JNK scaffold protein, JIP-1, followed by PBOX-6 treatment. JIP-1,

which is located in the cytoplasm, creates a functional signalling module by interaction of components of the JNK signalling pathway with other proteins. For example, it has been shown that JIP-1 specifically binds JNK, MKK7 and the mixed-lineage protein kinase (MLK) group of MAPKKKs (Yasuda *et al.*, 1999). This selectivity indicates that JIP scaffold complexes represent only one pathway leading to JNK activation. Signals mediated by MEKK protein kinases and MKK4 function independently of the JIP scaffold complexes (Yasuda *et al.*, 1999). Overexpression of the JIP-1 scaffold protein acts as a potent inhibitor of the downstream JNK signalling pathway. This inhibition is due to cytoplasmic retention of JNK and may also reflect the sequestration of limiting JNK pathway components (Dickens *et al.*, 1997; Whitmarsh *et al.*, 1998; Yasuda *et al.*, 1999). In the present study, K562 cells were co-transfected with JIP-1 and the ATF-2-dependent luciferase reporting system, followed by treatment with PBOX-6. Results revealed that while PBOX-6 caused stimulation in ATF-2-luciferase activity, co-transfection of JIP-1 completely abolished PBOX-6-induced stimulation of ATF-2. These results are consistent with that reported by Dickens *et al.* (1997) where co-transfection of JIP-1 into CHO cells was found to inhibit the transcriptional activity of ATF-2. Transfection of JIP-1 was also found to significantly reduce PBOX-6-induced apoptosis in K562 cells, as determined by morphological examination. These results present further evidence for an essential role of JNK activity in the apoptotic pathway induced by PBOX-6 in K562 cells and confirm the earlier findings from Western blot analysis using the JNK signalling inhibitors, CEP-1347 and dicumarol. Furthermore, the selectivity of the JIP-1 scaffold protein for the MLK-MKK7-JNK pathway suggests that this may be the signalling cascade utilised by PBOX-6 in the mechanism in which it induces apoptosis in K562 cells. The mixed-lineage kinase (MLK) family consists of five members, MLK-1, -2 and -3, DLK and LZK. With the exception of MLK-1, all family members function as MAPKKKs and predominantly activate the JNK signalling pathway. The JIP-1 scaffold protein has been shown to interact specifically with MLK-2, MLK-3 and DLK all of which are capable of activating the MKK7-JNK pathway (Leung and Lassam, 2001). A summary of MAP kinase signalling cascades is outlined in Fig. 1.6.

A number of proteins exist upstream, that interact with the MLKs and have been shown to regulate activation of the JNK signalling cascade. These include the GTP-binding proteins Rac and Cdc42 and a subgroup of Ste20-related kinases known as germinal centre kinases (GCKs). Some members of the MLK family interact with Rac and Cdc42 through a

binding domain known as Cdc42/Rac interactive binding (CRIB) domain. This domain is similar to that found in a subgroup of the Ste20-related kinases known as PAKs, which are downstream effectors of Rac and Cdc42 in the JNK signalling pathway (Knaus and Bokoch, 1998). Interaction of Rac and Cdc42 with MLKs results in homodimerisation and autophosphorylation (Leung and Lassam, 2001). For example, overexpression of MLK-3 in COS-7 cells was sufficient to activate the JNK signalling pathway (Teramoto *et al.*, 1996). These authors showed that MLK-3 associated with activated Rac and Cdc42 and activated the MEKK-SEK pathway leading to JNK activation. In addition, GTPases including Ras, Rac and Cdc42 have been shown to activate the JNK signalling pathway in response to a variety of stimuli. For instance, Cdc42 and PAKs have been shown to mediate JNK activation in IL-1 treated COS-1 cells (Bagrodia *et al.*, 1995). In addition, angiotensin-mediated activation of JNK in cardiac fibroblast cells was blocked by dominant negative mutants of Rac and MEKK1 (Murasawa *et al.*, 2000). The GTPase Ras, although primarily involved in activation of the ERK MAP kinase pathway, has also been shown to activate the JNK pathway in response to epidermal growth factor (EGF) and nerve growth factor (NGF) (Minden *et al.*, 1994). Therefore, the presence of the small GTPases Ras, Rac and Cdc42 as regulatory proteins acting upstream of JNK in the PBOX-6-induced signalling cascade was examined. Co-transfection of dominant negative mutants of Ras, Rac or Cdc42, and the ATF-2-dependent luciferase reporter gene into K562 cells, failed to prevent PBOX-6-induced activation of the ATF-2-dependent luciferase activity. These results suggest that these GTPases are not involved in the upstream signalling pathway leading to JNK activation. Furthermore, co-transfection of constitutively active forms of Ras and Rac into K562 cells without any treatment was capable of stimulating ATF-2-dependent luciferase activity, and treatment with PBOX-6 resulted in an increase in this effect. The synergy between constitutively active forms of Ras/Rac and PBOX-6 strongly suggests that the GTPase and PBOX-6 activated JNK via independent signalling pathways. These results are in agreement with many reports, which suggest that alternative GTPase-independent mechanisms exist, that lead to JNK activation. For example, dominant negative mutants of Rac and Cdc42 had no effect on anisomycin-induced JNK activation in COS-7 cells (Coso *et al.*, 1995). In addition, activation of JNK by IL-1 seems to be dependent on Rac/Cdc42 in some cases, for example in COS-1 cells (Bagrodia *et al.*, 1995) but not in others, as shown by the lack of effect of dominant negative mutants of Rac and Cdc42 on IL-1 and PDGF induced JNK

activation in PAE cells (Davis *et al.*, 1999). Furthermore, Minden *et al.* (1994) reported that the activation of JNK by EGF or NGF was dependent on Ras activation, whereas JNK activation by TNFα was Ras-independent in PC12 cells. These discrepancies may be explained by the possibility that the GTPases may only modulate JNK activity in certain cell types and under certain conditions (Kjoller and Hall, 1999).

The use of bacterial toxins, which glycosylate and inhibit the activity of certain GTPases, are often used to confirm data obtained using reporter gene assays. For example, the lack of effect of dominant negative mutants of Rac and Cdc42 on IL-1 and PDGF induced JNK activation in PAE cells was confirmed by the lack of effect observed when cells were treated with bacterial toxins (Davis *et al.*, 1999). In the present study, pretreatment of K562 cells with lethal toxin, which inhibits activity of Ras and Rac, prior to treatment with PBOX-6 had no effect on PBOX-6-induced activation of JNK, whereas it was shown to prevent PMA-induced activation of the ERK MAP kinase. In contrast, the toxin itself induced activation of JNK, which complicates interpretation of the data, but suggests that at the concentrations used the toxin may induce stress in the cells. However, treatment of K562 cells with lethal toxin at similar concentrations did not induce apoptosis, nor did it prevent PBOX-6-induced apoptosis as determined by morphological examination. The lack of any observable inhibition of PBOX-6-induced JNK activity or inhibition of apoptosis following pretreatment of K562 with lethal toxin presents further evidence to suggest that apoptosis occurs independently of Ras and Rac in these cells.

As outlined earlier, in addition to GTPases, MLKs are activated by a subgroup of the Ste20-related kinases known as GCKs. This group of kinases, which consists of several family members, is thought to activate MLKs and MEKKs through direct recruitment of the MAPKKKs (Yuasa *et al.*, 1998). They do not activate the ERK or p38 MAP kinase pathways (Pombo *et al.*, 1995) and are involved in TNFα- and UV-induced JNK activation (Yao *et al.*, 1999). Although little is known about the upstream regulation of GCKs, they lack a Cdc42 and Rac binding domain (Su *et al.*, 1997). This suggests that MLKs can be regulated by GCKs in a GTPase-independent manner, which is consistent with reports that the MLK family member, DLK, lacks a Cdc42/Rac binding domain (Teramoto *et al.*, 1996). Therefore GCKs, which are located upstream of JNK and are not under the control of small GTPases, may participate in the apoptotic pathway induced by PBOX-6 in K562 cells. A recent publication by Maroney *et al.* (2001) outlines the cellular target of CEP-1347, the selective

and potent inhibitor of JNK activity. CEP-1347 inhibits the kinase activity of all MLK family members and JNK activation driven by overexpression of members of the GCK family. The MLKs are shown to function downstream of the GCKs in the pathway leading to JNK activation. CEP-1347 appears to selectively target the MLKs as it has no inhibitory effect on JNK activation as a result of over-expressing members of the MEKK, Raf, or MKK families. In the present study, it has been shown that in K562 cells, PBOX-6-induced JNK activation and apoptosis is inhibited by CEP-1347 and by the JNK scaffold protein, JIP-1. The selectivity of CEP-1347 for members of the MLK and GCK families together with the selectivity of JIP-1 for the MLK/MKK7/JNK pathway, strongly suggests that MLKs represent the tier of MAPKKKs upstream of JNK in the apoptotic pathway induced by PBOX-6. Furthermore, a GCK family member, HPK1, has also been shown to associate with JIP-1 (Whitmarsh *et al.,* 1998). Together, these reports lend further support to the idea that PBOX-6-induced activation of the JNK MAP kinase is regulated upstream by members of the GCK family. Further work is required to investigate this hypothesis.

In summary, an attempt to delineate the biochemical pathway activated during PBOX-6-induced apoptosis in K562 cells has revealed that activation of the JNK MAP kinase is an early and essential step in the apoptotic pathway. A number of downstream substrates of JNK became activated in response to PBOX-6, including the nuclear transcription factors c-Jun, ATF-2 and NFκB. In addition, inactivation of some members of the Bcl-2 family with concurrent apoptosis in K562 cells suggests that they may participate in the Bcr-Abl-mediated anti-apoptotic pathway responsible for the resistant properties of CML cells. PBOX-6-mediated activation of JNK occurs independently of GTPases, and recent data outlining the selectivity of the JNK signalling inhibitors CEP-1347 and JIP-1 for members of the GCK and MLK kinase families strongly support a role of these kinases in the upstream pathway leading to JNK activation and apoptosis in K562 cells in response to this novel compound. Fig. 5.26 represents a proposed pathway of PBOX-6-induced apoptosis in K562 cells.

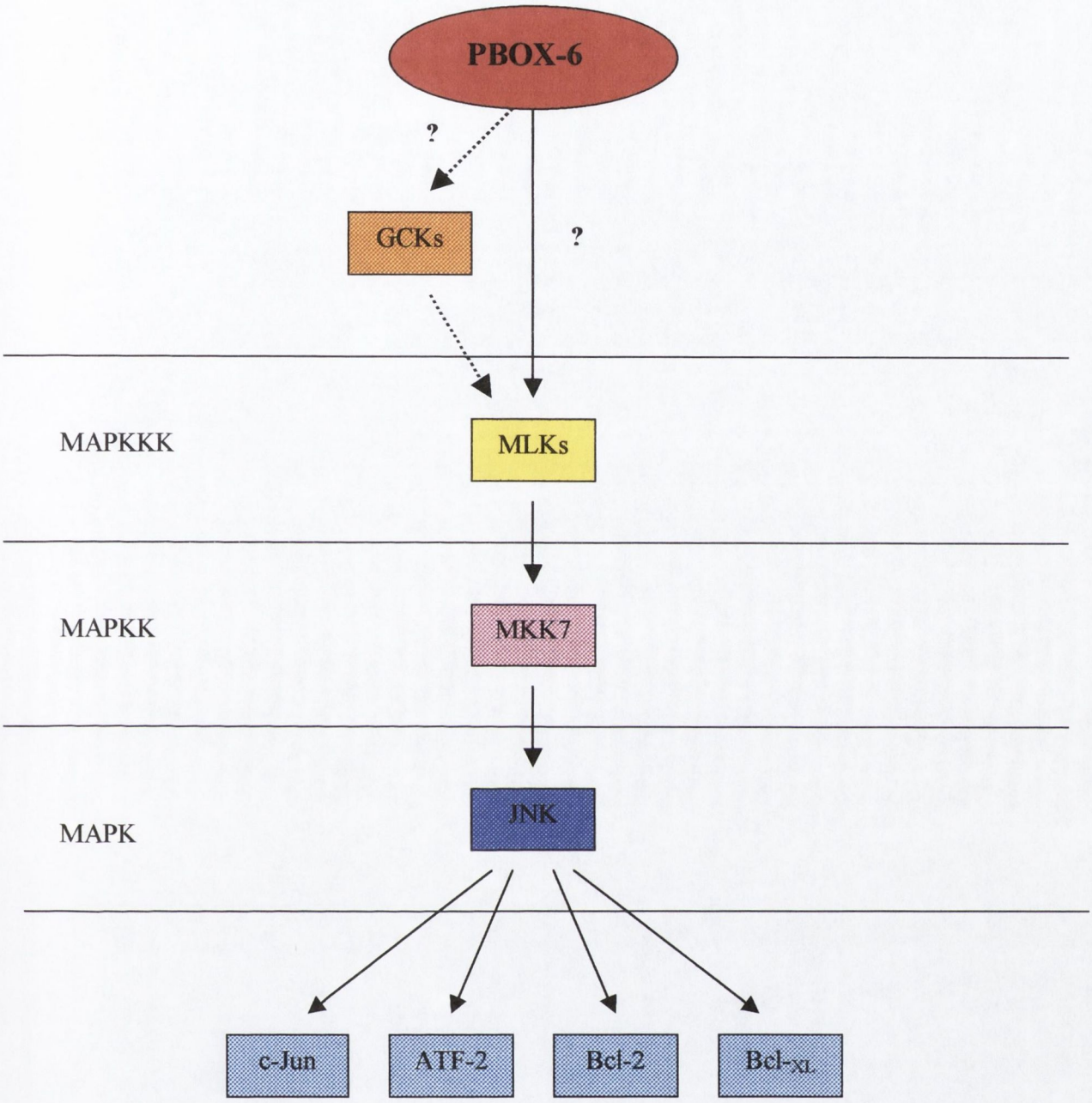

Fig. 5.26 Schematic representation of the proposed pathway of PBOX-6-induced apoptosis in K562 cells

Chapter 6
Concluding Remarks

Although CML is probably the most extensively studied human malignancy, it is not currently curable by conventional chemotherapy. To date, the only known curative therapy for CML is an allogenic bone marrow transplant in the chronic phase. As this option is not available to the majority of patients, due to lack of a suitable donor and to age restrictions (Deininger *et al.*, 2000), the search for novel drugs with reduced toxicity and increased specificity over conventional therapies is of utmost importance. This study has concentrated on determining the therapeutic potential of a novel series of pyrrolo-1,5-benzoxazepine compounds in the treatment of CML. The first part of the study focused on determining the ability of members from this series of pyrrolo,1,5-benzoxazepines to induce apoptotic cell death in CML cells.

It has been found that some members of this series of pyrrolo-1,5-benzoxazepines potently induce apoptosis in the extremely resistant K562 cell line. A representative compound, PBOX-6, has been found to induce apoptosis with similar potencies in K562, KYO.1 and LAMA 84 cells, which represent different stages in the progression of CML. The ability of PBOX-6 to potently induce apoptosis in a number of CML cells suggests its potential as a novel agent in the therapy of CML. The induction of apoptosis in CML cells by PBOX-6 is accompanied by many the morphological features typical of apoptotic cell death, including chromatin condensation, DNA fragmentation and Parp cleavage. However, apoptosis is independent of mitochondrial events such as cytochrome c release and oxidative stress, and the activity of caspases is dispensable for apoptosis induced by PBOX-6 in K562 cells. Apoptosis-inducing factor (AIF), which is released from the mitochondria during apoptosis, has been shown to be involved in many caspase-independent pathways (Zamzami and Kroemer, 1999). Any involvement of AIF during PBOX-6-induced apoptosis remains to be determined by Western blot analysis. The induction of apoptosis by PBOX-6 in K562 cells was accompanied by an increase in the tyrosine phosphorylation status of two, as yet, unidentified proteins. The phosphorylation of these proteins did not become apparent until 16 hours following treatment with PBOX-6, suggesting that this event is not involved in the upstream apoptotic pathway triggered by PBOX-6, but rather accompanies apoptosis. Identification of these proteins would involve two-dimensional gel electrophoresis and the isolated proteins would then be excised from the gel and subjected to mass spectrometry fragmentation and analysis, producing spectra for sequence interpretation and database correlation.

The second part of this study focused on elucidating the mechanism by which PBOX-6 induces apoptosis in CML cells. Over the past few decades the approach to cancer therapy has changed significantly. Conventional chemotherapeutic agents are largely anti-mitotic and act by interfering with the basic machinery of DNA synthesis and cell division and not by targeting the specific lesions responsible for deregulated tumour growth. Advances in molecular biology has allowed us to identify genes involved in oncogenesis, and offer the opportunity to dissect the molecular mechanism underlying the disease. This includes the identification of mutated genes and cellular signalling pathways, which may be exploited as potential drug targets. The Philadelphia chromosome, present in 95% of cases of CML, presented the first example of a consistent chromosomal abnormality associated with a specific type of leukaemia. The requirement for Bcr-Abl kinase activity in transformation made this protein an ideal candidate for therapeutic targeting. Pharmaceutical efforts have also focused on developing FPTase inhibitors, which inhibit cellular transformation by the Ras oncoprotein (Bamford *et al.*, 2000), and antisense technologies that alter gene expression. Antisense oligonucleotides targeted against Bcr-Abl, which was first reported in 1991, inhibited the growth of CML cells (Szczylik *et al.*, 1991). However, many non-specific toxic effects have been reported with antisense technologies (Vaerman *et al.*, 1995). In recent years, a competitive ATP inhibitor of the Bcr-Abl tyrosine kinase, STI571, has been developed and has shown initial encouraging results in the treatment of CML (Drucker *et al.*, 1996). However, in an alternative mechanism to STI571, PBOX-6 has been found to bypass the apoptotic suppressor, Bcr-Abl, present in CML cells. Down-regulation of Bcr-Abl or its tyrosine kinase activity is not part of the upstream signalling pathway initiated by PBOX-6 and leading to apoptosis in CML cells. Thus, PBOX-6 represents a novel strategy for the treatment of CML and related diseases.

The binding of PBOX-6 to a number of alternative and potential drug targets was investigated. Pyrrolo-1,5-benzoxazepines are high affinity ligands to the PBR, and of the members tested, all were found to bind with similar affinities to the receptor in CML cells. However, the lack of correlation observed between binding affinities for the PBR and the apoptotic effect of this series of pyrrolo-1,5-benzoxazepines, suggests that the mechanism in which these compounds induce apoptosis in K562 cells does not involve their specific interaction with the PBR.

Pyrrolo-1,5-benzoxazepines share structural similarity with a series of compounds known as benzodiazepines, which have also been shown to bind to the PBR (Braestrup and Squires, 1977). A novel series of benzodiazepine-based peptidomimetics have been synthesised that potently inhibit farnesylation of Ras and slow the growth of transformed cells (James *et al.*, 1993). It has been previously shown that activation of Ras function is an important component of Bcr-Abl-mediated transformation (Pendergast *et al.*, 1993), and the ability of PBOX-6 to bypass Bcr-Abl in the mechanism by which it induces apoptosis in CML cells suggests that it may inhibit a point further downstream in the Bcr-Abl mediated signalling pathway. These findings prompted speculation that PBOX-6 might act as a farnesyl protein transferase inhibitor of Ras farnesylation, and thus Ras activity. However, in contrast to the benzodiazepine-based peptidomimetics, PBOX-6 does not inhibit H-Ras farnesylation, indicating that although these compounds share structural similarities, they do not function in a similar manner, and PBOX-6 does not target Ras as part of the mechanism in which it induces apoptosis in K562 cells.

A wide variety of chemotherapeutic agents used in the treatment of diseases of the hematopoietic system target the mammalian topoisomerase II enzyme (Topo II) and induce DNA damage. In contrast, PBOX-6 does not induce DNA strand breaks in K562 cells. Compounds that inhibit Topo II activity at a point in the catalytic cycle earlier than the DNA damaging drugs, do not induce DNA damage but have been shown to attenuate strand breaks induced by DNA damaging agents such as etoposide (Tanabe *et al.*, 1991). However, PBOX-6 did not prevent strand breaks induced by etoposide. These results indicate that PBOX-6 does not function in a manner similar to the Topo II poisons that induce DNA strand breaks, such as etoposide and daunorubicin, or compounds that inhibit at an earlier point in the catalytic cycle, such as the bis-2,6-dioxopiperazine derivatives, staurosporine, merbarone and aclarubicin. However, the ability of a number of Topo II inhibitors to prevent PBOX-6-induced apoptosis raises speculation that PBOX-6 requires Topo II at some stage in the pathway in which it induces apoptosis. Further work is required to establish the specific involvement of Topo II in the apoptotic pathway mediated by PBOX-6. This includes an assessment of the involvement of PBOX-6 at different stages in the Topo II catalytic cycle and an assessment of its ability to decatenate kinetoplast DNA. Kinetoplast DNA is a massive network consisting of thousands of interlocked closed circular DNA molecules called minicircles. Since the transient double strand break is necessary to release the

minicircle from the network, the decatenation of kinetoplast DNA is one of the highly specific assays of Topo II, and can be detected by analysis of the migration profile of released minicircle DNA on an agarose gel.

The final part of this study focused on dissecting biochemical components of the signalling pathway initiated by PBOX-6, which results in the induction of apoptosis in K562 cells. It has been found that PBOX-6 induces the rapid and transient activation of the JNK MAP kinase in K562 cells, whereas the p38 and ERK MAP kinase pathways are not activated. Activation of the JNK MAP kinase is an essential component of the apoptotic pathway induced by PBOX-6 in K562 cells. Furthermore, PBOX-6 induces the activation of a number of downstream substrates of JNK, such as the transcription factors c-Jun, ATF-2 and NFκB, in K562 cells.

Components of the anti-apoptotic signalling pathway mediated by Bcr-Abl in CML cells remain unclear. Although a number of Bcr-Abl substrates have been identified, it seems that the intracellular pathway responsible for the anti-apoptotic effects of Bcr-Abl differ depending on cell type. The induction of apoptosis in K562 cells by PBOX-6 was found to involve the phosphorylation and inactivation of Bcl-2 and Bcl-$_{XL}$, which occurs downstream of JNK activation. This suggests that expression of these anti-apoptotic proteins may be a component of the Bcr-Abl signalling pathway responsible for the resistant properties of CML cells. However, inactivation of Bcl-2 by PBOX-6 does not appear to result in the translocation of the pro-apoptotic protein, Bax, into the mitochondria. Future work will include an assessment of the effect of PBOX-6 on the extent of heterodimer formation between pro- and anti-apoptotic Bcl-2 family members, using co-immunoprecipitation experiments, and implications it may have on the apoptotic process.

Inhibitors of the JNK signalling pathway, dicumarol, CEP-1347 and the scaffold protein, JIP-1, prevent PBOX-6-induced apoptosis demonstrating the essential role of JNK in the apoptotic pathway. PBOX-6-induced activation of the JNK MAP kinase in K562 cells was found to be independent of GTPase activity. These results are consistent with a recent report that identifies members of mixed-lineage (MLK) kinase and germinal centre kinase (GCK) as selective targets of CEP-1347 (Maroney *et al.*, 2001). Furthermore, JIP-1 has been shown to selectively scaffold the MLK-MKK7-JNK signalling pathway, and does not interact with small GTPases (Yasuda *et al.*, 1999). These recent reports, together with the lack of involvement of GTPases in PBOX-6-induced JNK activation, strongly support a role

of the MLK and GCK kinase families in the upstream signalling pathway leading to JNK activation in K562 cells. Future work to further investigate this hypothesis will involve examining the effect of dominant negative mutants of MLK and GCK family members on PBOX-6-induced apoptosis.

The apoptotic activity of members of the pyrrolo-1,5-benzozazepine series is dependent on their structure. Some, but not all members from this series induced apoptosis in K562 cells, suggesting a structure-activity relationship. The pro-apoptotic members were found to contain a naphthyl side chain, which may be important in the mechanism in which these compounds induce apoptosis. The synthesis of additional pyrrolo-1,5-benzoxazepines derivatives, will provide further insights into the importance of the naphthyl group.

A number of approaches that will aid in uncovering the biological target of PBOX-6 have been initiated. These include the synthesis of a non-penetrating carboxylated derivative of PBOX-6 that will determine whether the apoptotic effects are mediated from the cell surface, as is the case with many membrane receptors, or whether the compound gains access into the cells and targets intracellular proteins directly. A second approach involves the use of microarray technologies, which allow the rapid profiling of cellular mRNA transcript levels. Various human cDNA expression array chips are now commercially available including chips that represent key genes known to control apoptosis. This technique would allow the detection of changes in expression of many pro- and anti-apoptotic genes in CML cells following treatment with PBOX-6. And finally, a proteomic approach could aid in identifying the biological target of PBOX-6. This would involve the generation of a PBOX-6 affinity matrix using cross-linked agarose resin, which would be incubated with K562 cell lysates. Specific PBOX-6-binding proteins could then be eluted and separated by SDS-PAGE and further characterised by mass spectrometry. Alternatively, a photoaffinity labelling technique may be used to identify the drug target. An azido-biotinylated derivative of PBOX-6 would be incubated with cell lysates, and would bind to the drug target. Upon irradiation with UV light, the photoaffinity probe would covalently cross-link to its target protein, which would be subsequently analysed by SDS-PAGE using high affinity avidin-biotin binding.

All forms of cancer therapy carry the danger of selection for drug resistance. A recent study reported that, like many conventional drugs, patients in the advanced "blast crisis" stage of CML are beginning to gain resistance to the Bcr-Abl tyrosine kinase inhibitor, STI571 (Gorre *et al.*, 2001). Early in the chronic phase of CML it is likely that Bcr-Abl is the

sole oncogenic abnormality and STI571 has shown promising results against chronic phase CML. However, results from patients treated in the accelerated and blast crisis phase of CML support the concept of only a partial dependence of the malignant clones on Bcr-Abl tyrosine kinase activity with the probable acquisition of further genetic defects resulting in the development of resistant disease (Mauro and Drucker, 2001). Therefore, current efforts focus on the potential of STI571 in combination therapy regimens. Possibilities for future combination therapies include STI571 with additional tyrosine kinases or drugs with alternative targets. In the present study, the therapeutic potential of pyrrolo-1,5-benzoxazepine compounds in the treatment of CML has been highlighted. An assessment of the apoptotic effect of PBOX-6 in combination with STI571, in K562 cells, would identify any synergistic apoptotic effects that could be exploited in combination therapy regimens. *Ex vivo* work is currently underway to determine the effect of PBOX-6 on early hematopoietic progenitor cells. Mononuclear cells, isolated by density gradient centrifugation from the peripheral blood of normal donor and CML patients, are treated with PBOX-6 for up to 72 hours and the effect on CFU-GEMM (granulocyte, erythrocyte, monocyte, megakaryocyte) progenitor colony formation in soft agar is assessed. In addition to myeloid cells, the effect of PBOX-6 on the viability of hematopoietic cells such as human lymphocytes, both normal and cancerous, will provide additional information on the potential of this compound as an anti-cancer agent in the treatment of various leukaemias and lymphomas.

A number of therapies including antisense oligonucleotides and novel drugs have been studied as agents for purging hematopoietic cell harvests prior to autologous transplantation (Clark, 2000). The present study outlines the potential of PBOX-6 as a purging agent to eradicate CML cells from bone marrow and peripheral blood stem cell collections *ex vivo*.

In addition to CML cells, PBOX-6 has been show to induce apoptosis in variety of cancerous cells derived from the hematopoietic system such as the human promyelocytic leukaemia HL-60 cells, Jurkat T lymphoma and subcutaneous Hut-78 lymphoma cells (Zisterer *et al.,* 2000). Preliminary data have also shown that PBOX-6 potently induces apoptosis in the human breast carcinoma cell line, MCF-7, and the human prostate carcinoma cell line, LNCap. The apoptotic effect of PBOX-6 on a wide variety of tumour cell lines in culture is promising and future work includes an *in vivo* assessment of the apoptotic activity of this novel compound. A number of *in vivo* murine models have been successfully

generated for studying CML, such as the engraftment of severe combined immunodeficiency (SCID) mice with human Bcr-Abl-positive cells (Deininger *et al.,* 2000). *In vivo* studies, which will evaluate the ability of PBOX-6 to reduce tumour growth, will provide valuable insights into the therapeutic potential of this novel compound.

In summary, the current study has revealed the therapeutic potential of a novel agent, PBOX-6, in the treatment of CML and related diseases. Part of the mechanism in which PBOX-6 induces apoptosis in CML cells has been uncovered. Further characterisation of the apoptotic pathway, coupled with *ex vivo* and *in vivo* experiments, will provide further insights into the use of this novel agent in the treatment of CML.

References

Adjei, A.A., Erlichman, C., Davis, J.N., Cutler, D.L., Sloan, J.A., Marks, R.S., Hanson, L.J., Svingen, P.A., Atherton, P., Bishop, W.R., Kirschmeier, P. & Kaufmann, S.H. (2000). A Phase I trial of the farnesyl transferase inhibitor SCH66336: evidence for biological and clinical activity. *Cancer Res.* **60,** 1871-7.

Afar, D.E., Goga, A., McLaughlin, J., Witte, O.N. & Sawyers, C.L. (1994). Differential complementation of Bcr-Abl point mutants with c-Myc. *Science* **264,** 424-6.

Aggarwal, B.B. (2000). Apoptosis and nuclear factor-kappa B: a tale of association and dissociation. *Biochem. Pharmacol.* **60,** 1033-9.

Amarante-Mendes, G.P., McGahon, A.J., Nishioka, W.K., Afar, D.E., Witte, O.N. & Green, D.R. (1998a). Bcl-2-independent Bcr-Abl-mediated resistance to apoptosis: protection is correlated with up-regulation of Bcl-xL. *Oncogene* **16,** 1383-90.

Amarante-Mendes, G.P., Naekyung Kim, C., Liu, L., Huang, Y., Perkins, C.L., Green, D.R. & Bhalla, K. (1998b). Bcr-Abl exerts its antiapoptotic effect against diverse apoptotic stimuli through blockage of mitochondrial release of cytochrome C and activation of caspase-3. *Blood* **91,** 1700-5.

Azuma, Y., Onishi, Y., Sato, Y. & Kizaki, H. (1995). Effects of protein tyrosine kinase inhibitors with different modes of action on topoisomerase activity and death of IL-2-dependent CTLL-2 cells. *J. Biochem.* **118,** 312-8.

Bagrodia, S., Derijard, B., Davis, R.J. & Cerione, R.A. (1995). Cdc42 and PAK-mediated signaling leads to Jun kinase and p38 mitogen-activated protein kinase activation. *J. Biol. Chem.* **270,** 27995-8.

Baikie, A.G., C.B.W., Buckton, KE. (1960). A possible specific chromosome abnormality in human chronic myeloid leukemia. *Nature* **188,** 1165-1166.

Balla, A., Toth, B., Timar, G., Bak, J. & Krajcsi, P. (2001). Molecular targets for

pharmacological cytoprotection. *Biochem. Pharmacol.* **61,** 769-77.

Bamford, M., Walkinshaw, G. & Brown, R. (2000). Therapeutic applications of apoptosis research. *Exp. Cell Res.* **256,** 1-11.

Barrington, R.E., Subler, M.A., Rands, E., Omer, C.A., Miller, P.J., Hundley, J.E., Koester, S.K., Troyer, D.A., Bearss, D.J., Conner, M.W., Gibbs, J.B., Hamilton, K., Koblan, K.S., Mosser, S.D., O'Neill, T.J., Schaber, M.D., Senderak, E.T., Windle, J.J., Oliff, A. & Kohl, N.E. (1998). A farnesyltransferase inhibitor induces tumor regression in transgenic mice harboring multiple oncogenic mutations by mediating alterations in both cell cycle control and apoptosis. *Mol. Cell Biol.* **18,** 85-92.

Bergamaschi, G., Rosti, V., Danova, M., Ponchio, L., Lucotti, C. & Cazzola, M. (1993). Inhibitors of tyrosine phosphorylation induce apoptosis in human leukemic cell lines. *Leukemia* **7,** 2012-8.

Bergan, R.C., Kyle, E., Connell, Y. & Neckers, L. (1995). Inhibition of protein-tyrosine kinase activity in intact cells by the aptameric action of oligodeoxynucleotides. *Antisense Res. Dev.* **5,** 33-8.

Bessho, R., Matsubara, K., Kubota, M., Kuwakado, K., Hirota, H., Wakazono, Y., Lin, Y.W., Okuda, A., Kawai, M., Nishikomori, R. & et al. (1994). Pyrrolidine dithiocarbamate, a potent inhibitor of nuclear factor kappa B (NF-kappa B) activation, prevents apoptosis in human promyelocytic leukemia HL-60 cells and thymocytes. *Biochem. Pharmacol.* **48,** 1883-9.

Bhatia, R., Verfaillie, C.M., Miller, J.S. & McGlave, P.B. (1997). Autologous transplantation therapy for chronic myelogenous leukemia. *Blood* **89,** 2623-34.

Bird, T.A., Kyriakis, J.M., Tyshler, L., Gayle, M., Milne, A. & Virca, G.D. (1994). Interleukin-1 activates p54 mitogen-activated protein (MAP) kinase/stress-activated protein kinase by a pathway that is independent of p21ras, Raf-1, and MAP kinase kinase. *J. Biol. Chem.* **269,** 31836-44.

Bishop, W.R., Bond, R., Petrin, J., Wang, L., Patton, R., Doll, R., Njoroge, G., Catino, J., Schwartz, J., Windsor, W. & et al. (1995). Novel tricyclic inhibitors of farnesyl protein transferase. Biochemical characterization and inhibition of Ras modification in transfected Cos cells. *J. Biol. Chem.* **270,** 30611-8.

Blume-Jensen, P. & Hunter, T. (2001). Oncogenic kinase signalling. *Nature*, **411,** 355-65.

Bock, B.C., Vacratsis, P.O., Qamirani, E. & Gallo, K.A. (2000). Cdc42-induced activation of the mixed-lineage kinase SPRK *in vivo*. Requirement of the Cdc42/Rac interactive binding motif and changes in phosphorylation. *J. Biol. Chem.* **275,** 14231-41.

Bono, F., Lamarche, I., Prabonnaud, V., Le Fur, G. & Herbert, J.M. (1999). Peripheral benzodiazepine receptor agonists exhibit potent antiapoptotic activities. *Biochem. Biophys. Res. Commun.* **265,** 457-61.

Bours, V., Bentires-Alj, M., Hellin, A.C., Viatour, P., Robe, P., Delhalle, S., Benoit, V. & Merville, M.P. (2000). Nuclear factor-kappa B, cancer, and apoptosis. *Biochem. Pharmacol.* **60,** 1085-9.

Bradford, M.M. (1976). A rapid and sensitive method for the quantitation of microgram quantities of protein utilizing the principle of protein-dye binding. *Anal. Biochem.* **72,** 248-54.

Braestrup, C. & Squires, R.F. (1977). Specific benzodiazepine receptors in rat brain characterized by high- affinity (^{3}H)diazepam binding. *Proc. Natl. Acad. Sci. U S A* **74,** 3805-9.

Bratton, S.B., MacFarlane, M., Cain, K. & Cohen, G.M. (2000). Protein complexes activate distinct caspase cascades in death receptor and stress-induced apoptosis. *Exp. Cell Res.* **256,** 27-33.

Buchdunger, E., Cioffi, C.L., Law, N., Stover, D., Ohno-Jones, S., Druker, B.J. & Lydon, N.B. (2000). Abl protein-tyrosine kinase inhibitor STI571 inhibits *in vitro* signal transduction

mediated by c-kit and platelet-derived growth factor receptors. *J. Pharmacol. Exp. Ther.* **295,** 139-45.

Buchdunger, E., Zimmermann, J., Mett, H., Meyer, T., Muller, M., Druker, B.J. & Lydon, N.B. (1996). Inhibition of the Abl protein-tyrosine kinase *in vitro* and *in vivo* by a 2-phenylaminopyrimidine derivative. *Cancer Res.* **56,** 100-4.

Burden, D.A. & Osheroff, N. (1998). Mechanism of action of eukaryotic topoisomerase II and drugs targeted to the enzyme. *Biochim. Biophys. Acta.* **1400,** 139-54.

Buschmann, T., Yin, Z., Bhoumik, A. & Ronai, Z. (2000). Amino-terminal-derived JNK fragment alters expression and activity of c- Jun, ATF2, and p53 and increases H_2O_2-induced cell death. *J. Biol. Chem.* **275,** 16590-6.

Campiani, G., Nacci, V., Fiorini, I., De Filippis, M.P., Garofalo, A., Ciani, S.M., Greco, G., Novellino, E., Williams, D.C., Zisterer, D.M., Woods, M.J., Mihai, C., Manzoni, C. & Mennini, T. (1996). Synthesis, biological activity, and SARs of pyrrolobenzoxazepine derivatives, a new class of specific "peripheral-type" benzodiazepine receptor ligands. *J. Med. Chem.* **39,** 3435-50.

Cans, C., Mangano, R., Barila, D., Neubauer, G. & Superti-Furga, G. (2000). Nuclear tyrosine phosphorylation: the beginning of a map. *Biochem. Pharmacol.* **60,** 1203-15.

Capranico, G. & Binaschi, M. (1998). DNA sequence selectivity of topoisomerases and topoisomerase poisons. *Biochim. Biophys. Acta.* **1400,** 185-94.

Chan-Hui, P.Y. & Weaver, R. (1998). Human mitogen-activated protein kinase kinase kinase mediates the stress-induced activation of mitogen-activated protein kinase cascades. *Biochem. J.* **336,** 599-609.

Chauhan, D., Pandey, P., Ogata, A., Teoh, G., Krett, N., Halgren, R., Rosen, S., Kufe, D., Kharbanda, S. & Anderson, K. (1997). Cytochrome c-dependent and -independent induction

of apoptosis in multiple myeloma cells. *J. Biol. Chem.* **272,** 29995-7.

Chelli, B., Falleni, A., Salvetti, F., Gremigni, V., Lucacchini, A. & Martini, C. (2001). Peripheral-type benzodiazepine receptor ligands: mitochondrial permeability transition induction in rat cardiac tissue. *Biochem. Pharmacol.* **61,** 695-705.

Chen, C.Y., Liou, J., Forman, L.W. & Faller, D.V. (1998). Differential regulation of discrete apoptotic pathways by Ras. *J. Biol. Chem.* **273,** 16700-9.

Chinnaiyan, A.M., Orth, K., O'Rourke, K., Duan, H., Poirier, G.G. & Dixit, V.M. (1996). Molecular ordering of the cell death pathway. Bcl-2 and Bcl-xL function upstream of the CED-3-like apoptotic proteases. *J. Biol. Chem.* **271,** 4573-6.

Clark, R.E. (2000). Antisense therapeutics in chronic myeloid leukaemia: the promise, the progress and the problems. *Leukemia* **14,** 347-55.

Clarkson, B.D., Strife, A., Wisniewski, D., Lambek, C. & Carpino, N. (1997). New understanding of the pathogenesis of CML: a prototype of early neoplasia. *Leukemia* **11,** 1404-28.

Cortez, D., Reuther, G. & Pendergast, A.M. (1997). The Bcr-Abl tyrosine kinase activates mitogenic signaling pathways and stimulates G1-to-S phase transition in hematopoietic cells. *Oncogene* **15,** 2333-42.

Cory, S. & Adams, J.M. (1998). Matters of life and death: programmed cell death at Cold Spring Harbor. *Biochim. Biophys. Acta.* **1377,** R25-44.

Coso, O.A., Chiariello, M., Yu, J.C., Teramoto, H., Crespo, P., Xu, N., Miki, T. & Gutkind, J.S. (1995). The small GTP-binding proteins Rac1 and Cdc42 regulate the activity of the JNK/SAPK signaling pathway. *Cell* **81,** 1137-46.

Croce, C.M., Huebner, K., Isobe, M., Fainstain, E., Lifshitz, B., Shtivelman, E. & Canaani, E.

(1987). Mapping of four distinct BCR-related loci to chromosome region 22q11: order of BCR loci relative to chronic myelogenous leukemia and acute lymphoblastic leukemia breakpoints. *Proc. Natl. Acad. Sci. U S A* **84,** 7174-8.

Cross, J.V., Deak, J.C., Rich, E.A., Qian, Y., Lewis, M., Parrott, L.A., Mochida, K., Gustafson, D., Vande Pol, S. & Templeton, D.J. (1999). Quinone reductase inhibitors block SAPK/JNK and NFkappaB pathways and potentiate apoptosis. *J. Biol. Chem.* **274,** 31150-4.

Cross, T.G., Scheel-Toellner, D., Henriquez, N.V., Deacon, E., Salmon, M. & Lord, J.M. (2000). Serine/threonine protein kinases and apoptosis. *Exp. Cell Res.* **256,** 34-41.

Crul, M., de Klerk, G.J., Beijnen, J.H. & Schellens, J.H. (2001). Ras biochemistry and farnesyl transferase inhibitors: a literature survey. *Anticancer Drugs* **12,** 163-84.

Cuvillier, O., Rosenthal, D.S., Smulson, M.E. & Spiegel, S. (1998). Sphingosine 1-phosphate inhibits activation of caspases that cleave poly(ADP-ribose) polymerase and lamins during Fas- and ceramide- mediated apoptosis in Jurkat T lymphocytes. *J. Biol. Chem.* **273,** 2910-6.

Daugas, E., Nochy, D., Ravagnan, L., Loeffler, M., Susin, S.A., Zamzami, N. & Kroemer, G. (2000). Apoptosis-inducing factor (AIF): a ubiquitous mitochondrial oxidoreductase involved in apoptosis. *FEBS Lett.* **476,** 118-23.

Davis, L., Stephens, L.R., Hawkins, P.T. and Saklatvala, J. (1999). Synergistic activation of JNK/SAPK by interleukin-1 and platelet-derived growth factor is independent of Rac and Cdc42. *Biochem. J.* **338,** 387-392.

Deininger, M.W., Goldman, J.M., Lydon, N. & Melo, J.V. (1997). The tyrosine kinase inhibitor CGP57148B selectively inhibits the growth of BCR-ABL-positive cells. *Blood* **90,** 3691-8.

Deininger, M.W., Goldman, J.M. & Melo, J.V. (2000). The molecular biology of chronic myeloid leukemia. *Blood* **96,** 3343-56.

Denhardt, D.T. (1996). Signal-transducing protein phosphorylation cascades mediated by Ras/Rho proteins in the mammalian cell: the potential for multiplex signalling. *Biochem. J.* **318,** 729-47.

Deutsch, E., Dugray, A., AbdulKarim, B., Marangoni, E., Maggiorella, L., Vaganay, S., M'Kacher, R., Rasy, S.D., Eschwege, F., Vainchenker, W., Turhan, A.G. & Bourhis, J. (2001). BCR-ABL down-regulates the DNA repair protein DNA-PKcs. *Blood* **97,** 2084-90.

Dickens, M., Rogers, J.S., Cavanagh, J., Raitano, A., Xia, Z., Halpern, J.R., Greenberg, M.E., Sawyers, C.L. & Davis, R.J. (1997). A cytoplasmic inhibitor of the JNK signal transduction pathway. *Science* **277,** 693-6.

Diener, K., Wang, X.S., Chen, C., Meyer, C.F., Keesler, G., Zukowski, M., Tan, T.H. & Yao, Z. (1997). Activation of the c-Jun N-terminal kinase pathway by a novel protein kinase related to human germinal center kinase. *Proc. Natl. Acad. Sci. U S A* **94,** 9687-92.

Dou, Q.P., Mcguire, T.F., Peng, Y. and An, B. (1999). Proteasome inhibition leads to significant reduction of Bcr-Abl expression and subsequent induction of apoptosis in K562 chronic myelogenous leukemia cells. *J. Pharm. Exp. Ther.* **289,** 781-790.

Druker, B.J., Tamura, S., Buchdunger, E., Ohno, S., Segal, G.M., Fanning, S., Zimmermann, J. & Lydon, N.B. (1996). Effects of a selective inhibitor of the Abl tyrosine kinase on the growth of Bcr-Abl positive cells. *Nat. Med.* **2,** 561-6.

Du, W., Thanos, D. and Maniatis, T. (1993). Mechanisms of transcriptional synergism between distinct virus-inducible enhancer elements. *Cell* **74,** 887-898.

Duan, H., Orth, K., Chinnaiyan, A.M., Poirier, G.G., Froelich, C.J., He, W.W. & Dixit, V.M. (1996). ICE-LAP6, a novel member of the ICE/Ced-3 gene family, is activated by the cytotoxic T cell protease granzyme B. *J. Biol. Chem.* **271,** 16720-4.

Dubrez, L., Eymin, B., Sordet, O., Droin, N., Turhan, A.G. & Solary, E. (1998). BCR-ABL

delays apoptosis upstream of procaspase-3 activation. *Blood.* **91,** 2415-22.

Dubrez, L., Goldwasser, F., Genne, P., Pommier, Y. & Solary, E. (1995). The role of cell cycle regulation and apoptosis triggering in determining the sensitivity of leukemic cells to topoisomerase I and II inhibitors. *Leukemia* **9,** 1013-24.

Duke, R.C., Ojcius, D.M. & Young, J.D. (1996). Cell suicide in health and disease. *Sci. Am.* **275,** 80-7.

Dumont, C., Durrbach, A., Bidere, N., Rouleau, M., Kroemer, G., Bernard, G., Hirsch, F., Charpentier, B., Susin, S.A. & Senik, A. (2000). Caspase-independent commitment phase to apoptosis in activated blood T lymphocytes: reversibility at low apoptotic insult. *Blood* **96,** 1030-8.

Dunant, N.M., Wisniewski, D., Strife, A., Clarkson, B. & Resh, M.D. (2000). The phosphatidylinositol polyphosphate 5-phosphatase SHIP1 associates with the dok1 phosphoprotein in bcr-Abl transformed cells. *Cell Signal* **12,** 317-26.

Eischen, C.M., Dick, C.J. & Leibson, P.J. (1994). Tyrosine kinase activation provides an early and requisite signal for Fas-induced apoptosis. *J. Immunol.* **153,** 1947-54.

Ellis, H.M. & Horvitz, H.R. (1986). Genetic control of programmed cell death in the nematode *C. elegans*. *Cell* **44,** 817-29.

Emanuel, P.D., Snyder, R.C., Wiley, T., Gopurala, B. & Castleberry, R.P. (2000). Inhibition of juvenile myelomonocytic leukemia cell growth *in vitro* by farnesyltransferase inhibitors. *Blood* **95,** 639-45.

Enari, M., Sakahira, H., Yokoyama, H., Okawa, K., Iwamatsu, A. & Nagata, S. (1998). A caspase-activated DNase that degrades DNA during apoptosis, and its inhibitor ICAD. *Nature* **391,** 43-50.

Eskes, R., Antonsson, B., Osen-Sand, A., Montessuit, S., Richter, C., Sadoul, R., Mazzei, G., Nichols, A. & Martinou, J.C. (1998). Bax-induced cytochrome C release from mitochondria is independent of the permeability transition pore but highly dependent on Mg^{2+} ions. *J. Cell Biol.* **143,** 217-24.

Evan, G.I. & Vousden, K.H. (2001). Proliferation, cell cycle and apoptosis in cancer. *Nature* **411,** 342-8.

Evans, C.A., Owen-Lynch, P.J., Whetton, A.D. & Dive, C. (1993). Activation of the Abelson tyrosine kinase activity is associated with suppression of apoptosis in hemopoietic cells. *Cancer Res.* **53,** 1735-8.

Fadeel, B., Hassan, Z., Hellstrom-Lindberg, E., Henter, J.I., Orrenius, S. & Zhivotovsky, B. (1999). Cleavage of Bcl-2 is an early event in chemotherapy-induced apoptosis of human myeloid leukemia cells. *Leukemia* **13,** 719-28.

Faderl, S., Talpaz, M., Estrov, Z. & Kantarjian, H.M. (1999). Chronic myelogenous leukemia: biology and therapy. *Ann. Intern. Med.* **131,** 207-19.

Faltynek, C.R., Schroeder, J., Mauvais, P., Miller, D., Wang, S., Murphy, D., Lehr, R., Kelley, M., Maycock, A., Michne, W. & et al. (1995). Damnacanthal is a highly potent, selective inhibitor of p56lck tyrosine kinase activity. *Biochemistry* **34,** 12404-10.

Fan, M., Goodwin, M., Vu, T., Brantley-Finley, C., Gaarde, W.A. & Chambers, T.C. (2000). Vinblastine-induced phosphorylation of Bcl-2 and Bcl-XL is mediated by JNK and occurs in parallel with inactivation of the Raf-1/MEK/ERK cascade. *J. Biol. Chem.* **275,** 29980-5.

Fattman, C.L., Allan, W.P., Hasinoff, B.B. & Yalowich, J.C. (1996). Collateral sensitivity to the bisdioxopiperazine dexrazoxane (ICRF-187) in etoposide (VP-16)-resistant human leukemia K562 cells. *Biochem. Pharmacol.* **52,** 635-42.

Feldkamp, M.M., Lau, N., Roncari, L. & Guha, A. (2001). Isotype-specific Ras.GTP-levels

predict the efficacy of farnesyl transferase inhibitors against human astrocytomas regardless of Ras mutational status. *Cancer Res.* **61,** 4425-31.

Fernandes, R.S., Gorman, A.M., McGahon, A., Lawlor, M., McCann, S. & Cotter, T.G. (1996). The repression of apoptosis by activated abl oncogenes in chronic myelogenous leukaemia. *Leukemia* **10 Suppl 2,** s17-21.

Finkel, E. (2001). The mitochondrion: is it central to apoptosis? *Science* **292,** 624-6.

Fortune, J.M. & Osheroff, N. (1998). Merbarone inhibits the catalytic activity of human topoisomerase IIalpha by blocking DNA cleavage. *J. Biol. Chem.* **273,** 17643-50.

Fuchs, S.Y., Tappin, I. & Ronai, Z. (2000). Stability of the ATF2 transcription factor is regulated by phosphorylation and dephosphorylation. *J. Biol. Chem.* **275,** 12560-4.

Fulda, S., Susin, S.A., Kroemer, G. & Debatin, K.M. (1998). Molecular ordering of apoptosis induced by anticancer drugs in neuroblastoma cells. *Cancer Res.* **58,** 4453-60.

Gambacorti-Passerini, C., le Coutre, P., Mologni, L., Fanelli, M., Bertazzoli, C., Marchesi, E., Di Nicola, M., Biondi, A., Corneo, G.M., Belotti, D., Pogliani, E. & Lydon, N.B. (1997). Inhibition of the ABL kinase activity blocks the proliferation of BCR/ABL+ leukemic cells and induces apoptosis. *Blood Cells Mol. Dis.* **23,** 380-94.

Garcia-Calvo, M., Peterson, E.P., Leiting, B., Ruel, R., Nicholson, D.W. & Thornberry, N.A. (1998). Inhibition of human caspases by peptide-based and macromolecular inhibitors. *J. Biol. Chem.* **273,** 32608-13.

Gavish, M., Bachman, I., Shoukrun, R., Katz, Y., Veenman, L., Weisinger, G. & Weizman, A. (1999). Enigma of the peripheral benzodiazepine receptor. *Pharmacol. Rev.* **51,** 629-50.

Gesbert, F. & Griffin, J.D. (2000). Bcr/Abl activates transcription of the Bcl-X gene through STAT5. *Blood* **96,** 2269-76.

Gibbs, J.B. (2000). Mechanism-based target identification and drug discovery in cancer research. *Science* **287,** 1969-73.

Gibbs, J.B., Oliff, A. & Kohl, N.E. (1994). Farnesyltransferase inhibitors: Ras research yields a potential cancer therapeutic. *Cell* **77,** 175-8.

Goga, A., McLaughlin, J., Afar, D.E., Saffran, D.C. & Witte, O.N. (1995). Alternative signals to RAS for hematopoietic transformation by the BCR-ABL oncogene. *Cell* **82,** 981-8.

Goping, I.S., Gross, A., Lavoie, J.N., Nguyen, M., Jemmerson, R., Roth, K., Korsmeyer, S.J. & Shore, G.C. (1998). Regulated targeting of BAX to mitochondria. *J. Cell Biol.* **143,** 207-15.

Gorre, M.E., Mohammed, M., Ellwood, K., Hsu, N., Paquette, R., Rao, P.N. & Sawyers, C.L. (2001). Clinical Resistance to STI-571 Cancer Therapy Caused by BCR-ABL Gene Mutation or Amplification. *Science* **293,** 876-80.

Green, D.R. & Reed, J.C. (1998). Mitochondria and apoptosis. *Science* **281,** 1309-12.

Gross, A., Jockel, J., Wei, M.C. & Korsmeyer, S.J. (1998). Enforced dimerization of BAX results in its translocation, mitochondrial dysfunction and apoptosis. *Embo. J.* **17,** 3878-85.

Gross, A., McDonnell, J.M. & Korsmeyer, S.J. (1999). BCL-2 family members and the mitochondria in apoptosis. *Genes Dev.* **13,** 1899-911.

Gu, Y., Sarnecki, C., Aldape, R.A., Livingston, D.J. & Su, M.S. (1995). Cleavage of poly(ADP-ribose) polymerase by interleukin-1 beta converting enzyme and its homologs TX and Nedd-2. *J. Biol. Chem.* **270,** 18715-8.

Gupta, S., Campbell, D., Derijard, B. & Davis, R.J. (1995). Transcription factor ATF2 regulation by the JNK signal transduction pathway. *Science* **267,** 389-93.

Haldar, S., Chintapalli, J. & Croce, C.M. (1996). Taxol induces bcl-2 phosphorylation and

death of prostate cancer cells. *Cancer Res.* **56,** 1253-5.

Haldar, S., Jena, N. & Croce, C.M. (1995). Inactivation of Bcl-2 by phosphorylation. *Proc. Natl. Acad. Sci. U S A* **92,** 4507-11.

Hara, M., Akasaka, K., Akinaga, S., Okabe, M., Nakano, H., Gomez, R., Wood, D., Uh, M. & Tamanoi, F. (1993). Identification of Ras farnesyltransferase inhibitors by microbial screening. *Proc. Natl. Acad. Sci. U S A* **90,** 2281-5.

Hasinoff, B.B., Abram, M.E., Barnabe, N., khelifa, T., Allan, W.P. and Yalowich, J.C. (2001). The catalytic DNA Topoisomerase II inhibitor Dexrazoxane (ICRF-187) induces differentiation and apoptosis in human leukemia K562 cells. *Molecular Pharmacology* **59,** 453-461.

Heimbrook, D.C. & Oliff, A. (1998). Therapeutic intervention and signaling. *Curr. Opin. Cell Biol.* **10,** 284-8.

Heinrich, M.C., Griffith, D.J., Druker, B.J., Wait, C.L., Ott, K.A. & Zigler, A.J. (2000). Inhibition of c-kit receptor tyrosine kinase activity by STI 571, a selective tyrosine kinase inhibitor. *Blood* **96,** 925-32.

Hengartner, M.O. (2000). The biochemistry of apoptosis. *Nature* **407,** 770-6.

Hirsch, T., Decaudin, D., Susin, S.A., Marchetti, P., Larochette, N., Resche-Rigon, M. & Kroemer, G. (1998). PK11195, a ligand of the mitochondrial benzodiazepine receptor, facilitates the induction of apoptosis and reverses Bcl-2-mediated cytoprotection. *Exp. Cell Res.* **241,** 426-34.

Hishita, T., Tada-Oikawa, S., Tohyama, K., Miura, Y., Nishihara, T., Tohyama, Y., Yoshida, Y., Uchiyama, T. & Kawanishi, S. (2001). Caspase-3 activation by lysosomal enzymes in cytochrome c-independent apoptosis in myelodysplastic syndrome-derived cell line P39. *Cancer Res.* **61,** 2878-84.

Ichijo, H. (1999). From receptors to stress-activated MAP kinases. *Oncogene* **18,** 6087-93.

Ishida, R., Miki, T., Narita, T., Yui, R., Sato, M., Utsumi, K.R., Tanabe, K. & Andoh, T. (1991). Inhibition of intracellular topoisomerase II by antitumor bis(2,6- dioxopiperazine) derivatives: mode of cell growth inhibition distinct from that of cleavable complex-forming type inhibitors. *Cancer Res.* **51,** 4909-16.

Jacobson, M.D. (1996). Reactive oxygen species and programmed cell death. *Trends Biochem. Sci.* **21,** 83-6.

Jacobson, M.D. & Raff, M.C. (1995). Programmed cell death and Bcl-2 protection in very low oxygen. *Nature* **374,** 814-6.

James, G.L., Brown, M.S., Cobb, M.H. & Goldstein, J.L. (1994). Benzodiazepine peptidomimetic BZA-5B interrupts the MAP kinase activation pathway in H-Ras-transformed Rat-1 cells, but not in untransformed cells. *J. Biol. Chem.* **269,** 27705-14.

James, G.L., Goldstein, J.L. & Brown, M.S. (1995). Polylysine and CVIM sequences of K-RasB dictate specificity of prenylation and confer resistance to benzodiazepine peptidomimetic in vitro. *J. Biol. Chem.* **270,** 6221-6.

James, G.L., Goldstein, J.L., Brown, M.S., Rawson, T.E., Somers, T.C., McDowell, R.S., Crowley, C.W., Lucas, B.K., Levinson, A.D. & Marsters, J.C., Jr. (1993). Benzodiazepine peptidomimetics: potent inhibitors of Ras farnesylation in animal cells. *Science* **260,** 1937-42.

Janicke, R.U., Ng, P., Sprengart, M.L. & Porter, A.G. (1998). Caspase-3 is required for alpha-fodrin cleavage but dispensable for cleavage of other death substrates in apoptosis. *J. Biol. Chem.* **273,** 15540-5.

Jensen, P.B., Sorensen, B.S., Demant, E.J., Sehested, M., Jensen, P.S., Vindelov, L. & Hansen, H.H. (1990). Antagonistic effect of aclarubicin on the cytotoxicity of etoposide and 4'-(9-acridinylamino)methanesulfon-m-anisidide in human small cell lung cancer cell lines

and on topoisomerase II-mediated DNA cleavage. *Cancer Res.* **50,** 3311-6.

Johnson, K.L., Vaillant, F. & Lawen, A. (1996). Protein tyrosine kinase inhibitors prevent didemnin B-induced apoptosis in HL-60 cells. *FEBS Lett.* **383,** 1-5.

Juo, P., Kuo, C.J., Yuan, J. & Blenis, J. (1998). Essential requirement for caspase-8/FLICE in the initiation of the Fas- induced apoptotic cascade. *Curr. Biol.* **8,** 1001-8.

Kabarowski, J.H., Allen, P.B. & Wiedemann, L.M. (1994). A temperature sensitive p210 BCR-ABL mutant defines the primary consequences of BCR-ABL tyrosine kinase expression in growth factor dependent cells. *Embo. J.* **13,** 5887-95.

Kamata, H. & Hirata, H. (1999). Redox regulation of cellular signalling. *Cell Signal* **11,** 1-14.

Kamesaki, S., Kamesaki, H., Jorgensen, T.J., Tanizawa, A., Pommier, Y. & Cossman, J. (1993). Bcl-2 protein inhibits etoposide-induced apoptosis through its effects on events subsequent to topoisomerase II-induced DNA strand breaks and their repair. *Cancer Res.* **53,** 4251-6.

Kang, C.D., Yoo, S.D., Hwang, B.W., Kim, K.W., Kim, D.W., Kim, C.M., Kim, S.H. & Chung, B.S. (2000). The inhibition of ERK/MAPK not the activation of JNK/SAPK is primarily required to induce apoptosis in chronic myelogenous leukemic K562 cells. *Leuk. Res.* **24,** 527-34.

Kannan K and Jain, S. (2000). Oxidative stress and apoptosis. *Pathophysiology*, **7,** 153-163.

Karin, M. (1995). The regulation of AP-1 activity by mitogen-activated protein kinases. *J. Biol. Chem.* **270,** 16483-6.

Kaufmann, S.H., Desnoyers, S., Ottaviano, Y., Davidson, N.E. & Poirier, G.G. (1993). Specific proteolytic cleavage of poly(ADP-ribose) polymerase: an early marker of chemotherapy-induced apoptosis. *Cancer Res.* **53,** 3976-85.

Kaufmann, S.H. & Earnshaw, W.C. (2000). Induction of apoptosis by cancer chemotherapy. *Exp. Cell Res.* **256,** 42-9.

Kaufmann, W.K. (1998). Human topoisomerase II function, tyrosine phosphorylation and cell cycle checkpoints. *Proc. Soc. Exp. Biol. Med.* **217,** 327-34.

Kerr, J.F., Wyllie, A.H. & Currie, A.R. (1972). Apoptosis: a basic biological phenomenon with wide-ranging implications in tissue kinetics. *Br. J. Cancer* **26,** 239-57.

Khaled, A.R., Kim, K., Hofmeister, R., Muegge, K. & Durum, S.K. (1999). Withdrawal of IL-7 induces Bax translocation from cytosol to mitochondria through a rise in intracellular pH. *Proc. Natl. Acad. Sci. U S A* **96,** 14476-81.

Kharbanda, S., Yuan, Z.M., Weichselbaum, R. & Kufe, D. (1997). Functional role for the c-Abl protein tyrosine kinase in the cellular response to genotoxic stress. *Biochim. Biophys. Acta.* **1333,** O1-7.

Khelifa, T. & Beck, W.T. (1999). Merbarone, a catalytic inhibitor of DNA topoisomerase II, induces apoptosis in CEM cells through activation of ICE/CED-3-like protease. *Mol. Pharmacol.* **55,** 548-56.

Kjoller, L. & Hall, A. (1999). Signaling to Rho GTPases. *Exp. Cell Res.* **253,** 166-79.

Knaus, U.G. & Bokoch, G.M. (1998). The p21Rac/Cdc42-activated kinases (PAKs). *Int. J. Biochem. Cell Biol.* **30,** 857-62.

Kohn, K.W., Erickson, L.C., Ewig, R.A. & Friedman, C.A. (1976). Fractionation of DNA from mammalian cells by alkaline elution. *Biochemistry* **15,** 4629-37.

Kouchi, H., Nakamura, K., Fushimi, K., Sakaguchi, M., Miyazaki, M., Ohe, T. & Namba, M. (1999). Manumycin A, inhibitor of ras farnesyltransferase, inhibits proliferation and migration of rat vascular smooth muscle cells. *Biochem. Biophys. Res. Commun.* **264,** 915-20.

Krause, D., Lyons, A., Fennelly, C. & O'Connor, R. (2001). Transient activation of Jun N-terminal kinases and protection from apoptosis by the insulin-like growth factor I receptor can be suppressed by dicumarol. *J. Biol. Chem.* **276,** 19244-52.

Kuwakado, K., Kubota, M., Bessho, R., Kataoka, A., Usami, I., Lin, Y.W., Okuda, A. & Wakazono, Y. (1995). Augmentation by aphidicolin of 1-beta-D-arabinofuranosylcytosine-induced c-jun and NF-kappa B activation in a human myeloid leukemia cell line: correlation with apoptosis. *Leuk. Res.* **19,** 645-50.

Kyriakis, J.M. & Avruch, J. (1996). Sounding the alarm: protein kinase cascades activated by stress and inflammation. *J. Biol. Chem.* **271,** 24313-6.

Laurent, E., Talpaz, M., Kantarjian, H. & Kurzrock, R. (2001). The BCR gene and philadelphia chromosome-positive leukemogenesis. *Cancer Res.* **61,** 2343-55.

Lennon, S.V., Martin, S.J. & Cotter, T.G. (1991). Dose-dependent induction of apoptosis in human tumour cell lines by widely diverging stimuli. *Cell Prolif.* **24,** 203-14.

Leppa, S. & Bohmann, D. (1999). Diverse functions of JNK signaling and c-Jun in stress response and apoptosis. *Oncogene* **18,** 6158-62.

Lerner, E.C., Qian, Y., Blaskovich, M.A., Fossum, R.D., Vogt, A., Sun, J., Cox, A.D., Der, C.J., Hamilton, A.D. & Sebti, S.M. (1995). Ras CAAX peptidomimetic FTI-277 selectively blocks oncogenic Ras signaling by inducing cytoplasmic accumulation of inactive Ras-Raf complexes. *J. Biol. Chem.* **270,** 26802-6.

Leung, I.W. & Lassam, N. (2001). The kinase activation loop is the key to mixed lineage kinase-3 activation via both autophosphorylation and hematopoietic progenitor kinase 1 phosphorylation. *J. Biol. Chem.* **276,** 1961-7.

Li, H. & Papadopoulos, V. (1998). Peripheral-type benzodiazepine receptor function in cholesterol transport. Identification of a putative cholesterol recognition/interaction amino

acid sequence and consensus pattern. *Endocrinology* **139,** 4991-7.

Li, H., Yao, Z., Degenhardt, B., Teper, G. & Papadopoulos, V. (2001a). Cholesterol binding at the cholesterol recognition/ interaction amino acid consensus (CRAC) of the peripheral-type benzodiazepine receptor and inhibition of steroidogenesis by an HIV TAT-CRAC peptide. *Proc. Natl. Acad. Sci. U S A* **98,** 1267-72.

Li, H., Zhu, H., Xu, C.J. & Yuan, J. (1998). Cleavage of BID by caspase 8 mediates the mitochondrial damage in the Fas pathway of apoptosis. *Cell.* **94,** 491-501.

Li, L.Y., Luo, X. & Wang, X. (2001b). Endonuclease G is an apoptotic DNase when released from mitochondria. *Nature* **412,** 95-9.

Li, P., Nijhawan, D., Budihardjo, I., Srinivasula, S.M., Ahmad, M., Alnemri, E.S. & Wang, X. (1997). Cytochrome c and dATP-dependent formation of Apaf-1/caspase-9 complex initiates an apoptotic protease cascade. *Cell* **91,** 479-89.

Liu, A., Cerniglia, G.J., Bernhard, E.J. and Prendergast, G.C. (2001). RhoB is required to mediate apoptosis in neoplastically transformed cells after DNA damage. *Proc. Natl. Acad. Sci. U S A* **98,** 6192-6197.

Liu, J., Wu, Y. & Arlinghaus, R.B. (1996). Sequences within the first exon of BCR inhibit the activated tyrosine kinases of c-Abl and the Bcr-Abl oncoprotein. *Cancer Res.* **56,** 5120-4.

Liu, L.F. & Miller, K.G. (1981). Eukaryotic DNA topoisomerases: two forms of type I DNA topoisomerases from HeLa cell nuclei. *Proc. Natl. Acad. Sci. U S A* **78,** 3487-91.

Loeffler, M. & Kroemer, G. (2000). The mitochondrion in cell death control: certainties and incognita. *Exp. Cell. Res.* **256,** 19-26.

Lown, J.W. & Joshua, A.V. (1979). Molecular mechanism of binding of pyrrolo(1,4)benzodiazepine antitumour agents to deoxyribonucleic acid--anthramycin and

tomaymycin. *Biochem. Pharmacol.* **28,** 2017-26.

Lown, J.W., Morgan, A.R., Yen, S.F., Wang, Y.H. & Wilson, W.D. (1985). Characteristics of the binding of the anticancer agents mitoxantrone and ametantrone and related structures to deoxyribonucleic acids. *Biochemistry* **24,** 4028-35.

Lozzio, B.B. & Lozzio, C.B. (1979). Properties and usefulness of the original K-562 human myelogenous leukemia cell line. *Leuk. Res.* **3,** 363-70.

Lozzio, C.B. & Lozzio, B.B. (1975). Human chronic myelogenous leukemia cell-line with positive Philadelphia chromosome. *Blood* **45,** 321-34.

Lugo, T.G. & Witte, O.N. (1989). The BCR-ABL oncogene transforms Rat-1 cells and cooperates with v-myc. *Mol. Cell. Biol.* **9,** 1263-70.

Mackay, D.J. & Hall, A. (1998). Rho GTPases. *J. Biol. Chem.* **273,** 20685-8.

Mahon, F.X., Deininger, M.W., Schultheis, B., Chabrol, J., Reiffers, J., Goldman, J.M. & Melo, J.V. (2000). Selection and characterization of BCR-ABL positive cell lines with differential sensitivity to the tyrosine kinase inhibitor STI571: diverse mechanisms of resistance. *Blood* **96,** 1070-9.

Mancini, M., Nicholson, D.W., Roy, S., Thornberry, N.A., Peterson, E.P., Casciola-Rosen, L.A. & Rosen, A. (1998). The caspase-3 precursor has a cytosolic and mitochondrial distribution: implications for apoptotic signaling. *J. Cell Biol.* **140,** 1485-95.

Markwell, M.A., Haas, S.M., Bieber, L.L. & Tolbert, N.E. (1978). A modification of the Lowry procedure to simplify protein determination in membrane and lipoprotein samples. *Anal. Biochem.* **87,** 206-10.

Maroney, A.C., Finn, J.P., Connors, T.J., Durkin, J.T., Angeles, T., Gessner, G., Xu, Z., Meyer, S.L., Savage, M.J., Greene, L.A., Scott, R.W. & Vaught, J.L. (2001). Cep-1347

(kt7515), a semisynthetic inhibitor of the mixed lineage kinase family. *J. Biol. Chem.* **276,** 25302-8.

Maroney, A.C., Glicksman, M.A., Basma, A.N., Walton, K.M., Knight, E., Jr., Murphy, C.A., Bartlett, B.A., Finn, J.P., Angeles, T., Matsuda, Y., Neff, N.T. & Dionne, C.A. (1998). Motoneuron apoptosis is blocked by CEP-1347 (KT 7515), a novel inhibitor of the JNK signaling pathway. *J. Neurosci.* **18,** 104-11.

Martin, S.J., O'Brien, G.A., Nishioka, W.K., McGahon, A.J., Mahboubi, A., Saido, T.C. & Green, D.R. (1995). Proteolysis of fodrin (non-erythroid spectrin) during apoptosis. *J. Biol. Chem.* **270,** 6425-8.

Martinou, J.C. (1999). Apoptosis. Key to the mitochondrial gate. *Nature* **399,** 411-2.

Martins, L.M., Mesner, P.W., Kottke, T.J., Basi, G.S., Sinha, S., Tung, J.S., Svingen, P.A., Madden, B.J., Takahashi, A., McCormick, D.J., Earnshaw, W.C. & Kaufmann, S.H. (1997). Comparison of caspase activation and subcellular localization in HL-60 and K562 cells undergoing etoposide-induced apoptosis. *Blood* **90,** 4283-96.

Marzo, I., Brenner, C., Zamzami, N., Jurgensmeier, J.M., Susin, S.A., Vieira, H.L., Prevost, M.C., Xie, Z., Matsuyama, S., Reed, J.C. & Kroemer, G. (1998). Bax and adenine nucleotide translocator cooperate in the mitochondrial control of apoptosis. *Science* **281,** 2027-31.

Matozaki, T., Nakanishi, H. & Takai, Y. (2000). Small G-protein networks: their crosstalk and signal cascades. *Cell Signal* **12,** 515-24.

Maundrell, K., Antonsson, B., Magnenat, E., Camps, M., Muda, M., Chabert, C., Gillieron, C., Boschert, U., Vial-Knecht, E., Martinou, J.C. & Arkinstall, S. (1997). Bcl-2 undergoes phosphorylation by c-Jun N-terminal kinase/stress- activated protein kinases in the presence of the constitutively active GTP-binding protein Rac1. *J. Biol. Chem.* **272,** 25238-42.

Mauro, M.J. & Druker, B.J. (2001). STI571: targeting bcr-abl as therapy for CML. *Oncologist*

6, 233-8.

Mayo, M.W. & Baldwin, A.S. (2000). The transcription factor NF-kappaB: control of oncogenesis and cancer therapy resistance. *Biochim. Biophys. Acta.* **1470,** M55-62.

McGahon, A., Cotter, T.G. and Green, D.R. (1994a). The abl oncogene family and apoptosis. *Cell Death Diff.* **1,** 77-83.

McGahon, A., Bissonnette, R., Schmitt, M., Cotter, K.M., Green, D.R. & Cotter, T.G. (1994b). BCR-ABL maintains resistance of chronic myelogenous leukemia cells to apoptotic cell death. *Blood* **83,** 1179-87.

McGowan, A.J., Ruiz-Ruiz, M.C., Gorman, A.M., Lopez-Rivas, A. & Cotter, T.G. (1996). Reactive oxygen intermediate(s) (ROI): common mediator(s) of poly(ADP-ribose)polymerase (PARP) cleavage and apoptosis. *FEBS Lett.* **392,** 299-303.

McWhirter, J.R. & Wang, J.Y. (1993). An actin-binding function contributes to transformation by the Bcr-Abl oncoprotein of Philadelphia chromosome-positive human leukemias. *Embo. J.* **12,** 1533-46.

Mehmet, H. (2000). Caspases find a new place to hide. *Nature* **403,** 29-30.

Meier, P., Finch, A. & Evan, G. (2000). Apoptosis in development. *Nature* **407,** 796-801.

Million, R.P. & Van Etten, R.A. (2000). The Grb2 binding site is required for the induction of chronic myeloid leukemia-like disease in mice by the Bcr/Abl tyrosine kinase. *Blood* **96,** 664-70.

Milne, D.M., Campbell, L.E., Campbell, D.G. & Meek, D.W. (1995). p53 is phosphorylated *in vitro* and *in vivo* by an ultraviolet radiation- induced protein kinase characteristic of the c-Jun kinase, JNK1. *J. Biol. Chem.* **270,** 5511-8.

Minden, A. & Karin, M. (1997). Regulation and function of the JNK subgroup of MAP kinases. *Biochim. Biophys. Acta.* **1333,** F85-104.

Minden, A., Lin, A., McMahon, M., Lange-Carter, C., Derijard, B., Davis, R.J., Johnson, G.L. & Karin, M. (1994). Differential activation of ERK and JNK mitogen-activated protein kinases by Raf-1 and MEKK. *Science* **266,** 1719-23.

Miramar, M.D., Costantini, P., Ravagnan, L., Saraiva, L.M., Haouzi, D., Brothers, G., Penninger, J.M., Peleato, M.L., Kroemer, G. & Susin, S.A. (2001). NADH oxidase activity of mitochondrial apoptosis-inducing factor. *J. Biol. Chem.* **276,** 16391-8.

Missy, K., Van Poucke, V., Raynal, P., Viala, C., Mauco, G., Plantavid, M., Chap, H. & Payrastre, B. (1998). Lipid products of phosphoinositide 3-kinase interact with Rac1 GTPase and stimulate GDP dissociation. *J. Biol. Chem.* **273,** 30279-86.

Mo, Y.Y. & Beck, W.T. (1999). DNA damage signals induction of fas ligand in tumor cells. *Mol. Pharmacol.* **55,** 216-22.

Morgan, S.E., Cadena, R.S., Raimondi, S.C. & Beck, W.T. (2000). Selection of human leukemic CEM cells for resistance to the DNA topoisomerase II catalytic inhibitor ICRF-187 results in increased levels of topoisomerase IIalpha and altered G(2)/M checkpoint and apoptotic responses. *Mol. Pharmacol.* **57,** 296-307.

Muchmore, S.W., Sattler, M., Liang, H., Meadows, R.P., Harlan, J.E., Yoon, H.S., Nettesheim, D., Chang, B.S., Thompson, C.B., Wong, S.L., Ng, S.L. & Fesik, S.W. (1996). X-ray and NMR structure of human Bcl-xL, an inhibitor of programmed cell death. *Nature* **381,** 335-41.

Muhlenbeck, F., Haas, E., Schwenzer, R., Schubert, G., Grell, M., Smith, C., Scheurich, P. & Wajant, H. (1998). TRAIL/Apo2L activates c-Jun NH_2-terminal kinase (JNK) via caspase-dependent and caspase-independent pathways. *J. Biol. Chem.* **273,** 33091-8.

Mulvaney, J.M. & Roberson, M.S. (2000). Divergent signaling pathways requiring discrete calcium signals mediate concurrent activation of two mitogen-activated protein kinases by gonadotropin-releasing hormone. *J. Biol. Chem.* **275,** 14182-9.

Murasawa, S., Matsubara, H., Mori, Y., Masaki, H., Tsutsumi, Y., Shibasaki, Y., Kitabayashi, I., Tanaka, Y., Fujiyama, S., Koyama, Y., Fujiyama, A., Iba, S. & Iwasaka, T. (2000). Angiotensin II initiates tyrosine kinase Pyk2-dependent signalings leading to activation of Rac1-mediated c-Jun NH2-terminal kinase. *J. Biol. Chem.* **275,** 26856-63.

Nicholson, D.W. (2000). From bench to clinic with apoptosis-based therapeutic agents. *Nature* **407,** 810-6.

Nicholson, D.W., Ali, A., Thornberry, N.A., Vaillancourt, J.P., Ding, C.K., Gallant, M., Gareau, Y., Griffin, P.R., Labelle, M., Lazebnik, Y.A. & et al. (1995). Identification and inhibition of the ICE/CED-3 protease necessary for mammalian apoptosis. *Nature* **376,** 37-43.

Nicholson, D.W. & Thornberry, N.A. (1997). Caspases: killer proteases. *Trends Biochem. Sci.* **22,** 299-306.

Nigam, M., Seong, C.M., Qian, Y., Hamilton, A.D. & Sebti, S.M. (1993). Potent inhibition of human tumor p21ras farnesyltransferase by A1A2- lacking p21ras CA1A2X peptidomimetics. *J. Biol. Chem.* **268,** 20695-8.

Nomura, M., Shimizu, S., Ito, T., Narita, M., Matsuda, H. & Tsujimoto, Y. (1999). Apoptotic cytosol facilitates Bax translocation to mitochondria that involves cytosolic factor regulated by Bcl-2. *Cancer Res.* **59,** 5542-8.

Nouraini, S., Six, E., Matsuyama, S., Krajewski, S. & Reed, J.C. (2000). The putative pore-forming domain of Bax regulates mitochondrial localization and interaction with Bcl-X(L). *Mol. Cell Biol.* **20,** 1604-15.

Oetzel, C., Jonuleit, T., Gotz, A., van der Kuip, H., Michels, H., Duyster, J., Hallek, M. &

Aulitzky, W.E. (2000). The tyrosine kinase inhibitor CGP 57148 (ST1 571) induces apoptosis in BCR-ABL-positive cells by down-regulating BCL-X. *Clin. Cancer Res.* **6,** 1958-68.

Ohkubo, T., Kamamoto, T., Kita, K., Hiraoka, A., Yoshida, Y. & Uchino, H. (1985). A novel Ph1 chromosome positive cell line established from a patient with chronic myelogenous leukemia in blastic crisis. *Leuk. Res.* **9,** 921-6.

Oliff, A. (1999). Farnesyltransferase inhibitors: targeting the molecular basis of cancer. *Biochim. Biophys. Acta.* **1423,** C19-30.

Oltvai, Z.N., Milliman, C.L. & Korsmeyer, S.J. (1993). Bcl-2 heterodimerizes in vivo with a conserved homolog, Bax, that accelerates programmed cell death. *Cell* **74,** 609-19.

Ono, K. & Han, J. (2000). The p38 signal transduction pathway: activation and function. *Cell Signal* **12,** 1-13.

Orth, K., Chinnaiyan, A.M., Garg, M., Froelich, C.J. & Dixit, V.M. (1996). The CED-3/ICE-like protease Mch2 is activated during apoptosis and cleaves the death substrate lamin A. *J. Biol. Chem.* **271,** 16443-6.

Osborn, L., Kunkel, S. and Nabel, G.J. (1986). TNF alpha and IL-1 stimulate the human immunodeficiency virus enhancer by activation of NFκB. *Proc. Natl. Acad. Sci. U S A* **86,** 2336-2340.

Osborn, M.T. & Chambers, T.C. (1996). Role of the stress-activated/c-Jun NH2-terminal protein kinase pathway in the cellular response to adriamycin and other chemotherapeutic drugs. *J. Biol. Chem.* **271,** 30950-5.

Pan, G., O'Rourke, K. & Dixit, V.M. (1998). Caspase-9, Bcl-XL, and Apaf-1 form a ternary complex. *J. Biol. Chem.* **273,** 5841-5.

Papadopoulos, V., Boujrad. N., Ikonomovic M.D., Ferrara, P. and Vidic B. (1994).

Topography of the leydig cell mitochondrial peripheral-type benzodiazepine receptor. *Mol. Cell. Endocrinology* **104,** R5-R9.

Papadopoulos, V., Amri, H., boujrad, N., Cascio, C., Culty, M., Garnier, M., Hardwick, M., Li, H., Vidic, B., Brown, A.S., Reversa J.L., Bernassau, J.M. and Drieu, K. (1997). peripheral benzodiazepine receptor in cholesterol transport and steroidogenesis. *Steroids* **62,** 21-28.

Pastorino, J.G., Simbula, G., Yamamoto, K., Glascott, P.A., Jr., Rothman, R.J. & Farber, J.L. (1996). The cytotoxicity of tumor necrosis factor depends on induction of the mitochondrial permeability transition. *J. Biol. Chem.* **271,** 29792-8.

Payne, D.M., Rossomando, A.J., Martino, P., Erickson, A.K., Her, J.H., Shabanowitz, J., Hunt, D.F., Weber, M.J. & Sturgill, T.W. (1991). Identification of the regulatory phosphorylation sites in pp42/mitogen- activated protein kinase (MAP kinase). *Embo. J.* **10,** 885-92.

Pendergast, A.M., Muller, A.J., Havlik, M.H., Maru, Y. & Witte, O.N. (1991). BCR sequences essential for transformation by the BCR-ABL oncogene bind to the ABL SH2 regulatory domain in a non-phosphotyrosine-dependent manner. *Cell* **66,** 161-71.

Pendergast, A.M., Quilliam, L.A., Cripe, L.D., Bassing, C.H., Dai, Z., Li, N., Batzer, A., Rabun, K.M., Der, C.J., Schlessinger, J., Mikhail, L. & Gishizky, M.L. (1993). BCR-ABL-induced oncogenesis is mediated by direct interaction with the SH2 domain of the GRB-2 adaptor protein. *Cell* **75,** 175-85.

Perez, C., Vilaboa, N.E., Garcia-Bermejo, L., de Blas, E., Creighton, A.M. & Aller, P. (1997). Differentiation of U-937 promonocytic cells by etoposide and ICRF-193, two antitumour DNA topoisomerase II inhibitors with different mechanisms of action. *J. Cell Sci.* **110,** 337-43.

Peters, D.G., Hoover, R.R., Gerlach, M.J., Koh, E.Y., Zhang, H., Choe, K., Kirschmeier, P., Bishop, W.R. & Daley, G.Q. (2001). Activity of the farnesyl protein transferase inhibitor

SCH66336 against BCR/ABL-induced murine leukemia and primary cells from patients with chronic myeloid leukemia. *Blood* **97,** 1404-12.

Pombo, C.M., Kehrl, J.H., Sanchez, I., Katz, P., Avruch, J., Zon, L.I., Woodgett, J.R., Force, T. & Kyriakis, J.M. (1995). Activation of the SAPK pathway by the human STE20 homologue germinal centre kinase. *Nature* **377,** 750-4.

Pommier, Y., Pourquier, P., Fan, Y. & Strumberg, D. (1998). Mechanism of action of eukaryotic DNA topoisomerase I and drugs targeted to the enzyme. *Biochim. Biophys. Acta.* **1400,** 83-105.

Prendergast, G.C. & Oliff, A. (2000). Farnesyltransferase inhibitors: antineoplastic properties, mechanisms of action, and clinical prospects. *Semin. Cancer Biol.* **10,** 443-52.

Puil, L., Liu, J., Gish, G., Mbamalu, G., Bowtell, D., Pelicci, P.G., Arlinghaus, R. & Pawson, T. (1994). Bcr-Abl oncoproteins bind directly to activators of the Ras signalling pathway. *Embo. J.* **13,** 764-73.

Puls, A., Eliopoulos, A.G., Nobes, C.D., Bridges, T., Young, L.S. & Hall, A. (1999). Activation of the small GTPase Cdc42 by the inflammatory cytokines TNF(alpha) and IL-1, and by the Epstein-Barr virus transforming protein LMP1. *J. Cell Sci.* **112,** 2983-92.

Qian, Y., Blaskovich, M.A., Saleem, M., Seong, C.M., Wathen, S.P., Hamilton, A.D. & Sebti, S.M. (1994). Design and structural requirements of potent peptidomimetic inhibitors of p21ras farnesyltransferase. *J. Biol. Chem.* **269,** 12410-3.

Qiu, R.G., Abo, A., McCormick, F. & Symons, M. (1997). Cdc42 regulates anchorage-independent growth and is necessary for Ras transformation. *Mol. Cell Biol.* **17,** 3449-58.

Raff, M. (1998). Cell suicide for beginners. *Nature*. **396,** 119-22.

Raitano, A.B., Halpern, J.R., Hambuch, T.M. & Sawyers, C.L. (1995). The Bcr-Abl leukemia

oncogene activates Jun kinase and requires Jun for transformation. *Proc. Natl. Acad. Sci. USA* **92,** 11746-50.

Ray, S., Bullock, G., Nunez, G., Tang, C., Ibrado, A.M., Huang, Y. & Bhalla, K. (1996). Enforced expression of Bcl-XS induces differentiation and sensitizes chronic myelogenous leukemia-blast crisis K562 cells to 1-beta-D-arabinofuranosylcytosine-mediated differentiation and apoptosis. *Cell Growth Differ.* **7,** 1617-23.

Reiss, Y., Goldstein, J.L., Seabra, M.C., Casey, P.J. & Brown, M.S. (1990). Inhibition of purified p21ras farnesyl:protein transferase by Cys-AAX tetrapeptides. *Cell* **62,** 81-8.

Resh, M.D. (1990). Membrane interactions of pp60v-src: a model for myristylated tyrosine protein kinases. *Oncogene* **5,** 1437-44.

Rey, C., Mauduit, C., Naureils, O., Benahmed, M., Louisot, P. & Gasnier, F. (2000). Up-regulation of mitochondrial peripheral benzodiazepine receptor expression by tumor necrosis factor alpha in testicular leydig cells. Possible involvement in cell survival. *Biochem. Pharmacol.* **60,** 1639-46.

Riordan, F.A., Bravery, C.A., Mengubas, K., Ray, N., Borthwick, N.J., Akbar, A.N., Hart, S.M., Hoffbrand, A.V., Mehta, A.B. & Wickremasinghe, R.G. (1998). Herbimycin A accelerates the induction of apoptosis following etoposide treatment or gamma-irradiation of bcr/abl-positive leukaemia cells. *Oncogene* **16,** 1533-42.

Ritke, M.K., Allan, W.P., Fattman, C., Gunduz, N.N. & Yalowich, J.C. (1994a). Reduced phosphorylation of topoisomerase II in etoposide-resistant human leukemia K562 cells. *Mol. Pharmacol.* **46,** 58-66.

Ritke, M.K., Murray, N.R., Allan, W.P., Fields, A.P. & Yalowich, J.C. (1995). Hypophosphorylation of topoisomerase II in etoposide (VP-16)-resistant human leukemia K562 cells associated with reduced levels of beta II protein kinase C. *Mol. Pharmacol.* **48,** 798-805.

Ritke, M.K., Rusnak, J.M., Lazo, J.S., Allan, W.P., Dive, C., Heer, S. & Yalowich, J.C. (1994b). Differential induction of etoposide-mediated apoptosis in human leukemia HL-60 and K562 cells. *Mol. Pharmacol.* **46,** 605-11.

Roberge, M., Tudan, C., Hung, S.M., Harder, K.W., Jirik, F.R. & Anderson, H. (1994). Antitumor drug fostriecin inhibits the mitotic entry checkpoint and protein phosphatases 1 and 2A. *Cancer Res.* **54,** 6115-21.

Roca, J., Ishida, R., Berger, J.M., Andoh, T. & Wang, J.C. (1994). Antitumor bisdioxopiperazines inhibit yeast DNA topoisomerase II by trapping the enzyme in the form of a closed protein clamp. *Proc. Natl. Acad. Sci. U S A* **91,** 1781-5.

Rowe, T.C., Chen, G.L., Hsiang, Y.H. & Liu, L.F. (1986). DNA damage by antitumor acridines mediated by mammalian DNA topoisomerase II. *Cancer Res.* **46,** 2021-6.

Rowley, P.T., Keng, P.C. & Kosciolek, B.A. (1996). The effect of bcr-abl antisense oligonucleotide on DNA synthesis and apoptosis in K562 chronic myeloid leukemia cells. *Leuk. Res.* **20,** 473-80.

Sakai, N., Ogiso, Y., Fujita, H., Watari, H., Koike, T. & Kuzumaki, N. (1994). Induction of apoptosis by a dominant negative H-RAS mutant (116Y) in K562 cells. *Exp. Cell Res.* **215,** 131-6.

Salomoni, P., Condorelli, F., Sweeney, S.M. & Calabretta, B. (2000). Versatility of BCR/ABL-expressing leukemic cells in circumventing proapoptotic BAD effects. *Blood* **96,** 676-84.

Salomoni, P., Wasik, M.A., Riedel, R.F., Reiss, K., Choi, J.K., Skorski, T. & Calabretta, B. (1998). Expression of constitutively active Raf-1 in the mitochondria restores antiapoptotic and leukemogenic potential of a transformation-deficient BCR/ABL mutant. *J. Exp. Med.* **187,** 1995-2007.

Samali, A., Gorman, A.M. & Cotter, T.G. (1997). Role of Bcr-Abl kinase in resistance to apoptosis. *Adv. Pharmacol.* **41,** 533-52.

Sanchez, I., Hughes, R.T., Mayer, B.J., Yee, K., Woodgett, J.R., Avruch, J., Kyriakis, J.M. & Zon, L.I. (1994). Role of SAPK/ERK kinase-1 in the stress-activated pathway regulating transcription factor c-Jun. *Nature* **372,** 794-8.

Sanchez-Garcia, I. & Grutz, G. (1995). Tumorigenic activity of the BCR-ABL oncogenes is mediated by BCL2. *Proc. Natl. Acad. Sci. U S A* **92,** 5287-91.

Sattler, M., Liang, H., Nettesheim, D., Meadows, R.P., Harlan, J.E., Eberstadt, M., Yoon, H.S., Shuker, S.B., Chang, B.S., Minn, A.J., Thompson, C.B. & Fesik, S.W. (1997). Structure of Bcl-xL-Bak peptide complex: recognition between regulators of apoptosis. *Science* **275,** 983-6.

Scarlett, J.L. & Murphy, M.P. (1997). Release of apoptogenic proteins from the mitochondrial intermembrane space during the mitochondrial permeability transition. *FEBS Lett.* **418,** 282-6.

Schendel, S.L., Xie, Z., Montal, M.O., Matsuyama, S., Montal, M. & Reed, J.C. (1997). Channel formation by antiapoptotic protein Bcl-2. *Proc. Natl. Acad. Sci. U S A* **94,** 5113-8.

Schindler, T., Bornmann, W., Pellicena, P., Miller, W.T., Clarkson, B. & Kuriyan, J. (2000). Structural mechanism for STI-571 inhibition of abelson tyrosine kinase. *Science* **289,** 1938-42.

Seimiya, H., Mashima, T., Toho, M. & Tsuruo, T. (1997). c-Jun NH_2-terminal kinase-mediated activation of interleukin-1beta converting enzyme/CED-3-like protease during anticancer drug-induced apoptosis. *J. Biol. Chem.* **272,** 4631-6.

Sen, R. & Baltimore, D. (1986). Inducibility of kappa immunoglobulin enhancer-binding protein Nf-kappa B by a posttranslational mechanism. *Cell* **47,** 921-8.

Senechal, K. & Sawyers, C.L. (1996). Signal transduction-based strategies for the treatment of chronic myelogenous leukemia. *Mol. Med. Today* **2,** 503-9.

Shao, J., Sheng, H., DuBois, R.N. & Beauchamp, R.D. (2000). Oncogenic Ras-mediated cell growth arrest and apoptosis are associated with increased ubiquitin-dependent cyclin D1 degradation. *J. Biol. Chem.* **275,** 22916-24.

Shaulian, E. & Karin, M. (1999). Stress-induced JNK activation is independent of Gadd45 induction. *J. Biol. Chem.* **274,** 29595-8.

Shi, C.S. & Kehrl, J.H. (1997). Activation of stress-activated protein kinase/c-Jun N-terminal kinase, but not NF-kappaB, by the tumor necrosis factor (TNF) receptor 1 through a TNF receptor-associated factor 2- and germinal center kinase related-dependent pathway. *J. Biol. Chem.* **272,** 32102-7.

Shimizu, S., Narita, M. & Tsujimoto, Y. (1999). Bcl-2 family proteins regulate the release of apoptogenic cytochrome c by the mitochondrial channel VDAC. *Nature* **399,** 483-7.

Shuai, K., Halpern, J., ten Hoeve, J., Rao, X. & Sawyers, C.L. (1996). Constitutive activation of STAT5 by the BCR-ABL oncogene in chronic myelogenous leukemia. *Oncogene* **13,** 247-54.

Sillaber, C., Gesbert, F., Frank, D.A., Sattler, M. & Griffin, J.D. (2000). STAT5 activation contributes to growth and viability in Bcr/Abl- transformed cells. *Blood* **95,** 2118-25.

Singh, N.P. (2000). A simple method for accurate estimation of apoptotic cells. *Exp. Cell Res.* **256,** 328-37.

Srivastava, R.K., Mi, Q.S., Hardwick, J.M. & Longo, D.L. (1999). Deletion of the loop region of Bcl-2 completely blocks paclitaxel-induced apoptosis. *Proc. Natl. Acad. Sci. U S A* **96,** 3775-80.

Steller, H. (1995). Mechanisms and genes of cellular suicide. *Science* **267,** 1445-9.

Su, Y.C., Han, J., Xu, S., Cobb, M. & Skolnik, E.Y. (1997). NIK is a new Ste20-related kinase that binds NCK and MEKK1 and activates the SAPK/JNK cascade via a conserved regulatory domain. *Embo. J.* **16,** 1279-90.

Sun, X.M., MacFarlane, M., Zhuang, J., Wolf, B.B., Green, D.R. & Cohen, G.M. (1999). Distinct caspase cascades are initiated in receptor-mediated and chemical-induced apoptosis. *J. Biol. Chem.* **274,** 5053-60.

Susin, S.A., Lorenzo, H.K., Zamzami, N., Marzo, I., Brenner, C., Larochette, N., Prevost, M.C., Alzari, P.M. & Kroemer, G. (1999a). Mitochondrial release of caspase-2 and -9 during the apoptotic process. *J. Exp. Med.* **189,** 381-94.

Susin, S.A., Lorenzo, H.K., Zamzami, N., Marzo, I., Snow, B.E., Brothers, G.M., Mangion, J., Jacotot, E., Costantini, P., Loeffler, M., Larochette, N., Goodlett, D.R., Aebersold, R., Siderovski, D.P., Penninger, J.M. & Kroemer, G. (1999b). Molecular characterization of mitochondrial apoptosis-inducing factor. *Nature* **397,** 441-6.

Suzuki, N., Urano, J. & Tamanoi, F. (1998). Farnesyltransferase inhibitors induce cytochrome c release and caspase 3 activation preferentially in transformed cells. *Proc. Natl. Acad. Sci. U S A* **95,** 15356-61.

Szczylik, C., Skorski, T., Nicolaides, N.C., Manzella, L., Malaguarnera, L., Venturelli, D., Gewirtz, A.M. & Calabretta, B. (1991). Selective inhibition of leukemia cell proliferation by BCR-ABL antisense oligodeoxynucleotides. *Science* **253,** 562-5.

Tafani, M., Minchenko, D.A., Serroni, A. & Farber, J.L. (2001). Induction of the mitochondrial permeability transition mediates the killing of HeLa cells by staurosporine. *Cancer Res.* **61,** 2459-66.

Talanian, R.V., Quinlan, C., Trautz, S., Hackett, M.C., Mankovich, J.A., Banach, D., Ghayur,

T., Brady, K.D. & Wong, W.W. (1997). Substrate specificities of caspase family proteases. *J. Biol. Chem.* **272,** 9677-82.

Tanabe, K., Ikegami, Y., Ishida, R. & Andoh, T. (1991). Inhibition of topoisomerase II by antitumor agents bis(2,6- dioxopiperazine) derivatives. *Cancer Res.* **51,** 4903-8.

Teramoto, H., Coso, O.A., Miyata, H., Igishi, T., Miki, T. & Gutkind, J.S. (1996). Signaling from the small GTP-binding proteins Rac1 and Cdc42 to the c- Jun N-terminal kinase/stress-activated protein kinase pathway. A role for mixed lineage kinase 3/protein-tyrosine kinase 1, a novel member of the mixed lineage kinase family. *J. Biol. Chem.* **271,** 27225-8.

Thornberry, N.A. & Lazebnik, Y. (1998). Caspases: enemies within. *Science* **281,** 1312-6.

To, L.B., Haylock, D.N., Simmons, P.J. & Juttner, C.A. (1997). The biology and clinical uses of blood stem cells. *Blood* **89,** 2233-58.

Tolias, K.F., Cantley, L.C. & Carpenter, C.L. (1995). Rho family GTPases bind to phosphoinositide kinases. *J. Biol. Chem.* **270,** 17656-9.

Tsujimoto, Y. (1998). Role of Bcl-2 family proteins in apoptosis: apoptosomes or mitochondria? *Genes Cell* **3,** 697-707.

Tsujimoto, Y. & Shimizu, S. (2000). Bcl-2 family: life-or-death switch. *FEBS Lett.* **466,** 6-10.

Uckun, F.M., Tuel-Ahlgren, L., Song, C.W., Waddick, K., Myers, D.E., Kirihara, J., Ledbetter, J.A. & Schieven, G.L. (1992). Ionizing radiation stimulates unidentified tyrosine-specific protein kinases in human B-lymphocyte precursors, triggering apoptosis and clonogenic cell death. *Proc. Natl. Acad. Sci. U S A* **89,** 9005-9.

Urbano, A., Koc, Y. & Foss, F.M. (1998). Arginine butyrate downregulates p210 bcr-abl expression and induces apoptosis in chronic myelogenous leukemia cells. *Leukemia* **12,** 930-6.

Vaerman, J.L., Lammineur, C., Moureau, P., Lewalle, P., Deldime, F., Blumenfeld, M. & Martiat, P. (1995). BCR-ABL antisense oligodeoxyribonucleotides suppress the growth of leukemic and normal hematopoietic cells by a sequence-specific but nonantisense mechanism. *Blood* **86,** 3891-6.

Vaux, D.L., Weissman, I.L. & Kim, S.K. (1992). Prevention of programmed cell death in Caenorhabditis elegans by human bcl-2. *Science* **258,** 1955-7.

Vogt, A., Qian, Y., Blaskovich, M.A., Fossum, R.D., Hamilton, A.D. & Sebti, S.M. (1995). A non-peptide mimetic of Ras-CAAX: selective inhibition of farnesyltransferase and Ras processing. *J. Biol. Chem.* **270,** 660-4.

Wang, Y., Zhou, R., Liliemark, J., Gruber, A., Lindemalm, S., Albertioni, F. & Liliemark, E. (2001). *In vitro* topo II--DNA complex accumulation and cytotoxicity of etoposide in leukaemic cells from patients with acute myelogenous and chronic lymphocytic leukaemia. *Leuk. Res.* **25,** 133-40.

Weisberg, E. & Griffin, J.D. (2000). Mechanism of resistance to the ABL tyrosine kinase inhibitor STI571 in BCR/ABL-transformed hematopoietic cell lines. *Blood* **95,** 3498-505.

Weng, L.P., Yuan, J. & Yu, Q. (1998). Overexpression of the transmembrane tyrosine phosphatase LAR activates the caspase pathway and induces apoptosis. *Curr. Biol.* **8,** 247-56.

Whitmarsh, A.J., Cavanagh, J., Tournier, C., Yasuda, J. & Davis, R.J. (1998). A mammalian scaffold complex that selectively mediates MAP kinase activation. *Science* **281,** 1671-4.

Wilkinson, G.N. (1961). *Biochem. J.* **80,** 324-332.

Wolf, B.B. & Green, D.R. (1999). Suicidal tendencies: apoptotic cell death by caspase family proteinases. *J. Biol. Chem.* **274,** 20049-52.

Wolf, B.B., Schuler, M., Echeverri, F. & Green, D.R. (1999). Caspase-3 is the primary

activator of apoptotic DNA fragmentation via DNA fragmentation factor-45/inhibitor of caspase-activated DNase inactivation. *J. Biol. Chem.* **274,** 30651-6.

Wu, Y., Ma, G., Lu, D., Lin, F., Xu, H.J., Liu, J. & Arlinghaus, R.B. (1999). Bcr: a negative regulator of the Bcr-Abl oncoprotein. *Oncogene* **18,** 4416-24.

Xia, Z., Dickens, M., Raingeaud, J., Davis, R.J. & Greenberg, M.E. (1995). Opposing effects of ERK and JNK-p38 MAP kinases on apoptosis. *Science* **270,** 1326-31.

Xiang, J., Chao, D.T. & Korsmeyer, S.J. (1996). BAX-induced cell death may not require interleukin 1 beta-converting enzyme-like proteases. *Proc. Natl. Acad. Sci. U S A* **93,** 14559-63.

Yamamoto, K., Ichijo, H. & Korsmeyer, S.J. (1999). BCL-2 is phosphorylated and inactivated by an ASK1/Jun N-terminal protein kinase pathway normally activated at G(2)/M. *Mol. Cell. Biol.* **19,** 8469-78.

Yang, E., Zha, J., Jockel, J., Boise, L.H., Thompson, C.B. & Korsmeyer, S.J. (1995). Bad, a heterodimeric partner for Bcl-XL and Bcl-2, displaces Bax and promotes cell death. *Cell* **80,** 285-91.

Yao, Z., Zhou, G., Wang, X.S., Brown, A., Diener, K., Gan, H. & Tan, T.H. (1999). A novel human STE20-related protein kinase, HGK, that specifically activates the c-Jun N-terminal kinase signaling pathway. *J. Biol. Chem.* **274,** 2118-25.

Yasuda, J., Whitmarsh, A.J., Cavanagh, J., Sharma, M. & Davis, R.J. (1999). The JIP group of mitogen-activated protein kinase scaffold proteins. *Mol. Cell Biol.* **19,** 7245-54.

Yousefi, S., Green, D.R., Blaser, K. & Simon, H.U. (1994). Protein-tyrosine phosphorylation regulates apoptosis in human eosinophils and neutrophils. *Proc. Natl. Acad. Sci. U S A* **91,** 10868-72.

Yuasa, T., Ohno, S., Kehrl, J.H. & Kyriakis, J.M. (1998). Tumor necrosis factor signaling to stress-activated protein kinase (SAPK)/Jun NH_2-terminal kinase (JNK) and p38. Germinal center kinase couples TRAF2 to mitogen-activated protein kinase/ERK kinase kinase 1 and SAPK while receptor interacting protein associates with a mitogen- activated protein kinase kinase kinase upstream of MKK6 and p38. *J. Biol. Chem.* **273,** 22681-92.

Zamzami, N. & Kroemer, G. (1999). Condensed matter in cell death. *Nature* **401,** 127-8.

Zanke, B.W., Boudreau, K., Rubie, E., Winnett, E., Tibbles, L.A., Zon, L., Kyriakis, J., Liu, F.F. & Woodgett, J.R. (1996). The stress-activated protein kinase pathway mediates cell death following injury induced by cis-platinum, UV irradiation or heat. *Curr. Biol.* **6,** 606-13.

Zhang, S., Han, J., Sells, M.A., Chernoff, J., Knaus, U.G., Ulevitch, R.J. & Bokoch, G.M. (1995). Rho family GTPases regulate p38 mitogen-activated protein kinase through the downstream mediator Pak1. *J. Biol. Chem.* **270,** 23934-6.

Zisterer, D.M., Campiani, G., Nacci, V. & Williams, D.C. (2000). Pyrrolo-1,5-benzoxazepines induce apoptosis in HL-60, Jurkat, and Hut- 78 cells: a new class of apoptotic agents. *J. Pharmacol. Exp. Ther.* **293,** 48-59.

Zisterer, D.M., Hance, N., Campiani, G., Garofalo, A., Nacci, V. & Williams, D.C. (1998). Antiproliferative action of pyrrolobenzoxazepine derivatives in cultured cells: absence of correlation with binding to the peripheral- type benzodiazepine binding site. *Biochem. Pharmacol.* **55,** 397-403.

Zisterer, D.M. & Williams, D.C. (1997). Peripheral-type benzodiazepine receptors. *Gen. Pharmacol.* **29,** 305-14.

Zwelling, L.A., Hinds, M., Chan, D., Mayes, J., Sie, K.L., Parker, E., Silberman, L., Radcliffe, A., Beran, M. & Blick, M. (1989). Characterization of an amsacrine-resistant line of human leukemia cells. Evidence for a drug-resistant form of topoisomerase II. *J. Biol. Chem.* **264,** 16411-20.

Publications

Mc Gee, M.M., Campiani, G., Ramunno, A., Fattorusso, C., Nacci, V., Lawler, M., Williams, D.C. & Zisterer, D.M. (2001) Pyrrolo-1,5-benzoxazepines Induce Apoptosis in Chronic Myelogenous Leukemia (CML) Cells by Bypassing the Apoptotic Suppressor Bcr-Abl. *J. Pharmacol. Exp. Ther.* **296,** 31-40.

Zisterer, D.M., McGee, M.M., Campiani, G., Ramunno, A., Fattorusso, C., Nacci, V., Lawler, M. & Williams, D.C. Pyrrolo-1,5-benzoxazepines: A new class of apoptotic agents. *Biochem. Soc. Trans*. (2001, In Press).

0022-3565/01/2961-31–40$3.00
THE JOURNAL OF PHARMACOLOGY AND EXPERIMENTAL THERAPEUTICS
JPET 296:31–40, 2001
Copyright © 2001 by The American Society for Pharmacology and Experimental Therapeutics
Vol. 296, No. 1
0/869988
Printed in U.S.A.

Pyrrolo-1,5-benzoxazepines Induce Apoptosis in Chronic Myelogenous Leukemia (CML) Cells by Bypassing the Apoptotic Suppressor Bcr-Abl

MARGARET M. MC GEE, GIUSEPPE CAMPIANI, ANNA RAMUNNO, CATERINA FATTORUSSO, VITO NACCI, MARK LAWLER, D. CLIVE WILLIAMS, and DANIELA M. ZISTERER

Department of Biochemistry, Trinity College, Dublin, Ireland (M.M.M.G., D.C.W., D.M.Z.); Dipartimento Farmaco Chimico Tecnologico, Universita' degli Studi di Siena, Siena, Italy (G.C., V.N.); Dipartimento di Scienze Farmaceutiche, Universita' degli Studi di Salerno, Fisciano, Italy (A.R., C.F.); and Department of Haematology, Sir Patrick Dun Research Labs, St. James's Hospital and Trinity College, Dublin, Ireland (M.L.)

Received July 13, 2000; accepted September 13, 2000 This paper is available online at http://jpet.aspetjournals.org

ABSTRACT

Expression of the transforming oncogene *bcr-abl* in chronic myelogenous leukemia (CML) cells is reported to confer resistance against apoptosis induced by many chemotherapeutic agents such as etoposide, ara-C, and staurosporine. In the present study some members of a series of novel pyrrolo-1,5-benzoxazepines potently induce apoptosis, as shown by cell shrinkage, chromatin condensation, DNA fragmentation, and poly(ADP-ribose) polymerase (PARP) cleavage, in three CML cell lines, K562, KYO.1, and LAMA 84. Induction of apoptosis by a representative member of this series, PBOX-6, was not accompanied by either the down-regulation of Bcr-Abl or by the attenuation of its protein tyrosine kinase activity up to 24 h after treatment, when approximately 50% of the cells had undergone apoptosis. These results suggest that down-regulation of Bcr-Abl is not part of the upstream apoptotic death program activated by PBOX-6. By characterizing the mechanism in which this novel agent executes apoptosis, this study has revealed that PBOX-6 caused activation of caspase 3-like proteases in only two of the three CML cell lines. In addition, inhibition of caspase 3-like protease activity using the inhibitor z-DEVD-fmk blocked caspase 3-like protease activity but did not prevent the induction of apoptosis, suggesting that caspase 3-like proteases are not essential in the mechanism by which PBOX-6 induces apoptosis in CML cells. In conclusion, this study demonstrates that PBOX-6 can bypass Bcr-Abl-mediated suppression of apoptosis, suggesting an important potential use of these compounds in the treatment of CML.

Chronic myelogenous leukemia (CML) is a member of a group of diseases classed as myeloproliferative disorders, which account for 20% of all leukemias. CML is a clonal disorder that is usually easily recognized because the leukemia cells of more than 95% of patients suffering from CML have a distinctive cytogenetic abnormality, the Philadelphia chromosome. This results from a reciprocal translocation between the long arms of chromosomes 9 and 22. This translocation results in the transfer of the Abelson (*abl*) oncogene on chromosome 9 to an area of chromosome 22 that includes the breakpoint cluster region (*bcr*) gene. This results in the presentation of a leukemia-specific fusion gene (*bcr-abl*) that gives rise to an abnormal tyrosine kinase protein, p210, with increased activity (Clarkson et al., 1997; Cortez et al., 1997).

The tyrosine phosphorylation status of a protein is controlled by two antagonistic families of enzymes, protein tyrosine kinases and phosphatases. Phosphorylation and dephosphorylation of cellular proteins are implicated in many important processes such as cell growth and differentiation (Weng et al., 1998). The products of several proto-oncogenes, such as *bcr-abl,* are tyrosine kinases, and kinase activities are either increased or constitutively activated in the corresponding oncogenes (Bergamaschi et al., 1993).

Bcr-Abl expressing leukemic blasts are highly resistant to different classes of chemotherapeutic drugs. K562 cells, derived from patients with CML in blast crisis (Lozzio and Lozzio, 1975), which express p210 Bcr-Abl, have been shown to be highly resistant to apoptosis induced by many chemotherapeutic agents (McGahon et al., 1994; Amarante-Mendes et al., 1998). Overexpression of Bcr-Abl has been implicated in inhibiting apoptosis induced by cytokine deprivation, DNA damage, and a variety of chemotherapeutic drugs (Cortez et al., 1997). Thus, the Bcr-Abl fusion protein has been sug-

This study was supported by BioResearch Ireland, National Pharmaceutical Biotechnology Centre.

ABBREVIATIONS: CML, chronic myeloid leukemia; *abl,* Abelson; *bcr*, breakpoint cluster region; PARP, poly(ADP-ribose) polymerase; PBOX, pyrrolo-1,5-benzoxazepine; NAC, *N*-acetylcysteine; AMC, amino-4-methyl coumarin; fmk, fluoromethyl ketone; ROI, reactive oxygen intermediate; PAGE, polyacrylamide gel electrophoresis.

gested to function as does bcl-2, as an antiapoptotic factor and overexpression of the Bcr-Abl protein in K562 cells may in part account for the resistance of these cells to apoptosis, thereby leading to the accumulation of leukemic blasts in patients with chronic myeloid leukemia (Urbano et al., 1998).

Programmed cell death or apoptosis is an evolutionary conserved and genetically regulated biological process that plays an important role in the development and homeostasis of multicellular organisms (Wyllie et al., 1980). It is widely reported that mitochondria play a critical role in apoptosis. Mitochondria are the primary site of reactive oxygen species production within the cell. Many reports suggest an increase in the production of reactive oxygen species such as peroxides during apoptosis (McGowan et al., 1996), which may be prevented by antioxidants such as *N*-acetylcysteine.

The execution of apoptosis requires specific molecular machinery, the central component of which is a family of proteases called caspases. Caspases are cysteine proteases that cleave proteins after specific aspartate residues, in response to proapoptotic signals (Nicholson and Thornberry, 1997). During apoptosis caspases are thought to be activated in an amplifying proteolytic cascade, cleaving one another in sequence (Raff, 1998). One of the most widely studied caspases, caspase 3, is classed as an effector caspase and cleaves death substrates such as the structural proteins lamin and fodrin, and the nuclear protein poly(ADP-ribose) polymerase (PARP) (McGowan et al., 1996).

Recently a novel series of pyrrolo-1,5-benzoxazepines were synthesized (Campiani et al., 1996) and some of these compounds induce apoptosis in a number of cancerous cells such as the human promyelocytic leukemia HL-60 cell line, the human lymphoma Hut-78 cell line, and the human lymphoblast Jurkat cell line (Zisterer et al., 2000). The search for novel compounds that induce apoptosis in CML cells and that may be useful in the therapy of patients with CML is of importance. In the present study, a number of these novel pyrrolo-1,5-benzoxazepines (Fig. 1) were found to induce apoptosis in CML cells, including the extremely resistant K562 cell line. The *bcr-abl* oncogene is believed to be responsible for mediating the resistance of CML cells to the induction of apoptosis. We examined whether Bcr-Abl becomes down-regulated during PBOX-6-mediated apoptosis, and whether protein tyrosine kinase activity is altered. Zisterer et al. (2000) has recently shown that activation of caspase 3-like proteases is essential in the mechanism by which PBOX-6 induces apoptosis in HL-60 and Jurkat cells. In the current study, we tested the hypothesis that caspase 3-like proteases might play a role in PBOX-6-induced apoptosis in CML cells. We also examined the involvement of reactive oxygen intermediates in the apoptotic death program activated by PBOX-6. Finally, we discuss the potential of PBOX-6 as a novel anticancer drug for the treatment of chronic myeloid leukemia.

Experimental Procedures

Materials. The CML cells K562, KYO.1, and LAMA 84 were kindly supplied by Dr. Jane Apperley and Dr. Junia Melo, Department of Hematology, Imperial College, London, UK. These cell lines represent the different stages in the progression of CML. K562 and KYO.1 cells are derived from patients in blast crisis stage, whereas the LAMA 84 cells are derived from a patient in the accelerated stage. Human promyelocytic leukemia (HL-60), and human T-cell lymphoma (Jurkat T) cells were obtained from the European Collection of Animal Cell Culture, Salisbury, UK. CML and Jurkat T cells were grown in RPMI-1640 supplemented with 10% fetal calf serum, gentamicin (0.1 mg/ml), and L-glutamine (2 mM), all obtained from Sigma (Poole, Dorset, UK). HL-60 cells were maintained in similar medium containing 20% fetal calf serum. All cells were maintained in a humidified incubator with 95% air and 5% CO_2 at 37°C. The PBOX compounds were prepared as 1 mM stocks in ethanol and stored at −20°C. A 20 mM stock of etoposide (Sigma) was dissolved in ethanol:dimethyl sulfoxide (1:1) and stored at −20°C. Mitoxanthrone, 50 μM stock, and ara-C, 10 mM stock (Sigma), were dissolved in H_2O and stored at −20°C. *N*-Acetylcysteine (NAC) (100 mM) and vitamin E (1 mM) (Sigma) were dissolved in 25 mM Tris (pH 7.2) and PBS, respectively, whereas H_2O_2 (Sigma) was diluted in growth medium. The caspase 3-like fluorogenic substrate Ac-DEVD-AMC was obtained from Alexis (Nottingham, UK). The caspase 3-like inhibitor z-DEVD-fmk, and the caspase 6-like fluorogenic substrate Ac-VEID-AMC were supplied by Calbiochem-Novabiochem (Nottingham, UK). The RapiDiff kit was purchased from Diagnostic Developments (Burscough, Lancashire, UK). The enhanced chemiluminescence reagent was from Amersham Pharmacia Biotech (Aylesbury, UK). The anti-c-abl, anti-phosphotyrosine, and anti-PARP antibodies were supplied by Calbiochem-Novabiochem. The pro-caspase 3 and pro-caspase 7 antibodies were obtained from Transduction Laboratories (Lexington, KY). Anti β-actin was obtained from Sigma.

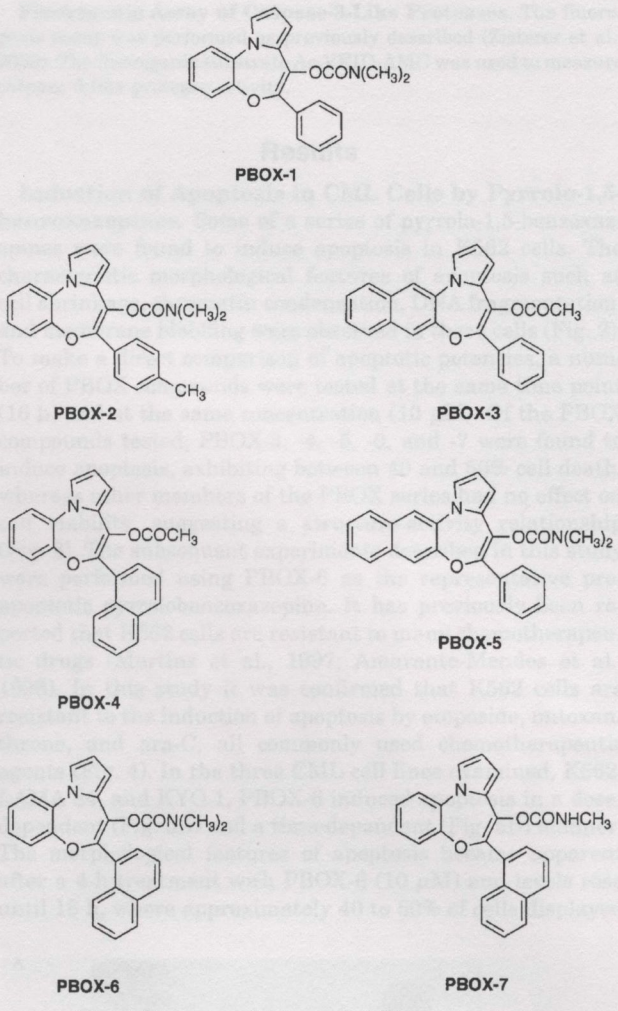

Fig. 1. Structures of the pyrrolo-1,5-benzoxazepines.

Apoptosis and DNA Fragmentation Assays. Cells were seeded at 3×10^5 cells/ml and after treatment with the indicated compound, an

aliquot (150 μl) was removed and cytocentrifuged onto poly(L-lysine)-coated glass slides. The slides were stained using the RapiDiff kit following manufacturer's instructions. The extent of apoptosis and necrosis was determined by counting approximately 300 cells under 40× magnification using a light microscope. At least three fields of view per slide, with approximately 100 cells/field, were counted. Apoptotic cells were characterized by cell shrinkage, membrane blebbing, nuclear condensation, and DNA fragmentation. Cell swelling and loss of cell membrane identified necrotic cells. For the DNA fragmentation assay 1×10^7 cells were seeded in 20 ml of growth medium and treated with ethanol (1% v/v) or PBOX-6 (10 μM) for the required time period at 37°C. Cells were centrifuged at 500*g* for 5 min and the supernatant removed. The pellet was resuspended in lysis buffer (1 ml) [20 mM EDTA, 100 mM Tris, pH 8.0, 0.8% (w/v) sodium lauryl sarcosinate] and incubated at 37°C for 1 h. After incubation RNase A was added to each tube (0.5 mg/ml) and left at 37°C for a further 2 h. Proteinase K (6 mg/ml) was then added to each sample and tubes were incubated overnight at 37°C. An aliquot of each sample (45 μl) was mixed with 5 μl of loading dye (0.25% bromophenol blue, 30% glycerol in Tris borate) and samples were resolved on a 1.5% agarose gel in Tris borate for 4 h at 55 V. Ethidium bromide (10 μl of a 10-mg/ml stock) had been previously added into 100 ml of agarose. DNA ladders were visible under UV light using a UVP gel documentation system.

Measurement of Bcr-Abl and Protein Tyrosine Phosphorylation by Western Blotting. Cells (6×10^6) were harvested by centrifugation at 500*g* for 5 min followed by washing in ice-cold PBS. Pellets were resuspended in 200 μl of Harvesting buffer for assay of Bcr-Abl [20 mM HEPES, pH 7.5, 10% (w/v) sucrose, 0.1% (w/v) 3-[(3-cholamidopropyl)dimethylammino]propanesulfonate, 2 mM dithiothreitol, 0.1% (v/v) Nonidet P-40, 1 mM sodium EDTA, and 1 mM phenylmethylsulfonyl fluoride] supplemented with protease inhibitors (1 μg/ml pepstatin A and 1 μg/ml leupeptin). For the measurement of protein tyrosine phosphorylation the cell pellet was suspended in 100 μl of ice-cold lysis buffer [50 mM Tris-HCl, pH 8.0, 150 mM NaCl, 0.1% (w/v) SDS, 1% (w/v) Triton X-100, 1 mM sodium orthovanadate, 1 μg/ml leupeptin, 1 mM phenylmethylsulfonyl fluoride, and 10 μg/ml aprotinin]. In both cases, cells were incubated on ice for 10 min followed by passage 12 times through a 21-gauge needle. After a further 10-min incubation on ice the homogenates were centrifuged at 20,000*g* for 20 min at 4°C. Supernatants were removed and protein concentration was determined using a Bradford assay (Bradford, 1976). Equal amounts of protein were resolved on an 8% SDS-polyacrylamide gel and transferred onto polyvinylidene difluoride. After transfer, the membranes were blocked in PBS containing 5% (w/v) dried milk and probed with anti-c-abl or anti-phosphotyrosine antibodies. Blots were washed and probed with goat anti-mouse horseradish peroxidase-coupled secondary antibody and developed using enhanced chemiluminescence detection according to manufacturer's instructions. The Bcr-Abl blots were stripped of the antibody by incubating at 50°C for 30 min in a stripping buffer (62.5 mM Tris, 100 mM β-mercaptoethanol, and 2% SDS) and reprobed with anti-β-actin as a loading control.

Western Blot Analysis of PARP Cleavage. Cells (2×10^6) were harvested by centrifugation at 500*g* for 5 min, the supernatant was removed, and the pellets resuspended in 200 μl of PARP sample buffer [62.5 mM Tris-HCl, pH 6.8, containing 6 M urea, 10% (w/v) glycerol, 2% (w/v) SDS, 0.00125% bromophenol blue, and 5% (v/v) β-mercaptoethanol]. Samples were sonicated for 15 s and heated at 65°C for 15 min. Equal amounts of sample (15 μl) were resolved directly on a 10% SDS-polyacrylamide gel and transferred onto polyvinylidene difluoride membrane. The membrane was blocked overnight in PBS containing 5% (w/v) dried milk followed by incubation with anti-PARP antibody (2 μg/ml) for 1 h. After incubation, the membrane was washed and incubated with goat anti-mouse horseradish peroxidase-conjugated secondary antibody and enhanced chemiluminescence was used to visualize the proteins. The intact enzyme is represented by a 116-kDa band, whereas the cleavage products are represented by 29- and 87-kDa bands.

Fluorogenic Assay of Caspase-3-Like Proteases. The fluorogenic assay was performed as previously described (Zisterer et al., 2000). The fluorogenic substrate Ac-VEID-AMC was used to measure caspase 6-like protease activity.

Results

Induction of Apoptosis in CML Cells by Pyrrolo-1,5-benzoxazepines. Some of a series of pyrrolo-1,5-benzoxazepines were found to induce apoptosis in K562 cells. The characteristic morphological features of apoptosis such as cell shrinkage, chromatin condensation, DNA fragmentation, and membrane blebbing were observed in these cells (Fig. 2). To make a direct comparison of apoptotic potencies, a number of PBOX compounds were tested at the same time point (16 h) and at the same concentration (10 μM). Of the PBOX compounds tested, PBOX-3, -4, -5, -6, and -7 were found to induce apoptosis, exhibiting between 40 and 50% cell death, whereas other members of the PBOX series had no effect on cell viability, suggesting a structure-activity relationship (Fig. 3). The subsequent experiments described in this study were performed using PBOX-6 as the representative pro-apoptotic pyrrolobenzoxazepine. It has previously been reported that K562 cells are resistant to many chemotherapeutic drugs (Martins et al., 1997; Amarante-Mendes et al., 1998). In this study it was confirmed that K562 cells are resistant to the induction of apoptosis by etoposide, mitoxanthrone, and ara-C, all commonly used chemotherapeutic agents (Fig. 4). In the three CML cell lines examined, K562, LAMA 84, and KYO.1, PBOX-6 induced apoptosis in a dose-dependent (Fig. 5A) and a time-dependent (Fig. 5B) manner. The morphological features of apoptosis became apparent after a 4-h treatment with PBOX-6 (10 μM) and levels rose until 16 h, where approximately 40 to 50% of cells displayed

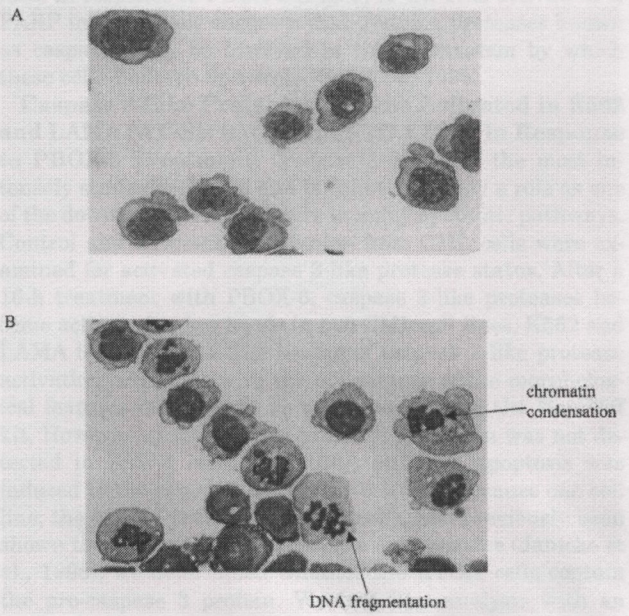

Fig. 2. Morphological features of K562 cells undergoing apoptosis after treatment with PBOX-6. Microscopic analysis of K562 cells was performed on cytospin samples. Vehicle (1% ethanol)-treated cells (A) are characterized by a continuous plasma membrane and an intact nucleus. PBOX-6-treated cells (B) display the morphological features of apoptosis, which include chromatin condensation and DNA fragmentation.

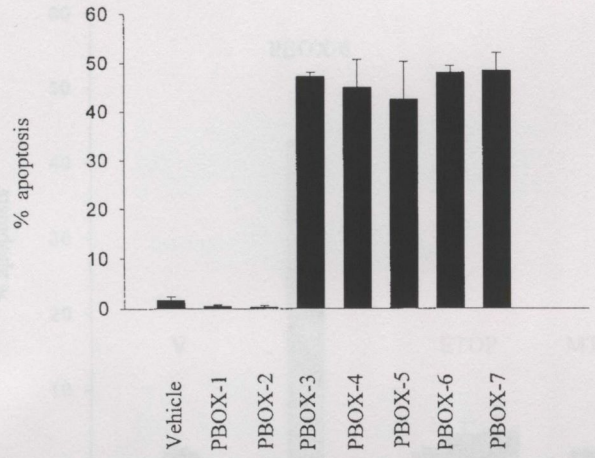

Fig. 3. Some pyrrolo-1,5-benzoxazepines induce apoptosis in K562 cells. K562 cells were seeded at 3×10^5 cells/ml and treated with the indicated PBOX compound (10 μM) for 16 h. The extent of apoptosis was determined by cytospinning an aliquot (150 μl) onto a glass slide and staining the cells with the RapiDiff kit. Values represent the mean ± the range of two separate experiments.

apoptotic features. When CML cells were treated with a concentration range of PBOX-6 for 16 h, apoptotic features were not visible with PBOX-6 concentrations of 1 μM or less. DNA fragmentation is considered to be the hallmark of apoptosis, and produces 180- to 200-base pair internucleosomal DNA fragments that are visible as "DNA ladders" on a gel. This DNA laddering pattern was visible on agarose gel when DNA was extracted from all three CML cell lines after a 48-h treatment with PBOX-6 (Fig. 5C).

PBOX-6-Induced Apoptosis Is Not Preceded by a Down-Regulation of Bcr-Abl Expression. Expression of the Bcr-Abl fusion protein in CML cells has been suggested to be responsible for the resistance of CML cells to many apoptotic agents (Martins et al., 1997). To investigate the effect of PBOX-6 on Bcr-Abl expression, levels of p210 were determined by Western blot analysis of protein extracts isolated from control and PBOX-6-treated CML cells. In the three CML cell lines, any down-regulation of Bcr-Abl was not detected up to 24 h after treatment with PBOX-6 where approximately 50% of cells had undergone apoptosis. (Fig. 6, A–C). A decrease in Bcr-Abl expression was detected in K562 and LAMA 84 cells, but only after a 24-h treatment. These results suggest that down-regulation of Bcr-Abl is not involved in the induction of apoptosis by PBOX-6.

PBOX-6-Induced Apoptosis Is Not Mediated by a Decrease in Protein Tyrosine Phosphorylation. Tyrosine phosphorylation is involved in the regulation of some apoptotic pathways. Protein tyrosine kinases and phosphatases jointly maintain the tyrosine phosphorylation status of cellular proteins (Yousefi et al., 1994). To determine the effect of PBOX-6 on the tyrosine phosphorylation status of proteins in CML cells, a Western blot assay was set up using an antibody directed against the phosphorylated form of tyrosine residues. In the three cell lines examined, the tyrosine phosphorylation status of proteins was unchanged up to 24 h after treatment with PBOX-6 (Fig. 7). We also did not detect a decrease in tyrosine phosphorylation in K562 and KYO.1 cells even up to 48 h after PBOX-6 treatment. In LAMA 84 cells, a decrease in the tyrosine phosphorylation status of some proteins was detected after a 24-h treatment with PBOX-6, at which point approximately 50% of the cells had undergone apoptosis. These results further suggest that down-regulation of Bcr-Abl or inhibition of the Abl tyrosine kinase activity is not part of the upstream events associated with PBOX-6-induced apoptosis.

PBOX-6-Induced Apoptosis in K562 Cells Does Not Involve the Production of Reactive Oxygen Intermediates (ROIs). Several observations suggest an involvement of ROIs in the signal transduction pathway leading to apoptosis (Jacobson, 1996). To determine whether the induction of apoptosis in K562 cells by PBOX-6 involved the production of ROIs, cells were pretreated with vitamin E or *N*-acetylcysteine for 1 or 24 h, respectively, before treatment with PBOX-6 for a further 16 h. The extent of apoptosis was determined by cytospinning the cells onto slides and staining with the RapiDiff kit. These compounds did not protect against PBOX-6-induced apoptosis (Fig. 8, A and B), suggesting that the production of ROIs is not involved in the mechanism by which PBOX-6 induces apoptosis in K562 cells. As a positive control HL-60 cells were pretreated with the antioxidants vitamin E or *N*-acetylcysteine before treatment with the apoptosis-inducing agents, UV irradiation, or H_2O_2, respectively. Results showed that pretreatment of HL-60 cells with these antioxidants before either UV-irradiation or H_2O_2 treatment reduced the level of apoptosis induced in these cells (Fig. 8, C and D).

PBOX-6 Treatment of CML Cells Results in PARP Cleavage. In some cell lines, PARP (116 kDa) is cleaved during apoptosis into its 87- and 29-kDa fragments, which can be detected by Western blot analysis of cell lysates. Control and PBOX-6-treated cell lysates of CML cells were examined for evidence of PARP cleavage. Results show that PARP cleavage occurs to a small extent in all three CML cell lines in response to PBOX-6 (Fig. 9, A–C). This activation of PARP in these cells suggests that cysteine proteases known as caspases may be involved in the mechanism by which these cells undergo apoptosis (Gu et al., 1995).

Caspase 3-Like Proteases Become Activated in K562 and LAMA 84 Cells but Not in KYO.1 Cells in Response to PBOX-6 Treatment. Caspase 3 is one of the most intensely studied caspases and is believed to play a role as one of the downstream executioners in many apoptotic pathways. Control and apoptotic cell lysates from CML cells were examined for activated caspase 3-like protease status. After a 16-h treatment with PBOX-6, caspase 3-like proteases become activated to low levels in two CML cell lines, K562 and LAMA 84 (Fig. 10A). The timing of caspase 3-like protease activation correlates with the appearance of the morphological features of apoptosis as determined using the RapiDiff kit. However, caspase 3-like protease activation was not detected in KYO.1 cells (Fig. 10A), although apoptosis was induced to the same extent in this cell line. Because one cell line, the MCF-7 breast carcinoma cells, had previously been shown to be deficient in the caspase 3 proenzyme (Janicke et al., 1998), we determined whether the KYO.1 cells contain the pro-caspase 3 protein. Western blot analysis with an antibody directed against the pro-enzyme form of caspase 3 was used to demonstrate the presence of this protein in all three CML cell lines (Fig. 10B).

Cells were pretreated with a caspase 3-like protease inhibitor, z-DEVD-fmk (200 μM), for 1 h followed by treatment

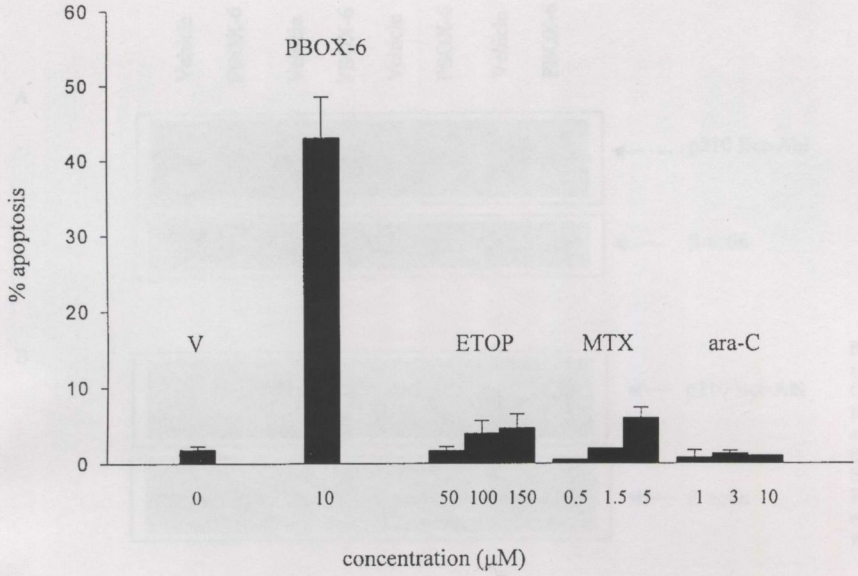

Fig. 4. K562 cells are resistant to apoptosis induced by etoposide, mitoxanthrone, and ara-C. K562 cells were seeded at a density of 3×10^5 cells/ml and treated for 16 h with either vehicle (V) PBOX-6 (10 μM), etoposide (ETOP), (50, 100, or 150 μM), mitoxanthrone (MTX) (0.5, 1.5, or 5 μM), or ara-C (1, 3, or 10 μM). The extent of apoptosis was determined by cytospinning and staining the slides using the RapiDiff kit. Results represent the mean ± S.E. of three separate experiments.

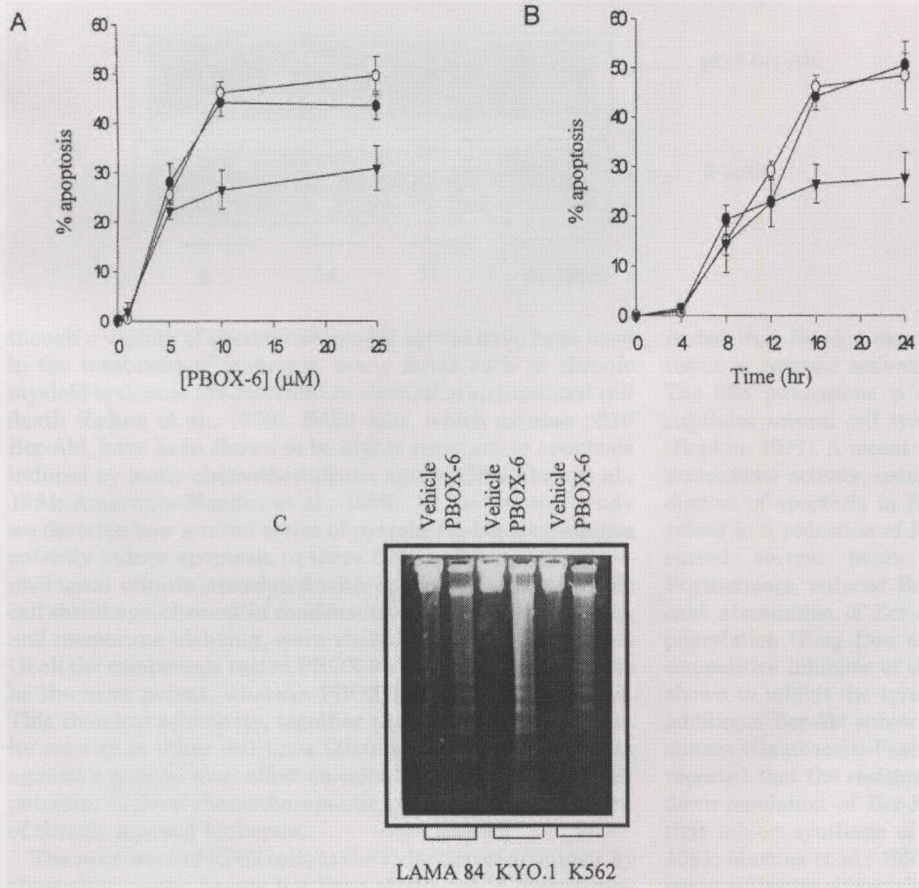

Fig. 5. PBOX-6 induces apoptosis in CML cells in a dose- and time-dependent manner and results in DNA fragmentation. Cells were seeded at 3×10^5 cells/ml and were treated with a range (0–25 μM) of PBOX-6 concentrations for 16 h (A) or PBOX-6 (10 μM) for a period of 4, 8, 12, 16, and 24 h (B). The extent of apoptosis was determined by cytospinning and staining cells with the RapiDiff kit. Values represent the mean ± S.E. of three separate experiments. In C, CML cells were treated with either vehicle [1% (v/v) ethanol] or PBOX-6 (10 μM) for 48 h and DNA (45 μl) was resolved by gel electrophoresis. Results are representative of at least two separate experiments. ●, K562; ○, KYO.1; ▼, LAMA 84.

with PBOX-6 for a further 8 h. Results show that pretreatment of K562 and LAMA 84 cells with z-DEVD-fmk inhibited the activity of caspase 3-like proteases (Fig. 10C) but did not prevent the induction of apoptosis by PBOX-6 (Fig. 10D). These results would suggest that although during apoptosis a low level of caspase 3-like protease activation was detected in two of the CML cell lines, this activation is not an essential step in the pathway under which PBOX-6 induces apoptosis in any of the three cell lines.

Discussion

The efficacy of chemotherapeutic agents depends on their effectiveness at inducing apoptosis in malignant cells. Al-

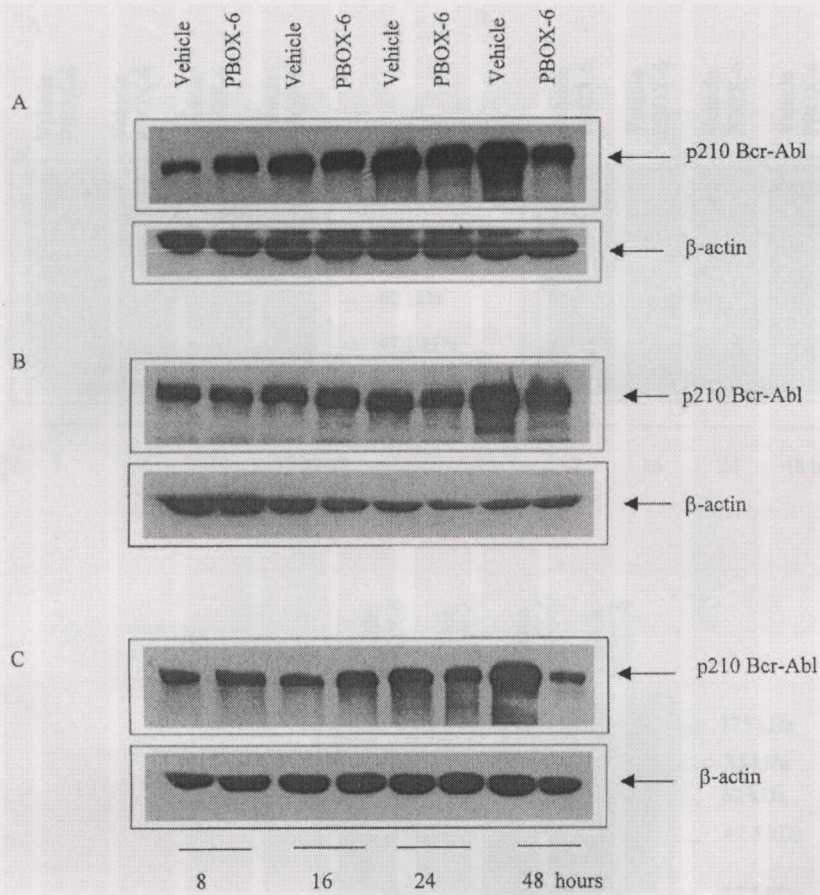

Fig. 6. PBOX-6-induced apoptosis in CML cells is not preceded by the down-regulation of Bcr-Abl. Cytosolic extracts were prepared from K562 (A), KYO.1 (B), and LAMA 84 (C) after treatment with either vehicle (1% ethanol) or PBOX-6 (10 μM) for 8, 16, 24, and 48 h. Protein (40 μg) was resolved by SDS-PAGE and probed with anti-c-abl antibody. Results are representative of at least two separate experiments. Blots were stripped and reprobed with β-actin as a loading control.

though a variety of chemotherapeutic agents have been used in the treatment of leukemia, many forms such as chronic myeloid leukemia are resistant to chemotherapy-induced cell death (Lehne et al., 1998). K562 cells, which express p210 Bcr-Abl, have been shown to be highly resistant to apoptosis induced by many chemotherapeutic agents (McGahon et al., 1994; Amarante-Mendes et al., 1998). In the present study we describe how a novel series of pyrrolo-1,5-benzoxazepines potently induce apoptosis in three CML cell lines. The morphological criteria associated with apoptosis, which include cell shrinkage, chromatin condensation, DNA fragmentation, and membrane blebbing, were visible in all three cell lines. Of all the compounds tested PBOX-3, -6, and -7 were found to be the most potent, whereas PBOX-1 and -2 had no effect. This chemical selectivity, together with their lack of apoptotic activity in other cell lines (Zisterer et al., 2000), argues against a general toxic effect on cells. This may suggest their potential as novel chemotherapeutic agents for the treatment of chronic myeloid leukemia.

The resistance of K562 cells to the induction of apoptosis by chemotherapeutic agents has been attributed to overexpression of the *bcr-abl* gene (McGahon et al., 1994, 1995; Martins et al., 1997). It is widely agreed that the mechanism by which Bcr-Abl may cause the accumulation of leukemic blasts is by inhibition of apoptosis, rather than by increasing the rate of cell division (Kabarowski et al., 1994; Rowley et al., 1996). The mechanism or the step at which this antiapoptotic effect is exerted has not been clearly defined. However, it is reported that Bcr-Abl exerts its effect upstream of events that result in caspase activation (Amarante-Mendes et al., 1998). The 26S proteasome is a large multicatalytic protease that regulates several cell cycle and apoptosis regulatory proteins (Hopkin, 1997). A recent report suggests that inhibition of the proteasome activity, using selective inhibitors, causes the induction of apoptosis in K562 cells. Proteasome inhibition resulted in a reduction of Bcr-Abl protein expression, which occurred several hours before the onset of apoptosis. Furthermore, reduced Bcr-Abl expression resulted in significant attenuation of Bcr-Abl-mediated protein tyrosine phosphorylation (Ping Dou et al., 1999). CGP57148B, the ATP-competitive inhibitor of the Abl protein kinase, has also been shown to inhibit the tyrosine phosphorylation of Bcr-Abl and additional Bcr-Abl substrates within minutes, resulting in apoptosis (Gambacorti-Passerini et al., 1997). It has also been reported that the resistance of K562 cells can be reversed by down-regulation of Bcr-Abl using antisense oligonucleotides that inhibit synthesis of the Bcr-Abl kinase (Szczylik et al., 1991; Martins et al., 1997). Studies by McGahon et al. (1994) using antisense oligonucleotides reveal that down-regulation of p210 Bcr-Abl expression rendered the cells more susceptible to apoptosis induced by chemotherapeutic agents. However, some studies have revealed conflicting reports. It has been reported that down-regulation is not caused by an antisense mechanism, but is due to a nonspecific effect brought about by the DNA sequence (Vaerman et al., 1995).

Our results show that a representative pyrrolo-1,5-benzo-

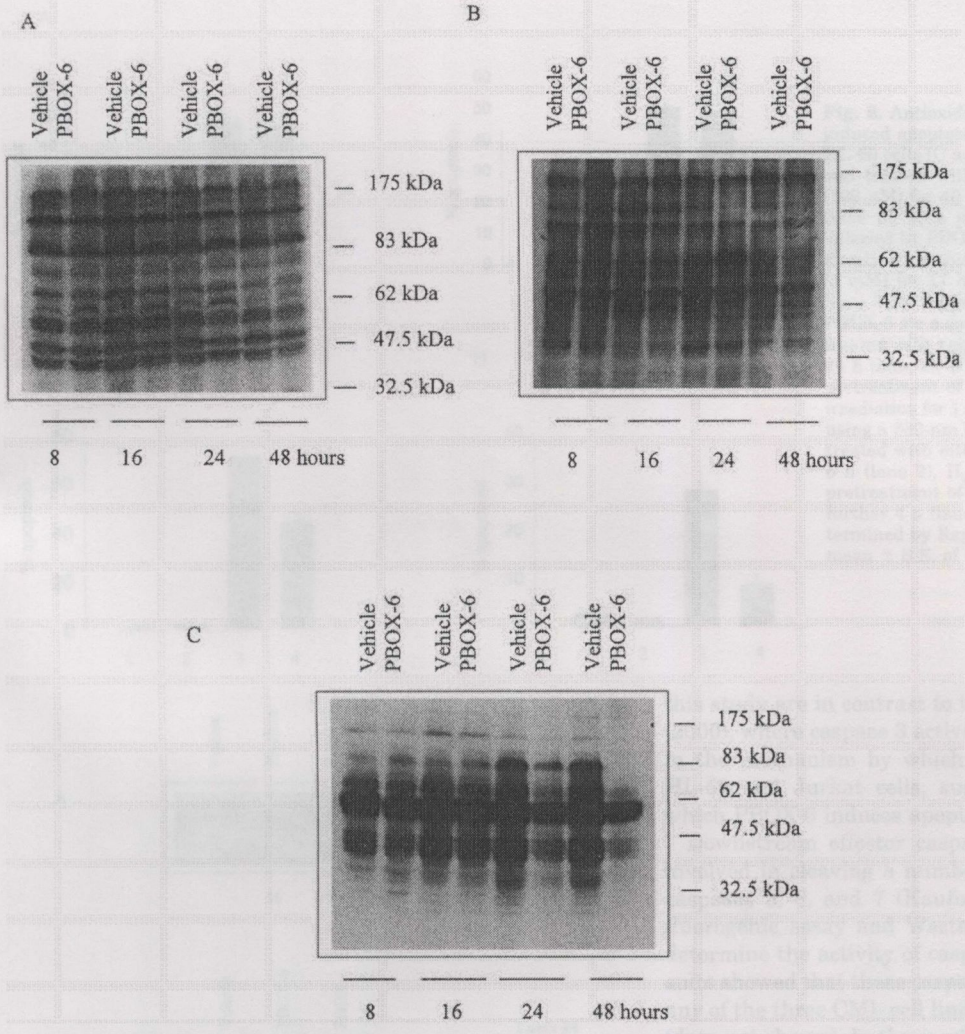

Fig. 7. PBOX-6-induced apoptosis is not mediated by a change in the tyrosine phosphorylation status of proteins. Whole-cell extracts were prepared from K562 (A), KYO.1 (B), and LAMA 84 (C) after treatment with either vehicle (1% ethanol) or PBOX-6 (10 μM) for 8, 16, 24, and 48 h. Protein was resolved by SDS-PAGE and probed with anti-phosphotyrosine antibody. Results are representative of at least two separate experiments.

xazepine, PBOX-6, induces a time- and dose-dependent induction of apoptosis in three CML cell lines. In the present study, PBOX-6 was able to bypass Bcr-Abl-mediated resistance to apoptosis in the three CML cell lines. Any down-regulation of Bcr-Abl did not accompany, but rather followed apoptosis in these cells. Any down-regulation was not detected until after a 24-h treatment with PBOX-6 when approximately 50% of cells displayed the morphological features of apoptosis. This would suggest that down-regulation of Bcr-Abl is not involved in the upstream events associated with PBOX-6-induced apoptosis. The tyrosine phosphorylation status of proteins remained unchanged up to 24 h after treatment with PBOX-6, suggesting that inhibition of Bcr-Abl activity is not responsible for execution of the apoptotic cascade after PBOX-6 treatment. Results from this study suggest that a reduction in p210 expression, or inhibition of Bcr-Abl activity, is not the only mechanism by which cells can escape the antiapoptotic effect of the *bcr-abl* gene.

Several observations suggest an involvement of ROIs in the signal transduction pathway leading to apoptosis. This mode of cell death is sometimes associated with increases in intracellular ROI levels and the addition of various exogenous antioxidants, such as NAC, can inhibit apoptosis (McGowan et al., 1996). This work has shown that PBOX-6-induced apoptosis in K562 cells was unaffected by the presence of NAC or vitamin E. This would suggest that PBOX-6-induced apoptosis is not mediated by ROIs. Similar findings were reported by Zisterer et al. (2000) after treatment of HL-60 cells with PBOX-6. This is in agreement with recent reports, which have indicated that ROIs are not necessarily a requirement for apoptosis (Jacobson and Raff, 1995).

A unique family of cysteine proteases called caspases appear to play a critical role in initiating and sustaining the biochemical events that occur during apoptotic cell death. This family of proteases, which contain at least 12 human members, cleaves after aspartate residues (Martins et al., 1997). Janicke et al. (1998) and others have shown that activation of caspase 3 is not essential for tumor necrosis factor-, staurosporine-, or Fas-induced apoptosis. Although a low level of activation of caspase 3-like proteases was detected in K562 and LAMA 84 cells, inhibition of this caspase 3-like protease activity using the inhibitor z-DEVD-fmk did not inhibit the induction of apoptosis. In addition, caspase 3-like protease activity was not detected in KYO.1 cells undergoing apoptosis. The lack of activation of caspase 3-like proteases in KYO.1 cells was not due to the absence of the

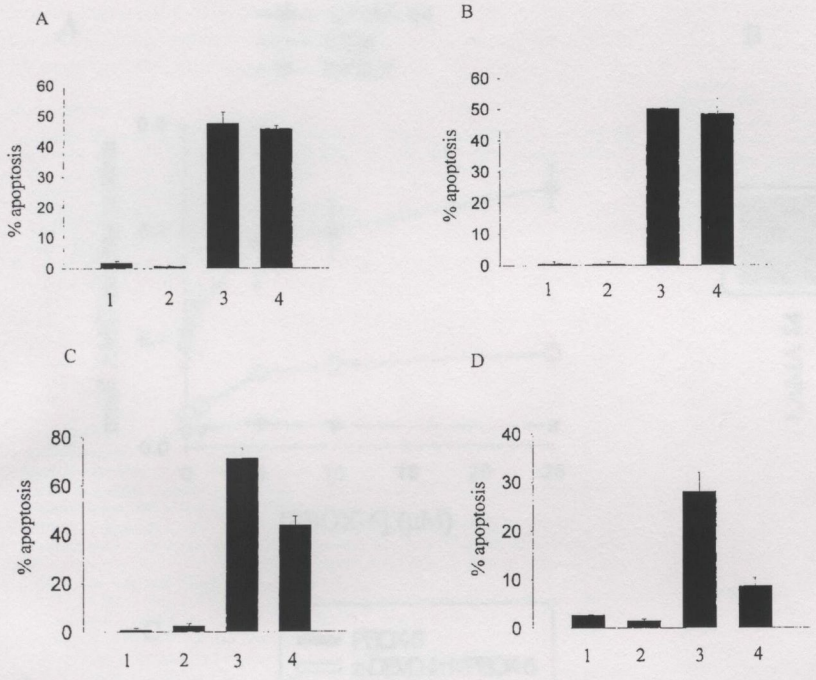

Fig. 8. Antioxidants do not protect against PBOX-6-induced apoptosis in K562 cells. K562 (A and B) and HL-60 cells (C and D) were seeded at 3×10^5 cells/ml and treated with either vehicle (lane 1), vitamin E (100 μM) for 40 h (lane 2), PBOX-6 (10 μM) for 16 h (lane 3), or a pretreatment of vitamin E for 24 h followed by PBOX-6 for a further 16 h (lane 4) (A). In B, cells were treated with either vehicle (lane 1), NAC (5 mM) for 17 h (lane 2), PBOX-6 (10 μM) for 16 h (lane 3), or a pretreatment of NAC for 1 h followed by PBOX-6 for a further 16 h (lane 4). HL-60 cells were treated with vehicle (lane 1), vitamin E (100 μM) for 24 h (lane 2), UV-irradiation for 1 min (lane 3), or a pretreatment of vitamin E for 24 h followed by UV-irradiation for 1 min (lane 4) (C). Cells were irradiated using a 302-nm UV transilluminator. In D, cells were treated with either vehicle (lane 1), NAC (5 mM) for 5 h (lane 2), H_2O_2 (0.01 μM) for 4 h (lane 3), or a pretreatment of NAC for 1 h followed by H_2O_2 for a further 4 h (lane 4). The extent of apoptosis was determined by RapiDiff staining. Results represent the mean ± S.E. of three separate experiments.

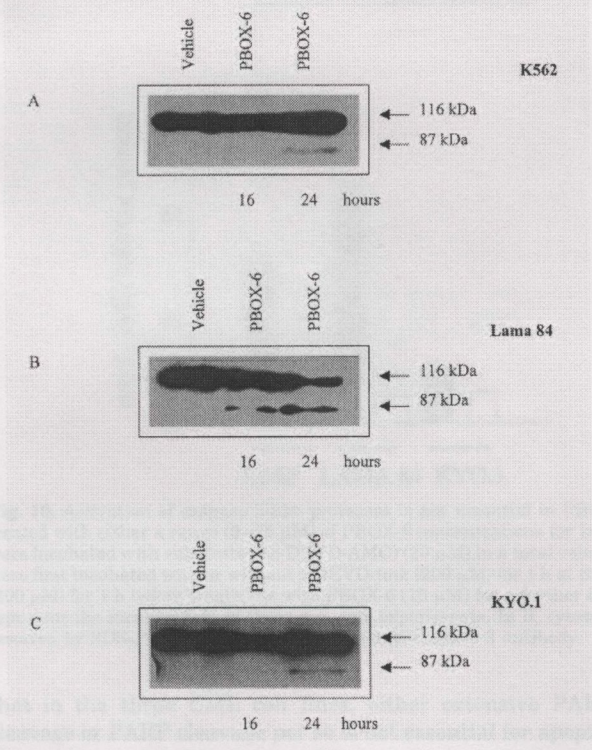

Fig. 9. PBOX-6 induces PARP cleavage in CML cells. Whole-cell extracts from K562 (A), LAMA 84 (B), and KYO.1 (C) were prepared after treatment with vehicle (1% ethanol) or PBOX-6 (10 μM) for 16 and 24 h. Samples were resolved by SDS-PAGE and probed with anti-PARP. Results are representative of at least two experiments.

proenzyme form of caspase 3, as demonstrated by Western blotting. Therefore, in this study it has been shown that activation of caspase 3-like proteases is not required for the induction of apoptosis by PBOX-6 in CML cells. Results from this study are in contrast to those reported by Zisterer et al. (2000), where caspase 3 activation was shown to be essential in the mechanism by which PBOX-6 induces apoptosis in HL-60 and Jurkat cells, suggesting that the pathway in which PBOX-6 induces apoptosis is cell-type specific.

Downstream effector caspases, which are thought to be involved in cleaving a number of death substrates, include caspases 3, 6, and 7 (Kaufmann and Earnshaw, 2000). A fluorogenic assay and Western blot analysis were used to determine the activity of caspases 6 and 7, respectively. Results showed that these caspases did not become activated in any of the three CML cell lines after treatment with PBOX-6 (data not shown). In these cells, alternative, as yet unknown effector caspases may be involved in the induction of apoptosis or a caspase-independent mechanism for commitment cell death may exist. For example, a recent report indicates that inhibition of the activity of the transcription factor nuclear factor-κB in human T lymphocytes resulted in apoptosis without detectable activation of caspase 1-, 3-, or 6-like proteases, suggesting either low level of activation is required or different caspases are involved (Kolenko et al., 1999). Caspase-independent pathways have also been reported, for example, overexpression of the proapoptotic protein Bax in mammalian cells induces DNA condensation and membrane alterations leading to cell death without caspase activation (Xiang et al., 1996).

In the present study Western blot analysis has shown only a small degree of PARP cleavage into its 87-kDa cleavage product. Although Western blotting may not provide an accurate quantitative assessment of cleavage, this low level of cleavage is consistent with low or no caspase 3-like protease activation because caspase 3 is thought to be the major protease cleaving this substrate (Cuvillier et al., 1998). As mentioned above, caspase-independent apoptosis can occur, which would in turn suggest that PARP cleavage is not essential for apoptosis in these cases. Our results suggest

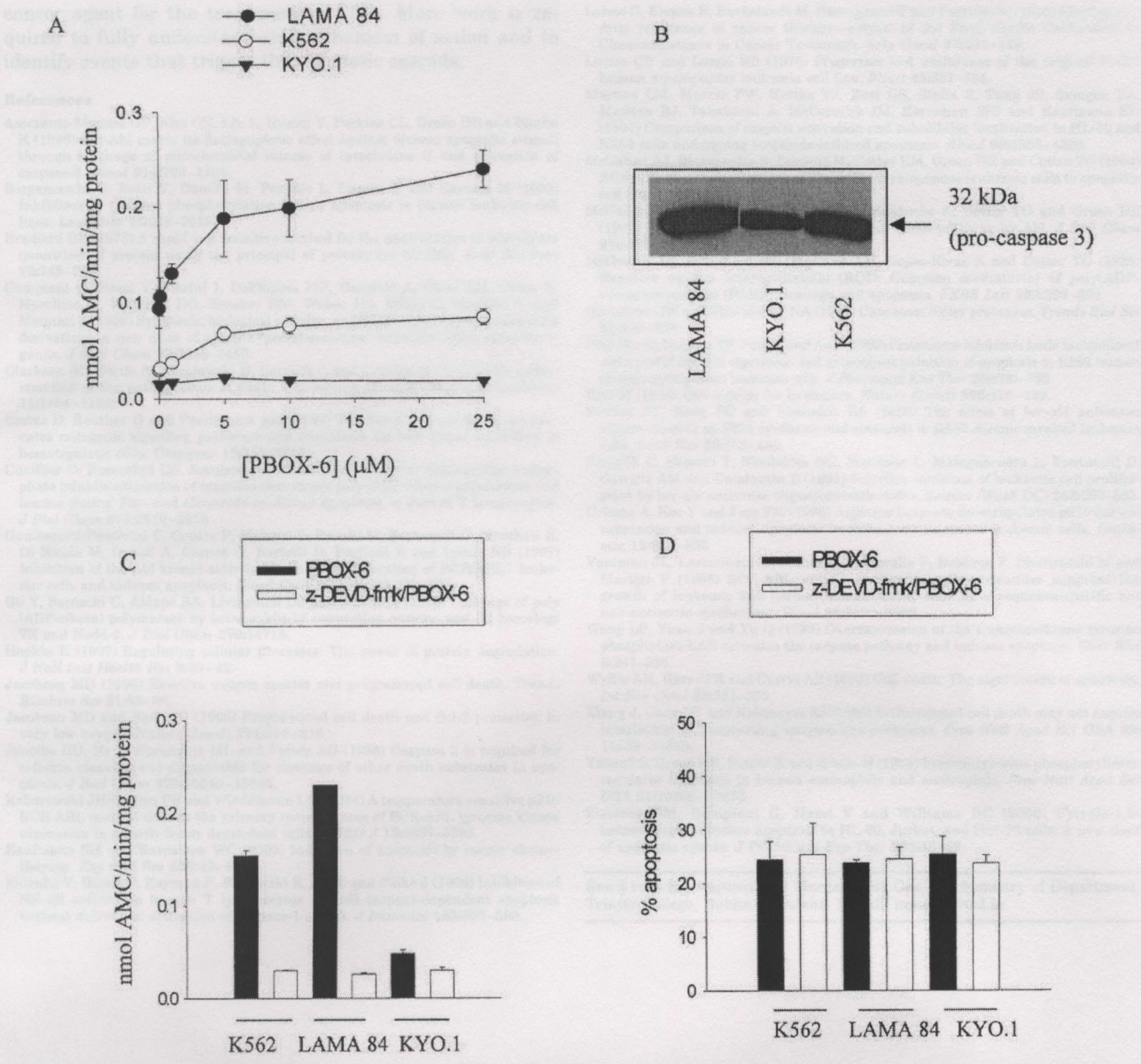

Fig. 10. Activation of caspase 3-like proteases is not essential in PBOX-6-mediated apoptosis. CML cells were seeded at 5×10^6 cells/sample and treated with either a range (0–25 μM) of PBOX-6 concentrations for 16 h (A) or PBOX-6 (10 μM) for 16 h (C). In both cases, enzyme extracts (100 μg) were incubated with substrate (Ac-DEVD-AMC) (20 μM) in a total volume of 3 ml and caspase 3-like protease activity was measured, but in C extracts were first incubated with or without z-DEVD-fmk (200 μM) for 1 h at room temperature. In D, CML cells were pretreated with or without z-DEVD-fmk (200 μM) for 1 h before treatment with PBOX-6 (10 μM) for a further 8 h and the extent of apoptosis was determined by RapiDiff staining. All values represent the mean ± S.E. of three separate experiments. In B, cytosolic extracts from untreated CML cells were prepared and protein (45 μg) was resolved by SDS-PAGE before probing with anti-caspase 3 antibody.

that in the three CML cell lines, either extensive PARP cleavage or PARP cleavage per se is not essential for apoptosis.

In agreement with previous reports, we have shown that K562 cells are resistant to apoptosis induced by many chemotherapeutic agents (Amarante-Mendes et al., 1998). Pyrrolo-1,5-benzoxazepines have recently been described as a novel class of apoptotic agent based on their ability to induce apoptosis in a number of leukemia and lymphoma cell lines derived from the hematopoietic system such as HL-60, Jurkat, and Hut 78 cells (Zisterer et al., 2000). In the present work it has been shown that a number of these novel pyrrolo-1,5-benzoxazepine derivatives are also potent inducers of apoptosis in drug-resistant CML cells. These compounds induce apoptosis with similar potencies to that reported in HL-60 cells, which are often used as a model for the induction of apoptosis (Zisterer et al., 2000). The resistance of CML cells has been attributed to the expression of the transforming oncogene *bcr-abl*. Results from the current study suggest that this novel compound, PBOX-6, can induce apoptosis in CML cells by bypassing Bcr-Abl-mediated resistance. This may suggest the potential of this compound as a novel anti-

cancer agent for the treatment of CML. More work is required to fully understand its mechanism of action and to identify events that trigger the apoptotic cascade.

References

Amarante-Mendes GP, Kim CN, Liu L, Huang Y, Perkins CL, Green DR and Bhalla K (1998) Bcr-Abl exerts its antiapoptotic effect against diverse apoptotic stimuli through blockage of mitochondrial release of cytochrome C and activation of caspase-3. *Blood* **91:**1700–1705.

Bergamaschi G, Rosti V, Danova M, Ponchio L, Lucotti C and Cazzola M (1993) Inhibitors of tyrosine phosphorylation induce apoptosis in human leukemic cell lines. *Leukemia* **7:**2012–2018.

Bradford BB (1976) A rapid and sensitive method for the quantitation of microgram quantities of protein using the principal of protein-dye binding. *Anal Biochem* **72:**248–253.

Campiani G, Nacci V, Fiorini I, DeFilippis MP, Garofalo A, Ciani SM, Greco G, Novellion E, Williams DC, Zisterer DM, Woods MJ, Mihai C, Manzoni C and Mennini T (1996) Synthesis, biological activity, and SARs of pyrrolobenzoxazepine derivatives, a new class of specific "peripheral-type" benzodiazepine receptor ligands. *J Med Chem* **39:**3435–3450.

Clarkson BD, Strife A, Wisniewski D, Lambek C and Carpino N (1997) New understanding of the pathogenesis of CML: A prototype of early neoplasia. *Leukemia* **11:**1404–1428.

Cortez D, Reuther G and Pendergast AM (1997) The Bcr-Abl tyrosine kinase activates mitogenic signaling pathways and stimulates G1-to-S phase transition in hematopoietic cells. *Oncogene* **15:**333–2342.

Cuvillier O, Rosenthal DS, Smulson ME and Spiegel S (1998) Sphingsoine 1-phosphate inhibits activation of caspases that cleave poly (ADP-ribose) polymerase and lamins during Fas- and Ceramide-mediated apoptosis in Jurkat T lymphocytes. *J Biol Chem* **273:**2910–2916.

Gambacorti-Passerini C, Coutre P, Mologni L, Fanelli M, Bertazzoli C, Marchesi E, Di Nicola M, Biondi A, Corneo G, Berlotti D, Pogliani E and Lydon NB (1997) Inhibition of the Abl kinase activity blocks the proliferation of BCR/ABL$^+$ leukemic cells and induces apoptosis. *Blood Cells Mol Dis* **23**:380–394.

Gu Y, Sarnecki C, Aldape RA, Livingston DJ and Su MS-S (1995) Cleavage of poly (ADP-ribose) polymerase by interleukin-1β converting enzyme and its homologs TX and Nedd-2. *J Biol Chem* **270:**18715.

Hopkin K (1997) Regulating cellular processes: The power of protein degradation. *J Natl Inst Health Res* **9:**36–42.

Jacobson MD (1996) Reactive oxygen species and programmed cell death. *Trends Biochem Sci* **21:**83–86.

Jacobson MD and Raff MC (1995) Programmed cell death and Bcl-2 protection in very low oxygen. *Nature (Lond)* **374:**814–816.

Janicke RU, Ng P, Sprengart ML and Porter AG (1998) Caspase 3 is required for α-fodrin cleavage but dispensable for cleavage of other death substrates in apoptosis. *J Biol Chem* **273:**15540–15545.

Kabarowski JHS, Allen PB and Wiedemann LM (1994) A temperature sensitive p210 BCR-ABL mutant defines the primary consequences of BCR-ABL tyrosine kinase expression in growth factor dependent cells. *EMBO J* **13:**5887–5895.

Kaufmann SH and Earnshaw WC (2000) Induction of apoptosis by cancer chemotherapy. *Exp Cell Res* **256:**42–49.

Kolenko V, Bloom T, Rayman P, Bukowski R, His E and Finke J (1999) Inhibition of NK-κB activity in human T lymphocytes induces caspase-dependent apoptosis without detectable activation of caspase-1 and -3. *J Immunol* **163:**590–598.

Lehne G, Elonen E, Baekelandt M, Skovsgaard T and Peterson C (1998) Challenging drug resistance in cancer therapy—review of the First Nordic Conference on Chemoresistance in Cancer Treatment. *Acta Oncol* **37:**431–439.

Lozzio CB and Lozzio BB (1975) Properties and usefulness of the original K-562 human myelogenous leukemia cell line. *Blood* **45:**321–334.

Martins LM, Mesver PW, Kottke TJ, Basi GS, Sinha S, Tung JS, Svingen PA, Madden BJ, Takahashi A, McCormick DJ, Earnshaw WC and Kaufmann SH (1997) Comparison of caspase activation and subcellular localization in HL-60 and K562 cells undergoing etoposide-induced apoptosis. *Blood* **90:**4283–4296.

McGahon AJ, Bissonnette R, Schmitt M, Cotter KM, Green DR and Cotter TG (1994) BCR-ABL maintains resistance of chronic myelogenous leukemia cells to apoptotic cell death. *Blood* **83:**1179–1187.

McGahon AJ, Nishioka WK, Martin SJ, Mahboubi A, Cotter TG and Green DR (1995) Regulation of the Fas apoptotic cell death pathway by Abl. *J Biol Chem* **270:**22625–22631.

McGowan AJ, Ruiz-Ruiz MC, Gorman AM, Lopez-Rivas A and Cotter TG (1996) Reactive oxygen intermediate(s) (ROI): Common mediator(s) of poly(ADP-ribose)polymerase (PARP) cleavage and apoptosis. *FEBS Lett* **392:**299–303.

Nicholson DW and Thornberry NA (1997) Caspases: Killer proteases. *Trends Biol Sci* **22:**299–306.

Ping Dou Q, Mcguire TF, Peng Y and An B (1999) Proteasome inhibition leads to significant reduction of Bcr-Abl expression and subsequent induction of apoptosis in K562 human chronic myelogenous leukemia cells. *J Pharmacol Exp Ther* **289:**781–790.

Raff M (1998) Cell suicide for beginners. *Nature (Lond)* **396:**119–122.

Rowley PT, Keng PC and Kosciolek BA (1996) The effect of *bcr-abl* antisense oligonucleotide on DNA synthesis and apoptosis in K562 chronic myeloid leukemia cells. *Leuk Res* **20:**473–480.

Szczylik C, Skorski T, Nicolaides NC, Manzella L, Malaguarnera L, Venturelli D, Gewirtz AM and Calabretta B (1991) Selective inhibiton of leukemia cell proliferation by bcr-abl antisense oligodeoxynucleotides. *Science (Wash DC)* **253:**562–565.

Urbano A, Koc Y and Foss FM (1998) Arginine butyrate downregulates p210 bcr-abl expression and induces apoptosis in chronic myelogenous leukemia cells. *Leukemia* **12:**930–936.

Vaerman JL, Lammineur C, Moureau P, Lewalle P, Deldime F, Blumenfeld M and Martiat P (1995) BCR-ABL antisense oligodeoxyribonucleotides suppress the growth of leukemic and normal hematopoeitic cells by a sequence-specific but non-antisense mechanism. *Blood* **86:**3891–3896.

Weng LP, Yuan J and Yu Q (1998) Overexpression of the transmembrane tyrosine phosphatase LAR activates the caspase pathway and induces apoptosis. *Curr Biol* **8:**247–256.

Wyllie AH, Kerr JFR and Currie AR (1980) Cell death: The significance of apoptosis. *Int Rev Cytol* **68:**251–306.

Xiang J, Chao DT and Kolsmeyer SJ (1996) BAX-induced cell death may not require interleukin 1 β-converting enzyme-like proteases. *Proc Natl Acad Sci USA* **93:** 14559–14563.

Yousefi S, Green DR, Blaser K and Simon H (1994) Protein-tyrosine phosphorylation regulates apoptosis in human eosinophils and neutrophils. *Proc Natl Acad Sci USA* **91:**10868–10872.

Zisterer DM, Campiani G, Nacci V and Williams DC (2000) Pyrrolo-1,5-benzoxazepines induce apoptosis in HL-60, Jurkat, and Hut-78 cells: A new class of apoptotic agents. *J Pharmacol Exp Ther* **293:**48–59.

Send reprint requests to: Margaret Mc Gee, Biochemistry of Department, Trinity College, Dublin 2, Ireland. E-mail: mmcgee@tcd.ie